

Controlled Drug Delivery

August 16, 2012 | <http://pubs.acs.org>
Publication Date: May 15, 2000 | doi: 10.1021/bk-2000-0752.fw001

ACS SYMPOSIUM SERIES 752

Controlled Drug Delivery

Designing Technologies for the Future

Kinam Park, EDITOR
Purdue University

Randall J. Mersny, EDITOR
Genentech, Inc.



American Chemical Society, Washington, DC

iii



Library of Congress Cataloging-in-Publication Data

Controlled drug delivery : designing technologies for the future / Kinam Park, Randy J. Mrsny, [editors].

p. cm.—(ACS symposium series , ISSN 0097-6156 ; 752)

Includes bibliographical references and index.

ISBN 0-8412-3625-9

1. Drug delivery systems—Congresses. 2. Drug targeting—Congresses.

I. Park, Kinam., 1952- . II. Mrsny, Randy J., 1955- . III. Series.

RS199.5.C664 2000

615'.7—dc21

99-58688

The paper used in this publication meets the minimum requirements of American National Standard for Information Sciences—Permanence of Paper for Printed Library Materials, ANSI Z39.48-1984.

Copyright © 2000 American Chemical Society

Distributed by Oxford University Press

All Rights Reserved. Reprographic copying beyond that permitted by Sections 107 or 108 of the U.S. Copyright Act is allowed for internal use only, provided that a per-chapter fee of \$20.00 plus \$0.75 per page is paid to the Copyright Clearance Center, Inc., 222 Rosewood Drive, Danvers, MA 01923, USA. Republication or reproduction for sale of pages in this book is permitted only under license from ACS. Direct these and other permissions requests to ACS Copyright Office, Publications Division, 1155 16th Street, N.W., Washington, DC 20036.

The citation of trade names and/or names of manufacturers in this publication is not to be construed as an endorsement or as approval by ACS of the commercial products or services referenced herein; nor should the mere reference herein to any drawing, specification, chemical process, or other data be regarded as a license or as a conveyance of any right or permission to the holder, reader, or any other person or corporation, to manufacture, reproduce, use, or sell any patented invention or copyrighted work that may in any way be related thereto. Registered names, trademarks, etc., used in this publication, even without specific indication thereof, are not to be considered unprotected by law.

PRINTED IN THE UNITED STATES OF AMERICA

**American Chemical Society
Library**

1155 16th St., N.W.

Washington, D.C. 20036

In Controlled Drug Delivery; Park, K., et al.;

ACS Symposium Series; American Chemical Society: Washington, DC, 2000.

Foreword

THE ACS SYMPOSIUM SERIES was first published in 1974 to provide a mechanism for publishing symposia quickly in book form. The purpose of the series is to publish timely, comprehensive books developed from ACS sponsored symposia based on current scientific research. Occasionally, books are developed from symposia sponsored by other organizations when the topic is of keen interest to the chemistry audience.

Before agreeing to publish a book, the proposed table of contents is reviewed for appropriate and comprehensive coverage and for interest to the audience. Some papers may be excluded in order to better focus the book; others may be added to provide comprehensiveness. When appropriate, overview or introductory chapters are added. Drafts of chapters are peer-reviewed prior to final acceptance or rejection, and manuscripts are prepared in camera-ready format.

As a rule, only original research papers and original review papers are included in the volumes. Verbatim reproductions of previously published papers are not accepted.

ACS BOOKS DEPARTMENT

Preface

The advent of a new millennium provides a somewhat unique opportunity for both reflection and projection. It seems that everyone awaits the beginning of the new millennium with some degree of anticipation. Indeed, great expectations have been imposed for significant advances in areas ranging from aquaculture to the Unified Field Theory. With similar expectations, a symposium entitled “Drug Delivery in the 21st Century” was held at a recent meeting of the American Chemical Society (ACS) (March 1999 in Anaheim, California). An outstanding group of research scientists from both academics and industry were brought together and given the opportunity to express not only their views of what has been accomplished in various delivery technologies but also prophetic views of drug delivery possibilities for the next millennium. Their common focus of future drug delivery possibilities was driven by expectations that advances made by the medical research community will allow improvements in both the quality of life and the duration of life expectancy. As with previous medical advances, the success of future treatments will require the demonstration of both safety and efficacy. It was anticipated that, more than ever before, the clinical success of future advances made by medical research will require the application of drug delivery technologies.

As one might imagine, it is also assumed that as more complex medical technologies are developed, more creative forms of delivery will be required for their successful clinical application to ensure maximum efficacy and minimal side effects. The speakers brought together for this symposium did a magnificent job of providing that spark of creativity. Their concepts have now been incorporated into the chapters of this book.

We have divided the many topics of these presentations into six sections. The first section focuses on design considerations and challenges in oral drug delivery. In the second section, strategies to improve drug delivery are highlighted. Drug targeting approaches is the topic for the third section. Self-regulated and modulated drug delivery technologies are the focus of the fourth section. Delivery of hydrophobic drugs using new delivery vehicles is discussed in the fifth section. Polymeric therapeutics in the next century is the subject of the final section.

Background information in each chapter allows the novice to gain an appreciation for that particular area while state-of-the-art data is presented as a platform for future projections.

In the past, numerous advances in medical technology were made that never came to fruition due to inadequate drug delivery. Frequently, timing was a major culprit. As a new medical advance is identified, the required need for drug delivery for its clinical success is identified only at a late stage in its development. Thus, the successful application of a drug delivery technology typically requires that it be ready at the same time as an advance occurs in a medical technology so

that the two technologies can be melded at an early stage of development. This timing issue is not a simple one to overcome. It is relatively easy to look back on these missed opportunities and identify what should have been done. The problem becomes much more challenging when future drug delivery needs must be anticipated so they can be available for cohesive integration as new medical technologies are identified. Without a crystal ball, this task of identifying drug delivery technologies needed for the future requires astute anticipation. This book is a platform where some of the brightest and most far-thinking researchers in drug delivery have been given the opportunity to state where they feel future needs will be in their specific area of study.

Motivation for this book at this time comes from the upcoming transition from the 20th to the 21st century. Such a momentous occasion seems appropriate for evaluating the past and making plans for the future. The past and future of drug delivery, however, is different for everyone who is involved in this field. It is different for everyone because they not only view drug delivery from different perspectives but also with different time frames. For example, a chemist may focus on synthetic events that take months to accomplish whereas a biologist may focus on biocompatibility studies that take years to complete. Only through a combination of efforts using multiple disciplines does a new drug delivery technology obtain acceptability for clinical application. All together, these efforts take several to many years to complete. So when one thinks of the title of this book, a question of how far into the next millennium can one look becomes valid. In reality, it would be hard to imagine looking farther than the first century of the next millennium. In essence that may be as far as our current disciplines, current understanding of biological processes, and current synthetic capabilities can allow us to look. Thus, this book is a testament to what has been and what can be achieved through innovative drug delivery technologies. But no one really knows how far this can take us into the next millennium.

Our deepest appreciation goes to Abbott Laboratories (Hospital Products Division), the ACS Division of Polymer Chemistry, Inc., Amgen, Bristol-Myers Squibb Company, Glaxo Wellcome Inc., Genentech Inc., GeneMedicine Inc., Immunex Inc., Merck Research Labs, Pharmacia and Upjohn, Schering-Plough Corp., Soffinova Inc., and Yamanouchi Shaklee Pharma. Without the generous support of these institutions, the "Drug Delivery in the 21st Century" symposium and this book could not have been possible. Their contributions have allowed us to peer into the future.

KINAM PARK
Purdue University School of Pharmacy
West Lafayette, IN 47907

RANDALL J. MRSNY
Department of Pharmaceutical Research and Development
Genentech Inc.
South San Francisco, CA 94080

Chapter 1

Controlled Drug Delivery: Present and Future

Kinam Park¹ and Randall J. Mrsny²

¹Purdue University School of Pharmacy, West Lafayette, IN 47907

²Department of Pharmaceutical Research and Development, Genentech Inc.,
South San Francisco, CA 94080

Advances in controlled release drug delivery systems have been largely based on advances in functional polymers. However, the future of controlled release dosage forms will likely be heavily dependent upon an increased understanding of protein chemistry and cell biology principles. As our understanding increases on how cells function in normal and disease states and what limits the actions of potential therapeutics, the possibility of designing delivery technologies into a therapeutic offers tremendous potential for clinical interventions with maximal efficacy and minimal side effects. Genes and gene products and peptide and protein drugs will be the drugs of choice in the future due to their exquisitely specific bioactivities. Delivery approaches for these classes of therapeutics will likely come in many forms, some of which may be radically new. As in the current millennium, the success of delivery approaches in the next millenium will require interdisciplinary approaches.

Controlled release drug delivery technologies have made quantum advances in the last three decades from primitive delayed-release dosage forms in 1960's to highly sophisticated self-regulated delivery systems in 1990's¹. Drugs can now be delivered at zero-order for periods ranging from days to years. Such technology advances have produced many clinically useful controlled release dosage forms and have provided new lives for many existing drugs. Injectable lipid-based systems have recently been shown to have striking clinical advantages over previous formulations for reducing the overt side-effects associated with the administration of several existing therapeutic agents that are extremely toxic. Advances in areas such as biotechnology have now brought new and more difficult challenges (or opportunities) in controlled drug

delivery that will require more than the sustained release approaches previously provided by the highly successful lipid-based systems. It is now possible to produce oligonucleotide, peptide and protein drugs in large quantities, and non-parenteral delivery of such drugs has become a major issue²⁻⁴. Gene therapy also now appears to be clinically feasible and effective delivery of genes to specific target sites is an unmet medical need. Scientists in the controlled release area have been very creative and effective in developing new technologies for such new challenges. On the occasion of transitioning into a new millennium, we examine the current status and future prospects of the controlled release technologies and their potential applications.

Issues in the Development of Controlled Release Dosage Forms

Development of controlled release drug delivery systems requires simultaneous consideration of several factors, such as the drug property, route of administration, nature of delivery vehicle, mechanism of drug release, ability of targeting, and biocompatibility (Fig. 1). Due to extensive interdependency of those factors, it is not easy to establish a sequential process for designing a controlled release dosage form. Choice of one factor in Fig. 1 is likely to affect and/or to be affected by other factors. Let's consider developing a gene delivery system. Genes are macromolecules and successful gene therapy requires more specific cellular targeting than therapies which use other forms of drugs. An ideal gene delivery system should allow gene to find the target cell, penetrate the cell membrane, and go into the nucleus. Since genes should not be released until they reach the target cellular component, release has to be delayed. Furthermore, one has to decide whether to release genes only once or repeatedly through a predetermined period of time. Currently, attenuated, living viruses are most effective in cell transfection, and the use of live vectors leads to the issue of neutralizing immunological responses. To relieve such issues of biocompatibility, one can employ non-living vectors, but then the targeting and transfection efficiency will be low. At present (at least for now before in the 21st Century), the most common route of gene therapy administration is by parenteral injection and syringable microparticulate delivery systems are a reasonable choice. In the future, it may be possible for other delivery technologies to be used if the size, composition or targeting capacity of genes can be modified. In any regard, the selection of a delivery system involves an iterative process where factors of administration route and dose are critical.

Current Controlled Release Technologies

Smart Polymers

Much of the current technology of controlled drug delivery is primarily based on polymers having various properties. Polymer, commonly known as "plastic" to the

public, has been one of the main driving forces shaping the cultural history of the 20th Century⁵. The history of controlled drug delivery, of course, has been based on the evolution of polymers. From simple pH-sensitive polymers commonly used for enteric coating to so-called “smart” polymers used in self-regulated (or modulated) drug delivery systems, polymers have made it possible to design controlled release dosage forms with a variety of release profiles⁶. It is the polymer that has also made it possible to deliver heterologous cells releasing desired bioactive agents without immune responses in humans⁷. Undoubtedly, future advances in controlled drug delivery will continue to depend on the advances in new polymeric materials, such as synthetic polymers with novel functions⁸ and protein mimetics⁹.

There are a number of polymers that have been used in drug delivery and known to be safe which are comprised of generally regarded as safe (GRAS) materials. Since few pharmaceutical companies want to go through the lengthy regulatory processes required for approval of new polymers by Food and Drug Administration (FDA), only a limited number of polymers are currently used in the development of clinical controlled release drug delivery systems. Unfortunately, most of the recently developed smart polymers do not have a long history of safe use. Thus these materials are not considered as GRAS materials, which puts serious limitations in the practical application of smart polymers. Despite this, numerous new polymers have been developed and tested for controlled drug delivery. Since the benefit of using smart polymers should be much greater than the potential risk, one may justify the use of these new polymers for advanced controlled drug delivery.

Factors Important to Controlled Drug Delivery

Of the many routes of drug delivery, oral administration has been dominant. Oral delivery is simply the most convenient mode of drug delivery, and the first choice in selecting the delivery route. This will not change anytime soon. Oral controlled drug delivery, however, has a number of limitations posed by human physiology. Only small molecular drugs stable in the hostile environment of the gut can be delivered by the oral route. Appreciable amounts of large molecular drugs, such as proteins, cannot be absorbed intact from the GI tract. In addition, relatively short GI transit time, in the order of several hours, limits the drug delivery to only 12 hours or so, except for drugs that are absorbed well in the large intestine. Limitations in oral delivery have had a significant influence in developing small molecular drugs based on protein drugs (see below). Recent efforts exploring alternative routes for peptide and protein drug delivery have resulted in some promising outcomes. Clinical studies with selected macromolecular drugs (including insulin) have suggested that both pulmonary and gastrointestinal routes may in fact be useful in the delivery of drugs previously considered too large for significant absorption.

Targeting of drugs/delivery systems to specific tissues and cells in the body is an area requiring major breakthroughs. History shows that targeting of cancer drugs to tumors and genes to defected cells requires much more than simply attaching

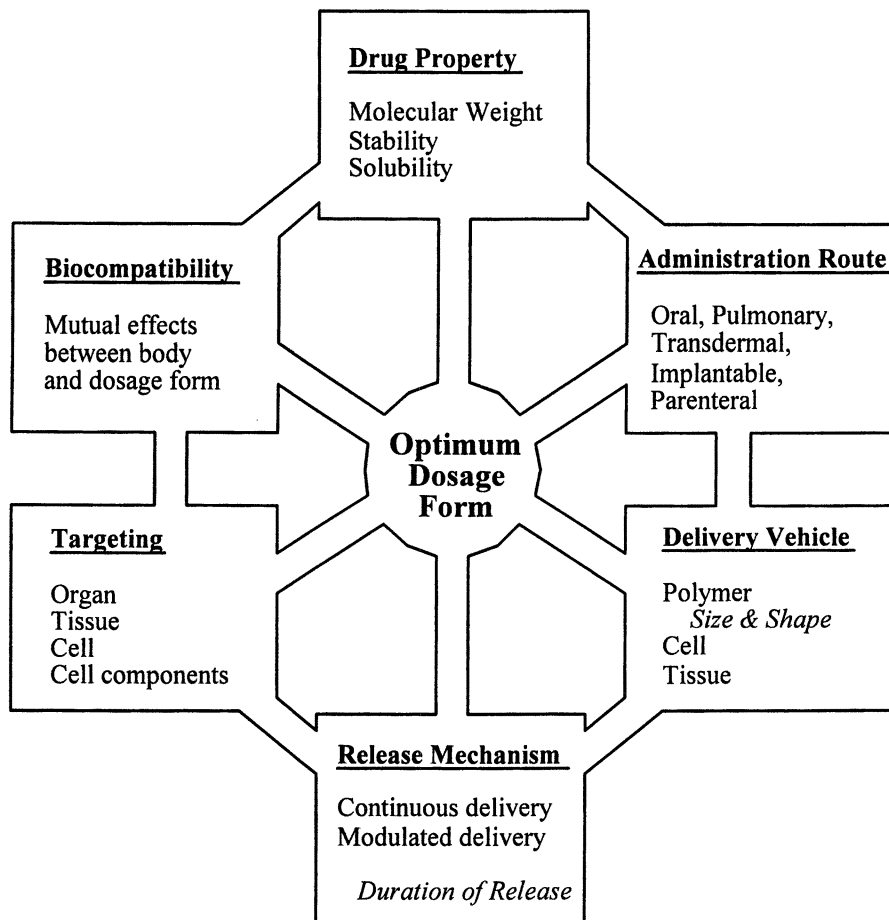


Figure 1. Interdependent factors important in the design of controlled drug delivery systems. The pathophysiology of a disease also plays a critical role in the definition of the final goal of this scheme - development of an optimal dosage form.

antibodies against molecules present on target cells. Coating delivery systems, which are most likely nano- and micro-particulates, with poly(ethylene glycol) (PEG) is known to increase the blood circulation time substantially¹⁰. PEGylated dosage forms, if equipped with a proper homing mechanism, may have a better chance of targeting due to their longer circulation times.

The issue of biocompatibility was brought to our attention after recent episodes associated with silicone rubber-based implantable devices (e.g., Norplant). Silicone rubber has long been presumed to be totally biocompatible. Yet, the body responds to silicone implants by forming a fibrous capsule around the implanted device similar to any foreign body. Since long-term drug delivery on the order of months and years inevitably requires implantation of controlled release dosage forms, biocompatibility of implanted material may be the determining factor for the success of their clinical use. Development of new polymers or modification of existing polymers for improved biocompatibility requires a better understanding on the body's reaction toward an implanted artificial material¹¹.

Tissue Engineering as Drug Delivery Vehicles

Tissue engineering has made landmark advances in the recent past¹². Not only has there been a new appreciation for geometries of the framework required to recreate vital tissue and organ architecture, but cell culture methods to allow for the simultaneous growth of several cell types have been identified. With such recent successes in organ and tissue replacement efforts, it is easy to be extremely optimistic about what the next millennium might hold in this area. Not only have complex organs been prepared in the lab and been shown to function properly following implantation¹³, the knowledge base obtained from other arenas will feed important information into this field. For example, a number of genetic manipulation studies in mice where specific genes are either knocked out or knocked in have led to the identification of factors critical to the growth and development of various organs and tissues. Many of these observations came as a surprise because the role played by these factors is many times very transient and not sustained in the mature organ or tissue. With such knowledge it may soon be possible to build artificial pancreas releasing insulin in response to changes in glucose levels in blood for diabetic patients. Thus, tissue engineering holds great promise in the future of controlled drug delivery.

Challenges in Controlled Release Technologies

Non-parenteral Delivery of Peptide and Protein Drugs

Although extensive efforts have been and will be made to reduce critical peptide and protein functions to orally bioavailable small molecular mimetics, many peptide and protein therapeutics will not be able to be easily emulated in this way. Recent, extensive efforts have gone into identifying and validating non-parenteral delivery methods that provide an improved delivery of peptide and protein drugs. These

approaches have demonstrated that the mucosal barriers (primarily respiratory and gastrointestinal tract) can be a site of successful peptide and protein delivery where significant biochemical, physiological and physical barriers established by these mucosal surfaces have been surmounted. The actual mechanisms by which these barriers have been overcome is not completely clear at this time and additional studies may better define critical components which might be manipulated to make trans-mucosal delivery a primary method of delivering peptide and protein therapeutics. Although inroads have been made to overcome mucosal barriers for the delivery of peptides and proteins, the desired delivery profile is typically rapid and short-lived. Delivery of peptide and protein drugs by non-parenteral route needs to be followed by more continuous or long-lived delivery profiles using biodegradable polymer-based systems.

Targeting of Peptide and Protein Drugs

Adequate controlled delivery of peptides and proteins is frequently critical to their clinical success. Up to this point successful peptide and protein therapeutics are typically endocrine factors which are secreted at one location in the body but which act at distant, and frequently multiple, sites of the body. Such molecules can be equally effective in their biological actions relative to their side-effect profiles whether they are delivered by traditional parenteral injections, polymer-based depots, or trans-mucosal methods. Many peptides and proteins, however, act more locally, being secreted by a cell to act on itself as an autocrine factor or on adjacent cells as a paracrine factor. These factors are not typically intended to circulate systemically as typical endocrine factors, and the serious side effects associated with the systemic delivery of such factors have severely limited the clinical utility of many promising molecules (e.g., interferons and interleukins). Presently, an improved appreciation of these systemic side effect issues has driven interest in peptide and protein delivery approaches other than parenteral injection. The capacity to potentially deliver peptides and proteins at specific epithelia could provide highly focused concentrations similar to that achieved by a local delivery. The delivery profile desired for maximal therapeutic use of peptides and proteins may be possible through improved targeting.

Delivery of Oligonucleotides and Genes.

The human genome project will not only drive the identification of new protein and peptide entities for therapeutic application, but also result in the identification of disease-causing defective genes. Replacing of a defective gene or merely introducing the correct form is the promise of gene therapy. These therapeutic approaches are likely to have tremendous impact in the next millennium since they would hopefully eliminate the need for continued therapy to deal with disease symptoms or could be used to prophylactically protect an individual against a condition (e.g., cancer, heart disease, etc.) for which they are genetically pre-disposed. The uptake, integration and expression of introduced genetic material, however, is extremely challenging. As one might imagine, the body has established significant barriers to the random uptake of

genetic materials. This is an important protective mechanism since various cells of the body are confronted daily with the genetic material from disrupted pathogens and/or diseased cells¹⁴. A number of approaches, such as liposomes, lipid complexes, polymers and viral vectors, have been taken to overcome the challenges of genetic material delivery and uptake¹⁵. To date, viral vectors have demonstrated promise in clinical settings but have been used under controlled conditions where the transfection either occurred *in vitro* and the transfected cells were returned to the body or where the vector was applied *in vivo* to a mucosal surface. Only a few viral vectors have been used to date, but great advances may come from the identification and application of viral vectors with highly specific tropisms. For example, specific delivery of genes encoding pain-killing proteins to the central nervous system for patients suffering from conditions of chronic pain appears to be possible¹⁶. The success of cloning of mammals from somatic cells brought new possibilities in gene delivery. The introduction of components associated with sperm nuclei has been shown to facilitate the expression of introduced somatic genetic material. Conjugation of oligonucleotides with peptides can improve cellular uptake in antisense applications. Many of these findings were unanticipated and point to the likelihood of even more unanticipated, but extremely useful findings in the near future. Some of these findings will likely come in the progression of knowledge gained about the use of viral vectors to deliver genetic material.

Future Prospects

Development of Non-protein Mimetic Drugs

Over the last millennium, two forms of drug delivery have dominated. Small, easily absorbed agents have been the more readily acceptable form while injection of macromolecules has been a less desired, but tolerated form of delivery. Small molecules can readily enter the body at a mucosal surface or across the skin through passive mechanisms. Small molecular drugs are frequently identified surreptitiously through screens of massive chemical libraries. Ultimate success of these compounds in clinical settings commonly requires satisfying two general parameters. The first parameter is that once the drug is absorbed it has to reach the target cell, tissue or organ without extensive modification or destruction and induce an action at the target sufficient for the desired activity. Appropriate pharmacokinetic and pharmacodynamic profiles are typically obtained for only a few of the hundreds or thousands of potential compounds identified in these screens. All too often additional chemical modification of otherwise promising compounds is required and to obtain lead molecules with desired (or even acceptable) pharmacokinetic and pharmacodynamic profiles. The second parameter of clinical success for a small molecule is the identification of an acceptable therapeutic window. This is a range of drug concentrations bracketed by a lack of effect at one extreme and toxicity at the other. The chances of finding an acceptable therapeutic window for a new small

molecule drug is positively correlated with the selectivity of action by that drug. Although initial drug screening using *in vitro* model systems can sometimes be used to select for certain aspects of drug selectivity, ultimately *in vivo* studies are required to identify or rule out unanticipated drug actions and this approach has become a primary screening approach for drug selection.

Advances in recombinant biotechnology over the last twenty years have allowed for the development of new peptide and protein therapeutics and have also provided a much different approach to the identification of promising small molecular drug candidates. Instead of random screening of chemical libraries *in vivo* using various animal models, the identification and large-scale production of critical therapeutic peptide and protein targets can now be accomplished. This new approach of drug screening is currently being used to establish mechanism(s) of drug action but also to provide a clearer understanding of potential side effect profiles. From these studies, it has become clear that the peptide and protein therapeutics are dramatically more selective than small molecular drugs which emulate their actions. A likely explanation for this outcome is that most peptide and proteins function selectively by initiating multiple contact sites on a target or targets to achieve the desired action. One parameter of small molecular drugs is that of size, with an upper limit in size of about 400 g/mole. Molecules constrained by this size limitation cannot typically bridge required molecular distances essential to establish such specificity¹⁷. Efforts to reduce the size of molecules while maintaining specificity have further established apparent limits in the molecular requirements of non-protein mimetics.

New Drug Modalities – New Drug Delivery Approaches

The prospects of better defining the specificity of small molecular drugs and improving the delivery options of peptides and proteins appears promising. Such advances will be driven not only by a wealth of critical information generated by the Human Genome Project but also by the identification of technologies which allow for new and/or better screening methods and a clarification of therapeutic targets. As secrets of the human genome become known, not only will new therapeutic targets be identified but it will be possible to better clarify the actions of current therapeutics to drive their refinement. Additionally, the information derived from sequencing the human genome will provide the basis to advances in critical areas of information associated with the development of new proteins and peptides as well as small molecule therapeutics and even new classes of therapeutic agents. Thus, we would anticipate that the spectrum of drug modalities utilized in the next millennium will likely include new applications for carbohydrates, lipids and nucleotide-based drug molecules. Novel physical and chemical characteristics of these new classes of compounds should drive new approaches in drug delivery and a re-examination of established methods. Ultimately, successful therapeutic application(s) from each of these chemical classes will likely rely on appropriate local and/or targeted drug delivery technologies to add selectively and increase therapeutic opportunities.

Understanding Structures of Peptide and Protein Drugs

Peptides and proteins are composed of linear polymers of amino acids, with peptides containing usually less than 20 residues and proteins being composed of more. Although stable solution structures for peptides of less than 20 amino acids have been determined, this break-point roughly relates to the presumed differences between proteins and peptides where the former is likely to have a more defined and stable solution structure than the latter. A critical role for the application of any protein or peptide therapeutic is that it can either acquire and/or maintain the proper structure for its desired biological activity¹⁸. One area where advances in the next millennium will significantly impact the field of therapeutic proteins and peptides is that of solution structure calculations. Currently, only a few poorly defined rules of protein folding based upon amino acid sequence are understood; but even the exceptions to these rules are poorly understood. At present, solution structure information has been obtained for some peptides and crystal structure information has been acquired for some proteins. However, critical rules of the protein and peptide structure/function will likely come from solution structures of proteins during interactions with their functional mate (e.g., a receptor, enzyme substrate, etc.) since these interactions could easily involve induced fit events.

Established rules of protein folding will expedite the identification and development of protein and peptide therapeutics as well as small molecule drugs designed to best emulate critical actions of these proteins and peptides. Such structure/function information about peptides and proteins may lead to the optimization of stability both in formulations and following administration. Further, defective or altered proteins such as enzymes, ion channels and cell-surface receptors involved in the modified cellular pathways associated with disease states will be better defined. With this more complete data set, a clearer understanding of disease will be possible and the selection of optimal sites for therapeutic intervention will be better appreciated. This more complete understanding may also lead to a more logical effort to identify effective small molecule therapeutics capable of affecting or modulating a disease state previously defined only by these protein and peptide interactions. All information will be critical in formulation of long-term delivery systems for protein drugs and non-protein mimetics.

Targeting to Intracellular Sites

Many opportunities for drug delivery in the next millennium will likely come from unanticipated scientific observations. In the area of intracellular delivery and targeting, one of those surprising findings was already made in this millennium. The observation that some growth factors and polypeptide hormones and toxins can target intracellular targets such as the nucleus of cells following interaction with the external surface of the plasma membrane opens up an unprecedented possibility to access the cytoplasm of cells. No longer would small molecules be required to access the interior of cells. With the additional knowledge of how proteins can be sequestered at specific organelles and structures within cells, it seems likely that pharmaceuticals of the new millennium may include protein conjugate or chimera molecules which can cross the plasma membrane, access the cell's cytoplasm and target to specific

intracellular sites. Although many questions remain to be answered before significant applications of such an approach can be used to delivery a therapeutic agent, the concept of such a delivery approach is indicative of what may be possible in the next millennium.

Acknowledgments

We thank the sponsors of the symposium: Abbott Laboratories (Hospital Products Division), the ACS Polymer Chemistry Division, Amgen, Bristol-Myers Squibb Co., Glaxo Wellcome Inc., Genentech Inc., GeneMedicine Inc., Immunex Inc., Merck Research Labs, Pharmacia & Upjohn, Schering-Plough Corp., Soffinova Inc., and Yamanouchi Shaklee Pharma.

References

- 1 Park, K. *Controlled Drug Delivery: Challenges and Strategies*, American Chemical Society: Washington, DC, 1997.
- 2 Sanders, L. M.; Hendren, R. W. *Protein Delivery. Physical Systems*, Plenum Press: New York, 1997.
- 3 Shahrokh, Z.; Sluzky, V.; Cleland, J. L.; Shire, S. J.; Randolph, T. W. *Therapeutic Protein and Peptide Formulation and Delivery*, American Chemical Society: Washington, DC, 1997.
- 4 Cleland, J. L.; Langer, R. *Formulation and Delivery of Proteins and Peptides*, American Chemical Society: Washington, DC, 1994.
- 5 Meikle, J. L. *American Plastic. A Cultural History*, Rutgers University Press, New Brunswick, NJ, 1995, Pages.
- 6 Okano, T. *Biorelated Polymers and Gels. Controlled Release and Applications in Biomedical Engineering*, Academic Press: Bonton, MA, 1998.
- 7 Mikos, A. G.; Murphy, R. M.; Bernstein, H.; Peppas, N. A. *Biomaterials for Drug and Cell Delivery*, Materials Research Society: Pittsburgh, PA, 1994.
- 8 Akaike, T.; Okano, T.; Akashi, M.; Terano, M.; Yui, N. *Advances in Polymeric Biomaterials Science*, CMC Co., Ltd.: Tokyo, Japan, 1997.
- 9 McGrath, K.; Kaplan, D. *Protein-Based Materials*, Birkhäuser: Boston, MA, 1997.
- 10 Harris, J. M.; Zalipsky, S. *Poly(ethylene glycol) Chemistry and Biological Applications*, American Chemical Society: Washington, DC, 1997.
- 11 Braybrook, J. H. *Biocompatibility Assessment of Medical Devices and Materials*, John Wiley & Sons: New York, NY, 1997.
- 12 Lanza, R. P.; Langer, R.; Chick, W. L. *Principles of Tissue Engineering*, R.G. Landes Company: Austin, TX, 1997.
- 13 Oberpenning, F.; Meng, J.; Yoo, J. J.; Atala, A. *Nature Biotech.* **1999**, 17, 149-155.
- 14 Stein, C. A. *Nature Biotech.* **1999**, 17, 209.
- 15 Lasic, D. L. *Liposomes in Gene Delivery*, CRC Press, Boca Raton, FL, 1997.

- 16 Wilson, S. P.; Yeomans, D. C.; Bender, M. A.; Lu, Y.; Goins, W. F.; Glorioso, J. C. *Proc. Natl. Acad. Sci. USA* **1999**, *96*, 3211-3216.
- 17 Reineke, U.; Sabat, R.; Misselwitz, R.; Welfe, H.; Volk, H.-D.; Schneider-Mergener, J. *Nature Biotech.* **1999**, *17*, 271-275.
- 18 Feher, V. A.; Cavanagh, J. *Nature* **1999**, *400*, 289-293.

Chapter 2

Controlled-Release Oral Delivery Systems

Joseph A. Fix¹, Kazuhiro Sako², and Toyohiro Sawada²

¹Yamanouchi Shaklee Pharma, 1050 Arastradero Road, Palo Alto, CA 94304

²Novel Pharmaceutical Laboratories, Yamanouchi Pharmaceutical Company, Ltd., 180 Ozumi, Yaizu-shi, Shizuoka-ken 425, Japan

The advantages of controlled-release oral delivery systems, particularly those achieving once-a-day efficacy, have long been recognized. Outcomes can include better therapeutic efficacy via improved control of plasma drug levels and reduced peak-associated side effects. Oral controlled-release dosage forms can also afford advantages in drug stability, patient compliance, and reduced total drug exposure. Applications for once-a-day administration must balance release kinetics, dosage form and in vivo drug stability, absorption kinetics and variable physiologic parameters such as g.i. transit, enzymes, pH, motility and fluid level. In spite of major efforts to develop once-a-day oral dosage forms, relatively few products have been introduced. In many cases, once daily therapeutic efficacy cannot be easily achieved due to poor control of drug release or poor drug absorption in the colon. Food effects can also introduce significant variability. OCAS is an oral controlled absorption gel matrix system that exhibits pH-independent, pseudo-zero order drug release with minimal food effects. The rapid hydration and formation of a rigid gel leads to effective drug release in the colon. Future advances in once-a-day oral delivery systems must address improving drug absorption in the colon and may extend applications of controlled-release technology to biomolecules.

Controlled-release oral delivery systems have been an integral part of pharmaceutical technology for several decades (1). Within the pharmaceutical industry, delivery systems and formulations have been developed which can provide

a wide variety of drug release profiles, including systems designed for immediate, continuous, pulsatile, and delayed administration (2-4). For most traditional small molecule drug candidates, delivery systems can be designed which will release the candidate drug in the desired profile. In recent years, much of the focus in oral controlled-release technology has been directed toward site specific delivery in the gastrointestinal tract, chronobiology as related to oral delivery systems (5), and the development of technology to control the release and delivery of non-traditional drug candidates, i.e. peptides and proteins. Included in these various technologies are osmotically-controlled devices, matrix tablets, hydrogels, polymeric systems, multiparticulates, and erosion systems regulated by geometric design. Figure 1 depicts illustrative plasma profiles that can be achieved with existing oral technology.

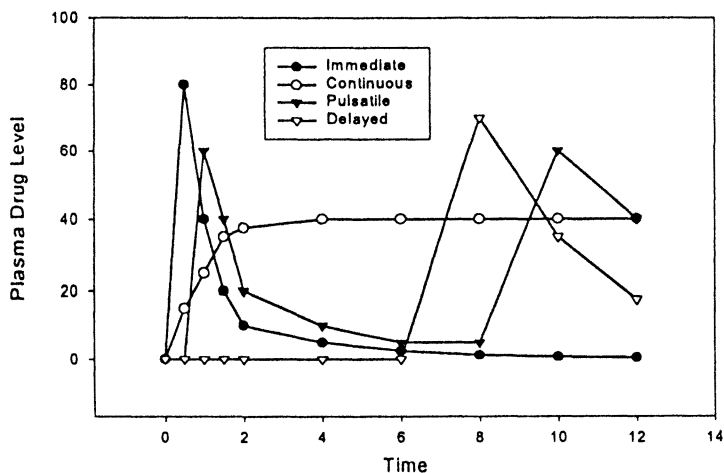


Figure 1: Representative plasma profiles for immediate, continuous, pulsatile, and delayed oral delivery systems.

In spite of the availability of numerous technologies to achieve up to 24 hour controlled drug release, relatively few products that are efficacious for once-a-day dosing have reached the market. Table I, although not inclusive, lists some of the products currently available where the recommended dose and administration guidelines indicate once-a-day efficacy.

In some cases, controlled-release dosage forms that provide up to 24 hour in vitro drug release do not achieve the same release profile in vivo due to influences from the milieu of the gastrointestinal tract. Also, poor colonic drug absorption can effectively limit the once daily efficacy of dosage forms that otherwise afford 24 hour drug release.

Table I: Representative Once-a-Day Oral Products

Indocin SR® (Merck)	Verelan® (Lederle)
DynaCirc CR® (Novartis)	Glucotrol XL® (Pfizer)
Toprol XL® (Astra USA)	Calan SR® (Searle)
Adalat CC® (Bayer)	Theo-24® (UCB Pharma)
Prelu-2® (Boehringer Ingelheim)	Dilacor XR® (Watson)
Cardizem CD® (Hoechst Marion Roussel)	Lodine XL® (Wyeth Ayerst)
Theo-Dur® (Key)	

SOURCE: Physician's Desk Reference, 52nd Edition, 1998, Medical Economics Co., Inc., Montvale, NJ

Physiologic Influences

Once-a-day controlled release dosage forms are subject to numerous physiologic influences in the gastrointestinal tract, including pH, bile salts, fluidity, motility, enzyme activity, and absorption windows. Ideally, a once-a-day dosage form should function independent of variations in the parameters shown in Figure 2.

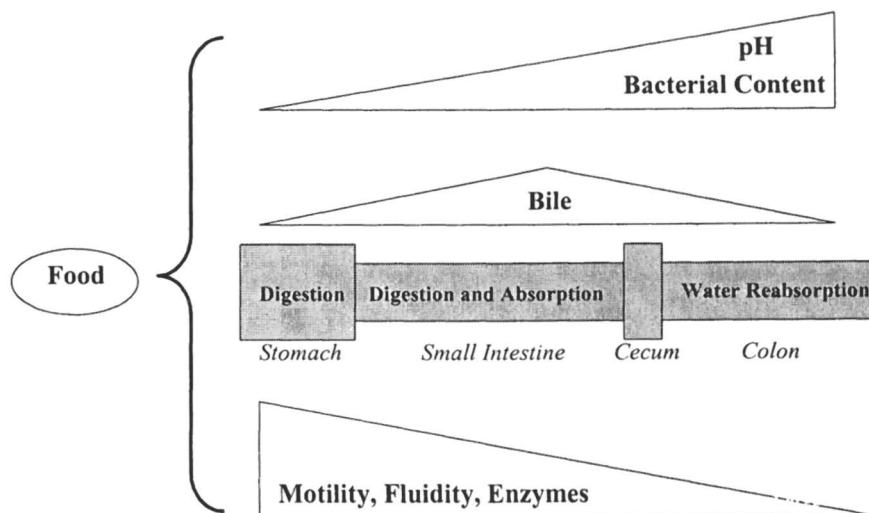


Figure 2: Quantitative trend analysis of gastrointestinal parameters that effect the performance of once-a-day dosage forms.

During transit from stomach to lower colon, the pH exposure can range from pH 1.0 to pH 7.5 or greater. Bile salts and degradative enzymes are present in relatively high concentrations in the small intestine. Fluid content and gastrointestinal motility

are high in the upper intestine and diminish in a distal direction. In order to reliably control drug release in an extended release product, the formulation would ideally function independent of these changing variables. Additionally, the decrease in fluid content in the colon, which is a water re-absorption site, can lead to altered drug release profiles (normally a decrease in the release rate if the release mechanism is dependent on the continued presence of high water content). The osmotically driven delivery systems pioneered by Alza have been quite effective in performing in a uniform fashion even in the presence of limited water availability (6). Other types of dosage forms do not always perform as well. Two examples are shown in Figure 3 where prospective once-a-day dosage forms do not achieve continuous drug release once the formulation reaches the colon.

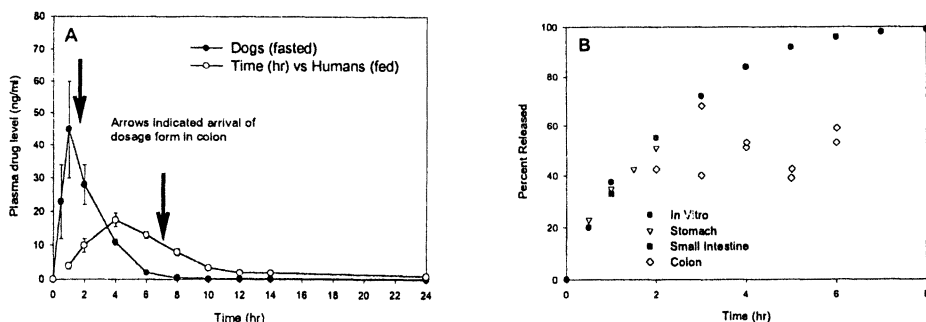


Figure 3: A: Plasma nifedipine levels after oral dosing of controlled-release nifedipine hydrochloride to dogs and humans. B: In vitro and in vivo acetaminophen release from HPMC matrix sustained release tablets.

In Figure 3A, the absorptive phase for nifedipine terminates upon arrival of the dosage form in the colon (as determined by scintigraphic imaging) of both dogs and humans. In Figure 3B, the in vivo release of acetaminophen (determined by deconvolution of plasma acetaminophen levels) only correlates with in vitro release while the dosage form is in the stomach or small intestine. Acetaminophen release dramatically decreased when the dosage form reached the colon. These data suggest that the release characteristics of these matrix tablets are not consistently maintained throughout the entire gastrointestinal tract.

Several reasons may account for the discrepancies between in vitro and in vivo drug release, including effects of the gastrointestinal milieu on the controlled-release dosage form. In the colon, very little free water exists since the colon is a water absorptive region of the gastrointestinal tract. Those once-a-day dosage forms that are dependent on the continued presence of relatively significant amounts of water may be expected to experience altered drug release profiles once the dosage form reaches the colon. The osmotic systems developed by Alza Corporation have been shown to function well in low water environments, but other sustained release dosage forms (i.e. certain matrix tablets, hydrogels) are not always so robust in their

performance characteristics. The future development of once-a-day dosage forms depends on the ability to design and develop sustained-release dosage forms that will function independent of influences from the gastrointestinal milieu. Since sustained-release dosage forms spend the majority of their residence time in the colon, future once-a-day dosage forms must be designed to release drug in a predictable fashion in the relatively low water content of the colon.

Oral Controlled Absorption System (OCAS™)

In an effort to design a sustained-release formulation suitable for once-a-day dosing that will perform reproducibly whether in the small intestine or colon, modifications to gel-forming matrix tablets were investigated. The OCAS system described here contains, as its major components, the active drug, a gel-forming polymer (polyethylene oxide, PEO), and a gel-enhancing agent (polyethylene glycol, PEG). The design concept is to achieve rapid gelation, pseudo first-order drug release, consistent colonic drug release, and ease of manufacturing. A schematic, shown in Figure 4, describes the basic performance characteristics of OCAS.

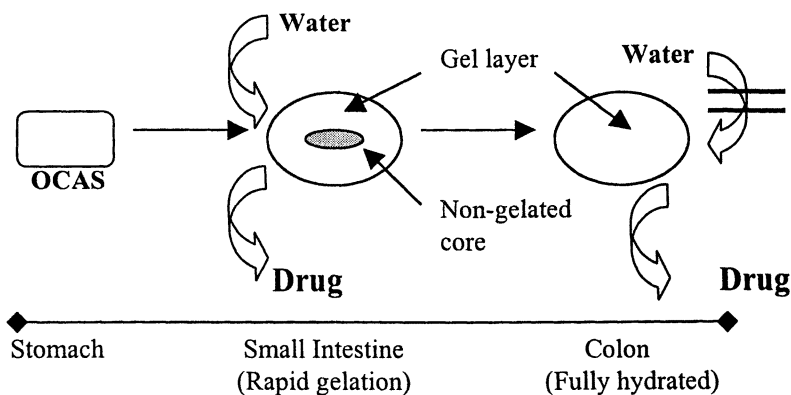


Figure 4: Schematic of OCAS hydration and drug release in small intestine and colon.

The schematic in Figure 4 depicts the design concept of OCAS in that the formulation achieves nearly complete hydration in the small intestine. Unlike OCAS, other gel-forming matrix tablets may only achieve incomplete hydration in the small intestine, resulting in a dosage form that retains a significant volume of residual non-hydrated drug/polymer core in the colon. In the absence of significant free water in the colon, drug release from these formulations may significantly decrease, resulting in a lack of correlation between in vitro drug release and in vivo drug absorption.

The key to sustaining consistent drug release, as designed in the OCAS dosage form, is very rapid hydration of the gel matrix such that nearly complete hydration occurs prior to arrival of the dosage form at the colon. In most cases, the transit time for dosage forms from the stomach to the colon is approximately 3-4 hours, perhaps longer in the fed state depending on the extent of gastric retention. In order to ensure nearly complete pre-colonic hydration, fillers that could be combined with the gel-forming polymer (PEO) were examined for their effects on gelation index (extent of gelation occurring within 2 hours). The results are summarized in Table II.

Table II: Effect of Fillers on Gelation Index of 1:1 PEO-Filler Matrix Tablets

<i>Additive</i>	<i>Gelation Index (Percent at 2 hours)</i>
Lactose	24.4 ± 3.3
D-Mannitol	26.8 ± 3.3
PVP K30	82.2 ± 4.3
PEG6000	87.1 ± 0.4
D-Sorbitol	97.0 ± 0.8
None	29.7 ± 5.0

Tablets were immersed in dissolution media for two hours. Gelation index was calculated by comparing ratios of the gel layer and non-gelated residual core thicknesses.

Without added filler, PEO matrix tablets exhibited only 30% gelation within two hours. This control gelation index was not significantly increased by the addition of lactose or mannitol. PVP K30, PEG6000 and D-sorbitol each significantly increased OCAS gelation index, although PVP K30 required 2 ml of water per 1 g of solute whereas PEG6000 and D-sorbitol required only 1 ml of water per 1 g of solute to achieve similar results. PEG6000 was chosen as the desired filler because of its high gelation index and pharmaceutical acceptability.

Utilizing PEG6000 as the filler for the gel-forming matrix tablets, four different gel-forming polymers were examined for their ability to achieve pseudo zero-order drug release for 12 hours. Matrix tablets were prepared from acetaminophen:PEG:polymer (1:1:2) and their in vitro release profiles determined by the paddle method. In addition, the release mechanism was described according to the following equation,

$$D = kt^n$$

where D is drug release at time t, k is the drug release rate constant, t is time, and n is the diffusional exponent number. As an approximation, $n < 0.66$ indicates diffusion dominated drug release while $n > 0.66$ indicates erosion dominated drug release ($n =$

0.5 for Fickian diffusion control and $n = 1.0$ for solvent front penetration control). The results from these studies are summarized in Table III.

Table III: Determination of In Vitro Release Mechanism of Acetaminophen from Drug:PEG:Polymer (1:1:2) Matrix Tablets

<i>Gel-Forming Polymer</i>	<i>Diffusional Exponent Number (n)</i>
Hydroxypropylcellulose (HPC)	0.59
Hydroxyethylcellulose (HEC)	0.61
Hydroxypropylmethylcellulose (HPMC)	0.61
Polyethyleneoxide (PEO)	0.76

PEG6000 used as filler in matrix tablet.

The data shown in Table III indicate that tablets made from PEO were the only ones tested that exhibited erosion dominated drug release ($n > 0.66$). The other three polymers tablets (HPC, HEC, and HPMC) exhibited diffusion dominated drug release ($n < 0.66$). The actual release profiles (shown in Figure 5 for PEO and HPMC) also demonstrated these differences in that a pseudo-zero order release profile was achieved only with PEO while the other polymers resulted in tablets exhibiting more non-linear release profiles.

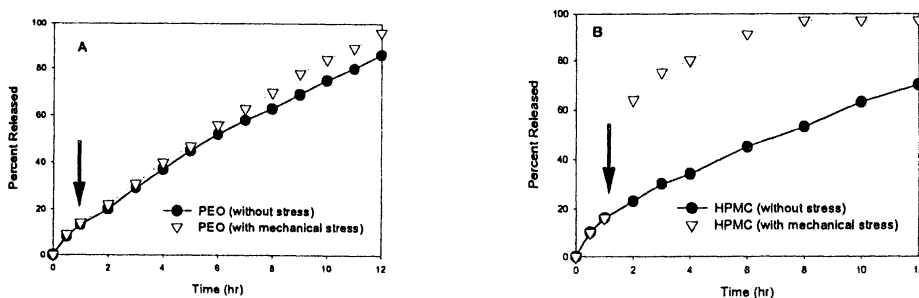


Figure 5: In vitro acetaminophen release profile from PEO and HPMC matrix tablets. The arrow shows the time of initiation (1 hour) of mechanical stress as described in the text.

The data shown in Figure 5 also demonstrate an additional important characteristic of the OCAS formulation. The arrows indicate the initiation of mechanical stress on the formulations. The mechanical stress involved shaking the formulations in dissolution medium at 320 strokes/min in the presence of 50 g of

glass beads. Only a very minimal increase in drug release was observed utilizing PEO whereas an abrupt and dramatic increase in drug release was seen when HPMC was used as the gel-forming polymer. These data indicate that the gel formed with PEO possesses significant structural rigidity that is important in maintaining both physical integrity and consistent drug release during contractile activity present in the gastrointestinal tract.

While *in vitro* release data are important in developing and characterizing sustained release dosage forms, the *in vivo* performance is the critical test of functionality. A comparison of *in vitro* and *in vivo* performance can be utilized to demonstrate that the dosage forms performs independent of gastrointestinal variables. Conventional PEO matrix tablets (gelation index = 21%) and OCAS PEO/PEG tablets (gelation index = 76%) were prepared and evaluated in both *in vitro* and *in vivo* models. Both formulations demonstrated reasonably pH-independent *in vitro* drug release between pH 1.2 and pH 6.8 over a 12 hour dissolution time. The release profile for OCAS was somewhat more linear than that observed with the conventional gel matrix tablet, especially between 8 and 12 hours, but both formulations achieved greater than 85% drug release within 10 hours. Two different *in vivo* experiments were conducted in dog models. In one study, both conventional and OCAS tablets were dosed at various times prior to necropsy and the tablets then retrieved and analyzed for *in vivo* drug release. In another experimental model, dogs received either conventional or OCAS tablets containing acetaminophen and plasma drug profiles determined. The pharmacokinetic parameters from this study are summarized in Table IV and a graphic summarization of all results is shown in Figure 6.

The data presented in Table IV and Figure 6 clearly indicate that this conventional gel matrix tablet exhibits decreased *in vivo* drug release in the colon. In contrast, drug release from OCAS appears to remain consistent even when the dosage form enters the colonic region. It is proposed that the reason for the consistent OCAS performance is the fully hydrated state of the dosage form prior to its arrival in the "water-deficient" colon region.

As mentioned in the introduction, the gastrointestinal variables that can impact the performance sustained-release once-a-day dosage forms are generally influenced by the presence of food. Enzyme activity, motility, pH, fluid content, and bile salts are all modified in the fed state versus the fasted state. In order to determine whether OCAS would perform independent of the effects of food, a dog study was conducted comparing nifedipine hydrochloride absorption from OCAS and conventional gel tablets. The resultant pharmacokinetic parameters are summarized in Table V.

The data presented in Table V indicate that significantly greater absorption (AUC) is achieved with OCAS compared to the conventional gel and that the OCAS system is relatively free of food effects (547 vs 681 ng.hr./ml AUC for fasted vs fed, respectively). By contrast, an approximate 2-fold food effect was observed with the conventional gel formulation. Again, it is likely that the very rapid hydration of the OCAS formulation is an underlying cause for the relative food effect independence.

Table IV: Pharmacokinetic Parameters

Formulation	AUC 0-24hr (ng.hr./ml)	C _{max} (ng/ml)	T _{max} (hr)	MRT (hr)
OCAS	2702 ± 151	350 ± 36.1	1.5 ± 0.3	7.0 ± 0.3
Conventional	1470 ± 537	344 ± 21.7	1.3 ± 0.3	4.0 ± 1.2

Mean ± S.E.

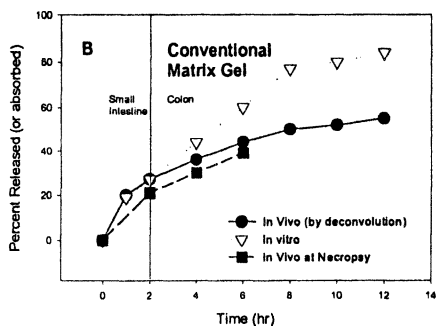
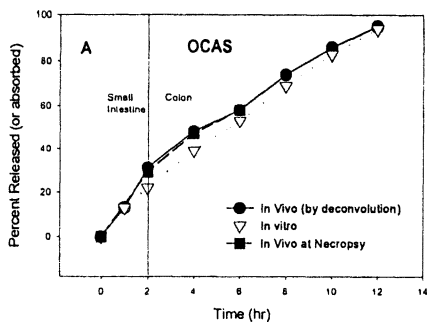


Figure 6: In vitro and in vivo release performance of OCAS and conventional gel tablets.

Table V: Pharmacokinetic Parameters of OCAS and Conventional Gel Nicardipine Hydrochloride Tablets in Fed and Fasted Dogs

<i>Formulation</i>	<i>Food</i>	<i>AUC</i> 0-24hr (ng.hr./ml)	<i>C</i> _{max} (ng/ml)	<i>T</i> _{max} (hr)
OCAS	Fasted	547 ± 180	82 ± 14.8	3.9 ± 1.1
	Fed	681 ± 108	87 ± 17.8	4.7 ± 1.5
Conventional	Fasted	125 ± 32	54 ± 12.5	1.3 ± 0.2
	Fed	239 ± 62	47 ± 12.6	4.3 ± 1.2

N = 6, mean ± S.E.

In summary, OCAS is a rapidly hydrating gel matrix tablet that performs relatively independent of the effects of pH, mechanical stress, and location in the gastrointestinal tract. In addition, at least with the model compound employed, food effects appear minimal. As such, the technology represents an advance in sustained release formulations that might have applications in once-a-day drug therapy.

Future Challenges and Opportunities

Sustained-release formulations for once-a-day therapy have been a target of pharmaceutical research and development for several decades with a limited variety available as marketed products. Advances as those described with OCAS represent attempts to further refine and develop new applications. Significant challenges and opportunities, however, still remain in this field and are summarized in Table VI.

Although significant advances have been made in developing and commercializing once-a-day dosage forms, the field is still amenable to continued improvement and applications. Probably the two most critical fields for investigation are technologies for improving colonic absorption and applications of once-a-day technologies for biomolecules.

Technologies such as OCAS can effectively achieve drug release in the colon. However, until pharmaceutical approaches are available to improve colonic absorption, once-a-day products will be limited to those few drugs that exhibit high colonic permeability. In normal gastrointestinal transit, it can be expected that dosage forms will have approximately 4-6 hours available for drug release prior to arrival at the colon. This time window will continue to limit development of once-a-day dosage forms unless colonic absorption improvement is adequately addressed.

Finally, little progress has been achieved in oral delivery systems for biotechnology products, even with immediate release or targeted delivery systems. As more progress is achieved with this class of compounds, their *in vivo* behavior will be more fully understood. One can then anticipate extending that knowledge to once-a-day dosage forms in a manner similar to what has been done with traditional organic drug candidates.

Table VI: Future Challenges and Opportunities for Once-a-Day Oral Delivery Systems

Formulation design to optimize 24 hour absorption
Biopharmaceutical techniques for improved colonic absorption
Gastric retention techniques to minimize large intestine residence time
Chronopharmaceutics
Matching release/absorption profiles with therapeutic needs
Technology improvements to minimize effects of gastrointestinal variables
Applications to biotechnology products (i.e. peptides, proteins, genes, etc)
Formulation strategies
Stability
Local therapy or systemic absorption

References

1. Chien, Y.C. *Prog. Technol.* **1989** 15,21.
2. Shah, A.J.; Britten, N.J., Olanoff, L.S.; Badalamenti, J.N. *J. Controlled Rel.* **1989** 9,169.
3. Lee, V.H.L.; Yamamoto, A. *Adv. Drug Del. Reviews* **1990** 4, 171.
4. Chien, Y.W. *Novel Drug Delivery Systems*; Marcel Dekker, Inc. New York, NY, 1992, pp 139-196.
5. Lemmer, B. *J. Controlled Rel.* **1991** 16,63.
6. Theeuwes, F. *Drug Dev. Ind. Pharm.* **1983** 9,1331.

Chapter 3

Safe Mucosal Penetration Enhancers: A Fiction?

Polymers as Absorption Enhancers for Transmucosal Drug Delivery

H. E. Junginger, M. Thanou, H. L. Lueßen¹, A. F. Kotzé²,
and J. C. Verhoef

Leiden/Amsterdam Center for Drug Research, Department of Pharmaceutical
Technology, Leiden University, Leiden, the Netherlands

Polyacrylate and chitosan derivatives are able to increase the transmucosal absorption of hydrophilic macromolecules. Different absorption profiles suggest different mechanism of action. While the normally used penetration enhancers and native polymers show features that may be disadvantageous for drug delivery and absorption, the derivatives show superior physico-chemical properties well correlated with in vivo absorption enhancement. Carbopol 934P[®] and TMC (N-trimethyl chitosan chloride) have been proven to be efficient enhancers with promising safety aspects of the transmucosal absorption of peptide drugs, as tested in rats

Peroral Delivery of Hydrophilic Macromolecules

The peroral route of peptide or protein administration is currently the greatest challenge in developing suitable dosage forms, because it offers the highest ease of application to the patient. However, particular difficulties are met in designing effective delivery systems for gastro-intestinal application. The challenge to achieve sufficient peptide or protein drug absorption is to overcome the very efficient absorption barriers of the gastro-intestinal tract. These barriers can be divided into three main parts: 1) the metabolic barrier consisting of the proteolytic activity of luminal and membrane-bound enzymes, 2) the mucosal transport barrier whereby the passive absorption of hydrophilic macromolecules such as peptides is mainly

¹Current address: Octopus, Leiden, the Netherlands

²Current address: Department of Pharmaceutics, Potchefstroom University for Christian Higher Education, Potchefstroom, Republic of South Africa

controlled by the integrity of intercellular junctions, and 3) the mucus layer which covers the epithelial cells as a blanket and forms a highly viscous network of glycoproteins, hampering the diffusion of peptides. Although different enzyme inhibitors and absorption enhancers, with the disadvantage to display undesired systemic side effects, have been shown to improve the absorption of various peptide drugs, there is still a need for the search of safe absorption enhancing excipients for peroral delivery of peptide drugs.

Polymers as Safe Absorption Enhancers for “Delicate” Macromolecules

Polymers are considered as “safe” drug carriers, since they are not absorbed through the mucosa because of their high molecular size and do not show systemic side effects. In order to increase the contact time of the therapeutic substance at the site of absorption, polymers that show mucoadhesive properties are preferred. These polymers carry specific chemical moieties, which facilitate binding interactions with the mucus components. In addition, they should also show absorption enhancing properties independently on mucoadhesion. These properties may be facilitation of the paracellular permeation of the hydrophilic peptides and/or protection from proteolytic degradation. Two classes of mucoadhesive polymers are studied in our Department. Crosslinked poly (acrylic acid) derivatives and chitosans both proved to be promising absorption enhancers when studied in vitro (Caco-2 cells) and showed to be able to positively influence the luminal absorption conditions of macromolecules and to alter the intestinal barrier properties to improve peptide drug absorption.

Crosslinked Poly(Acrylic Acid) Derivatives

Carbomer (Carpopol[®] 934P) and polycarbophil (Noveon[®] AA1, both supplied by BF Goodrich, Cleveland, OH, USA) are crosslinked polyacrylates. Noveon[®] AA1 is weakly crosslinked with divinylglycol, while carbomer is relatively stronger crosslinked with allyl sucrose. The chemical representation of crosslinked polyacrylates is shown at Figure 1. Unfortunately, exact data about the structure and degree of crosslinking are not available from the manufacturer. Both polyacrylate derivatives show strong binding interactions with mucosal tissues, which is in favor for increased residence time of the drug at the site of absorption and subsequently for enhanced absorption. In addition to these mucoadhesion properties, it was shown that these poly(acrylic acid) derivatives have enzyme inhibition properties.

As it has been referred, one of the main obstacles for peptide and protein absorption is the enzymatic barrier. According to their location, intestinal proteases can be divided into three main groups: luminal, membrane-bound and cytosolic enzymes. Luminal enzymes, which are serine proteases like trypsin and α -chymotrypsin, often initiate the degradation of perorally administered peptides. The resulting peptidic fragments are further degraded by a variety of exopeptidases such as carboxy-peptidases, aminopeptidases and di- and oligopeptidases, which are

mainly embedded in the brush border membrane of the intestinal epithelium but are also present in the lumen of the gut.

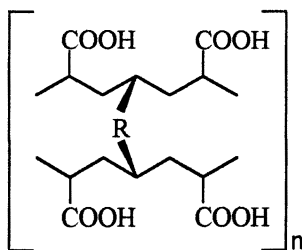


Figure 1. Structure of crosslinked poly (acrylic acid) derivatives. The crosslinking agent (*R*) is in case of Polycarbophil divinylglycol and for Carbomer allylsucrose.

It has been shown that the use of protease inhibitors like aprotinin and soybean trypsin inhibitor can lead to increased peptide drug absorption (1). A major drawback of these inhibitors is their toxicity, especially in chronic drug therapy. An alternative to these toxic enzyme inhibitors may be polymers, which have the ability to inactivate the proteolytic enzymes.

At first the potency of mucoadhesive excipients to inhibit intestinal proteases has been evaluated (2,3). Among the different mucoadhesive polymers investigated, uniquely the poly(acrylates) polycarbophil and Carbomer 934P were able to inhibit the activities of trypsin, α -chymotrypsin, carboxypeptidase A and B as well as of cytosolic leucine aminopeptidase. However, they failed to inhibit microsomal leucine aminopeptidase and pyroglutamyl aminopeptidase. Carbomer was found to be more efficient to reduce proteolytic activity than polycarbophil. The pronounced binding properties of polycarbophil and carbomer for bivalent cations such as zinc and calcium were demonstrated to be a major reason for the observed inhibitory effect. These polymers were able to deprive Ca^{2+} and Zn^{2+} , respectively, from the enzyme structures, thereby inhibiting their activities. Carboxypeptidase A and α -chymotrypsin activities were observed to be reversible upon addition of Zn^{2+} and Ca^{2+} ions, respectively. Therefore, it was concluded that poly(acrylates) may be promising excipients to protect peptide drugs from intestinal degradation (2,3).

In vitro studies, using the Caco-2 cell intestinal epithelium model, showed that carbomer was able to increase the transport of the paracellular radiolabelled marker ^{14}C -mannitol (Mw 180Da) and the fluorescently labelled dextran (FITC-dextran Mw 4400Da) at significantly higher levels than the controls in which monolayers were incubated only with the paracellular markers. Using the same in vitro model carbomer was found to increase the paracellular transport of the peptide DGAVP(9-desglycinamide, 8-L-arginine vasopressin) (4).

In vivo studies in rats were performed in order to investigate the absorption enhancing effect of carbomer (5). The peptide analogue buserelin, a LHRH

superagonist, was chosen to be tested *in vivo*. Buserelin (donated by Hoechst, Germany) was administered with and without the polymer intraduodenally in rats. In this study another modification of the carbomer (C934P) was investigated as well. This modification consisted of a gel solution of carbomer, neutralized and subsequently freeze-dried in order to obtain a fast swelling hydrogel. Absorption profiles of buserelin revealed elevated plasma levels of the peptide, as shown in Figure 2.

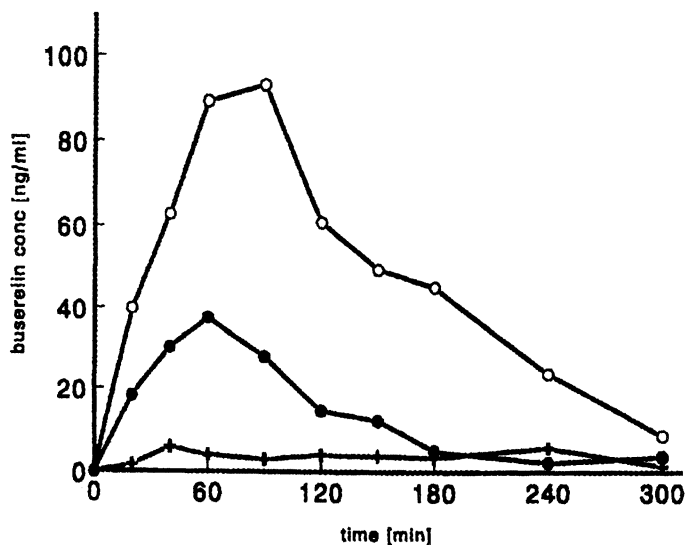


Figure 2. Mean serum concentrations after intraduodenal application of buserelin; +, control (MES-KOH buffer pH 6.7); ● 0.5% (w/v) freeze-dried carbomer; ○ 0.5% (w/v) carbomer. (SOURCE: Reproduced with permission from reference 5. Copyright 1996 Pharm. Res.)

The native carbomer was proven to be more potent than its fast swelling, freeze-dried modification. Co-application of buserelin with carbomer resulted in 1.9 % bioavailability while buserelin only (control cases) gave 0.1% bioavailability (Table I). In addition, the residence time of the drug in the blood was also significantly increased, as evident from the T_{90} values. The increased bioavailabilities are probably due to the mucoadhesive and enzyme inhibitory properties of carbomer (5).

Chitosan a "precious" waste material

Chitosan is a natural-origin polymer obtained from chitin, waste material from the sea food industry, by alkaline or enzymatic deacetylation. Chitosan consists of glucosamine units ((1,4)-linked poly (2-amino-2 deoxy- β -D-glucose or poly (D-glucosamine)) and its chemical structure is depicted at Figure 3.

Chitosan has been investigated in the pharmaceutical field as the excipient in granules and tablets, gels, coacervates or microspheres, and sponge-like formulations

of chitosan have been referred as sustained release drug carriers(6). A very interesting application of chitosan is its use as a carrier of plasmids in gene delivery. Being a cationic polymer, easily available at a wide range of molecular sizes, it forms complexes with DNA (polyplexes) which are able to permeate the cell membrane and transfer genetic material into the cell (7). Chitosan's biocompatibility and biodegradation suggest its safe use. Several studies have been performed showing that chitosan lacks toxic effects when applied in vivo. On the contrary, it has also been referred that chitosan possesses wound healing and bone regenerating properties.

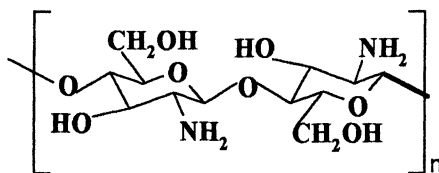


Figure 3. Chemical representation of chitosan

Table I. Intraduodenal administration of busserelin in rats

Polymer	T_{max}	T_{90}	C_{max} (ng/ml)	F (%)	(n)
Control	60-90	n.d	6.7±1.7	0.1±0.1	(6)
FNa C934P gel 0.5% (w/v)	40-60	95± 25	45.8±20.8	0.6± 0.2	(5)
C934P gel 0.5%(w/v)	40-90	165± 80	112.1± 53.4	1.9± 1.3	(5)
Chitosan -HCl gel 1.5%(w/v)	40-90	76± 29	364±140	5.1± 1.5	(6)

NOTE: Pharmacokinetic parameters after intraduodenal administration of busserelin (500µg/rat). Data are presented as mean ± S.D. for the number of animals indicated (n). T_{max} : time to reach serum peak concentration ; T_{90} time to reach 90% of the total amount absorbed; C_{max} serum peak concentration; F, absolute bioavailability; n.d. not determined.

SOURCE:Reproduced with permission from reference 5. Copyright 1996 Pharm. Res.

Another characteristic of this polymer is its mucoadhesion. It has been demonstrated, in repeated adhesion studies, that chitosan is fairly mucoadhesive in comparison to polycarboxophil (8). Chitosan has been observed to promote the nasal absorption of insulin in rats and sheep (9). Chitosan capsules, containing various additives such as absorption enhancers (sodium glycocholate) and protease

inhibitors, are able to promote the colonic absorption of insulin. These capsules were shown to be stable in the stomach and small intestine, but were specifically degraded by microorganisms in the cecal contents of the rat.

In our Department studies have been performed *in vitro* and *in vivo* to investigate the absorption enhancing effect of chitosans. *In vitro* experiments concerning the enzyme inhibitory properties of chitosan revealed that chitosan salts were unable to inhibit the proteolytic enzymes like trypsin (10). In studies using the Caco-2 intestinal epithelium model, chitosan HCl and chitosan glutamate managed to increase the permeability of paracellular markers (e.g. mannitol) at a slightly acidic pH. The levels of the transported paracellular markers were significantly higher than the control and carbomer cases (10). It was suggested that chitosan had a higher efficiency in opening the intestinal tight junctions at this pH value (6-6.5). However, chitosan failed to increase the paracellular permeability at neutral pH values. Chitosan HCl has an apparent pK_a of 5.6, which means that in slight acidic pH values chitosan is protonated, and well soluble, having a certain charge density. These positive charges interact with anionic components of the pores in between the cells that are sealed by the tight junctions, leading to tight junction opening and facilitation of paracellular permeation. At neutral pH values, chitosan aggregates and the charge density is diminished as such that it has less effect on the tight junctions.

In vivo studies were performed to investigate the potency of chitosan HCl to increase the absorption of the peptide analogue buserelin. Chitosan was administered intraduodenally in combination with buserelin in rats (5). The pharmacokinetic parameters are shown in Table I. Chitosan managed to increase the absorption of the peptidic drug buserelin at higher levels than the control and the carbomer cases. Chitosan HCl resulted in a buserelin bioavailability of 5.1%. The buserelin absorption profiles in the presence of chitosan HCl are given at Figure 4. The absorption profiles of control cases and the combination of chitosan/freeze dried neutralized carbomer are shown as well. The combination of the two polymers did not manage to increase the absorption of buserelin, probably due to strong electrostatic interactions. The absorption enhancing effect of chitosan is caused predominantly by its effect on the tight junctions, whereas its mucoadhesive properties play only a secondary role.

Chitosan Derivatives; Novel Permeation Enhancers?

Despite all the aforementioned “desired” properties of chitosan, this polymer still lacks the advantage of good solubility at neutral pH values. It aggregates in solutions at pH values above 6.5. The polymer is therefore only soluble in acidic solutions (pH 1-6.5) where most of the amino groups are protonated. Studies have shown that only protonated chitosan, i.e. in its uncoiled configuration, can trigger the opening of the tight junctions, thereby facilitating the paracellular transport of hydrophilic compounds (11). This property implies that chitosan can be effective as an absorption enhancer only in a limited area of the intestinal lumen where the pH values are close to its pK_a . For that reason, it may not be a suitable carrier for targeted peptide drug delivery to specific sites of the intestine, for instance jejunum or ileum.

To overcome this problem the chitosan derivative N,N,N- trimethyl chitosan chloride (TMC) has been synthesized and characterized. The synthesis of TMC is shown in Figure 5. It is a reductive methylation procedure, which yields quaternized chitosan as iodide salts. The counterion is exchanged to chloride in an aqueous NaCl solution. TMC chloride is subsequently isolated by precipitation in an ethanol solution. TMC can be quaternized in different degrees, dependent upon the conditions, steps and duration of the synthesis reaction (12).

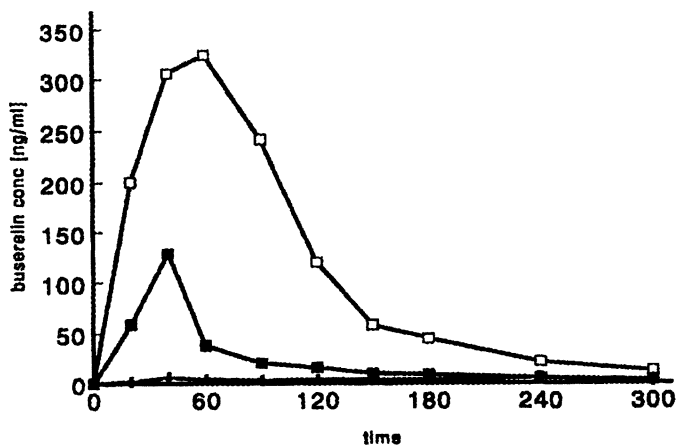


Figure 4. Mean serum concentrations after intraduodenal application of buserelin. + control (MES/KOH buffer pH 6.7); ■, 0.5% (w/v) freeze-dried carbomer 934P/1.5% chitosan HCl mixture (1:1); □, 1.5% (w/v) chitosan HCl. (SOURCE: Reproduced with permission from reference 5. Copyright Pharm. Res.)

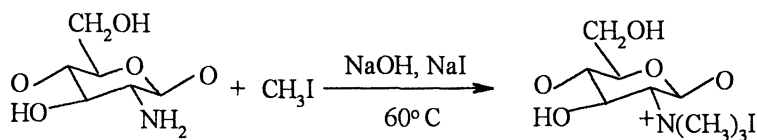


Figure 5. Synthesis of N-trimethyl chitosan

The quaternized chitosan showed higher solubility than chitosan in a broader pH range. TMC was characterized for the degree of substitution with $^1\text{H-NMR}$ spectroscopy and potentiometric titration (12).

If the charge density on the sugar moiety would have been the key to open the tight junctions, one would expect the degree of molar substitution of TMC to play an important role on its property to interact with the tight junctions and to increase the permeability of the intestinal epithelia.

Chitosan HCl and TMCs of different degrees of substitution were tested for enhancing the permeability of the radiolabelled marker ^{14}C -mannitol in Caco-2 intestinal epithelia at neutral pH values (7.2). TMC20, TMC40 and TMC60, having degrees of trimethylation 20, 40 and 60% were chosen to be screened (13,14). The permeability was calculated as follows: $P_{\text{app}} = (dc/dt) \cdot (1/A \cdot 60 \cdot C_o)$, where P_{app} is the apparent permeability coefficient (cm/s), dc/dt the permeability rate, A the diffusion area of the cell monolayer (cm^2) and C_o the initial concentration of the radiomarker. Transport enhancement ratios R were calculated from these P_{app} values :

$$R = P_{\text{app polymer}} / P_{\text{app control}}$$

Chitosan HCl failed to increase the permeation of monolayers and so did TMC20, indicating that a threshold value at the charge density of the polymer is necessary to trigger the opening of the tight junctions. In Figure 6 the enhancement ratios for ^{14}C -mannitol transport obtained by TMC40 and TMC60 are shown. TMC60 reached higher enhancement ratios than TMC40 at every concentration tested, indicating that the charge density plays an important role on the opening of the tight junctions at more “intestinal like” pH values (14).

TMCs with higher degrees of substitution were synthesized as well but the extended methylation at 3-OH and 6-OH positions decreased the solubility and the efficiency to open the tight junctions. TMC60 has the highest effect on the intercellular junctions from all TMC polymers tested.

These novel polymers were investigated also for possible toxic effects on the Caco-2 cells. The cells were incubated with the paracellular marker Texas red dextran of Mw 10000Da and an impermeable nucleic acid probe. If TMCs would disrupt the membrane, the nucleic probe would have entered the cells, then bound to nucleic DNA and emitted a specific fluorescence signal. From visualization studies with confocal laser scanning microscopy only the paracellular fluorescence could be observed. Intracellular fluorescence could not be detected, either from the complex nucleic probe –DNA or from the paracellular marker. Experiments using ciliated tissue of embryo chicken trachea incubated with TMCs solutions (TMC20, 40 and 60) showed complete absence of ciliostatic effects, and measurements of the mitochondrial dehydrogenase activity (MTT) revealed no deviations from normal levels when TMCs were applied on cells (to be published).

Safety is the major issue in the search for drug excipients. So far monomeric absorption enhancers have shown that the effective concentrations are very close to their toxic concentrations. Furthermore, these enhancers are of low M.W. and are absorbed as well with increased possibility of systemic toxic effects.

TMCs as novel chitosan derivatives have demonstrated to be efficient in facilitating the paracellular permeation of hydrophilic compounds. The effective TMCs provoked a redistribution of the F-actin, the main component of the cytoskeleton, which is an indication of opening the tight junctions. In the same study it could be shown that the microvillar actin was not influenced by the application of the polymer (to be published).

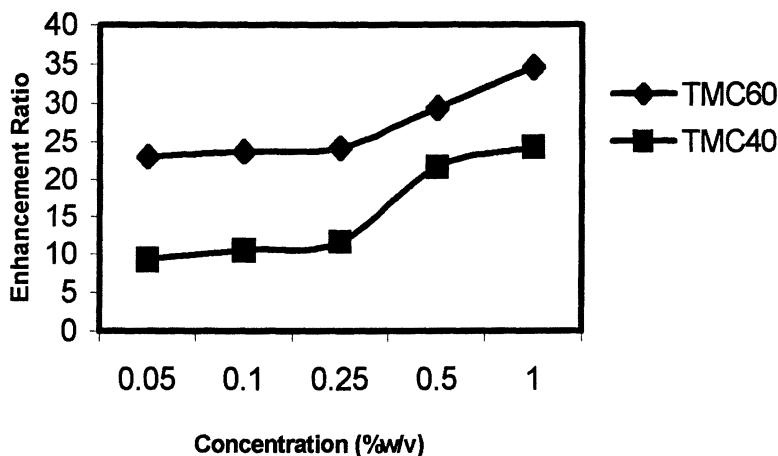


Figure 6. Concentration-dependent transport enhancement ratios of the most effective TMCs at pH = 7.2

Enhancement of the nasal insulin absorption by TMC in rats

The nasal route of administration was chosen to test the absorption efficiency of the TMCs (15). Chitosan HCl, TMC-L (20% trimethylation) and TMC-H (60% trimethylation) were coadministered with insulin (donated by Eli-Lilly) in the nasal cavity of Sprague-Dawley rats, and plasma insulin and blood glucose levels were monitored with time.

From all applications tested only the highly substituted TMC60 was able to substantially enhance the absorption of insulin (Figure 7). These results are in accordance with the previous *in vitro* results, verifying the power of *in vitro* cell culture systems to screen absorption enhancers and the potential of TMC60 as an effective and safe absorption enhancer. These modified chitosans are at the beginning on the development of novel functional chitosan derivatives for different pharmaceutical applications. Small chemical modifications at the chitosan structure can modify the physicochemical properties of the polymer and lead to desirable, tailor-made derivatives. These derivatives may be applicable as drug carriers in all cases where chitosan itself is not suitable. For instance, substitution at the $-NH_2$ group with alkyl-carboxylic groups can switch the polymer from a cationic to an anionic type, and therefore applicable for delivery of anionic macromolecules.

Conclusions

Modified and native polyacrylates and chitosans have been studied in order to obtain macromolecular, non-absorbable penetration enhancers. Both native and modified polymers showed enhanced permeation *in vitro* and absorption *in vivo*.

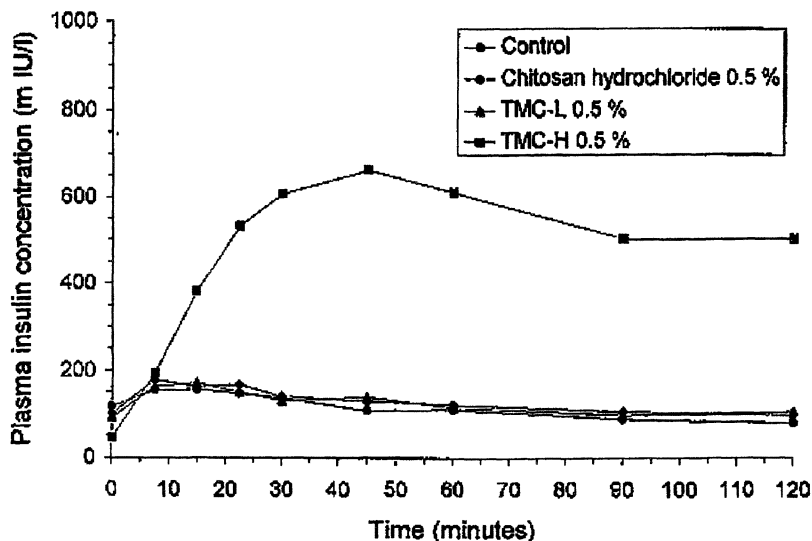


Figure 7. Plasma concentrations of insulin after nasal administration (pH=7.4)

Carbomer as an anionic polymer shows mucoadhesive, proteolytic enzyme inhibiting and paracellular permeation enhancing properties. The freeze dried modification proved to be less potent than the native polymer (absorption enhancement), but it showed better swelling properties. In the case of chitosan, the chemically modified polymer TMC showed even better absorption enhancing effects than the native polymer at neutral pH values. All above mentioned polymers are considered to be safe, as they are not absorbed (because of high molecular weight) through mucosal epithelia. Based on the results obtained so far, safe transmucosal macromolecular penetration enhancers may not be longer a contradiction as such, but the fiction may become a fact. Since polymers are widely used in solid dosage forms, it is expected that these multifunctional polyacrylate and chitosan polymers will be a useful tool for nasal, peroral and pulmonary delivery of peptide and protein drugs.

References

1. Bernkop-Schnurch A., *J. Controlled Release* **1998**, *52*, 1-16.
2. Lueßen, H. L.; Verhoef, J. C.; Borchard, G.; Lehr, C.-M.; De Boer, A. G.; Junginger, H. E., *Pharm. Res.* **1995**, *12*, 1293-1298.

3. Lueßen, H. L.; De Leeuw, B. J.; Pérard, D.; Lehr, C.-M.; De Boer, A. G.; Verhoef, J. C.; Junginger, H. E., *Eur. J. Pharm. Sci.* **1996**, *4*, 117-128.
4. Lueßen, H. L.; Rentel, C.-O.; Kotzé, A. F.; Lehr, C.-M.; De Boer, A. G.; Verhoef, J. C.; Junginger, H. E., *J. Controlled Release* **1997**, *45*, 15-23.
5. Lueßen, H. L.; De Leeuw, B. J.; Langemeijer, M. W.; De Boer, A. G.; Verhoef, J. C.; Junginger, H. E., *Pharm. Res.* **1996**, *13*, 1668-1672.
6. Oungbho, K.; Muller, B. W., *Int. J. Pharm.* **1997**, *156*, 229-237.
7. MacLaughlin, F. C.; Mumper, R. J.; Wang, J. J.; Tagliaferri, J. M.; Gill, I.; Hinchcliffe, M.; Rolland, A. P., *J. Controlled Release* **1998**, *56*, 259-272.
8. Lehr, C.-M.; Bouwstra, J. A.; Schacht, E. H.; Junginger, H. E., *Int. J. Pharm.* **1992**, 43-48.
9. Illum, L.; Farraj, N. F.; Davis, S. S., *Pharm. Res.* **1994**, *11*, 1186-1189.
10. Kotzé, A. F.; De Leeuw, B. J.; Lueßen, H. L.; De Boer, A. G.; Verhoef, J. C.; Junginger, H. E., *Int. J. Pharm.* **1997**, *159*, 243-253.
11. Kotzé, A. F.; Lueßen, H. L.; De Boer, A. G.; Verhoef, J. C.; Junginger, H. E., *Eur. J. Pharm. Sci.* **1999**, *7*, 145-151.
12. Sieval, A. B.; Thanou, M.; Kotzé, A. F.; Verhoef, J. E.; Brussee, J.; Junginger, H. E., *Carbohydr. Polym.* **1998**, *36*, 157-165.
13. Kotzé, A. F.; Thanou, M. M.; Lueßen, H. L.; De Boer, A. G.; Verhoef, J. C.; Junginger, H. E., *J. Pharm. Sci.* **1999**, *88*, 253-257.
14. Thanou, M.; Kotzé, A. F.; Scharringhausen, T.; Lueßen, H. L.; De Boer, A. G.; Verhoef, J. C., and Junginger, H. E., *J. Controlled Release* **1999**, *In Press*.
15. Kotzé, A. F., Thanou, M., Verhoef, J. C., and Junginger, H. E., *Proceed. Intern. Control. Rel. Bioact. Mater* **1998**, *25*, 479-480.

Chapter 4

Prodrug Strategies to Improve the Oral Absorption of Peptides and Peptide Mimetics

Ronald T. Borchardt¹ and Binghe Wang²

¹Department of Pharmaceutical Chemistry,
The University of Kansas, Lawrence, KS 66047

²Department of Chemistry, North Carolina State University, Raleigh, NC 27695

Recently, our laboratories have introduced the concept of preparing cyclic prodrugs of peptides and peptide mimetics as a means of modifying their physicochemical properties sufficiently to allow them to permeate biological barriers (i.e., intestinal mucosa). These cyclization strategies employ new chemical linkers that were designed to be susceptible to esterase metabolism, leading to a cascade of chemical reactions that result in release of the peptide or peptide mimetic. These cyclic prodrug strategies have been applied to opioid peptides and RGD peptide mimetics to stabilize them to metabolism and/or to improve their intestinal mucosal permeation.

In recent years, many structurally diverse peptides and peptide mimetics possessing a broad spectrum of pharmacological effects have been synthesized by medicinal chemists (1). Many of these peptides and peptide mimetics have unique therapeutic indications that warrant their clinical development. However, in many cases, the clinical development of these molecules has been prevented because of their unfavorable biopharmaceutical properties, which include (i) metabolic lability and (ii) poor permeation of cell membranes (e.g., intestinal mucosa) (2,3). The problem of metabolic lability by hydrolytic pathways (e.g., peptidases) has, for all practical purposes, been resolved by medicinal chemists through structural manipulation of the peptide (i.e., introducing peptidase-resistant bonds) to produce peptide mimetics (2,3). Until recently, medicinal chemists have had less success in manipulating the structures of peptides and peptide mimetics to achieve good permeation of cell membranes (i.e., intestinal mucosa) while still retaining high affinity for the macromolecular target (2,3).

Permeation of peptides and peptide mimetics across the intestinal mucosa can occur via the paracellular pathway (pathway A, Figure 1) or transcellular pathway

(pathway B, Figure 1). In general, hydrophilic peptides (e.g., opioid peptides) and peptide mimetics (e.g., RGD peptide mimetics) are restricted to the paracellular pathway, which consists of aqueous pores (average size in the small intestine, approx. 7–9 Å) created by the cellular tight junctions (3). These aqueous pores restrict peptide and peptide mimetic permeation based on size and charge (4). Hydrophilic peptides and peptide mimetics, whose permeation is restricted to the paracellular pathway, typically exhibit oral bioavailabilities of <1–2% (3). It should be noted that some hydrophilic molecules that structurally resemble di- and tripeptides (e.g., β -lactam antibiotics) show good intestinal permeation and good oral bioavailability (>50%) because they serve as substrates for the oligopeptide transporter (pathway C, Figure 1) (5).

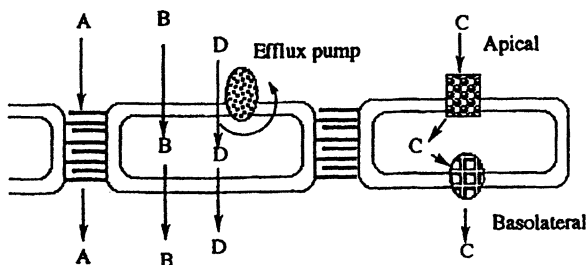


Figure 1. Pathways of peptide mimetic transport across the intestinal mucosa: A, passive diffusion via paracellular route; B, passive diffusion via transcellular route; C, transporter-facilitated (e.g., oligopeptide transporter); D, transport-restricted (e.g., efflux transporters).

In contrast to hydrophilic molecules, hydrophobic peptides, peptide mimetics or prodrugs of these molecules that lack charge and exhibit low hydrogen bonding potential can traverse the intestinal mucosa by passive diffusion via the transcellular pathway. Previously, it was thought that the enzymatic barrier to peptide transport consisted only of brush border membrane and cytoplasmic peptidases (6). Recently, however, it was shown that a specific isozyme (3A4) of cytochrome P450 plays an important role in the metabolism of peptides (e.g., cyclosporin) and peptide mimetics (e.g., HIV protease inhibitors) (7,8). In addition, the intestinal mucosa has been shown to contain efflux transporters [e.g., multidrug resistance protein (MDR1 in humans, also called P-glycoprotein)] that restrict transcellular permeation of hydrophilic peptides (e.g., cyclosporin) and peptide mimetics (e.g., HIV protease inhibitors) (8,9), as well as hydrophobic prodrugs of peptides and peptide mimetics (10).

To succeed in developing orally bioavailable peptides and peptide mimetics, it will be necessary to incorporate structural features into the molecules that will optimize their pharmacological (e.g., high receptor affinity) as well as their biopharmaceutical (e.g., intestinal mucosal permeation) properties. As an alternative approach, unfavorable biopharmaceutical properties of peptides and peptide mimetics can be

transiently modified using prodrug strategies. In general, prodrug strategies applied to peptides and peptide mimetics have focused on modification of a single functional group (e.g., N-terminal amino group or C-terminal carboxyl group) (3,11,12). More recently, our laboratories have introduced the concept of preparing cyclic prodrugs of peptides (e.g., opioid peptides) and peptide mimetics (e.g., RGD peptide mimetics) as a way to modify their physicochemical properties sufficiently to overcome their undesirable biopharmaceutical properties (e.g., poor intestinal mucosal permeation). Our progress to date on this strategy is the subject of this chapter.

Results and Discussion

Chemical Linkers Used to Prepare Cyclic Prodrugs

From a membrane permeation perspective, there are several possible advantages to considering cyclization strategies for making prodrugs of peptides and peptide mimetics (11,13). These include: (i) derivatization of key functional groups (e.g., N-terminal amino and C-terminal carboxyl groups) would reduce the overall charge of the molecule; (ii) cyclization could lead to the creation of unique solution structures that reduce the hydrogen bonding potential of the molecule; and (iii) cyclization could lead to a reduction in the size of the molecule. Key to the success of these cyclic prodrug strategies was the identification of chemical linkers that were susceptible to esterase metabolism, leading to a cascade of chemical reactions and resulting in release of the therapeutic peptide or peptide mimetic (Figure 2). Recently, Borchardt's laboratory has described synthetic methodologies for linking the N-terminal amino group to the C-terminal carboxyl group of peptides using an acyloxyalkoxy promoiety (Figure 2A) (14,15) or a 3-(2'-hydroxy-4',6'-dimethylphenyl)-3,3-

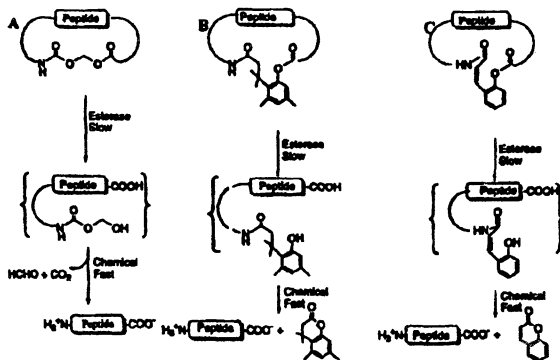


Figure 2. Cyclic prodrug strategies. Panel A, acyloxyalkoxy-based prodrug; panel B, phenylpropionic acid-based prodrug; Panel C, coumarinic acid-based prodrug.

dimethylpropionic acid promoiety (Figure 2B) (16,17). In a similar manner, Wang's laboratory (18–20) has used coumarinic acid (Figure 2C) as a chemical linker to make cyclic prodrugs of peptides.

Using a model hexapeptide, Borchardt's laboratory showed that an acyloxyalkoxy cyclic prodrug (21) and a phenylpropionic acid prodrug (22) were converted to the parent peptide more rapidly in human blood than in physiological buffer, supporting the involvement of esterases in their bioconversion. In addition, in transport studies conducted using Caco-2 cell monolayers, an *in vitro* model of the intestinal mucosa, both cyclic prodrugs were shown to permeate at least 70 times better than the parent hexapeptide (21,22). The enhanced permeation of the acyloxyalkoxy cyclic prodrug could be explained by formation of unique solution structures that reduced the hydrogen bonding potential of the molecule (23).

Applications to Opioid Peptides

Recently, our laboratories have applied the cyclic prodrug strategies shown in Figure 2 to opioid peptides. [Leu⁵]-enkephalin (H-Tyr-Gly-Gly-Phe-Leu-OH) and its metabolically stable analog DADLE (H-Tyr-D-Ala-Gly-Phe-D-Leu-OH) were chosen as model opioid peptides because many of the structural features of these molecules (e.g., free N-terminal amino and C-terminal carboxyl groups) that bestow upon them affinity and specificity for the opioid receptors also endow these molecules with undesirable physicochemical properties (e.g., charge, hydrophilicity, high hydrogen bonding potential) that limit their permeation via the transcellular route. Consistent with the enzymatic/chemical pathway of degradation of the coumarinic acid-based cyclic prodrugs shown in Figure 2C, the [Leu⁵]-enkephalin and DADLE prodrugs using this linker were shown to release the parent peptides more rapidly in biological media containing esterase activity than in pH 7.4 Hanks' balanced salt solution (HBSS) (24,25).

When [Leu⁵]-enkephalin was applied to the apical (AP) side of Caco-2 cell monolayers, no detectable levels of this opioid peptide were observed in the basolateral (BL) side of the monolayer (25). A maximum apparent permeability (P_{app}) value of 0.31×10^{-8} cm/s was calculated based on the limit of detection of our analytical method for [Leu⁵]-enkephalin. In contrast, DADLE, when applied to the AP side of the Caco-2 monolayer, was relatively stable and could be detected on the BL side ($P_{app} = 7.8 \pm 0.7 \times 10^{-8}$ cm/s). When the coumarinic acid-based cyclic prodrugs were applied to the AP side of Caco-2 monolayers, significant quantities of these cyclic prodrugs were detected on the BL side of the monolayer (25). Based on the estimated P_{app} value for [Leu⁵]-enkephalin and the determined P_{app} value of the corresponding [Leu⁵]-enkephalin cyclic prodrug, the prodrug was shown to be approx. 665-fold more able to permeate the cell monolayer than was the opioid peptide itself. In comparison, the cyclic prodrug of DADLE was approx. 31-fold more able to permeate the monolayer than was DADLE itself. Characterization of the membrane interaction potentials ($\log k'_{IAM}$) of the cyclic prodrugs and the opioid peptides by immobilized artificial membrane (IAM) chromatography revealed that

the cyclic prodrugs had significantly higher tendency to partition into the artificial membrane than did the opioid peptides (24). Therefore, a good correlation was observed between this physicochemical property ($\log k'_{IAM}$) and the cell permeation characteristics of the prodrugs. In fact, the membrane interaction potentials of the coumarinic acid-based cyclic prodrugs were sufficiently favorable to allow these prodrugs to traverse the monolayer via the transcellular pathway without interacting with polarized efflux transporters (e.g., MDR1) (25). In contrast, the opioid peptides themselves could only permeate via the paracellular pathway.

In an attempt to understand how the solution structures of the coumarinic acid-based cyclic prodrugs influenced their passive diffusion, conformational studies using spectroscopic techniques (2D-NMR, CD) and molecular dynamics were performed (26). These studies indicated that the cyclic prodrugs had compact and rigid secondary structures composed of β -turns that are partially stabilized by formation of intramolecular hydrogen bonds. The existence of these well-defined secondary structures in the cyclic prodrugs, particularly the presence of intramolecular hydrogen bonds, correlates well with the ability of these prodrugs to partition into an artificial membrane and to permeate the Caco-2 cell monolayers.

Like the coumarinic acid-based cyclic prodrugs described above, the phenylpropionic acid-based cyclic prodrugs were shown to release [Leu⁵]-enkephalin and DADLE by enzymatic hydrolysis of the ester promoity to form an intermediate that would then undergo lactonization to release the parent peptides (24,27). When the phenylpropionic acid-based cyclic prodrugs of [Leu⁵]-enkephalin and DADLE were applied to the AP side of Caco-2 cell monolayers, no significant degradation by chemical or enzymatic (peptidases, esterases) processes was observed (27). However, both cyclic prodrugs showed excellent cell permeation characteristics. For example, based on the estimated P_{app} value for [Leu⁵]-enkephalin (see above) and the determined P_{app} value of the corresponding phenylpropionic acid-based [Leu⁵]-enkephalin cyclic prodrug, the prodrug was approx. 1680-fold more able to permeate the cell monolayer than was the opioid peptide itself. In comparison, the cyclic prodrug of DADLE was approx. 72-fold more able to permeate the monolayer than was DADLE. Characterization of the membrane interaction potentials ($\log k'_{IAM}$) of the cyclic prodrugs by IAM chromatography revealed that the cyclic prodrugs had significantly higher tendency to partition into the artificial membrane than did the opioid peptides (24). Therefore, a good correlation was observed between this physicochemical property ($\log k'_{IAM}$) and the actual cell permeation characteristics of the prodrugs. Similar to those of the coumarinic acid-based prodrugs, the membrane interaction potentials of the phenylpropionic acid-based cyclic prodrugs were sufficiently favorable to allow these prodrugs to traverse the monolayer via the transcellular pathway without interacting with polarized efflux transporters (e.g., MDR1) (27).

To better understand their lipophilic character and their ability to permeate cell membranes, we conducted conformational studies on these phenylpropionic acid-based cyclic prodrugs using 1D- and 2D-NMR and CD (26). These studies revealed that the phenylpropionic acid-based cyclic prodrugs exhibited more well-defined, rigid and compact secondary structures composed of β -turns than did the opioid peptides. The formation of the intramolecular hydrogen bonds, as well as the incor-

poration of the lipophilic phenylpropionic acid moiety into the relatively hydrophobic peptide sequence, may account for the ability of the prodrugs to partition into an artificial membrane as determined by IAM chromatography. Furthermore, the existence of these well-defined secondary structures in cyclic prodrugs, particularly the presence of intramolecular hydrogen bonds, correlates well with their membrane interaction potential and their ability to permeate the Caco-2 cell monolayers.

Like the coumarinic acid-based and phenylpropionic acid-based cyclic prodrugs described above, the acyloxyalkoxy cyclic prodrugs were shown to rapidly release [Leu⁵]-enkephalin and DADLE by an esterase-catalyzed reaction (10,28). Because of the physicochemical properties (e.g., high membrane interaction potential, low hydrogen bonding potential) of the acyloxyalkoxy-based cyclic prodrugs (28), it was expected that these cyclic prodrugs of [Leu⁵]-enkephalin and DADLE would have favorable permeation characteristics across Caco-2 cell monolayers. This hypothesis was based on our earlier observations with the phenylpropionic acid- and coumarinic acid-based cyclic prodrugs of the same opioid peptides. These cyclic prodrugs exhibited favorable physicochemical properties (e.g., $\log k'_{IAM}$) that correlated well with their excellent Caco-2 permeation characteristics (see discussion above). However, it should be noted that, while these phenylpropionic acid- and coumarinic acid-based cyclic prodrugs of [Leu⁵]-enkephalin and DADLE had favorable $\log k'_{IAM}$ values, they were not shown to be substrates for apically polarized efflux systems in Caco-2 cells, which could have restricted their transcellular permeation.

Therefore, it was very surprising to observe that the acyloxyalkoxy-based cyclic prodrugs of [Leu⁵]-enkephalin and DADLE exhibited P_{app} values across Caco-2 cell monolayers in the AP-to-BL direction that were approximately 200–300 times lower than the values observed previously with the phenylpropionic acid- and coumarinic acid-based cyclic prodrugs of the same opioid peptides (10,25,27). In fact, the acyloxyalkoxy-based cyclic prodrug of DADLE had a $P_{app\ AP-BL}$ value approx. four times lower than that of DADLE itself, in spite of having a membrane interaction potential ($\log k'_{IAM}$) approx. four times higher (10). However, an explanation for the lower permeation of acyloxyalkoxy-based cyclic prodrugs across Caco-2 cells became obvious when the P_{app} values in the BL-to-AP direction for these prodrugs were determined. The much higher $P_{app\ BL-to-AP}$ values compared to the $P_{app\ AP-to-BL}$ values for cyclic prodrugs ([Leu⁵]-enkephalin prodrug, 36 times greater; DADLE prodrug, 52 times greater) suggest that these acyloxyalkoxy-based prodrugs are substrates for apically polarized efflux systems (10). Further evidence in support of this hypothesis was obtained by conducting competition experiments using cyclosporin, a known inhibitor of P-glycoprotein (10).

The substrate activity of the acyloxyalkoxy-based cyclic prodrugs of [Leu⁵]-enkephalin and DADLE for efflux systems in Caco-2 cells versus the nonsubstrate activity of the phenylpropionic acid- and coumarinic acid-based cyclic prodrugs of the same opioid peptides is very intriguing. Based on their membrane interaction potentials ($\log k'_{IAM}$) as measured by their abilities to partition into an immobilized artificial membrane, the acyloxyalkoxy-based prodrugs had the least favorable membrane partition characteristics (low $\log k'_{IAM}$ values) (28) and the phenylpropionic acid-based prodrugs had the most favorable membrane partition characteristics (high

log k'_{IAM} values) (24). These results would suggest, based on what is known about the substrate activity of P-glycoprotein, that the phenylpropionic acid- and coumarinic acid-based prodrugs would be more likely to be substrates for P-glycoprotein than the acyloxyalkoxy-based prodrugs. Obviously, these predictions were wrong because neither the phenylpropionic acid- nor the coumarinic acid-based prodrugs were substrates for efflux systems (e.g., P-glycoprotein), whereas the acyloxyalkoxy-based prodrugs were excellent substrates. These results suggest that, for this series of compounds, the membrane interaction potential alone was not a good predictor of substrate activity for P-glycoprotein. One possible difference between the acyloxyalkoxy-based prodrugs and the phenylpropionic acid- and coumarinic acid-based prodrugs is their solution conformations. While the phenylpropionic acid- and coumarinic acid-based prodrugs exist in well-defined solution conformations with significant secondary structure (e.g., β -turns) (26), the acyloxyalkoxy-based prodrugs have two major conformers that exist in equilibrium as determined by NMR (29). These conformers arise from the cis-trans isomerization of the carbamate junction between the promoity and the peptide. Therefore, it may be possible that the acyloxyalkoxy-based prodrugs in the lipid environment of the cell membrane adopt structures more conducive to interactions with P-glycoprotein. Alternately, the acyloxyalkoxy linker itself cannot be rule out at this time as the structural feature recognized by P-glycoprotein.

Application to RGD Peptide Mimetics

Our laboratories have also applied the coumarinic acid-based cyclic prodrug strategy to RGD peptide mimetics. For these studies, we used MK-383 (**4c**, tirofiban) and several of its analogs (**4a**, **4b**) (30). The corresponding cyclic prodrugs **1a–c** were designed to be sensitive to esterases and were shown to undergo bioconversion as illustrated in Figure 3 (31). The cell transport characteristics of the RGD peptide mimetics (**4a–b**) and the corresponding cyclic prodrugs (**1a–b**) were determined in Caco-2 cell monolayers (32). The apparent membrane permeability of RGD analogs **4a** and **4b** were determined to be $3.94 \pm 0.05 \times 10^{-7}$ and $3.88 \pm 0.10 \times 10^{-7}$ cm/s, respectively. The coumarinic acid-based prodrugs **1a** and **1b** exhibited apparent membrane permeabilities that were approximately sixfold ($2.42 \pm 0.29 \times 10^{-6}$ cm/s) and fivefold ($1.90 \pm 0.21 \times 10^{-6}$ cm/s) higher than their corresponding RGD analogs, respectively (32). These data indicate that the coumarinic acid-based prodrug strategy can indeed be used to improve the ability of such RGD analogs to permeate membranes. However, the magnitude of the improvement was less than what we observed with a cyclic prodrug of a metabolically stable opioid peptide, DADLE, which was 31 times more able to permeate than was the peptide itself (25). One possible explanation for this difference is that intramolecular hydrogen bond formation in the cyclic prodrug of DADLE could help to improve membrane permeation (26), while similar intramolecular hydrogen bonds cannot be formed with the cyclic

prodrugs **1a,b** of the RGD peptide mimetics because of the lack of the regularly spaced amide bonds.

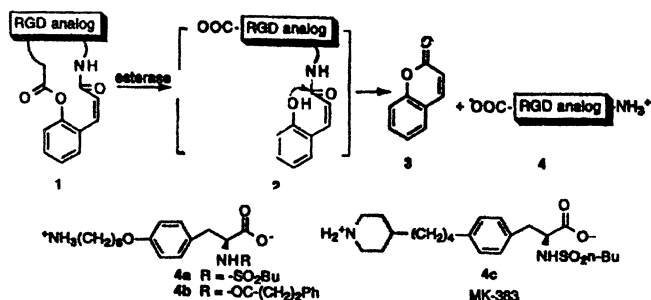


Figure 3. Esterase-sensitive cyclic prodrugs of RGD analogs.

The ultimate objective of our prodrug research with RGD peptide mimetics is to identify an orally bioavailable derivative that exhibits *in vivo* efficacy. Therefore, the *ex vivo* pharmacological effect of one prodrug (**1c**) was evaluated after oral administration in dog (Binghe Wang, David C. Sane, Guy L. Wheeler and Che-Ping Cheng, unpublished data). In a very preliminary study using a single beagle dog, the prodrug was administered using a gelatin capsule. Blood samples drawn at different intervals were examined for indications of altered platelet aggregation patterns due to the administration of the prodrug. In this particular experiment the prodrug of tirofiban (**1c**), was used because it is a potent antiplatelet agent and is known to be orally unavailable (33). Significant and prolonged antiplatelet activity after oral administration of prodrug **1c** was observed. In contrast, administration of an equivalent dose of MK-383 to the same dog had a minimal effect on ADP-induced platelet aggregation. However, it must be emphasized that these results are preliminary. More studies will be needed to further confirm the observed effects.

Conclusion

The results of our studies have shown that cyclization of linear peptides produces a dramatic effect on their metabolic stability and their ability to permeate a biological barrier (e.g., intestinal mucosa). Therefore, the chemical linkers described in this chapter can be used to prepare cyclic prodrugs of therapeutically important peptides (e.g., opioid peptides) and peptide mimetics (e.g., RGD peptide mimetics) so as to transiently alter their physicochemical properties, thereby potentially improving their membrane permeation. However, because these prodrugs are designed to partition significantly into the lipid bilayer, they will be exposed to polarized efflux systems and cytochrome P-450-3A4 that could restrict their overall cell permeation. Currently, we have the knowledge to predict the physicochemical properties that would

optimize the partitioning of a peptide or peptideomimetic prodrug into a lipid bilayer. However, we lack the knowledge to predict which structural features will induce substrate activity for apically polarized efflux systems and cytochrome P450-3A4.

Acknowledgments

Financial support from the American Heart Association (BW), the Presbyterian Health Foundation (BW), United States Public Health Service (DA09315) (RTB), and the Costar Corporation (RTB) is gratefully acknowledged.

References

1. *Proceedings of the 15th American Peptide Symposium*; Tam, J. P.; Kaumaya, P. T. P., Eds.; Kluwer Academic Publisher: Dordrecht, The Netherlands, 1998.
2. *Peptide-Based Drug Design: Controlling Transport and Metabolism*; Taylor, M. D.; Amidon, G. L., Eds.; American Chemical Society: Washington, DC, 1995.
3. Pauletti, G. M.; Gangwar, S.; Siahaan, T. J.; Aube, J.; Borchardt, R. T. *Adv. Drug Del. Rev.* **1997**, *27*, 235.
4. Pauletti, G. M.; Okumu, F. W.; Borchardt, R. T. *Pharm. Res.* **1997**, *14*, 164.
5. Tsuji, A. In *Peptide-Based Drug Design: Controlling Transport and Metabolism*; Taylor, M. D.; Amidon, G. L., Eds.; American Chemical Society: Washington, DC, 1995, pp. 101–117.
6. Krishnamoorthy, R.; Mitra, A. K. In *Peptide-Based Drug Design: Controlling Transport and Metabolism*; Taylor, M. D.; Amidon, G. L., Eds.; American Chemical Society: Washington, DC, 1995, pp. 47–68.
7. Thummel, K. E.; Wilkinson, G. R. *Annu. Rev. Pharmacol. Toxicol.* **1998**, *38*, 389.
8. Watkins, P. B. *Adv. Drug Del. Rev.* **1997**, *27*, 161.
9. Wachter, V. J.; Salphati, L.; Benet, L. Z. *Adv. Drug Del. Rev.* **1996**, *20*, 99.
10. Bak, A.; Gudmundsson, O. S.; Friis, G. J.; Siahaan, T. J.; Borchardt, R. T. *Pharm. Res.* **1999**, *16*, 24.
11. Gangwar, S.; Pauletti, G. M.; Wang, B.; Siahaan, T. J.; Stella, V. J.; Borchardt, R. T. *Drug Discovery Today* **1997**, *2*, 148.
12. Oliyai, R. *Adv. Drug Del. Rev.* **1996**, *19*, 275.
13. Shan, D.; Nicolaou, M. G.; Borchardt, R. T.; Wang, B. *J. Pharm. Sci.* **1997**, *86*, 765.
14. Gangwar, S.; Pauletti, G. M.; Siahaan, T. J.; Stella, V. J.; Borchardt, R. T. *J. Org. Chem.* **1997**, *62*, 1356.

15. Gangwar, S.; Pauletti, G. M.; Siahaan, T. J.; Stella, V. J.; Borchardt, R. T. In *Peptidomimetics Protocols*; Kazmierski, W. M. Ed.; Humana Press: Totowa, NJ, 1998, pp. 37–59.
16. Wang, B.; Gangwar, S.; Pauletti, G. M.; Siahaan, T. J.; Borchardt, R. T. *J. Org. Chem.* **1997**, *62*, 1363.
17. Wang, B.; Gangwar, S.; Pauletti, G.; Siahaan, T. J.; Borchardt, R. T. In *Peptidomimetics Protocols*; Kazmierski, W. M. Ed.; Humana Press: Totowa, NJ, 1998, pp. 53–69.
18. Wang, B.; Zhang, H.; Wang, W. *Bioorg. Med. Chem. Lett.* **1996**, *6*, 945.
19. Wang, B.; Wang, W.; Zhang, H.; Shan, D.; Smith, T. D. *Bioorg. Med. Chem. Lett.* **1996**, *6*, 2823.
20. Wang, B.; Shan, D.; Wang, W.; Zhang, H.; Gudmundsson, O. In *Peptidomimetics Protocols*; Kazmierski, W. M. Ed.; Humana Press: Totowa, NJ, 1998, pp. 71–85.
21. Pauletti, G. M.; Gangwar, S.; Okumu, F. W.; Siahaan, T. J.; Stella, V. J.; Borchardt, R. T. *Pharm. Res.* **1996**, *13*, 1615.
22. Pauletti, G. M.; Gangwar, S.; Wang, B.; Borchardt, R. T. *Pharm. Res.* **1997**, *14*, 11.
23. Gangwar, S.; Jois, S. D. S.; Siahaan, T. J.; Vander Velde, D. G.; Stella, V. J.; Borchardt, R. T. *Pharm. Res.* **1996**, *13*, 1657.
24. Wang, B.; Nimkar, K.; Wang, W.; Zhang, H.; Shan, D.; Gudmundsson, O.; Gangwar, S.; Siahaan, T. J.; Borchardt, R. T. *J. Peptide Res.* **1999**, *53*, 370.
25. Gudmundsson, O.; Pauletti, G. M.; Wang, W.; Shan, D.; Zhang, H.; Wang, B.; Borchardt, R. T. *Pharm. Res.* **1999**, *16*, 7.
26. Gudmundsson, O.; Jois, S. D. S.; Vander Velde, D. G.; Siahaan, T. J.; Wang, B.; Borchardt, R. T. *J. Peptide Res.* **1999**, *53*, 383.
27. Gudmundsson, O.; Nimkar, K.; Gangwar, S.; Siahaan, T. J.; Borchardt, R. T. *Pharm. Res.* **1999**, *16*, 16.
28. Bak, A.; Siahaan, T. J.; Gudmundsson, O.; Gangwar, S.; Friis, G. J.; Borchardt, R. T. *J. Peptide Res.* **1999**, *53*, 393.
29. Gudmundsson, O.; Vander Velde, D. G.; Jois, S. D. S.; Bak, A.; Siahaan, T. J.; Borchardt, R. T. *J. Peptide Res.* **1999**, *53*, 403.
30. Hartman, G. D.; Egbertson, M. S.; Halczenko, W.; Laswell, W. L.; Duggan, M. E.; Smith, R. L.; Naylor, A. M.; Manno, P. D.; Lynch, R. J.; Zhang, G.; Chang, C. T.-C.; Gould, R. J. *J. Med. Chem.* **1992**, *32*, 4640.
31. Wang, B.; Wang, W.; Camenisch, G. P.; Elmo, J.; Zhang, H.; Borchardt, R. T. *Chem. Pharm. Bull. (Tokyo)* **1999**, *47*, 90.
32. Camenisch, G. P.; Wang, W.; Wang, B.; Borchardt, R. T. *Pharm. Res.* **1998**, *15*, 1174.
33. Peerlinck, K.; De Lepeleire, I.; Goldberg, M.; Farrell, D.; Barrett, J.; Hand, E.; Panebianco, D.; Deckmyn, H.; Vermylen, J.; Arnout, J. *Circulation* **1993**, *88*, 1512.

Chapter 5

Designing Prodrugs for the hPEPT1 Transporter

Hyo-kyung Han and Gordon L. Amidon

College of Pharmacy, The University of Michigan, Ann Arbor, MI 48109-1065

Prodrug delivery has generally utilized a passive membrane transport to enhance cellular membrane permeability and, hence, uptake. This, however, generally enhances uptake into all cells. An alternative strategy, that we have developed, focuses on enhancing the uptake via cellular transporters, in particular the hPEPT1 peptide transporter found in mucosal epithelial cells. We have designed a variety of prodrugs that utilize this transporter for uptake and shown that these antiviral prodrugs, both in vitro and in vivo, show saturation and competition characteristics of carrier-mediated transport via the hPEPT1 transporter. These results indicate that design of drugs for specific membrane transporters can achieve enhanced membrane permeability and drug efficacy.

Intestinal drug absorption and first-pass drug metabolism have been the main concern in oral drug delivery to assure sufficient oral bioavailability for the adequate therapeutic effect of drugs. Among many attempts to overcome the pharmaceutical and pharmacokinetic barriers causing low oral bioavailability, the chemical approach using drug derivatization offers the highest flexibility and has been recognized as an important means of producing better pharmaceuticals. The prodrug approach which is a chemical approach using reversible derivatives could be useful to enhance the intestinal absorption of polar drugs. Whereas the classical prodrug design utilizes lipophilic derivatives to increase the passive membrane permeability, 'targeted-prodrug design' utilizes the membrane transporters for polar nutrients such as amino acids, nucleosides or peptide transporters (1-3). This type of 'targeted prodrug design' requires considerable knowledge of the particular carrier system including

their molecular and functional characteristics. Recently, the advances in gene cloning and controlled gene expression techniques in mammalian cells can be used to elucidate the molecular nature of carrier proteins and make possible more rational design of 'targeted prodrugs'.

Compared to other transporters, peptide transporters have broad substrate specificity (4, 5) and could be a good target for chemical modification to improve oral drug absorption of polar drugs (6-8). Peptide transporters have been extensively studied to optimize the structural modification of drugs and their substrate specificity has been discussed in major reviews (1, 9-11). However, recently, novel findings on the substrate specificity of peptide transporters (12-20), strongly suggest the re-evaluation of structural requirements for these transporters. In this manuscript, we will briefly summarize the peptidyl substrates of peptide transporters and then mainly discuss the new structural features for peptide transporters focused on our new findings with amino acid ester prodrugs and other non-peptide substrates.

PEPTIDYL SUBSTRATES OF PEPTIDE TRANSPORTERS

In addition to the endogenous peptides, various therapeutic drugs are known as substrates of peptide transporters. As shown in Fig. 1, β -lactam antibiotics, angiotensin-converting enzyme inhibitors, renin inhibitors and bestatin are well-known substrates for peptide transporters (2, 4, 21) and possess peptide-like chemical structures with a peptide bond, an α -amino group and a C-terminal carboxyl group. Substitution of N-terminal α -amino group or C-terminal carboxyl group of the peptidyl substrates greatly influences the affinity for the peptide transport system (10, 22, 23). Blocking of these groups reduces the affinity to a significant extent but they still can be recognized as substrates of peptide transporters. For example, several β -lactam antibiotics (e.g., cefixime, cefdinir) and ACE inhibitors (e.g., captopril, enalapril, quinapril, benazepril) have been shown to be transported via the intestinal peptide transport system even though they do not have an N-terminal α -amino group (24-26). Also, thyrotropin releasing hormone (TRH) and some renin inhibitors which do not have a free C-terminal carboxyl group are reported to be transported by the peptide transporters (27, 28). Therefore, an N-terminal α -amino group and a C-terminal carboxyl group do not appear to be critical requirements for the peptide transporters although modification of these groups generally diminishes the substrate affinity to the transporters.

Several studies have indicated that the intestinal and renal peptide transporters are stereoselective (29-31). Peptides containing L-amino acids interact with the peptide transporter with greater affinity than do peptides containing D-amino acids. The same is true with peptidomimetic drugs, which are substrates for the peptide transporters. In addition, a D-amino acid at the N-terminal end of a peptide may have more effect on transport than one at the carboxyl terminal end (32).

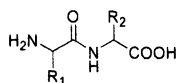
On the other hand, until recently, the presence of a peptide bond in the substrate has been considered as a prerequisite for the recognition by peptide transporters. However, recent findings on the non-peptidyl substrates of peptide transporters such

American Chemical Society
Library
1155 16th St., N.W.

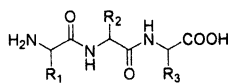
In *Chemical Biology*, Vol. 1, No. 1, 2000, pp. 47-54. © 2000 American Chemical Society, et al.;

ACS Symposium Series; American Chemical Society: Washington, DC, 2000.

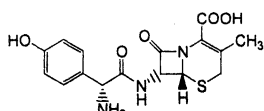
(a) Di-/Tripeptides



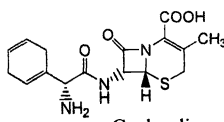
Dipeptide



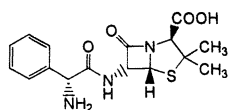
Tripeptide

(b) β -Lactam antibiotics

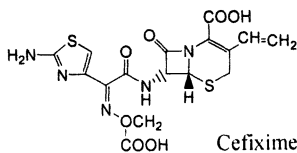
Cefadroxil



Cephadrine

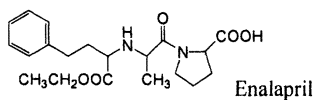


Ampicillin

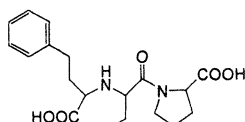


Cefixime

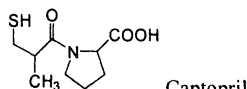
(c) ACE inhibitors



Enalapril

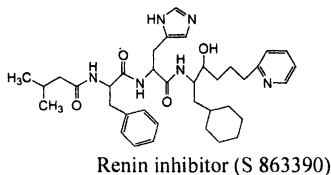


Lisinopril

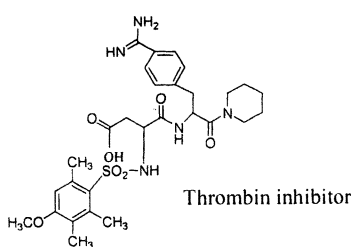


Captopril

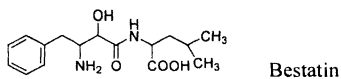
(d) Miscellaneous



Renin inhibitor (S 863390)



Thrombin inhibitor



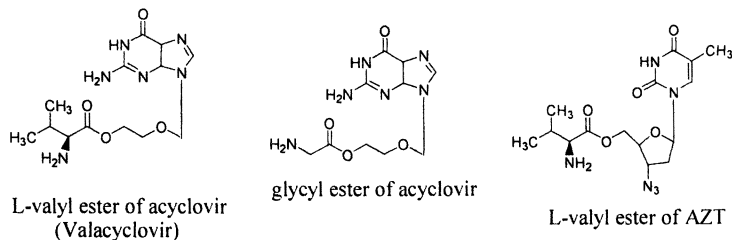
Bestatin

Fig. 1: Peptidyl substrates of peptide transporters

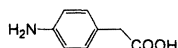
as Arpharmenine A (12, 13), amino acid ester prodrugs of acyclovir and AZT (14, 15), and 4-aminophenylacetic acid (16) (Fig. 2), strongly challenge the obligatory

need for a peptide bond. Therefore, in the following section, the recent studies on the non-peptidyl substrates will be discussed in detail.

(a) Amino acid ester prodrugs of acyclovir and AZT



(b) 4-aminophenylacetic acid



(c) Arphamenine A

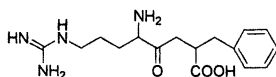


Fig. 2: Non-peptidyl substrates of peptide transporters

NON-PEPTIDYL SUBSTRATES OF PEPTIDE TRANSPORTERS

Amino acid ester prodrugs of acyclovir and zidovudine

In our present study, two nucleoside antiviral drugs, acyclovir (ACV) and Zidovudine (AZT) were converted to the amino acid ester prodrugs such as L-valyl esters of ACV and AZT (L-Val-ACV and L-Val-AZT), D-valyl ester of ACV (D-Val-ACV) and glycyl ester of ACV (Gly-ACV). The intestinal absorption mechanism of these amino acid ester prodrugs was characterized in three different experimental systems; *in situ* rat perfusion model, CHO/hPEPT1 cells and Caco-2/hPEPT1 cells.

Intestinal membrane permeability studies in the *in situ*-perfused rat jejunum indicated that the membrane permeabilities (P_w) of glycyl ester (Gly-ACV) and L-valyl ester prodrugs (L-Val-ACV and L-Val-AZT) were three to ten fold higher than those of the parent drugs (ACV and AZT) but there was no differences in P_w values between D-valyl ester prodrug (D-Val-ACV) and acyclovir (ACV) (Table I). Furthermore, transport of the prodrugs was concentration dependent supporting a carrier-mediated transport mechanism (14). Studies with competitive inhibitors of the intestinal peptide transporter, cephalixin and various dipeptides, significantly reduced the permeability of L-Val-ACV, while the free amino acid, L-valine, had no effect. In addition, L-Val-AZT and Gly-ACV strongly inhibited the transport of the L-Val-ACV, indicating a common transport pathway (14). These results suggest that the peptide transporter is primarily responsible for the transport of these amino acid ester prodrugs across the apical membrane of the intestinal epithelial cell.

Table I: Wall permeability of amino acid ester prodrugs and their parent drugs in rats (0.01mM, Mean \pm SE)

Drugs	N	P_w ($\times 10^{-3}$, cm/sec)
ACV	4	1.3 \pm 0.2
L-Val-ACV	6	13.5 \pm 3.1
D-Val-ACV	4	1.9 \pm 0.3
Gly-ACV	4	6.6 \pm 1.3
AZT	6	1.7 \pm 0.3
L-Val-AZT	6	6.5 \pm 0.6

Data are from reference 14.

A peptide carrier mediated membrane transport of the amino acid esters was confirmed by competitive uptake studies with stably transfected Chinese Hamster Ovary (CHO) cells overexpressing the hPEPT1 transporter. The amino acid ester prodrugs showed strong inhibition of the uptake of a standard peptide substrate Gly-Sar and their IC_{50} values were similar to that of Gly-Sar while lower than those for cephradine and enalapril (14). Thus, these non-peptide amino acid-nucleoside esters display surprisingly good affinity for the hPEPT1 transporter. We also studied the stability and uptake characteristics of these prodrugs in Caco-2/hPEPT1 cells. After 30-min incubation, the hydrolysis of amino acid ester prodrugs was less than 10 % in the supernatant, while it was above 95 % inside the cells except for D-Val-ACV which was relatively stable against the enzymatic hydrolysis (15). These data indicate that L- amino acid ester prodrugs are rapidly converted to the parent drugs by the intracellular hydrolysis following the apical membrane transport. In addition to the inhibition effect on the cellular uptake of L-Val-ACV by peptidyl substrates (15), the membrane transport mechanism of these prodrugs was further supported by the

enhanced cellular uptake of L-Val-ACV following the overexpression of hPEPT1 transporters in the Caco-2 cells (Table II).

Table II: Initial uptake rate of L-Val-ACV in the untransfected Caco-2 cells and the transfected Caco-2/hPEPT1 cells (Mean \pm SD)

	<i>N</i>	<i>Uptake rate (pmol/min/cm²)</i>
Caco-2 cells	4	13.9 \pm 3.2
Caco-2/hPEPT1 cells	6	63.8 \pm 9.2

Data are from reference 15.

The results from three different model systems were very consistent in all cases and can be summarized as follows. First, amino acid ester prodrugs significantly (three to ten fold) increase membrane permeability compared to their parent drugs; second, the L-configuration of amino acid showed more favorable membrane transport and faster reconversion to the parent drug than the D-configuration, and; third, the intestinal absorption of amino acid ester prodrugs is peptide transporter-mediated, even though there is no peptide bond in their structures.

Recently, other research groups independently reported the peptide transporter-mediated absorption mechanism of valacyclovir (L-Val-ACV) (17-20). However, distinguished from other studies, our present study examined several amino acid ester prodrugs as well as valacyclovir and demonstrates that the hPEPT1 transporter can recognize various amino acid progroups with stereoselectivity and also the nucleoside component can be variable. The present study demonstrates that amino acid ester prodrugs can be a good approach to targeting a peptide transporter for improving oral drug absorption of polar nucleoside analogs.

Other non-peptidyl substrates

Daniel *et al.* (12) has shown that Arphamenine A, a Arg-Phe analogue without a peptide bond (the peptide bond (CONH) is replaced by a ketomethylene function (COCH₂)), could be a potent inhibitor for peptide transporters in the renal brush border membrane vesicles and subsequently, Enjoh *et al.* (13) demonstrated that Arphamenine A is transepithelially transported by a peptide transporter in Caco-2 cells. 4-Aminophenylacetic acid (4-APAA), a small totally non-peptidyl drug, has been shown to interact with a proton-coupled oligopeptide transporter by Temple *et al.* (16). 4-APAA transport across the rat intact intestine was stimulated 18-fold by luminal acidification (to pH 6.8) and using renal brush border membrane vesicles and *Xenopus* oocytes expressing PepT1, 4-APAA was shown as a substrate for

translocation by peptide transporters. These studies on the non-peptidyl substrates of peptide transporters further support the suggestion that a peptide bond is not prerequisite for recognition by peptide transporters.

CONCLUSION

The previously proposed substrate specificity on peptide transporters has been challenged by the recent new findings on non-peptidyl substrates and needs to be re-evaluated with more direct evidence at the molecular level. It is still difficult to clearly visualize the structure-transport relationship on peptide transporters, even though these transporters have been extensively studied for several decades. Furthermore, the basolateral membrane transport of dipeptides seems to be different from the apical membrane transport, adding to the complexity of characterizing the minimal structural requirements for peptide transporters. However, as shown in our studies on the amino-acid ester prodrugs, 'targeted-prodrug design' utilizing the peptide transporters can be an efficient strategy to improve oral drug absorption of polar drugs. For rational prodrug design to develop the efficient oral drug delivery systems, the structure-transport relationship of peptide transporters needs to be further investigated at the molecular level.

REFERENCE

1. Walter, E.; Kissel, T.; Amidon, G.L. *Adv. Drug Del. Rev.* **1996**, *20*, 33-58
2. Bai, J.P.F.; Stewart, B.H.; Amidon, G.L. *Handbk. Exp. Pharmacol.* **1994**, *110*, 189-206
3. Stewart, B.H.; Kugler, A.R.; Thompson, P.R.; Bockbrader, H.N. *Pharm. Res.* **1993**, *10*, 276-281
4. Leibach, F.H.; Ganapathy, V. *Annu. Rev. Nutr.* **1996**, *16*, 99-119
5. Smith, P.L.; Eddy, E.P.; Lee, C-P.; Wilson, G. *Drug. Del.* **1993**, *1*, 103-111
6. Hu, M.; Subramanian, P.; Mosberg, H.I.; Amidon, G.L. *Pharm. Res.* **1989**, *6*, 66-70
7. Bai, J.P.F.; Hu, M.; Subramanian, P.; Mosberg, H.I.; Amidon, G.L. *J. Pharm. Sci.* **1992**, *81*, 113-116
8. Yee, S.; Amidon, G.L. In *Peptide-based Drug Design: Controlling Transport and Metabolism*; Taylor, M.D.; Amidon, G.L., Eds.; American Chemical Society: Washington, DC, 1995; pp 135-147
9. Matthews, D.M. *Protein absorption. Development and Present State of the Subject*; Wiley-Liss: New York, 1991
10. Bai, J.P.F.; Amidon, G.L. *Pharm. Res.* **1992**, *9*, 969-978
11. Kramer, W.; Girbig, F.; Gutjahr, U.; Kowalewski, S. In *Peptide-based Drug Design*; Taylor, M.D.; Amidon, G.L., Eds.; American Chemical Society: Washington, DC, 1995; pp 149-180
12. Daniel, H.; Adibi, S.A. *FASEB* **1994**, *8*, 753-759

13. Enjoh, M.; Hashimoto, K.; Arai, S.; Shimizu, M. *Biosci. Biotech. Biochem.* **1996**, 60, 1893-1895
14. Han, H-k.; de Vruhe, R.L.A.; Rhie, J.K.; Covitz, K-M. Y.; Smith, P.L.; Lee, C-P.; Oh, D-M.; Sadée, W.; Amidon, G.L. *Pharm. Res.* **1998**, 15, 1154-1159
15. Han, H-k.; Oh, D-M.; Amidon, G.L. *Pharm. Res.* **1998**, 15, 1382-1386
16. Temple, C.S.; Stewart, A.K.; Meredith, D.; Lister, N.A.; Morgan, K.M.; Collier, I.D.; Vaughan-Jones, R.D.; Boyd, C.A.R.; Bailey, P.D.; Bronk, J.R. *J. Biol. Chem.* **1998**, 273, 20-22
17. Ganapathy, M.E.; Huang, W.; Wang, H.; Ganapathy, V.; Leibach, F.H. *Biochem. Biophys. Res. Commun.* **1998**, 246, 470-475
18. Sinko, P.J.; Balimane, P.V. *Biopharm. Drug. Dispos.* **1998**, 19, 209-217
19. Balimane, P.V.; Tamai, I.; Guo, A.; Nakanishi, T.; Kitada, H.; Leibach, F.H.; Tsuji, A.; Sinko, P.J. *Biochem. Biophys. Res. Commun.* **1998**, 250, 246-251
20. DE Vruhe, R.L.A.; Smith, P.L.; Lee, C-P. *J. Pharmacol. Exp. Ther.* **1998**, 286, 1166-1170
21. Tsuji, A.; Tamai, I. *Pharm. Res.* **1996**, 13, 963-977
22. Hidalgo, I.J.; Bhatnagar, P.; Lee, C-P.; Miller, J.; Cucullino, G.; Smith, P.L. *Pharm. Res.* **1995**, 12, 317-319
23. Samanen, J.; Wilson, G.; Smith, P.L.; Lee, C-P.; Bondinell, W.; Ku, T.; Rhodes, G.; Nichols, A. *J. Pharm. Pharmacol.* **1996**, 48, 119-135
24. Tsuji, A.; Tamai, I.; Nakanish, M.; Terasaki, T.; Hamano, S. *J. Pharm. Pharmacol.*, **1993**, 45, 996-998
25. Tsuji, A.; Terasaki, T.; Tamai, I.; Hirooka, H. *J. Pharmacol. Exp. Ther.* **1987**, 241, 594-601
26. Friedman, D.I.; Amidon, G.L. *Pharm. Res.*, **1989**, 6, 1043-1047
27. Humphrey, M.J.; Ringrose, P.S. *Drug Metab. Rev.* **1986**, 17, 283-310
28. Kramer, W.; Girbig, F.; Gutjaha, U.; Kleemann, H-W.; Leipe, I.; Urbach, H.; Wagner, A. *Biochem. Biophys. Acta.* **1990**, 1027, 25-30
29. Tamai, I.; Ling, H.Y.; Timbul, S.M.; Nishikido, J.; Tsuji, A. *J. Pharm. Pharmacol.* **1988**, 40, 320-324
30. Lister, N.; Sykes, A.P.; Bailey, P.D.; Boyd, C.A.; Bronk, J.R. *J. Physiol.(Lond)* **1995**, 484, 173-182
31. Ganapathy, V.; Leibach, F.H. *Biochem. Biophys. Acta.* **1982**, 691, 362-366
32. Boyd, CA.; Ward, MR. *J. Physiol.* **1982**, 324, 411-428

Chapter 6

Oral Delivery of Heparin

Andrea Leone-Bay¹, Theresa Rivera-Schaub¹, Rajesh Agarwal¹,
Mark Gonze², Sam Money², Connie Rosado-Gray¹,
and Robert A. Baughman¹

¹Emisphere Technologies, Inc., 765 Old Saw Mill River Road,
Tarrytown, NY 10591

²Ocshner Medical Institutes, New Orleans, LA 70121

During the past decade, dramatic progress in the field of biotechnology has resulted in a large increase in the number of commercially available macromolecular drugs that require parenteral dosing. These new drugs have enormous therapeutic potential, but their use is often limited by their invasive route of administration and with it the complications of patient discomfort and noncompliance. Nonparenteral macromolecular drug delivery has obvious benefits but represents a major clinical challenge because these drugs are plagued by poor absorption, rapid metabolism, and biological and chemical instability. A variety of noninvasive routes of administration for these new therapeutics are currently under investigation including pulmonary, nasal, transdermal, buccal, and oral. Of these methodologies, the most desirable route is the oral route, but it is also the most difficult because the gastrointestinal tract is designed to degrade large molecules and to prevent their absorption.

Heparin

Heparin is a heterogeneous mixture of oligosaccharides with an average molecular weight of about 20,000 Da. It is an anticoagulant drug administered parenterally to hospitalized patients to prevent deep venous thrombosis (DVT) and pulmonary embolism (PE), two common post-surgical complications. Heparin is favored over antivitamin K oral anticoagulants because it produces a rapid onset of anticoagulant activity and has a short physiological half-life (1). Heparin therapy also results in a significantly lower incidence of drug-drug interactions. These pharmacological properties facilitate uncomplicated dose adjustment and contribute to heparin's relatively large margin of safety.

The biological response to heparin is increased blood clotting time typically measured by the activated partial thromboplastin time (APTT) assay. The therapeutic target range is 1.5-2.5 times baseline. Heparin levels in the systemic circulation are measured by the anti-Factor Xa assay. Adequate anticoagulation is achieved when plasma heparin levels are 0.1-0.2 IU/mL.

The major disadvantage of heparin therapy is the requirement for parenteral administration. Oral heparin is ineffective because its highly anionic character and large molecular weight preclude its absorption from the gastrointestinal tract (2). Thus, heparin is usually replaced by the oral anticoagulant warfarin for outpatient therapy.

Warfarin has an extended physiological half-life, is almost completely bound to plasma proteins (3), and requires multiple days for the onset or termination of its activity. Due to its high protein binding, warfarin is the source of numerous unfavorable drug interactions. The switch from heparin to warfarin therapy requires 5-6 days because the delayed onset of action and the prolonged half-life of the latter necessitates a gradual increase in dose as the heparin dose is slowly decreased. Throughout this period of multiple drug exposure, careful patient monitoring is imperative (1). In addition, establishing an appropriate dose can be a long process because equilibration of clotting time may not be achieved for 1-2 weeks after dose adjustment. Daily monitoring is ultimately reduced to several times per month in well-controlled patients receiving long-term therapy. Given these therapeutic problems associated with the current oral anticoagulants, and given that heparin is considered the therapy of choice for preventing DVT and PE, an oral heparin formulation could have tremendous clinical importance.

Oral Heparin

Numerous attempts to develop oral heparin formulations have been reported. Formulations using enteric-coated heparin-amine combinations, heparin complexes or salts prepared with organic acids, heparin derivatives produced by partial desulfation and methylation, mixed micelles, oil/water emulsions, and absorption enhancers such as EDTA have been described (4). Dosage forms based on hydrophobic organic bases (5, 6), spermine and lysine salts (7), liposomes (8, 9), hydrogel nanospheres (10), or bile salts (11, 12) have also been investigated. These approaches have been largely unsuccessful. Consequently, the need for an oral heparin dosage form remains.

We have chosen a new approach to oral heparin delivery that can be described as the design and synthesis of novel, peptide-like delivery agents that facilitate the gastrointestinal absorption of macromolecular drugs including interferon (13), recombinant human growth hormone (14), and heparin (15). These delivery agents can be administered in combination with macromolecular drugs to effect their oral absorption.

We previously demonstrated limited absorption of heparin in rats (16) following the oral administration of microsphere-encapsulated heparin. These microspheres were prepared from either complex, uncharacterized mixtures of thermally condensed α -amino acids (17) or acylated α -amino acids, both of which undergo spontaneous molecular self-assembly to form microspheres under acidic conditions. To improve the efficiency of this oral heparin delivery, we have now developed novel delivery agents based on non- α -amino acids. These compounds promote the oral absorption of heparin at physiological pH and offer several advantages over our earlier systems. Most importantly, these current delivery agents are well-characterized chemical entities, and the preparation of microsphere

suspensions is no longer required to elicit enhanced absorption. Following oral administration of a solution containing a combination of heparin and a selected delivery agent to rats, monkeys, or healthy, human subjects therapeutic levels of anticoagulation can be obtained (18, 19).

Oral SNAC/Heparin

A family of delivery agents (Figure 1) was prepared and screened for their ability to facilitate the gastrointestinal absorption of heparin in rats. These data are reported in Figure 2 in which mean peak APTT values are plotted against the number of methylene units in the acid chain. The data show that the delivery agents having 7 (SNAC), 8, or 9 methylenes connecting the amide and acid functions are the most efficient at promoting oral heparin absorption. The compounds having either a fewer or a greater number of carbons do not effect the oral delivery of heparin as well. One possible explanation for this observation is that the delivery agents are acting as surfactants or "traditional penetration enhancers" (20-22). However, surfactants cause damage to the gastrointestinal membranes at the concentrations required to effect drug delivery. Here, however, the increased absorption of heparin in the presence of delivery agents was not the result of frank damage to the intestinal tissue (23). Histological evaluation of the gastrointestinal tracts of rats was performed following a single oral administration of SNAC to ensure that the increased absorption of heparin observed in these studies was not due to tissue damage. At no time point was there detectable pathology caused by SNAC. These data confirm that the increased absorption of heparin in the presence of SNAC was not due to disruption of the intestinal epithelium.

Based on these studies, the SNAC/heparin combination was selected to confirm oral heparin delivery in a second species, cynomolgus monkeys. Monkeys that received a single oral dose of 150 mg/kg SNAC in combination with 30 mg/kg heparin had APTT levels above the detectable range of the assay (>240 sec). This response is about 12 times the baseline value of 20 seconds. In humans, therapeutic anticoagulation is achieved at 1.5-2.5 times baseline. The pharmacodynamic response following oral administration of 150 mg/kg SNAC and 30 mg/kg heparin is shown in Figure 3a. A large increase in clotting time demonstrated that significant absorption of heparin was achieved in the presence of SNAC. Neither SNAC (300 mg/kg) nor heparin (100 mg/kg) dosed alone elicited any change in APTT.

When the dose of heparin was reduced by one-half (150 mg/kg SNAC and 15 mg/kg heparin), the pharmacodynamic response was greatly reduced (Figure 3a). However, the direct plasma heparin measurement by anti-Factor Xa activity showed that drug levels were approximately half those measured following a heparin dose of 30 mg/kg (Figure 3b). The dependence of the pharmacological response (clotting time) to increasing heparin concentration is not a linear function due to heparin's dose-dependent clearance (24,25). At higher heparin doses, relatively small changes in plasma heparin concentrations will lead to proportionately larger changes in APTT.

Given the effective oral delivery of heparin in the presence of SNAC in two species, the safety of this combination dosing solution was evaluated in monkeys. Cynomolgus monkeys dosed orally with SNAC and heparin (30 mg/kg) in

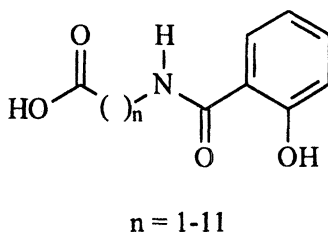


Figure 1. Chemical Structures of Oral Heparin Delivery Agents

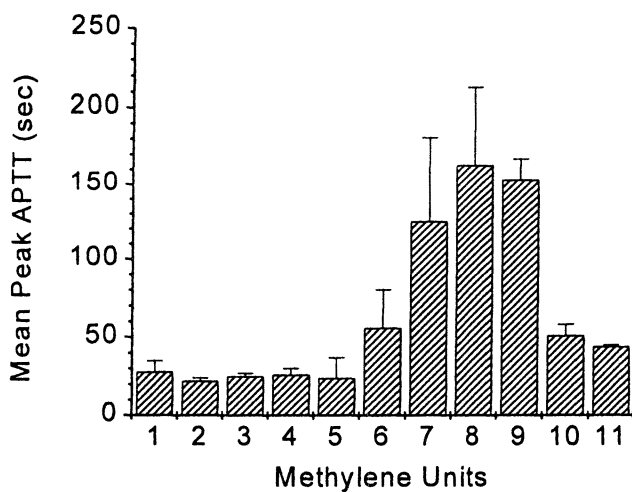
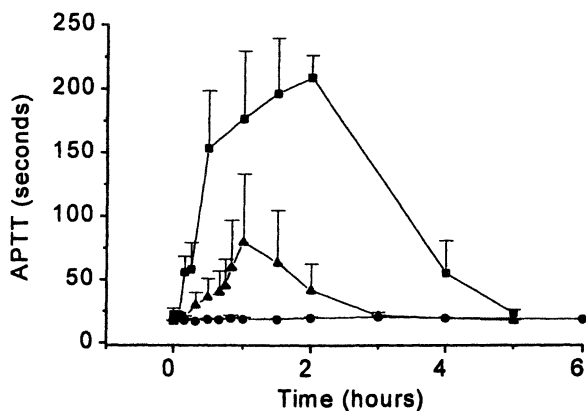


Figure 2. APTT response in rats following a single, colonic dose of heparin in combination with one of the delivery agents 1-11. The data are plotted as mean \pm SEM.

a



b

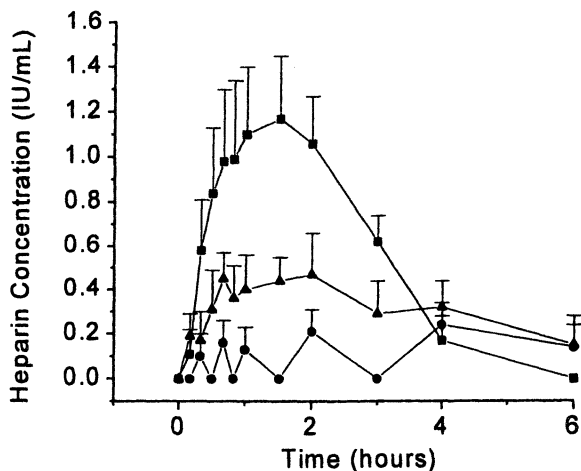


Figure 3. (a) Pharmacodynamic profile following the oral administration of SNAC in combination with varying heparin doses in monkeys. (b) Pharmacokinetic profile following the oral administration of SNAC in combination with varying heparin doses in monkeys. Squares represent 150 mg/kg SNAC in combination with 30 mg/kg heparin. Triangles represent 150 mg/kg SNAC in combination with 15 mg/kg heparin. Circles represent 100 mg/kg heparin alone.

combination for 28 consecutive days showed no observable effects at a SNAC dose of up to 800 mg/kg. Microscopic examination of the gastrointestinal tract at the end of this period did not reveal pathological changes in the tissue. Also, there were no significant changes in serum chemistries.

Efficacy Studies

To confirm the biological efficacy of heparin delivered orally, as compared to heparin administered parenterally, the efficacy of the oral SNAC/heparin combination was evaluated in a rat model of venous thrombosis (26). The ability of SNAC/heparin to prevent DVT and to treat DVT was studied independently in this model.

In the DVT prevention model, rats were dosed by oral gavage with either oral heparin alone (30 mg/kg), oral SNAC alone (300 mg/kg), intravenous heparin (10 mg/kg), or SNAC/heparin (300 mg/kg SNAC; 30 mg/kg heparin). Control animals received oral saline only. Thirty minutes after treatment, the rats were anesthetized and thrombosis formation was induced surgically by exposure of the jugular vein to ethanol and formalin. The surgical incision was closed and after 2 hours was reexplored and examined for the absence or presence of thrombus. The control group demonstrated an 89% (8 of 9) incidence of DVT compared to 25% (2 of 8) for the oral SNAC/heparin group (Figure 4a). The intravenous heparin group demonstrated an 11% (1 of 9) rate of thrombus formation and the oral heparin alone group showed 44% (4 of 9) thrombus formation. The incidence of thrombus in the oral SNAC alone group was 100% (9 of 9). These data show that there is a significant reduction in the rate of DVT formation in both the intravenous heparin and the oral SNAC/heparin groups. Thus, oral SNAC/heparin is effective for preventing DVT in this rat model (27).

Those veins containing thrombi were harvested and the clots were removed and weighed (Figure 4b). In the control group, the mean thrombus weight was 5.7 ± 1.3 mg and in the oral heparin alone group, the mean thrombus weight was 2.3 ± 1.0 mg. The rats in the oral SNAC alone group presented with clots averaged 4.9 ± 0.4 mg. In contrast, the rats in the oral SNAC/heparin and intravenous heparin group had mean clot weights of 0.8 ± 0.5 mg and 0.4 ± 0.2 mg, respectively. Thus, oral SNAC/heparin is comparable to intravenous heparin for the prevention of DVT in this rat model.

SNAC/heparin was further evaluated in a rat model of DVT dissolution. In these studies, DVT formation was induced surgically as described above. Following visual confirmation of thrombi in the jugular veins, the rats were divided into 5 groups and administered by oral gavage either oral heparin alone (30 mg/kg), oral SNAC alone (300 mg/kg), subcutaneous heparin (3 mg/kg), or SNAC/heparin (300 mg/kg SNAC; 30 mg/kg heparin). Control animals received oral saline. At the end of the treatment period, 100% of the rats in the control, oral heparin alone, and oral SNAC alone groups presented with large, well-formed clots (Figure 5a and b). In comparison, only 20% of the rats in the subcutaneous heparin group had clots and 10% of the rats in the oral SNAC/heparin group had small, friable clots. These data

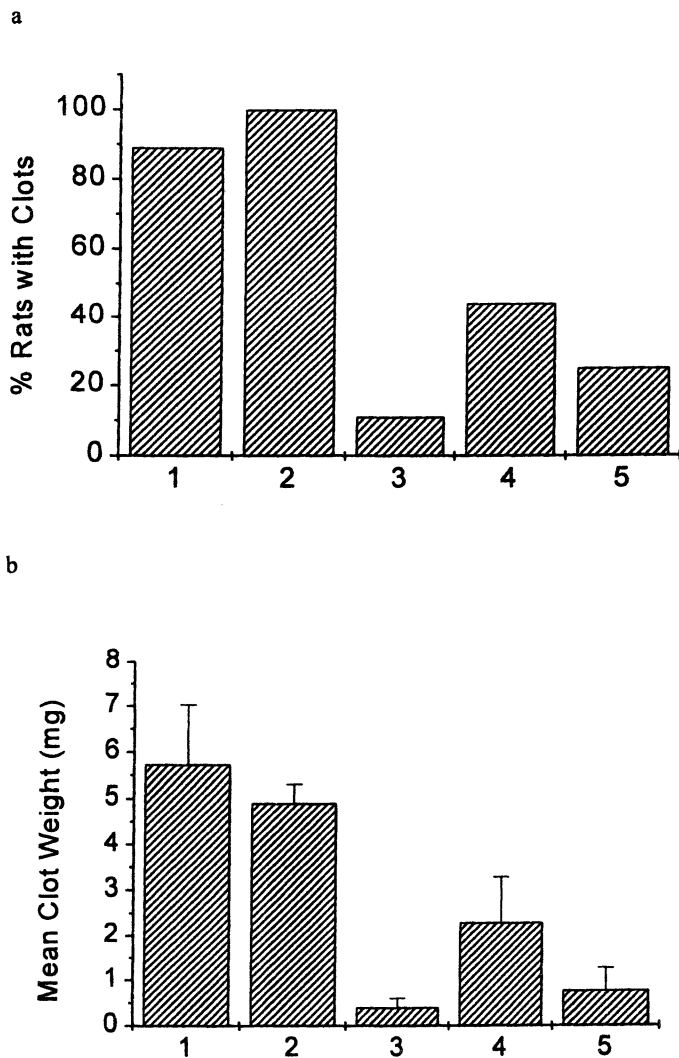
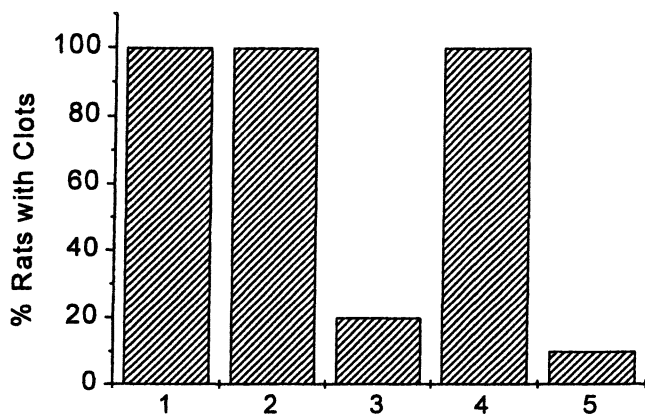


Figure 4. (a) Percentage of rats having DVT's and (b) mean clot weights following surgical induction of clot formation and treatment. Bar 1 represent the control group. Bar 2 represents the oral SNAC alone group. Bar 3 represents the intravenous heparin group. Bar 4 represents the oral heparin alone group. Bar 5 represents the oral SNAC/heparin group.

a



b

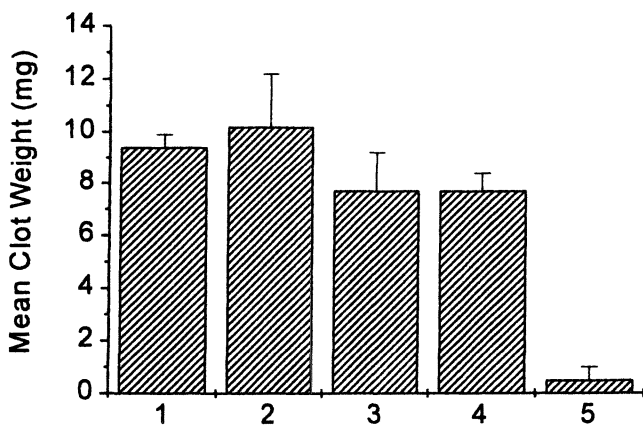


Figure 5. (a) Percentage of rats having DVT's and (b) mean clot weights following treatment for DVT dissolution. Bar 1 represent the control group. Bar 2 represents the oral SNAC alone group. Bar 3 represents the subcutaneous heparin group. Bar 4 represents the oral heparin alone group. Bar 5 represents the oral SNAC/heparin group.

also show that oral SNAC/heparin is comparable to injectable heparin for the treatment of DVT in this rat model.

Clinical Studies

The oral SNAC/heparin combination was next evaluated in healthy, human subjects (28). Thus, SNAC and heparin were formulated into a flavored syrup and administered orally in two tablespoon doses (30 mL). In one study, a fixed dose of SNAC was used with escalating doses (30K, 60K, 90K, and 120K IU) of heparin. These subjects exhibited clinically significant and dose-dependent elevations in APTT and anti-Factor Xa levels at all heparin doses (Figure 6). There were no clinically important adverse events in these subjects. Oral administration of SNAC alone or heparin alone did not alter either APTT or anti-factor Xa. This study establishes the feasibility of oral heparin delivery in humans.

SNAC/heparin was further evaluated in a Phase II clinical trial for the prevention of DVT following hip arthroplasty. Three groups (40/group) of surgical patients were treated with either subcutaneous heparin, oral SNAC/heparin (2.25 g SNAC with 90,000 U heparin), or oral SNAC/heparin (1.5 g SNAC with 60,000 U heparin). The results of this study indicate that oral SNAC/heparin is comparable to subcutaneous heparin for the prevention of DVT in hip replacement patients.

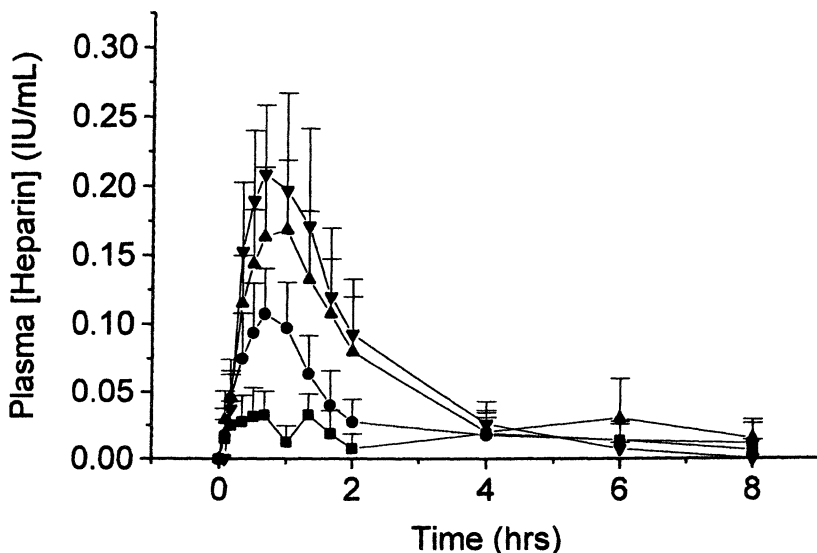


Figure 6. Mean dose-dependent prolongation of anti-Factor Xa activity in response to oral dosing of a taste-masked syrup containing SNAC (2.25 g) and rising doses of heparin. Squares represent 30,000 IU heparin, circles represent 60,000 IU heparin, up triangles represent 90,000 IU heparin, and down triangles represent 120,000 IU heparin.

Mechanism of Action

The mechanism by which SNAC facilitates the gastrointestinal absorption of heparin in rats, monkeys, and humans is not yet fully elucidated. However, studies conducted to date suggest that a non-covalent interaction between SNAC and heparin enables membrane transport of the drug (15, 29, 30).

Conclusion

The oral delivery of heparin has been demonstrated in rats, monkeys, healthy human subjects, and surgical patients following PO administration of SNAC/heparin as a flavored syrup. The efficacy of heparin delivered orally for the prevention and treatment of DVT in a rat model has also been shown. Finally, the SNAC/heparin combination is comparable to injectable heparin for the prevention of DVT in surgical patients following hip arthroplasty.

References

1. *Goodman and Gilman's The Pharmacological Basis of Therapeutics*; Hardman, J.B.; Limbird, L.E., Eds.; 9th Ed.; Macmillan Publishing Co.: New York, NY, 1996; pp1344-1346.
2. Heibert, L.M.; Wice, S.M.; Jacques, L.B. *J Cardiovasc. Pharm.* **1996**, *28*, 26-29.
3. Griffin, J.P.; D'Arcy, P.F.; Speirs, C.J. *A Manual of Adverse Drug Interactions*; John Wright: London, 1988; 137-158.
4. Andriuolo, G.; Bossi, M.; Caramazza, I.; Zoppetti, G. *Haemostasis* **1990**, *20*, 154-158 and references cited therein.
5. Dal Pozzo, A.; Acquasaliente, M.; Geron, M.R. *Thromb. Res.* **1989**, *56*, 119-124.
6. Caramazza, I.; D'Atri, G.; Bossi, M.L.; De Ponti, F.; D'Angelo, L.; Crema, A. *Thromb. Res.* **1991**, *62*, 785-789.
7. Morton, A.K.; Edwards, H.E.; Allen, J.C.; Phillips, G.O. *Int. J. Pharm.* **1981**, *9*, 321-335.
8. Kim, T.D.; Sakon, M.; Kawasaki, T.; Kambayashi, J.; Ohshiro, T.; Mori, T. *Thromb. Res.* **1986**, *43*, 603-612.
9. Ueno, M.; Nakasaki, T.; Horikoshi, I.; Sakuragawa, N. *Chem. Pharm. Bull.* **1982**, *30*, 2245-2247.
10. Dunn, J. M.; Hollister, A.S. *Cur. Therap. Res.* **1995**, *56*, 738-745.
11. Ziv, E.; Eldor, A.; Kleinman, Y.; Bar-on, H.; Kidron, M. *Biochem. Pharmacol.* **1983**, *32*, 773-776.
12. Guarini, S.; Ferrari, W. *Experientia* **1985**, *41*, 350-352.
13. Leone-Bay, A.; Santiago, N.; Achan, D.; Chaudhary, K.; DeMorin, F.; Falzarano, L.; Haas, S.; Kalbag, S.; Kaplan, D.; Leipold, H.; Lercara, C.; O'Toole, D.; Rivera, T.; Rosado, C.; Sarubbi, D.; Vuocolo, E.; Wang, N-F.; Baughman, R.A. *J. Med. Chem.* **1995**, *38*, 4263-4269.
14. Leone-Bay, A.; Ho, K-K.; Agarwal, R.; Baughman, R.A.; Chaudhary, K.; DeMorin, F.; Genoble, L.; McInnes, C.; Lercara, C.; Milstein, S.; O'Toole, D.; Sarubbi, D.; Variano, B.; Paton, D.R. *J. Med. Chem.* **1996**, *39*, 2571-2758.
15. Leone-Bay, A.; Paton, D.; Freeman, J.; Lercara, C.; O'Toole, D.; Gschneidner, D.; Wang, E.; Harris, E.; Rosado, C.; Rivera, T.; DeVincent, A.; Tai, M.; Mercogliano, F.; Agarwal, R.; Leipold, H.; Baughman, R.A. *J. Med. Chem.* **1998**, *41*, 1163-1171.
16. Steiner, S.; Rosen, R. U. S. Patent 4,925,678, 1990.

17. Ma, X.; Santiago, N.; Chen, Y.; Chaudhary, K.; Milstein, S.J.; Baughman, R.A. *J. Drug Targ.* **1994**, *2*, 9-21.
18. Leone-Bay, A.; Leipold, H.; Agarwal, R.; Rivera, T.; Baughman, R.A. *Drugs Future* **1997**, *22*, 885-891.
19. Leone-Bay, A.; Paton, D.; Variano, B.; Leipold, H.; Rivera, T.; Miura-Fraboni, J.; Baughman, R.A.; Santiago, N. *J. Cont. Rel.* **1998**, *50*, 41-49.
20. Nerurkar, M.M.; Surton, P.S.; Borchart, R.T. *Pharm. Res.* **1996**, *13*, 528-534.
21. Michniak, B.B.; Player, M.R.; Godwin, D.A.; Sowell, J. W.; *Drug Del.* **1995**, *2*, 117-122.
22. Takahashe, K.; Murakami, T.; Kamata, A.; Yumoto, R.; Higashi, Y.; Yata, N. *Pharm. Res.* **1994**, *11*, 388-392.
23. Rivera, T.; Leone-Bay, A.; Paton, D.; Leipold, H.; Baughman, R.A. *Pharm. Res.* **1997**, *14*, 1830-1834.
24. Bjornsson, T.D. *J. Pharm. Sci.* **1982**, *71*, 1186-1188.
25. Mungall, D.; Raskob, G.; Coleman, D.; Rosenbloom, D.; Ludden, T.; Hull, R. J. *Clin. Pharmacol.* **1989**, *29*, 890-900.
26. Blake, A.; Ashwin, T.; Jacques, L.B. *J. Clin. Pathol.* **1959**, *12*, 118-122.
27. Gonze, M.D.; Manord, J.D.; Leone-Bay, A.; Baughman, R.A.; Garrard, C.L.; Sternbergh, W.C.; Money, S.R. *Am. J. Surg.* **1998**, *176*, 176-178.
28. Baughman, R.A.; Kapoor, S.C.; Agarwal, R.K.; Kisicki, J.; Catella-Lawson, F.; Fitzgerald, G.A. *Circulation* **1998**, *98*, 610-1615.
29. Mlynek, G.M. Ph.D. thesis, University of Wisconsin, Madison, WI, 1995.
30. Brayden, D.; Creed, E.; O'Connell, A.; Leipold, H.; Agarwal, R.; Leone-Bay, A. *Pharm. Res.* **1997**, *14*, 1772-1779.

Chapter 7

Hypoglycemic Effect of Insulin in Oil Preparation by Oral Administration

M. X. Duan, J. H. Guo, H. Ma, Y. Zuo, and C. X. Zheng

Department of Biological Sciences and Biotechnology, Tsinghua University,
Beijing, 100084, Peoples Republic of China

Since the discovery of insulin, attempts have been made to find the best route of administration of insulin. In addition to injection, various routes^{[1],[2]} of administration have been proposed to control diabetes. However, oral administration of insulin is most convenient, if insulin is protected from proteolytic degradation in the gastrointestinal tract and transported into the circulation system effectively. An oil formulation^[3] was developed and it seemed to be effective by oral route.

The use of oil solution for insulin delivery has recently been tested. A system, called IIOP, involves amphiphiles to maintain insulin fully dispersed in oil. The stability of insulin in oil was studied in different pH buffers. This kind of oil phase solution was found to be effective in diabetic rats and normal mice.

Experimental

Materials.

Crystalline porcine insulin was purchased from Xuzhou Biopharmaceutical Company, PRC. Amphiphiles were purchased from Sigma. The oil (such as PECEOL, LABRAFAC CC, LABRAFIL M 1944 CS, PLUROL OLEIQUE CC 497, etc.) was generously donated by GATTEFOSSE Company, France. The insulin radioimmunoassay (RIA) kit was purchased from Beijing Nuclear Energy Institute. The glucose analysis kit was purchased from Beijing Zhongsheng High-tech Bioengineering Company, PRC.

Methods.

The insulin, amphiphiles, and oil were carefully mixed together to obtain a clear oil solution (IIOP) in the absence of water. Each male Wistar rat was injected with streptozocin (65 mg/kg body weight) to destroy β cells in pancreas islets. The rats were considered diabetic when fasted glycemia was more than 300 mg/dl two weeks after the treatment⁽⁴⁾.

The IIOP was dispersed and stirred in 0.1M HCl (pH=1.0) solution, PBS buffer (pH=7.4) and Na_2CO_3 - NaHCO_3 buffer (pH=11.8), respectively, up to 24 hours. Samples were extracted at 0, 1, 2, 24 hours after dispersion. The mixture was then centrifuged at 15,000 rpm for 10 minutes until complete separation of the oil phase from the water phase. The amount of insulin in the water phase was measured with RIA by the method described by RIA kit instruction.

Diabetic rats were treated with 0.5 ml of IIOP at the dose of 50 IU/kg body weight after over night fasting. The concentration of serum glucose was measured with glucose and RIA kits.

Normal mice were fed with glucose orally and then with IIOP at the dose of 50 IU/kg body weight. Their serum glucose level was also measured with the glucose analysis kit.

Results and Discussion

As shown in Table 1, insulin was not released from the oil solution even after being dispersed in bulk buffer of different pH over 24 hours. This might explain why the activity of insulin in IIOP is still retained after flowing through the gastrointestinal tract. When dispersed in the aqueous environment of the gut, the oil is emulsified to small droplets which still contain insulin.

Table 1. Effects of Buffer of Different pH on the Stability of IIOP

	Percentage of Total Insulin Entering into the Aqueous Phase			
	0 hour	1 hour	2 hours	24 hours
pH=1 HCl	< 5	< 5	< 5	< 5
pH=7.4 PBS	0.14	0.84	1.22	1.71
pH=11.8 Na_2CO_3 - NaHCO_3	0.68	0.74	0.65	0.73

As illustrated in Fig. 1, IIOP administered orally by force-feeding to the stomach in diabetic rats (n=7) induced an approximately 40% decrease of serum glucose concentration measured at 1.5 hours after feeding and the effect lasted at least 3 hours. Compared with i.v. injection (data not shown here), the oil-base insulin shows a relatively long lasting effect. The long-term hypoglycemic effect of the oil-base

insulin may be attributed to the progressive degradation of oil droplets during metabolism. The control group (n=6) took IIOP without insulin.

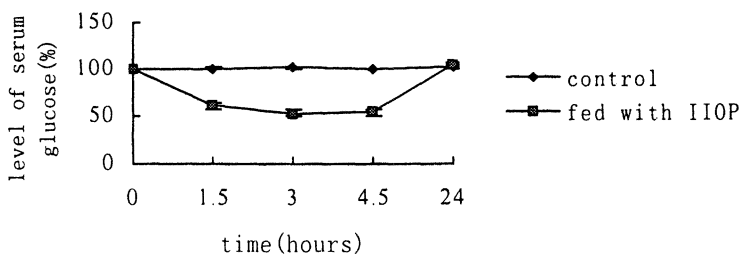


Figure 1. Effect of IIOP on Serum Glucose of Diabetic Rats

As shown in Fig 2, the serum insulin level of diabetic rats (n=8) was increased about 65% at 1.5 hours after feeding with IIOP. The time that the increased insulin level lasted is in accordance with that of the hypoglycemic effect. The control group (n=3) received no insulin.

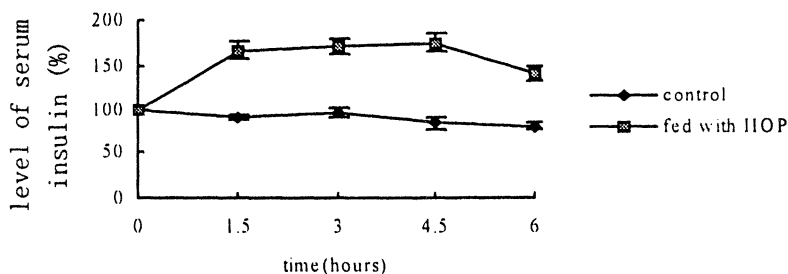


Figure 2. Effect of IIOP on Serum Insulin of Diabetic Rats

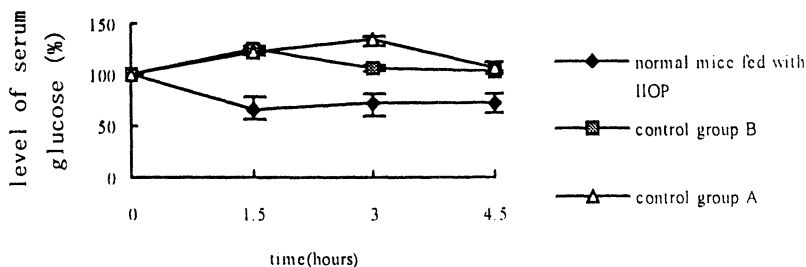


Figure 3. Effect of IIOP on Serum Glucose of Normal Mice

Normal mice (n=6) were subjected to an oral glucose tolerance test at a dose of 800 mg glucose/kg body weight. Then each mouse in the test group was given with insulin 50 IU/kg body weight contained in IOP. Two control groups were also included.

As illustrated in Fig.3, each mouse in the control group A (n=6) was treated with glucose at the dose of 800 mg/kg body weight only. Each mouse in control group B (n=5) was administrated with glucose at the same dose as the control group A followed by free insulin solution. Obvious decrease of serum glucose in normal mice fed with IOP was observed compared with the control groups.

Conclusion

IOP was effective in the protection of insulin from the proteolytic degradation in the gastrointestinal tract, and showed obvious effect on hyperglycemia of diabetic rats. So, IOP might be a prospective oral route of protein drug delivery.

Acknowledgement

The work was supported by National Biotechnology Center of China and Fosse Bio-Engineering Development Limited.

References

- [1] Banting F.G., Best C.H: The internal secretion of the pancreas. *J Lab Clin Med* 7:251-66,1922
- [2] Irsigler K, et al.: Long-term continuous intraperitoneal insulin infusion with an implanted remote-controlled insulin infusion device. *Diabetes* 30: 1072-75, 1981
- [3] New R.R.C., Kirby C.J: Solubilisation of hydrophilic drugs in oily formulations. *Advanced Drug Delivery Reviews* 25: 59-69, 1997
- [4] Dange C, et al.: New approach for oral administration of insulin with polyalkylcyanoacrylate nanocapsules as drug carrier. *Diabetes* vol. 37, 246-251 1988

Chapter 8

Feasibility Assessment and Rapid Development of Oral Controlled Release Prototypes

Avinash G. Thombre

Pfizer Inc., Central Research Division, Eastern Point Road, Groton, CT 06340

Several essential data and predictive methods are available to assess the feasibility of controlled release for a drug candidate in early development. These include physicochemical properties such as solubility and partition coefficient, and biopharmaceutical properties such as Caco-2 permeability. Feasibility assessment is important to aid in the selection of appropriate drug candidates that will benefit from novel drug-delivery approaches. The strategies to rapidly progress prototype oral controlled release dosage forms into clinical evaluation in the context of drug development in a large pharmaceutical company are discussed.

Advances in areas of combinatorial chemistry and high throughput screening (HTS) using receptor-site binding assays have made the drug discovery process increasingly efficient [1,2,3,4]. The efficiency has also been boosted by advances in the areas of bioinformatics, data mining, molecular modeling, and quantitative structure-activity relationships (QSAR). Thus, there are an unprecedented number of drug candidates in the development pipelines of major pharmaceutical companies. Although the emphasis is on orally absorbed compounds, not all drug candidates have the optimal solubility, permeability, and potency characteristics required for oral absorption. Furthermore, when one or more key physicochemical or biopharmaceutical property, e.g., the half-life of the drug candidate is not appropriate, then drug delivery approaches are frequently considered for these candidates as an alternative to the traditional discovery approach of seeking new drug candidates with an appropriate half-life. The drug delivery option is also increasingly being considered for early drug candidates to improve the efficacy and safety profiles including reduction of side-effects.

The consideration of the drug delivery or sustained release option for early drug candidates has resulted in the need to assess the feasibility of controlled release based on physicochemical and physiological measurements and to rapidly develop prototype dosage forms for clinical evaluation [5,6]. Frequently, physicochemical data such as solubility and partition coefficient are available for the drug candidate at an early stage of development as are some of the biopharmaceutical data such as Caco-2 permeability and bioavailability. In the absence of experimental data, predictive methods are available which can be used. For sustained release formulations, information on the regional absorption of the drug as a function of position in the gastrointestinal tract, and, in particular, colonic absorption is an important factor that may determine whether a long delivery duration corresponding to once-daily dosing is feasible or whether a shorter delivery duration with twice-daily dosing is the best option. Also, it is important to know the extent of first pass metabolism in relation to the rate of drug release as this may impact the bioavailability of the drug candidate from a sustained release dosage form.

This paper presents an overview of the factors that should be considered as part of feasibility assessment and the strategies that can be employed to rapidly progress prototype controlled release dosage forms to clinical evaluation. The issues arising in the context of drug development in a large pharmaceutical company are discussed.

Discussion

Key considerations in early drug candidate development

The key considerations in the development of early drug candidates in a global pharmaceutical company and the strategy that can be employed are given in Table 1. In addition to the constraints of unknown dose strengths and unknown optimal release profiles, the quantity of bulk drug available for development is generally limited. Also, because of the team focus on the clinical testing of new hypotheses with molecules that exhibit a new pharmacology (i.e., first-in-class), the time available for development is short. The dosage form patent issues are less critical at this stage because the drug candidate is generally covered by a composition-of-matter patent.

The recommended development strategy is as follows:

- First, conduct a feasibility assessment of controlled release (CR) based on available physicochemical and biopharmaceutical data. The feasibility report should list the approaches considered and recommend the best approach to progress a CR formulation. It should provide a timeline and request that additional work be done to obtain key pieces of information that may not be available.

- Second, conduct an experimental feasibility evaluation to confirm the “paper” feasibility analysis. The objective of the experimental evaluation is to determine the range of possible delivery durations and the doses that can be delivered.
- Third, develop prototype CR dosage forms for clinical evaluation. In the development of prototype formulations, the focus is on performance attributes such as the range of doses and release rates available, the chemical and physical stability of the dosage form, and, to a somewhat lesser extent, the manufacturability and scale-up of the formulation. The manufacturability considerations obviously become extremely important during the later stages of development.

Table 1. Key Considerations in Early Drug Candidate Development

<u>Consideration</u>	<u>Strategy</u>
Pharmacology of the active agent is unknown. Unknown dose strengths and delivery duration.	Progress a dosage form rapidly into a human clinical study with prototypes if necessary. Choose technologies that allow dose flexibility.
Available quantity of bulk drug is small. Timing is critical.	Develop controlled release formulations in an efficient, optimized fashion. Consider prototypes.
Development process occurs in a team environment.	Manage team expectations. Educate what controlled release dosage forms can and cannot do.
Dosage form patent issues are less critical because the candidate molecule is generally patented.	Consider unpatented or “low tech” dosage forms. Remember that this can change at a later date.

Controlled Release Feasibility Assessment

The feasibility of a controlled release dosage form of an early drug candidate can be considered at many different levels. The ability of the formulation to control the release rate of the drug with judicious choice of rate-controlling excipients and specific delivery technology or drug release device assures the *in vitro* feasibility. On the other hand, for *in vivo* feasibility, one has to consider drug absorption or biopharmaceutics, pharmacokinetic, and metabolism-related issues. From the standpoint of eventual commercialization of the formulation, factors such as the reliability and reproducibility of the dosage form, and the robustness of the manufacturing process as it is scaled up from the laboratory to pilot plant and then to production are critical issues. Finally, the pharmacological or clinical feasibility

includes the medical rationale for controlled release and the pharmacodynamic aspects of the drug candidate.

Physicochemical Feasibility

The physicochemical properties that have an impact of the feasibility of a controlled release formulation include molecular weight or size, partition coefficient, solubility, pKa, pH solubility profile, potential for solubilization, salt forms, polymorphs, particle size/distribution, and stability. In most cases, these properties directly influence whether it is possible to obtain the desired *in vitro* release profile utilizing a given controlled release technology. For example, the aqueous solubility of the drug will influence the rate of drug diffusion across a membrane barrier or a polymer gel. Thus, for commonly used hydrophilic matrix devices which release the drug by diffusion through a swollen polymer or by erosion of the matrix tablet, it may be difficult to obtain sustained release of a high dose over a prolonged duration for a highly water soluble drug. Osmotic systems that release the drug as a solution by a pumping mechanism may be limited by the availability of excipients with the proper solubility and osmotic properties. Such relationships between the excipients, delivery technology, and *in vitro* performance of the dosage form are generally well known to formulation scientists through the literature and from their own experiences.

Most of the physicochemical property data required to assess the *in vitro* feasibility of controlled release is readily available for a given compound in the development pipeline. Generally, it is included in the Pharmaceuticals Profile or equivalent report for the drug candidate. If a particular drug delivery technology requires a parameter that has not been measured, this can easily be accommodated. Experimental and computational approaches for estimating properties such as solubility and permeability have been extensively reviewed [7,8,9].

Biopharmaceutical Feasibility

The biopharmaceutical and pharmacokinetic properties that have an impact of the feasibility of a controlled release formulation include gastrointestinal transit of the dosage form, food effect, intrinsic permeability, extent of first pass metabolism and oral bioavailability. The bioavailability and, hence, the biopharmaceutical feasibility is also dependent upon efflux mechanisms that may be relevant and the colonic absorption of the drug candidate. For example, if there is poor colonic drug absorption, it may not be feasible to have a long duration formulation for q.d. dosing without a significant loss of bioavailability, and, only a formulation with a short delivery duration suitable for b.i.d. dosing should be considered.

The regional permeability of drugs in the rat jejunum, ileum, and colon have been determined for several drugs and attempts have been made to correlate the permeability values to physicochemical properties such as molecular weight and octanol-water partition coefficient [10,11,12,13]. A literature survey also reveals that

the regional absorption of several drugs has been studied in humans by intubation methods (see Fig. 1) although formulations and protocols vary a lot between studies.

Flux measurements through Caco-2 monolayers have been used to predict absorption in humans [14,15,16,17,18] and there is a good understanding of the circumstances under which the predictions are less accurate. Many companies routinely determine Caco-2 permeability of drug candidates. Therefore, it is worthwhile to compile available data and correlate with performance of controlled release dosage forms. Depending on the available database and the correlation, "rules of thumb" can be developed for selection of controlled release candidates.

The metabolism of the drug, particularly, its first pass extraction by hepatic and intestinal enzymes will also influence bioavailability and, hence, the feasibility of controlled release. Several *in vitro* and *in vivo* models are available to determine whether a given drug candidate is a substrate for cytochrome P 450 oxidation. The role of isoenzymes CYP3A4 and CYP2C9 has also been recognized. [19]

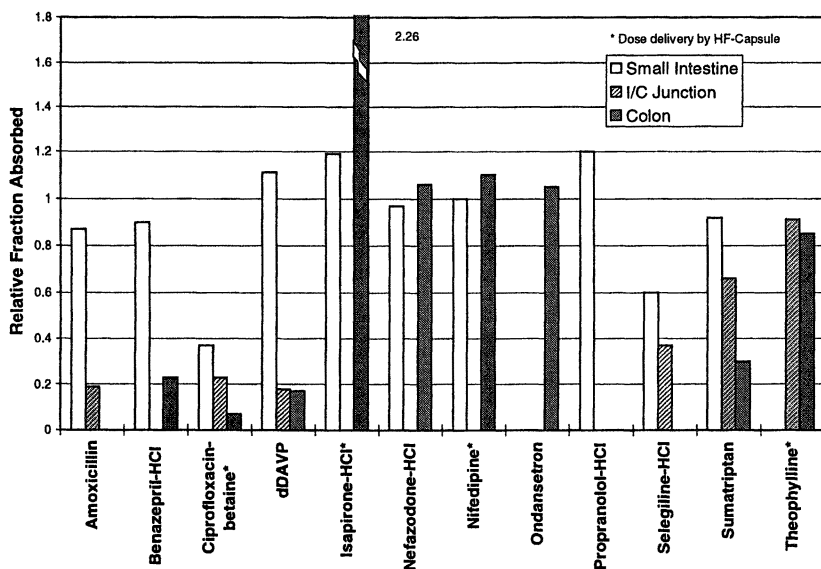


Figure 1. Regional absorption of selected drugs in the human gastrointestinal tract.

If pharmacokinetic data from an immediate release dosage form is available, the plasma concentrations following administration of various controlled release dosage forms can be simulated. Based on these simulations, it may be possible to select the recommended drug delivery profile. For example, a mathematical model using STELLA® has been used to calculate drug absorption from the duodenum, jejunum, ileum, and colon. [20] Other models that take into account pH-dependent dissolution as well as GI transit times and regional absorption are also available. [21,22]

Compared to the physicochemical feasibility, there is a somewhat greater uncertainty in determining the biopharmaceutical or *in vivo* feasibility. This is because the *in vitro* - *in vivo* correlation may be complex for many dosage forms and because of the added complexities of an *in vivo* situation compared to a well characterized *in vitro* system.

Technological Feasibility

Selection of the drug delivery platform and the technology often depends on the physicochemical and biopharmaceutical properties of the drug candidate as well as the design parameters of the dose, delivery duration, and release profile. In addition to the drug and design parameters, prior experience with a technology and availability of in-house equipment and expertise may be important, as are financial constraints such as the need for the purchase of capital equipment for production. Depending on the in-house expertise and equipment availability, it may be necessary to consider an external collaboration with a drug delivery company.

As stated earlier, the patent issues for early drug candidates may not be as important a factor as are reliability and reproducibility of dosage form performance, i.e., no dose-dumping or incomplete release, a robust manufacturing process, scale-up experience, and speed of development. Several oral drug delivery technologies are now available including those based on diffusion and erosion such as hydrophilic matrix tablets and osmotic systems such as Alza's OROS™ and GITS™.

Pharmacological Feasibility

The rationale for controlled release is generally based on an assumption. For example, a slow drug input rate will result in reducing the blood level fluctuations, which may be expected to decrease the side effects of a drug. However, it is possible that the peaks are pharmacologically important indicating the need for pulsatile delivery. Also, in certain cases, sustained release can cause down regulation or decrease in the number of receptors resulting from over-stimulation. In these cases, a controlled release dosage form may not be feasible. The continuous blood level of a hormone such as a corticosteroid might suppress adrenocorticotropic hormone (ACTH) release from the pituitary gland, resulting in atrophy of the adrenal gland [23]. In most cases, such effects are difficult to predict a priori for early drug candidates and they become known only after extensive clinical testing.

Feasibility Assessment Report

The Feasibility Assessment Report is a “paper” study to assess the feasibility of controlled release of a particular drug candidate. Ideally it is based on actual data, however, depending on when such a report is issued, it may have to rely on best guess estimates and institutional experience with similar compounds. The objectives of the feasibility report are to manage expectations of the candidate management team and educate its members on the pros and cons controlled release dosage forms. In addition to a discussion of the relevant physicochemical and biopharmaceutical properties that impact the feasibility of controlled release, the feasibility assessment should also include an estimate of the degree of difficulty and probability of success of the recommended approach. This is important information for line management for analyzing whether this represents the best use of available resources. Furthermore, because the development generally occurs in a team environment, the feasibility assessment report should also address the quantity of bulk active that will be required and the timing for the various milestones. Information regarding the approaches considered versus those recommended is valuable to the formulator, as they will provide good starting points for the formulation development project.

Depending on the stage of development of the compound, some key pieces of data may not be available when the controlled release feasibility assessment is performed. Therefore, the report should also include a recommended experimental plan. In particular, the experimental plan should address areas such as colonic intubation to determine whether a long duration sustained release formulation would be feasible.

The major portion of the feasibility assessment report will provide physicochemical and biopharmaceutical data on the candidate and interpretation of these data in light of the performance of a controlled release formulation. Thus, for example, if the predicted (or actual) colonic permeability is poor, it may not be feasible to consider a long delivery duration (once-daily) for the compound and resources should be focused on a shorter delivery duration formulation that is likely to be dosed twice-daily.

The feasibility assessment report should also include the biopharmaceutics classification system (BCS) for the candidate drugs. In this system, drugs are divided into four classes depending on their solubility and permeability [24,25].

Rapid Development of Controlled Release Prototypes

The next step in the development of a drug candidate is to experimentally verify the controlled release feasibility assessment and to rapidly develop prototype formulations for clinical studies. In this phase, the important issues are speed (to shorten development time) and the quantity of bulk active required (to minimize resource/costs). Having prototype dosage forms for clinical evaluation is particularly

important in the case of compounds that are “first-in-class” or “best-in-class” because of the time pressure to move forward rapidly with such candidates.

Typical experiments that are conducted in this phase include the following:

(a) an excipient compatibility screen; (b) the *in vitro* and *in vivo* (animal models such as dog or monkey) performance studies with prototype formulations; (c) accelerated stability with the prototype formulations; and (d) a determination of scale-up issues and ease of manufacture. Based on the results of this experimentation, the range of feasible doses and delivery durations are determined. Also, the components of the formulations are identified although their quantity in the formulations may change somewhat later on during process development.

A worthwhile investment that can be made to reduce prototype development timelines is research geared towards developing a generic controlled release technology that is broadly applicable to a variety of potential drugs with a range of physicochemical properties. If such a technology were available for the majority of the early drug candidates under consideration, the few drugs that required other technologies could be easily handled.

Conclusions

The recommended strategy for the development of early drug candidates consists of assessing the feasibility of oral controlled release dosage forms followed by rapid development of prototype formulations for clinical testing. The state of the art for predicting whether the desired dose and delivery duration are feasible allows for a reliable assessment. Several tools are also available to determine the *in vivo* feasibility based upon biopharmaceutical factors. However, the data available in the literature needs to be analyzed further to ideally determine a set of rules that will help predict regional drug absorption for controlled release feasibility. Rapid development of oral controlled release prototypes for clinical testing is challenging in the case of early candidates given the various constraints imposed on development, including short timelines.

Acknowledgments

The author would like to thank his colleagues in the Oral Controlled Release and Biopharmaceutics group for their contributions and useful discussions and Hope Carter for compiling the intubation data.

References

1. Lipper, R. A., *Modern Drug Discovery*, **1999**, Jan/Feb, 55-60.
2. Lensey, M. S. *Today's Chemist at Work*, **1999**, pp 36-43.
3. Smith, P. *Adv. Drug Delivery Rev.*, **1997**, 23, 1.
4. See PhRMA Facts on <http://www.pharma.org/facts/>
5. Lipinski, C. A.; Lombardo, F.; Dominy, B. W.; Feeney, P. J. *Adv. Drug Delivery Rev.*, **1997** 23, 3-25.
6. Stewart, B. H.; Chan, O. H.; Jezyk, N.; Fleisher, D. *Adv. Drug Delivery Rev.*, **1997** 23, 27-45.
7. Yalkowsky, S. H.; Banerjee, S. *Aqueous solubility*; Marcel Dekker: New York, 1992.
8. Wessel, M. D.; Jurs, P. C.; Tolan, J. W.; Muskal, S. M.; *J. Com. Inf. Comput. Sci.*, **1998**, 38, 726-735.
9. Meylan, W. M.; Howard, P. H.; Boethling, R. S.; *Environ. Tox. Chem.*, **1996** 15, 100-106.
10. Ungell, A.-L.; Bergstrand, N. S.; Sjoberg, A.; Lennernas, H. *J. Pharm. Sci.*, **1998** 87, 360-366.
11. Fagerholm, U.; Lindahl, A.; Lennernas, H. *J. Pharm. Pharmacol.*, **1997**, 49, 687-690.
12. Lennernas, H. *J. Pharm. Pharmacol.*, **1997**, 49, 627-638.
13. Lennernas, H.; Lee, I.-D.; Fagerholm, U.; Amidon, G. L. *J. Pharm. Pharmacol.*, **1997**, 49, 682-686.
14. Rubas W; Cromwell, M. E. M.; *Adv. Drug Delivery Rev.*, **1997** 23, 157-162.
15. Rubas, W.; Cromwell M. E. M.; Shahrokh, Z.; Villagran, J.; Nguyen, T.-N.; Wellton, M.; Nguyen, T.-H.; Mrsny, R. J. *J. Pharm. Sci.*, **1996**, 85, 165-169.
16. Yee, S. *Pharm. Res.*, **1997**, 14, 763-766.
17. Irvine, J. D.; Takahashi, L.; Lockhart, K.; Cheong, J.; Tolan, J. W.; Selick, H. E.; Grove, J. R. *J. Pharm. Sci.*, **1999**, 88 28-33.
18. Gan, L.-S. L.; Thakker, D. R. *Adv. Drug Delivery Rev.*, **1997**, 23, 77-98.
19. Thummel, K. E.; Kunze, K. L.; Shen, D. D. *Adv. Drug Delivery Rev.*, **1997**, 27, 99-127.
20. Grass, G. M. *Adv. Drug Delivery Rev.*, **1997**, 23, 199-219.
21. Yu, L. X.; Lipka, E.; Crison, J. R.; Amidon, G. L. *Adv. Drug Delivery Rev.*, **1996**, 19, 359-376.
22. GastroPlus™ Software from Simulations Plus, Inc., Lancaster, CA.
23. Shargel, L.; Yu, A.B.C. *Applied Biopharmaceutics and Pharmacokinetics*, Appleton & Lange, CT, 1993, p.248.
24. Amidon, G. L.; Lennernas, H.; Shah, V. P.; Crison, J. R. *Pharm. Res.*, **1995**, 12, 413-420.
25. Waterbeemd, H. *Eur. J. Pharm. Sci.*, **1998**, 7, 1-3.

Chapter 9

The Effect of Adhesive Antioxidant Enzymes on Experimental Colitis in the Rat

Abraham Rubinstein¹, Sigal Blau¹, Paul Bass², and Ron Kohen¹

¹The Hebrew University of Jerusalem, Faculty of Medicine, School of Pharmacy, P.O. Box 12065, Jerusalem 91120, Israel

²The University of Wisconsin, School of Pharmacy, Madison, WI 53706

The overall antioxidant activity of sections along the small intestine and colon of the rat was evaluated by determining its reducing power, which reflects the total antioxidant activity derived from low molecular weight antioxidant (LMWA), using cyclic voltammetry. In addition, the activity of the antioxidant enzymes catalase and superoxide dismutase (SOD), was measured in the same sections. It was found that the reducing power was higher in the mucosa/submucosa of the small intestine as compared to that of the colon. Similarly, catalase and SOD activity in the mucosa/submucosa of the small intestine was significantly higher than that of the colon. To improve their local antioxidant action catalase and SOD were cationized and their ability to treat colitis was compared to that of native enzyme preparations. The cationized antioxidant enzymes were found to be more effective than the native enzymes as a result of their ability to non-specifically adhere to the colonic mucosa. In most studies the cationized enzymes were more effective than 5-aminosalicylic acid and betamethasone.

Gastrointestinal (GI) tissues are constantly exposed to reactive oxygen species (ROS) originating from endogenous and exogenous sources (1). This ROS efflux is increased in disease states (e.g. colitis) (2). Gut tissues cope with the exposure to oxidative stress by several defense mechanisms including antioxidant system. The latter can be classified into two major groups: antioxidant enzymes, such as superoxide dismutase (SOD), catalase and peroxidases, and low molecular weight antioxidant (LMWA) compounds which act indirectly (e.g., chelators) or directly (e.g., scavengers) (3). The fact that the colon is more susceptible to inflammatory processes than the small bowel may be, partially, due to differences in the antioxidant profiles of the organs' tissues. In the past, such differences were related to specific antioxidant compounds (4-6). One goal of the present study was to measure the differences in the total endogenous tissue antioxidants along the intestine by measuring the reducing power (total antioxidant capacity) of various tissues.

Enrichment of the colonic tissue with antioxidants (e.g., antioxidant enzymes, such as SOD and catalase) was suggested as an effective tool for minimizing the oxidative damage caused by ROS. Previous studies already showed that systemic treatment with SOD reduced the severity of inflammation in experimental colitis, as well as in Crohn's disease patients (7, 8). However, the major drawback of systemic administration of antioxidant enzymes such as SOD is their ultra-short elimination half-life. Also, the damage induced by ROS is characterized by site-specific events. Therefore, if antioxidant enzymes are to be used for the treatment of IBD, they should be located in a close proximity to the site of inflammation. In this study we hypothesized that the attachment of antioxidant enzymes to the colonic mucosa (by changing their surface electric charge from negative to positive, i.e., cationization) could increase the efficacy of the antioxidant treatment.

The advantage of cationized catalase and SOD over the native enzyme has already been demonstrated (9-11). For example, in previous studies we reported that cationization of catalase significantly increased its ability to prevent tissue damage caused by hydroxyl radicals, hydrogen peroxide and superoxide radicals when applied topically in the small intestine of the rat (12,13). In the present study we checked the ability of cationized catalase and cationized SOD to serve as novel therapeutic agents for the treatment of experimental colitis. More specifically, the goals of the present study were: (a) to delineate, longitudinally, the endogenous activity of the antioxidant enzymes catalase and SOD as well as the total antioxidant profile of LMWA; (b) to cationize catalase and SOD while maintaining their activity; (c) to verify that cationization caused the enzymes to adhere to the colonic mucosa of the rat, and (d) to examine if cationized antioxidant enzymes are superior to the native ones in the treatment of experimental colitis after intracolonic administration.

METHODOLOGY

Evaluation of the Total Antioxidant Capacity of The Rat Intestine

The colon and the small intestine of anesthetized male Sprague-Dawley rats (200-250 g) were removed and divided into three equal segments: distal (DC), medial (MC) and proximal (PC). The small intestine was removed and cut into two sections (40 cm each): distal (DSI) and proximal (PSI). The mucosa and submucosa of all segments were carefully scraped, homogenized in 0.02M phosphate buffer, pH 7.4, at 4 °C (dilution of 1:10 w/v), and stored at -74 °C until analysis. The anesthetized rats were sacrificed by chest wall puncture. Each group consisted of at least seven animals.

Catalase and SOD activities were determined according to the procedures described by Aebi (14) and McCord (15), respectively.

Total levels of tissue direct-acting water-soluble LMWA (scavengers) were measured by cyclic voltammetry (CV) as described elsewhere (16-21). The method allows for rapid examination of the ability of a tested biological specimen to donate electron(s), and enables an estimation of the overall amount of scavengers present in

the tested tissues without measuring specific compounds. In CV, voltammograms are plotted for each tested tissue and the reducing power is characterized by the peak potential of each anodic wave at its $E_{p(a)}/2$ value and quantified by the amplitude of the anodic current (AC) which correlates to the LMWA levels (22).

Cationization of Catalase, SOD and BSA

Cationization was performed by coupling the protein carboxyl groups with 1,6-diaminohexane using 1-ethyl-3(3-dimethylaminopropyl)-carbodiimide HCl as a catalyst (23,24).

Characterization of the Cationized Proteins

Net molecular charge was assessed qualitatively on a cation exchange (24). Amine substitution assay was performed by the fluorescamine method (25). Catalase and SOD activity after cationization was measured as described above.

Assessment of the Attachment Properties of the Cationized Proteins to Rat Intestinal Mucosa

This assessment was performed qualitatively and quantitatively. In the former, fluoresceine isothiocyanate (FITC) stained BSA (F-BSA) served as a model protein for the two cationized enzymes. It was incubated for 10 minutes with a suspension of isolated epithelial cells (26) and then rinsed twice with HEPES buffer. Native (non-cationized) F-BSA served as a control in a similar protocol. The suspensions were immediately visualized using a laser scanning confocal microscope. In the latter assessment, the colon of male Sprague-Dawley rats was cut open, rinsed with ice-cold PBS, pH 7.4 and divided into 6-10 segments, each 1 cm long. The segments were then incubated for 10 minutes with cationized or native enzymes or PBS. The tissue specimens were then rinsed with PBS and shaken in 5 ml of the same buffer for 1 and 24 hours for SOD and 24 hours for catalase. At the end of each study, the mucosa of each colonic segment was carefully scraped and homogenized in 0.02 M phosphate-buffer, pH 7.4, at 4 °C and stored at -74 °C for SOD and catalase activity analysis, which was performed as described above.

Induction of Experimental Colitis

The induction was performed by intracolonic administration of 30 mg of dinitrobenzensulfonic acid (DNBS) dissolved in 1 ml of ethanol 25 % (v/v) under light ether inhalation anesthesia, via a flexible, perforated Foley catheter (24,27).

Local Treatments with Cationized Catalase, Cationized SOD, 5-ASA and Betamethasone

In separate studies, rats were dosed intracolonicly with 1 ml of cationized catalase solution (activity: 9,600U), or 1 ml of cationized SOD solution (activity: 1,600U) or cationized BSA or 67 mg/ml 5-ASA or 50 µg/ml betamethasone (retention enema preparations from Rafa, Israel and Glaxo UK, respectively). The administration was carried out for 1 hour following colitis induction and repeated

every 12 hours over three days. The rats were sacrificed 4 days after colitis induction.

Quantification of Colonic Inflammation

The distal 10 cm of the colon from the treated rats was removed. Ulcerated and inflamed regions were located, separated and immediately frozen in liquid nitrogen. At a later stage the specimens were homogenized in 0.02M phosphate-buffer, pH 7.4. Inflammation was quantified by measuring tissue MPO activity and TNF α concentration. MPO activity was determined according to the procedures described by Grisham (28). TNF α tissue concentrations were measured by ELISA according to the manufacturer's instructions (Genzyme Co., Cambridge, MA, USA). Tissue protein was measured by the Bradford method and the results were expressed in mg protein (29).

Statistical Analysis

The results were expressed as mean values \pm S.E.M. The Mann-Whitney test was conducted to identify differences in the antioxidant levels along the GI tract and following treatment with 5-ASA and betamethasone compared to the saline treated group. The Kruskal Wallis test (30) was conducted to check whether the differences among the various treated groups were significant. The Dunn's test (30) was used to identify differences among the results obtained following treatment with the antioxidant enzymes. In all cases $p < 0.05$ was considered to be significant.

RESULTS

Relative Reducing Power Along the Rat Intestine

In all CV measurements two typical anodic waves with $E_{p(a)/2}$ values of 0.45 ± 0.02 V and 0.84 ± 0.02 V were identified. The reproducibility of the $E_{p(a)/2}$ values in different experiments indicates that similar types of reducing LMWA are responsible for the observed anodic waves. An overall increase in antioxidant activity, as measured by CV, was observed from the distal to orad direction of the mucosa/submucosa layer of the small intestine and colon of the rat (Table 1). A similar observation was noted when the activity of the tissue antioxidant enzymes catalase and SOD was measured. The conclusion of this part of the study is that in the rat the activities of antioxidant enzymes in the mucosa/submucosa of the proximal small intestine are significantly higher than those in the distal colonic mucosa/submucosa (Table 1).

Cationization Quantification

The amounts of the primary amines on the surface of the modified proteins were higher compared to the native proteins. Primary amine group ratios of 1.29, 3.28 and 1.37 for cationized catalase, cationized SOD and cationized BSA respectively over the native proteins were obtained. The results demonstrated that cationization was most efficient for SOD. The protein cationization was verified by net charge measurements as summarized in Table 2.

Table 1: The first and the second anodic wave currents (antioxidant concentrations) calculated from the cyclic voltammogram and antioxidant enzymes (catalase and SOD) activities in the mucosa/submucosa layer along (five different segments) the rat intestine. Shown are the mean values \pm SEM, $n = 7$ rats.

	Intestinal Segment				
	DC	MD	PC	DSI	PSI
<i>1st Anodic Wave Current [$\mu\text{A}/(\text{mg protein/ml})$]</i>	0.74 \pm 0.07	0.57 \pm 0.07	0.61 \pm 0.12	1.20 \pm 0.08*	1.34 \pm 0.17*
<i>2nd Anodic Wave Current [$\mu\text{A}/(\text{mg protein/ml})$]</i>	1.21 \pm 0.12	1.24 \pm 0.14	1.10 \pm 0.18	1.73 \pm 0.11*	1.88 \pm 0.24*
<i>Catalase Activity [$\mu\text{A}/(\text{mg protein/ml})$]</i>	11.5 \pm 1.4	14.2 \pm 0.8	14.9 \pm 1.2	18.9 \pm 1.2*	20.2 \pm 2.4*
<i>SOD Activity ($\mu\text{A}/\text{mg protein}$)</i>	5.6 \pm 1.0	5.9 \pm 0.6	6.4 \pm 0.6	8.9 \pm 0.7*	10.4 \pm 1.5*

DC = distal colon, MD = medial colon, PC = proximal colon, DSI = distal small intestine, PSI = proximal small intestine.

- $p < 0.05$ when compared to the mucosa/submucosa of the distal/medial/proximal segment of the colon.

Table 2: Activity and net charge of the cationized proteins used in the study.

	Activity (% of native enzyme)	Net Charge
Catalase		
Native		-
Cationized	36	+
SOD		
Native		-
Cationized	38.2	+
BSA		
Native		-
Cationized		+

Assessment of the Attachment Properties of the Cationized Proteins to the Rat Intestinal Mucosa

Microscopic visualization of the adherence of the model probe F-BSA to the isolated colonic epithelium cells is shown in Figure 1. Large amounts of the cationized F-BSA adhered to the cell membrane and in some cases were internalized into the cell cytoplasm. No adherence was observed when the non-cationized F-BSA was examined (data not shown).

The extent of attachment of the cationized catalase and the cationized SOD to the colonic mucosa of the rat is shown in Figure 2, which shows the total mucosal activity of the enzymes normalized to the basal levels. The results demonstrate that the native enzymes were unable to adhere to the tissues while the cationized enzymes did. A gradual decrease in the cationized catalase and SOD activities was observed during 24 or 26 hours of rinsing.

Local Treatments with Cationized Catalase, Cationized SOD, 5-ASA and Betamethasone

Treatment with cationized catalase and SOD significantly attenuated the inflammatory response caused by DNBS, as assessed by both MPO activity and TNF α concentration measurements in the inflamed (non-ulcerated) colonic tissue. Cationized catalase caused a reduction of 39% in tissue MPO activity and 33% reduction in tissue TNF α concentration compared with the saline treatment controls. A 46% reduction in tissue MPO activity and 38% reduction in tissue TNF α concentration were observed after treatment with cationized SOD compared to the saline treatment controls (Table 3). No significant effect could be detected when the native (non-cationized) enzymes were used. Table 3 also shows the tissue MPO activity and TNF α concentration after treatment with BSA. The enzyme activities were similar after BSA, cationized BSA or saline treatments. These findings prove that the protecting effect observed was not a result of the change in the surface electric charge of the enzymes. After treatment with betamethasone, MPO activity and TNF α tissue levels were significantly lower. Treatment with 5-ASA resulted in a significant reduction in TNF α concentration with no significant change in MPO activity (Table 3).

DISCUSSION

In this study we found that in the rat the colonic mucosa/submucosa possesses low endogenous antioxidant capacity when compared to similar layers in the upper regions of its intestine. It was speculated that this relatively low antioxidant capacity is a possible reason for the susceptibility of the colon to oxidative stress and to inflammatory processes. This led to the assumption that local attachment of antioxidant enzymes to the colonic mucosa could improve disease states of this organ. Indeed, the next step was to check whether cationized catalase and SOD could improve colitis.

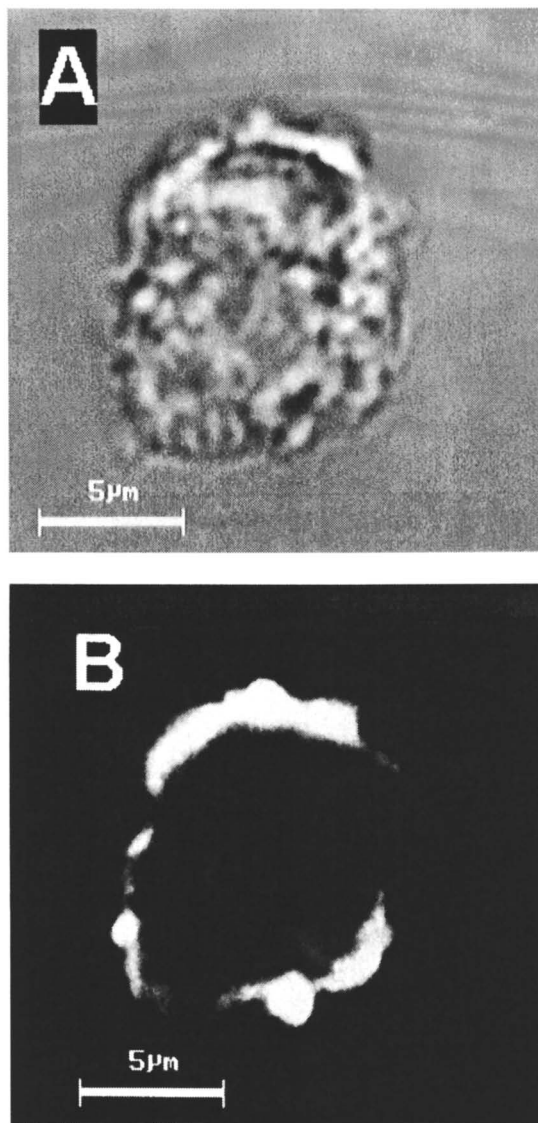


Figure 1: A microphotograph of FITC labeled cationized BSA (F-BSA) attached to a single isolated colonocyte from the rat colon.
Top: light microscope; **Bottom:** confocal microscope.

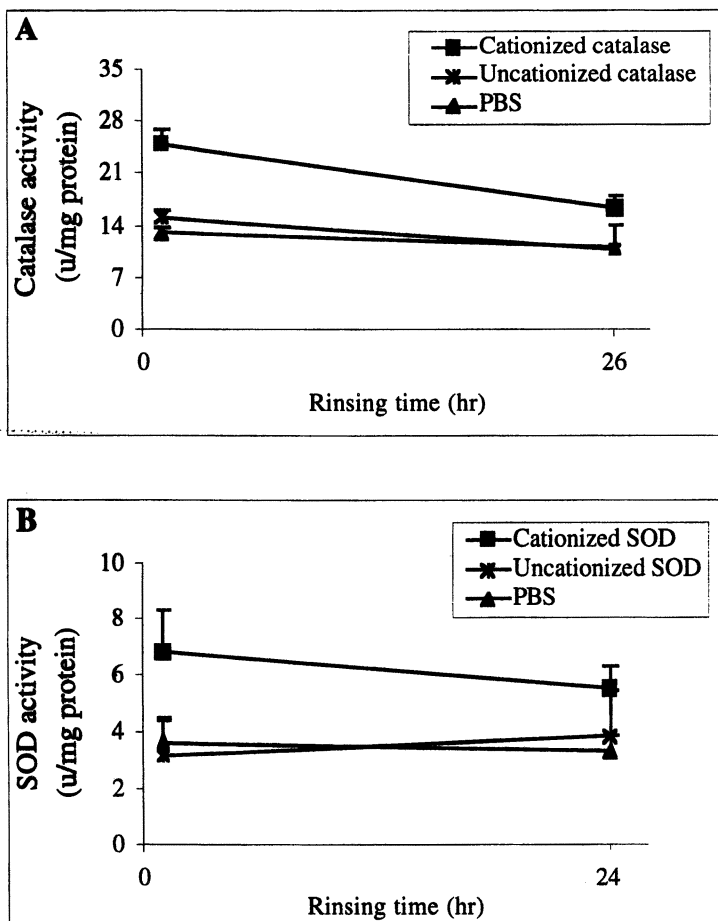


Figure 2: The attachment of cationized and non-cationized catalase (top) and SOD (bottom) to the colonic mucosa of the rat as assessed by measuring the overall tissue activity of the enzymes. Shown also are the enzyme mucosal activity after PBS control. Shown are the mean values of at least 4 segments \pm S.E.M.

Table 3: Effects of cationized and native catalase, SOD, BSA, and commercial drugs (5-ASA and betamethasone) on the severity of colon inflammation.

Treatment	Relative MPO Activity	Relative TNF α Activity
Catalase		
Cationized	61.5 \pm 6.9 ^{*,**}	67.3 \pm 6.9 *
Native	110.8 \pm 13.9	73.7 \pm 8.0
SOD		
Cationized	54.0 \pm 5.4 ^{*,**}	62.4 \pm 4.9 *
Native	110.0 \pm 13.3	76.1 \pm 8.6
BSA		
Cationized	120.7 \pm 18.8	105.4 \pm 6.5
Native	97.1 \pm 27.9	94.5 \pm 6.4
Commercial Drugs		
5-ASA	106.9 \pm 21.0	74.6 \pm 10.0 *
Betamethasone	66.6 \pm 7.3 *	68.7 \pm 8.3 *
Saline	100.0 \pm 15.4	100.0 \pm 8.8

The inflammation was assessed by measuring tissue MPO activity and tissue TNF α concentrations. Results are expressed in percentage of the measurements taken in saline treated rats (controls). Thus, the activity of MPO in the colonic tissues averaged at 12.00 \pm 2.18 U/g protein, and the concentration of TNF α averaged at 0.754 \pm 0.083 ng/g protein. Shown are the mean values of at least 6 rats \pm SEM.

* $p < 0.05$ compared to saline treatment.

** $p < 0.05$ compared to native enzymes treatment.

Cationization of proteins as a tool to increase their residence time in target organs has been suggested in the past. For example, it was found that cationized proteins accumulated in the liver, kidney and joints in larger extent than their related native proteins (11,31). This increased accumulation was explained by either the change in the elimination (clearance and degradation) of the proteins or by their interaction with the negatively charged cell membranes in the target organs. The ability of cationized proteins to adhere to negatively-charged membranes poses an interesting potential in drug delivery. Local treatment of colonic inflammation with antioxidant enzymes is a rational example because of the accessibility of the injured epithelium to the lumen of the colon. The ultra-short half-life of the superoxide radical and hydrogen peroxide which are formed at the site of inflammation requires that antioxidant enzymes should reside as close as possible to that location to prevent the damage caused by the decomposition of these two reactive oxygen species. For that purpose, the anionic side carboxyl groups of the enzymes were substituted with positively-charged hexadamine to allow the enzymes to adhere to the negatively-charged mucosa. These cationized enzymes were found to be superior to the native ones only in the inflamed regions of the rat colon, a finding which may indicate that ulcerated tissues are injured far beyond antioxidant enzyme therapy capabilities. It may also indicate that the cationized enzymes cannot adhere to ulcerated tissues as evidenced in duodenal and gastric ulcers. Ulcerated tissues were found to possess high concentrations of positively charged proteins that increase the affinity to negatively charged substances, such as sucralfate (32). It is speculated that if similar changes in the electric charge occur in ulcerated regions of the colon, the ability of cationized antioxidant enzymes to adhere to those regions will be lost.

Two types of biochemical markers were used in the present study to assess inflammation severity, MPO and TNF α . In both cases a significant reduction in tissue activity and levels (respectively) was observed following treatment with the cationized enzymes compared to saline control treatment (Table 3). MPO, an enzyme found predominantly in activated neutrophils and to a lesser extent in eosinophils and macrophages, is commonly used to quantify acute colonic inflammation (33). TNF α is a mediator released mainly from macrophages or lymphocytes (34), which accumulates in the inflamed colon at advanced stages of the inflammatory process (35).

The clinical implication of the cationized antioxidant enzymes for the treatment of IBD was estimated, in our study, by comparing their efficacy to the efficacy of 5-ASA and betamethasone in similar experimental treatment protocols. Betamethasone significantly reduced MPO activity levels and TNF α concentrations following treatment. 5-ASA significantly reduced TNF α concentrations but was unable to reduce MPO activity. Although the results are promising, problems and constraints must not be ignored. For example, cationization can enhance protein immunogenicity by increasing the production of antibodies to the modified macromolecules (36,37).

In conclusion, cationized antioxidant enzymes are effective and efficient for the local treatment of colitis. In the experimental colitis model used, the enrichment of the low antioxidant capacity colonic tissue with cationized enzymes was found to be more effective than the native enzymes. This study is significant because it

demonstrates that the local attachment of antioxidant enzymes is a feasible method to improve the anti-inflammatory effect of antioxidant enzyme therapy.

Acknowledgments

The study was supported by a research grant from the American-Israeli Binational Foundation number 93-56. The results reported here are included in the dissertation thesis of S.B. as partial fulfillment of her Ph.D. degree requirements at The Hebrew University of Jerusalem. The skillful technical assistance of Ms. Naama Levin is greatly acknowledged.

LITERATURE CITED

- 1 Harris M. L.; Schiller H. J.; Reilly P. M.; Donowitz M.; Grisham M. B.; Bulkley G. B. *Pharmacol Ther* **1992**, *53*, 375-408.
- 2 Grisham M. B. *Lancet* **1994**, *344*, 859-61.
- 3 *Free Radicals in Biology and Medicine*; 2nd ed.; Halliwell B.; Gutteridge J. M. C., Eds.; Clarendon: Oxford, 1989.
- 4 Grisham M. B.; MacDermott R. P.; Deitch E. A. *Inflammation* **1990**, *14*, 669-80.
- 5 Moghadasian M. H.; Godin D. V. *Mol Cell Biochem* **1996**, *155*, 43-9.
- 6 Siegers C. P.; Bartels L.; Riemann D. *Pharmacology* **1989**, *38*, 121-8.
- 7 Emerit J.; Pelletier S.; Likforman J.; Pasquier C.; Thuillier A. *Free Radic Res Commun* **1991**, *2*, 563-9.
- 8 Keshavarzian A.; Haydek J.; Zabihi R.; Doria M.; D'Astice M.; Sorenson J. R. *Dig Dis Sci* **1992**, *37*, 1866-73.
- 9 Kohen R.; Shalhoub R. *Free Radic Biol Med* **1994**, *16*, 571-80.
- 10 Gibbs D.; Varani J.; Ginsburg I. *Inflammation* **1989**, *13*, 465-74.
- 11 Schalkwijk J.; Van den Berg W. B.; Van de Putte L. B.; Joosten L. A.; Van den Bersselaar L. *J Clin Invest* **1985**, *76*, 198-205.
- 12 Kohen R.; Kakunda A.; Rubinstein A. *J Biol Chem* **1992**, *267*, 21349-54.
- 13 Rubinstein A.; Kakunda A.; Kohen R. *J Pharm Sci* **1993**, *82*, 1285-7
- 14 Aebi H. In *Methods Enzymol.*, **1984**; Vol. 105; pp 121-6.
- 15 McCord J. M.; Fridovich I. *J Biol Chem* **1969**, *244*, 6049-55.
- 16 Kohen R.; Tirosh O.; Kopolovich K. *Exp Gerontol* **1992**, *27*, 161-8.
- 17 Kohen R. *J Pharmacol Toxicol Methods* **1993**, *29*, 185-93.
- 18 Kohen R.; Beit Yannai E.; Berry E. M.; Tirosh O. *Methods Enzymol* **1999**, *300*, 285-96.
- 19 Kohen R.; Fanberstain D.; Tirosh O. *Arch Gerontol Geriatr* **1997**, *24*, 103-23.
- 20 Chevion S.; Berry E. M.; Kitrossky N.; Kohen R. *Free Radic Biol Med* **1997**, *22*, 411-21.

- 21 Lomnitski L.; Kohen R.; Chen Y.; Shohami E.; Trembovler V.; Vogel T.; Michaelson D. M. *Pharmacol Biochem Behav* **1997**, *56*, 669-73.
- 22 Blau S.; Kohen R.; Bass P.; Rubinstein A. *Dig Dis Sci* **1999**, *Submitted*.
- 23 Danon D.; Goldstein L.; Marikovsky Y.; Skutelsky E. *J Ultrastruct Res*, 1972, *38*, 500-10.
- 24 Blau S.; Bass P.; Rubinstein A.; Kohen R. *Gastroenterology* **1999**, *Submitted*.
- 25 De Bernardo S.; Weigele M.; Toome V.; Manhart K.; Leimgruber W.; Bohlen P.; Stein S.; Udenfriend S. *Archives of Biochemistry and Biophysics* **1974**, *163*, 390-9.
- 26 Schwartz B.; Avivi C.; Lamprecht S. A. *Gastroenterology* **1991**, *100*, 692-702.
- 27 Wallace J. L.; Le T.; Carter L.; Appleyard C. B.; Beck P. L. *J Pharmacol Toxicol Methods* **1995**, *33*, 237-9.
- 28 Grisham M. B.; Benoit J. N.; Granger D. N. In *Methods Enzymol*, **1986**; Vol. 186; pp 729-33.
- 29 Bradford M. M. *Anal Biochem* **1976**, *72*, 248-54.
- 30 Zar J. H. *Biostatistical Analysis*. Prentice-Hall: Englewood Cliffs, NJ, 1984.
- 31 Mihara K.; Mori M.; Hojo T.; Takakura Y.; Sezaki H.; Hashida M. *Biol Pharm Bull* **1993**, *16*, 158-62.
- 32 Nagashima R. *J Clin Gastroenterol* **1981**, *3*, 117-27.
- 33 Krawisz J. E.; Sharon P.; Stenson W. F. *Gastroenterology* **1984**, *87*, 1344-50.
- 34 Murch S. H.; Braegger C. P.; Walker Smith J. A.; MacDonald T. T. *Gut* **1993**, *34*, 1705-9.
- 35 Hawkins J. V.; Emmel E. L.; Feuer J. J.; Nedelman M. A.; Harvey C. J.; Klein H. J.; Rozmiarek H.; Kennedy A. R.; Lichtenstein G. R.; Billings P. C. *Dig Dis Sci* **1997**, *42*, 1969-80.
- 36 Farmer J. L.; Roberts L. A.; Rydzinski M. E.; Hilty M. D. *Cell Immunol* **1993**, *146*, 186-97.
- 37 Muckerheide A.; Pesce A. J.; Michael J. G. *Cell Immunol* **1990**, *127*, 67-77.

Chapter 10

Oral Dosage Forms with Controlled Release for Constant Plasma Drug Level

A. Ainaoui, E. M. Ouriemchi, and J. M. Vergnaud

Laboratory of Materials and Chemical Engineering, Faculty of Sciences,
University of Saint-Etienne, 42023 Saint-Etienne, France

Oral dosage forms with drug release controlled by erosion, with various shapes and dimensions, are considered. The kinetics of drug release, as well as the plasma drug level, are calculated in various cases by using a numerical model. The effect of the time of retention of the dosage forms in the gastrointestinal on the plasma drug level is especially determined. Bioadhesive dosage forms able to remain in the gastrointestinal over a long period of time appear to be of interest, when the time of full release of the drug out of the dosage forms exceeds 24 hours. Thus rather constant plasma drug level is achieved, whatever the shape given to the dosage form and the dose frequency, and particularly with once a day dosage.

Introduction

The best way to cure the patient is to deliver the drug in such a way that the plasma drug level is nearly constant over a long period of time. This will be the objective for oral dosage forms with controlled release of drug. The compliance will also be easier, with dosage forms taken every day, following a once day dosage. This objective is not so easy to achieve, and three problems should be resolved :

- i) preparation of dosage forms delivering the drug with an about constant rate ;
- ii) in vitro/in vivo correlation or rather, assessment of the plasma drug level associated with a kinetics of drug release ;
- iii) dosage forms releasing the drug over a period of time much longer than the usual gastrointestinal tract time, using adhesion.

Therapeutic systems that release a controlled amount of drug over a defined period of time represent a significant pathway for optimizing drug effects. They offer

important advantages over traditional dosage forms with immediate drug release in diseases requiring the most constant possible blood levels over prolonged durations of therapy. They can decrease the total daily dosage of drug and in so doing decrease the number and frequency of side effects ; they also facilitate the dosage regimen and thus the compliance of the patient [1]. The most simple therapeutic systems are monolithic dosage forms where the drug is dispersed through a biocompatible polymer which can be either stable or erodible along the gastrointestinal tract [2]. With stable polymers the process of drug release is controlled by diffusion, while it is controlled by diffusion-erosion [3] or simply by erosion with bioerodible polymers [2]. Dosage forms with erodible polymers exhibit some advantages over their diffusion-controlled counterparts : the rate of drug release is more constant, and all the drug is released after a finite time [4].

In vitro/in vivo correlations were managed by the Food and Drug Administration through two workshops (5, 6), but "no meaningful data were obtained at that time" (7). In fact these correlations are made with three levels A, B, and C. The problem is of great interest as in vitro experiments giving the kinetics of drug release out of the dosage form are easy to do while in vivo experiments leading to the plasma drug level on healthy volunteers are costly and highly time-consuming. A new way was laid by building numerical models taking all the known facts into account, namely, the kinetics of drug release out of the dosage form, the stages of absorption into- and of elimination out of the plasma (8). Using these models makes possible to assess the plasma drug level, even in the following complex cases provided that they are known : changes in the kinetics of drug release with the pH along the gastrointestinal (GI) tract, change in the value of the rate constant of absorption along the GI tract time, change in the value of the rate constant of elimination with the plasma drug level, metabolism with the first-pass hepatic. Thus the effect of well known parameters such as the dose frequency (9), the GI tract time (10), the value of the rate constant of elimination (11), on the plasma drug level has been precisely defined.

Various new studies are made in order to extend the time over which the dosage form remains in the GI, so that it becomes much longer than the usual GI tract time. Bioadhesion of the dosage forms on the GI wall is the main principle and the dosage form is erodible, in order to make sure that the GI wall will be free after the time of full erosion.

The main purpose in this paper is to assess the plasma drug level obtained with erodible dosage forms of given shapes and given times of full erosion. Emphasis is placed upon the plasma drug level associated with dosage forms taken once a day, either when they remain 24h in the GI or when they remain a much longer time resulting from adhesion to the GI wall. Thus the interest of the bioadhesion of dosage forms can be clearly shown, especially when the time of full release and full erosion is much longer than the usual GI tract time.

Theoretical

Two parts are considered, with the kinetics of drug release, and calculation of the plasma drug level.

Kinetics of drug release.

The main assumptions are that the drug release is controlled by erosion and that the rate of erosion does not vary along the GI tract. The kinetics is expressed in terms of time of full erosion t_r , instead of the rate of erosion (4). The amount of drug released after time t , M_t , as the fraction of the amount of drug initially in the dosage form, is expressed as a function of times t and t_r as follows :

in the sphere and in the cube, by :

$$\frac{M_t}{M_{in}} = 1 - \left(1 - \frac{t}{t_r}\right)^3 \quad (1)$$

in the cylinder of radius R_0 and height $2H_0$:

$$\frac{M_t}{M_{in}} = 1 - \left[1 - \frac{H_0}{R_0} \cdot \frac{t}{t_r}\right]^2 \left[1 - \frac{t}{t_r}\right] \quad (2)$$

in the parallelepiped of sides $2a$, $2b$, $2c$, when a is the smaller dimension :

$$\frac{M_t}{M_{in}} = 1 - \left[1 - \frac{t}{t_r}\right] \left[1 - \frac{a}{b} \cdot \frac{t}{t_r}\right] \left[1 - \frac{a}{c} \cdot \frac{t}{t_r}\right] \quad (3)$$

Plasma drug level.

The following assumptions are made :

- i) The stages of absorption into- and elimination out of the plasma are controlled by first-order kinetics with the rate constants k_a and k_e .
- ii) The rate constant of absorption k_a does not vary along the GI tract time (12).
- iii) The rate constant of elimination k_e does not vary with the plasma drug level.
- iv) No first-pass hepatic is considered.

The rate of drug release out of dosage form at time t is $\frac{dM}{dt}$.

The amount of drug in the GI at time t , is X_t :

$$\frac{dX}{dt} = \frac{dM}{dt} - k_a \cdot X \quad (4)$$

The amount of drug in the plasma, at time t , Y_t , is :

$$\frac{dY}{dt} = k_a \cdot X - k_e \cdot Y \quad (5)$$

The problem is resolved by using a numerical method with constant time increment.

Results

Three types of results are given : the plasma drug level obtained with an erodible dosage form in order to show the accuracy of the method of calculation, the kinetics of

drug release out of erodible dosage forms of various shapes and dimensions, the plasma drug level obtained with these dosage forms. Of course, the amount of drug is also obtained in the GI compartment.

Plasma drug level with an erodible dosage form.

The kinetics of drug release and the plasma drug level are calculated by using interesting results shown in the literature (13). The dosage form is a tablet whose release is controlled by erosion following eq. 3. The drug, salbutamol sulphate, is dispersed through a mixture of hydroxypropylmethylcellulose (Methocel K 100 M) and of sodium carboxymethylcellulose (Blanose 7 HFD). The kinetics of drug release are determined in water at 37°C. In vivo experiments are made by delivering 9.6 mg. of drug to five dogs, and making analysis of the drug in blood samples at intervals.

The plasma drug levels obtained either by experiments (13) or calculation using the numerical model are drawn in Fig. 1 with the immediate release dosage form Ventolin (curve 2) and the erosion-controlled dosage form (curve 1). The parameters evaluated from the experiments (13) and used for calculation are : $k_a = 1.5/h$; $k_e = 0.22/h$; $V_d = 10 \text{ l.}$; $t_r = 10 \pm 1 \text{ h.}$

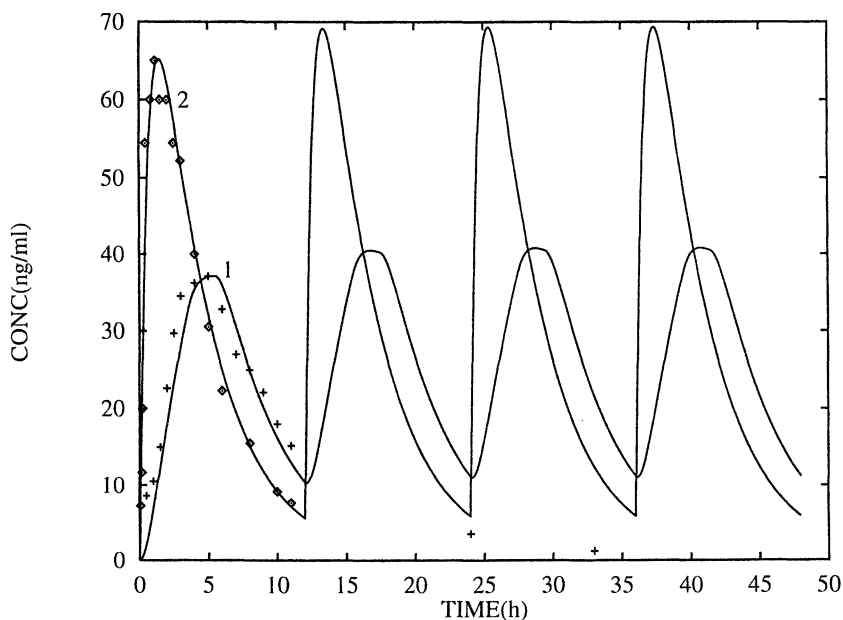


Figure 1. Plasma drug (salbutamol sulphate) level with Ventolin (2) and erosion-controlled release dosage form (1) taken twice a day. $t_r = 10 \text{ h.}$

Some conclusions can be drawn from these curves :

- i) Rather good agreement is observed between the experimental and theoretical curves with a correlation coefficient of 0.985 for Ventolin and 0.96 for the other dosage form.
- ii) The interest of the controlled release clearly appears with a more constant plasma drug level.
- iii) The plasma drug level is far from being constant, even with a twice a day dosage, showing the interest of a long time of full release.

Kinetics of drug release out of dosage forms.

The dosage forms are made of the same polymer and drug, with the same rate of erosion. They are of same volume whatever their shapes and dimensions, with $R_0 = H_0$ for the cylinder, and $b = c = 2a$ for the parallelepiped. The dimensions and time of full release are given in Table 1 for the spheres of types A, B and C.

Table 1 - Dimensions and t_r for the spheres.

Type	A	B	C
Dimension (μm)	87.1	348.8	696.8
t_r (h)	12.8	51.2	102.4

The kinetics of drug release are drawn in Fig. 2 for the three types A, B, C and the various shapes (noted 2 - 5), as they are usually obtained through in-vitro tests.

The following remarks are worth noting :

- i) Of course, the dimension of the dosage form is of prime importance, the time of full drug release being proportional to the radius of the sphere, and to the smaller dimension for other shapes.
- ii) A full release of the drug is attained within a finite time, while infinite time is theoretically necessary with a diffusional process.
- iii) The effect of the shape is of secondary importance. Nevertheless, the time of full release is in decreasing order with the sphere, cylinder, cube and parallelepiped.
- iv) Increasing the residence time of the dosage form in the GI by bioadhesion is of prime interest. Otherwise, the drug is partly released along the GI tract time.

Plasma drug level in simple and multidose.

As shown in the theoretical part, the amount of drug is determined at every time not only in the plasma with eq. 5, but also in the GI with eq. 4. In the same way the kinetics of elimination is obtained. These pieces of information are of interest for curing the patient. The drug is aspirin : $k_a = 2.77/h$; $k_e = 0.23/h$ (11)

The plasma drug levels obtained by calculation are drawn for the type of large dosage forms C and the various shapes in two different cases : (Fig. 3) when the residence time in the GI of the dosage forms is so long that all the drug can be released

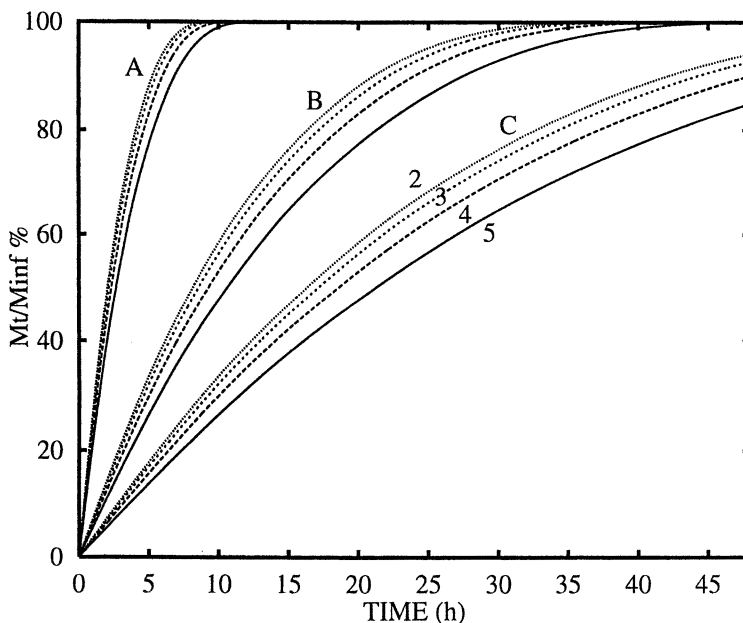


Figure 2. Kinetics of drug release from dosage forms of various shapes and same volume (5 : sphere ; 4 : cylinder ; 3 : cube ; 2 : parallelepiped) with three dimensions and three times of full release (A, B, C).

out of the dosage form in the GI ; (Fig. 4) when the same dosage forms remains in the GI over a period of time of 24 h. Comparison between these plasma drug levels obtained in Figs. 3 and 4 enables to draw conclusions of interest :

i) With a GI tract time of 24 h, a rather large amount of drug remains in the dosage form at the end of the tractus.

ii) Because of the fact said in i), the so-called steady-state is attained after the 1st dose in Fig. 4. On the contrary when these dosage forms adhering to the GI wall remain in the GI over a period of time much longer than 24 h, the drug level increases from the 1st to the 3rd dose and then the steady-state is reached.

iii) The effect of the shape given to the dosage form is of slight importance with regard to the effect of the dimension and time of full release. Nevertheless, it clearly appears that the sphere (curve 5) either in Figs. 3 or 4 is associated with the most constant plasma drug level.

Conclusions

Calculation of the plasma drug level associated with dosage forms with controlled release is of great interest. With the *in vitro/in vivo* correlation method, another way has been developed, based on a numerical model taking all the known facts into

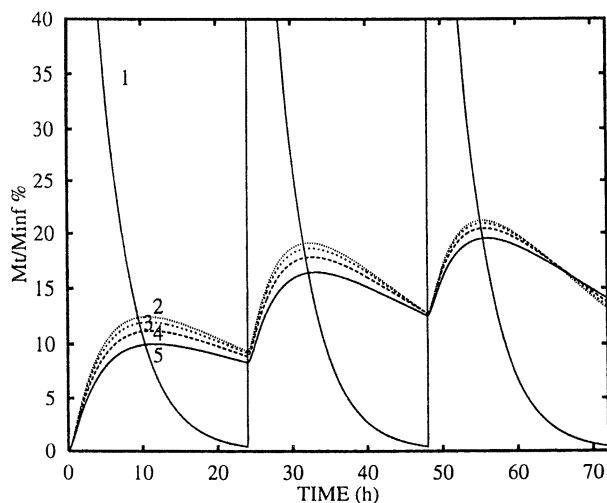


Figure 3. Plasma drug (aspirin) level obtained with dosage forms of type C, and various shapes : immediate release (1) ; controlled release : parallelepiped (2) ; cube (3) ; cylinder (4) ; sphere (5), with a GI residence time much larger than 24 h. $t_r = 102.4$ h for the sphere.

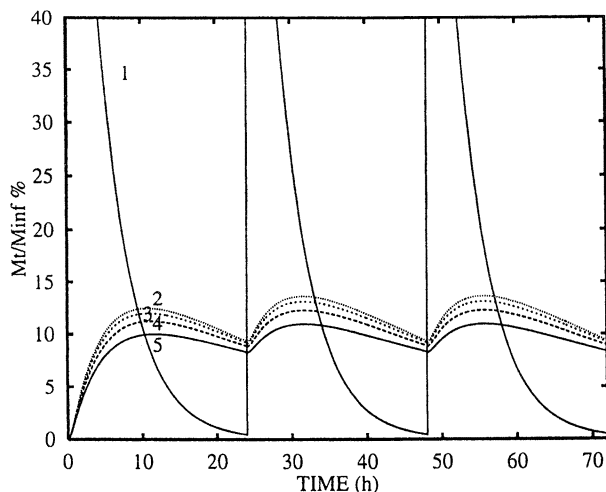


Figure 4. Plasma drug (aspirin) level obtained with dosage forms of type C, and various shapes : immediate release (1) ; controlled release : parallelepiped (2) ; cube (3) ; cylinder (4) ; sphere (5), with a GI residence time of 24 h. $t_r = 102.4$ h for the sphere.

account. Moreover, extending these models enabled one to determine the drug profile not only in the plasma, but also in various tissues such as the blister fluid (14), the lung tissue (15) and bronchial secretion (16).

Dosage forms with release controlled by erosion have been especially considered for two reasons : they deliver the drug with a nearly constant rate in the GI within a given time ; they can be used in bioadhesion systems without harm.

The interest of having these dosage forms adhere to the GI wall has been explored. Thus some main advantages are found : all the drug in the dosage form can be released even when the time of full release is much longer than the GI tract time ; the plasma drug level is nearly constant whatever the dose frequency, once a day dose being acceptable ; omission of a dosage form does not lead to a low trough for the plasma drug level. These results should encourage people working in the field of erodible polymers capable of adhering to the GI wall.

References

1. *Therapeutic Systems* ; Heilmann, K. ; Georg. Thieme Verlag, Eds. ; New-York, 1984, pp. 5 - 23.
2. *Oral Dosage Forms with controlled release* ; Vergnaud, J.M. ; Horwood, E. Eds. ; New-York, 1993, pp. 199 - 251.
3. Feijen, J. ; 14th Meet. French Polymer Group. Rouen, France, Nov. 1984.
4. Ainaoui, A., Ouriemchi, E.M. ; Vergnaud, J.M. *J. Reinforced Plastics Composites*, 1999, 18, in press.
5. Skelly, J.P. ; Barr, W.H. et al. *Pharm. Res.*, 1987, 4, 75.
6. Skelly, J.P. ; Amidon, G.L. et al. *Int. J. Pharm.*, 1990, 7, 975.
7. Skelly J. P. ; Shiu, G. F. *Europ. J. Drug Metabol. Pharmacok.*, 1993, 18, 121.
8. Nia, B. ; Ouriemchi, E. M. ; Vergnaud, J. M. *Int. J. Pharm.*, 1995, 119, 165.
9. Ouriemchi, E. M. ; Vergnaud, J. M. *Int. J. Pharm.*, 1996, 127, 177.
10. Ouriemchi, E. M. ; Vergnaud, J. M. *J. Pharm. Pharmacol.*, 1996, 48, 391.
11. Ainaoui, A. ; Vergnaud, J.M. *Europ. J. Drug Metabol. Pharmacok.*, 1998, 23, 383.
12. Amidon, G.L. ; Lennernäs, H. ; Shah, V.P. ; Crison, R. *J. Pharm. Res.*, 1995, 12, 413.
13. Hernandez, R.M. ; Gasco, A.R. ; Calvo, M.B. ; Caramella, C. ; Conte, U. ; Domingez-Jil, A. ; Pedraz, J.L. *Int. J. Pharm.*, 1996, 139, 45.
14. Bakhouya, A. ; Saïdna, M. ; Vergnaud, J. M. *Int. J. Pharm.*, 1997, 146, 225.
15. Saïdna, M. ; Ouriemchi, E.M. ; Vergnaud, J.M. *Eur. J. Drug Metabol. Pharmacok.*, 1997, 22, 237.
16. Saïdna, M. ; Ouriemchi, E.M. ; Vergnaud, J.M. *Inflammopharmacology*, 1998, 6, 321.

Chapter 11

Solving Drug Delivery Problems with Liposomal Carriers

Theresa M. Allen

Department of Pharmacology, University of Alberta,
Edmonton, Alberta T6G 2H7, Canada

Liposomes are beginning to achieve widespread acceptance as drug carriers, with several products in the clinic and many more in clinical development. Particularly useful is the ability of liposomes to solublize drugs and protect them from degradation. Furthermore, liposomal association of drugs can result in substantial changes in drug clearance, volume of distribution and biodistribution which can help to solve delivery problems associated with unfavorable drug pharmacokinetics. This can lead to increased drug efficacy and decreased drug-associated toxicities. In addition to their use as carriers for chemotherapeutic drugs, liposomes are receiving attention for their use as non-viral delivery systems for gene therapy and as carriers in vaccines.

There is no such thing as a perfect drug. A 'perfect' drug would cure or prevent disease in a highly selective manner by homing only to specific target tissue(s) with no side effects, i.e. it would function as a "magic bullet". It would, arguably, be water soluble and orally active, with pharmacokinetics permitting a once per day administration schedule. We can also fantasize about other properties which we would impart to our perfect drug. In the real world, however, we have to deal with problems like poor solubilities, rapid degradation, unfavorable pharmacokinetics, and poor selective toxicities with attendant side effects. Many novel drug entities fail clinical trials because of these considerations. Other drugs have made it into the clinic, but still have significant problems associated with their administration and/or selectivity.

Liposomal Drug Delivery Systems in Clinical Development

Several drug delivery systems are being researched as a means of solving problems associated with drug delivery, including: liposomes, polymer drug carriers, microspheres, antibody-drug conjugates and immunotoxins. Amongst the drug carriers, liposomes (phospholipid bilayer spheres) are the most developed¹. There

are currently four liposome-based products in the clinic: a liposomal formulation of the antifungal drug amphoterecin B (AmBisome®, NeXstar Pharmaceuticals), and two liposomal anticancer anthracycline formulations, Stealth liposomal doxorubicin (Caelyx® or Doxil®, SEQUUS Pharmaceuticals), liposomal daunorubicin (DaunoXome®, NeXstar Pharmaceuticals) and a liposome-based photosensitizer porfimer sodium (Photofrin®, QLT Phototherapeutics). Approval for another liposomal doxorubicin formulation (Evacet®, The Liposome Company) is currently being sought from the FDA.

Several more liposomal drugs are currently in clinical development including several additional anticancer drugs (vincristine, annamycin, cis-platin, camptothecins, taxanes, tretinoin) antibiotics (amikacin, gentamicin), immune modulators (IL-2, muramyl tripeptide) and photosensitizers (benzophorphrin derivatives in age-related macular degeneration). Furthermore, liposomes are being developed for delivery of antigens for vaccines and as non-viral vectors for gene therapy. The high level of commercial activity surrounding liposomal drug delivery is a result, in part, of the low toxicity of liposomal components, their biodegradability, their excellent storage stability, and relative ease of manufacture. This paper will provide a brief review of the current state of liposomal drug delivery and suggest some future directions for the field.

Choice of Drugs for Liposomal Delivery

How can it be decided whether or not a drug is a candidate for liposomal delivery? A variety of drugs can achieve stable association with liposomes, but not all (Figure 1). Hydrophilic drugs, i.e. those with low octanol:water partition coefficients, can be readily accommodated within the aqueous interior of liposomes². Drugs in the liposome interior are protected from enzymatic degradation and will be slowly released over a period of hours to days, depending on liposome composition and osmotic strength of the drug solution. On the other hand, the entrapment efficiency of hydrophilic drugs may be low which could be a problem for expensive compounds such as proteins and peptides. In addition, the rate of drug release is non-linear.

Hydrophobic drugs may also be associated with liposomes². These drugs, having high octanol:water partition coefficients, can be accommodated within the hydrophobic acyl chain region of the phospholipid bilayer. The association can be very rapid and efficient, allowing the liposomes to function as solubilizers for drugs having low solubilities. Following *in vivo* administration, hydrophobic drugs appear to rapidly transfer to lipoproteins or other biological membranes³.

Association with liposomes of drugs of intermediate solubility can be problematic. Drugs in this category often transfer rapidly between the liposome aqueous interior, the liposome membrane and the external medium (Figure 1). However, clever manipulation of the conditions of entrapment may allow even some of these drugs to be efficiently entrapped. Weak acids and bases can be entrapped with high efficiency by liposomes exhibiting a pH gradient across the liposome bilayer, or drugs can be complexed with substances in the liposome interior which render them more stable and less soluble^{4,5}. For example, very efficient loading of

doxorubicin can occur through the formation of a doxorubicin sulfate precipitate in the liposome interior and these liposomes show high stability and low leakage rates⁵.

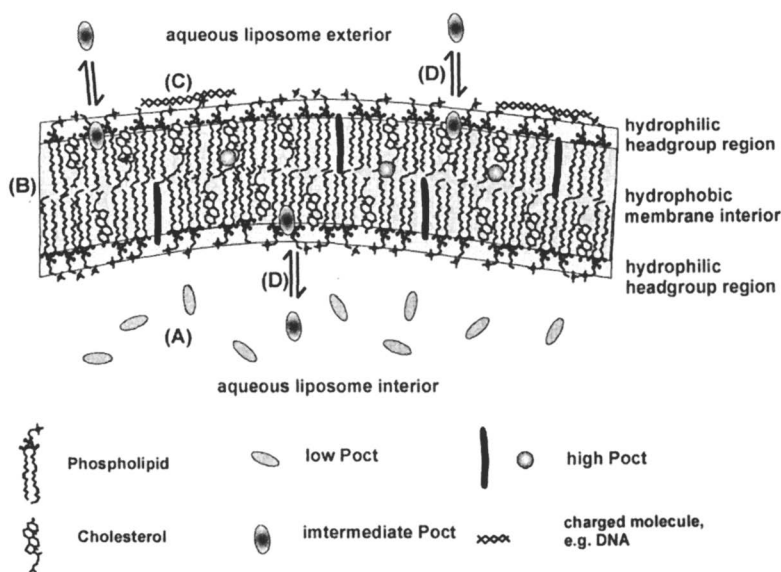


Figure 1. *Interactions of drugs with liposomes. (A) Hydrophilic drugs are encapsulated in the aqueous compartment(s). (B) Hydrophobic molecules can be accommodated in bilayer interior. (C) Charged molecules, e.g. DNA, associate with the bilayer surface through Van der Waal's interactions. (D) Molecules with intermediate solubilities will be in equilibrium between the membrane interior and exterior and will not easily form a stable association with liposomes*

Pharmacokinetics of Liposomal Drugs

One of the most compelling reasons for the use of liposomal drugs is the often dramatic changes in drug pharmacokinetics which result from liposome encapsulation⁶. Because liposomes are large (on the scale of a drug molecule), and particulate in nature, they have difficulty in extravasating through normal vasculature. This results in volumes of distribution (V_D) which are similar to plasma volumes *in vivo*, i.e. approximately 4 L in humans⁷. Since many free, i.e. non-encapsulated, drugs have large V_D , often over 100-200 L in humans, this represents a substantial change. Thus liposomal delivery can result in decreased drug concentrations in normal tissues, e.g. heart, GI tract or kidney, and consequently decreased drug toxicities. Decreased drug toxicities accompanying liposome encapsulation of drugs may be particularly relevant for anticancer drugs or antiviral drugs. On the other hand, liposomal delivery may impede the delivery of drug from liposomes to some

tissues because of poor extravasation of the liposomes. Fortunately, some diseased tissues have increased vasculature permeability which can lead to increased uptake of liposomal drugs into those tissues (see below)⁸.

While liposome composition will have little influence on the volume of distribution of liposomal carriers per se, the volume of distribution for liposome-entrapped drugs may appear to change with drug release rate, which is itself dependent on liposome composition. For example, the anticancer drug doxorubicin has a V_D in humans of 254 L humans⁹. When entrapped in liposomes with very low release rates, the V_D decreases to 4.1 L. However, for a formulation with higher drug release rates, the V_D is a combination of the V_D for the liposomal carrier and the V_D for the released (now free) drug and could be anywhere between 4.1 L and 254 L depending on the release rate of drug⁶.

Liposome composition can also have significant effects on the clearance rate of liposomal drugs. Size, surface charge, phospholipid composition, the presence or absence of cholesterol, and the presence or absence of surface hydrophilic polymers can all affect the clearance of liposomes and their associated drugs¹⁰. Clearance half-lives as low as a few minutes have been described for some "classical" liposome formulations. Liposomes are cleared from blood primarily by uptake into the mononuclear phagocyte system (MPS, i.e., reticuloendothelial system) and are found principally in Kupffer cells in liver and in fixed macrophages in spleen because these organs receive the largest blood flows¹¹. Particularly if one is delivering cytotoxic drugs, this has implications for impairment of MPS function. Classical liposomes are cleared into liver with Michaelis-Menten (saturable) pharmacokinetics¹².

More recent research has resulted in the description of long-circulating (Stealth) liposomes which have a reduced rate and extent of uptake into MPS tissues. These liposomes have hydrophilic polymers such as polyethylene glycol (PEG) grafted at the liposome surface (reviewed in ^{13,14}). The polymers repel opsonins involved in the MPS uptake of liposomes and significantly reduce the clearance rate of liposomes. These liposomes are cleared with log-linear (non-saturable) pharmacokinetics¹⁵. Clearance half-lives for PEG-grafted liposomes of up to 2 days in humans have been described¹⁶. Decreased clearance rates for liposomal drugs and reduced volumes of distribution, lead to increased areas under the plasma concentration versus time curve (AUC).

When the clearance rate of liposomal drugs is reduced, i.e. if the liposomes can circulate long enough, they can begin to extravasate through leaky vasculature, which is characteristic of several diseased tissues, in a process called passive targeting¹⁷. Examples of tissues with increased vascular permeability include solid tumours undergoing angiogenesis (recruitment of new blood vessels) and tissues exposed to various cytokines as might occur during the process of bacterial infections. The concentration of liposomal drugs in tumours, relative to free drug tumour concentrations, can be increased up to 10-fold or higher through the passive targeting mechanism. This increased localization of drugs to diseased tissues can lead to increases in the efficacy of the drugs. For example, the efficacy of Stealth liposomal doxorubicin (Caelyx/Doxil®) in the treatment of Kaposi's sarcoma approximately doubled with a complete plus partial response rate (PR/CR) of 46.2 % for the liposomal drug compared to 25.6% for a free drug schedule consisting of adriamycin (doxorubicin), bleomycin, vincristine (ABV)¹⁸.

Potential Uses for Liposomal Drugs

Liposomes cannot solve all drug delivery problems, but, based on the physical and pharmacokinetic properties of liposomes, many possible applications for liposomal drugs can be suggested. In general, liposomes are very versatile drug carriers¹⁹. They can be given by a number of routes of administration, although administration via the oral route has, until now, been less successful than other routes²⁰. Non-toxic, non-immunogenic and biodegradable liposomes are easy to formulate and can be manufactured with relative ease. Storage stabilities of up to two years have been achieved. When a currently approved drug is placed in a liposome it is considered to be a new drug and must go through the approval process again, with the attendant cost in time and money, but, on the positive side, the liposomal drug can then receive patent protection even after this protection has expired on the conventional form of the drug.

Because liposomes can readily solubilize hydrophobic drugs within the fatty acyl chain region of their bilayers, their use to formulate such drugs would be an obvious application²¹. Lipid components can be chosen which are non-toxic and biodegradable and such systems may have advantages over traditional excipients such as dimethyl sulfoxide (DMSO), Cremphor EL or surfactants. Hydrophobic compounds, like photosensitizers, have been reported to transfer rapidly from liposomes to lipoproteins upon *in vivo* administration³. More research is needed into the factors which govern the pharmacokinetics and biodistribution of drugs 'solubilized' in liposomal membranes.

Liposomes have many actual and potential applications for hydrophilic drugs which are entrapped in the aqueous interior of liposomes. Many examples exist of applications in which liposomes function as sustained release systems for drugs (see also below)²². The rate of drug release can be manipulated over a wide range, depending on how the liposomal drugs are formulated. However, more research is needed into the relationship between drug release rate and therapeutic efficacy²³. Is a faster drug release rate or a slower one more efficacious in treating, for example, a solid tumour? Are there factors, such as tumour doubling times, which can be used to predict optimum drug release rates? Are there simple, inexpensive ways of formulating liposomes which demonstrate triggered release of drugs once they reach the site of drug action? Would this lead to improved therapeutic effects?

When drugs are sequestered in the liposome aqueous interior they are protected from enzymatic and other process of degradation, thus the half-life of the drugs can be prolonged. Consequently, another application for liposomes is in the 'protection' of drugs which are degraded rapidly. For example, the half-life of cytosine arabinoside, an anticancer drug, is increased from a few minutes to several hours upon liposome encapsulation as the drug is sequestered away from the degrading enzyme cytosine deaminase²⁴. This effect can lead to a decrease in the maximum tolerated dose of the drug because drug is available over significantly longer periods of time. Because liposome can maintain a pH gradient across their membranes, drugs which are sensitive to pH-mediated breakdown, such as the camptothecins, can be protected from degradation within liposomes²⁵. Similarly,

liposomes should be considered in applications involving proteins and peptides, many of which have short half-lives *in vivo*. Smaller peptides can be easily accommodated within the aqueous space of liposomes, although it is difficult to entrap larger proteins within the small liposomes required for many therapeutic applications. More work on how to increase the entrapment efficiency of proteins and peptides needs to be done.

The ability of liposomal carriers to alter the biodistribution of drugs leads to other possible applications. Since liposomes do not readily exit through normal, tight, vascular endothelium, they can be used to reduce the exposure of sensitive normal tissues to damaging drugs. For example, liposomal encapsulation of doxorubicin results in a decrease in cardiac toxicities and liposomal association of amphotericin leads to a reduction in dose-limiting kidney toxicities^{16,26}. The pharmacokinetic profile of liposomes suggests that they would be particularly well suited for applications involving drug delivery within the vasculature. Applications of liposomal drugs which take advantage of the 'passive targeting' abilities should also be considered. Liposomal drugs can localize to tissues which have increased vascular permeabilities accompanying the disease process and this is the basis of the clinical approval of two liposomal formulations of anthracyclines and the pending approval of a further liposomal anthracycline for use in the treatment of solid tumours (see above)¹⁷. In at least one instance however, liposomes may extravasate into normal tissues. The tendency of small liposomes to be 'squeezed' out into skin in regions experiencing pressure or rubbing, has been reported to cause 'hand and foot' syndrome in patients being treated with Stealth liposomal doxorubicin¹⁶.

Liposomes have received considerable attention for their potential as non-viral delivery vehicles for plasmid DNA or antisense oligonucleotides (asODNs) for gene therapy^{27,28}. Liposomal vectors are considered to be safer than viral vectors, but, on the whole, they lack the transfection efficiency of the viral vectors. More than one clinical trial is currently underway for intrapulmonary and intratumoral administration of liposomal vectors^{29,30}. AsODNs are small enough to be treated like other hydrophilic drugs and they can be passively entrapped in the aqueous interior of liposomes³¹. Plasmid DNA presents more difficulties because of its large size. In some applications plasmid DNA has been associated with cationic liposomes, forming large heterogeneous complexes. Although these cationic lipid-DNA complexes can be very efficient as transfecting cells *in vitro*, their size and charge guarantees their rapid removal into the MPS *in vivo* following intravenous administration²⁷. In addition, cationic lipids, which are not normal components of cell membranes, have considerable toxicity compared to neutral or negative phospholipids. Techniques for condensing DNA and associating it with lipid particles have been described which should improve the outlook for non-viral liposomal vectors, and investigators are exploring alternatives to cationic lipids²⁸. However, considerable work remains to be done to develop liposomal vectors which are non-toxic, and have good *in vivo* transfection efficiency.

Even though non-immunogenic liposomes can be readily formulated, liposomes can also be good antigen carriers for stimulating immune responses for the purposes of vaccines^{32,33}. The liposome membrane can effectively mimic natural membranes which present proteins, peptides and carbohydrates to the immune system. Many studies have demonstrated that antigens incorporated into liposomal

bilayers or sequestered into the liposome interior can generate vigorous immune responses^{34,35}. Sometimes an immune-stimulating substance or adjuvant is incorporated into the liposome to facilitate the generation of an immune response, e.g. muramyl tripeptide or lipid A.

Improving on the Current Generation of Liposomes

There are several ways in which liposomal carriers might be improved. The next generation of liposomal carriers is likely to be specifically targeted to diseased cells via target-specific ligands attached at the liposome surface³⁶. A number of the steps toward this goal have already been achieved. Methods for attaching antibodies and other ligands to both classical and Stealth liposomes have been described³⁷. Although antibody-targeted classical liposomes are removed very rapidly from circulation into the MPS, it has been shown that antibody-targeted Stealth liposomes retain long circulation times. When the antibodies are coupled to the terminus of PEG in Stealth liposomes they are also able to retain binding affinities for their respective antigens. Liposomes are also to restore multivalent binding to antibody fragments, which may help improve the binding avidity of fragments.

The therapeutic efficacy of targeted liposomes has been examined in several experimental models of haematological and solid tumours^{38,39}. Some tentative conclusions can be drawn from these experiments. The best therapeutic results in the treatment of cancers appear to come from liposomes with modest, rather than high, antibody densities where the targeting moiety has good affinity for its antigen and is targeted against an internalizing receptor on the target cell. In this case, binding of the liposomal ligand to its receptor triggers the internalization of the liposome package into the lysosomal apparatus⁴⁰. However, more effective techniques to promote release of the drug or genetic material from endosomes need to be found. The antigen (receptor) should preferably be expressed uniquely in high concentrations by the target cell and not be down-regulated or sloughed into circulation. Targets which are readily accessible from the vasculature or peritoneal cavity appear to result in better therapeutic effects. Large solid tumours generally do not respond as well to ligand-targeted liposomes as they do to passively targeted liposomes, perhaps because of the 'binding site barrier' which traps the ligand-targeted liposomes at the tumour exterior, preventing them from penetrating into the tumour interior⁴¹.

Targeted liposomal anticancer drugs have resulted in significant improvements over non-targeted therapy in haematological malignancies such as B cell lymphoma, and in 'adjuvant' models of solid tumours where individual metastatic cells are destroyed by the targeted therapy during migration or just after settling down to form new colonies in sites of metastases^{39,42}. It appears that targeted liposomal therapy will be most successful when the liposomes have ready access to their target cells.

Other improvements in liposome therapy will undoubtedly follow improvements in our understanding of how liposomal drugs are trafficked in cells after different routes of presentation, i.e., free drug *versus* non-targeted liposomal drug *versus* targeted liposomal drug (no endocytosis) *versus* targeted liposomal drug

internalized by receptor-mediated endocytosis⁴³. An understanding of how different routes of trafficking of liposomal drugs within cells would affect drug resistance mechanisms would, for example, allow a better choice of a liposomal anticancer drug formulation which might overcome drug resistance.

Further improvements in the ability of liposomal delivery systems to overcome problems of drug delivery will come with a better understanding of how to optimize the rate of drug release from liposomes for each particular application. For example, for a schedule-dependent anticancer drug being used in the treatment of a cancer with a rapid doubling time (like leukemias), liposomes with very slow rates of drug release are less effective than liposomes with more rapid drug release²³. On the other hand, for treating slow-growing solid tumours, the drug should be retained in the liposomes until the liposomes can localize in the tumour by the passive targeting mechanism mentioned above, in order to reduce the distribution of any released drug to normal tissues. Once the liposomal drug localizes to the solid tumour we really don't understand whether it would be better to trigger a rapid burst of drug release within the tumour, or to have a slower sustained release of drug over a period or several weeks, or to have a release rate somewhere in between.

In the area of gene delivery using non-viral, liposomal vectors, significant improvements in the transfection ability, stability and pharmacokinetics of the vectors are needed. Currently, other than via injection directly into the target site, there is no way to target gene delivery to selective *in vivo* targets. Nor do we have a good understanding of how plasmid DNA and asODNs are trafficked within cells once they reach the target cell. If they are delivered to specific cells via receptor-mediated endocytosis, can we find better ways of releasing the material from endosomes before extensive degradation takes place?

Summary

Many significant developments have taken place over the last three decades in the field of liposomal drug delivery and several products have reached the clinic in recent years. Liposomes are proving themselves capable of solving a variety of drug delivery problems and their use will continue to grow in the future as many exciting new drugs and genes are being found from the human genome project, combinatorial chemistry, high throughput screening, etc. Many of these drugs will have problems of pharmacokinetics, solubility, toxicity, etc., some of which can be solved by liposomal delivery. The decision of whether to go to a liposomal drug delivery system for a particular drug requires an excellent understanding of the physical properties of the drug to be delivered as well as those of the liposomal carrier and how the two will interact. The effect of liposome association on the pharmacokinetics and biodistribution of the chosen drug must also be well understood. Finally, in order to make the best decisions about drug formulation, we should have a clear appreciation of the biology and physiology of the disease to be treated. Only in the light of this background knowledge can sensible, rational decisions be made about liposomal drug delivery systems which will lead to new clinical products.

References

- 1) Ranson, M.; Howell, A.; Cheeseman, S.; Margison, J. *Cancer Treatment Rev.* **1996**, *22*, 365-379.
- 2) Defrise-Quertain, F.; Chatelain, P.; Delmelle, M.; Ruyschaert, J. *Model studies for drug entrapment and liposome stability*; Gregoriadis, G., Ed.; CRC Press, Inc.: Boca Raton, FL, 1984; Vol. 2, pp 1-17.
- 3) Ginevra, F.; Biffanti, S.; Pagnan, A.; Biolo, R.; Reddi, E.; Jori, G. *Cancer Lett* **1990**, *49*, 59-65.
- 4) Mayer, L. D.; Bally, M. B.; Cullis, P. R. *Biochim. Biophys. Acta* **1986**, *857*, 123-126.
- 5) Haran, G.; Cohen, R.; Bar, L. K.; Barenholz, Y. *Biochim. Biophys. Acta* **1993**, *1151*, 201-315.
- 6) Allen, T. M.; Hansen, C. B.; Lopes de Menezes, D. E. *Adv. Drug Del. Rev.* **1995**, *16*, 267-284.
- 7) Northfelt, D. W.; Martin, F. J.; Kaplan, L. D.; Russell, J.; Andersen, M.; Lang, J.; Volberding, P. A. *Proc. Am. Soc. Clin. Oncol.* **1993**, *12*, 51.
- 8) Jain, R. K. *Cancer Metastasis Rev.* **1987**, 559-593.
- 9) Gabizon, A.; Catane, R.; Uziely, B.; Kaufman, B.; Safra, T.; Cohen, R.; Martin, F.; Huang, A.; Barenholz, Y. *Cancer Res.* **1994**, *54*, 987-992.
- 10) Sharma, A.; Sharma, U. S. *Int J Pharm* **1997**, *154*, 123-140.
- 11) Scherphof, G. L.; Velinova, M.; Kamps, J.; Donga, J.; van der Want, H.; Kuipers, F.; Havekes, L.; Daeman, T. *Adv. Drug Del. Rev.* **1997**, *24*, 179-191.
- 12) Hwang, K. J. *Liposome pharmacokinetics*; Marcel Dekker: New York, NY, 1987.
- 13) Allen, T. M. *Adv. Drug Del. Rev.* **1994**, *13*, 285-309.
- 14) Ceh, B.; Winterhalter, M.; Frederik, P. M.; Vallner, J. J.; Lasic, D. D. *Adv. Drug Del. Rev.* **1997**, *24*, 165-177.
- 15) Papahadjopoulos, D.; Allen, T. M.; Gabizon, A.; Mayhew, E.; Matthay, K.; Huang, S. K.; Lee, K. D.; Woodle, M. C.; Lasic, D. D.; Redemann, C.; Martin, F. J. *Proc. Natl. Acad. Sci. USA* **1991**, *88*, 11460-11464.
- 16) Coukell, A. J.; Spencer, C. M. *Drugs* **1997**, *53*, 520-538.
- 17) Gabizon, A.; Goren, D.; Horowitz, A. T.; Tzemach, D.; Lossos, A.; Siegal, T. *Adv. Drug Del. Rev.* **1997**, *24*, 337-344.
- 18) Northfelt, D. W.; Dezube, B. J.; Thommes, J. A.; Levine, R.; Von Roenn, J. H.; Dosik, G. M.; Rios, A.; Crown, S. E.; DuMond, C.; Mamelok, R. D. *J. Clin. Oncol.* **1997**, *15*, 653-659.
- 19) Allen, T. M. *Drugs* **1998**, *56*, 747-756.
- 20) Rogers, J. A.; Anderson, K. E. *Crit. Rev. in Therap. Drug Carrier Sys.* **1998**, *15*, 421-480.
- 21) Reddi, E. J. *Photochem. Photobiol.* **1997**, *37*, 189-195.
- 22) Woodle, M. C.; Storm, G. *Long-Circulating Liposomes: Old Drugs, New Therapeutics*; Landes Bioscience: Georgetown, TX, 1998.
- 23) Allen, T. M.; Newman, M. S.; Woodle, M. C.; Mayhew, E.; Uster, P. S. *Int. J. Cancer* **1995**, *62*, 199-204.

- 24) Allen, T. M.; Mehra, T.; Hansen, C. B.; Chin, Y. C. *Cancer Res.* **1992**, *52*, 2431-2439.
- 25) Subramanian, D.; Muller, M. T. *Oncol. Res.* **1995**, *7*, 461-469.
- 26) de Marie, S.; Janknegt, R.; Bakkerwoudenberg, I. A. J. M. *Antimicrob. Chemother.* **1994**, *33*, 907-916.
- 27) Mahato, R. I.; Takakura, Y.; Hasida, M. *Crit. Rev. Therap. Drug Carrier Sys.* **1997**, *14*, 133-172.
- 28) Lee, R. J.; Huang, L. *Crit. Rev. in Therap. Drug Carrier Sys.* **1997**, *14*, 173-206.
- 29) Schreier, H.; Sawyer, S. M. *Adv. Drug Del. Rev.* **1996**, *19*, 73-87.
- 30) Rolland, A. P. *Crit. Rev. in Therap. Drug Carrier Sys.* **1998**, *15*, 143-198.
- 31) Woodle, M. C.; Huang, S. K.; Meyer, Q.; Brown, B. D.; Dizik, M.; Hong, K.; Papahadjopoulos, D. *Adv. Drug Del. Rev.* **1997**, *24*, 273.
- 32) Gregoriadis, G. *Trends Biotechnol.* **1995**, *13*, 527-537.
- 33) Gould-Fogerite, S.; Kheiri, M. T.; Zhang, F.; Wang, Z.; Scolpino, A. J.; Feketeova, E.; Canki, M.; Mannino, R. J. *Adv. Drug Del. Rev.* **1998**, *32*, 273-287.
- 34) Kersten, G. F. A.; Crommelin, D. J. A. *Biochim. Biophys. Acta* **1995**, *124*, 117-138.
- 35) Guan, H. H.; Budzynski, W.; Koganty, R. R.; Krantz, M. J.; Reddish, M. A.; Rogers, J. A.; Longenecker, B. M.; Samuel, J. *Bioconjugate Chem.* **1998**, *9*, 451-458.
- 36) Allen, T. M.; Hansen, C. B.; Stuart, D. D. *Targeted sterically stabilized liposomal drug delivery*; Lasic, D. D. and Papahadjopoulos, D., Ed.; Elsevier Science Publishers: Amsterdam, 1998, pp 297-323.
- 37) Allen, T. M.; Moase, E. H. *Adv. Drug Del. Rev.* **1996**, *21*, 117-133.
- 38) MacLean, A. L.; Symonds, G.; Ward, R. *Int. J. Oncol.* **1997**, *11*, 325-332.
- 39) Lopes de Menezes, D. E.; Pilarski, L. M.; Allen, T. M. *Cancer Res.* **1998**, *58*, 3320-3330.
- 40) Park, J. W.; Hong, K.; Kirpotin, D. B.; Meyer, O.; Papahadjopoulos, D.; Benz, C. *Cancer Lett.* **1997**, *118*, 153-160.
- 41) Osdol, W. V.; Fujimori, K.; Weinstein, J. N. *Cancer Res.* **1991**, *51*, 4776-4784.
- 42) Ahmad, I.; Longenecker, M.; Samuel, J.; Allen, T. M. *Cancer Res.* **1993**, *53*, 1484-1488.
- 43) Lopes de Menezes, D. E.; Pilarski, L. M.; Allen, T. M. *J. Liposome Res.* **1999**, *9*, 199-228.

Chapter 12

PEGylation: A Tool to Enhance Protein Delivery

Wayne R. Gombotz and Dean K. Pettit

Department of Analytical Chemistry and Formulation, Immunex Corporation,
51 University Street, Seattle, WA 98101

The process of conjugation of proteins to polyethylene glycol (PEGylation) has been utilized to enhance solubility, reduce immunogenicity, reduce proteolytic degradation and prolong in vivo circulation half-life. PEG-conjugation can also lead to a reduction or alteration in biological activity. Purification and characterization of PEGylated proteins can also be difficult due to the heterogeneity of the product. This manuscript will review protein PEGylation highlighting potential advantages and challenges of the technology. Emphasis will be given to methods used to preserve the biological function of PEG conjugated proteins using three recombinant proteins as examples; granulocyte macrophage colony stimulating factor (GM-CSF), p75 tumor necrosis factor receptor IgG1 Fc fusion protein (TNFR:Fc, etanercept), and interleukin-15 (IL-15).

PEG Chemistry and Solubility

Poly(ethylene oxide) (PEO) is a synthetic, non-toxic, water soluble polymer with the general formula $\text{HO}-(\text{CH}_2\text{CH}_2\text{-O})_n\text{-H}$. PEO molecules are available in a wide range of molecular weights, varying from several hundred up to ten million or more. The lower molecular weight members of the series with n up to about 150 are generally called polyethylene glycols (PEGs) (1). PEO is soluble in water at room temperature in all proportions for a wide range of molecular weights. Water molecules are hydrogen bonded to the ether oxygens of the PEO molecule and three water molecules are associated with each ethylene oxide unit (2). These water molecules are believed to form a protective hydration shell around the PEO (3).

PEG in the Biomedical Field and Rationale for PEGylation

The extreme water solubility of PEG combined with its excellent safety profile (4) have generated much interest in the use of this molecule in the biomedical field (5). Surfaces that have been coated with PEG having a molecular weight of 2000 Daltons or more exhibit the ability to repel proteins (6,7). The pioneering work of Davis and Abuchowski demonstrated the utility of conjugation of proteins to

polyethylene glycol (PEGylation) for use as therapeutic agents (8). PEGylation has been utilized to enhance solubility, reduce immunogenicity, reduce proteolytic degradation (9) and prolong *in vivo* circulation half-life of therapeutic proteins (10). Although the circulation half-lives of some proteins and peptides has been increased 50-fold through the use of PEGylation (11), PEG-conjugation can also lead to a reduction or alteration in biological activity. This is usually due to steric interference of the conjugated PEG with biologically relevant regions of the protein and can depend on the degree of conjugation, the type of conjugation chemistry utilized, and the specific location on the protein where the conjugation has occurred. Several approaches have been taken to minimize the activity loss associated with protein PEGylation and are listed in Table I.

Table I. Approaches to Minimize the Activity Loss Associated with PEGylation

1. Minimize PEG chains per protein
2. Use a few high mw PEG chains
3. Use a few branched PEG chains
4. N-terminal conjugation
5. Carbohydrate conjugation
6. Sulfhydryl conjugation
7. Site-protection
8. Lysine mutagenesis

A variety of PEG reagents have also been developed which allow one to select the specific type of PEG molecule (mw and structure) and chemistry of PEG conjugation to a protein. These commercially available reagents include PEG molecules with different backbone structures as well as a PEGs derivatized with different functional end groups, some of which are listed in Table II (12).

Table II. Different PEG Backbones and Conjugation Chemistries Available for PEGylation

PEG Backbones	Conjugation Chemistries
Methoxy PEGs	Nucleophilic PEGs
Mono-acid PEGs	Carboxyl PEGs
Branched PEGs	Electrophilically activated PEGs
Star and dendritic PEGs	Sulfhydryl-selective PEGs
Pendant PEGs	Heterofunctional PEGs
Comb PEGs	Biotinylated PEGs
EO/PO copolymers	Vinyl PEGs
Forked PEGs	PEG silanes
Degradable PEGs	PEG phospholipids

Purification of PEGylated Proteins

Purification of PEGylated proteins can also be difficult due to the heterogeneity of the product. Any PEGylation reaction will generate several molecular species which must be removed. These species include reaction byproducts from the conjugation chemistry such as free PEG or N-hydroxysuccinimide, unPEGylated protein, and over PEGylated product. Several chromatographic techniques are commonly used for purification of PEGylated proteins. Size exclusion chromatography (SEC) separates the product based on size. Attachment of PEG to a protein results in a significant increase in the hydrodynamic radius of the molecule which can be readily resolved from the native protein on a sizing column. Ion exchange chromatography is a charge based separation. Since PEGylation can shield a protein's charge this method can be used effectively to separate PEGylated from non-PEGylated product. PEG will contribute to the hydrophilicity/hydrophobicity of a protein and methods which can take advantage of these differences include hydrophobic interaction chromatography (HIC) and reversed phase chromatography (RPLC). HIC will separate proteins based on hydrophobicity in aqueous solution while RPLC works on a similar principle in an organic solvent. Aqueous two-phase partitioning has also been used for purification of PEGylated proteins.

Characterization of PEGylated Proteins

Once a product has been PEGylated and purified the final challenge lies in the characterization of the molecule. PEGylated proteins are generally comprised of a heterogeneous mixture of several species which may vary in both the number and site of the attached PEG molecules. In addition the PEG molecules themselves are polydisperse which further adds to product heterogeneity. Characterization of the PEGylated product involves an understanding of (i) the properties of the individual species; (ii) the reproducibility of the heterogeneity and; (iii) the structural integrity of the product. Many analytical techniques are available for characterization of PEGylated proteins. Electrophoretic techniques include sodium dodecyl sulfate polyacrylamide gel electrophoresis (SDS-PAGE), isoelectric focusing, and capillary electrophoresis. SDS-PAGE provides a general indication of whether or not PEGylation has occurred as seen by an increase in the apparent molecular weight of the protein on the gel. This method, however, is not quantitative and provides no information about the site of attachment of the PEG on the protein. Capillary electrophoresis can better discriminate between the different heterogeneous species in a product. Other chromatographic techniques such as SEC are also useful for characterization of the molecular weight of the product. Both ion exchange chromatography and reversed phase HPLC can provide some information about the consistency of the product.

Peptide mapping is a more sensitive technique which can be used to determine the precise locations of the PEG chains on the peptide backbone (13). Matrix-assisted laser desorption ionization time of flight (MALDI-TOF) mass spectrometry is a method which can quickly and accurately determine the molecular weight and heterogeneity of a PEGylated product (14). This method also allows one to readily determine the amount of molecular weight heterogeneity in a product due to differences in the number of PEG chains attached to the protein.

Other biophysical characterization methods such as differential scanning calorimetry, circular dichroism, and fluorescence spectroscopy, Raman spectroscopy and UV-vis spectroscopy can provide information about the structural integrity of a PEGylated molecule (15, 16). An *in vitro* bioassay is also essential to determine the effect of PEGylation on the product's bioactivity.

PEGylated Proteins in the Clinic

Despite the challenges of producing and characterizing biologically active PEG-protein conjugates, several PEGylated proteins are approved biopharmaceutical products including PEG-L-asparaginase (Oncospar™) and PEG-adenosine-deamidase (Adagen™). Numerous others are currently progressing through clinical trials such as PEG- α -interferon, PEG-interleukin-2, PEG-hemoglobin, PEG-granulocyte colony stimulating factor, and PEG human growth hormone antagonist. In this manuscript the PEGylation of three recombinant proteins will be presented; granulocyte macrophage colony stimulating factor (GM-CSF), p75 tumor necrosis factor receptor IgG1 Fc fusion protein (TNFR:Fc, etanercept), and interleukin-15 (IL-15).

Material and Methods

N-Terminal PEGylation of muPEG-GM-CSF

GM-CSF is a cytokine which exhibits pleiotropic activity in the hematopoietic and immune systems. The drug is currently used clinically to accelerate myeloid recovery in patients undergoing bone marrow transplantation or for peripheral blood stem cell expansion. Previous reports in the literature have shown that PEGylation of GM-CSF increased the ability of this protein to prime neutrophils *in vitro* (17) while increasing the *in vivo* circulation half-life (18). Sherman et al., showed that PEGylation of murine (mu)GM-CSF with high molecular weight PEG enhanced the *in vivo* bioactivity and circulation half-life (19).

In this study recombinant muGM-CSF was produced in yeast (*Saccharomyces cerevisiae*) as described (20). N-terminal PEG conjugation was carried out with 20 kDa PEG which was obtained in aldehyde terminated form (PEG-aldehyde) (Shearwater Polymers, Huntsville, AL). A six fold molar excess of PEG-aldehyde was added to a solution of muGM-CSF in 20 mM Na₂HPO₄, 50 mM cyanoborohydride, pH 6.0, and the reaction was allowed to proceed overnight at 2-8 °C. The PEGylation reaction was carried out at a pH of 6.0 to take advantage of the greater reactivity of the N-terminal amino acid residue toward the aldehyde group on the PEG under these conditions (21). Mono-PEG conjugated muGM-CSF was purified from the reaction mixture by anion exchange chromatography with Q Sepharose High Performance resin (Pharmacia, Uppsala Sweden) using a 0-150 mM NaCl elution gradient on a Perceptive Integral HPLC system. Purified protein solutions were concentrated and buffer exchanged into PBS. PEG-muGM-CSF was then tested for endotoxin levels by the LAL method and total protein concentration by amino acid analysis. The material was characterized by SDS-PAGE, SEC, and tryptic peptide mapping. The PEGylated protein was compared to native muGM-CSF in a murine model. Mice were injected with 5 μ g of protein daily for seven days with

native muGM-CSF, PEGmuGM-CSF or a buffer control. The effect of these molecules on both the spleen weight and cellularity was then evaluated.

Site-Specific PEGylation of Etanercept

The extracellular domain of p75 TNFR linked to the Fc portion of a human IgG1 (etanercept) has been recently approved by the FDA for treatment of patients suffering from rheumatoid arthritis (22). Conjugation of PEG to this molecule was investigated as a way to increase its half-life and ultimately decrease the dosing frequency and total dose required to achieve clinical efficacy. Etanercept was expressed in Chinese hamster ovary (CHO) cells and purified with a protein A affinity chromatography step. Two methods of PEGylation were carried out, both utilizing succinimidyl carbonate (SC) PEG-5000 (Shearwater Polymers, Birmingham, AL), a solution method and an affinity column method.

In the solution PEGylation method etanercept was reacted with SC-PEG-5000 at molar ratios of 1.25:1, 0.625:1, 0.313:1, 0.156:1, and 0.078:1 (PEG: lysine) in 50 mM Na₂HPO₄ (pH 8.5) overnight at 4°C. The PEGylated etanercept was purified via SEC (Bio-Sil SEC 400 column, BioRad, Hercules, CA).

In the affinity column method, a column was prepared by conjugating a TNFR:Fc neutralizing monoclonal antibody, M1 (Immunex designation), onto Emphaze™ biosupport beads (Pierce, Rockford, IL). Five milligrams of antibody was reacted with 250 mgs of beads. The antibody conjugated beads were packed in a 2 mL stainless steel column. Etanercept was allowed to bind to the column by passing 0.5 mg of protein over the column in PBS (pH 7.4) at a flow rate of 0.1 ml/min. The bound etanercept was then reacted with SC-PEG-5000 by circulating 10 mg of the reagent in Na₂HPO₄ (pH 8.5) at 1 ml/min overnight at 25°C. PEGylated material was eluted from the column by flowing 50 mM NaCitrate (pH 3.0) over the column at 1 ml/min. The PEGylated protein was collected and neutralized with 0.1N NaOH.

The concentration of each of the protein solutions was measured by amino acid analysis (AAA). The number of PEG conjugates per protein molecule was estimated by fluorescence (23). PEGylated etanercept was characterized by SEC, tryptic peptide mapping and an A375 bioassay (A375 human melanoma cells are sensitive to TNFα and protected by bioactive etanercept) (24).

To further direct the PEGylation of etanercept away from the active TNFα binding site, TNFR:Fc muteins were prepared in which lysine (K) 108 and K120 were mutated to arginine (R) which would not react with the SC-PEG. The protein was characterized by SDS-PAGE, SEC, tryptic peptide mapping and bioassay. *In vivo* pharmacokinetics were also determined in a murine model.

A PEG-IL-15 Antagonist

IL-15 is a multifunctional cytokine which shares many biological activities with IL-2. This functional overlap, as well as receptor binding units shared by IL-15 and IL-2, suggest tertiary structural similarities between these two cytokines (11). The recombinant form of IL-15 is a CHO-derived glycoprotein composed of 126 amino acids with a peptide molecular weight of approximately 14 kDa. IL-15 and IL-2 are

structurally homologous molecules which bind to at least three distinct receptor subunits on the T-cell membrane surface (α , β , and γ). IL-15 was PEGylated via lysine-specific conjugation chemistry in order to extend the circulation half-life of this cytokine. IL-15 was reacted with SC-PEG-5000 (Shearwater Polymers) at PEG:lysine ratios of 1:1, 3:1, 10:1, and 100:1. Reactions were carried out overnight at 4 °C in 50 mM NaH₂PO₄, pH 8.5. PEG-IL-15 was then dialyzed against PBS to remove residual N-hydroxysuccinimide, a byproduct of SC-PEG hydrolysis. Protein concentration was determined by amino acid analysis. The conjugated proteins were characterized by SDS-PAGE, SEC, and MALDI-TOF mass spectrometry. The bioactivity of the PEG-IL-15 was tested in an *in vitro* T-cell proliferation assay (CTLL)(25) and compared to the bioactivity of IL-2 in the same assay. Experiments were also performed to compare the pharmacokinetics of IL-15 to PEG-IL-15 (PEG:lysine ratio of 10:1). Three groups of mice per timepoint were injected with 10 μ g of protein. Following the injections the mice were sacrificed and blood samples collected out to 48 hrs. The amount of IL-15 or PEG-IL-15 was determined in the serum using an IL-15 specific ELISA.

Results and Discussion

N-Terminal PEGylation of PEG-muGM-CSF

Both SDS-PAGE and SEC showed that the molecular weight of the muGM-CSF was increased through PEGylation and that populations of mono- and di-PEG-GM-CSF species were present. Tryptic peptide mapping revealed that the majority of the PEG was attached to the N-terminus of the muGM-CSF. *In vivo* studies showed that the half-life of the PEG-muGM-CSF was significantly increased. Unlike native muGM-CSF, the PEG-conjugated protein dramatically increased the spleen weight (Figure 1) and splenic cellularity of the myeloid dendritic cell lineage. The high molecular weight PEG (mw 20 kDa) chosen for the N-terminal conjugation offset the fact that only one or two PEG chains were attached to the molecule. The mono- and di-PEGylated conjugates are more homogeneous than the more heterodisperse species obtained by coupling many lower molecular weight PEGs to multiple sites on the protein. This results in a molecule that is easier to purify and characterize.

Site-Specific PEGylation of Etanercept

The results of the fluorescamine, SEC and A375 bioassay are shown in Table III. Note that when etanercept is PEGylated in solution without the aid of the affinity column that the number of PEG chains per protein molecule increased as did the molecular weight estimated by SEC. The increase in PEG modification and molecular weight was inversely related to the biological activity of etanercept as measured by the A375 bioassay. When etanercept was PEGylated on the affinity column approximately 5-6 PEG modifications were detected and a large molecular weight was estimated by SEC. However, in contrast to the solution PEGylated etanercept, these physical changes were not accompanied by a reduction in bioactivity.

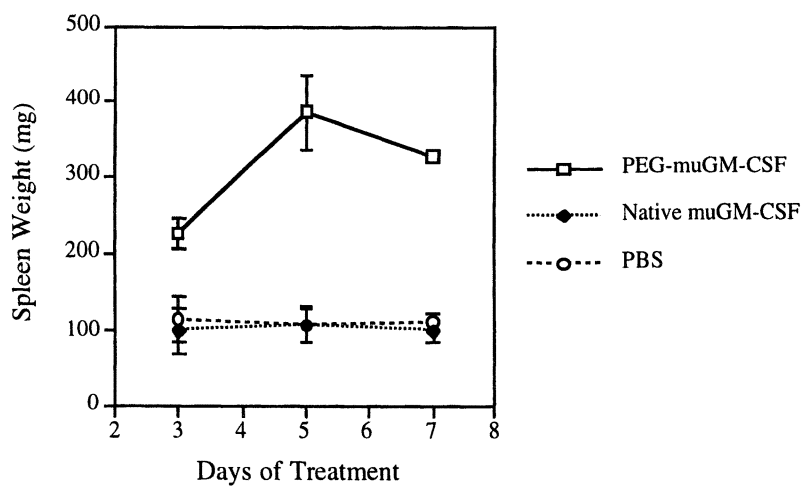


Figure 1. Spleen weight of mice treated with PEG-muGM-CSF, muGM-CSF or PBS. Mice were injected with 5 μ g of protein, once daily for 7 days.

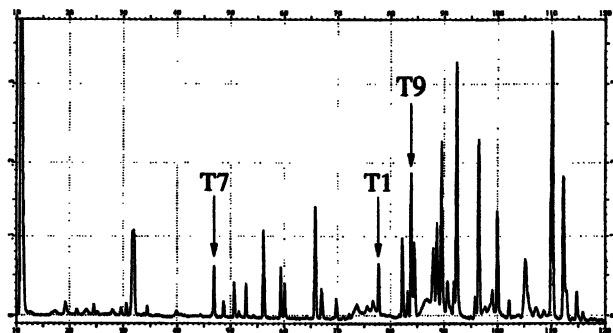
Table III. Characterization of Solution and Affinity PEGylated Etanercept by Fluorescamine Assay, SEC, and A375 Bioassay

Sample (PEG:lysine)	# of PEG chains per TNFR:Fc	Molecular Weight (via Size Exclusion)	% Bioactivity
<i>PEGylated in solution:</i>			
0:1 (control)	0	370,960	100
0.078:1	1.8	494,937	74
0.156:1	3.2	648,335	60
0.313:1	4.7	865,013	38
0.625:1	4.5	1,092,262	10
1.25:1	ND	1,174,221	0
<i>PEGylated on affinity column:</i>			
Run #1	6.5	833,829	131
Run #2	5.4	ND	124
Run #3	5.2	ND	110
Run #4	ND	ND	120

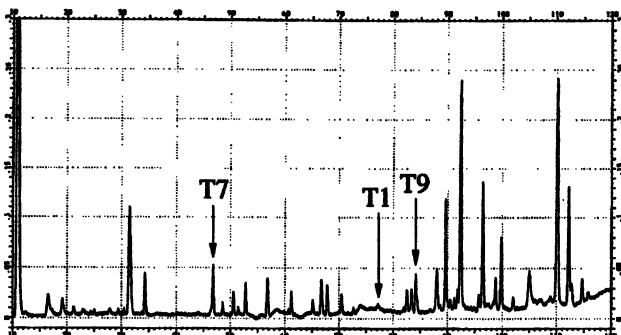
A tryptic peptide map of etanercept is shown in Figure 2. Trypsin cleavage results in 39 peptide fragments which are detected by RP-HPLC. PEGylation resulted in either the disappearance of peaks from the map or a reduction in peak height. Note in Figures 2 A, B, and C the peaks identified as T7, T1, and T9. Each of the chromatograms were normalized using the height of peak T7 which is flanked by arginine (R) on both ends (R*CSSDQVETQACTR*). This peak is not expected to be effected by PEGylation since it contains no lysine residues. The N-terminus of etanercept is represented by T1 (LPAQVAFTPYAPEPGSTCR*) and is readily observed in the peptide map of the unPEGylated material (Figure 2A), but absent in the maps of both the solution and affinity PEGylated proteins (Figures 2B and 1C respectively). Peak T9 (R*ICTCRPGWYCALS*) includes amino acid residue K108 which may be involved in interaction with TNF α . This peak is significantly reduced in the map of solution PEGylated etanercept (Figure 2B) but unaffected in the map of affinity PEGylated etanercept (Figure 2C). In summary, high levels of PEG modification were achieved with minimal effect on biological activity using the affinity column technique.

The conservation of bioactivity in the affinity PEGylated etanercept is likely due to the protection of lysine residue 108 from PEGylation. To further test this hypothesis TNFR:Fc were prepared in which K108 and K120 were mutated to arginine. Solution PEGylation of this mutein resulted in retention of high levels of bioactivity. An *in vivo* pharmacokinetic study demonstrated that the half-life of the PEG-TNFR:Fc K108 and K120 mutein was doubled when compared to the native protein (Figure 3). Studies are ongoing in a collagen induced arthritis model in mice to determine whether a significant reduction in the dosing frequency may be achieved while retaining the anti-inflammatory activity of this molecule.

A



B



C

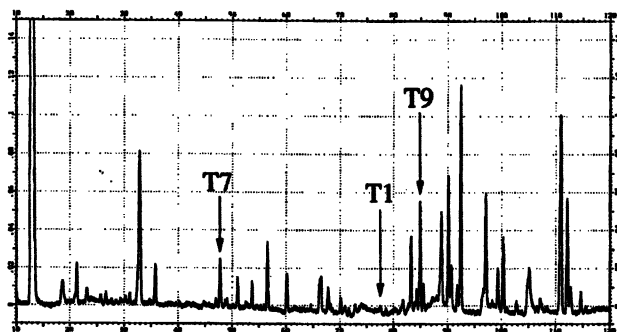


Figure 2. Tryptic peptide maps of : (A) Etanercept control; (B) Etanercept PEGylated in solution (PEG:lysine ratio 1.25:1); and (C) etanercept PEGylated on the affinity column. Three tryptic peptides are identified as T7, T1, and T9 (see text for description).

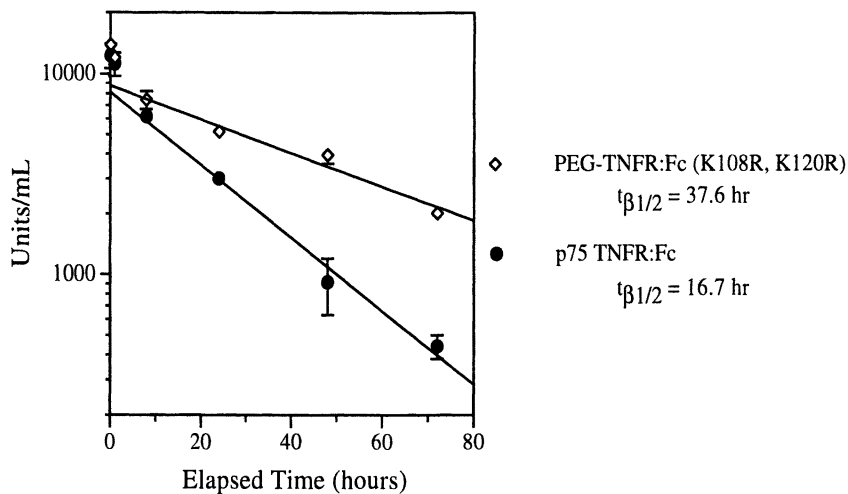


Figure 3. Pharmacokinetics of PEG-TNFR:Fc K108 and K120 mutein following intravenous injection in mice. Serum levels were determined by ELISA. The PEGylated molecule had a beta elimination half-life of 38 hours compared to etanercept with a half-life of approximately 17 hours.

A PEG-IL-15 Antagonist

PEGylation of IL-15 resulted in a high degree of modification as demonstrated by SDS-PAGE and SEC. An increase in the ratio of PEG to lysine residues resulted in higher molecular weight bands on the gel and a shift to later eluting peaks in the SEC profile (Figure 4). MALDI-TOF mass spectrometry of PEG-IL-15 (PEG:lysine ratio of 100:1) indicated that the PEGylated IL-15 was heterogeneous with at least seven distinct species ranging in size from 14 kDa (unmodified IL-15) to approximately 50 kDa in intervals of about 5 kDa (Figure 5).

The results of the pharmacokinetic studies which compared the circulating serum concentrations of IL-15 and PEG-IL-15 showed a significant increase in the half-life of the PEGylated molecule. For the unmodified IL-15 the beta elimination half-life was 16 min compared to 2470 (41 hrs) for the PEG-IL-15.

PEGylation of IL-15 also significantly reduced the ability of IL-15 to stimulate the proliferation of T-cells in the CTLL bioassay. Upon further investigation it was discovered that the PEG-IL-15 acted as a specific antagonist of IL-15. In comparing the sequence alignments and molecular models for IL-2 and IL-15, it was noted that lysine residues resided in regions of IL-15 that may have selectively disrupted receptor subunit binding. Further studies with site-specific mutants of IL-15

suggested that PEGylation of IL-15 interferes with β but not α receptor subunit binding, resulting in the IL-15 antagonist activity observed *in vitro*. This study shows the importance role that the attachment site of a PEG molecule to protein can play in the modification of the protein's bioactivity.

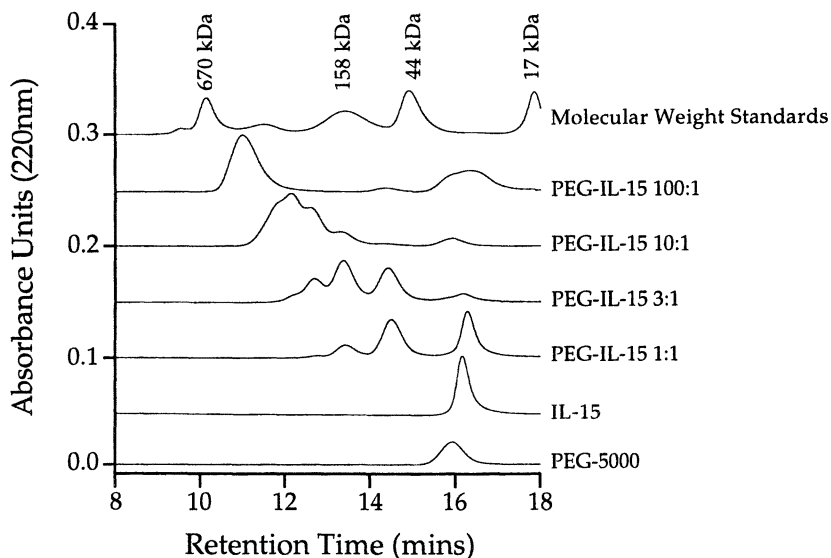


Figure 4. Size exclusion HPLC of PEG-500, IL-15 and PEG-IL-15 at PEG:lysine ratios of 1:1, 3:1, 10:1, and 100:1. Protein molecular mass standards are shown in top chromatogram. Reproduced with permission from reference 11.

Conclusions

Protein PEGylation is a technique which is growing rapidly within the biotechnology industry. Several PEGylated protein products are currently on the market and many more are under clinical investigation and likely to be approved. PEGylation can provide many advantages to the delivery of therapeutic proteins by significantly increasing their serum half-life and many studies have demonstrated that the *in vitro* and *in vivo* function of proteins can be dramatically altered by PEG-modification. PEGylation of proteins can often lead to a reduction in their *in vitro* specific activity. This loss of activity can be minimized by controlling the site of PEGylation through the use of different PEG conjugation chemistries, different PEG molecular weights or by protection of the active site on the protein. A wide variety of PEG reagents are commercially available which can provide a great deal of flexibility in the degree and type of chemistry with which to modify a product. The development of successful PEGylated products will result from a thorough understanding a protein's structure and function, and specifically how the attachment

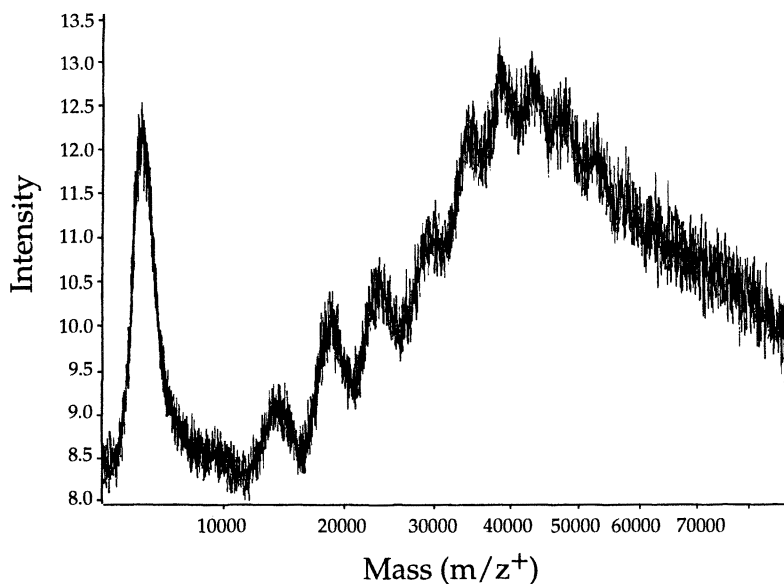


Figure.5. MALDI-TOF mass spectroscopy results for PEG-IL-15 (PEG:lysine ratio of 100:1). Mass per cationic charge (m/z^+) peaks correspond to unconjugated PEG at m/z^+ of 5,000 kDa, unconjugated IL-15 at m/z^+ of approximately 14,000 kDa, and PEG-IL-15 with 1 PEG per IL-15 molecule at m/z^+ of 19,000 kDa, 2 PEGs per IL-15 molecule at m/z^+ of 24,000, 3 PEGs per IL-15 molecule at m/z^+ of 29,000, etc. Reproduced with permission from reference 11.

of PEG affects the protein's bioactivity. PEGylated products of the future may benefit from site directed attachment of the PEG molecules to the peptide backbone which can be controlled by the chemistry on the PEG and/or modification of the amino acid residues on the protein itself.

Literature Cited

1. Bailey, F.E.; Koleske, J.V. *Poly(ethylene oxide)*; Academic Press: New York, NY, 1976.
2. Liu, K.J.; Parsons, J.C. *Macromolecules*. **1969**, *2*, 529-533.
3. Kjellander, R. J. *Chem. Soc. Faraday Trans.* **1982**, *2*, 2025-2042.
4. Working, P.K.; Newmann, M.S.; Johnson, J.; Cornacoff, J.B. In *Poly(ethylene glycol) Chemistry and Biological Applications*; Harris, J.M.; Zalipsky, S.; ACS Symposium Series 680, American Chemical Society: Washington, DC, 1997; pp 45-57.
5. Harris, J.M. *Poly(ethylene glycol) Chemistry Biotechnical and Biomedical Applications*; Plenum Press: New York, NY, 1992. pp 1-385.
6. Mori, Y.; Nagaoka, S.; Takiuchi, H.; Kikuchi, T.; Noguchi, N.; Tanzawa, H.; Noishiki, Y. *Trans. Amer. Soc. Artif. Int. Organs*. **1982**, *28*, 459-463.
7. Gombotz, W.R.; Guanghui, W.; Horbett, T.A.; Hoffman, A.S. *J. Biomed. Mater. Res.* **1991**, *25*, 1547-1562.
8. Abuchowski, A.; Van Es, T.; Palczuk, N.C.; Davis, F.F. *J. Biol. Chem.* **1977**, *252*, 3578-3581.
9. Cunningham-Rundles, C.; Zhuo, Z.; Griffith, B.; Keenan, J. *J. Immunol. Methods*. **1992**, *152*, 177-190.
10. Delgado, C.; Francis, G.E.; Fisher, D. *Crit. Rev. Ther. Drug Carrier Sys.* **1992**, *9*, 249.
11. Pettit, D.K.; Bonnert, T.P.; Eisenman, J.; Srinivasan, S.; Paxton, R.; Beers, C.; Lynch, D.; Miller, B.; Yost, J.; Grabstein, K.H.; Gombotz, W.R. *J. Biol. Chem.* **1997**, *272*, 2312-2318.
12. Harris, J.M. *J. Macromol. Sci. -Rev. Macromol. Chem. Phys.* **1985**, *C25*, 325-373.
13. Clark, R.; Olson, K.; Fuh, G.; Marian, M.; Mortensen, D.; Teshima, G.; Chang, S.; Chu, H.; Mukku, V.; Canova-Davis, E.; Somers, T.; Cronin, M.; Winkler, M.; Wells, J.A. *J. Biol. Chem.* **1996**, *36*, 21969-21977.
14. Watson, E.; Shah, B.; DePrince, R.; Hendren, R.W.; Nelson, R. *BioTechniques*, **1994**, *16*, 278-281.
15. Tuma, R.; Russell, M.; Rosendahl, M.; Thomas G.J. *Biochemistry*. **1995**, *34*, 15150-15156.
16. Mabrouk, P.A. *Bioconjugate Chem.* **1994**, *5*, 236-241.
17. Knusli, C.; Delgado, C.; Malik, F.; Domine, M.; Tejedor, M.C.; Irvine, A.E.; Fisher, D.; Francis, G.E. *British J. Hematol.*, **1992**, *82*, 654-663.
18. Malik, F.; Delgado, C.; Knusli, C.; Irvine, A.E.; Fisher, D.; Francis, G.E. *Exp. Hematol.*, **1992**, *20*, 1028-1035.
19. Sherman, M.; Williams, L.D.; Saifer, M.G.; French, J.A.; Kwak, L.W.; Oppenheim, J.J. In *Poly(ethylene glycol) Chemistry and Biological Applications*; Harris, J.M.; Zalipsky, S.; ACS Symposium Series 680, American Chemical Society: Washington, DC, 1997; pp 155-169.

20. Price, V.; Mochizuki, S.; March, C.J.; Cosman, D.; Deeley, M.C.; Klinke, R.; Clevenger, W.; Gillis, S.; Baker, P.; Urdal, D. *Gene*, **1987**, *55*, 287-293.
21. Kinstler, O.B.; Brems, D.N.; Lauren, S.L.; Paige, A.G.; Hamburger, J.B.; Treuheit, M.J.; *Pharm. Res.* **1996**, *13*, 996-1002.
22. Weinblatt, M.E.; Kremer, J.M.; Bankhurst, A.D.; Bulpitt, K.J.; Fleischmann, R.M.; Fox, R.I.; Jackson, C.G.; Lange, M.; Burge, D.J. *New England J. Medicine.* **1999**, *340*, 253-259..
23. Sartore, L.; Caliceti, P.; Schiavon, O.; Monfardini, C.; Veronese, F.M. *Appl. Biochem. Biotech.* **1991**, *31*, 213-222.
24. Nakai, S.; Mizuno, K.; Kaneta, M.; Hirai, Y. *Biochem. Biophys. Res. Comm.* **1988**, *154*, 1189-1196.
25. Gillis, S.; Ferm, M.M.; Ou, W.; Smith, K.A.; *J. Immunol.* **1978**, *120*, 2027-2032.

Chapter 13

Polymeric Delivery Vehicles for Bone Growth Factors

Lichun Lu, Susan J. Peter, Georgios N. Stamatias,
and Antonios G. Mikos¹

Departments of Bioengineering and Chemical Engineering, Rice University,
6100 Main Street, Houston, TX 77005-1892

Recombinant human transforming growth factor- β 1 (TGF- β 1) was incorporated into biodegradable microparticles of blends of poly(DL-lactic-co-glycolic acid) (PLGA) and poly(ethylene glycol) (PEG) at 6 ng per mg microparticle. Fluorescein isothiocyanate-labelled bovine serum albumin (FITC-BSA) was co-encapsulated as a porogen. The effects of PEG content (0, 1, or 5 wt%) and buffer pH (3, 5, or 7.4) on TGF- β 1 release kinetics and PLGA degradation were determined *in vitro* for up to 28 days. TGF- β 1 was released in a multi-phasic fashion including an initial burst effect. Increasing the PEG content resulted in decreased cumulative mass of released proteins. Aggregation of FITC-BSA occurred at acidic buffer pH, which led to decreased protein release rates. PLGA degradation was also enhanced at 5% PEG, which was significantly accelerated at acidic pH conditions. Co-encapsulation of TGF- β 1 with FITC-Dextran reduced the initial burst effect as compared to FITC-BSA. The TGF- β 1 released from PLGA/PEG microparticles enhanced the proliferation and osteoblastic differentiation of marrow stromal cells cultured on poly(propylene fumarate) (PPF) substrates. The cells showed significantly increased total cell number, alkaline phosphatase (ALPase) activity, and osteocalcin production after 21 days, as compared to cells cultured under control conditions without TGF- β 1. These results suggest that PLGA/PEG blend microparticles can serve as delivery vehicles for controlled release of TGF- β 1, which may find applications in modulating cellular response during bone healing at a skeletal defect site.

Many afflictions require controlled delivery of therapeutic molecules for effective treatment. Transforming growth factor- β 1 (TGF- β 1) has been studied as a potential

¹Corresponding author.

induction factor for bone tissue engineering¹⁻⁴. TGF- β 1 is a multifunctional protein that regulates many aspects of cellular activity including cell proliferation, differentiation, and extracellular matrix metabolism, in a time- and concentration-dependent fashion⁴. It plays a significant role in regulating bone formation at a fracture callus⁵, and has been shown to increase osteoblast proliferation and differentiation during fracture healing in a rat femur model⁶. Furthermore, TGF- β 1 was used to enhance healing *in vivo* in a canine total joint replacement model⁷. Controlled release of TGF- β 1 to a bone defect may therefore be beneficial for the induction of a bone regeneration cascade.

Microparticles made of biodegradable polymers have been widely utilized as vehicles for drug delivery. They can be implanted at an afflicted site during surgery or injected as a suspension to a wound area. Alternatively, microparticles can be impregnated into polymer scaffolds and then transplanted⁸. Among different polymers, poly(DL-lactic-co-glycolic acid) (PLGA) copolymers have been extensively studied as microparticle carriers for many bioactive molecules⁹⁻¹². PLGA copolymers are biocompatible, biodegradable, and approved by the FDA for certain human clinical uses¹³.

Release rates of bioactive molecules can be modulated by altering the molecular weight of PLGA as well as the ratio of lactic to glycolic acid in the copolymer¹⁰. The combination of poly(ethylene glycol) (PEG) and PLGA as a blend to form microparticle carriers allows further attenuation of the release profile of the loaded compound¹⁴. In addition, the release of compounds is also affected by co-encapsulation of other molecules in the microparticle formulations¹⁵. Furthermore, the protein release profiles are also dependent on environmental conditions such as the acidity of the release medium. For example, the inflammatory response following implantation of devices or the release of acidic PLGA degradation products at late stages of microparticle degradation often results in decrease in local pH^{10,16}. This decrease in pH can affect the structure, solubility, diffusivity, and activity of the loaded compound.

A novel injectable, *in situ* polymerizable, biodegradable orthopaedic material based on poly(propylene fumarate) (PPF) for filling skeletal defects has recently been developed in our laboratory¹⁷. PPF, combined with a vinyl monomer (*N*-vinyl pyrrolidinone) and an initiator (benzoyl peroxide), forms an injectable paste that can be polymerized *in situ*, filling skeletal defects of any shape or size¹⁸. Additionally, incorporation of solid phase components including β -tricalcium phosphate (β -TCP) and sodium chloride can result in a porous composite material possessing mechanical properties sufficient for the replacement of human trabecular bone¹⁹. Furthermore, marrow stromal cells were shown to attach, proliferate, and express differentiated osteoblastic function when cultured on PPF/ β -TCP substrates *in vitro*²⁰. It is an objective of our laboratory to develop an injectable formulation that may provide a vehicle for delivery of microparticle carriers of growth factors to the defect site and induce bone regeneration.

The present study addresses the effects of PEG content and buffer pH on the release kinetics of TGF- β 1 from biodegradable PLGA/PEG blend microparticles and the degradation of PLGA, as well as the effects of TGF- β 1 released from these microparticles on the proliferation and differentiation of primary rat marrow stromal cells seeded on PPF substrates.

Controlled Release of Transforming Growth Factor- β 1 from Biodegradable Polymer Microparticles

Biodegradable Polymer Microparticles

Microparticles of blends of poly(DL-lactic-*co*-glycolic acid) (PLGA; Medisorb[®], Alkermes, Cincinnati, OH) with a 50:50 lactic to glycolic acid copolymer ratio and poly(ethylene glycol) (PEG; Aldrich, Milwaukee, WI) were fabricated using a double-emulsion-solvent-extraction technique ((water-in-oil)-in-water) as previously described^{14,21}. PLGA had a weight average molecular weight (Mw) of 46,700 and a polydispersity index (PI) of 1.73, as determined by gel permeation chromatography (GPC)¹⁶. PEG with a Mw of 10,700 was incorporated at 0, 1, and 5 wt% in the microparticles. Recombinant human transforming growth factor- β 1 (TGF- β 1; R&D Systems, Minneapolis, MN) with a molecular weight of 25,000 was loaded at 6 ng per mg microparticle. Fluorescein isothiocyanate-labelled bovine serum albumin (FITC-BSA; Sigma, St. Louis, MO) with a molecular weight of 68,000 was co-encapsulated as a porogen at 4 μ g per mg microparticle.

The average diameter of the microparticles containing 0, 1, or 5 wt% initial PEG, reported as mean \pm standard deviation (SD) based on normal distribution, was 20.0 ± 11.9 , 18.8 ± 9.9 , and 23.3 ± 13.7 μ m, respectively. The entrapment efficiency of the proteins in the microparticles was determined by normalizing the amount actually entrapped to the starting amount, using an established solvent extraction technique¹⁴. The entrapment yields of TGF- β 1 were $83.4 (\pm 13.1)$, $84.6 (\pm 16.4)$, and $54.2 (\pm 12.1)$ % ($n = 4$) for PEG contents of 0, 1, and 5 wt%, respectively. Single factor analysis of variance (ANOVA) was used to assess statistical significance of results. Scheffé's test showed the entrapment efficiency at 5% PEG was significantly lower ($p < 0.05$), which may be due to the leaching of compounds with soluble PEG during microparticle fabrication.

Scanning electron microscopy (SEM) revealed that the fabricated PLGA/PEG microparticles were spherical in shape, with smooth, non-porous surfaces (Fig. 1a). In addition, fluorescence images indicated fairly uniform distribution of FITC-BSA (and probably TGF- β 1) throughout the microparticles (Fig. 1b).

TGF- β 1 Release Kinetics

The release kinetics of TGF- β 1 from PLGA/PEG microparticles were studied under six experimental conditions. Microparticles with varied initial PEG contents (0, 1, and 5 wt%) were placed in pH 7.4 phosphate buffered saline (PBS) for up to 28 days. Additional microparticles containing 5% PEG were incubated in buffers of pH 3, 5, or 7.4. At the end of various time points, the amounts of TGF- β 1 in the releasing media were analyzed by enzyme-linked immunosorbent assay (ELISA).

Both microparticle PEG content (Fig. 2a) and medium acidity (Fig. 2b) were found to affect the release of TGF- β 1 from the microparticles. After 2 days in PBS, 2.9 ± 0.2 , 2.7 ± 0.3 , and 1.9 ± 0.3 ng of the compound per mg microparticle were released for initial PEG content of 0, 1, and 5 wt%, respectively. While in buffers of

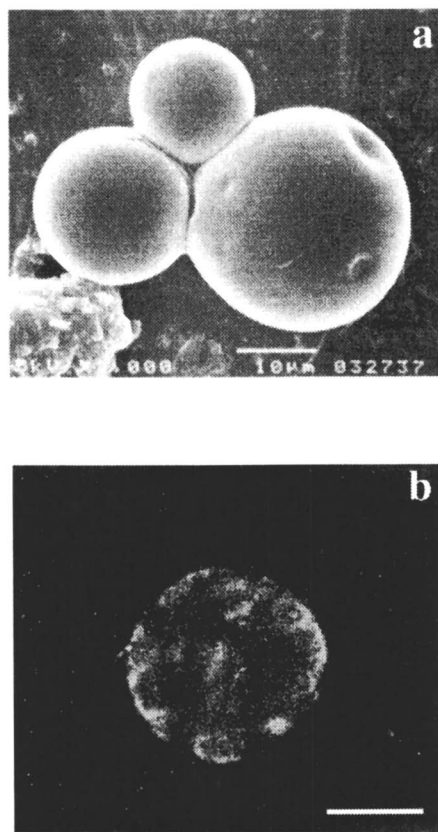


Figure 1. Fabricated PLGA/PEG blend microparticles with 5 wt% PEG: (a) scanning electron micrograph and (b) fluorescence micrograph. Scale bar is 20 μm for (b).

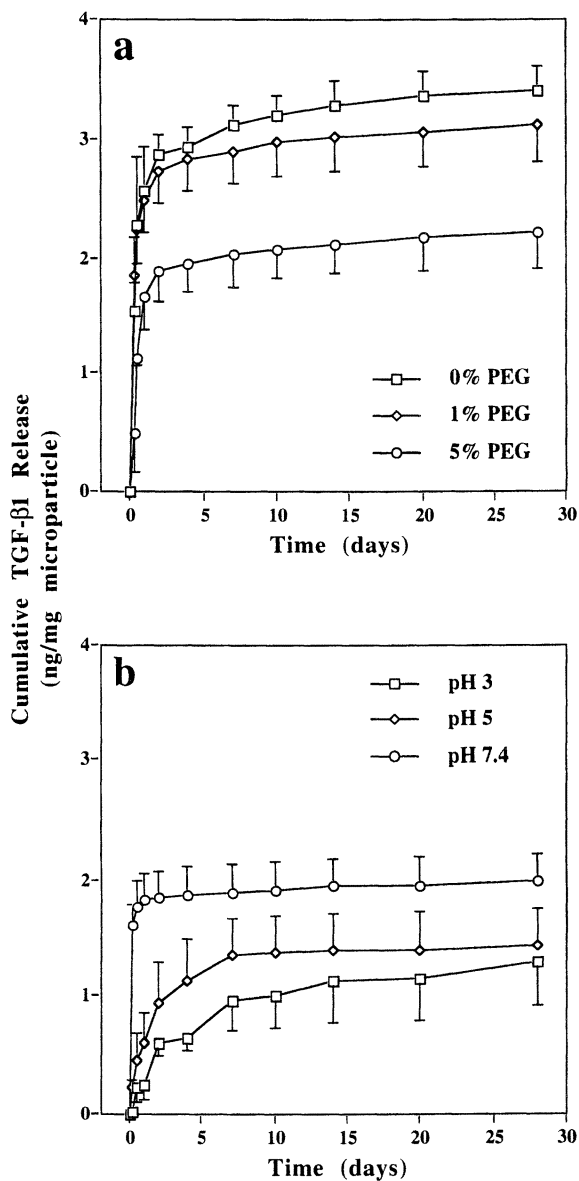


Figure 2. Cumulative release kinetics of TGF- β 1 (co-encapsulated with FITC-BSA) from PLGA/PEG microparticles for different (a) PEG content and (b) buffer pH. Error bars represent means \pm SD for $n = 4$.

pH 3, 5, and 7.4, 0.6 ± 0.1 , 0.9 ± 0.4 , and 1.9 ± 0.2 ng of TGF- β 1 per mg of microparticle were released from microparticles containing 5% PEG, respectively. At pH 7.4 (either PBS or pH buffer), the initial burst was followed by a linear phase of slow release rate reaching a plateau. In acidic pH, however, the initial burst was followed by a fast linear release phase (days 1-8) and then by a slower one (days 9-28). The cumulative mass of released TGF- β 1 was increased at lower PEG content or higher buffer pH. After 28 days, 3.4 ± 0.2 and 2.2 ± 0.3 ng of loaded TGF- β 1 were released from microparticles with 0 and 5% PEG in pH 7.4 PBS, and 2.0 ± 0.2 and 1.3 ± 0.4 ng released for 5% PEG in pH 7.4 and 3 buffers, respectively.

***In vitro* degradation of microparticles**

The degradation of PLGA/PEG microparticles (loaded with TGF- β 1 and FITC-BSA) were studied under the same conditions as in the protein release experiments. The Mw of PLGA, evaluated by GPC, decreased continuously throughout the time course for microparticles with varied PEG content placed in pH 7.4 PBS (Fig. 3a). By day 28, $35.6 (\pm 0.5)$, $34.4 (\pm 1.3)$, and $29.5 (\pm 1.5)$ % of the day 0 Mw remained for microparticles with 0, 1, and 5 wt% PEG, respectively. The half-life of PLGA, calculated by fitting the data for Mw to an exponential function of time¹⁴, was 15.9 ± 1.2 days for microparticles with 5% PEG, significantly lower ($p < 0.05$) than that for 0 and 1% PEG (20.3 ± 0.9 and 18.9 ± 0.5 days, respectively).

Degradation profiles of PLGA microparticles with 5% initial PEG content in various pH buffers are shown in Fig. 3b. By day 28, the remaining Mw of PLGA placed in pH 3, 5, and 7.4 buffers was $3.1 (\pm 0.3)$, $14.0 (\pm 0.8)$, and $25.6 (\pm 4.6)$ % of the day 0 value, respectively. The corresponding half-lives of PLGA were 5.5 ± 0.1 , 10.9 ± 0.4 , and 14.8 ± 0.4 days, significantly dependent on the environmental pH ($p < 0.01$).

Fluorescence images showed that the distribution of FITC-BSA was mainly at the peripheral of the microparticles after 14 days of degradation in pH 7.4 buffers (Fig. 4a). Most of the protein was released by day 28 (Fig. 4b). However, under acidic conditions such as pH 3, FITC-BSA had limited solubility. This led to aggregation of FITC-BSA in the polymer matrix, as confirmed by enhanced fluorescence after 14 days (Fig. 4c). The aggregated FITC-BSA formed a paste-like structure after complete PLGA degradation at 28 days (Fig. 4d). The decreased release of both TGF- β 1 and FITC-BSA at lower pH is believed to result from this aggregation of insoluble compounds.

Effects of TGF- β 1 Released from Biodegradable Polymer Microparticles on Marrow Stromal Osteoblast Culture

Biodegradable Polymer Substrates

Poly(propylene fumarate) (PPF) was synthesized from fumaryl chloride and propylene glycol in the presence of potassium carbonate, a proton scavenger. The

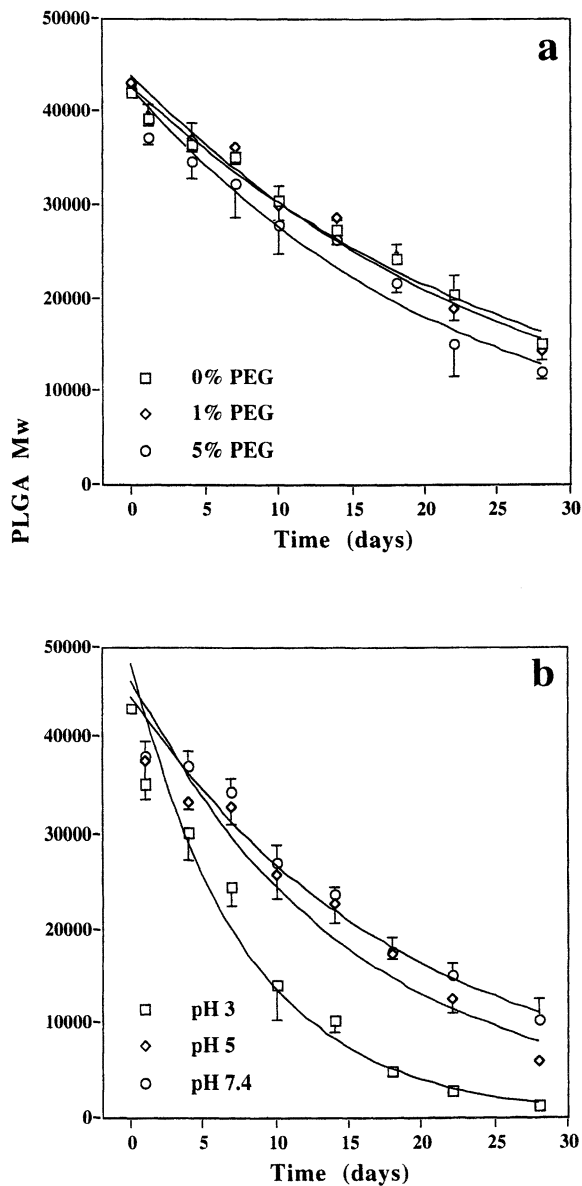


Figure 3. Decrease of weight average molecular weight (M_w) of PLGA in PLGA/PEG microparticles for different (a) PEG content and (b) buffer pH. Error bars represent means \pm SD for $n = 4$.

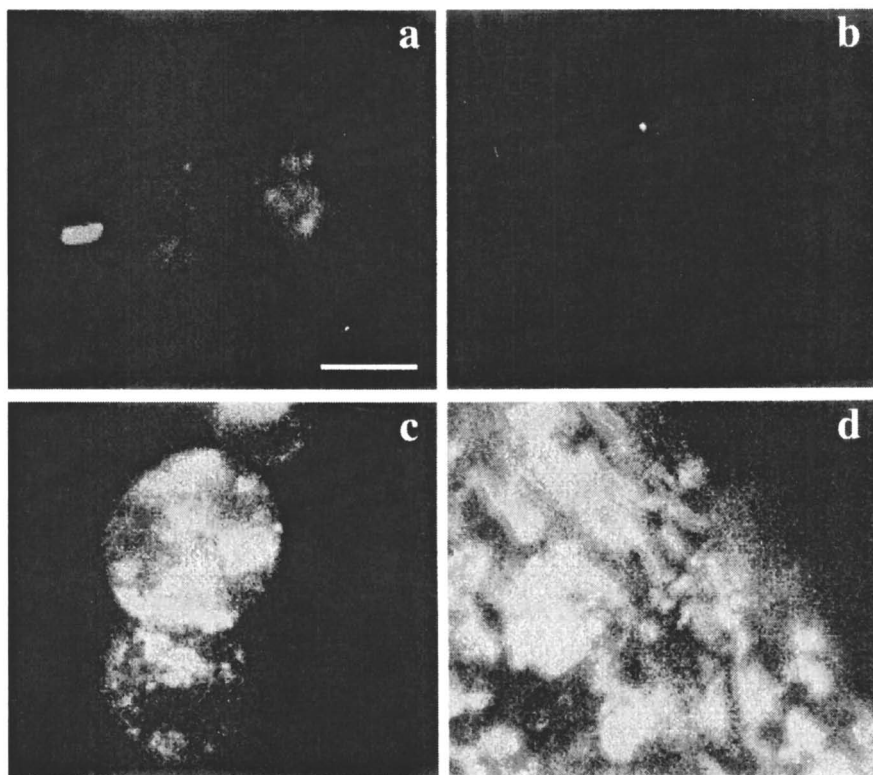


Figure 4. Fluorescence micrographs showing the distribution of FITC-BSA within PLGA/PEG microparticles with 5 wt% PEG after (a,c) 14 and (b,d) 28 days of in vitro degradation in (a,b) pH 7.4, and (c,d) pH 3 buffers. Scale bar is 20 μm .

resulted PPF (1 g) was then mixed with *N*-vinyl pyrrolidinone (0.33 mL) and benzoyl peroxide (0.005 g) in a cylindrical mold (1.8 cm diameter). Cured cylinders were sectioned into 1.5-mm thick disks. These discs, after leaching out unreacted material, drying, sterilization by ethylene oxide, and prewetting with sterile PBS, were used as substrates for cell culture.

TGF- β 1 Release Kinetics

TGF- β 1 was incorporated into PLGA/PEG blend microparticles with 5 wt% PEG at 6 ng per mg microparticle. FITC-Dextran was co-encapsulated as a porogen at 1 wt%. The entrapment efficiency of TGF- β 1 was 40.3 (\pm 1.2) % (n = 3), corresponding to an actual loading of 2.42 ng per mg microparticle. The release kinetics showed that 17.9 (\pm 0.6) and 32.1 (\pm 2.5) % of loaded TGF- β 1 was released after 1 and 8 days, respectively, followed by a plateau for the remaining 3 weeks (Fig. 5). FITC-Dextran allowed modulation of TGF- β 1 release profiles with a smaller burst effect as compared to FITC-BSA described in the previous section. After 24 h, 54% of the total released TGF- β 1 was freed from the microparticles, in contrast to a value of 75% when co-encapsulated with FITC-BSA.

Marrow Stromal Cell Function in Response to Released TGF- β 1

The femurs and tibias of 6-week-old male Sprague-Dawley rats were harvested as previously described to isolate marrow stromal cells²². After 10 days of expansion in tissue culture flasks, the marrow-derived cells were seeded at 24,000 cells/cm² onto tissue culture polystyrene (TCPS) and PPF substrates placed at the bottom of transwell plates. Complete media containing Dulbecco's modified eagle medium (DMEM) supplemented with 10% fetal bovine serum (FBS), 20 μ g/mL penicillin/streptomycin/neomycin (PSN), 20 μ g/mL fungizone, 1×10^{-7} M dexamethasone, 10 mM Na β -glycerol phosphate, and 50 μ g/mL L-ascorbic acid were added to each well. The cells were subsequently maintained in complete media for 24 h to induce the osteoblastic phenotype of the marrow stromal cells²³. Microparticles with encapsulated TGF- β 1 and FITC-Dextran were suspended in primary media (DMEM supplemented with 10% FBS, 20 μ g/mL PSN, and 20 μ g/mL fungizone) and added to the top portion of transwell plates. Cells seeded on PPF substrates and treated with blank microparticles with neither TGF- β 1 nor FITC-Dextran, as well as cells seeded on PPF and TCPS and cultured in the absence of any microparticles served as controls. The effects of TGF- β 1 released from PLGA/PEG microparticles on marrow stromal cell proliferation and function were assessed during a 21-day period.

Cell Number

Cell proliferation was assessed by measuring the total cell numbers using the DNA assay²⁴ (Fig. 6). The cell numbers increased rapidly for all sample sets through day 7, indicating high proliferative activity of the cells. This was followed by a plateau for the rest of the time course with little cell proliferation. The sample sets exposed to released TGF- β 1 had significantly higher cell counts after day 7. By day

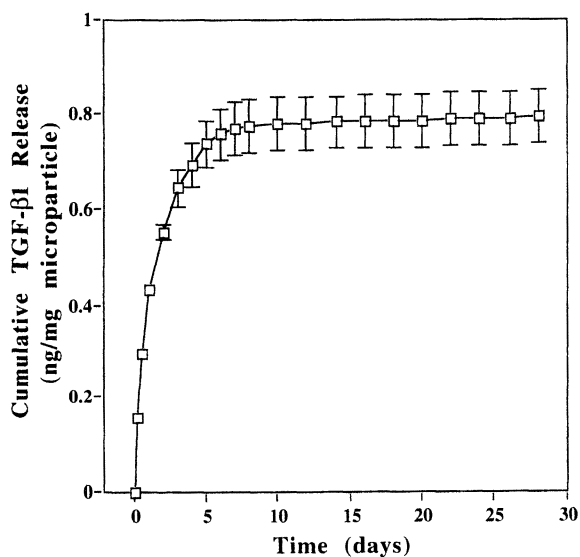


Figure 5. Cumulative release kinetics of TGF- β 1 (co-encapsulated with FITC-Dextran) from PLGA/PEG microparticles into pH 7.4 PBS. Error bars represent means \pm SD for $n = 3$.

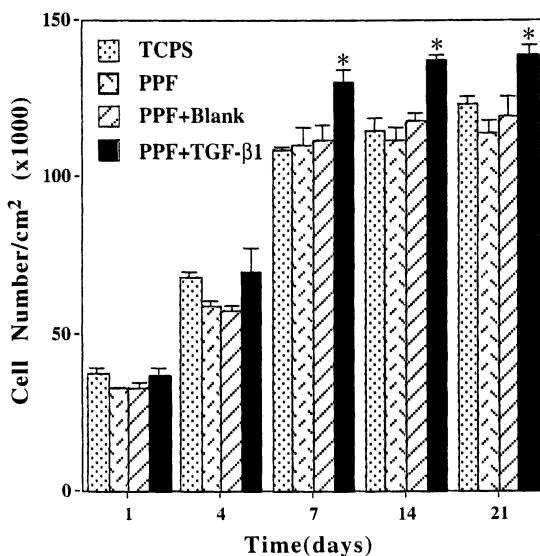


Figure 6. Total number of marrow stromal cells cultured on PPF substrates in the presence of TGF- β 1-loaded PLGA/PEG microparticles during 21 days of in vitro culture. PPF substrates with blank microparticles, PPF, and TCPS served as controls. Error bars represent means \pm SD for $n = 3$. Star indicates values significantly higher than all the control groups.

21, the total number of cells cultured on PPF in the presence of TGF- β 1 had reached $138,700 \pm 3,300$ cells/cm², while those for control sample sets TCPS, PPF, and blank microparticles were $123,700 \pm 2,300$, $114,300 \pm 3,900$ and $119,600 \pm 6,100$ cells/cm², respectively.

Alkaline Phosphatase Activity

Cell function was monitored by determining the expression of two markers of osteoblastic phenotype: alkaline phosphatase (ALPase) activity and osteocalcin production²⁴. At day 7, all sample sets had a moderate level of ALPase activity, with no difference in activity between sample sets (Fig. 7). However, at both day 14 and 21, the ALPase activity was significantly higher ($p < 0.05$) for the cells maintained in the presence of TGF- β 1 than all control conditions. The ALPase activity for this sample set at day 21 was $22.8 (\pm 1.5) \times 10^{-7}$ μ mole/min/cell, significantly higher than the next highest value of $16.3 (\pm 2.9) \times 10^{-7}$ μ mole/min/cell for the cells cultured on PPF with blank microparticles.

Osteocalcin Production

The effect of TGF- β 1 on osteocalcin production of marrow stromal cells was similar to that observed for ALPase activity. The cells exposed to TGF- β 1 had a significantly higher ($p < 0.05$) level of osteocalcin released into the medium than those maintained in the absence of TGF- β 1 (Fig. 8), reaching $15.9 (\pm 1.5) \times 10^{-6}$ ng/cell at this time point. The control cultures had values of $13.0 (\pm 1.0) \times 10^{-6}$ ng/cell for TCPS substrates, $12.5 (\pm 1.6) \times 10^{-6}$ ng/cell for PPF substrates, and $12.2 (\pm 1.2) \times 10^{-6}$ ng/cell for the PPF cultures exposed to blank microparticles.

Conclusions

TGF- β 1 was encapsulated along with FITC-BSA into PLGA/PEG blend microparticles and released in a controlled fashion *in vitro* for up to 28 days. Increasing the initial PEG content resulted in lower entrapment efficiency of TGF- β 1 and decreased cumulative mass of released compound. Protein release was decreased under acidic pH due to aggregation of FITC-BSA. The degradation of PLGA was increased at higher PEG content, and significantly accelerated at lower buffer pH. Co-encapsulation with FITC-Dextran resulted in reduced initial burst effect of released TGF- β 1. The TGF- β 1 released from the microparticles enhanced the proliferation and osteoblastic differentiation of marrow stromal cells cultured on PPF substrates, as indicated by the increased total cell number, ALPase activity, and osteocalcin production over a period of 21 days.

Acknowledgments

This work was completed through funding provided by the National Institutes of Health (R01-AR44381). S.J. Peter acknowledges financial support by the National Institutes of Health Biotechnology Training Grant 5T32GM08362.

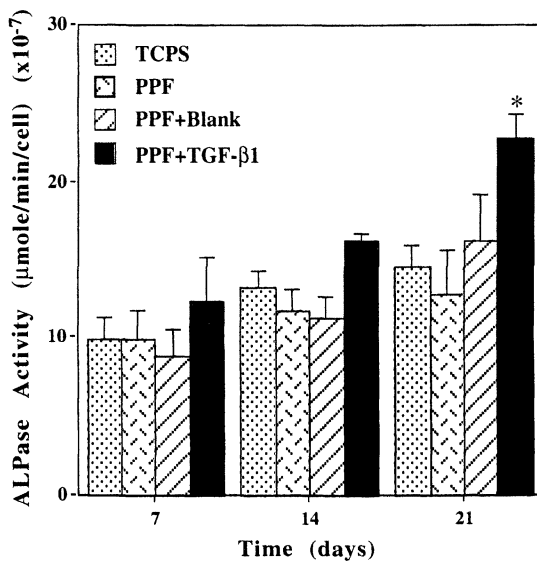


Figure 7. Alkaline phosphatase (ALPase) activity of marrow stromal cells cultured on PPF substrates in the presence of TGF- β 1-loaded PLGA/PEG microparticles during 21 days of *in vitro* culture. PPF substrates with blank microparticles, PPF, and TCPS served as controls. Error bars represent means \pm SD for $n = 3$. Star indicates values significantly higher than all the control groups.

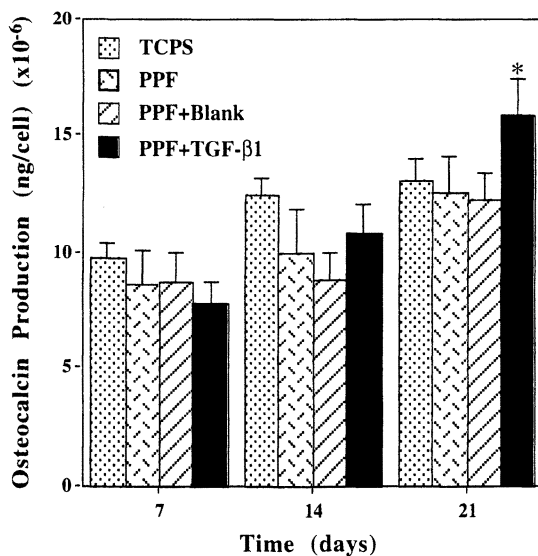


Figure 8. Osteocalcin production of marrow stromal cells cultured on PPF substrates in the presence of TGF- β 1-loaded PLGA/PEG microparticles during 21 days of *in vitro* culture. PPF substrates with blank microparticles, PPF, and TCPS served as controls. Error bars represent means \pm SD for $n = 3$. Star indicates values significantly higher than all the control groups.

References

1. Hock, J. M.; Canalis, E.; Centrella, M. *Endocrin* **1990**, *126*, 491-426.
2. Beck, L. S.; Deguzman, L.; Lee, W. P.; Xu, Y.; McFatrige, L. A.; Gillett, N. A.; Amento, E. P. *J Bone Min Res* **1991**, *6*, 1257-1265.
3. Hollinger, J. O.; Leong, K. *Biomaterials* **1996**, *17*, 187-194.
4. Nimni, M. E. *Biomaterials* **1997**, *18*, 1201-1225.
5. Sandberg, M. M.; Aro, H. T.; Vuorio, E. I. *Clin Orthop Rel Res* **1993**, *289*, 292-312.
6. Joyce, M., A. Roberts, M. Sporn, and M. Bolander. *J Cell Biology* **1990**, *110*, 2195-2207.
7. Sumner, D. R.; Turner, T. M.; Purchio, A. F.; Gombotz, W. R.; Urban, R. M.; Galante, J. O. *J Bone Joint Surg* **1995**, *77-A*, 1135-1147.
8. Lu, L.; Mikos, A. G. *Science Med* **1999**, *6*, 6-7.
9. Cohen, S.; Yoshioka, T.; Lucarelli, M.; Hwang, L. H.; Langer, R. *Pharm Res* **1991**, *8*, 713-720.
10. Anderson, J. M.; Shive, M. S. *Adv Drug Deliv Rev* **1997**, *28*, 5-24.
11. Crotts, G.; Park, T. G. *J Microencapsul* **1998**, *15*, 699-713.
12. Cao, X.; Shoichet, M. S. *Biomaterials* **1999**, *20*, 329-339.
13. Suggs, L. J.; Mikos, A. G. *Physical Properties of Polymers Handbook*; Mark, J. E., Ed.; American Institute of Physics: Woodbury, New York, 1996, pp 615-624.
14. Cleek, R. L.; Ting, K. C.; Eskin, S. G.; Mikos, A. G. *J Control Release* **1997**, *48*, 259-268.
15. Krewson, C. E.; Dause, R.; Mak, M.; Saltzman, W. M. *J Biomater Sci Polym Ed* **1996**, *8*, 103-117.
16. Lu, L.; Garcia, C. A.; Mikos, A. G. *J Biomed Mater Res* **1999**, *46*, 236-244.
17. Peter, S. J.; Suggs, L. J.; Yaszemski, M. J.; Engel, P. S.; Mikos, A. G. *J Biomater Sci Polym Ed* **1999**, *10*, 363-373.
18. Yaszemski, M. J.; Payne, R. G.; Hayes, W. C.; Langer, R. S.; Aufdemorte, T. B.; Mikos, A. G. *Tissue Eng* **1995**, *1*, 41-52.
19. Peter, S. J.; Kim, P.; Yasko, A. W.; Yaszemski, M. J.; Mikos, A. G. *J Biomed Mater Res* **1999**, *44*, 314-321.
20. Peter, S. J.; Lu, L.; Kim, D. J.; Mikos, A. G. *Biomaterials*, submitted.
21. Cleek, R. L.; Rege, A. A.; Denner, L. A.; Eskin, S. G.; Mikos, A. G. *J Biomed Mater Res* **1997**, *35*, 525-530.
22. Ishaug, S. L.; Crane, G. M.; Miller, M. J.; Yasko, A. W.; Yaszemski, M. J.; Mikos, A. G. *J Biomed Mater Res* **1997**, *36*, 17-28.
23. Jaiswal, N.; Bruder, S. P. *J Bone Min. Res* **1996**, *11*, S-259.
24. Peter, S. J.; Liang, C. R.; Kim, D. J.; Widmer, M. S.; Mikos, A. G. *J Cell Biochem* **1998**, *71*, 55-62.

Chapter 14

De Novo Design and Synthesis of a Small Globular Protein That Forms a Pore in Lipid Bilayers

Sannamu Lee¹, H. Michael Ellerby², Taira Kiyota¹,
and Gohsuke Sugihara¹

¹Department of Chemistry, Faculty of Science, Fukuoka University,
Fukuoka 814-0180, Japan

²Program on Aging and Cancer, The Burnham Institute,
La Jolla Cancer Research Center, La Jolla, CA 92121

We report here the design and synthesis of a native-like and pore-forming small protein (SGP) and its related analogs. SGP consists of 69 amino acid residues divided over four helical parts, 3 basic amphiphilic helices surrounding a central hydrophobic helix. SGP takes a stable globular-like structure in aqueous solution. In the SGP proteins, the hydrophobic central α -helix is able to enter spontaneously into lipid bilayers, and the Trp in central α -helix is located about in the middle of the alkyl chain in the outer layer of the phospholipid bilayer. The protein is also able to increase the membrane permeability with two modes of current in planar phospholipid bilayers, indicating that the spontaneous insertion of the protein into lipid bilayers, and then the formation of channel pores. SGP also induced apoptosis (Apoptosis is an evolutionarily conserved form of cell suicide).

Design, synthesis and characterization of SGP

Colicins, water-soluble toxic proteins have been investigated in order to understand how they enter spontaneously into a nonpolar membrane environment. The C-terminal of colicin A is a folding structure composed of 10 α -helices, two of them forming a hydrophobic helical hairpin buried in the soluble protein (1). In the first phase of the membrane penetration, the protein unfolds into a flexible conformation, so called molten globular state. The molten globular structure lowers the energy required for the hydrophobic hairpin to slip in, leaving an opened umbrella-like structure. This insertion mechanism appears common to all pore-forming colicins (2). However, the picture of protein translocation and pore-formation is not complete yet, because good model systems to obtain details of the mechanism of lipid bilayer insertion are not available. Thus we designed and synthesized a small globular protein

(SGP) to better understand the insertion of membrane targeting proteins into biomembranes, and studied the folding structure in aqueous solution as well as the actual penetration mechanism into lipid bilayers (3).

The protein designed and synthesized has four helices with a short hydrophobic helix and three long basic amphiphilic helices in 69 amino acid residues, and is expected to spontaneously insert itself into membrane (Fig 1A). SGP is divided over four helical parts; 3 basic amphiphilic helices composed of Leu and Lys and a hydrophobic helix composed of oligoalanine in the middle (Fig 1B). The appropriate periodical distribution of Leu and Lys along chains can induce a stable amphiphilic helical structure at apolar surfaces such as the hydrophobic sites of protein and phospholipid membrane (4). The oligoalanine (n=10) was selected as the hydrophobic central helix, which is the smallest in size and shorter in chain length than the other three helices (n = 15). The three helices composed of Lys and Leu residues take an amphiphilic structure when represented as α -helical wheels. To look at the folding structures, one Trp was introduced in the hydrophobic helix and one Tyr in each amphiphilic helix; the Tyr residue in α -2 is located in hydrophobic region of amphiphilic helix and the two Tyr in α -3 and α -4 are located in hydrophobic ones (Fig. 1C). The α -1 and α -2 helices were connected by a β -turn-forming sequence, Gly-Pro-Asn-Gly to tightly fold, while for connections between the other helices (α -2, α -3 and α -4), a β -turn-unfavorable one, Gly-Asn-Pro-Gly was employed to afford flexibility for bending at need. It is reasonable to consider that the hydrophobic helix of SGP will be located to make a hydrophobic core in the central part of the protein as the hydrophobic core is surrounded by amphiphilic helices. In aqueous solution, SGP is expected to take a globular protein-like structure as shown in Fig. 1A.

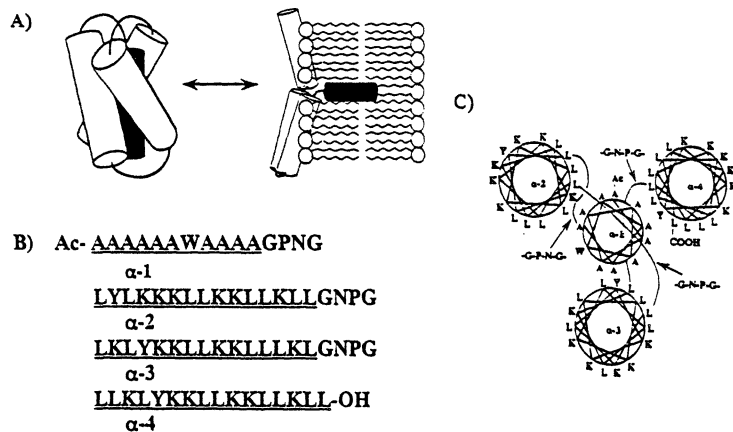


Figure 1. (A) A schematic illustration of expected folding state and open umbrella state of SGP in buffer and in membrane, respectively. (B) Amino acid sequence of SGP, and (C) helical wheel representation of SGP.

SGP was synthesized according to 9-fluorenylmethoxycarbonyl (Fmoc)-chemical procedure starting from Fmoc-Leu-PEG (polyethylene glycol)-resin by using a Miligen automatic peptide synthesizer model 9050. After the cleavage from the resin by trifluoroacetic acid, the crude peptide obtained was purified by HPLC chromatography. To demonstrate whether SGP is monomeric or oligomeric in buffer solution, size-exclusion chromatography was performed using a packed column for HPLC. Several natural proteins, known to form compact globular structures, were used as calibration standard. SGP was eluted as a single peak with some tailing from the gel filtration column. The location of this peak is consistent with the expected molecular mass of this protein, indicating that it is monomeric. This is also supported from analytical ultracentrifugation. The observed molecular weight is about 7600 at a concentration of about 50 μ M (Table I).

Table I. α -Helical contents and molecular weights of SGP and its related peptides.

<i>Peptide</i>	<i>α-Helical contents (%)</i>	<i>Theoretical</i>	<i>M. W. SED^a</i>	<i>HPLC^b</i>
SGP	52.2	7555	7500	6000
SGP-L	53.4	7979	25000	30000
SGP-E	50.4	7522	16000	27000
SGP-G	49.1	7263	10000	–

a) The sedimentation equilibrium experiments were carried out in a Beckman XLA-TG-2 analytical ultracentrifuge at 30 000 rpm, 20 °C in 5 mM Tris, 100 mM NaCl, pH 7.4). The data were analyzed by using XLAEQ program algorithm and molecular weight (M) was calculated from the following equation, $M_b(\text{molecular buoyant})=M(1-\nu r)$. The values of 0.75 and 1 were used as ν (partial specific volume of the particle) and r (density of the solvent), respectively. b) Size-exclusion chromatography was performed using Tris buffer (10 mM Tris, 150 mM NaCl, pH 5.0) on a packed column for HPLC, COSMOSIL 5DIOL-120 (Nakalai Tesk, Japan).

The conformations of SGP were studied by ultraviolet CD spectroscopic methods (Fig. 2A). The dichroic spectrum in 80% trifluoroethanol exhibits negative minima at 206 and 222 nm, characteristic of α -helical structure. In buffer solution, SGP also has a significant content (50%) of helical residues. Interestingly, the presence of egg PC liposomes increased the helical content to 60%.

To understand the stability of SGP, CD and fluorescence spectra were measured as functions of temperature and of guanidine-HCl (Gu·HCl) concentration (Fig. 2B and 2C, respectively). The intensities of minimum trough at 222 nm were decreased linearly with increasing temperature in the range of 20-90 °C. However 100 % unfolding was not observed even at 90 °C, at which the α -helical content was 35 %. With increasing concentration, unfolding started at about 4 M Gu·HCl and completed unfolding at 6 M Gu·HCl (Fig. 2C). The emission maxima of Trp-fluorescence shifted gradually to red wavelength with increasing concentration of Gu·HCl. A relatively strong change was observed in the range of 3 M to 5 M Gu·HCl (Fig. 3C), suggesting that the brief conformational change around Trp residue starts just before the starting of unfolding of α -helical structure.

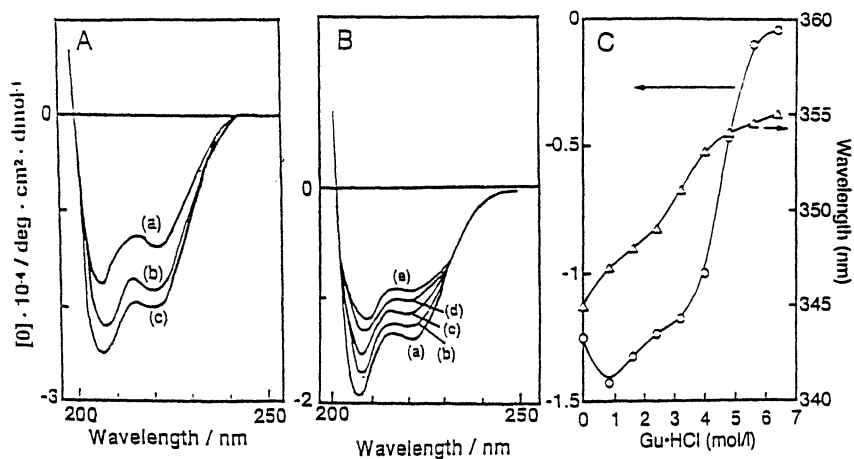


Figure 2. Circular dichroism and Trp-fluorescence behavior of SGP (A) CD spectra of the peptide in buffer (5 mM Tes HCl, and 100 mM NaCl at pH 7.4) (a), in the presence of egg PC liposomes (b) and in trifluoroethanol (c) (B) Temperature dependence of CD spectra in Tes buffer. Curves / °C: a, 20; b, 40; c, 60; d, 80; e, 90. (C) Gu·HCl denaturation profiles at 25 °C plotted on the basis of the ellipticity at 222 nm (circle, left y-axis) and emission maximum of Trp-fluorescence excited at 285 nm (triangle, right y-axis).

Next, to examine the translocation of peptide into membrane and to collect detailed information of the position of the helices within the lipid bilayers, the quenching behavior of n-doxylstearic acids in egg PC vesicles was investigated (Fig. 3A) (5). Depth-dependent fluorescent quenching of a Trp located at the hydrophobic helices was checked using a set of n-doxylstearic acids ($n=5, 10, 16$). The n-stearic acid bearing the nitroxide label at position 10 (10-NS) incorporated into egg PC liposomes drastically quenched the Trp fluorophore, but 5-NS and 16-NS did weakly. Titrating study of the peptide by n-doxylstearic acids incorporated into outer layer of egg PC liposomes was performed at several lipid concentrations; the results showed that the quenching efficiency is in the order $10\text{-NS} \gg 16\text{-NS} > 5\text{-NS}$. From these fluorescence experiments we concluded that the central helix is localized in lipid bilayers perpendicularly, in which the Trp residue is present at intermediate depth of lipid core at outer layer of lipid bilayers, while the three amphiphilic helices may be left at lipid surface, horizontally. This conclusion was also confirmed from the quenching experiment using the lipid bilayers containing 1,2-bis(9,10-dibromostearoyl)phosphatidylcholine (9,10-DBrPC). As shown in Fig. 3B, the fluorescence quenching caused by bromines attached to the 9 and 10 positions of the twin acyl chains of phospholipid was gradually increased with increasing content of DBrPC in egg PC liposomes (6). SGP undergoes a conformational change that results in transferring the Trp position from the protein interior to the area near the 9, 10 positions of the phospholipid acyl chain.

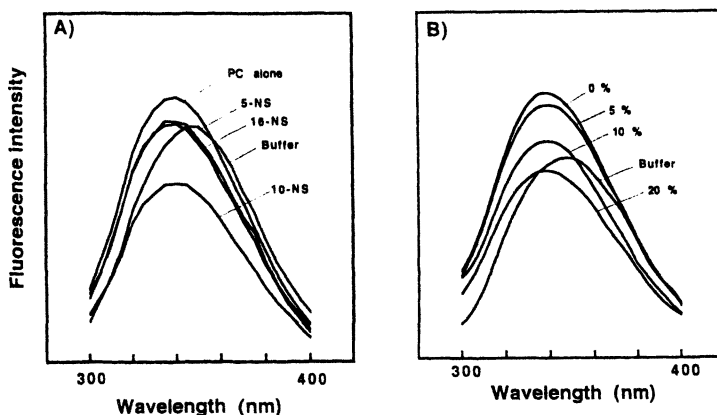


Figure 3. (A) Quenching of Trp fluorescence by various *n*-doxylstearic acids in the presence of egg PC liposomes at 25 °C. Peptide (5 μ M) was added to egg PC liposome (100 μ M) solution containing 4% *n*-doxylstearic acids. (B) Quenching of Trp fluorescence by egg PC liposomes containing different concentrations of DBrPC at 25 °C. Peptide concentration is 5 μ M. Lipid concentration is 200 μ M.

Finally, the planar bilayer method (7) was employed to further examine whether the peptide is able to move into the lipid bilayers and to increase the membrane permeability by forming something like an ion channel. When the methanol solution of SGP was added, the membrane current was rapidly increased at first and the rate of the increase was gradually slowed down (Fig. 4A). Here, the current is referred to as basal current. After the basal current reached a certain level, discrete current changes corresponding to channel-event appeared overlapping the basal current. The channels increased in multiples of the single channel level (Fig. 4B) with time at the later part of the trace of Fig. 4A. When the concentration of KCl was asymmetrical (cis: 600 mM, trans: 150 mM), SGP also induced two types of membrane currents (basal current and channel current) at almost zero membrane potential. Interestingly, the ion selectivity between the basal current and channel event is different. Although no exact ion selectivity of both currents was determined yet, the basal current was a little anion-selective while the channel event was cation-selective.

Synthesis of three SGP-related proteins

According to the physicochemical study, SGP was expected to fold in aqueous solution as shown in Fig. 1A, and spontaneously insert itself into membranes. Specifically, SGP can shed light on the process of selecting the appropriate location for the hydrophobic and hydrophilic regions, for observing space filling of the amino acid residues in the protein interior, and for estimating hydrophilic interaction at the

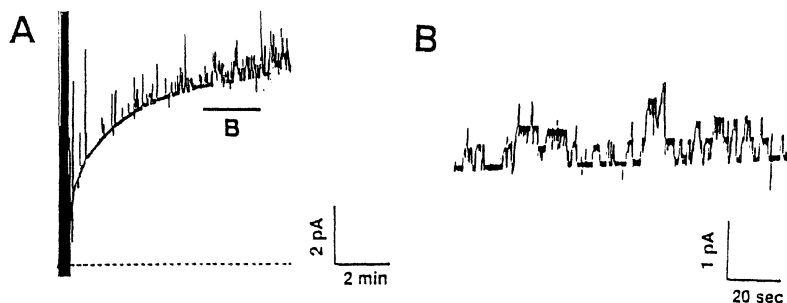


Figure 4. Electric current profiles of a bilayer membrane holding SGP. (A) Effect of SGP on the conductance of a planar bilayer membrane. The bilayer was formed by the folding method using egg PE/brain PS = 2:1 in symmetrical 1M KCl and 10 mM Tris-Hepes (pH 7.4). The dashed line indicates the zero current level. (B) A part of the current trace in the Fig. 4A was expanded as B

protein surface. It is also useful for the investigation of trans-location mechanisms from aqueous solution into lipid bilayers. Thus, we undertook the de novo design, synthesis and characterization of three SGP derivatives.

Protein design is ultimately sequence selection. In this connection, Bealy and Hecht (8) have recently reviewed how the choice of de novo sequences affects protein design, by dividing the process into four parts; a) binary patterning of polar and non-polar amino acids; b) packing; c) turns; and d) negative design. Based on this review, we decided to study de novo protein design more practically, by modifying the following three parts in SGP as shown in Fig. 5 : 1) All Ala residues in hydrophobic helix were replaced by Leu (SGP-L) in order to investigate the packing effect of the hydrophobic core; 2) some of the Lys residues in hydrophilic regions of amphipathic helices were replaced by Glu (SGP-E) in order to investigate the role of surface charge on folding and stability; 3) four amino acid residues of β -turns were replaced by Gly₄ (SGP-G) to determine whether or not a specific sequence is required for folding. The Glu residues of SGP-E were located in a position, which stabilizes α -helical structure through the charge interactions with Lys residues of the neighboring α -helical turn.

The molecular weights and the conformations of model peptides are determined by size-exclusion chromatography and analytical ultracentrifugation, and by ultraviolet CD spectroscopic method (Table 1). The SGP-L and SGP-E are present at trimeric and dimeric in buffer solution, respectively, and SGP-G is in the middle of the monomeric and dimeric states. All the peptides in 2,2,2-trifluoroethanol and buffer solution took α -helical structure (about 50%). To understand the stability of SGP, spectra were measured as function of guanidine-HCl (Gu-HCl) concentration. These temperature behavior was almost comparable with that of SGP, whereas those of a protein denaturant, Gu-HCl, were considerably different. With increasing concentration, unfolding started at about 5.6 M Gu-HCl for SGP-G and 6.4 mM for SGP-E. The complete unfolding of SGP-G was observed at about 7.2 M Gu-HCl, but not for SGP-E at the same concentration. Surprisingly, the denaturation of SGP-L

began at a concentration of 7.2 M Gu-HCl. These results indicate that the stability in the solutions of the SGP and its analogs increases in the order of SGP, SGP-G, SGP-E and SGP-L.

SGP-L

-L-K-L-Y-K-K-L-L-K-K-L-L-K-L-L-G-N-P-G-
-L-K-L-Y-K-K-L-L-K-K-L-L-L-K-L-L-G-N-P-G-
-L-L-K-L-Y-K-K-L-L-K-K-L-L-K-L-L-COOH

SGP-E

Ac-A-A-A-A-A-W-A-A-A-A-G-N-P-G-
-L-E-L-L-K-K-L-Y-K-K-L-L-E-L-L-G-N-P-G-
-L-E-L-L-K-K-Y-L-K-K-L-L-E-L-L-G-N-P-G-
-L-L-E-L-L-K-K-Y-L-K-K-L-L-E-L-L-COOH

SGP-G

Ac-A-A-A-A-A-W-A-A-A-A-G-G-G-G-
-L-K-L-L-K-K-L-Y-K-K-L-L-K-L-L-G-G-G-G-
-L-K-L-L-K-K-Y-L-K-K-L-L-K-L-L-G-G-G-G-
-L-L-K-L-L-K-K-Y-L-K-K-L-L-K-L-L-COOH

Figure 5. Amino acid sequence of three mutants of SGP.

To examine the translocation of proteins into membrane, a Trp-quenching experiment using the lipid bilayers containing 9,10-DBrPC in egg PC vesicles was completed. In analogy with SGP, the three analogs undergo a conformational change that results in the transference of the Trp position from the protein interior to the area near the 9 and 10 positions of the phospholipid acyl chains. From these fluorescence experiments, we conclude that the hydrophobic helices of SGP-related peptides are also localized in lipid bilayers perpendicularly. The Trp residues are present at intermediate depth of lipid core at outer layer of lipid bilayers, while the three amphipathic helices may be left at lipid surface, horizontally.

To further examine whether the peptides are able to form ion channels as observed for SGP, the planar bilayer method was also employed. When the methanol solutions of SGP-E and SGP-G were added, the discrete current changes corresponding to channel-event were observed in multiples of the single channel level (Fig. 6) with time, at the later part of the trace of Figs. 6B and C. On the other hand, the membrane current for SGP-L gradually increased at first, and then the rate of the increase gradually slowed down, reaching a plateau (Fig. 6A), never exhibiting channel events. Interestingly the SGP-L showed a current corresponding to basal current and no channel-like current, while SGP-G and SGP-E showed a channel-like current but no basal current. It has been suggested for SGP that the basal current was induced by the insertion of the central α -helix into planar lipid bilayer and the protein accumulation

into lipid bilayers caused the channel current. The insertion mechanism might be similar to those for colicins that spontaneously insert the hydrophobic central helices

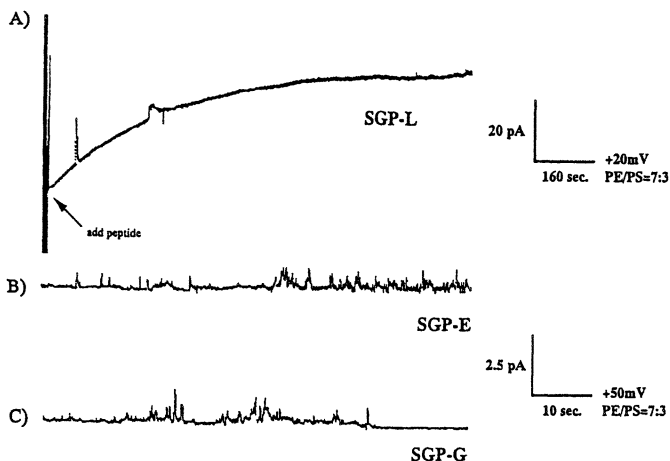


Figure 6. Electric current profiles of a bilayer membrane holding SGP-L, -E and -G. The bilayer was formed by the folding method using egg PE/ brain PS =2:1 in symmetrical 1M KCl and 10 mM Tris-Hepes (pH 7.4).

into the lipid bilayer by taking on an open umbrella-like structure, and then making a pore. The channel-formation of SGP-related three proteins may be explained as follows. The hydrophobic α -helix of SGP-L first inserted itself into lipid bilayers, but because it bound so strongly to the phospholipid core, the protein could not make a pore structure. However, because the hydrophobic helices of SGP-E and -G also bind to lipid more weakly than SGP-L, they can make channel smoothly by taking open-umbrella-like structure without their accumulation of bilayers (resulting in no basal current).

To evaluate the interaction of the proteins with biomembranes, the ability of the peptides to leak hemoglobin from human blood cells was measured. SGP and SGP-G have almost the same hemolytic ability (EC_{50} , about 0.5 μ M). It should be mentioned that both peptides show slightly stronger hemolytic activity than melittin, naturally occurring bee venom, which is one of the highest hemolysis-inducing peptide. However, the SGP-L and SGP-E have only very low hemolytic activity even at the high concentration of 100 μ M.

The abilities of membrane perturbation and channel formation have been closely related to the biological activity. SGP and SGP-G, which have channel-forming ability for model-membranes, have exhibited the strong hemolytic activity, but SGP-L with no channel forming ability, exhibited very weak hemolytic activity. SGP-L as well as other SGP related proteins insert their hydrophobic helices into lipid bilayers. Thus the binding of SGP-L to lipid bilayers may stabilize membranes rather than perturbing them. In this connection, we have previously shown that α -helical

oligoleucine can stabilize the packing structure of acyl chains in lipid bilayers, while oligoalanine can destabilize them (9).

The present study clearly revealed that SGP and its analogs consisting of 69 residues exhibit the different aggregation modes in buffer, but almost the same interaction modes in lipid bilayers. SGP and its analogs may be useful models to investigate the role of the hydrophobic and hydrophilic regions in the formation of protein monomers versus oligomers, and to observe the space filling of amino acid residues in protein interiors.

Induction of Apoptosis

Cell death is typically described as necrosis, a passive process, or apoptosis (from the Greek *apo* = away + *ptosis* = falling), an active process that follows an intrinsic cellular program (10). Apoptosis is a widespread form of cell death, occurring during development, involution, carcinogenesis, viral infections, and no doubt aging, among others (11). Cells undergoing apoptosis *in vivo* proceed through an orderly process of disassembly, with cellular components, proteinases, etc, remaining confined within apoptotic bodies up to the stage of phagocytosis. This prevents damage to the surrounding healthy cells. Thus, apoptosis is the preferred mode of induction for any cell death-based therapy.

Importantly, SGP induced apoptosis in mammalian cells within a concentration of 1-5 μM (Fig. 7). As Fig. 7B shows, the pore-forming ability of SGP caused widespread apoptosis in Kaposi's sarcoma cells (reference below), with evident nuclear condensation and membrane blebbing. Keeping this in mind, it is natural to wonder if analogs of SGP could be made to specifically disrupt the membranes of cancer cells, or if it might be possible to create a "targeted-form" of SGP to treat cancer.

The apoptosis induced by SGP might be explained relating to Bcl-2-related proteins that are critical regulators of cell survival in the outer mitochondrial membranes. The three-dimensional structure of BCL-XL, an inhibitor of apoptosis, was recently shown to be similar to the pore-forming domains of bacteriotoxins. A key feature of these pore forming domains is the ability to form ion channels into planar lipid (11). It causes two types of membrane current similar SGP; one is a basal current and the other is a channel-like open-closed current. Both proteins are also cation selective. These suggest that the apoptosis induced by SGP may be due to ion channel formation into biomembranes.

References

1. Parker, M. W.; Pattus, F.; Tucker, A. D.; Tsernoglou, D. *Nature* **1989**, *337*, 93.
2. van der Goot, F. G.; González-Mañas, J. M.; Lakey, J. H.; Pattus, F. *Nature* **1991**, *354*, 408
3. Lee, S.; Kiyota, T.; Kunitake, T.; Matsumoto, E.; Yamashita, S.; Anzai, K.; Sugihara, G. *Biochemistry* **1997**, *36*, 3782.
4. Kaiser, E.T.; Kézdy, F. J. *Science* **1984**, *223*
5. Voges, K.-P.; Jung, G.; Sawyer, W. H. *Biochim. Biophys. Acta* **1987**, *896*, 64.
6. Dawidowicz E.A.; Rothman, J. E. *Biochim. Biophys. Acta* **1976**, *455*, 621.

7. Montal, M.; Mueller, P. *Proc. Natl. Acad. Sci. USA* 1972, 69, 3561.
8. Beasley, JR.; Hecht, M.H. *J. Biol. Chem.* 1997, 272, 2031.
9. Lee, S.; Yoshitomi, H.; Morikawa, M.; Ando, S.; Takiguchi, H.; Inoue, T.; Sugihara, G. *Biopolymers* 1995 36, 391.
10. Wyllie, A.. *A new classification separating apoptosis from necrosis*; In *Cell death in biology and pathology* ;Bowen, I.D.; Lucksin, R.A., Eds.; , Chapman and Hall:New York, 1980, pp 9.
11. *Definition and incidence of apoptosis: A historical perspective* ; In *Apoptosis: The molecular basis of cell death*. Kerr, J.; Harmon, B., Eds.; Cold Spring Harbor Laboratory Press, 1991.
12. Minn, A. J.; Velez, P.; Shendel, S. L.; Liang, H.; Muchmore, S. W.; Fesik, S. W.; Fill, M.; Thompson, C. B. *Nature*, 1997, 385,353.

Chapter 15

Natural Pore Forming Proteins: Paneth Cell Cryptdins

W. I. Lencer¹, D. Merlin², A. J. Ouellette³, M. E. Selsted³,
and J. L. Madara²

¹Pediatric Gastroenterology and Nutrition, Children's Hospital,
Department of Pediatrics, Harvard Medical School,
and the Harvard Digestive Diseases Center, Boston, MA 02115

²Department of Pathology,

Emory University School of Medicine, Atlanta, GA 30322

³Department of Pathology,

University of California College of Medicine, Irvine, CA 92697

The antimicrobial peptides, cryptdins 2 and 3, secreted from Paneth cells at the base of the murine small intestinal crypts, stimulate Cl⁻ secretion from polarized monolayers of human intestinal T84 cells. The response is reversible and dose dependent. The secretory response correlates with the establishment of an apically located anion conductive channel permeable to carboxyfluorescein (450 Da). Thus cryptdins 2 and 3 can selectively permeabilize the apical cell membrane of epithelial cells in culture to elicit a physiologic Cl⁻ secretory response. Though the structure of the cryptdin channel is unknown, other highly homologous defensins form stable pores of 25Å in model membranes. If cryptdins 2 and 3 form similar pores, they may be capable of mediating transport of therapeutic molecules.

Cryptdins: antimicrobial α -defensins produced by Paneth cells

Paneth cells reside at the base of the crypts of lieberkuhn in intestinal epithelia. Among products produced by this unique cell type are novel peptides termed cryptdins. Cryptdins are intestinal epithelial specific α -defensins - cationic peptides first recognized as neutrophil products which exhibit potent antimicrobial properties. Twenty cryptdin isoforms have been described and cryptdins 1 - 6 have been purified to homogeneity (1,2).

α -defensins: Structure and Function

α -defensins are small (3-4 kD) highly cationic peptides which contain six conserved cysteine residues that form three disulfide bonds (in a characteristic pattern) thus rigidly stabilizing a cyclic amphipathic beta-sheet conformation of these molecules (3-5). Except for cryptidins and the human cryptidin homologues HD5 and HD6, α -defensins are generally expressed by neutrophils and macrophages (as components of exocytic granules) and exhibit potent antimicrobial activity as well as antiviral and antifungal activities (6). Abundant evidence indicate that α -defensins have a primary role in host defense against microbes and play a major role in the oxygen-independent killing of bacteria by neutrophils (along with other non-related cationic peptides) (7-9). It is not proven how α -defensins exert such antimicrobial properties. Available data indicate that α -defensins likely exert such antimicrobial properties by partitioning into biomembranes to form anion conductive channels (3,10-13).

Using planar lipid bilayers, it has been shown that purified rabbit defensin NP-1 partitions into the membrane and, under conditions in which the trans side of the membrane is clamped at a negative voltage, forms ion conductive "pores" which exhibit selectivity for Cl over Na or K (at ratios ~ 2-3:1). The single channel conductances of these defensin-associated pores were 10-1000 pS and varied as a function of membrane voltage (effects seen at voltages as low as 20 mV) and defensin concentration (effects seen at protein concentrations as low as 0.1 μ g/ml) (12). The ability of neutrophil α -defensins to assemble into anion conductive channels within liposomes of defined compositions has now been confirmed (10,11,13). In addition, the crystal and solution structures of rabbit and human α -defensins NP-1 and 5 (4) and HNP-1 and 3 (3) have been solved and a model for oligomerization and membrane insertion of the α -defensin channel has been proposed (3,7,11,13).

Paneth cell cryptidins are not the only antimicrobial peptides produced by epithelial cells. Recently, another class of neutrophil and epithelial defensins closely related to α -defensins have been identified (14,15). These peptides exhibit a different pattern of disulfide bond formation and have been termed β -defensins. β -defensins are expressed and secreted by epithelial cells of the intestine and respiratory tract. They also exhibit antimicrobial activities (16-18). β -defensins are not, however, expressed in Paneth cells, and the abilities of these peptides to form anion conductive channels in eukaryotic cell or artificial lipid membranes have not yet been examined. The function of β -defensins is not addressed in this review.

Paneth Cells and the Anatomy of the Intestinal Crypt

Cryptidins are known to be released from Paneth cells into the crypt lumen and thus other crypt cell types, the major one being the Cl⁻ secreting "undifferentiated" crypt cell (19), are naturally exposed to cryptidins. These cells, express the necessary ion channels, pumps, and cotransporters on their basolateral membranes to amass Cl⁻ ions inside the

cell (19). Activation of Cl⁻ channels in the apical membrane allows Cl⁻ to flow out of the cell down its electrochemical gradient into the crypt lumen. This ion flux hyperpolarizes the crypt lumen which drives Na⁺ and then water across the epithelial barrier to produce a secretory response. Movement of Cl⁻ out of the cell through apical membrane Cl⁻ channels is the rate limiting step in the secretory response, and it is subject normally to regulation by neurotransmitters and signaling peptides or nucleotides on the activity of Cl⁻ channels existent in the apical membrane of the undifferentiated crypt cell (20).

Effect of Paneth Cell α -defensins on Model Intestinal Cl⁻ secreting Crypt Epithelial Cells

Using the polarized human intestinal cell line T84, we have now found that Paneth cell α -defensins can act as soluble inducers of channel-like activity when applied to apical membranes of Cl⁻ secreting epithelial cells in culture (21).

T84 cells grown as confluent monolayers have been well characterized as a model system for the study of regulated Cl⁻ secretion in intestinal epithelia (21). Confluent monolayers of T84 cells form intercellular tight junctions with high transepithelial resistance (typically > 1000 ohms·cm²), and well defined charge and size selectivity (22). When grown on collagen coated permeable supports, the cells form morphologically well differentiated monolayers with a crypt cell-like phenotype and express the necessary ion channels, symporters, and pumps in the appropriate membrane domains for vectorial transport of Cl⁻. Furthermore, the monolayers respond to cAMP and Ca⁺⁺ agonists with regulated Cl⁻ secretion analogous to that found in intact intestine (21).

Cryptdins 2 and 3 induce a reversible Cl⁻ Secretory Response from Polarized Human Intestinal T84 cells *in vitro*

Our initial studies identified cryptdins 2 and 3 as novel paracrine inducers of epithelial Cl⁻ secretion (23). Of the six purified mouse cryptdins tested, only cryptdins 2 and 3 stimulated Cl⁻ secretion from polarized monolayers of human intestinal T84 cells. The response was reversible and dose dependent (See Figure 1).

Cryptdins 1, 4, 5, and 6 lacked this activity, demonstrating that Paneth cell defensins with very similar primary structures may exhibit a high degree of specificity in their capacity to elicit Cl⁻ secretion (see discussion below). The secretory response was not inhibited by pretreatment with 8-phenyltheophylline (1 μ M), or dependent on a concomitant rise in intracellular cAMP or cGMP, indicating that the apically located adenosine and guanylin receptors were not involved. On the other hand, cryptdin 3 elicited a secretory response that correlated with the establishment of an apically located anion conductive channel permeable to carboxyfluorescein (See Figure 2). These data suggested that cryptdins 2 and 3 can selectively permeabilize the apical cell membrane of epithelial cells in culture to elicit a physiologic Cl⁻ secretory response.

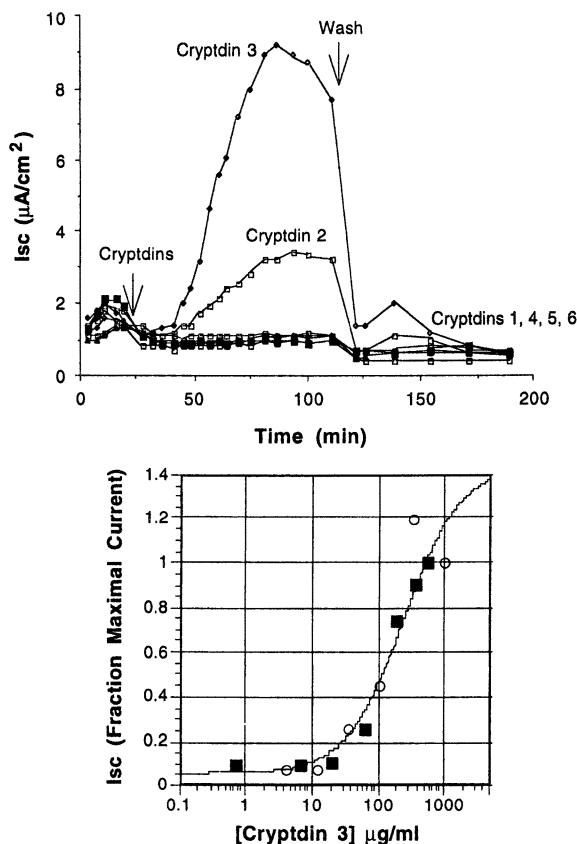


Figure 1: Cryptidins 2 and 3 elicit a reversible Cl^- secretory response from human intestinal T84 cell monolayers. Upper Panel: Time course of Cl^- secretion elicited by purified murine cryptidins 1 - 6. Cryptidin 1 (20 $\mu\text{g}/\text{ml}$) or cryptidins 2 - 6 (40 $\mu\text{g}/\text{ml}$) in Hank's balanced salt solution (HBSS) were applied to apical membranes of T84 cell monolayers at 37°C. At 120 min, cryptidins were removed from the apical reservoir by washout in > 100 vols. of HBSS containing 0.1% bovine serum albumin. Lower Panel: Dose dependency of Cl^- secretion for cryptidin 3. Data represent peak currents 30 min after apical administration of cryptidin 3 (circles and squares represent two independent experiments). Data were fit to Michaelis Menten model ($R^2 = 0.98$). Reproduced with permission Proc. Natl Acad. Sci. USA 1997, 94: 8585-8589.

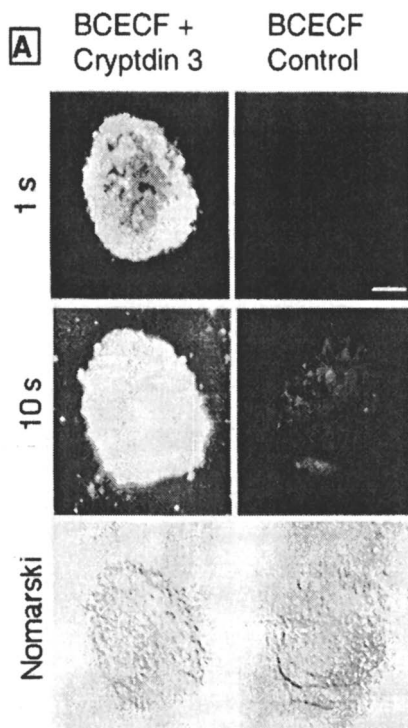


Figure 2: *Cryptdin 3 forms channels in T84 cell membranes. Cryptdin 3 (280 $\mu\text{g/ml}$) permeabilizes T84 cells to the membrane impermeant fluorophore BCECF-acid. Photographs were taken at 1 and 10 s exposures. Bar = 11 μm . Reproduced with permission Proc. Natl Acad. Sci. USA 1997, 94: 8585-8589..*

Studies in Progress

We have recently utilized T84 monolayers selectively permeabilized to monovalent ions at the basolateral membrane by treatment with amphotericin B to measure apical membrane ion conductances directly. These preliminary data provide evidence that cryptdin 3 elicits ion conductances with biophysical characteristics distinct from cAMP-dependent Cl⁻ channels endogenous to T84 cells. We also examined the ability of cryptdin 3 to elicit Cl⁻ secretion from intact cystic fibrosis affected nasal airway cells lacking endogenous CFTR, and in collaboration with Dr. D. Eaton (Professor in Physiology, Emory University, Atlanta), we have obtained single channel recordings of cryptdin 3 channels formed in inside-out patches of human embryonic kidney cells. These experiments indicate that when applied in effective concentrations, cryptdin 3 forms unique cryptdin-based anion conductive pores in cell membranes.

Cryptdin Peptides: Structure-Function Relationships

The secretory activities elicited by interaction between cryptdins and T84 cells were highly specific for individual peptides, as cryptdin 1 and cryptdins 4 - 6 were inactive under these *in vitro* conditions. These data identified specific residues of the cryptdin molecule which appear to confer bioactivity. Cryptdins 1, 2, 3 and 6 differ only at residue positions 10, 15, 29, and 31 (See Figure 3) (1). The two biologically active peptides, cryptdins 2 and 3, contain Arg at position 15 while cryptdins 1 and 6 contain Gly side chains at that position and they are inactive. Thus, Arg15 in cryptdins 2 and 3 may be important for channel formation in human T84 cells. As cryptdins 2 and 3, but not cryptdins 1 and 6, display antimicrobial activity against trophozoites of *Giardia lamblia* (24), the bulky, cationic arginine on the surface turn at position 15 may facilitate interaction of enteric defensins with eukaryotic membranes.

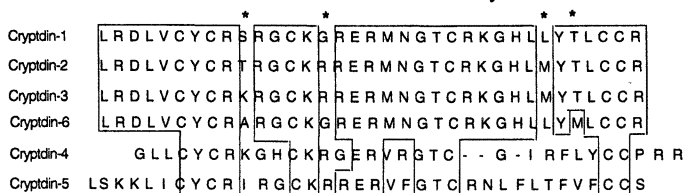


Figure 3: Amino acid sequences of cryptdins 1 - 6. Primary structures are shown in single letter amino acid code, and aligned to maximize sequence similarity with hyphens denoting gaps in the cryptdin-4 sequence. Asterisks identify the amino acid positions where cryptdins 1, 2, 3, and 6 differ. By analogy with the neutrophil defensins HNP-1, HNP-3, NP-2, and NP-5, amino acids at positions 10 and 15 are predicted to be located at conserved turns on the surface of the molecule (1). Variations at these positions have been shown to confer effects on the potency of antimicrobial activities (1,24). Reproduced from Proc. Natl Acad. Sci. USA 1997, 94: 8585-8589.

Our studies also show that the secretory response elicited by cryptdin 3 was more extensive than that induced by cryptdin 2. Since cryptdins 2 and 3 differ only at residue position 10 (Thr vs. Lys respectively), residues at position 10 may also be important in cryptdin action on T84 cells. By analogy with the known crystal or solution structures of human neutrophil defensins HNP-1 and -3 and rabbit defensins NP-1 and-5, the amino acids at position 10 are predicted to be involved in a conserved turn on the peptide surface and, we hypothesize, are positioned to influence the interaction between cryptdin and cell membranes.

Summary and Hypothesis

Our published and preliminary data show that cryptdin 3 forms anion selective channels in eukaryotic cell membranes *in vitro*. Thus, cryptdins may act *in vivo* as novel paracrine regulators of epithelial Cl⁻ secretion. After discharge from Paneth cells at the base of the crypt, cryptdins may insert into apical membranes of adjacent epithelial cells which, like polarized T84 cells in culture, are electrochemically poised for Cl⁻ secretion. Our data show that formation of cryptdin-based channels at this site will lead to a secretory response. Such a response would ensure that the crypt lumen is flushed after Paneth cell discharge. As cryptdin-based channel formation appears to depend on mass action (our studies and (12,25)), we propose that such flushing would reverse the cryptdin-induced secretory response, protect crypt epithelia from cytotoxicity, and ensure delivery of these anti-microbial peptides to the gut lumen. Based on the similarities in primary structure, we hypothesize that human Paneth cell α -defensin HD5 and possibly HD6 will exhibit similar bioactivities.

In the context of drug delivery, these studies show that cryptdins can reversibly permeabilize apical membranes of epithelial cells to solute transport. Such an effect may be harnessed for drug delivery to the cytosol of epithelial cells lining the intestine, lung or other mucosal surfaces. We know the channel formed by cryptdin 3 in T84 cells conducts 450 Da negatively charged fluorophores. Though the structure of the cryptdin 3 channel is unknown, other highly homologous α -defensins form stable pores of 25Å in model membranes (11,13). If cryptdins 2 and 3 form similar pores, they may be capable of mediating transport of therapeutic molecules into target epithelial cells.

References

1. Ouellette, A. J., Hsieh, M. M., Nosek, M. T., Cano-Gauci, D. F., Huttner, K. M., Buick, R. N., and Selsted, M. E. *Infect. Immun.* **1994**, *62*, 5040-5047.
2. Ouellette, A. J., Miller, S. I., Henschen, A. H., and Selsted, M. E. *FEBS Lett.* **1992**, *304*, 146-148.
3. Hill, C. P., Yee, J., Selsted, M. E., and Eisenberg, D. *Science (Wash. D. C.)* **1991**, *251*, 1481-1485.

4. Pardi, A., Hare, D. R., Selsted, M. E., Morrison, R. D., Bassolino, D. A., and Bach, A. C. *J. Mol. Biol.* **1988**, 201, 625-636.
5. Selsted, M. E., and Harwig, S. S. L. *J. Biol. Chem.* **1989**, 264, 4003-4007
6. Ganz, T., Selsted, M. E., and Lehrer, R. I. *Eur. J. Haematol.* **1990**, 44, 1-8
7. Ouellette, A. J., and Selsted, M. E. *FASEB J.* **1996**, 10, 1280-1289.
8. Ouellette, A. J. *J. Med. Microbiol.* **1998**, 47, 941-942.
9. Selsted, M. E., Miller, S. I., Henschen, A. H., and Ouellette, A. J. *J. Cell Biol.* **1992**, 118, 929-936.
10. Wimley, W. C., Selsted, M. E., and White, S. H. *Protein Sci* **1994**, 3, 1362-1373.
11. White, S. H., Wimley, W. C., and Selsted, M. E. *Curr. Opin. Struct. Biol.* **1995**, 5, 521-527.
12. Kagan, B. L., Selsted, M. E., Ganz, T., and Lehrer, R. I. *Proc. Natl. Acad. Sci. USA* **1990**, 87, 210-214.
13. Hiristova, K., Selsted, M. E., and White, S. H. *J. Biol. Chem.* **1997**, 272, 24224-24233.
14. Tang, Y.-Q., and Selsted, M. E. *J. Biol. Chem.* **1993**, 268, 6649-6653.
15. Selsted, M. E., Tang, Y.-Q., Morris, W. L., McGuire, P. A., Novotny, M. J., Smith, W., Henschen, A. H., and Cullor, J. S. *J. Biol. Chem.* **1993**, 268, 6641-6648.
16. Schonwetter, B. S., Stolzenberg, E. D., and Zasloff, M. A. *Science* **1995**, 267, 1645-1648.
17. Stolzenberg, E. D., Anderson, G. M., Ackermann, M. R., Whitlock, R. H., and Zasloff, M. *Proc. Natl. Acad. Sci. USA* **1997**, 94, 8686-8690.
18. Goldman, M. J., Anderson, G. M., Stolzenberg, E. D., Kari, U. P., Zasloff, M., and Wilson, J. M. *Cell* **1997**, 88, 553-560.
19. Madara, J. L., and Trier, J. S. in *Physiology of the gastrointestinal tract*; Johnson, L. R., ed; Raven Press: New York, NY 1987; Vol. 2, pp 1209-1250.
20. Donowitz, M., and Welsh, M. J. in *Physiology of the gastrointestinal tract*; Johnson, J. R., ed; Raven Press: New York, NY 1987; Vol. 2, pp. 1351-1388.
21. Dharmasathaphorn, K., and Madara, J. L. *Meth. Enzymol.* **1990**, 192, 354-359.
22. Madara, J. L., and Dharmasathaphorn, K. *J. Cell Biol.* **1985**, 101, 2124-2133.
23. Lencer, W. I., Cheung, G., Strohmeier, G. R., Currie, M., Ouellette, A. J., Selsted, M. E., and Madara, J. L. *Proc. Natl. Acad. Sci. USA* **1997**, 94, 8585-8589.
24. Aley, S. B., Zimmerman, M., Hetsko, M., Selsted, M. E., and Gillin, F. D. *Infect. Immun.* **1994**, 62, 5397-5403.
25. Cociancich, S., Ghazi, A., Hetru, C., Hoffmann, J. A., and Letellier, L. *J. Biol. Chem.* **1993**, 268, 19239-19245

Chapter 16

Growth Factor Delivery from Tissue Engineering Matrices: Inducing Angiogenesis to Enhance Transplanted Cell Engraftment

Martin C. Peters¹ and David J. Mooney¹⁻⁴

Departments of ¹Biomedical Engineering, ²Biologic and Materials Sciences, and ³Chemical Engineering, University of Michigan, Ann Arbor, MI 48109

Tissue engineering has been developed to address the increasing demand for replacement tissues and organs. It may be possible to guide the formation of new functional tissues by using three-dimensional biodegradable porous matrices for cell transplantation. One significant challenge facing tissue engineering is the lack of nutrients initially available to transplanted cells. A potential approach to address this nutrient transport limitation is to encourage the rapid formation of a functional vasculature within the transplanted matrix. Angiogenesis (blood vessel formation) can be promoted via the delivery of protein growth factors in the area of transplanted cells. Common tissue engineering materials (e.g., poly lactic-co-glycolic acid (PLGA), alginate) have been used successfully to encapsulate and release angiogenic growth factors. The localized delivery of growth factors from a tissue engineering matrix may provide a means to accelerate the vascularization process and bring the engineering of large metabolically active tissues one step closer to clinical application.

Engineering Organs with Cell Transplantation

The field of tissue engineering has developed due to the inadequate supply of organs and tissues for patients requiring organ/tissue replacement. For example, over 60,000 patients are currently on a waiting list to receive a new organ, and over 4000 patients die while waiting for an organ each year due to the shortage of donated organs¹. A promising alternative to organ transplantation that could greatly expand

⁴Corresponding author.

clinicians' ability to treat patients requiring new organs and tissues is the selective transplantation of the appropriate cell type(s), and the reconstitution of a functional tissue mass from these transplanted cells². Thus, cells from a single donated organ could be utilized to treat multiple patients, or a small biopsy from a living donor could yield a sufficient number of cells to engineer the necessary tissue mass. The concept of engineering organs using selective cell transplantation has recently been validated in animal models by the demonstrations that functional new intestinal tissue can be engineered and placed in-line with native intestine³, and functional new bladders can be similarly engineered and utilized to replace the native bladder⁴.

One promising approach to engineer new tissues using cell transplantation involves delivering cells on macroporous matrices, which become structurally integrated with the surrounding host tissue. These matrices can be fabricated from a number of different synthetic and naturally derived materials⁵. Synthetic polymers comprised of glycolic and lactic acid (PLGA) are especially attractive for this approach, as their degradation following tissue development will result in a completely natural new tissue. These polymers have been used in humans in the form of biodegradable sutures for over 20 years^{6,7}, and are considered to be biocompatible. They degrade to lactic and glycolic acid, which are natural metabolites, and the degradation rate of the polymer can be precisely controlled by varying the ratio of lactic:glycolic acid in the polymer⁵. These polymers have been processed into matrices with a number of physical forms, including non-woven fibrous arrays and foams, utilizing a variety of processing techniques⁸.

In this review we will discuss the challenges involved in vascularization of synthetic tissue engineering matrices, and we will focus on utilizing protein growth factor delivery to induce the formation of blood vessels. Discussions will include the characteristics of specific growth factors, materials and mechanisms for drug delivery, and strategies to apply current technology to tissue engineering.

Vascularization and Cell Survival

Transplantation of selected cell populations on biodegradable polymer matrices is an attractive approach to engineer a variety of tissue types (e.g., liver, intestine). However, the survival of transplanted cells is dependent on the diffusional transport of nutrients and waste products between these cells and the surrounding host tissue. Diffusion of oxygen is typically the limiting factor for cell survival in this situation, and it is estimated that cells more than several hundred microns from the capillaries in surrounding tissues will fail to engraft or rapidly die due to oxygen depletion⁹. Matrices utilized for cell transplantation are designed to address this mass transport issue as they contain large, interconnected pores that enhance diffusional transport of nutrients through the matrix. In addition, the macropores are intended to promote the ingrowth of granulation tissue from the host to provide for convective nutrient transport to the engineered tissue, and potentially allow for large tissue masses to be created. A variety of studies indicate that blood vessels will invade the macroporous matrices utilized for cell transplantation¹⁰⁻¹⁴. However, fibrovascular ingrowth into the matrix occurs at a rate less than 1 mm/day, and typically takes one to two weeks to completely penetrate even relatively thin (e.g., 3 mm thick)

matrices^{10,12}. The net result is that a high percentage of transplanted cells die within several days following transplantation¹⁴. This mass transport limitation currently limits the thickness of engineered tissues to the millimeter size scale, and this scale is clearly insufficient if one needs to replace an entire organ or a large mass of tissue. A critical challenge in the tissue engineering field is thus to develop strategies to achieve rapid and extensive vascularization of forming tissues.

Growth Factors

It has long been appreciated that a functional vasculature is an essential component of any metabolically active tissue which has a thickness in excess of a few millimeters¹⁵. The process of generating new microvasculature, termed angiogenesis, is a process observed physiologically in development and wound healing¹⁶. A variety of tissue-inducing substances (e.g., growth factors) that promote the formation of new microvasculature have been identified^{16,17} and they could potentially be utilized to accelerate the vascularization of engineered tissues. These substances stimulate the appropriate cells (e.g., endothelial cells), already present in the patient's body, to migrate from the surrounding tissue, proliferate, and finally differentiate into blood vessels¹⁶. By combining growth factor delivery, to induce angiogenesis, with tissue engineering matrices the engraftment of transplanted cells may be enhanced.

The search for potential growth factors regulating angiogenesis has yielded numerous candidates: basic fibroblast growth factor (bFGF), epidermal growth factor (EGF), angiogenin, prostoglandin E₂ (PGE₂), transforming factor-alpha (TGF- α), TGF- β , and vascular endothelial growth factor (VEGF) to name only a few¹⁸. All of these molecules are able to promote angiogenesis in certain *in vivo* model systems but with the exception of bFGF and VEGF these agents have little or no direct mitogenic effect on vascular endothelial cells¹⁹.

bFGF and its receptors can be found in nearly all tissues of the body^{20,21}. It is a single polypeptide of ~16kDa (146 amino acids) and part of a family of at least seven related heparin-binding peptides²². bFGF activity has been implicated in both normal and pathological processes including embryogenesis, limb regeneration, wound healing, diabetic retinopathy, and tumor angiogenesis²³. bFGF promotes the proliferation of a broad range of cells^{22,24} (e.g., fibroblasts, keratinocytes, smooth muscle cells, endothelial cells) and is intensely angiogenic, even at picomolar concentrations, *in vivo*²⁵.

VEGF is a homodimer with a molecular mass of 45 kDa and appears in four distinct isoforms: VEGF₁₂₁, VEGF₁₆₅, VEGF₁₈₉, and VEGF₂₀₆²⁶. VEGF is a key regulator of blood vessel formation during development and in neovascularization associated with tumors and intra-ocular disorders^{27,28}. VEGF₁₆₅ is a secreted heparin-binding protein that acts as a potent mitogen for micro and macrovascular endothelial cells from arteries and veins but lacks mitogenic activity for other cell types²⁹.

VEGF is an attractive molecule to enhance the vascularization of engineered tissues due to its endothelial cell specificity. To increase the survival of transplanted cells it will be critical to not only maximize the amount of vascularization, but also

the mass transport capability of the vasculature versus the metabolic needs of the forming tissues. The other growth factors identified to date which promote angiogenesis (e.g., FGF family) also increase the proliferation of other cell types (e.g., fibroblasts) present in connective tissue¹⁶. The increase in mass transport obtained with these other molecules may be offset by an increased need for nutrients due to non-desirable proliferation of host cells in the region of the engineered tissue. Systems for the sustained and localized delivery of bFGF and VEGF have been previously demonstrated³⁰⁻³³ but only preliminary work has been done to incorporate angiogenic factors into tissue engineering matrices^{34,35}.

Growth Factor Delivery

Previous studies have demonstrated that it is possible to promote angiogenesis through the delivery of peptide growth factors such as bFGF and VEGF^{17,36-38}. It may be possible to enhance angiogenesis at the site where a new tissue is engineered by locally delivering a high concentration of these growth factors in a sustained manner. Growth factors have promise for tissue engineering but the development of effective delivery mechanisms is essential to preserve their biological activity. Both bFGF and VEGF, though very potent, are rapidly degraded when injected or ingested³⁹. Growth factors are large molecular weight polypeptides which are susceptible to inactivation via a number of avenues including proteolysis, aggregation, deamidation, and oxidation^{40,41}. To avoid these pitfalls, investigators have developed a variety of encapsulation methods to release various growth factors with controlled kinetics while maintaining the growth factor's biological activity. PLGA and alginate, two materials utilized extensively for tissue engineering, have also met with success as growth factor delivery devices. We will briefly discuss these materials as they are used in the drug delivery realm and review strategies to adapt the positive aspects of each for tissue engineering.

PLGA Microspheres

A common approach to the delivery of growth factors is to encapsulate the protein in biodegradable polymer microspheres. These microspheres can be implanted in the body and release entrapped growth factors as they degrade. Like the sutures and tissue engineering matrices mentioned above, PLGA microspheres will degrade completely to natural metabolites so no retrieval of the microspheres is necessary following complete drug release. Polymer microspheres have been manufactured from PLGA and used to encapsulate a variety of proteins including EGF¹³, human growth hormone⁴², and VEGF⁴³. Growth factor encapsulation using a double emulsion (water-in-oil-in-water) technique yields loading efficiencies of approximately 50% (actual/theoretical) and controlled release kinetics for several weeks *in vitro*^{13,42,43}. The PLGA microsphere processing technology was improved through the development of a cryogenic non-aqueous process⁴⁴. This technique allows 95% of the protein to be loaded into the microspheres, and improved protein stability is also observed⁴⁵.

Microspheres have been utilized in tissue engineering by combining the microspheres with a cell suspension and seeding the mixture onto porous matrices¹³. This approach was used to deliver EGF to transplanted hepatocytes, and those matrices seeded with EGF-microspheres demonstrated approximately twice the hepatocyte engraftment of control samples¹³. Though effective, the use of microspheres for tissue engineering has its limitations. When microspheres are seeded onto matrices it is difficult to control their distribution after implantation. The microspheres may produce non-uniform drug distributions throughout the matrix, or the microspheres could be displaced from the matrix in which they were seeded and cause unwanted cellular responses (e.g., fibroblast proliferation, blood vessel leakage) in the host tissue.

Alginate Beads

Alginate, a natural material derived from seaweed, has also been utilized as an encapsulation system for growth factors such as bFGF^{30-32,46,47} and VEGF³³. Alginate has gentle gelling properties, and growth factor containing beads (~3 mm diameter) can be formed at room temperature without the use of organic solvents³³. bFGF and VEGF can be encapsulated within alginate beads with a protein loading efficiency of 30-70% depending on the concentration of the alginate solution and the presence of stabilizing molecules (e.g., heparin)^{31,33}. Alginate beads will release the incorporated growth factor in a controlled fashion for several weeks *in vitro* when maintained at physiologic conditions. Not only does the released growth factor retain its biologic activity, but some observations suggest that the negatively charged alginate interacts with the positively charged growth factor to stabilize the molecule and enhance its activity *in vitro*^{32,33}.

Alginate shows a promising interaction with growth factors and is being studied for tissue engineering applications⁴⁸. However, the alginate bead system for growth factor delivery has several disadvantages that make it non-ideal for tissue engineering. Alginate, in its native form, does not undergo biodegradation and the high molecular weight alginate typically utilized may be too large (>150 kDa) to pass through the kidneys. In addition, when the release of growth factors from alginate beads is monitored, for extended times (>70 days), it is apparent that 20-30% of the growth factor is retained in the bead^{31,33}. This remaining growth factor may aggregate within the hydrated bead, and in this case would not be released in a functional state. Recently novel alginate-derived polymers that degrade via hydrolysis to low molecular weight products have been developed⁴⁹. These polymers eliminate this problem, and could find great utility in growth factor delivery.

Release from PLGA Tissue Engineering Matrices

A more elegant approach to using growth factor delivery for tissue engineering is to incorporate growth factors directly into the porous matrix³⁴. A gas-foaming/particulate leaching method to fabricate tissue engineering matrices with controlled porosity, without the use of organic solvents or high temperatures has been developed using the same PLGA polymer used to fabricate microspheres⁵⁰ (Fig. 1). This represents a critical advance, as all other processing techniques utilized to date to

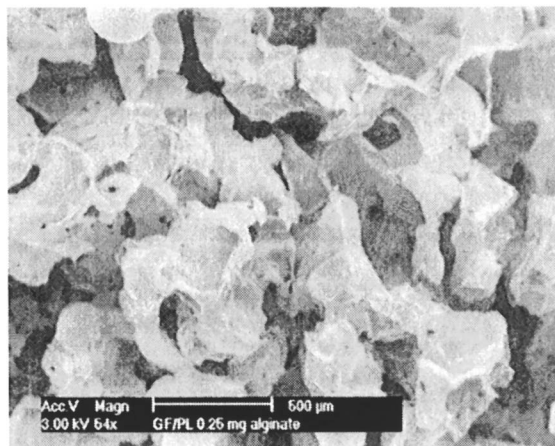


Figure 1. Scanning electron micrograph showing a cross-section of a 85:15 PLGA matrix containing 5% (w/w) sodium alginate formed by gas-foaming/particulate leaching process (500 μm size bar shown on photograph).

fabricate polymer matrices involve organic solvents and/or high temperatures^{8,51-53} which could potentially damage incorporated proteins during processing. Sheridan et al. demonstrated that lyophilized VEGF could be incorporated into the bulk of gas-foamed/particulate leached matrices (Fig. 2).

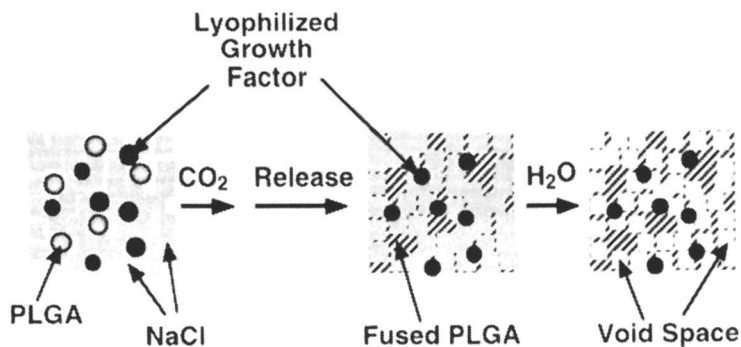


Figure 2. Process for fabricating PLGA matrices with incorporated growth factor. Lyophilized growth factor, (black circles), PLGA particles (shaded circles), and NaCl particles (gray squares) are mixed and compression molded to create a disk 3 mm in thickness. The compressed pellet is equilibrated with high-pressure carbon dioxide (800 psi), and then the gas pressure is rapidly released to ambient. The PLGA particles expand into the space between the NaCl particles (indicated by hatched

bars), and fuse. This expansion is caused by the formation of gas pores within the particles. The NaCl and growth factor are entrapped within the continuous PLGA phase. The NaCl can subsequently be removed by leaching with water (leaving void spaces) to yield macroporous matrices with entrapped growth factor.

The VEGF was released for over 2 months in vitro and found to retain over 90% of its bioactivity for the first 2 weeks (Fig. 3). However, the final VEGF loading was only 28% of the starting material due to the particulate-leaching step of matrix processing. In an effort to increase growth factor loading, alginate was added to the matrices prior to foaming³⁵. The addition of alginate increased the incorporation efficiency to approximately 60% while still providing controlled release kinetics for a variety of growth factors (Fig. 4).

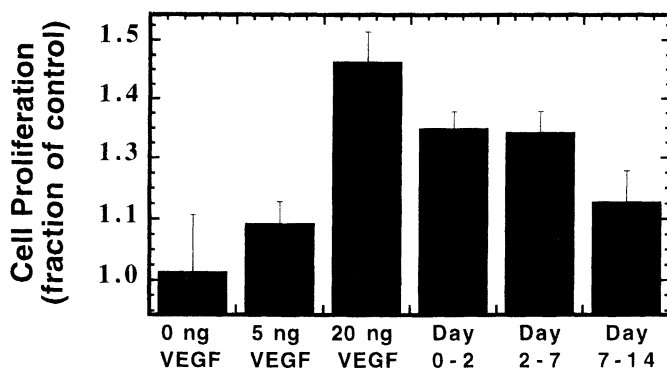


Figure 3. Biological activity of VEGF incorporated into 75:25 PLGA matrices. The bioactivity was determined by measuring the growth stimulation of cultured endothelial cells compared to endothelial cells grown in the presence of varying VEGF concentrations. Values represent mean and standard deviation ($n=3$)³⁴ divided by the average growth observed in control cultures.

Growth factor delivery from PLGA tissue engineering scaffolds provides several potential advantages over using different scaffolds for cell and drug delivery. The scaffold can be designed to degrade at a variety of rates, and releases growth factor throughout its life. The scaffold provides uniform growth factor concentrations in the tissue forming within the scaffold, and eliminates the need to introduce a second drug carrying material into the matrix. In addition, excipients such as alginate can easily be added to the sponge formulation prior to foaming to stabilize the growth factor and increase incorporation.

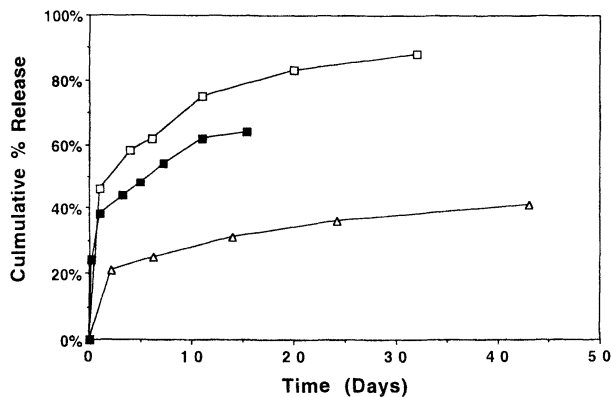


Figure 4. Release of I^{125} -labeled growth factors ((open triangles) VEGF, (closed squares) bFGF, and (open squares) EGF) from lyophilized alginate beads distributed throughout 85:15 PLGA matrices.³⁵

Conclusions

Engineering new tissues using cell transplantation on polymer matrices is an exciting approach to create a variety of organs and tissues. However, the rapid development of an appropriate vascular network throughout the matrix following cell transplantation is a critical, and currently unachieved, requirement for this approach to be applied to large organs and tissues. The localized delivery of angiogenic factors may provide a means to accelerate the vascularization process and bring the engineering of large metabolically active tissues (e.g., liver, kidney, and muscle) one step closer to clinical application.

The demonstration that VEGF can be delivered from porous tissue engineering scaffolds is a significant contribution with regard to developing transplant matrices that interact with cells by altering their soluble microenvironment. These growth factor releasing scaffolds must next be extensively evaluated *in vivo* to measure their ability to elicit physiologic responses. The development of this technology can hopefully help usher a new generation of tissue engineering matrices. These matrices could potentially interact with transplanted and native cells by presenting a host of spatially and temporally regulated signals to promote controlled tissue development (e.g., vascularization, enervation) and maturation (e.g., extracellular matrix remodeling, large blood vessel formation).

Acknowledgements

The authors would like to acknowledge the support of the NSF (Grant No. BES-9501376), NIH (Grant No. R29 DK50715), and Regeneration Inc. M.C.P was supported by a fellowship from the Whitaker Foundation.

Literature Cited

- 1) UNOS; Division of Organ Transplantation, H. R. a. S. A. "Annual Report of the U.S. Scientific Registry for Organ Transplantation and the Organ Procurement and Transplant Network," , 1997.
- 2) Langer, R.; Vacanti, J. P. *Science* **1993**, *260*, 920-6.
- 3) Kaihara, S.; Kim, S. S.; Benvenuto, M.; Choi, R.; Kim, B. S.; Mooney, D.; Tanaka, K.; Vacanti, J. P. *Transplantation* **1999**, *67*, 241-5.
- 4) Oberpenning, F.; Meng, J.; Yoo, J. J.; Atala, A. *Nat Biotechnol* **1999**, *17*, 149-55.
- 5) Wong, W. H.; Mooney, D. J. *Synthesis and properties of biodegradable polymers used in tissue engineering*; Atala, A. and Mooney, D. J., Ed.; Birkhauser Press, 1997, pp 51-82.
- 6) Katz, A. R.; Turner, R. J. *Surg Gynecol Obstet* **1970**, *131*, 701-16.
- 7) Frazza, E. J.; Schmitt, E. E. *J Biomed Mater Res* **1971**, *5*, 43-58.
- 8) Kim, B. S.; Mooney, D. J. *Trends Biotechnol* **1998**, *16*, 224-30.
- 9) Colton, C. K. *Cell Transplant* **1995**, *4*, 415-36.
- 10) Mikos, A. G.; Sarakinos, G.; M., L.; Ingber, E.; Vacanti, J.; Langer, R. *Biotech & Bioeng* **1993**, *42*, 716-723.
- 11) Wake, M. C.; Patrick, C. W., Jr.; Mikos, A. G. *Cell Transplant* **1994**, *3*, 339-43.
- 12) Mooney, D. J.; Kaufmann, P. M.; Sano, K.; McNamara, K. M.; Vacanti, J. P.; Langer, R. *Transplant Proc* **1994**, *26*, 3425-6.
- 13) Mooney, D. J.; Kaufmann, P. M.; Sano, K.; Schwendeman, S. P.; Majahod, K.; Schloo, B.; Vacanti, J. P.; Langer, R. *Biotech & Bioeng* **1996**, *50*, 422-429.
- 14) Mooney, D. J.; Sano, K.; Kaufmann, P. M.; Majahod, K.; Schloo, B.; Vacanti, J. P.; Langer, R. *J Biomed Mater Res* **1997**, *37*, 413-20.
- 15) Folkman, J. *Exs* **1997**, *79*, 1-8.
- 16) Polverini, P. J. *Crit Rev Oral Biol Med* **1996**, *6*, 230-47.
- 17) Klagsbrun, M.; D'Amore, P. A. *Annu Rev Physiol* **1991**, *53*, 217-39.
- 18) Folkman, J.; Shing, Y. *J Biol Chem* **1992**, *267*, 10931-10934.
- 19) Leung, D. W.; Cachianes, G.; Kuang, W.-J.; Goeddel, D. V.; Ferrara, N. *Science* **1989**, *246*, 1306-1309.
- 20) Rifkin, D. B.; Moscatelli, D. *J Cell Biol* **1989**, *109*, 1-6.
- 21) Burgess, W. H.; Maciag, T. *Annu Rev Biochem* **1989**, *58*, 575-606.
- 22) Baird, A.; Klagsbrun, M. *Cancer Cells* **1991**, *3*, 239-43.
- 23) Baird, A.; Walicke, P. A. *Br Med Bull* **1989**, *45*, 438-52.
- 24) Nimni, M. E. *Biomaterials* **1997**, *18*, 1201-1225.
- 25) Shing, Y.; Folkman, J.; Haudenschild, C.; Lund, D.; Crum, R.; Klagsbrun, M. *J Cell Biochem* **1985**, *29*, 275-87.
- 26) Park, J. E.; G-A., K.; Ferrara, N. *Mole Biol Cell* **1993**, *4*, 1317-1326.

- 27)Kim, K. J.; Li, B.; Winer, J.; Armanini, M.; Gillett, N.; Phillips, H. S.; Ferrara, N. *Nature* **1993**, *362*, 841-4.
- 28)Aiello, L. P.; Avery, R. L.; Arrigg, P. G.; Keyt, B. A.; Jampel, H. D.; Shah, S. T.; Pasquale, L. R.; Thieme, H.; Iwamoto, M. A.; Park, J. E.; et al. *N Engl J Med* **1994**, *331*, 1480-7.
- 29)Ferrara, N. *Eur J Cancer* **1996**, *32A*, 2413-22.
- 30)Edelman, E. R.; Mathiowitz, E.; Langer, R.; Klagsbrun, M. *Biomaterials* **1991**, *12*, 619-26.
- 31)Nugent, M. A.; Chen, O. S.; Edelman, E. R. *Mat. Res. Soc. Symp. Proc.* **1992**, *252*, 273-284.
- 32)Downs, E. C.; Robertson, N. E.; Riss, T. L.; Plunkett, M. L. *J Cell Physiol* **1992**, *152*, 422-9.
- 33)Peters, M. C.; Isenberg, B. C.; Rowley, J. A.; Mooney, D. J. *J Biomater Sci Polym Ed* **1998**, *9*, 1267-78.
- 34)Sheridan, M. E.; Shea, L. D.; Peters, M. C.; Mooney, D. J. *J Cont Rel (in press)*.
- 35)Peters, M. C.; Shea, L. D.; Mooney, D. J. *Polymer Preprints* **1999**, *40*, 273-274.
- 36)Ingber, D. E.; Folkman, J. *J Cell Biol* **1989**, *109*, 317-30.
- 37)Pepper, M. S.; Ferrara, N.; Orci, L.; Montesano, R. *Biochem Biophys Res Commun* **1992**, *189*, 824-31.
- 38)Goto, F.; Goto, K.; Weindel, K.; Folkman, J. *Lab Invest* **1993**, *69*, 508-17.
- 39)Gombotz, W. R.; Pettit, D. K. *Bioconjug Chem* **1995**, *6*, 332-51.
- 40)Manning, M. C.; Patel, K.; Borchardt, R. T. *Pharm Res* **1989**, *6*, 903-18.
- 41)Cleland, J. L.; Powell, M. F.; Shire, S. J. *Crit Rev Ther Drug Carrier Syst* **1993**, *10*, 307-77.
- 42)Cleland, J. L.; Mac, A.; Boyd, B.; Yang, J.; Duenas, E. T.; Yeung, D.; Brooks, D.; Hsu, C.; Chu, H.; Mukku, V.; Jones, A. J. *Pharm Res* **1997**, *14*, 420-5.
- 43)Eiselt, P.; Kim, B. S.; Chacko, B.; Isenberg, B.; Peters, M. C.; Greene, K. G.; Roland, W. D.; Loeb sack, A. B.; Burg, K. J.; Culberson, C.; Halberstadt, C. R.; Holder, W. D.; Mooney, D. J. *Biotechnol Prog* **1998**, *14*, 134-40.
- 44)Gombotz, W.; Healy, M.; Brown, L., U.S. Patent 5,019,400, 1991.
- 45)Johnson, O. L.; Jaworowicz, W.; Cleland, J. L.; Bailey, L.; Charnis, M.; Duenas, E.; Wu, C.; Shepard, D.; Magil, S.; Last, T.; Jones, A. J.; Putney, S. D. *Pharm Res* **1997**, *14*, 730-5.
- 46)Edelman, E. R.; Nugent, M. A.; Smith, L. T.; Karnovsky, M. J. *J Clin Invest* **1992**, *89*, 465-73.
- 47)Edelman, E. R.; Nugent, M. A.; Karnovsky, M. J. *Proc Natl Acad Sci U S A* **1993**, *90*, 1513-7.
- 48)Rowley, J. A.; Madlambayan, G.; Mooney, D. J. *Biomaterials* **1999**, *20*, 45-53.
- 49)Bouhadir, K. H.; Hausman, D. S.; Mooney, D. J. *Polymer* **1999**, *40*, 3575-3784.
- 50)Harris, L. D.; Kim, B. S.; Mooney, D. J. *J Biomed Mater Res* **1998**, *42*, 396-402.
- 51)Freed, L. E.; Vunjak-Novakovic, G.; Biron, R. J.; Eagles, D. B.; Lesnoy, D. C.; Barlow, S. K.; Langer, R. *Biotechnology (N Y)* **1994**, *12*, 689-93.
- 52)Mikos, A. G.; Thorsen, A. J.; Czerwonka, L. A.; Bao, Y.; Langer, R. *Polymer* **1994**, *35*, 1068-1077.
- 53)Lo, H.; Ponticciello, M. S.; Leong, K. W. *Tissue Engineering* **1995**, *1*, 15-28.

Chapter 17

Targeting Macromolecular Therapeutics to Specific Cell Organelles

Gilbert-André Keller¹, Wenlu Li¹, and Randall J. Mersny²

Departments of ¹Pharmacokinetics and Metabolism, Pharmacological Sciences, and ²Pharmaceutical Research and Development, Drug Delivery/Biology Group, 1 DNA Way, South San Francisco, CA 94080

Recent advances in cell biology and cell physiology have greatly improved our understanding of mechanisms involved in the dynamic events of intracellular protein trafficking. Additionally, some protein growth factors, binding proteins, receptors and polypeptide hormones have recently been shown to enter the cytoplasm of cells and target to the nucleus. Here, we describe how information on intracellular trafficking routes might be utilized to control the fate of conjugated or chimeric therapeutic molecules that can enter the cell cytoplasm to potentially target selected intracellular organelles. Delivery schemes utilizing intracellular trafficking pathways such as those discussed may result in the design of new drug entities as well as provide new applications for current drug molecules, possibly resulting in improved therapies.

Designing an optimal method for the delivery of any biologically active molecule requires the consideration of multiple factors. Whether the clinical disorder is limited or dispersed, therapeutic molecules would have maximum efficacy and minimal toxicity if they could be selectively targeted to specific cells in various tissues and organs. In essence, this describes the concept of magic bullets proposed by Ehrlich in 1900 (*1*) who suggested that a therapeutic treatment at specific cells or tissues might be achievable. Growth factors and polypeptide hormones that function by binding to highly specific cell surface receptors on selected cells define a subset of cell surface targets described by the Ehrlich concept. Use of growth factor and polypeptide hormone receptors in targeted cell delivery, however, requires an understanding of both the fate of ligands following receptor association and unique events associated with these receptor-ligand interactions.

Cellular Uptake Pathways for Proteins

Typically, binding of growth factors and polypeptide hormones to their cognate receptors at the surface of a target cell leads to the induction of an intracellular signal. Propagation of this signal results in a cellular response of varied duration. Following generation of an intracellular signal, a down-regulation mechanism is required to maintain the cell's responsiveness to that signaling event. A common cellular process for interruption of the intracellular signal involves the internalization of receptor-growth factor/peptide hormone complexes into the cell by a mechanism referred to as receptor-mediated endocytosis (RME). The process of RME involves the generation of nascent membrane-bound vesicles known as endosomes. A series of events in the endosome resulting from internal acidification or fusion with lysosomes often disrupts signaling events produced by growth factors and polypeptide hormones bound to their cognate receptors. RME is an efficient uptake pathway for growth factors and polypeptide hormones into cells that commonly results in their rapid destruction and typically precludes appreciable amounts of these molecules from accessing the cell cytoplasm. With this in mind, efforts have been made to develop prodrugs that become activated after reaching the acidic and hydrolytic environment of the lysosome (2). Applications of such an approach appear to be numerous (3).

Introduction of macromolecules into the cytoplasm of target cells can sometimes be achieved through another membrane-associated uptake pathway known as bulk-fluid endocytosis (BFE). This uptake pathway is constitutive (occurring continually rather than in response to a stimulus) and results in the indiscriminate trapping and ingestion of extracellular molecules. Small pinocytotic vesicles which bud from the plasma membrane in this process typically fuse with lysosomes. With some measurable frequency, however, BFE can result in macromolecular therapeutics such as peptides, proteins, antisense oligonucleotides and genes accessing the cell cytoplasm. Similar uptake into the cytoplasm is considered to be much more rare following RME. By comparison, BFE is much less efficient than RME and, unlike RME, is energy- and receptor-independent.

It has now become clear that a number of pathologies are associated with defects in specific intracellular organelles have been described (4). To optimally treat these conditions, it may be preferential to identify a delivery route with the efficiency of RME binding and uptake but with the increased cytoplasmic entry observed with BFE pathways. Recent observations that some protein growth factors, binding proteins, receptors and polypeptide hormones can cross the membrane of target cells to enter the cell cytoplasm and ultimately reach the nucleus have been reviewed (5). Nuclear targeting of these macromolecules can be positively correlated with specific nuclear localization amino acid sequences (NLSs) within these molecules. Presently, we describe known targeting signals for the nucleus and other organelles which might be used for the selective intracellular targeting of macromolecular therapeutics delivered as protein and peptide conjugates and discuss aspects of how membrane translocation mechanisms may one day be integrated into these delivery approaches.

Intracellular Trafficking Signals

Mammalian cells contain several types of membrane-bound organelles; mitochondria, the nucleus, peroxisomes, the endoplasmic reticulum and the Golgi apparatus. Newly synthesized proteins must reach specific destinations for optimal function within the cell. To this end, a series of domains defined by families of amino acid sequences provides at least one method for proteins to efficiently target to and be retained at specific organelles. Sometimes these trafficking signals are disrupted as in some cases of hyperoxaluria type I disease where an alanine:glyoxylate aminotransferase is mistargeted to the mitochondria (6). Although certainly not complete, a number of amino acid sequences have now been identified which affect the selective targeting of proteins to various cell organelles (Table I). Most sequences are simple; a few specific amino acids present at the carboxyl terminus of a protein. Other sequences are more complex; long bipartite domains buried within adjacent internal sites of a protein. Beyond these amino acid sequences, additional factors can control the intracellular trafficking of proteins. For example, molecules greater than ~50 kDa cannot readily transit through the pores that decorate the nuclear envelope. Targeting signals must also be accessible by molecules critical to trafficking and retention events at organelles.

Nuclear Targeting Signals

The nucleus, a large, usually centrally located organelle, is delimited by a double membrane envelope studded with 9 nm pores that control a series of import and export cycles for introduction and retention of nuclear-targeted proteins (7). Nuclear localization signals (NLSs) are frequently short clusters of the basic amino acids lysine and arginine positioned within a protein at sites where they can be recognized by nuclear binding proteins involved in their delivery to nuclear pores for transport into the nucleus (5). For example, the Pro-Lys-Lys-Lys-Arg-Lys-Val sequence of the SV40 large T antigen acts as a NLS (8). Mutation of a single amino acid of this sequence where a Lys within this sequence is mutated to either Thr or Asn causes a complete disruption of the NLS function. Other proteins have nucleoplasmin-like NLS motifs and although the consensus sequence of Lys-(Arg/Lys)-X-(Arg/Lys), where X is Lys, Arg, Pro, Val or Ala has been suggested (9), a clear picture for nuclear targeting by this mechanism has so far not emerged. An overview of recent data shows that some nuclear proteins do not contain any detectable nuclear targeting signal, whereas others may contain more than one signal (5).

A number of growth factors and polypeptide hormones including γ -interferon, growth hormone, insulin, nerve growth factor, epidermal growth factor, platelet-derived growth factor (PDGF), acidic fibroblast growth factor (a-FGF), basic fibroblast growth factor (b-FGF), the Schwannoma-derived growth factor, insulin-like growth factor-I (IGF-I) associated with IGF-I binding protein-3 and heregulin all contain NLS motifs (Figure 1). Further, many of these proteins access the nucleus and localize primarily in the nucleolus (10) where gene transcription, rRNA processing and nascent ribosomal subunit assembly take place. Although the pathway of nuclear delivery of these proteins is poorly understood, a few facts are

Table I. Examples of amino acid sequences capable of directing proteins to distinct organelles

Targeting Site	Targeting Sequence	Protein
Nucleus - monopartite	RRRGL	human angiogenin
	VSRKRPRPA	polyoma virus large T antigen
	PKKKRKY	SV40 large T antigen
Nucleus - bipartite	PRESGKKRRKR	human PGDF A
	KRPAATKKAGQAKKKLKD RLRRDAGGTGGVYEHGGAPRRRK	<i>Xenopus</i> nucleoplasmin mouse FGF-3
Peroxisome - matrix	SKL-COOH	acyl-CoA oxidase
	NH ₂ -MHRLQVVLGHL	3-ketoacyl-CoA thiolase
Mitochondria	MSESGKPIAKPIRKPGYTPALKALG IPALRLPSR	Yeast Tim54
	KKSL-COOH	glucose-6-phosphatase
Endoplasmic reticulum	DEKKMP-COOH	adenovirus 3 protein E19
	KPRRE-COOH	calnexin
	NH ₂ -MDVRRRSEKP	HMG-CoA Reductase
	NH ₂ -MHRRRRSRSCR	HLA Class II invariant chain
Golgi apparatus	KTKLL-COOH	yeast Emp47 protein
Lysosome - soluble	KFERQ	Ribonuclease A
Lysosome - membrane	GLKRHHHTGYEQF	Igp96

Abbreviations: COOH, carboxyl terminus; NH₂, amino terminus; PDGF, platelet-derived growth factor; Igp96, lysosomal associated membrane protein 2; HMG-CoA, 3-hydroxy-3-methylglutaryl-coenzyme A.

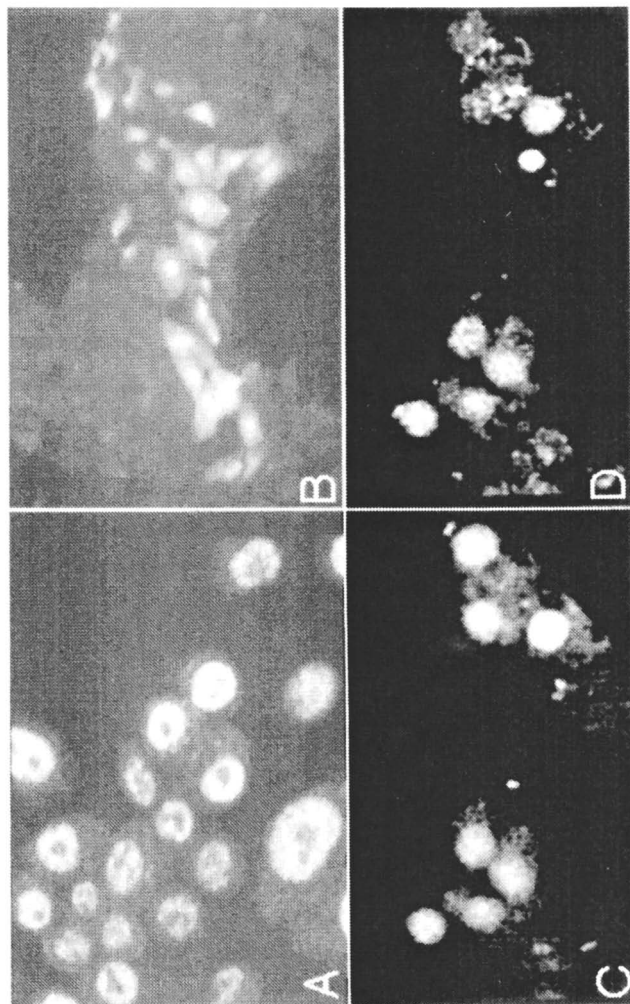


Figure 1 A) Confocal micrograph showing that fluorescent heregulin added to the culture medium is rapidly transported to the nuclei of breast cancer cells. B) Fluorescent IGF-I translocates to the nuclei of proliferating kidney cells at the periphery of a monolayer within three minutes after its addition to the medium. Confocal micrograph of the same field showing that IGF-I (C) and IGFBP3 (D) are targeted and accumulate in the nuclei of kidney cells.

clear. The process of plasma membrane and nuclear translocation can be very rapid. For example, a fluorescent form of IGF-I can be detected in the nuclei of cultured cells as early as 3 minutes after addition to the medium (11). Events associated with plasma membrane translocations and nuclear targeting appear to require stringent cellular conditions. PDGF and b-FGF transport to the nucleus appears to be cell cycle dependent, while IGF-I localization to the nucleus occurs only in proliferating cells at the periphery of a non-confluent monolayer or in cells at the edge of a physically induced wounding of cell monolayers in vitro (11). Diversity amongst nuclear targeting mechanisms is demonstrated by other proteins that target to the nucleus lack clear nuclear transport signals, such as IGF-1 and may be transported to the nucleus via interactions with other proteins such as binding proteins which do contain NLS motifs (Table I).

Mitochondrial Targeting Signals

Most cells contain hundreds of mitochondria that are responsible for lipid metabolism and the production of cellular ATP via oxidative phosphorylation. Mitochondria are double membrane structures that contain about 700 different proteins. More than 95% of mitochondrial proteins are encoded by nuclear genes and are thus synthesized outside of the mitochondria and must ultimately gain access to this organelle. Mitochondria contain two specialized compartments, the matrix and the inter-membrane space, separated by the inner mitochondrial membrane. Cytoplasmic proteins destined for an intra-mitochondrial location presumably interact with specific receptors on the outer mitochondrial membrane and cross at sites where the outer and inner membranes are in close apposition (12). Protein translocation appears to require a number of critical and integrated steps which include unfolding through the assistance of specific molecular chaperones, removal of signal domains by proteolytic cleavage and refolding events (13). A second signal peptide domain is involved in protein targeting of proteins from inter-membrane space to the mitochondrial matrix (14). Mitochondria-targeting sequences have been characterized (15) and putative receptor(s) for mitochondrial proteins have been identified (16). Antisera raised against these receptors interfere with protein uptake into isolated mitochondria. These sites are presumed to contain a pore or tunnel that facilitates the translocation of proteins with the correct targeting signal. The actual protein translocation step requires the maintenance of an electrical potential across the inner mitochondrial membrane.

Although proteins directed to the mitochondrial matrix are targeted by a 20-60 amino acid signal at the amino terminus, the minimum targeting signal can in fact be rather short (15). For the Cox IV presequence, only the first 12 residues of the 25 residue signal are required to direct this protein into the mitochondria matrix (17). Amino acid residues critical for mitochondrial targeting, however, are not always located at the extreme amino terminus. Sequence and structural requirements of mitochondrial protein signals have also been studied by saturation cassette mutagenesis (18) and by studies of randomly generated peptide sequences (19). Although leader sequences identified thus far have shown no primary amino acid sequence homology (Table I), predicted α -helix structures of these peptide

sequences have demonstrated several common features. Targeting signals of proteins destined to the mitochondrial matrix contain a high content in basic arginine and lysine amino acids (16), are devoid of acidic residues, and all of the positive charges appear to be expressed at one polar face (20).

Peroxisome Targeting Signals

Peroxisomes (also known as microbodies) are single membrane organelles composed of as many as 50 different proteins which include enzymes associated with a variety of oxidative reactions (21). Peroxisomal proteins are synthesized at their mature size on free polysomes and transported to the peroxisomes without further processing where they are delivered to either the membrane or matrix by distinct mechanisms (22). Advances in understanding how proteins are targeted to peroxisomes have led to the identification of a tripeptide peroxisomal signal located at the extreme carboxyl terminus of a majority of peroxisomal proteins (23). A tripeptide of the sequence Ser-Lys-Leu (SKL), or similar sequences where serine is substituted by either alanine or cysteine and lysine is substituted by either histidine or arginine (consensus sequence Ser/Ala/Cys-Lys/Arg/His-Leu/Met), is sufficient to target proteins to the peroxisomal compartment. For example, human serum albumin coupled covalently via its lysine side chain to a peptide ending in SKL is transported to peroxisomes (24,25). Alternately, an amino terminus sequence of 11 amino acids can also target proteins to the peroxisome (Table I). The fact that only 20-40% of peroxisomal proteins contains this tripeptide sequence indicates that other peroxisomal targeting signals must exist. A novel targeting signal has been identified in the peroxisomal thiolase. It consists of a 20 amino acid-long leader sequence situated at the amino terminus of the protein. Peroxisome membrane receptors for both peroxisome targeting signals have been identified (26). Thus, multiple peroxisomal-import mechanisms may exist and a number of studies have shown these to be novel and not simply variations of targeting mechanisms described for other organelles (21).

Endoplasmic Reticulum (ER) Targeting Signals

The ER is a highly convoluted continuous membrane structure that may constitute as much as 50% of the total membrane surface of a cell. It is continuous with the nuclear envelope. Playing a central role in cell function, the ER is a primary site of lipid biosynthesis, protein production and N-linked glycosylation. Signal peptides at the amino terminus of nascent polypeptide chains are recognized by the signal recognition particle of the ER to facilitate entry of growing proteins into the lumen of the ER. These signal peptides consistently have a high degree of hydrophobicity over a stretch of 20-30 amino acids. Retention of proteins in the ER is commonly accomplished by the presence of a carboxyl terminal His/Lys-Asp-Glu-Leu (H/KDEL) amino acid sequence (27). Additional ER retrieval motifs have been found to include Lys-Lys or Arg-Arg dibasic sequences located close to the terminus of the cytoplasmic domain of membrane proteins (28). In the case of the 3-

Hydroxy-3-methylglutaryl-Coenzyme A Reductase, a 39-residue domain of the amino terminus is involved in the retention of this protein in the ER membrane (29).

Golgi Apparatus Targeting Signals

The Golgi apparatus is a structurally and biochemically polarized organelle typically located near the nucleus that plays a pivotal role in processing and sorting of newly synthesized proteins through post-translational glycosylation and proteolysis. It is comprised of four compartments known as the cis, medial and trans domains and the trans Golgi network (reviewed in (30)). Functional differences, maintained through the restriction of resident enzymatic activities are used to delineate these Golgi domains. A vesicular-mediated process accomplishes migration of molecules from one compartment to the next. The first of these compartments, the cis-Golgi may also be involved in the sorting of misfolded proteins back to the ER where they are degraded. While initial oligosaccharide processing occurs in the ER, final sugar structures are positioned on lipids and proteins as they progress through the Golgi complex stacks. Removal of mannose and addition of N-acetylglucosamine occurs in the medial Golgi compartment. Addition of galactose and sialic acids is made in the trans Golgi cisternae. Ultimately, sorting occurs in the trans Golgi network that packages vesicular structures for final cellular targeting. Galactosyl transferase, glycosidase, nucleoside diphosphatase and acid phosphatase are examples of proteins which vectorially transport through the different subcompartments of the Golgi apparatus and become trans Golgi-resident proteins. Resident Golgi proteins contain specific signals that cause their retention in the appropriate compartment. For example, the first membrane spanning domain of the E1 glycoprotein from the avian corano virus can cause retention of a protein in the cis-Golgi which is normally transported to the plasma membrane (31). Reviews of Golgi apparatus protein targeting studies have suggested multiple signals to be involved in the specific localization of proteins retained within the various domains of the Golgi apparatus (32,33).

Lysosome Targeting Signals

Proteins reaching the trans-Golgi apparatus have shared a common pathway from the ER. Most of these proteins have been postranslationally modified and are segregated from one another in the trans-Golgi network. Depending on their final destinations in the cell, they are either i) aggregated in secretory granules that are transported to the cell surface and fuse with the plasma membrane, ii) targeted to the plasma membrane iii) or targeted to the lysosomes. Lysosomal proteins share a determinant that is recognized by a phosphorylating enzyme that adds a mannose-6-phosphate modification onto lysosomal hydrolases. This modification serves as a high affinity ligand to mannose-6-phosphate receptors in the trans-Golgi apparatus (34). Lysosomal enzyme-receptors exit the Golgi apparatus in a coated vesicle to be delivered into a prelysosomal compartment where the ligand and the receptor dissociate (35). The lysosomal enzyme is then released and packaged in a lysosome

while the receptors recycle to the Golgi apparatus or transits to the plasma membrane. Retention of these cytoplasmic proteins at the lysosome appears to require a selective targeting signal (36).

Additional Targeting Factors

Docking proteins, such as COPI, ARF and rab proteins, can be involved in the transport of proteins with targeting sequences for specific cell structures and organelles (37,38). Thus, emulation of specific organelle targeting sequences described above or identification of other methods of associating with selected docking proteins may provide additional routes of macromolecular delivery to specific intracellular sites. In any case, recognition by specific intracellular structures is a critical requirement when incorporating any targeting sequence (Table I) or specific docking protein component into a chimera delivery vehicle. For example, it is critical that some of these sequences are at the carboxyl terminus or the amino-terminus of the protein. Insertion at other locations will likely not work. In all cases, though, the targeting sequence must be exposed to the extent that it is accessible to whatever binding or docking structures are required to facilitate efficient targeting and retention at an organelle.

Protein Translocation Across Membranes

The migration of an amphipathic polymer such as a protein containing a critical three-dimensional structure across a membrane lipid bilayer membrane is extremely unfavorable from a thermodynamic standpoint. Indeed, upon synthesis, nascent proteins are assisted across the endoplasmic reticulum membrane in an unfolded state by a protein complex known as the translocon. Further, specific pores or transport structures exist in some organelles, such as the nucleus and mitochondria, to facilitate the uptake of protein molecules from the cytoplasm into these structures. Passage through at least some of these pores/pathways appears to require an unfolding step. The issue of re-folding is not a trivial one since initial protein folding occurring at the time of synthesis is directed either by the inherent amino acid sequence of the protein or through folding events assisted by chaperone proteins (39). Thus, growth factors and polypeptide hormones that associate with the external plasma membrane surface of a cell and target to the nucleus after somehow gaining access into the cell cytoplasm (40) may be able to undergo an unfolding-refolding step to allow passage across the lipid bilayer.

The requirements and events involved in growth factor and polypeptide hormone translocation across the plasma membrane are currently unclear. Do these events require co-factors at the plasma membrane? Are there peculiar cellular conditions required for translocation? Can a mutant form or a fragment of a growth factor or polypeptide hormone be used to enter into cells in a manner that is independent of these peculiar cellular conditions? Can inactive growth factor domains or mutant forms the protein be used to deliver therapeutic molecules associated through chimera production or chemical coupling? For many

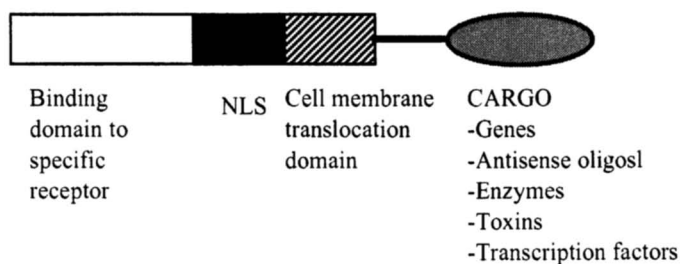
polypeptide hormones and growth factors, cellular responses require some critical step in this process of receptor-ligand internalization, ligand release, and receptor recoiling or degradation. Are any of these events required for translocation?

The exact mechanism(s) of polypeptide translocation across a lipid plasma membrane is unknown at present. However, several examples of cell membrane translocation that do not appear to involve the formation of vesicles have been described that may provide a paradigm of this form of protein transport. Some peptides, such as those referred to as penetratins, can facilitate the translocation of macromolecules across the plasma membrane of cells in a non-selective fashion (41). The antennapedia protein from *Drosophila* (42) and HIV-1 TAT protein (43) can transit across cellular membranes and into the cytoplasm. Although a specific domain appears to be involved in the translocation of the TAT protein, the mechanism of this internalization is unknown. The translocation of heregulin through the plasma membrane requires little energy and can not be inhibited by K^+ depletion and low temperature (44). Any or all of the mechanisms or protein translocation may involve the initial formation of an endosomal structure, as has been suggested for the translocation of IL-5 (5) and heregulin (44).

Design of Intracellular Targeting Vectors

As our ability to selectively target tissues and cells in the body increases, therapeutics such as that outlined in Figure 2 can be designed to achieve a very specific biological outcome. Although extensive practical applications remain to be explored, the key advantage of the intracellular targeting approach is not only the selective delivery to specific cells via surface-expressed structures, but also the ability to deliver a macromolecular cargo to the cytoplasm of specific cells. Some efforts in this area have already shown promise. For example, macromolecules conjugated to folic acid have been delivered into cells in a non-lysosomal and non-destructive fashion by taking advantage of the cellular uptake system for folate (45). The potential to deliver therapeutic macromolecules to specific cellular targets of selected cells opens the possibility to treat a variety of conditions associated with enzymatic imbalances, signaling pathway problems and intracellular pathogens such as viruses or invading bacteria. Delivered cargo might include genes, transcription factors, antisense oligonucleotides, toxins, enzymes etc. Based upon data showing membrane translocation of growth factors or polypeptide hormones and the ability to re-direct intracellular protein targeting, it would be attractive to consider a conjugate or chimera composed of these factors as a novel delivery approach. Indeed, the application of signals which mediate nuclear targeting for drug delivery has been previously discussed (40). One important aspect of such an approach involves the potential unwanted introduction of an active growth factor or polypeptide hormone. At present it is unclear what portions of these growth factors and polypeptide hormones are required for membrane translocation. It is also unclear if the portion(s) of growth factors and polypeptide hormones involved in membrane translocation into the cytoplasm can be separated from its biological activity on the target cell. Some growth factors and polypeptide hormones appear to directly access the cytoplasm and ultimately the nucleus of a target cell. Others,

A. Generic nuclear delivery vector



B. Generic cytoplasmic delivery vector

Mutant growth factor with NLS deleted



C. Generic mitochondrial delivery vector



Mitochondria targeting signal

D. Generic peroxisomal delivery vector



Peroxisome targeting signal 1

Alternatively, peroxisome targeting signal 2 can be used at the NH2 terminus

Figure 2. Cartoon of idealized targeting vectors for drug delivery to specific intracellular organelles.

however, such as IGF-I appear to enter into the cell in conjunction with specific circulating binding proteins which have NLS structures (44). Some receptors, such as those for IL-1 α and IL-1 β , have NLS structures and target to the nucleus along with their ligands (5). Thus, there are several scenarios where a macromolecule the size of a protein can associate with the plasma membrane of a cell and enter into the cytoplasm of that cell (Table II).

Chimeras for Targeted Delivery

A generic approach for the targeted delivery to specific intracellular organelles requires the construction of a chimeric protein which would contain at least three critical components; a binding domain, a translocation domain, and a cargo as shown in Figure 2a. To date, protein growth factors, binding proteins, receptors and polypeptide hormones which appear to be capable of entering the cytoplasm of cells have only been observed to have intracellular targeting signals for the nucleus and not other organelles. Thus, a generic chimera composed of binding and translocation domains useful for delivering a cargo component would likely deliver that cargo to the nucleus (Figure 2a). Appropriate deletion or mutation of the NLS motif from such binding and translocation domains should result in retention of the chimera in the cytoplasm as shown in Figure 2b. Alternately, introduction of a mitochondrial targeting motif at the amino terminus (Figure 2c) or a peroxisomal targeting motif at the carboxyl terminus (Figure 2d) of a chimera lacking an NLS should provide a mechanism for the specific delivery of cargo to these organelles, respectively. One critical aspect with the construction of any of these potential delivery vectors is that of antigenicity. Careful attention will have to be paid to insure that the introduction of non-self structures or induction of autoimmunity does not occur.

The ultimate construction of delivery vectors designed to target specific organelles will involve the identification of cargo components appropriate for that vector. For example, cargos of genes or antisense oligonucleotides would have optimal actions if they were targeted selectively and retained by the nucleus or mitochondria. Delivery to other organelles, which lack transcriptional activities, would be less effective. Correction of mitochondrial disorders (since 1988 more than 30 genetic point mutations on the mitochondrial DNA have been located) are sometimes complex since they may involve both mitochondrial and the nuclear DNA defects. In such cases, an NLS may be useful in a vector to affect an outcome in mitochondria. In many instances, toxins and enzymes delivered as cargo may already contain an intracellular targeting sequence. For example, toxins that induce apoptosis by interrupting a protein synthesis function primarily in the ER and usually have specific mechanisms of targeting to this site (46). Thus, if the KDEL sequence of these toxins is retained in a chimera, specific ER targeting would occur following selective cellular uptake through the binding and translocation domains.

Potential Clinical Applications

A number of storage diseases associated with either the ER, the Golgi apparatus

Table II. Classes of human proteins exhibiting nuclear targeting capacity

Protein Class	Examples	Presumed Targeting Signal
Polypeptide hormones		
	Atrial natriuretic peptide	Unknown
	insulin	Unknown
	growth hormone	Unknown
	growth hormone-releasing hormone	Unknown
	prothymosin α	TKKQKT
	proenkephalin	KRYGGFMRGLKR
	parathyroid hormone related protein	KTPKKKK-10 a.a.-KKKRR
Growth factors		
	platelet-derived growth factor A	PRESGKKRKRKR
	platelet-derived growth factor B	RVTIR.TVVRPPPKHRK
	fibroblast growth factor-1 α or 1 β	NYKKPKL
	fibroblast growth factor-2	GRGRPRERVGGRRGR
	vascular endothelial growth factor	KKSVRGKGGKQKRKKK
	Schwanoma-derived growth factor	KKGGKNGKGRNRKKK
	amphiregulin	KPKRKKGGKNGKNRNKKK
	angiogenin	RRRGL
Cytokines		
	γ -interferon	NSNKKR and KTGKRRS
	interleukin-1 α	KVLKRRRL
	interleukin-1 β	PKKKMEKRF
	interleukin-5	KKYIDGQKKKCGEERR
Receptors		
	growth hormone receptor	VRVRSQRN
	GM-CSF receptor α -subunit	RNSKRRREIR
Binding proteins		
	IGFBP3	KKGFYKKKQCRPSKGRK
	IGFBP5	RKGFYKRRQCKPSRGRK

Abbreviations: GM-CSF, granulocyte monocyte-colony stimulating factor; IGFBP, insulin-like growth factor I binding protein.

or lysosomes might be addressed clinically by the targeted delivery of enzymatic activities to these organelles using specific targeting motifs. Storage diseases typically result from the overproduction or reduced destruction of a particular protein, lipid or sugar which results in a toxic accumulation of that material. For example, Tangier disease may be caused by a defect in the release of lipids from the trans-Golgi into post-Golgi structures such as the lysosome (47). Niemann-Pick disease type C appears to result from a defect in the transfer of lipids from lysosomes to cell membranes. Delivery of lipid-degrading enzymes using targeting motifs for the Golgi apparatus or lysosomes might be useful in chimeras focused at treating Tangier and Niemann-Pick diseases, respectively. Several lysosomal storage diseases including α -N-acetylgalactosaminidase deficiency, G_{M2} gangliosidosis, galactosialidosis, Gaucher disease and mucopolysaccharidosis also might be treatable by the targeted delivery of an appropriate enzyme activity to lysosomes. Targeting enzyme-containing chimeras to mitochondria in a similar fashion might be useful to treat conditions involving defects in the respiratory chain and fatty acid oxidation. Peroxisomal targeting may be very effective with replacement enzymes to treat adrenoleukodystrophy, Refsum disease and hyperpipecolic acidemia where peroxisomes appear to be structurally intact but lack an enzymatic function. An overwhelming issue with any potential therapy for diseases involving storage defects is the potential need for prenatal intervention which represents another level of drug delivery complexity which will not be addressed in the present report.

Another potential application of an intracellular targeting technology would be to selectively destroy unwanted cells such as cancers or autoimmune lymphocytes. In both cases, delivery of a cytotoxic agent to the most sensitive location in the target cell would be optimal. Some toxins, as mentioned above, have such a targeting capacity to traffic to critical intracellular sites. An example of a cytotoxic cargo associated with a cell-selective delivery moiety is the IL-4(38-37)-PE38KDEL chimera (35). In this case IL-4 acts as the binding domain and *Pseudomonas aeruginosa* exotoxin A (PE) provides both the translocation domain and cargo components of the vectors shown in Figure 2. Additionally, the kill domain of PE also carries the KDEL sequence which allows for targeted ER delivery for the ultimate purpose of selective cell apoptosis. This approach was used successfully against Kaposi's sarcoma tumors. Overexpression of cancer-associated surface structures, such as the HER-2 receptors on breast cancer cells, should provide other potential applications for targeted cytotoxin delivery. In this case, a vector comprised of heregulin for binding and translocation associated with an apoptosis-inducing molecule might be a useful clinical approach.

Another layer of cell targeting specificity may be achieved by alterations in a cell's function based upon its status. For example, cells at the edge of a wound appear to more rapidly translocate VEGF to their nucleus compared to cells not directly associated with the wound. As stated previously, this enhanced nuclear targeting in wounds has also been demonstrated for IGF-I (11). Additionally, PDGF and b-FGF transport to the nucleus in a cell cycle-dependent fashion. Together, these observations support the possibility that, under certain cellular conditions, the mechanism(s) which facilitate the cytoplasmic delivery or uptake of specific growth

factors and polypeptide hormones can be modulated. Such information may result in additional improvements in the selectivity of therapeutic delivery to specific organelles.

Summary

As a result of recombinant biotechnology and innovative synthetic drug design, pharmaceutical research is now in a position to design and manufacture therapeutics that target to specific tissues. An ability to selectively target tissues and cells in the body and control the ultimate cellular fate of therapeutics may be crucial to achieve an optimal desired biological outcome. Efforts to better understand the biology and physiology of target cells have opened several new therapeutic avenues involving not only more efficient and selective cell killing but also points to the possibility of selective cell healing. Until recently it was thought that the physical and chemical properties of most proteins and peptides limited their ability to enter cells by routes that are different from the receptor-mediated endocytosis pathway, but it is now clear that a number of macromolecules can access the cytoplasm directly. Once in the cell, intracellular trafficking amino acid sequences may allow for the targeting of endocytosed structures to specific intracellular organelles. A key advantage of this approach is the versatility of the cargo molecule that can range from enzymes for enzyme replacement to carrying gene for gene therapy or toxins to poison the cell.

Acknowledgments

We apologize to our colleagues for the omission of many important papers which could not be cited due to limitation of the number of the references. We thank Drs. Tue Nguyen and Grant Schoenhard for their support of this work.

Literature Cited

1. Ehrlich, P. *Proc. R. Soc.* **1900**, *66*, 424-448.
2. Kopecek, J. *J. Controlled Rel.* **1990**, *11*, 279-290.
3. Duncan, R. *J. Drug Targeting* **1997**, *5*, 1-4.
4. Wallace, D. C. *Science* **1999**, *283*, 1482-1488.
5. Jans, D. A.; Hassan, G. *Bioessays* **1998**, *20*, 400-411.
6. Danpure, C. J.; Cooper, P. J.; Wise, P. J.; Jennings, P. R. *J. Cell Biol.* **1989**, *108*, 1345-1352.
7. Silver, P. A. *Cell* **1991**, *64*, 489-497.
8. Kalderon, D.; Roberts, B. L.; Richardson, W. D.; Smith, A. E. *Cell* **1984**, *39*, 499-509.
9. Chelsky, D.; Ralph, R.; Jonak, G. *J. Cell Biol.* **1989**, *9*, 2487-2492.
10. Pederson, T. *J. Cell Biol.* **1998**, *143*, 279-281.
11. Li, W.; Fawcett, J.; Widmer, R. H.; Rabkin, R.; Keller, G.-A. *Endocrinology* **1997**, *138*, 1763-1766.

12. Mori, M.; Terada, K. *Biochim. Biophys. Acta* **1998**, *1403*, 12-27.
13. Neupert, W. *Ann. Rev. Biochem.* **1997**, *66*, 863-917.
14. Rassow, J.; Dekker, P. J. T.; van Wilpe, S.; Meijer, M.; Soll, J. *J. Mol. Biol.* **1999**, *286*, 105-120.
15. Omura, T. *J. Biochem.* **1998**, *123*, 1010-1016.
16. Kurz, M.; Martin, H.; Rassow, J.; Pfanner, N.; Ryan, M. T. *Mol. Biol. Cell* **1999**, *10*, 2461-2474.
17. Hurt, E. C.; van Loon, A. P. G. M. *Trends Biochem. Sci.* **1986**, *11*, 204-207.
18. Bedwell, D. M.; Strobel, S. A.; Yun, K.; Jongeward, G. D.; Wmr, S. D. *Mol. Cell Biol.* **1989**, *9*, 1014-1025.
19. Lemire, B. D.; Fankhauser, C.; Baker, A.; Schatz, G. *J. Biol. Chem.* **1989**, *264*, 20206-20215.
20. von Heijne, G. *EMBO J.* **1986**, *5*, 1335-1342.
21. Waterham, H. R.; Cregg, J. M. *Bioessays* **1997**, *19*, 57-66.
22. Rehling, P.; Albertini, M.; Kunau, W. H. *Ann. New York Acad. Sci.* **1996**, *804*, 34-46.
23. Gould, S. J.; Keller, G. A.; Hosken, N.; Wilkinson, J.; Subramani, S. *J. Cell Biol.* **1989**, *108*, 1657-1664.
24. Walton, P. A.; Gould, S. J.; Feramisco, J. R.; Subramani, S. *Mol. Cell Biol.* **1992**, *12*, 531-541.
25. Wedland, M.; Subramani, S. *J. Cell Biol.* **1993**, *120*, 675-685.
26. Subramani, S. *Physiol. Rev.* **1998**, *78*, 171-188.
27. Munro, S.; Pelham, H. R. B. *Cell* **1987**, *48*, 899-907.
28. Teasdale, R. D.; Jackson, M. R. *Ann. Rev. Cell Develop. Biol.* **1996**, *12*, 27-54.
29. Olender, E. H.; Simon, R. D. *J. Biol. Chem.* **1992**, *267*, 4223-4235.
30. Allan, B. B.; Balch, W. E. *Science* **1999**, *285*, 63-66.
31. Swift, A. M.; Machamer, C. E. *J. Cell Biol.* **1991**, *115*, 19-30.
32. Munro, S. *Trends Cell Biol.* **1998**, *8*, 11-15.
33. Gleeson, P. A. *Histochem. Cell Biol.* **1998**, *109*, 517-532.
34. Dahms, N. M.; Lobel, P.; Kornfeld, S. *J. Biol. Chem.* **1989**, *264*, 12115-12118.
35. Pfeffer, S. R. *J. Membr. Biol.* **1988**, *103*, 7-16.
36. Cuervo, A. M.; Dice, J. F. *J. Molecular Medicine* **1998**, *76*, 6-12.
37. Lowe, M.; Kreis, T. E. *Biochim. Biophys. Acta* **1998**, *1404*, 53-66.
38. Martinez, O.; Goud, B. *Biochim. Biophys. Acta* **1998**, *1404*, 101-112.
39. Fedorov, A. N.; Baldwin, T. O. *J. Biol. Chem.* **1997**, *272*, 32715-32718.
40. Jans, D. A.; Chan, C. K.; Huebner, S. *Medicinal Research Reviews* **1998**, *18*, 189-223.
41. Derossi, D.; Chassaing, G.; Prochiantz, A. *Trends Cell Biol.* **1998**, *8*, 84-87.
42. Vives, E.; Brodin, P.; Leblus, B. *J. Biol. Chem.* **1997**, *272*, 1610-1617.
43. Green, M.; Loewenstein, P. M. *Cell* **1988**, *55*, 1179-1188.
44. Li, W.; Park, J. W.; Nuijens, A.; Sliwkowski, M. X.; Keller, G.-A. *Oncogene* **1996**, *6*, 2473-2477.
45. Kane, M. A.; Portillo, R. M.; Elwood, P. C.; Antony, A. C.; Kohlhouse, J. F. *J. Biol. Chem.* **1986**, *261*, 44-49.
46. Lord, J. M.; Roberts, L. M. *J. Cell Biol.* **1998**, *140*, 733-736.
47. Robenek, H.; Schmitz, G. *Arterioscler. Thromb.* **1991**, *11*, 1007-1020

Chapter 18

Modified Liposome Formulations for Cytosolic Delivery of Macromolecules

Kyung-Dall Lee and Gretchen M. Larson

Department of Pharmaceutical Sciences, College of Pharmacy,
University of Michigan, Ann Arbor, MI 48109-1065

Powerful therapeutic agents such as polypeptide-based drugs (1), antisense oligonucleotides (2,3), catalytic RNAs (4,5), and plasmid genes (6-8) represent the next generation of pharmaceuticals, but are limited thus far in their efficacy *in vivo* due to the difficulty in delivering them to the cytosolic space of target cells. The notion that these agents will exert their efficacy only with good delivery strategies that can place these macromolecules into the proper subcellular compartment of target cells is becoming more appreciated in academia, biotechnology, and pharmaceutical industries. Generally, the cytosolic space and the nucleus, which are topologically connected, are the desired target sites for therapeutic effectiveness of macromolecular drugs. Remarkable advances of biomedical research in recent years have identified numerous new targets and novel ammunitions to combat a variety of diseases, including cancer and AIDS; however, the weapons to deliver these potent agents to their targets at therapeutically effective concentrations *in vivo* are still lacking (9). Their intrinsic membrane impermeability is due to large molecular size or polyanionic characteristics. Such agents cannot cross the membrane barriers of cells, and thus, have limited access to the cytosol and nucleus. The development of a delivery strategy capable of specifically targeting and transporting these macromolecules across cell membranes into the appropriate subcellular compartments will dictate the potential for these drugs to achieve maximum efficacy.

We intend to primarily focus on liposomal drug delivery systems and their evolution from conventional formulations to next generation delivery vehicles, which can provide solutions to the problems of large molecular weight therapeutic agent delivery. The mechanism of liposome interaction with cells will be briefly examined in order to illustrate the limitations and unresolved issues associated with liposomal delivery system. Several recent approaches to overcome these limitations, including the effort in our laboratory, will then be discussed.

Background

From its inception in the sixties, liposome-based drug delivery research has survived the tortuous path common to many promising drug delivery schemes, and *en route* has seen significant transformation (10). While conceptually attractive, the dream of using liposomes made from naturally occurring lipids to serve as general drug carriers that can circulate much like red blood cells was quickly dismissed. Researchers soon discovered poor pharmacokinetic properties and rapid uptake of conventional liposomes by phagocytic cells in the reticuloendothelial system. Thus, formulation of sterically stabilized liposomes that show prolonged circulation in plasma was a long-sought solution to a critical obstacle (11-13). After many trials and failures, researchers in the liposome field recognized that the uptake of liposomes by macrophages can be drastically modulated or reduced by inclusion of specific lipids such as ganglioside GM₁, phosphatidylinositol, or a synthetic lipid, PEG-PE, which has polyethyleneglycol (PEG) attached to the headgroup of phosphatidylethanolamine (PE). The exact mechanism by which incorporation of one of these lipids induces longer circulation times is not entirely clear, although reduced binding of proteins, such as opsonizing plasma proteins or macrophage cell surface proteins, is implicated (14,15).

Due to the uptake by their natural target, macrophages of the reticuloendothelial system, efforts to target liposomes to other cell types failed until the advent of these long-circulating, sterically stabilized liposomes. The endocytic uptake of conventional liposomes by macrophages is so rapid that a targeting motif on the liposome surface has little opportunity to interact with the receptors on target cells, decreasing its potential effectiveness. The resurrected idea of targeting liposomes to specific cell types through increased plasma circulation and specific ligand-receptor interaction motivated many investigations of conjugated targeting motifs on long-circulating, sterically stabilized liposomes reporting increased efficiency of delivery to specific cells (16). We will not expand much further on this aspect, and refer to other existing reviews (13,17).

Interaction of Liposomes with Cells: Membranes as a Barrier

While targeting at the cellular or tissue level is clearly important, membrane-impermeant macromolecules cannot be effective without cytosolic delivery if their sites of action lie in the cytosol. Normal cellular interaction with its outside environment requires the cell to endocytose or phagocytose exogenous molecules or fluid into small, membrane-bounded vesicles called endocytic compartments. While this allows an effective reduction of the extracellular volume that cells must process, the endosomal membranes act as a physical barrier between the outside and the inside of cells. Thus the cytosol is topologically remote from both the cell exterior and the luminal space of the endosomal compartment. Although they appear to be within the cell, molecules internalized into the lumen of these endocytic compartments

technically still remain extracellular. Once the targeted liposomal vehicles transport the drugs to specific cells, most cells internalize them into these endocytic compartments. Membrane-impermeant macromolecules, however, remain trapped inside the endocytic pathway and are eventually delivered to the lysosomal compartments for degradation by hydrolases. Thus, even complete, specific delivery of drugs to the target cells has little therapeutic value if the majority of drug is routed to the lysosomal compartment and degraded.

Encapsulation of these macromolecules inside liposomes, either conventional or sterically stabilized, renders little advantage to favor their delivery into cytosol. Since the seminal work by Straubinger *et al.* demonstrating that liposomes are internalized by cells through the normal endocytic route, it has been well-established that liposomes and their contents are delivered to endosomes (18). These investigators prepared liposomes containing colloidal gold particles to follow the liposome's fate by electron microscopy. Their results definitively showed that the frequency of liposome fusion with cellular membranes, if it exists, is very low, thus liposomal cytosolic delivery is still minimal. Subsequent reports using the pyranine dye, HPTS, provided additional supporting evidence (19-21). Later work using the same techniques to follow PEG-PE-containing, sterically stabilized immunoliposomes also suggested that neutral or anionic liposomes in general have the tendency to be taken up by cells into endocytic compartments regardless of their binding mechanism, non-specific or ligand-receptor-mediated (16). An exception to these general findings is that direct destabilization or fusion with cellular membranes occurs quite extensively when liposomes are made of non-natural, cationic lipids (22); however, current research in this area is beyond the scope of this article. Yet, scattered reports suggest that we cannot entirely dismiss the possibility that a fraction of non-cationic liposomes can deliver their contents into the cytosol of cells under certain conditions and predominantly in complex *in vivo* cases (23,24). However, delivery in the range that is useful for most therapeutic purposes clearly requires greater efficiency and predictability of cytosolic delivery of liposomal contents.

Given such dogmatic generalizations, one might wonder how some pharmacological or therapeutic effects are observed with macromolecular drugs administered without special delivery systems or in conventional liposomal formulations. The cell biological mechanism of this phenomenon is not well understood, although it is speculated that intrinsic defects in the membranes' barrier function along the endocytic routes cause this limited leakage. If a minuscule amount of internalized material did leak out into the cytosol, a pharmacological effect could be achieved since these drugs are extremely potent once in the cytosol. Investigations addressing these fundamental questions are important and potentially beneficial for logical design of cytosolic delivery systems. Delivery via such mechanisms is far from the levels of predictability and effectiveness ideal for pharmaceutical applications, thus, we return our focus to the progress of liposomal formulations toward this goal.

Strategies for Cytosolic Delivery: Modified Liposome Formulations

Several approaches have been taken to reroute the cargo of endocytosed liposomes to the cytosolic space and away from the lysosomal compartment. One prominent strategy is to confer upon the liposomes a mechanism to overcome the membrane barrier of endocytic compartments. Temporarily breaching the endosomal membranes or inducing direct fusion between the internalized liposomal membrane and the endosomal membrane would allow the escape of endocytosed liposomal contents into the cytosolic space before they reach the highly degradative lysosomal compartments. If one envisions using targeted sterically stabilized liposomes which are designed to be delivered into the endocytic compartments of intended cells, such an approach seems particularly valid.

The most common paradigm for intracellular delivery has been to mimic viruses, which can efficiently introduce their contents into the cytosol of specific target cells. Viruses often achieve cell specificity by utilizing cell surface proteins as receptors for viral envelope proteins. Once bound to the cell surface, some viruses promote direct fusion between virus membrane and cell plasma membrane. Others are internalized into the endocytic compartment and trigger membrane fusion between the virus and endosome upon acidification of the endocytic compartment (25,26). Both types utilize the activity of the so called "fusion protein", which has the ability to coalesce two tightly apposed membranes.

Two main approaches have been proposed and tested in attempting to design liposomes that behave like viruses. One approach is the use of "pH-sensitive" or "acid-labile" liposomes (27-29). The other is incorporation of the function of the fusion protein into liposomal membranes. The former is achieved by incorporating into a lipid bilayer, made primarily of PE, lipids which have a protonatable moiety with a pKa near the acidic environment of endosomes. PE alone cannot form stable bilayers unless additional anionic lipid species are present in the bilayer. When the negative charge is neutralized upon protonation, the PE-containing bilayer collapses, which presumably results in fusion with adjacent membranes, as suggested by several *in vitro* liposome-based studies (30). However, no definitive experiment has been designed to test the events inside endosomes *in vivo*. Indirect evidence supports that these pH-sensitive liposomes induce a certain extent of leakage of endosomes, partly through this fusion event. Several experiments using antigen, fluorescent dye, toxin, or reporter genes show that the cytosolic delivery with pH-sensitive liposomes is greater than that with pH-insensitive liposomal formulations (31-33). However, the reported efficiency of cytosolic delivery indicates less frequent direct fusion between liposomal and endosomal membranes than the design hypothesized.

Reconstituting the whole viral fusion protein into liposomes to generate preteoliposomes or isolating the causative segment of fusion protein for incorporation into liposomes have been dominant methods for the second approach. Several delivery systems, particularly for oligonucleotides and plasmid genes, have been designed utilizing virus-derived fusion peptides or whole virus (34,35). In some instances, a viral envelope glycoprotein has been reconstituted into liposomes to

make artificial virus-like particles, called “viroosomes”, with a hollow aqueous compartment that can accommodate drugs (36). Similar formulations have been also generated by fusing liposomes with viruses. Viruses that have been exploited so far include influenza virus predominantly, as well as Adeno and Sendai viruses (37,38).

While most of these formulations augment cytosolic delivery via liposomes, their efficiency as delivery systems has not been at the level currently sought by the drug delivery field. Moreover, methods that use whole virus or reconstitution of viral membrane proteins are technically problematic for use in pharmaceutical formulations.

A New Delivery Strategy inspired from Intracellular Bacteria

A new paradigm that has recently been exploited is the cytosolic delivery of macromolecules by mimicking the escape of facultative intracellular bacteria from endocytic compartments into the cytosol. Parasitic bacteria or protozoa that survive by invading and multiplying within the cytoplasm of host cells must have the ability to escape from the endocytic vacuoles. By secreting specialized proteins, *Listeria*, *Shigella*, and *Trypanosoma cruzi* can effectively disrupt endosomal membranes (39-41). A different approach to macromolecular delivery and specifically gene delivery relies on the use of bacterial vectors to transfer exogenous genes, exploiting the cell biology of bacterial escape from endosomes (42). Facultative intracellular bacteria including *Shigella* and *Listeria* have been utilized in this manner (43-45). Attenuated mutant *Listeria monocytogenes* containing foreign plasmid DNA were introduced into a macrophage cell line and showed expression of reporter proteins and subsequent antigen presentation (45). Similarly, attenuated *Shigella flexneri* which is deficient in cell wall synthesis is also capable of DNA delivery (42,43). An *E. coli*-based bacterial carrier also represents a promising delivery route, with advantages including the improved safety of utilizing non-pathogenic *E. coli*, the ability to easily manipulate its genome, and the simplicity of attaining high plasmid copy number (42,55). *E. coli* is, however, still subject to the limitations of host immunity. Common to all these bacterial vectors is high enough efficiency to mediate therapeutically significant delivery of genes, as well as weaknesses shared by viral vectors including pathogenicity, immunogenicity, and difficulty in targeting.

Liposome Formulations with Bacterial Mechanisms: the Next Generation

Since risks and possible complications accompany the use of live bacteria, it is appealing to take only the necessary components from these intracellular invading organisms and design a non-bacterial delivery vehicle. The hemolysin of *Listeria monocytogenes*, listeriolysin O (LLO), is the well-characterized protein that is secreted by the intracellular parasite to escape from the endocytic compartment (46-48). LLO is a soluble protein of 58 kD that is suggested to form a pore in

membranes. It belongs to the “thiol-activated, pore-forming hemolysin” family, which includes perfringolysin O (PFO), pneumolysin O (PLO), and streptolysin O (SLO). These hemolysins share significant sequence homologies to each other, and all bind only to cholesterol-containing membranes, oligomerize within the lipid bilayer to form pores, and lyse membranes. LLO is unique among the thiol-activated hemolysins in that it possesses pH-dependent hemolytic activity; LLO is activated by low pH as well as reduction of the unique cysteine (Cys 484) in the amino acid sequence (48,49). The *Listeria* gene for LLO, *hly*, has been cloned and was the first virulence gene identified in *Listeria* (50,51). A mutant, *hly*⁻ *Listeria* cannot invade the cytosol of host cells; instead they die in the lysosomes, demonstrating that LLO is necessary for escape of *Listeria* into the cytosol (50,51). Portnoy and colleagues have demonstrated that when the *hly* gene is introduced into *Bacillus subtilis*, it confers the ability to escape from endocytic compartments (52), which is not inherently present in *B. subtilis*. This evidence suggests the hypothesis that a particulate carrier which releases LLO into the endosome may be able to disrupt endosomal membranes and deliver into the cytosol its internalized contents.

Early Work on a New Non-viral, Non-bacterial Liposome: *Listeriosomes*

This strategy has been recently tested by designing a new liposomal delivery vehicle that contains LLO (53). This new cytosolic delivery system incorporates the endosomolytic activity of LLO into pH-sensitive liposomes which can destabilize and leak their contents along with LLO upon protonation of their pH-sensitive component. The lipid formulation used does not interact with LLO and retains the LLO molecules inside liposomes at neutral pH, such that release is dictated by acidification in the endosomes, where LLO is then activated to form pores in the endosomal membranes. LLO is co-encapsulated inside liposomes with macromolecular cargo to create a LLO-containing liposome, or *listeriosome*, and its ability to deliver macromolecules into the cytosol of macrophages has been investigated. Testing of *listeriosomes* to deliver molecules of molecular mass up to 50 kD has shown dramatic enhancement of the release of fluorescent dyes, proteins (53), and 20-mer oligonucleotides from endosomes into the cytosol (unpublished data). This new delivery system can be utilized as a general delivery vehicle for many membrane-impermeant macromolecular drugs provided they can be encapsulated inside liposomes with reasonable efficiency. The unique ability of *listeriosomes* to put antigenic proteins into the cytosol makes them optimal for targeting antigens into the MHC class I-mediated cytosolic pathway of antigen presentation and T cell activation for vaccination applications. Additionally, targeted *listeriosomes* have the potential to serve as carriers of various toxins for use in chemotherapy. The versatility of *listeriosomes* would allow for the incorporation of a variety of cargos, from proteins to genes, without compromising delivery characteristics.

While LLO incorporation pioneered delivery using an isolated endosomolytic component of facultative intracellular bacteria, conjugation of PFO to DNA using a

biotin-streptavidin bridge has also been reported to yield enhanced levels of gene expression (54). However, the LLO protein has several beneficial inherent regulatory mechanisms including optimal activity at the pH of endosomes (48,49), which make it an ideal endosomolytic agent. Furthermore, since *Listeria* has evolved to be intracellular while *Streptococcus pyogenes* or *Clostridium perfringens* are extracellular bacteria, LLO should be better suited for endosome disruption for efficient and safe cytosolic delivery than SLO or PFO.

Conclusion

The ability to deliver a variety of drugs and macromolecules into the cytosol is essential to many areas of basic biology and pharmaceuticals. Potential applications include polypeptide delivery of antigenic proteins to induce cell-mediated immunity, chemotherapy using polypeptide- or recombinant protein-based drugs, delivery of oligonucleotide inhibitors in cell biology and in clinical settings, and plasmid DNA delivery in gene therapy. Liposomes in recent decades have gone through several transformations and will need significant further investigation to be used as a general delivery system for a variety of macromolecular therapeutic agents. In addition, modifications and customization for each application, depending on particular drugs and target cells, will be still necessary. Among the promising new strategies, the recent approach using the LLO-based mechanism presents an exciting solution to the limitations of liposomal cytosolic delivery. Several key questions, including (i) if the LLO-based delivery vehicles perform *in vivo* as well as in tissue culture and (ii) if nucleic acid-based macromolecules of various sizes can be delivered as efficiently as the proteinacious compounds, must be addressed in order to establish intracellular bacterial-based mechanisms of delivery as a new paradigm in the cytosolic delivery of macromolecules.

Acknowledgements

The authors would like to thank the University of Michigan and the College of Pharmacy for financial support (Rackham Faculty Research Award and Vahlteich Research Fund). Gretchen Larson is a Regent's Fellow at the University of Michigan and a F. Lyon's Fellow at the College of Pharmacy. This work has been also supported by the grants to K.-D. Lee from NIH (AI42084 and AI42657).

Literature Cited

1. Brugge, J. *Science* **1993**, *260*, 918-919.
2. Wagner, R. *Nature Med.* **1995**, *1*, 541-545.
3. Crooke, S. *Annu. Rev. Pharmacol. Toxicol.* **1992**, *32*, 329-376.

4. Castanotto, D.; Rossi, J.; Sarver, N. *Adv. Pharmacol.* **1994**, *25*, 289-317.
5. Cech, T. *The Journal of the American Medical Association* **1988**, *260*, 3030-3034.
6. Crystal, R. *Science* **1995**, *270*, 404-410.
7. Mulligan, R. *Science* **1993**, *260*, 926-932.
8. Felgner, P. L. *Laboratory Investigation* **1993**, *68*, 1-3.
9. Anonymous *Nature Biotechnology* **1998**, *16*, 115.
10. Papahadjopoulos, D. *J. of Liposome Research* **1995**, *5*, 9-14.
11. Papahadjopoulos, D.; Allen, T.; Gabizon, A.; Mayhew, E.; Matthay, K.; Huang, S. K.; Lee, K.-D.; Woodle, M. C.; Lasic, D. D.; Redemann, C.; Martin, F. J. *Proc. Natl. Acad. Sci. USA* **1991**, *88*, 11460-11464.
12. Allen, T. M. *Trends in Pharmacological Sciences* **1994**, *15*, 215-20.
13. Lasic, D.; Martin, F. *Stealth liposomes*; CRC: Boca Raton, FL, 1995.
14. Lasic, D. D.; Martin, F. J.; Gabizon, A.; Huang, S. K.; Papahadjopoulos, D. *Biochimica et Biophysica Acta* **1991**, *1070*, 187-92.
15. Lee, K. D.; Hong, K.; Papahadjopoulos, D. *Biochim Biophys Acta* **1992**, *1103*, 185-97.
16. Park, J. W.; Hong, K.; Carter, P.; Asgari, H.; Guo, L.; Keller, G.; Wirth, C.; Shalaby, R.; Kotts, C.; Wood, W.; Papahadjopoulos, D.; Benz, C. *Proc. Natl. Acad. Sci. USA* **1995**, *92*, 1327-1331.
17. Allen, T. M.; Brandeis, E.; Hansen, C. B.; Kao, G. Y.; Zalipsky, S. *Biochim Biophys Acta* **1995**, *1237*, 99-108.
18. Straubinger, R. M.; Hong, K.; Friend, D. S.; Papahadjopoulos, D. *Cell* **1983**, *32*, 1069-1079.
19. Straubinger, R. M.; Papahadjopoulos, D.; Hong, K. *Biochemistry* **1990**, *29*, 4929-4939.
20. Daleke, D. L.; Hong, K.; Papahadjopoulos, D. *Biochim Biophys Acta* **1990**, *1024*, 352-66.
21. Lee, K.-D.; Nir, S.; Papahadjopoulos, D. *Biochemistry* **1993**, *32*, 889-899.
22. Friend, D. S.; Papahadjopoulos, D.; Debs, R. J. *Biochim Biophys Acta* **1996**, *1278*, 41-50.
23. Zhou, F.; Huang, L. *Immunomethods* **1994**, *4*, 229-35.
24. Alving, C. R.; Wassef, N. M. *AIDS Research & Human Retroviruses* **1994**, *10*, S91-4.
25. Marsh, M.; Helenius, A. *Adv Virus Res* **1989**, *36*, 107-51.
26. White, J.; Kielian, M.; Helenius, A. *Quart. Rev. Biophys.* **1983**, *16*, 151-195.
27. Straubinger, R. M. *Methods in Enzymology* **1993**, *221*, 361-76.
28. Düzgünes, N.; Straubinger, R. M.; Baldwin, P. A.; Friend, D. S.; Papahadjopoulos, D. *Biochemistry* **1985**, *24*, 3091-3098.
29. Connor, J.; Huang, L. *J. Cell Biology* **1985**, *101*, 582-589.
30. Allen, T. M.; Hong, K.; Papahadjopoulos, D. *Biochemistry* **1990**, *29*, 2976-85.
31. Chu, C.-J.; Dijkstra, J.; Lai, M.-Z.; Hong, K.; Szoka, F. C. *Pharm. Res.* **1990**, *7*, 824-834.
32. Harding, C. V.; Collins, D. S.; Kanagawa, O.; Unanue, E. R. *J Immunology* **1991**, *147*, 2860-3.

33. Legendre, J. Y.; Szoka, F. J. *Pharm. Res.* **1992**, *9*, 1235-42.
34. Wagner, E.; Plank, C.; Zatloukal, K.; cotten, M.; Birnstiel, M. *Proc. Natl. Acad. Sci. USA* **1992**, *89*, 7934-7938.
35. Curiel, D. T.; Agarwal, S.; Wagner, E.; Cotten, M. *Proc. Natl. Acad. Sci. USA* **1991**, *88*, 8850-4.
36. Bron, R.; Ortiz, A.; Wilschut, J. *Biochemistry* **1994**, *33*, 9110-9117.
37. Uchida, T.; Kim, J.; Yamaizumi, M.; Miyake, Y.; Okada, Y. *J. Cell Biol.* **1979**, *80*, 10-20.
38. Dzau, V. J.; Mann, M. J.; Morishita, R.; Kaneda, Y. *Proc. Natl. Acad. Sci. USA* **1996**, *93*, 11421-5.
39. Portnoy, D.; Jacks, P.; Hinrichs, D. *J. Exp. Med.* **1988**, *167*, 1459-1471.
40. High, N.; Mounier, J.; Prevost, M. C.; Sansonetti, P. J. *EMBO Journal* **1992**, *11*, 1991-9.
41. Andrews, N. W. *Exp Parasitol* **1990**, *71*, 241-4.
42. Higgins, D.; Portnoy, D. *Nature Biotechnology* **1998**, *16*, 138-139.
43. Sizemore, D.; Branstrom, A.; Sadoff, J. *Science* **1995**, *270*, 299-302.
44. Ikonomidis, G.; Paterson, Y.; Kos, F. J.; Portnoy, D. A *J. Exp. Med* **1994**, *180*, 2209-18.
45. Dietrich, G.; Bubert, A.; Gentshev, I.; Sokolovic, Z.; Simm, A.; Catic, A.; Kaufmann, S.; Hess, J.; Szalay, A.; Goebel, W. *Nature Biotechnology* **1998**, *16*, 181-185.
46. Geoffroy, C.; Gaillard, J. L.; Alouf, J. E.; Berche, P. *Infection & Immunity* **1987**, *55*, 1641-6.
47. Goldfine, H.; Knob, C.; Alford, D.; Bentz, J. *Proc. Natl. Acad. Sci. USA* **1995**, *92*, 2979-83.
48. Portnoy, D. A.; Tweten, R. K.; Kehoe, M.; Bielecki, J. *Infection & Immunity* **1992**, *60*, 2710-7.
49. Jones, S.; Portnoy, D. A. *Infection & Immunity* **1994**, *62*, 5608-13.
50. Mengaud, J.; Chenevert, J.; Geoffroy, C.; Gaillard, J.; Cossart, P. *Infection & Immunity* **1987**, *55*, 3225-3227.
51. Cossart, P.; Vicente, M. F.; Mengaud, J.; Baquero, F.; Perez-Diaz, J. C.; Berche, P. *Infection & Immunity* **1989**, *57*, 3629-36.
52. Bielecki, J.; Youngman, P.; Connelly, P.; Portnoy, D. A. *Nature* **1990**, *345*, 175-6.
53. Lee, K.-D.; Oh, Y.; Portnoy, D.; Swanson, J. *J. Biol. Chem.* **1996**, *271*, 7249-7252.
54. Gottschalk, S.; Tweten, R.; Smith, L.; Woo, S. *Gene Therapy* **1995**, *2*, 498-503.
55. Higgins, D.E.; Shastri, N.; Portnoy, D.A. *Molecular Microbiology* **1999**, *31*, 1631-1641.

Chapter 19

Molecular Targeting of Nuclear Transcriptional Regulators

Yon Rojanasakul¹, Q. Luo¹, J. Ye², D. Faroonsargn³,
S. Dokka¹, and X. Shi²

¹Department of Basic Pharmaceutical Sciences,
West Virginia University, Morgantown, WV 26506

²Pathology and Physiology Research Branch, National Institute
for Occupational Safety and Health, Morgantown, WV 26505

³Department of Pharmaceutical Sciences,
Prince of Songkla University, Songkla, Thailand

Gene regulation by nuclear transcription factors involves intracellular interactions of nuclear transcriptors with specific transport carriers and/or DNA regulatory elements using sequence-specific recognition sites. In this study, we utilized a series of synthetic peptides carrying the nuclear localization sequence of the transcriptor NF- κ B p50 and p65 subunits to inhibit NF- κ B-mediated gene expression. Gene transfection and gel-shift assays showed that these peptides were effective in inhibiting the nuclear translocation and transcriptional activation of NF- κ B. However, their effects required the presence of a cell-permeable peptide which is covalently linked to the inhibitory peptides. These hybrid peptides may be used as novel therapeutic agents in diseases whose etiology is dependent on NF- κ B activation.

Gene activation by nuclear transcription factors represents a fundamental process in the cellular control of gene expression. This process involves intracellular interactions of nuclear proteins with specific transport carriers and/or DNA regulatory elements using recognition sequences. By exploiting these recognition sequences, a number of molecular therapeutic approaches has been developed to manipulate pathologic gene expression. In this study, we reported a gene inhibition method which

utilizes nuclear localization sequences (NLS) of the transcription factor NF- κ B to regulate the nuclear translocation and transcriptional activity of NF- κ B.

NF- κ B is a key transcription factor involved in immune and inflammatory disorders. It is frequently composed of two DNA-binding subunits, NF- κ B₁ (p50) and RelA (p65) (1, 2). It is normally kept in an inactive form in the cytoplasm by attachment of the inhibitory subunit I κ B, which masks the NLS of the NF- κ B subunits. The activation of NF- κ B is accomplished by phosphorylation of I κ B, which triggers the complete degradation of the inhibitor (3). This induced degradation of I κ B unmasks the NLS of the NF- κ B dimer and allows NF- κ B to enter the nucleus, to bind to its DNA target sequence, and to induce transcription. Because nuclear translocation of NF- κ B is crucial for its transcriptional activity and because this translocation is dependent on NLS, we rationalize that specific peptide sequences carrying the NLS signal may be used to selectively inhibit the nuclear translocation and thus transcriptional activity of NF- κ B. This was tested in the present study using various molecular techniques including electrophoretic mobility shift assay (EMSA), gene transfection, and enzyme linked immunosorbent assay (ELISA).

Experimental

Cells and Reagents

Macrophage RAW 264.7 cells were used throughout. The cells were maintained in DMEM supplemented with 5% fetal bovine serum, 2 mM glutamine, and 1,000 units/ml penicillin-streptomycin at 37°C in a humidified atmosphere at 5% CO₂. A specific antibody against NF- κ B (p50) was obtained from Santa Cruz Biotechnology Inc. (Santa Cruz, CA). Peptides were synthesized by a stepwise solid-phase peptide synthesis method (Quality Controlled Biochemicals, Hopkinton, MA). The peptides were purified by C₁₈ reverse-phase HPLC and verified by mass spectrometry.

Nuclear Extracts

Nuclear extracts were prepared as follows; 5x10⁷ cells were treated with 500 μ l lysis buffer (50 mM KCl, 0.5% NP-40, 25 mM Hepes, 1 mM PMSF, 10 mg/ml leupeptin, 20 μ l/ml aprotinin, 100 mM DTT) on ice for 4 min. Nuclei were pelleted by centrifugation at 14,000 rpm for 1 min and were resuspended in 300 μ l extraction buffer (500 mM KCl, 10% glycerol, 25 mM Hepes, 1 mM PMSF, 1 μ l/ml leupeptin, 20 μ g/ml aprotinin, 100 μ M DTT). After centrifugation at 14,000 rpm for 5 min, the

supernatant was harvested and stored at -70°C . The protein concentration of the resulting nuclear protein extract was determined by BCA protein assay reagent (Pierce, Rockford, IL).

Electrophoretic Mobility Shift Assay

The DNA-protein binding reaction was conducted in a 24 μl reaction mixture including 3 μg nuclear protein extract, 1 μg poly dI.dC (sigma), 3 μg BSA, 4×10^4 cpm of ^{32}P -labeled oligonucleotide probe, and 12 μl of 2xY buffer. The mixture was incubated on ice for 10 min without antibody, or 10 min with antibody, in the absence of radiolabeled probe, then 20 min at room temperature in the presence of radiolabeled probe. The mixture was resolved on a 5% polyacrylamide gel at 200 V for 90 min, then dried and placed on Kodak X-OMAT film (Eastman Kodak, Rochester, NY). This film was developed after an overnight exposure at -70°C . NF- κB binding sequence ($5'$ -TGGGATTTCCCATGAGTCT- $3'$) was used to synthesize the probe. The synthesized single-stranded oligonucleotide probe was denatured at 80°C for 5 min and annealed with its complementary sequence at room temperature. The double-stranded probe was labeled with ^{32}P -ATP (Amersham, Arlington Heights, IL) using T4 kinase (BRL, Gaithersburgh, MD).

Enzyme Linked Immunosorbent Assay

Analysis of TNF α levels was performed using the Genzyme TNF α ELISA kit (Genzyme Corp., Cambridge, MA) according to the manufacturer's instructions. Absorbance measurements of the enzyme product were performed at the wavelength of 450 nm using the Bio-Rad 500 microplate reader.

Transient Transfection and Luciferase Assay

The reporter plasmid used in this study was generously provided by Dr. J. Ye at the National Institute for Occupational Safety and Health. The luciferase reporter plasmid contains NF- κB binding sites derived from the -615/+15 promoter fragment of TNF α gene. The cells were plated in six-well plates 1 day before transfection. For transient transfection, 1 μg of the reporter DNA was mixed with 6 μg lipofectAMINE (GIBCO BRL) and 2 μg protamine sulfate (Sigma) in 200 μl Optimal medium (GIBCO BRL). The cells were incubated with the mixture of DNA and lipofectAMINE for 6 h at 37°C and then with 4 ml of the complete medium at 37°C for 24 h. After treatment, the cells were harvested and analyzed for luciferase activity using an assay kit (Promega, Madison, WI). To account for potential cytotoxicity caused by the transfecting agents or other test agents, total cell protein was determined and used to normalize the measured luciferase activity.

Results and Discussion

Design of Inhibitory Peptides

NF- κ B is a heterodimer nuclear protein that is formed by two common DNA-binding subunits p50 and p65. These two subunits have their individual NLS in the amino acid sequences (4). These NLS are involved in the nuclear translocation of NF- κ B; therefore, if peptides carrying the NLS of p50 and/or p65 are administered into cells, they should be able to compete with the NF- κ B for the nuclear transport carriers, and thus lead to an inhibition of NF- κ B activity. To aid the cellular delivery of NLS peptides, a cell-permeable import peptide (IP) derived from the hydrophobic region of the signal peptide fibroblast growth factor (5) was linked to the NLS peptides. This import peptide has been shown to facilitate the cellular entry of biomolecules into intact cells (6, 7). Accordingly, we synthesized a series of peptides comprising the IP (AAVALLPAVLLALLAP) and various NLS of NF- κ B:

IP50	=	IP + NLS of NF- κ B p50 (VQRKRQKLMP)
IP65	=	IP + NLS of NF- κ B p65 (HRIEEKRKRTYETF)
IP50/65	=	IP + NLS of NF- κ B p50 and p65

As comparative controls, the following peptides were used:

IP50M	=	IP + mutated NLS of NF- κ B p50 (VQRNGQKLMP)
IP	=	IP
P50	=	NLS of NF- κ B p50

Inhibition of Nuclear Translocation of NF- κ B

To test the effect of peptides on nuclear translocation of NF- κ B, EMSA studies were conducted. Nuclear proteins were made from RAW 264.7 cells after 2-h stimulation with 10 ng/ml of LPS in DMEM. The results showed that nuclear translocation of NF- κ B was induced by LPS and this translocation of NF- κ B was inhibited by IP50, IP65, and IP50/65 (Fig. 1A). The control peptides P50, IP50M, and IP (insoluble in the test medium) had no effect. To assess the binding specificity of NF- κ B in the EMSA studies, oligonucleotide competition and antibody supershift assays were conducted. The results of this study showed that the NF- κ B binding activity could be competed by a nonlabeled NF- κ B oligonucleotide probe but not by the non-specific AP1 probe, and the antibody specific to the p50 subunit of NF- κ B caused a band-shift of the NF- κ B complexes (Fig. 1B)). These results indicated the DNA binding specificity of NF- κ B under the experimental conditions. The lack of the inhibitory effect of IP50M indicated the sequence specificity for nuclear translocation of IP50. Likewise, the lack of the inhibitory effect of P50 indicated the requirement of the peptide carrier IP for efficient cellular uptake of the NLS peptides. Cellular

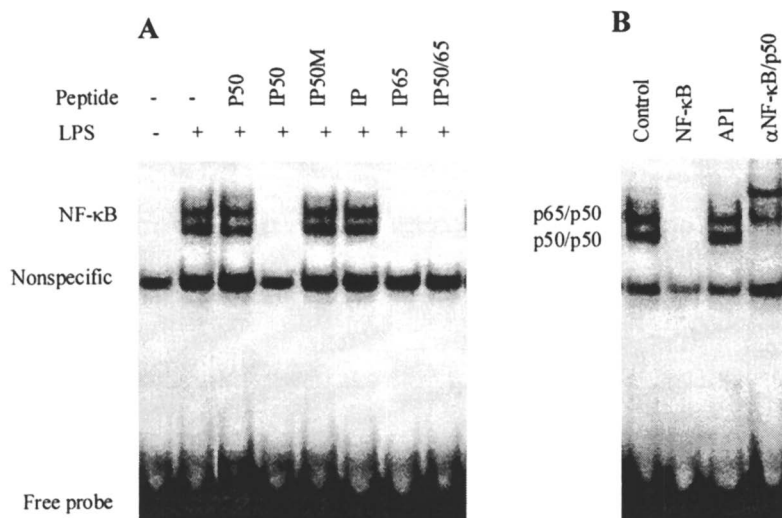


Figure 1. EMSA studies of NF-κB. Cells were pretreated with the indicated peptide (100 μg/ml) for 1 h followed by LPS (10 ng/ml) for 2 h. The assays were performed as described in the Materials and Methods. Competitor and antibody used in each lane as indicated.

uptake studies using fluorescently-labeled peptides in this laboratory supported this conclusion.

Inhibition of LPS-Induced TNF α Gene Expression

The inhibition of nuclear translocation of NF- κ B by inhibitory peptides should lead to transcriptional inactivation of NF- κ B-dependent genes. The cytokine TNF α gene is one of those genes whose expression is dependent on NF- κ B activation (8). To test the potential inhibitory effect of peptides on TNF α gene expression, ELISA studies were conducted. Our results showed that the inhibitory peptides IP50, IP65, and IP50/65 caused a complete inhibition in LPS-induced TNF α expression, whereas the control peptides IP50M had no effect (Fig. 2). These results are in good agreement with the EMSA studies and indicate that the transcriptional inactivation of TNF α gene can lead to an inhibition of its protein expression.

Inhibition of NF- κ B-Dependent Reporter Gene Expression

To confirm the inhibitory effect of peptides on NF- κ B-dependent gene expression, gene transfection assays using a reporter plasmid were conducted. The reporter plasmid contains luciferase gene under the control of NF- κ B gene promoters. Our results indicated that the IP50 was able to inhibit LPS-induced luciferase gene expression in transfected cells, whereas the mutated IP50M had no effect (Fig. 3). The inhibitory effect of IP50 was not due to its cytotoxicity as indicated by trypan blue dye exclusion assay. The percentage of cells viable after treatment with IP50 (100 μ g/ml) was 94 \pm 4 % which was not significantly different from the nontreated control (97 \pm 3 %) ($p < 0.05$).

Conclusions

Using synthetic peptides carrying the NLS of NF- κ B, we demonstrated that effective inhibition of the nuclear translocation of NF- κ B can be achieved. This inhibition required the presence of a cell-permeable peptide carrier which is linked to the NLS peptides. Control peptides lacking NLS or carrier sequences exhibited no inhibitory effect, as demonstrated by electrophoretic mobility shift assay. ELISA and transient gene transfection assays also showed that these peptides were effective in inhibiting NF- κ B-dependent gene expression. These inhibitory peptides may be used as novel therapeutic agents in diseases whose etiology is dependent on NF- κ B activation.

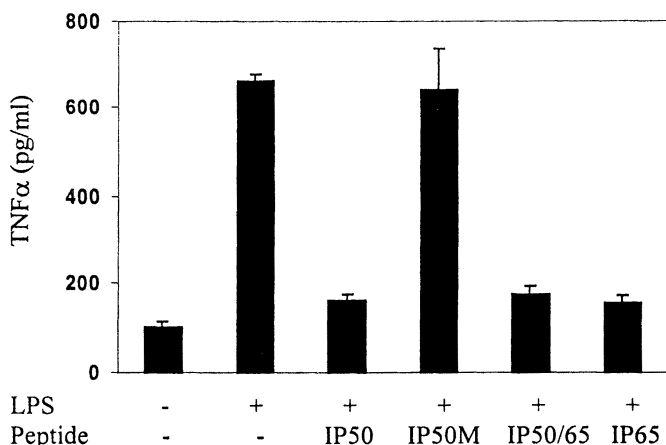


Figure 2. Suppression of LPS-Induced TNF α Production by Inhibitory Peptides. Cells were treated with the indicated peptide (100 μ g/ml) for 1 h prior to LPS stimulation (10 ng/ml). TNF α levels were detected 6 h after stimulation by an ELISA assay. The values represent mean \pm S.E., $n = 4$.

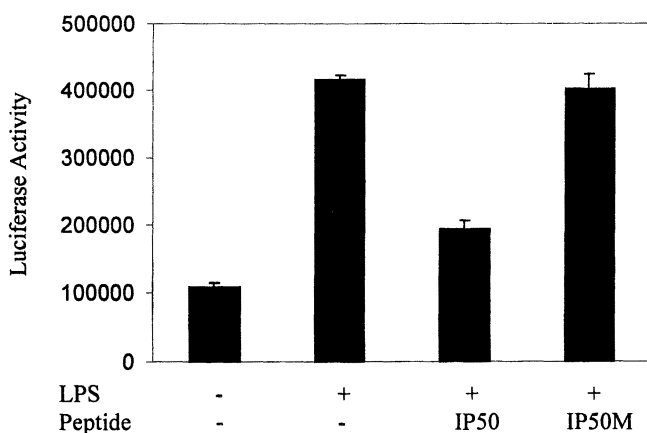


Figure 3. Effect of Inhibitory Peptides on NF- κ B-Dependent Luciferase Gene Expression. Transfected cells were treated with peptide (100 μ g/ml), followed by LPS stimulation (10 ng/ml). The values represent mean \pm S.E., $n = 4$.

References

1. Baeuerle, P.A. *Biochim. Biophys. Acta* **1991**, *1072*, 63.
2. Baeuerle, P.A.; Henkel, T. *Annu. Rev. Immunol.* **1994**, *12*, 141.
3. Traenkner, B.M.; Wilk, S.; Baeuerle, P.A. *EMBO J.* **1994**, *13*, 5433.
4. Henkel, T.; Zabel, K.; Zee, K.; Muller, J.; Fanning, E.; Baeuerle, P. *Cell* **1992**, *68*, 1121.
5. von Heijne, G. *J. Memb. Biol.* **1990**, *115*, 195.
6. Dokka, S.; Toledo, D.; Shi, X.; Wang, L.Y.; Rojanasakul, Y. *Pharm. Res.* **1997**, *14*, 1759.
7. Rojas, M.; Donahue, J.P.; Tan, Z.; Lin, Y.Z. *Nature Biotech.* **1998**, *6*, 370.
8. Collart, M.A.; Baeuerle, P.A.; Vassal, P. *Mol. Cell Biol.* **1990**, *10*, 1498.

Chapter 20

Cell-Specific Targeting of Drugs and Genes with Glycosylated Liposomes: Comparison with Glycosylated Poly(amino acids)

Mitsuru Hashida, Makiya Nishikawa, Fumiyoshi Yamashita,
and Yoshinobu Takakura

Graduate School of Pharmaceutical Sciences, Kyoto University,
Sakyo-ku, Kyoto 606-8501, Japan

Cell-specific targeting of drugs and genes with novel galactosylated liposomes was examined *in vitro* and *in vivo* and compared with that with galactosylated poly(amino acids). Galactosylated liposomes were largely recovered in liver parenchymal cells after intravenous injection as galactosylated poly(amino acids). DNA/galactosylated cationic liposome complexes showed higher transfection activity and DNA uptake in asialoglycoprotein receptor-positive cells than DNA complexes with conventional cationic liposomes. DNA complexes with galactosylated cationic liposomes were more efficient as far as *in vitro* gene transfer was concerned but their biodistribution was more difficult to control than that of DNA/galactosylated poly(amino acids) complexes. These results suggest that application of these galactosylated liposomes for cell-specific targeted delivery of low-molecular weight drugs and genes will be a useful advance.

Cell-specific targeting of pharmaceuticals is an effective strategy for improving their therapeutic efficacy. Using glycosylated delivery systems is a promising approach for the targeted delivery of drugs and genes to cells having the corresponding sugar receptors. Hepatocytes are well known to recognize galactose- and *N*-acetylgalactosamine-terminal glycoproteins via asialoglycoprotein receptors, whereas macrophages, like Kupffer cells and liver endothelial cells, possess mannose receptors that specifically recognize mannose and *N*-acetylglucosamine residues (1). Therefore, chemically glycosylated proteins, polymers and liposomes have been used

for cell-specific targeting of drugs and genes to these cells (2,3). In these approaches, carriers having sugar moieties were simply considered to be able to transport drugs and genes to cells possessing the corresponding receptors, and little attention was paid to the *in vivo* disposition properties of the drug- and gene-carrier complexes.

For the rational design of drug delivery systems, we have emphasized the importance of considering the pharmacokinetics of their biodistribution. In a series of investigations we showed that the physicochemical properties, such as molecular weight, particle size, and electrical charge, mainly determine the biodistribution of carriers after intravenous injection (for review, 4-6). Even in the case of glycosylated carriers, these properties have been found to affect the targeting efficiency to the liver (7-9). These findings indicate that not only ligands grafted to carriers but also the overall physicochemical properties of the carriers themselves determine the amount delivered to receptor-positive cells after their systemic administration. Carriers, even if they were extensively galactosylated, cannot deliver a pharmaceutical agent to hepatocytes without reaching the cells.

From a structural point of view, carriers can be divided into two categories: macromolecular and particulate carriers. As far as biodistribution is concerned, macromolecular carriers are more easy to control. However, particulate carriers such as liposomes may have some advantages as carriers for low molecular weight drugs (large loading capacity for lipophilic drugs) and for gene therapies (high transfection efficiency). These diverse properties that determine the efficacy of drug or gene targeting should both be considered when designing an appropriate carrier for drugs and genes. Recently, we synthesized a novel galactosylated cholesterol derivative with a carbohydrate spacer (Gal-C4-Chol) (Figure 1), and formulated galactosylated cationic liposomes (10). To evaluate the usefulness of these novel galactosylated liposomes for the targeted delivery of drugs and genes, we compared the results obtained with galactosylated liposomes with those of galactosylated poly(amino acids). In this paper, the biodistribution and cell-specific targeting of drugs and plasmid DNA by these carriers are discussed.

BIODISTRIBUTION OF GLYCOSYLATED CARRIERS

Galactosylated carriers are designed to deliver drugs and genes to hepatocytes through a recognition process via the asialoglycoprotein receptors. Although some branched (triantennary) galactose oligomers are the most useful targeting molecules for asialoglycoprotein receptors, the increase in the number of single galactose moieties on the carriers can take their hepatic uptake to the limit (7,8). However, galactosylated carriers do not reach hepatocytes after systemic administration due to their adverse biodistribution properties.

Glycosylated Poly(Amino Acids)

Poly(amino acids) are considered to possess advantages as drug carriers since they are soluble in water, biodegradable, are not significantly immunogenic, and have

multiple functional groups that are easily modified chemically. Therefore, great attention has been paid to the use of glycosylated poly(amino acids) as a carrier of low-molecular weight drugs (11-13) and poly- or oligonucleotides (14-17).

Of the various poly(amino acids) available, poly(L-glutamic acid) (PLGA) and poly(L-lysine) (PLL) have been widely used as carrier backbones. PLGA is an anionic polymer and PLL is a cationic one, so their biodistribution properties are very different. After intravenous injection into mice, PLL is largely delivered to liver parenchymal cells (PC) due to its positive charge, whereas PLGA is partially taken up by liver nonparenchymal cells (NPC), probably via a scavenger receptor-like mechanism (9,11). Glycosylation changes the biodistribution properties of these polymers, especially PLGA. Galactosylated (Gal-) and mannosylated (Man-) PLGAs were recovered mainly in the liver after intravenous injection. Furthermore, Gal-PLGA and Man-PLGA were selectively taken up by liver PC and NPC, respectively, indicating their receptor-mediated uptake (Figure 2). Their receptor-mediated uptake was also supported by the co-injection of Gal- or Man-bovine serum albumin (BSA) (9). On the other hand, both Gal-PLL and Man-PLL accumulated largely in PC. However, the PC/NPC ratios of Gal-PLL (4.7) and Man-PLL (1.6) were larger and smaller than that of PLL (3.2), respectively (Figure 2), suggesting that these glycosylated PLLs are also taken up by the liver cells through receptor-mediated recognition as glycosylated PLGAs.

From a pharmacokinetic point of view, PLL seems to be a promising hepatocyte-specific carrier, but galactosylated polymers have some advantages over cationic PLL. Since the hepatotropic nature of cationic polymers is likely due to their positive charge, neutralization of this charge abolishes its affinity for the cells. As discussed below, complex formation with nucleic acids like plasmid DNA reduces the positive charge of PLL. This, in turn, makes the recognition of glycosylated PLLs via receptors more evident. In addition, the internalization of galactosylated carriers is much faster than that of cationic ones (18), which could be an advantage for DNA and some drugs.

The degree of modification is an important factor determining the targeting efficiency of these glycosylated carriers. Increasing the number of galactose units increased the amount delivered to the liver and the hepatic clearance of Gal-PLGA (11). These features should be considered when designing polymeric carriers with sugar moieties.

Glycosylated Liposomes

To control the biodistribution of glycosylated liposomes, simple sugars, not asialoglycoproteins, would be more suitable. To this end, we synthesized a galactosylated cholesterol, Gal-C4-Chol, and formulated galactosylated liposomes (10). For hepatocyte-directed drug delivery, liposomes with long circulating half-lives are suitable for the preparation of galactosylated liposomes. Therefore, a liposome formulation composed of distearoylphosphatidylcholine and cholesterol was selected as a control liposome, and a portion of the cholesterol was replaced with Gal-C4-Chol to prepare a galactosylated liposome formulation. The control liposomes showed a

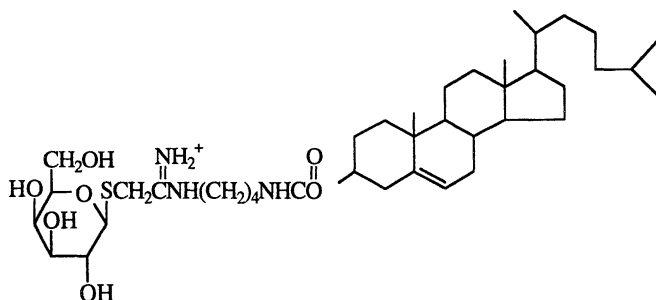


Figure 1. Chemical structure of cholesten-5-yloxy-N-(4-((1-imino-2- β -D-thiogalactosylethyl)amino)butyl)formamide (Gal-C4-Chol).

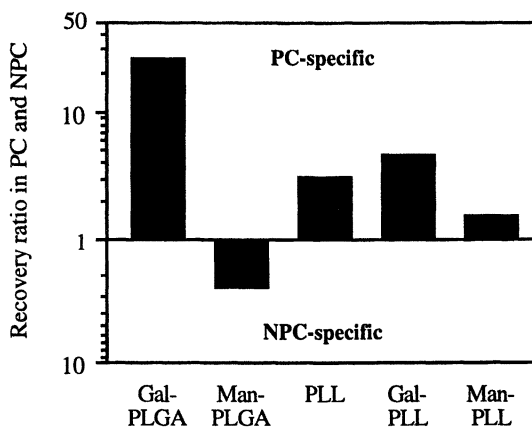


Figure 2. Recovery ratio of glycosylated poly(amino acids) in liver parenchymal (PC) and nonparenchymal cells (NPC) after intravenous injection. After intravenous injection of ^{111}In -glycosylated poly(amino acids), mouse liver was perfused with a solution containing collagenase to obtain cell suspensions. The cells were then separated into PC and NPC by differential centrifugation.

prolonged blood circulation, whereas the Gal-liposomes were selectively delivered to liver PC, indicating asialoglycoprotein receptor-mediated delivery.

In the case of particulate carriers like galactosylated liposomes, particle size is an important factor. For targeting to hepatocytes, the fenestrae of liver sinusoids larger than 200 nm in diameter are very small (19) and, therefore, carriers should be less than that size for efficient delivery to the cells.

DRUG DELIVERY WITH GLYCOSYLATED CARRIERS

Low-molecular weight drugs can be delivered to sugar receptor-positive cells by conjugating them to glycosylated carriers (in most cases, polymers) or by incorporating them into glycosylated particulate carriers. Both approaches are available, but the former requires conjugation for synthesis and the regeneration of the parent drug after administration.

Chemical Conjugation of Drugs

Drugs can be covalently bound to macromolecular carriers to form macromolecular prodrugs. In our previous studies, mitomycin C, cytosine arabinoside, vitamin K₃, prostaglandin E₁ (PGE₁), and FK506 were attached to carriers or glycosylated carriers. Macromolecular prodrugs should fulfill the following criteria: (i) drugs can be attached to carriers without significant loss of activity, (ii) the conjugation of drugs does not significantly alter the biodistribution of carriers, and (iii) active drugs are regenerated within the body.

Although PGE₁ is known to be effective on fulminant or subfulminant viral hepatitis, long-term administration of PGE₁ is required for treatment due to its low hydrophilicity and poor physiological stability. Therefore, delivery systems could increase the usefulness of PGE₁. To deliver PGE₁ to hepatocytes, we synthesized PGE₁ prodrugs with Gal-PLGA (4). When PGE₁ was attached to Gal-PLGA by the carbonyldiimidazole method (Gal-PLGA-PGE₁), the PGE₁ conjugate showed no pharmacological activity although the targeting of PGE₁ to hepatocytes was successful. This would be due to inactivation of the drug during the conjugation reaction by CDI. To retain the pharmacological activity of PGE₁ after conjugation, therefore, a different synthetic procedure is needed. To this end, a hydrazide group was introduced onto PLGA to couple PGE₁ through its ketone group (Gal-HZ-PLGA-HZ-PGE₁) in a weakly acidic buffer at room temperature, a condition where PGE₁ is expected to be chemically most stable (20). When investigated in mice with tetrachloride-induced hepatitis, the new PGE₁ conjugate showed a significant effect on the GPT level in plasma, suggesting that it has superior therapeutic activity against fulminant hepatitis (unpublished data).

Physical Entrapment of Drugs

Drugs, especially lipophilic ones, can be physically incorporated into particulate carriers such as liposomes and fat emulsions (21). In the cases of lipophilic drugs, their lipophilicity determines their retention in liposomes and emulsions. Although PGE₁ can be formulated in a liposomal formulation, the biodistribution of PGE₁ is quite different from that of the liposome itself, suggesting its rapid release within the body. However, our preliminary investigation suggests that a portion of PGE₁ can be delivered to hepatocytes by incorporating it into a Gal-liposome, which is effective in suppressing experimental hepatitis (unpublished data).

DNA DELIVERY WITH GLYCOSYLATED CARRIERS

Gene delivery is a critical issue for successful *in vivo* gene therapy. *In vivo* gene therapy requires the development of carriers (vectors) that can deliver therapeutic genes into a specific cell population and, there, efficiently express encoded proteins. Although viral systems such as retroviral and adenoviral vectors are potentially very efficient, nonviral gene delivery systems have a number of potential advantages: they are less toxic, less immunogenic, and easier to prepare (22,23). In most cases, cationic carriers are used for DNA delivery because they can form complexes with DNA.

Galactosylated Cationic Liposomes

Glycosylation of cationic carriers can be more effective in introducing DNA to cells possessing sugar receptors. For hepatocyte-specific gene transfer, we prepared a cationic liposome formulation using Gal-C4-Chol, 3 β [N',N',N'-dimethylaminoethane)-carbamoyl]cholesterol (DC-Chol), and dioleoylphosphatidylethanolamine (DOPE) (Gal-C4-Chol/DC-Chol/DOPE, 3:3:4) and mixed it with DNA encoding firefly luciferase gene (10). Figure 3 shows the expression of luciferase in HepG2 cells treated with DNA/cationic liposome complexes. Three cationic liposomes showed different optimal DNA/liposome ratios for gene expression. The greatest gene expression with DC-Chol/DOPE (6:4) liposomes was observed at a DNA/liposome ratio of 1:5, whereas that for Gal-C4-Chol/DC-Chol/DOPE (3:3:4) and Gal-C4-Chol/DOPE (6:4) liposomes was found at a ratio of 1:10. When gene expression was compared at their optimal ratios, Gal-C4-Chol/DC-Chol/DOPE (3:3:4) liposomes were the most effective. The maximum transfection activities of DC-Chol/DOPE (6:4) liposomes and Gal-C4-Chol/DOPE (6:4) liposomes were almost identical and half that of Gal-C4-Chol/DC-Chol/DOPE (3:3:4) liposomes. The presence of 20 mM galactose significantly inhibited the gene expression of Gal-C4-Chol/DC-Chol/DOPE (3:3:4) and Gal-C4-Chol/DOPE (6:4) liposomes, but not that of DC-Chol/DOPE (6:4) liposomes (Figure 4). In addition, no enhancement by galactosylated liposomes in gene expression was observed in NIH 3T3 cells, which have no specific receptors for galactose. These results suggest that DNA/galactosylated liposome complexes are recognized by the asialoglycoprotein receptors on HepG2 cells.

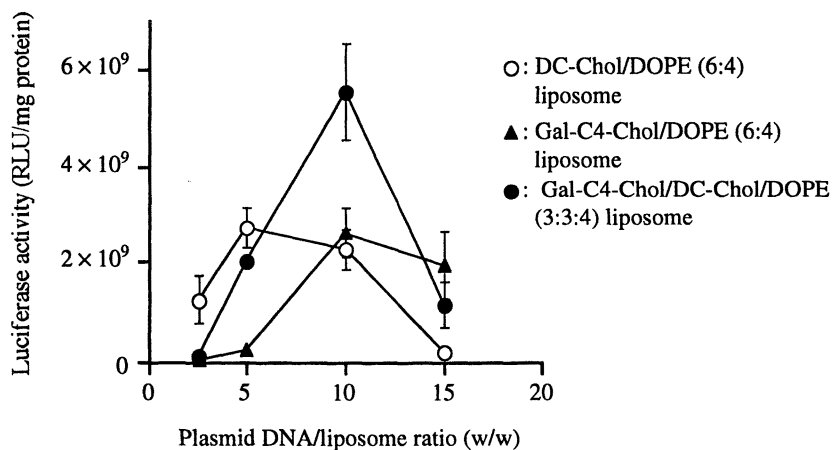


Figure 3. Transfection activity of DNA/liposome complexes at various ratios (w/w) in HepG2 cells. DNA encoding firefly luciferase gene mixed with various liposome formulations was applied to the cells for 6 h. After an additional 42 h, the gene expression was evaluated by luciferase assay.

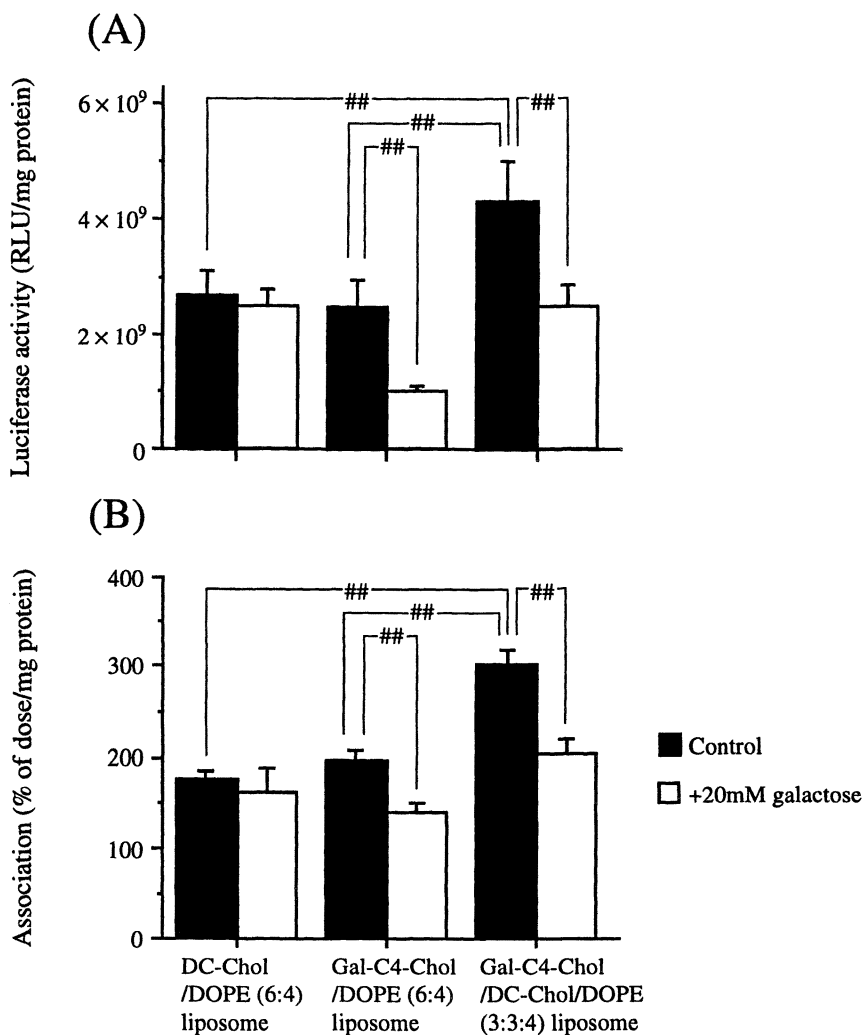


Figure 4. Inhibitory effect of the presence of 20 mM galactose on the transfection activity of DNA/liposome complexes (A) and on the cellular association of [32 P]DNA/liposome complexes at 3 h (B) in HepG2 cells. The cells were incubated with the complexes in the presence or absence of 20 mM galactose. Statistical analysis was performed by analysis of variance followed by Tukey-Kramer multiple comparisons test (## $P < 0.01$).

The cellular uptake time-courses of [32 P]DNA complexed with the liposomes were also examined in HepG2 cells (Figure 4). The highest uptake of [32 P]DNA was observed when it was complexed with Gal-C4-Chol/DC-Chol/DOPE (3:3:4) liposomes. The uptake of [32 P]DNA complexed with Gal-C4-Chol/DOPE (6:4) liposomes was comparable with that with DC-Chol/DOPE (6:4) liposomes. In the presence of 20 mM galactose, the uptake of [32 P]DNA with Gal-C4-Chol/DC-Chol/DOPE (3:3:4) and Gal-C4-Chol/DOPE (6:4) liposomes up to 3 h was significantly reduced, but this was not the case with DC-Chol/DOPE (6:4) (Figure 4). These results correspond to those of the transfection experiments.

Our preliminary data on *in vivo* gene transfer by these galactosylated cationic liposomes showed that DNA/galactosylated cationic liposome complexes of about 150 nm in diameter can be used for liver-specific gene transfer by intraportal injection. However, when injected intravenously, the complex showed a higher gene expression in the lung. This would be due to adverse biodistribution properties of the complex; interaction with blood components alters the physicochemical properties of DNA/galactosylated cationic liposome complexes, as observed for other conventional DNA/cationic liposome complexes (24).

Galactosylated Cationic Poly(Amino Acids)

The biodistribution of DNA complexes with macromolecular carriers was more easily controlled than that of DNA/liposome complexes. We have developed various Gal-PLLs with different molecular weights and different numbers of galactose units (17). Hepatocyte-specific delivery of DNA was successfully achieved by selecting the most suitable size of PLL and by controlling the galactose density on PLL. If a short PLL with a molecular weight of 1800 was used, a larger amount of PLL was required for complex formation than with PLLs with molecular weights of 13000 and 29000. In addition, there was hardly any DNA condensation by the short PLL. Increasing number of galactose units partially disturbed the complex formation between DNA and Gal-PLL. Intravenously administered DNA/Gal₁₃-PLL₁₃₀₀₀ and DNA/Gal₂₆-PLL₂₉₀₀₀ could reach hepatocytes, indicating that these DNA complexes have suitable biodistribution characteristics for hepatocyte-specific targeting. Compared with these complexes, DNA/Gal₅-PLL₁₈₀₀ and DNA/Gal₅-PLL₁₃₀₀₀ had a smaller hepatic uptake clearance, suggesting that both the molecular weight and the degree of galactose modification of PLL determine the hepatic targeting of DNA (17).

In vitro and *in vivo* gene expression studies revealed that DNA/Gal₁₃-PLL₁₃₀₀₀ and DNA/Gal₂₆-PLL₂₉₀₀₀ complexes are superior to the DNA/Gal₅-PLL₁₈₀₀ complex for introducing DNA into cells. However, the level of gene expression was low compared with that obtained with DNA/cationic liposome complexes (17). To improve the efficiency of galactosylated cationic poly(amino acids)-based gene transfer, the use of compounds that can enhance gene expression such as viruses or viral proteins, fusogenic lipids, and membrane-disruptive peptides can be considered. Fusogenic peptides could be promising materials for this purpose because the addition of these peptides to carrier systems strongly enhanced the *in vitro* gene transfer by several DNA/carrier complexes (25). However, their application to *in vivo* gene

transfer has not been reported so far. As far as their biodistribution is concerned, they should be firmly attached to carriers. Our preliminary experiments using a galactosylated polymeric carrier conjugated with a fusogenic peptide indicate that this approach is very effective in improving the level of gene transfer after intravenous injection of DNA/carrier complexes (unpublished data).

CONCLUSIONS

Galactosylated liposomes have been shown to be promising carriers of drugs and genes to cells possessing asialoglycoprotein receptors such as hepatocytes. These galactosylated liposomes are selectively delivered to liver parenchymal cells, and the receptor-mediated efficient uptake of these liposomes contributes their greater gene expression in HepG2 cells than that obtained with conventional cationic liposomes. DNA complexes with these galactosylated liposomes are more efficient for in vitro gene transfer but their biodistribution is more difficult to control than DNA/galactosylated polymer complexes. These results suggest that these galactosylated liposomes will be very useful for the cell-specific targeted delivery of low-molecular weight drugs and genes.

LITERATURE CITED

1. Ashwell, G.; Harford, J. *Annu. Rev. Biochem.* **1982**, *51*, 531.
2. Meijer, D. K. F.; van der Sluijs, P. *Pharm. Res.* **1989**, *6*, 105.
3. Wu, G. Y.; Wu, C. H. *Adv. Drug Delivery Rev.* **1998**, *29*, 243.
4. Sezaki, H.; Takakura, Y.; Hashida, M. *Adv. Drug Delivery Rev.* **1989**, *3*, 247.
5. Takakura, Y.; Mahato, R. I.; Nishikawa, M.; Hashida, M. *Adv. Drug Delivery Rev.* **1996**, *19*, 377.
6. Takakura, Y.; M.; Hashida, M. *Self-assembling Complexes for Gene Delivery: From Laboratory to Clinical Trial*; Kabanov, A. V.; Felgner, P. L.; Seymour, L. W., Eds.; John Wiley & Sons Ltd.: Chichester, UK, 1998, p 295.
7. Nishikawa M.; Hirabayashi, H.; Takakura, Y.; Hashida, M. *Pharm. Res.* **1995**, *12*, 209.
8. Nishikawa, M.; Miyazaki, C.; Yamashita, F.; Takakura, Y.; Hashida, M. *Am. J. Physiol.* **1995**, *268*, G849.
9. Akamatsu, K.; Imai, M.; Yamasaki, Y.; Nishikawa, M.; Takakura, Y.; Hashida, M. *J. Drug Targeting* **1998**, *6*, 229.
10. Kawakami, S.; Yamashita, F.; Nishikawa, M.; Takakura, T.; Hashida, M. *Biochem. Biophys. Res. Commun.* **1998**, *252*, 78.
11. Hirabayashi, H.; Nishikawa, M.; Takakura, Y.; Hashida, M. *Pharm. Res.* **1996**, *13*, 880.
12. Hashida, M.; Hirabayashi, H.; Nishikawa, M.; Takakura, Y. *J. Controlled Release* **1997**, *46*, 129.
13. Akamatsu, K.; Nishikawa, M.; Takakura, Y.; Hashida, M. *Int. J. Pharm.* **1997**, *155*, 65.

14. Midoux, P.; Mendes, C.; Legrand, A.; Raimond, J.; Mayer, R.; Monsigny, M.; Roche, C. *Nucl. Acids Res.* **1993**, *21*, 871.
15. Perales, J. C.; Ferkol, T.; Beegen, H.; Ratnoff, O. D.; Hanson, R. W. *Proc. Natl. Acad. Sci. USA* **1994**, *91*, 4086.
16. Mahato, R. I.; Takemura, S.; Akamatsu, K.; Nishikawa, M.; Takakura, Y.; Hashida, M. *Biochem. Pharmacol.* **1997**, *53*, 887.
17. Nishikawa, M.; Takemura, S.; Takakura, Y.; Hashida, M. *J. Pharmacol. Exp. Ther.* **1998**, *287*, 408.
18. Nishida, K.; Takino, T.; Eguchi, Y.; Yamashita, F.; Hashida, M.; Sezaki, H. *Int. J. Pharm.* **1992**, *80*, 101.
19. Wisse, E.; De Zanger, R. B.; Charels, K.; Van Der Smissen, P.; McCuskey, R. S. *Hepatology* **1985**, *5*, 683.
20. Hashida, M.; Akamatsu, K.; Nishikawa, M.; Yamashita, F.; Takakura, Y. *J. Controlled Release* **1999**, in press.
21. Takino, T.; Nakajima, C.; Takakura, Y.; Sezaki, H.; Hashida, M. *J. Drug Targeting* **1993**, *1*, 117.
22. Anderson, W.F. *Nature(London)* **1998**, *392(Supple.)*, 25.
23. Mahato, R. I.; Takakura, Y.; Hashida, M.; *Crit. Rev. Ther. Drug Carrier Syst.* **1997**, *14*, 133.
24. Litzinger, D. C.; Brown, J. M.; Wala, I.; Kaufman, S. A.; Van, G. Y.; Farrell, C. L.; Collins, D. *Biochim. Biophys. Acta* **1996**, *1281*, 139.
25. Wagner, E.; Plank, C.; Zatloukal, K.; Cotton, M.; Birnstiel, M. L. *Proc. Natl. Acad. Sci. USA* **1992**, *89*, 7934.

Chapter 21

Targeted Gene Delivery via the Folate Receptor

Wenjin Guo and Robert J. Lee

Division of Pharmaceutics and Pharmaceutical Chemistry, College of Pharmacy,
The Ohio State University, Columbus, OH 43210

A novel synthetic gene transfer vector system is developed based on targeting to the folate receptor. The folate receptor is a cellular marker overexpressed in over 90% of ovarian carcinomas and large percentages of other human tumors. Folic acid is a high affinity ligand for the folate receptor that retains its binding affinity upon derivatization at its gamma carboxyl. Folate conjugation, therefore, presents a novel strategy for tumor-specific targeted drug delivery. In the current study, we investigated novel folate conjugates of the cationic polymer polyethylenimine (PEI), for potential applications in receptor-mediated gene delivery. Unmodified PEI (M.W. 25,000) forms charge complexes with plasmid DNA carrying the luciferase reporter gene and was capable of cellular transfection, the efficiency of which depends on charge ratio (N/P ratio). Folate directly attached to PEI did not alter the transfection activity of its DNA complex compared to unmodified PEI. Modification of PEI by polyethyleneglycol (PEG) partially inhibited gene delivery. Attaching a folate to the distal terminus of PEG-modified PEI greatly increased the transfection activity in cultured folate receptor-positive human oral carcinoma KB cells at all N/P ratios. This increase was partially blocked by co-incubation with 200 μ M free folic acid, suggesting the involvement of folate receptor in gene transfer. Targeted synthetic vectors based on cationic polymer-folate conjugate may be useful in the tumor-specific delivery of therapeutic genes

The folate receptor is a GPI-anchored high affinity membrane folate binding protein overexpressed in a wide variety of human tumors, including > 90% ovarian carcinomas (1; 2). Meanwhile, the normal tissue distribution of folate receptor is highly restricted, making it a useful marker for targeted drug delivery to tumors (2). Mov18, a monoclonal antibody against the folate receptor has been evaluated for the scintigraphy and tomography imaging, radiotherapy, and immunotherapy of ovarian cancer in clinical studies (3-7). Folic acid, a high affinity ligand for the folate receptor

($K_d \sim 10^{-10}$ M) retains its receptor binding property when covalently derivatized via its γ -carboxyl. Folate conjugates have been shown to be taken into receptor-bearing tumor cells via folate receptor-mediated endocytosis (Figure 1). Folate-derivatization, therefore, presents a method for receptor-mediated targeted drug delivery into tumor cells. Folic acid is potentially superior to antibodies as a targeting ligand due to its small size, lack of immunogenicity, ready availability, and simple chemistry. Tumor cell specific delivery has been shown with folate conjugates of protein toxins, anti-T-cell receptor antibodies, liposomes, radioimaging agents, chemotherapy agents, and gene transfer vectors (8-15). Folate conjugated poly-L-lysine coupled with replication-defective adenovirus has been shown to mediate receptor-specific transfection in cultured tumor cells (16). Folate conjugated F_{ab} against adenoviral fiber has been shown to alter the tropism of the viruses towards receptor-bearing tumor cells (17). Folate-targeted pH-sensitive liposomes have been formulated as LPDII particles for the receptor-dependent cellular delivery of plasmid carrying a reporter gene or antisense oligonucleotides (11; 18).

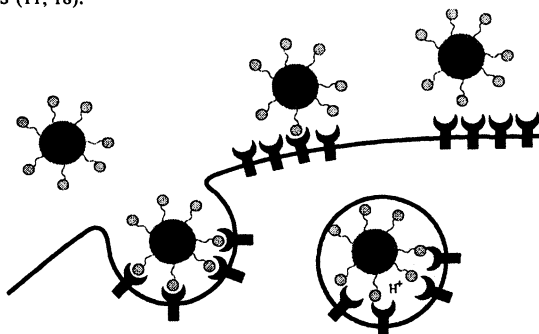


Figure 1. Receptor-mediated endocytosis of folate conjugates.

In the current study, we attempt to evaluate a simple system for targeted gene delivery via folate-conjugated polyethylenimine (PEI). Polyethylenimine (PEI), linear or branched, is a cationic polymer ideally suited for the formation of compact charge complexes with plasmid DNA. In addition to its DNA condensing properties, this polymer also possesses endosomallytic activities due to its strong buffering capacity at endosomal acidic pH. PEI-DNA polyplexes have been shown to mediate efficient transfection of cultured cells and targeting ligands such as transferrin and galactose have been used to facilitate the delivery of PEI polyplexes to specific cell types (19-20). Folate conjugates of polyethylenimine were synthesized and evaluated for their ability to mediate receptor-specific gene transfer *in vitro*.

Experimental

Materials. All reagents were used without further purification. Polyoxyethylenebis-amine (M.W. 3350) and Sephadex G-100 resin were purchased from Sigma Chemical Co. Polyethylenimine (M.W. 25,000), dicyclohexylcarbodiimide, *N*-hydroxysuccinimide, maleimidobenzoyl-*N*-hydroxysuccinimide ester (MBS), and Traut's Reagent (2-iminothiolane) were purchased from Aldrich Chemical Co. Luciferase assay kits were obtained from Promega, and BCA protein assay kits were

purchased from Pierce Chemical Co. Tissue culture media were purchased from Life Technologies.

Synthesis of Folate-PEI and Folate-PEG-PEI (Figure 2). Folic acid (1g) was converted to its *N*-hydroxysuccinimide ester (NHS-folate) by reacting with 1.1 molar excess of *N*-hydroxysuccinimide (NHS) in the presence of 1.1 molar excess of dicyclohexylcarbodiimide (DCC) in 50 mL dimethylsulfoxide (DMSO) at room temperature for 4 h. The insoluble by product, dicyclohexylurea was removed by filtration.

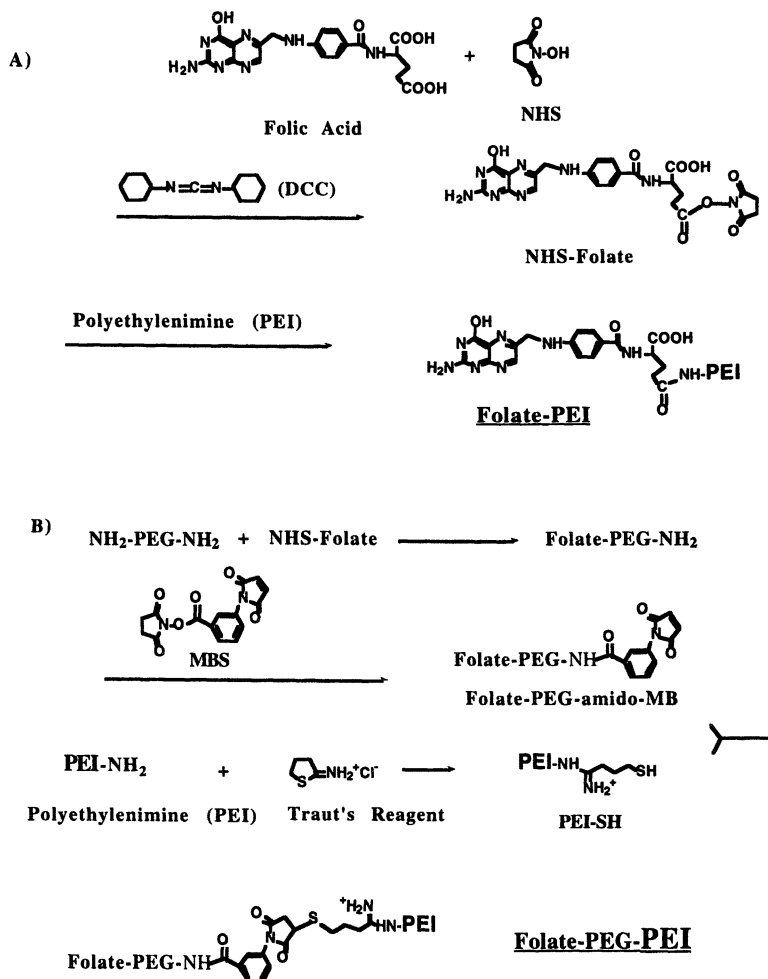


Figure 2. Synthesis of A) Folate-PEI and B) Folate-PEG-PEI.

Folate-PEI conjugate was then synthesized by reacting PEI (branched polymer, M.W. 25,000) with 5x excess of NHS-folate in DMSO (Figure 2A). The product, folate-PEI, was then diluted in 2 volumes of deionized water and passed through a Sephadex G-100 column equilibrated with phosphate-buffered saline (PBS, pH 7.4). The conjugate, which is high molecular weight, eluted in the early fractions. Product concentration and degree of derivatization were determined by assaying for residual primary amine content by a ninhydrin assay and measurement of folate content by ultraviolet absorption at 363 nm based on a molar extinction coefficient of 6500 for folate. Approximately 3 folates were attached to each molecule of PEI.

To synthesize folate-PEG-PEI, an intermediate, folate-PEG-amine, was first synthesized by reacting PEG-*bis*-amine (M.W. 3350) with 1x of NHS-folate in DMSO. The product was purified by gel-filtration on a Sephadex G-25 column equilibrated in deionized water and then lyophilized. Folate-PEG-amine was then dissolved in DMSO and converted to a maleimide derivative by reacting with 1.1 molar excess of maleimidobezoyl-*N*-hydroxysuccinimide ester (MBS). Meanwhile, PEI (branched polymer, M.W. 25,000) was converted to a thiol-derivative by reacting with Traut's Reagent in aqueous solution at pH 7.4. The thiol-PEI was purified by passing through a Sephadex G-100 column and then reacted to 1.5 molar excess of the folate-PEG-maleimide derivative to yield folate-PEG-PEI linked via a thioether bond. The product was purified from unreacted folate derivatives by passing through a Sephadex G-100 column equilibrated with PBS (Figure 2B). PEI and folate contents were determined as described for folate-PEI. An average of ~ 1.0 folate per molecule of PEI was found in the conjugate product. As a control, PEG-PEI conjugates was also synthesized by reacting PEI with 1.5 molar excess of methoxy-SSA-PEG 5000 (Shearwater Polymers).

Cell Culture. KB, a human oral cancer cell line which overexpresses the folate receptor, was cultured in folate-free RPMI media supplemented with 10% fetal bovine serum. This media contain a final folate concentration similar to that of human plasma. (Regular tissue culture media contains μM levels of folate which is unphysiological and interferes with receptor binding of folate conjugates). The cells were grown as a monolayer in a humidified 37°C CO₂ incubator.

In Vitro Transfection Studies. Supercoiled *pCMV-Luc* plasmid DNA (containing the firefly luciferase reporter gene under a cytomegalovirus promoter) was prepared by alkaline lysis of *E. Coli* followed by purification using a kit from Qiagen. DNA-polycation complexes were prepared by rapid addition of PEI or PEI conjugates to DNA at a series of PEI nitrogen to DNA phosphate (N/P) ratios, in 100 μL of deionized water. For transfection studies, cells were plated in 24-well plates at 50% initial confluence and incubated for 24 h prior to the experiment. During transfection, cells (in triplicates) were incubated with 1 μg /well of DNA complexes in 500 μL of serum-free media for 4 h at 37°C. The cells were then gently washed twice with cold PBS and incubated for a further 24 h in culture medium containing 10% fetal bovine serum. The cells were then lysed with a lysis buffer (0.5% Triton X-100, 0.1 M Tris-HCl, pH 7.8, 2 mM EDTA) and the lysate analyzed for protein content by a BCA protein assay and for luciferase activity using a kit from Promega on a Lumat LB9501-16 Luminometer (EG&G Berthold).

Results and Discussion

Folate-PEI (no spacer) and Folate-PEG-PEI. Cationic polymer polyethylenimine (PEI, M.W. 25 kDa, branched) has been shown to possess both DNA condensing and endosomal lytic activities. The later is presumably due to the high buffering capacity of PEI at the endosomal acidic pH. These properties make PEI ideally suited for forming transfection polyplex with plasmid DNA. Primary amino-groups on PEI, which accounts for ~ 25% of nitrogen atoms, can be readily derivatized with electrophilically-activated folate, PEG, or crosslinking agents. A previous study with folate derivatized liposomes (mean diameter ~ 67 nm) show a long PEG spacer was necessary to allow folate linked to the lipid molecule to be recognized by the folate receptor whereas folates attached to the lipid head group with short linkers were ineffective to mediate liposome targeting. Since PEI/DNA complexes (mean diameter ~ 50-100 nm) is in the similar size order as the liposomes, we anticipate a similar requirement for a long spacer for effective receptor targeting. Therefore, folate-PEG-PEI was synthesized incorporating a M.W. 3350 PEG-bis-amine-based spacer. Also, the presence of PEG may interfere with the PEI conjugate's ability to complex with DNA and interact with cells. A PEG-PEI conjugate was therefore synthesized to assess the effect of PEG derivatization on the transfection activity of PEI-DNA complexes.

Transfection Activities of Folate-PEI (no spacer) and Folate-PEG-PEI DNA Complexes. KB cells, which overexpress the folate receptor, grown in 24-well plates were incubated with DNA complexes with PEI, folate-PEI (no spacer), folate-PEG-PEI, or PEG-PEI at PEI nitrogen to DNA phosphate (N/P) ratios of 3, 5, 7.5, and 10, in serum free culture media. The *pCMV-Luc* plasmid was used as a reporter gene, and transfection efficiency determined by luciferase assay, as described in Experimental. The results in relative light units per mg of extracted protein (RLU/mg) are shown in Figure 3.

For each of the PEI conjugates and unmodified PEI, transfection activity was increased with an increase in N/P ratio. This could be due to the combination of an increase in the positive charge of the polyplex formed (which enhance cellular uptake) and increased PEI content in the DNA polyplex (which facilitates the endosomal escape of the polyplexes). At an N/P ratio of 3 where negatively charged DNA complexes were formed, PEI, folate-PEI (no spacer), and PEG-PEI DNA complexes showed very low transfection activity. Meanwhile, folate-PEG-PEI/DNA complexes had ~ 30–50 times higher activity. This suggest that transfection was facilitated by targeting to the folate receptor and that a spacer is required between folic acid and PEI for receptor binding of the DNA complexes, as we have anticipated. At higher N/P ratios, folate-PEG-PEI complexes were similarly active as underivatized PEI and folate-PEI (no spacer), and ~ 10 times more efficient than PEG-PEI complexes in transfection. It is possible that at these higher N/P ratios, charge-mediated cellular uptake is quite efficient for polyplexes formed with PEI or folate-PEI (no spacer) due to the presence of a net positive charge in these complexes. PEG-derivatization introduces steric barriers that could reduce the efficiency of charge interactions necessary for efficient transfection, resulting in an ~ 10-fold reduction of transfection activity of PEG-PEI compared to PEI complexes. Cellular uptake was then restored when folate was attached to the distal end of the PEG in folate-PEG-PEI.

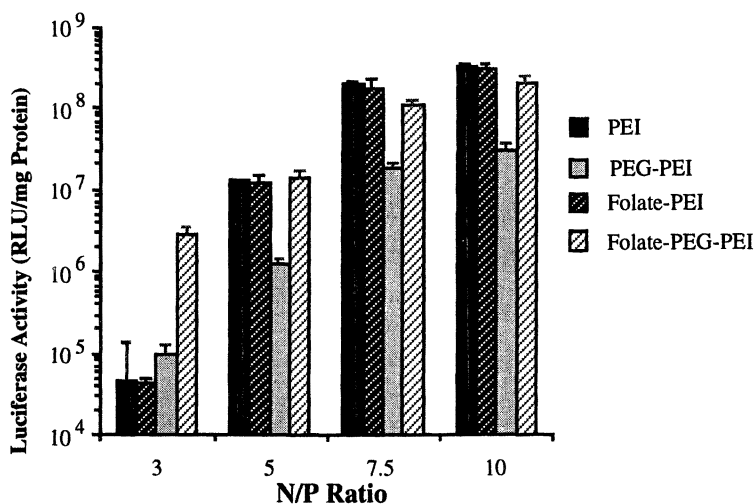


Figure 3. Transfection of KB Cells with Folate-conjugates of PEI

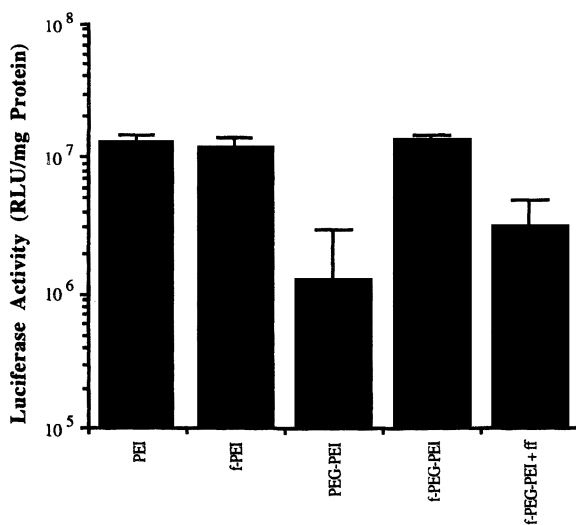


Figure 4. Effect of free folate on the transfection activities of DNA complexes.

To further define the role of targeting in gene delivery, transfection studies were performed either in the presence or the absence of 200 μ M folic acid at an N/P ratio of 5. As shown in **Figure 4**, 200 μ M free folate reduced the transfection activity of folate-PEG-PEI/DNA complexes by ~75%. Meanwhile, free folate had little effect on the transfection activity of PEI, folate-PEI/DNA, or PEG-PEI complexes (data not shown). These data suggest that receptor mediated transfection of folate-PEG-PEI polyplexes can be competitively blocked by excess free ligand folic acid.

Conclusions

Folate-PEG-PEI/DNA complexes were shown to mediate efficient transfection of culture tumor cells expressing the folate receptor in a receptor-dependent manner. Targeting effect was more evident at low N/P ratios with negatively charged DNA complexes. A spacer was necessary between folate and PEI to allow efficient receptor targeting. PEG-modification of PEI appears to reduce the charge-mediated transfection of polyplexes formed. Cellular transfection activity could be restored by the attachment of a folate at the distal end of the PEG. Transfection activity of folate-PEG-PEI could be partially blocked by free folate. Folate-PEG-PEI/DNA complexes may be potentially useful for tumor-specific targeted gene therapy and warrant further characterization.

Acknowledgments

This study is supported by a grant from the Parenteral Drug Association (PDA) and a grant (RPG-99-097-01-MGO) from the American Cancer Society.

References

1. Garin-Chesa, P., Campbell, I., Saigo, P.E., Lewis, J.L.J., Old, L.J. and Rettig, W.J., Trophoblast and ovarian cancer antigen LK26. Sensitivity and specificity in immunopathology and molecular identification as a folate-binding protein., *Am. J. Pathol.*, 142, 557-567, 1993.
2. Ross, J.F., Chaudhuri, P.K. and Ratnam, M., Differential regulation of folate receptor isoforms in normal and malignant tissues in vivo and in established cell lines, *cancer*, 73, 2432-2443, 1994.
3. Crippa, F., Buraggi, G., DiRe, M., Gasparini, M., Seregini, E., Canervari, S., Gadina, M., Presti, A., Marini, A. and Seccamani, E., Radioimmunoscintigraphy of ovarian cancer with the MOv18 monoclonal antibody, *Eur. J Cancer*, 27, 724, 1991.
4. Crippa, F., Bolis, G., Seregini, E., Gavoni, N., Scarfone, G., Ferraris, C., Buraggi, G. and Bombardieri, E., Single-dose intraperitoneal radioimmunotherapy with the murine monoclonal antibody I-131 MOv18: clinical results in patients with minimal residual disease of ovarian cancer, *Europ. J. Cancer*, 31A, 686-690, 1995.
5. Casalini, P., Luison, E., Menard, S., Colnaghi, M.I., Paganelli, G. and Canervari, S., Tumor pretargeting: role of avidin/streptavidin on monoclonal antibody internalization, *J. Nucl. Med.*, 38, 1378-1381, 1997.

6. Paganelli, G., Belloni, C., Magnani, P., Zito, F., Pasini, A., Sassi, I., Meroni, M., Mariani, M., Vignali, M., Siccardi, A. and Fazio, F., Two-step tumor targeting in ovarian cancer patients using biotinylated monoclonal antibodies and radioactive streptavidin, *Eur. J. Nucl. Med.*, 19, 322, 1992.
7. Molthoff, C., Buist, M., Kenemans, P., Pinedo, H. and Boven, E., Experimental and clinical analysis of the characteristics of a chimeric monoclonal antibody, MOv18 reactive with an ovarian cancer-associated antigen, *J. Nucl. Med.*, 33, 2000, 1992.
8. Leamon, C.P. and Low, P.S., Delivery of macromolecules into living cells: a method that exploits folate receptor endocytosis, *Proc. Natl. Acad. Sci. USA*, 88, 5572-5576, 1991.
9. Lee, R.J. and Low, P.S., Delivery of liposomes into cultured KB cells via folate receptor-mediated endocytosis, *J. Biol. Chem.*, 269, 3198-3204, 1994.
10. Lee, R.J. and Low, P.S., Folate-mediated tumor cell targeting of liposome-entrapped doxorubicin in vitro, *Biochim. Biophys. Acta*, 1233, 134-144, 1994.
11. Lee, R.J. and Huang, L., Folate-targeted, anionic liposome-entrapped polylysine-condensed DNA for tumor cell-specific gene transfer, *J. Biol. Chem.*, 271, 8481-8487, 1996.
12. Lee, R., Wang, S. and Low, P., Measurement of Endosomal pH Following Folate Receptor-Mediated Endocytosis, *Biochim. Biophys. Acta*, 1312, 237-242, 1996.
13. Wang, S., Lee, R.J., Cauchon, G., Gorenstein, D.G. and Low, P.S., Delivery of antisense oligodeoxynucleotides against the human epidermal growth factor receptor into cultured KB cells with liposomes conjugated to folate via polyethylene glycol, *Proc. Natl. Acad. Sci. USA*, 92, 3318-3322, 1995.
14. Ladino, C.A., Chari, R.V.J., Bourret, L.A., Kedersha, N.L. and Goldmacher, V.S., Folate-maytansinoids: Target-selective drugs of low molecular weight, *Int. J. Cancer*, 73, 859-864, 1997.
15. Kranz, D.M., Patrick, T.A., Brigle, K.E., Spinella, M.J. and Roy, E.J., Conjugates of folate and anti-T-cell receptor antibodies specifically target folate-receptor-positive tumor cells for lysis, *Proc. Natl. Acad. Sci. USA*, 92, 9057-9061, 1995.
16. Gottschalk, S., Cristiano, R., Smith, L. and Woo, S., Folate Receptor Mediated DNA Delivery into Tumor Cells: Potosomal disruption results in enhanced gene expression, *Gene Ther.*, 1, 185-191, 1994.
17. Douglas, J., Rogers, B., Rosenfeld, M., Michael, S., Feng, M. and Curiel, D., Targeted Gene Delivery by Tropism-Modified Adenoviral Vectors, *Nature Biotechnology*, 14, 1574-1578, 1996.
18. Li, S., Deshmukh, H. and Huang, L., Folate-Mediated Targeting of Antisense Oligodeoxynucleotides to Ovarian Cancer Cells, *Pharmaceut. Res.*, 15, 1540-1545, 1998.
19. Zanta, M.-A., Boussif, O., Adib, A., and Behr, J.-P., In Vitro Gene Delivery to Hepatocytes with Galactosylated Polyethylenimine, *Bioconj. Chem.* 8, 339-344, 1997.
20. Kircheis, R., Kichler, A., Wallner, G., Kursa, M., Ogris, M., Felzmann, T., Buchberger, M., and Wagner, E. Coupling of Cell-Binding Ligands to Polyethylenimine for Targeted Gene Delivery, *Gene Ther.*, 4, 409-418, 1997.

Chapter 22

Latest Advances in the Understanding of Active-Specific Immunotherapy for Brain Tumors

Yang Liu^{1,2}, Qingzhong Kong¹, Ka-yun Ng², and Kevin Lillehei^{1,3}

¹Division of Neurosurgery and ²Department of Pharmaceutical Sciences, University of Colorado Health Sciences Center, Denver, CO 80262

Over the years, numerous attempts have been tried to establish the effective use of immunotherapy for treatment of brain tumors. However, generation of active immune responses in most of these studies was only possible in the absence of viable tumor cells, suggesting that immunotherapy can only be used as preventive therapy. Few studies today have demonstrated success in using immunotherapy to treat an already established intracranial tumor. Using the Fischer 9L intracranial glioma model, we attempted to delineate the underlying mechanisms for these observations. Animals were vaccinated with irradiated 9L-glioma cells (i9L) together with interferon- γ (IFN- γ) before, at the same time, or after intracranial (IC) 9L tumor cell challenge. Survival of animals was then monitored for 60 days. In addition, developments of tumor-specific cytotoxicity and T lymphocyte proliferation at the various stages of vaccination were also studied. Animals vaccinated 14 and 7 days prior to intracranial tumor cell challenge showed a significant increase in survival. By contrast, vaccinations applied 5 days prior to, at the time of (i.e., day 0) or 7 days after IC tumor cell challenge failed to influence survival. Histological examination of brain tissue of vaccinated animals identified that vaccination increased mononuclear cell infiltration of the induced tumor. When spleen cells were stimulated with mitomycin C-treated i9L to generate cytotoxic lymphocytes (CTL), only CTL from animals primed with i9L plus IFN- γ killed 9L-glioma cells. CTL from non-primed rats or rats with established 9L intracranial tumor failed to affect 9L-glioma cells. Similarly, when stimulated with mitomycin-C treated i9L, only spleen cells from primed animals showed an increase in proliferation. These data suggest that the tumor itself may exert a strong immunomodulatory effect at the systemic and

³Corresponding author.

local levels. The exact mechanism of this immunomodulatory effect is currently unknown. Nevertheless, subversion of this immunosuppressive effect would be expected to enhance the therapeutic efficacy of active specific immunotherapy.

Introduction

The prognosis of patients with malignant glioma following conventional treatment is poor. Surgery, irradiation, and chemotherapeutic treatments rarely succeed in curing the disease. Among patients carrying a diagnosis of Glioblastoma Multiforme, average survival time is generally 12-18 months with few patients surviving beyond 2 years¹. The apparent lack of efficacy of conventional therapy has prompted a search for other potentially beneficial therapies. One of the more promising approaches for the treatment of brain tumors is the development of cancer vaccines.

Although cerebral tissue does not possess any HLA antigens² and a brain-tumor specific antigen has yet to be identified, glioma cells have been found to express low levels of MHC class I and class II molecules as well as tumor-associated antigens³. These antigens are capable of inducing cell-mediated immune responses, thus rendering glioma cells susceptible to immunotherapy⁴. These findings, when taken together with the recent observation that activated host immune cells are able to effectively infiltrate the blood-brain-barrier⁵, suggest the feasibility of applying an intensified active immunization strategy to treat malignant brain tumors.

For several decades, numerous attempts have been made to establish the use of immunotherapy for treatment of brain tumors. The approaches taken include tumor cells with adjuvant⁶, tumor cells transduced with specific viral and allogeneic MHC genes⁷ or tumor cells transduced with cytokine genes⁸ to augment or enhance their immunogenicity. Most of these experiments, however, demonstrated that antitumor immunity was effective only when generated in the absence of viable tumor cells. These approaches are only effective against subsequent tumor cell challenge or in preventive therapy. Few studies have demonstrated success in treating established intracranial tumors, with cures being especially hard to achieve when immunizations were launched several days after tumor cell challenges⁷. This explains why no one has been successful in prolonging survival in patients with high grade gliomas in controlled trials using manipulation of the immune system.

The ability to create antitumor immunity in the presence of an established intracranial tumor is clearly of clinical relevance. By employing a Fischer 9L intracranial glioma model as our model system, the present study was instigated to delineate the mechanisms underlying the ineffectiveness of antitumor immunity in treating an established intracranial tumor. Using an assay of survival studies, histological surveys and *in vitro* cytotoxicity and proliferation assays, the antitumor effect of immunization before or after intracranial tumor cell challenge was studied. Our results demonstrate that a modulating effect of tumor cells on the immune system may be an important factor contributing to the failure of vaccination against the established brain tumor.

Materials And Methods

Cell Line and Experimental Animal

9L gliosarcoma, a malignant glioma cell line syngeneic to the Fischer 344 rat, was used for the proposed studies. This cell is known to secrete transforming growth factor-beta (TGF- β), making it very similar to human gliomas⁹. The tumor cell line was cultured in RPMI-1640 medium (Life Tech. Inc., Bethesda, MD) supplemented with 10% fetal bovine serum (FBS), and 2 mM glutamine. The cells were grown in a incubator at 37°C with a 5% CO₂/air atmosphere. Fischer 344 male rats (Charles River Lab., Wilmington, MA) weighing 250 \pm 20 grams were used.

Subcutaneous Vaccination

0.8 ml of phosphate buffered saline (PBS) containing 5 x 10⁶ irradiated tumor cells (10,000 rad) and 10,000 U IFN- γ (R&D Systems, Minneapolis MN) were injected subcutaneously into the right hind leg of Fischer 344 rats. After the first injection, the rats received daily subcutaneous injections of IFN- γ (10,000 U in 0.3 ml) at the original site for 5 additional days. IFN- γ was chosen as the adjuvant in these vaccination studies for two reasons. Firstly, it can increase class I and class II MHC molecule expression on tumor cells¹⁰ and, therefore, act to enhance the development of cytotoxic T cells¹¹. Secondly, it has been shown to induce a potent antitumor immune response when used as an adjuvant¹² or in a genetically-engineered tumor vaccine⁵.

Intracranial Tumor Implantation

Using a stereotactic frame (Kopf, USA) and a Hamilton syringe, 10 μ l PBS containing 5 x 10³ tumor cells were injected into the right frontal lobe of the rat. After receiving IC injections, the animals were monitored twice a day for neurological signs and weighed every third day until the end of the experiment (60 days after tumor cell implantation). All animals were sacrificed when moribund or at Day 60. At the time of death, brains of all animals were harvested for histological evaluation.

Proliferation Assay And Cytotoxicity Assay

At various time intervals after vaccination, mononuclear cells were obtained from the spleens of Fischer 344 rats using a previously described method¹³.

To perform the proliferation assay, isolated nonadherent mononuclear cells (responder) were incubated with mitomycin C-treated 9L tumor cells (stimulator) at a stimulator:responder ratio of 0.4:1 in the wells of a 96-well microtiter plate (5x10⁴ responder cells/well). After 72 hours incubation, mononuclear cell proliferation was

determined using a CellTiter 96 AQ non-radioactive cell proliferation assay kit (Promega, Madison WI).

To perform the cytotoxicity assay, aliquots of isolated mononuclear cells were co-incubated with mitomycin C-treated 9L glioma cells for 5 days. 5×10^3 9L tumor cells (target cells) were then incubated in 5% FBS culture media with the 5-day cultured nonadherent mononuclear cells (effector cells) at an effector:target ratio of 10:1, for 4 hours at 37°C. At the end of the incubation, mononuclear cell-mediated cytotoxicity was determined by using the CytoTox 96 Non-Radioactive Cytotoxicity Assay kit (Promega). The data were calculated as:

$$\% \text{ Cytotoxicity} = (\text{EXR} - \text{ESR} - \text{TSR} + \text{CMB}) / (\text{TMR} - \text{TSR} - \text{VC} + \text{CMB}) \times 100.$$

(Where EXR is experimental LDH release, ESR is effector cell spontaneous LDH release, TSR is target cell spontaneous LDH release, TMR is target cell maximum LDH release, VC is volume correction, and CMB is culture medium LDH background.)

Histological detection of mononuclear cell infiltration

To detect mononuclear cell infiltration at the site of IC tumor cell challenge, two series of experiments were carried out. The first involved immunization prior to tumor cell challenge (prevention experiment), and the second involved immunization after tumor cell challenge (treatment experiment). In the first study, rats in each group were injected subcutaneously with i9L and IFN- γ on day 0, challenged intracranially on day 7 and euthanized at day 12, 17, or 22. For the treatment study, rats in each group were intracranially challenged on day 0, vaccinated on day 7 and euthanized at day 12, 17 or 22. The brain from each animal was removed, fixed in 10% formalin, and embedded in paraffin for histological examination. Four-micrometer tissue sections were stained with hemotoxylin and eosin according to standard procedures and evaluated for the presence of mononuclear cell infiltration by a neuropathologist blinded to the treatment groups.

Statistical Analysis

Log-rank analyses were used to determine statistical significance between the survival data of the treatment groups. Student's unpaired t-test was used to determine the differences between the various groups in proliferation assay. $P < 0.05$ was considered significant.

Results

Efficacy of Tumor Vaccine in Preventing Tumor Development

The ability of vaccinating the animals with a mixture of i9L and IFN- γ to elicit an antitumor immune response against a subsequent tumor challenge was studied.

Six rats per group were immunized with either i9L, IFN- γ , PBS or a mixture of i9L + IFN- γ . One week after immunization they were challenged with IC i9L implantation. The mean survival time (MST) of controls immunized with IFN- γ (28.5 days) was indistinguishable from animals receiving PBS (26.8 days), pointing to the need to have i9L to elicit antitumor immunity. In contrast, prolonged survival was observed in rats immunized with either i9L or i9L plus IFN- γ (MST: 45.8 days and 56.5 days, respectively; Figure 1). These results suggest that immunizing animals with either i9L or a mixture of i9L and IFN- γ resulted in generation of an antitumor immune response. However, the protective effect of i9L + IFN- γ was greater than that afforded by immunizing the animals with i9L alone.

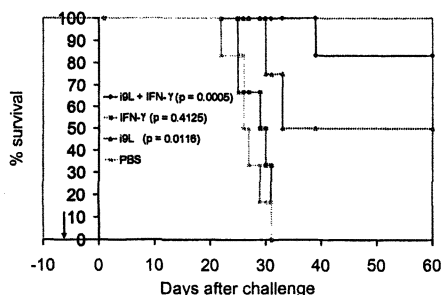


Figure 1. Effect of vaccination with i9L + IFN- γ on survival of animals challenged with intra-cranial tumor cells. Differences in survival between groups were determined by non-parametric log rank test. P values refer to comparison with PBS.

To test the effect of time of vaccination relative to tumor cell challenge on animal survival, groups of 5 rats were immunized with i9L + IFN- γ 14, 7, 5, 3 or 0 days prior to IC tumor cell challenge. The survival of rats immunized 5, 3 and 0 days prior to tumor challenge was not different from those receiving PBS. In contrast, rats immunized 14 and 7 days prior to tumor challenge demonstrated significant protective immunity (MST: 46.0 days and 54.2 days; $p = 0.0018$ and 0.0064 when compared to PBS). Histological examination of the surviving animals for all groups on Day 60 revealed no evidence of viable IC tumor cells. These results indicate that the optimum time period required to develop an effective antitumor immune response in rats using a subcutaneously injected tumor vaccine is 7 days or more.

Efficacy of Tumor Vaccine in Treating Established Tumor

Experiments were conducted to determine whether vaccinating animals with i9L + IFN- γ is effective in extending the survival of animals with established IC 9L gliomas. In these studies, animals were immunized at various times after IC 9L glioma tumor challenge. The survival of rats receiving immunization 0 or 7 days after tumor challenge was not significantly different from those receiving PBS (control). Therefore, vaccinating animals on the same day or 7 days after IC tumor cell challenge fails to increase survival. A number of mechanisms can be proposed to explain the failure of vaccination to show an impact on survival under these circumstances. It is possible that (a) a single vaccination of the animal in the presence of viable IC tumor cells is insufficient to generate a potent antitumor immune

response, or (b) an established brain tumor may exert an inhibitory influence on the development of an antitumor immune response. To examine the former possibility, an additional experiment was performed wherein animals received 4 vaccinations of i9L + IFN- γ on days 5, 8, 11 and 14 after IC tumor cell challenge. If our first possibility is correct, the increased number of vaccinations should enhance the immune response and extend the survival of animals. This does not appear to be the case, however, in that survival of this group of animals was similar to control (data not shown). It is clear from these studies that vaccination after IC tumor cell implantation is ineffective in altering the progression of an established tumor. The second possibility was considered in other experiments investigating potential immunomodulatory actions. The results of these experiments were outlined below.

Determination of mononuclear cell infiltration at the site of tumor cell challenge

To examine if established brain tumors can exert a repressive effect on the manifestation of the antitumor immune response, the extent of mononuclear cell infiltration at the IC site of tumor cell implantation was examined following various vaccination regimens, i.e., the prevention protocol and treatment protocols. In the prevention experiments (i.e., when vaccination was applied 7 days before IC tumor cell implantation), there was extensive mononuclear cell infiltration into tumor and surrounding areas 10 days after the tumor cell challenge. Five days after this observation (i.e., 15 days post tumor cell challenge), tumors in the vaccinated animals showed marked sign of regression. Ten days after tumor cell challenge, only a few mononuclear cells were observed at the tumor edge of PBS-vaccinated rats. The tumor in this group of animals continued to grow and showed no sign of regression even 15 days after tumor cell challenge (Table I-a).

When the tumor and its surrounding areas were examined in the treatment group of animals (i.e., when vaccination was initiated after tumor cell challenge), there was also extensive infiltration of the tumor by mononuclear cells, although their appearance took a slightly longer time when compared to the prevention protocol (17 days vs. 10 days). Despite this mononuclear cell infiltration, tumors in these animals appeared to continue to grow (Table I-b). As in the prevention study, far fewer mononuclear cells were observed at the tumor edge of PBS-vaccinated rats. In both the prevention and treatment studies, challenging the vaccinated animals with IC injection of PBS buffer did not result in any tumor development or mononuclear cell infiltration at the site of IC injection.

Together, these data demonstrate that subcutaneous immunization prior to (prevention) or after (treatment) IC tumor cell challenge results in infiltration of the tumor and its surrounding areas by mononuclear cells. However, it is only when vaccination is applied prior to tumor cell challenge that tumor cell growth is inhibited and the tumor cells eventually eradicated. Thus, our data indicate that suppression of mononuclear cell infiltration is not the mechanism by which the tumor inhibits the antitumor immune response. Rather, the most likely explanation for the failure of vaccine strategy to inhibit tumor cell growth in animals with established tumors may be related to an immunomodulatory effect of the tumor. This effect can be in the

form of an inhibitory factor secreted by the tumor, which abrogates the antitumor activity of stimulated mononuclear cells.

Table I. Mononuclear cell infiltration of tumor

a. Prevention ^a			Mononuclear cell infiltration ^b			Tumor size ^b		
			Days after Challenge			Days after Challenge		
Group	Vaccine	Challenge	5	10	15	5	10	15
1	i9L+IFN- γ	9L	+	+++	+++	+	++	+
2	i9L+IFN- γ	PBS	-	-	-	-	-	-
3	PBS	9L	+	+	+	+	+	++

b. Treatment ^a			Mononuclear cell infiltration ^b			Tumor size ^b		
			Days after Challenge			Days after Challenge		
Group	Challenge	Vaccine	12	17	22	12	17	22
1	9L	i9L+IFN- γ	+	+++	+++	++	+++	+++
2	PBS	i9L+IFN- γ	-	-	-	-	-	-
3	9L	PBS	-	++	++	+	++	+++

^aFor the prevention experiments, rats were immunized with i9L + IFN- γ subcutaneously 7 days prior to IC challenge. Animals were euthanized 5, 10, or 15 days thereafter. For the treatment experiments, rats were immunized 7 days after IC challenge and euthanized 12, 17, or 22 days thereafter.

^bTumors were quantitated by a blinded observer as follows: (-) no tumor, (+) ≤ 2 mm in maximum dimension, (++) ≥ 2 mm and < 4 mm in maximum dimension, (+++) > 4 mm in maximum dimension. Mononuclear cell infiltration: (-) almost none, (+) scarce at edge of tumor, (++) more at edge and few in tumor, (+++) more at edge and in tumor. Two animals were investigated in each group at each time point.

Role of immunomodulatory effect on antitumor immune response

To examine if established brain tumors can exert an immunomodulating effect, the cytotoxic and proliferative activity of mononuclear cells obtained from the spleens of immunized or non-immunized animals was studied. If an established tumor exerts an immunomodulatory effect on T lymphocytes, mononuclear cells obtained from animals that received vaccinations 7 days or 14 days prior to T cell harvest should exhibit greater cytotoxicity towards target 9L cells than those receiving vaccination 5 days, 3 days, 0 days prior to harvest. Similarly, mononuclear cells obtained from animals vaccinated 7 days prior to T cell harvest should also show greater proliferation than those obtained from the non-vaccinated group at all stimulator to responder ratios. In both cases, our data clearly demonstrate that mononuclear cells from animals vaccinated prior to tumor cell challenge exhibited greater cytotoxic and proliferative activity towards target 9L glioma cells (Figure 2 and 3). In contrast, minimal cytotoxic or proliferative activity was observed in effector cells (as in cytotoxicity studies) and responder cells (as in proliferative studies) obtained from animals that received no immunization but were challenged

intracranially with 9L glioma cells or from animals vaccinated 7 days after IC tumor cell challenge. These data agree with the results seen in our earlier survival experiments and support the premise that the antitumor immunity seen is the result of the development of tumor specific cytotoxic T cell. Further, our data suggest that established tumor might exert an inhibitory effect on the proliferation and cytotoxic activity of mononuclear cells in response to systemic vaccine therapy.

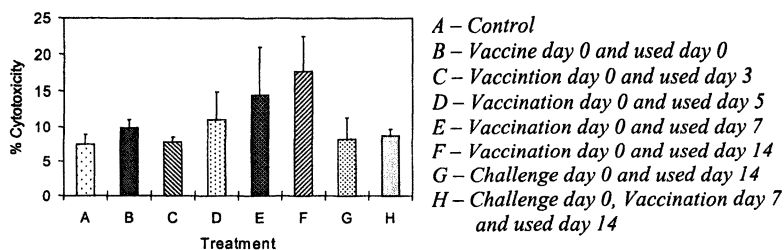


Figure 2. Cytotoxicity analysis of spleen cells from primed rats and unprimed rats. For these studies, rats ($n=2$) either received vaccination with i9L + IFN- γ on day 0, IC tumor cells challenge on day 0, IC tumor cell challenge on day 0 followed by vaccination with i9L + IFN- γ on day 7, or PBS on day 0 (controls). Effector cells from animals vaccinated 7 days and 14 days before harvest displayed greater cytotoxicity than those harvested from animals receiving vaccination at 0, 3, and 5 days prior to harvest. Effector cells from animals challenged IC with 9L glioma cells alone or vaccinated 7 days after IC tumor cell challenge showed minimal cytotoxicity.

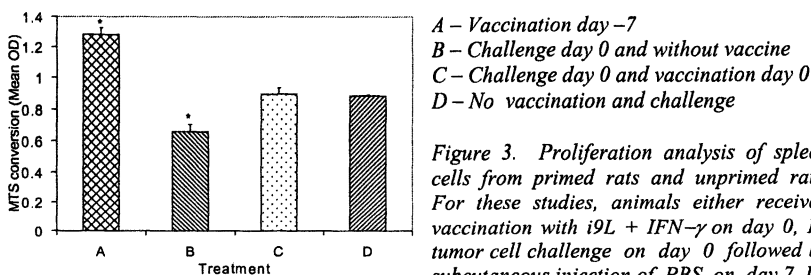


Figure 3. Proliferation analysis of spleen cells from primed rats and unprimed rats. For these studies, animals either received vaccination with i9L + IFN- γ on day 0, IC tumor cell challenge on day 0 followed by subcutaneous injection of PBS on day 7, IC tumor cell challenge on day 0 followed by i9L + IFN- γ vaccination on day 7, or vaccination with PBS on day 0 (control). Seven days after the various treatments, mononuclear cells were obtained from the spleens of the treated animals for proliferation analysis. Mononuclear cells from animals vaccinated 7 days prior to sacrifice showed more proliferation than those from either the controls, the animals challenged intracranially with 9L glioma cells, or animals that received vaccination 7 days after IC tumor cell challenge. Data represent mean \pm S.E. from 2 experiments. * $P < 0.001$ relative to MTS conversion of other treatment group.

Discussion

We have demonstrated that subcutaneous vaccination with i9L + IFN- γ can generate a potent protective antitumor effect against subsequent 9L glioma IC

challenge in the Fischer 344 rat. Thus, our current studies extend those findings by Jean et al.¹⁴, who reported similar results using a mixture of IL-12 and irradiated tumor cells for immunizing animals. The ability to generate an antitumor immune response by subcutaneous administration of irradiated tumor cells and cytokines circumvents the need for genetically engineered tumor cells to express particular cytokines. Unfortunately, despite the simplistic nature of this approach, we were unable to use this technique to extend the survival of animals with already established brain tumors.

In the present study, development of antitumor immune response followed a specific time course. Our data indicated that at least 7 days are required for the immune system to develop an effective antitumor immune response, with the optimal response being obtained when vaccination was applied 7 days prior to tumor cell challenge. This was reflected in increased survival in rats immunized at least 7 days prior to IC tumor cell challenge. The reason for a loss of antitumor effects when vaccination occurs within 5 days of tumor challenge is probably both quantitative and qualitative. At shorter periods of immunization (such as 3 days), the buildup of immune effector cells is probably not reaching a critical level to stage a successful attack on tumor cells. Tumor-induced immunosuppression has been well documented in patients with malignant glioma and in tumor-bearing animals¹⁵. Accordingly, tumor cells may release an immunomodulating factor, which functions to suppress the antitumor immune response. The release of such a factor may render the already poorly primed T-cells to a state of energy, allowing the injected tumor cells to escape the assault by the cytotoxic T cells. Application of vaccine at the time of or after tumor cell challenge also failed to exert an antitumor effect. Under these conditions, there would be no primed T-cells to begin with, and the tumor-derived suppressive factor may either inhibit the development of antitumor immune response or exert modulating influence on the antitumor immune response.

The most compelling data supporting the contention that the tumor cells are releasing a factor that modulates rather than inhibits the development of antitumor response came from our histological studies wherein mononuclear cell infiltration of the tumor occurred whether vaccination occurred 7 days prior to or 7 days after IC tumor cell challenge. Hence, recruitment of mononuclear cells to the tumor appeared to be independent of the time of vaccination relative to tumor cell implantation. Had a tumor-derived factor been suppressing development of the anti-tumor response, one would have expected reduced mononuclear cell infiltration of the tumor under conditions that failed to affect tumor development, i.e., vaccination after tumor cell challenge. The observation that mononuclear cells are present at the tumor site but ineffective in eliciting tumor repression (as was the case for vaccination after tumor cell challenge) leads to the intriguing possibility that the tumor cells may be locally repressing the cytotoxic activity of infiltrating mononuclear cells.

Another significant finding in our studies is the possibility that tumor cells may also be exerting a systemic immunosuppressive effect. Mononuclear cells isolated from the spleen of immunized animals exhibit cytotoxic and proliferative activity when exposed to immunogenic tumor cells. Our studies demonstrated that these activities are significantly reduced when the mononuclear cells are obtained from animals with established brain tumors. *In vitro* and *in vivo* studies in our laboratory

are currently in progress to identify and subsequently neutralize this immunosuppressive factor.

In summary, experiments reported herein suggest that established brain tumors have a strong repressive effect on the immune system at the systemic and local levels. This activity may be sufficient to diminish the activity of active immunotherapy to destroy an established tumor. It is anticipated that inhibition of this tumor suppressive factor should enhance the efficacy of active immunotherapy in the treatment of brain tumors.

Acknowledgements

We gratefully acknowledge the University of Colorado Cancer Center, Milheim Foundation for Brain Tumor Research, Pharmaceutical Research and Manufacturers of America Foundation for funding support. The authors also like to thank Drs. Bette DeMaster for performing the histological analysis, Pan Zhaoxing for statistical analysis and David Thompson for his helpful criticism.

References

1. Shapiro WR, Green SB, Burger PC, et al. *J Neurosurg.* 1989,71,1-9.
2. Berah M, Hors J, Dausset J. *Transplantation.* 1970,9,185-192.
3. Sawamura Y, de Tribolet N. *J Neurosurg.Sci.* 1990,34,265-278.
4. Holladay FP, Lopez G, De M, Morantz RA, Wood GW. *Neurosurgery.* 1992,30,499-504.
5. Wakimoto H, Abe J, Tsunoda R, Aoyagi M, Hirakawa K, Hamada H. *Cancer Res.* 1996;56:1828-1833.
6. Kida Y, Cravioto H, Hochwald GM, Hochgeschwender U, Ransohoff J. *J Neuropathol.Exp.Neurol.* 1983;42:122-135.
7. Yumitori K, Ito Y, Handa H. *Eur.J Cancer Clin.Oncol.* 1982,18,177-181.
8. Glick RP, Lichtor T, Kim TS, Ilangovan S, Cohen EP. *Neurosurgery.* 1995,36,548-555.
9. Fakhrai H, Dorigo O, Shawler DL, et al. *Proc.Natl.Acad.Sci.U.S.A.* 1996,93,2909-2914.
10. Wen PY, Lampson MA, Lampson LA. *J Neuroimmunol.* 1992,36,57-68.
11. Maraskovsky E, Chen WF, Shortman K. *J Immunol.* 1989,143,1210-1214.
12. Kruse CA, Molleston MC, Parks EP, Schiltz PM, Kleinschmidt-DeMasters BK, Hickey WF. *J Neurooncol.* 1994,22,191-200.
13. Tzeng, J.J., Barth, R.F., Clendenon, N.R. and Gordon, W.A. *Cancer Res.* 1990, 50,4338-4343.
14. Jean WC, Spellman SR, Wallenfriedman MA, Hall WA, Low WC. *Neurosurgery.* 1998,42,850-856.
15. Brooks WH, Netsky MG, Normansell DE, Horwitz DA. *J Exp.Med.* 1972,136,1631-1647.

Chapter 23

Application of pH- and Temperature-Sensitive Polymers for Controlled Drug Release Device

Soon Hong Yuk¹, Jung Ki Seo¹, Jin Ho Lee¹, and Sun Hang Cho²

¹Department of Polymer Science and Engineering, Han Nam University,
133 Ojeong Dong, Daedeog Ku, Taejeon 300-791, Korea

²Advanced Materials Division, Korea Research Institute of Chemical Technology,
P.O. Box 107, Yusung, Taejeon 305-600, Korea

A new pH/temperature-responsive polymer system with transitions resulting both from polymer-water and polymer-polymer interactions has been demonstrated using the copolymer composed of N,N'-dimethylaminoethyl methacrylate (DMAEMA) and ethyl acrylamide (EAAM) and the mixture of poly DMAEMA and poly EAAM. Based on the pH/temperature responsiveness of the copolymer and polymer mixture, glucose-controlled insulin delivery system and microsphere for temperature-sensitive solute release have been designed and characterized.

It has been recognized that the constant release is not the only way to maximum drug effect and minimum side effects and the assumption used for constant release rate sometimes fails its validity for physiological conditions. To overcome this difficulty, externally modulated or self-regulating drug delivery systems have been used as novel approaches to delivering drug as required. To achieve this drug delivery system, the phase transition polymers have been intensively exploited as a candidate materials. With the understanding of the phase transition in polymers, numerous polymer systems that show a phase transition in response to external stimuli such as temperature, pH (1-2), ionic strength (3), and electric potential (4-6) have been reported. For its remarkable properties, poly N-isopropylacrylamide has been studied widely for temperature-modulated device (7-14). Recently polymer systems that demonstrate the phase transition to more than one variable, in particular pH and temperature, have been studied intensively for realizing the more sophisticated device responding to external stimuli (15-16).

In this study, a new pH/temperature-responsive polymer system with transitions resulting both from polymer-water and polymer-polymer interactions has been demonstrated using the copolymer composed of N,N'-dimethylaminoethyl methacrylate (DMAEMA) and ethyl acrylamide (EAAM) and the mixture of poly DMAEMA and poly EAAM. Based on the pH/temperature responsiveness of copolymer and polymer mixture, glucose-controlled insulin delivery system and microsphere for temperature-sensitive solute release have been designed and characterized.

Experimental

Materials.

DMAEMA monomer, ammonium persulfate (APS), and tetramethylethylene diamine (TEMED) were purchased from Aldrich. Bovine insulin, N,N'-azobis(isobutyronitrile) (AIBN) and glucose oxidase (GOD) were purchased from Sigma Chemical Co. DMAEMA monomer was distilled before use. Other reagents were used as received.

Synthesis.

EAAM was synthesized in our laboratory as described previously (17). Poly(DMAEMA-co-EAAM) was prepared by free radical polymerization as follows: 7.8 g of distilled monomers (mixtures of DMAEMA and EAAM) and 0.02 g of AIBN as an initiator were dissolved in 100 mL of water/ethanol binary solvent (5/5 by volume). The ampoule containing the solution was sealed by conventional methods and immersed in a water bath held at 75 °C for 15 h. After polymerization, all polymers were dialyzed against distilled-deionized water at 4 °C and freeze-dried. PolyDMAEMA and polyEAAM were prepared using the preparation method of copolymer for the preparation of pH/temperature responsive polymer complex. To observe the effect of preparation method on polyDMAEMA, polyDMAEMA was prepared by free radical polymerization in water at room temperature using APS as initiator and TEMED as accelerator.

Transmittance Measurements.

The phase transition was traced by monitoring the transmittance of a 500 nm light beam on a Spectronic 20 spectrophotometer (Baush & Lomb). The concentration of the aqueous polymer solution was 5 wt%, and the temperature was raised from 15 to 70 °C in 2-deg increments every 10 min. To observe their pH/temperature dependence, the phase transitions of polymers in citric-phosphate buffer solution versus temperature at two pH values (4.0 and 7.4) were measured.

Preparation of Insulin-Loaded Matrix.

Lyophilized copolymer was ground down to colloidal dimensions (< 1 μm) using a laboratory planetary mill (Pulverisette, Fritsch GmbH). A 110 mg sample of copolymer powder, 20 mg of bovine insulin, and 20 mg of GOD were mixed, and the mixture was compressed into a disk-shaped matrix of 5-mm thickness and 15-mm diameter.

Measurement of Weight Loss of Insulin-Loaded Matrix in Response to Glucose.

After immersion in phosphate buffer solution (PBS) for desired time at 37 °C, the insulin-loaded matrix was removed and dried in a vacuum oven at room temperature. The percent of weight of the matrix was determined as a function of time.

Release Experiment for Insulin.

Insulin release from the insulin-loaded matrix was measured in response to alternating changes of glucose concentration when 150 mg of an insulin-loaded matrix was introduced to 100 mL of phosphate buffer solution (PBS) at 37 °C. The amount of released insulin was measured by taking 1 mL of the release medium at a specific time and immersing the matrix in a fresh medium. Insulin was determined by reverse-phase HPLC, using a Resolvex C₁₈ (Fisher Scientific) and 0.01 N HCl/acetonitrile (80/20-50/50, v/v%) mobile phase over 30 min at a flow rate of 1 mL/min. The eluate was monitored by optical absorption at 210 nm.

Preparation of Microsphere Using Temperature-Sensitive Polymers.

Using 5 ml syringe (26 gauge needle), polymer solution mixture composed of polyDMAEMA, poly EAAM and model drug was transferred dropwise to the water as shown in Figure 1. The temperature of water should be higher than the LCST of polymer for the coagulation of polymer and hydrocortisone was used as a model drug. The microsphere was dried in vacuum oven at 40 °C and the diameter of microsphere was approximately 2 mm. The loading amount is approximately 20 wt %.

Release Experiment for Hydrocortisone.

The release of hydrocortisone from the microsphere was measured in response to pulsatile changes of temperature. 500 mg of microspheres were introduced into 200 ml of release medium (pH 7.4 PBS) at desired temperature. The amount of released hydrocortisone was measured by taking 1 mL of the release medium at a specific time, replacing the total release medium with fresh PBS to maintain sink conditions and assaying the drug concentration at 248 nm using a UV spectrophotometer (Shimadzu, Japan).

Results and Discussions

pH/Temperature-Induced Phase Transition.

The temperature-induced behavior of poly(DMAEMA-co-EAAM) at two pHs (4.0 and 7.4) is observed as shown in Figure 2. At pH 7.4, the LCST of poly(DMAEMA-co-EAAM) was shifted to a lower temperature with the increase of EAAM content. In general, the LCST should increase with increasing hydrophilicity of the polymer (16). However, a LCST shift to a lower temperature was observed with the incorporation of the hydrophilic EAAM. This is due to the formation of hydrogen bonds, which protect (N,N-dimethylamino)ethyl groups from exposure to water and result in a hydrophobic contribution to the LCST (18-19) At pH 4, no LCST was observed with polyDMAEMA and the LCST of all copolymers was increased compared to that at pH 7.4. At pH 4.0, (N,N-dimethylamino)ethyl groups of DMAEMA are fully ionized. An increasing electrostatic repulsion between charged sites on DMAEMA disrupts the hydrogen bonds between EAAM and DMAEMA. These interfere with the

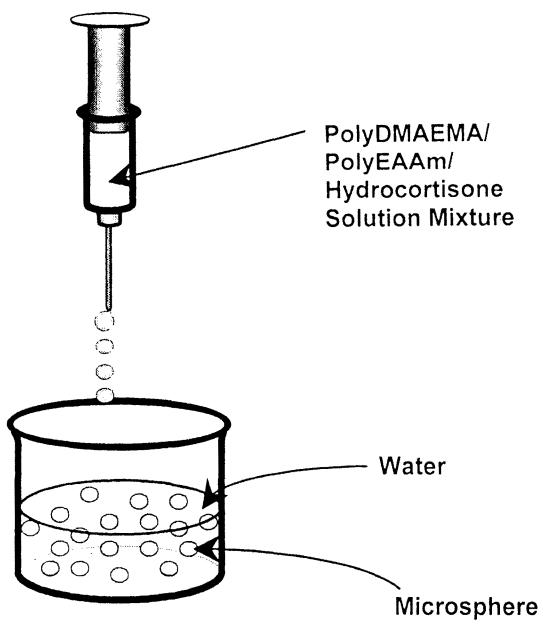


Figure 1. Preparation method of microsphere.

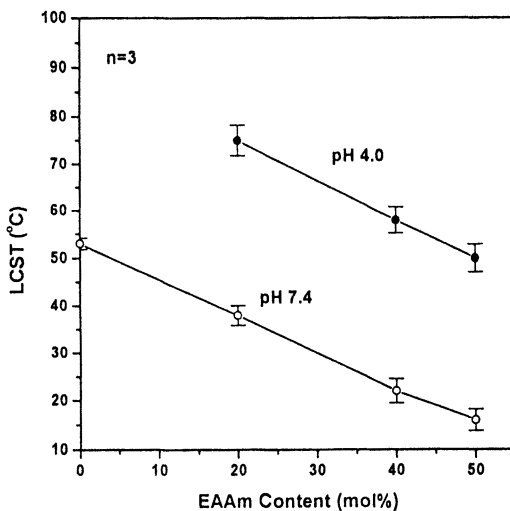


Figure 2. LCST of poly(DMAEMA-co-EAAM) in citric-phosphate buffer solution at pH 4.0 and 7.4.

hydrophobic interactions between (N,N- dimethylamino)ethyl groups above the LCST and the hydrophobic contribution to the LCST due to hydrogen bonding.

To prepare temperature-sensitive polymer complex, the mixtures of poly EAAm and polyDMAEMA in appropriate ratio with that of copolymer were prepared and their temperature-sensitive behaviors were observed. As presented previously, poly DMAEMA can be prepared in the water containing APS as an initiator and TEMED as an accelerator or water/ethanol solvent mixture containing AIBN as an initiator. Poly DMAEMA prepared in the water showed the LCST at 50 °C and that prepared in the water/ethanol mixture showed the LCST at 30 °C. The LCST of polyDMAEMA prepared in water was shifted to the lower temperature with the addition of polyEAAm, which was observed in the aqueous copolymer solution as shown Figure 2 (pH 7.4) and polymer aqueous solution became milky without aggregation above LCST. However, the polymer aggregate was formed with the addition of polyEAAm into the aqueous solution of polyDMAEMA prepared in the water/ethanol mixture above LCST. These indicate that there exists a difference in the stereochemical configuration of polyDMAEMA depending on the preparation method. To understand this behavior of polyDMAEMA, the tacticity of poly DMAEMA was investigated. Table 1 show the α -CH₃ portion of the ¹³C-NMR spectra of polyDMAEMA prepared at two different conditions. It shows that poly DMAEMA prepared in the water does not contain syndiotactic triads, however, the polymer prepared in water/ethanol mixture contains syndiotactic triads (13.6 ppm). According to the literature (20), the isotactic chain has no intramolecular interaction between side chains. On the other hand, every sequence in the syndiotactic chains brings two pendant groups into close proximity where they can form an intramolecular interaction which stabilizes the local chain conformation. This leads to the efficient formation of hydrogen bond between polyEAAm and polyDMAEMA prepared in water/ethanol mixture resulting in the formation of aggregation above LCST. The mechanism on this phenomenon is under investigation.

Glucose-Sensitive Insulin Release.

Figure 3 shows the rationale of glucose-controlled insulin delivery system schematically. In the presence of glucose, gluconic acid generated by the glucose-GOD reaction protonates dimethylamino groups of poly(DMAEMA-co-EAAm), inducing the LCST shift to higher temperature from the surface of the insulin-loaded matrix. This leads to the disintegration of the matrix with polymer dissociation from the surface with the insulin release.

Based on this concept, insulin-loaded matrix was designed and characterized. Poly(DMAEMA-co-EAAm) with 50 mol % of EAAm was selected as a model polymer for the preparation of an insulin-loaded matrix considering its pH/temperature responsiveness.

Figure 4 shows the weight loss of the matrix in PBS at two different glucose concentrations. We found that 100 % of initial weight had been lost at 5 g/L of glucose concentration during 24 hours, whereas 10 % of initial weight had been lost at 0.5 g/L of glucose concentration. These results indicate that this polymer system responds to the change of glucose concentration in the presence of GOD.

Table 1. Chemical shift for various α -CH₃

Polymer	$\delta\alpha$ -CH ₃ (ppm)			Area		
	i	h	s	i	h	s
Poly DMAEMA prepared in water/ethanol solvent mixture	18.36	16.49	13.63	3.28	5.49	2.95
Poly DMAEMA prepared in water	18.32	16.45	-	3.34	5.42	-

i: isotactic triads, h: atactic triads, s: syndiotactic triads

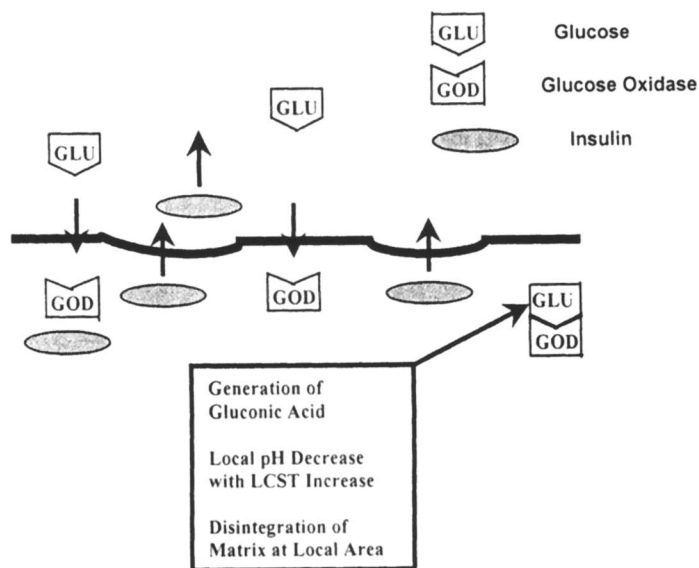


Figure 3. Schematic representation of the glucose-controlled insulin release using poly(DMAEMA-co-EAAm).

Figure 5 shows the alternating insulin release rate in response to an alternating exposure of the insulin-loaded matrix to high and low aqueous glucose solutions. Minimal release was observed at the lower concentration of glucose. The large deviation in the release rate was attributed to inhomogeneous mixing of the components in the insulin-loaded matrix causing its irregular dissolution.

Temperature-Sensitive Release of Hydrocortisone from Microsphere.

Firstly, poly(DMAEMA-co-EAAM) was used for the preparation of microsphere based on the preparation method presented previously. However, the formation of microsphere was not observed. The formation of microsphere was observed with the mixture of polyDMAEMA and polyEAAM.

To understand this phenomenon more in detail, temperature-induced phase transition of polymer was observed in the various forms of polymer networks. As present previously, the LCST of linear (noncrosslinked) poly(DMAEMA-co-EAAM) was shifted to a lower temperature with the increase of EAAM content. This is due to the formation of hydrogen bonds, which protect (N,N-dimethylamino)ethyl groups from exposure to water and result in a hydrophobic contribution to the LCST. With the formation of crosslinked network, the polymer gel exhibited the temperature-induced phase transition which was quite different from that of polymer aqueous solution. The transition temperature of poly(DMAEMA-co-EAAM) gel between the shrunken and swollen was shifted to the higher temperature with the increase of EAAM content, which was contrary to the LCST change of poly(DMAEMA-co-EAAM) aqueous solution as shown in Figure 6. This indicates that polymer-polymer interaction via hydrogen bond contributed hydrophobically to the LCST of poly(DMAEMA-co-EAAM) aqueous solution but it contributed hydrophilically to the temperature-responsive swelling behavior of poly(DMAEMA-co-EAAM) gel (21). With the formation of gel network, the degree of freedom of polymer chain is significantly decreased and this hinders the formation of the hydrogen bond between DMAEMA and EAAM. From this result, the temperature-induced phase transition of poly(DMAEMA-co-EAAM) is highly dependent on the change of hydrogen bond due to the structural difference. From this perspective, we can suggest that there exists the difference in the temperature-induced phase transition between poly(DMAEMA-co-EAAM) and the mixture of polyDMAEMA and polyEAAM. Poly(DMAEMA-co-EAAM) exhibit less drastic phase transition in response to temperature changes compared to the mixture of polyDMAEMA and polyEAAM. This arises from cooperative polymer-polymer interactions (zipper-like effect) in the mixture of polyDMAEMA and polyEAAM as shown schematically in Figure 7. Based on this characteristic of polymer complex, we can expect that the formation of microsphere using temperature-induced phase transition is observed with the polymer complex.

When we applied a step function of temperature to the microsphere, hydrocortisone was released in a stepwise manner. Figure 8 exhibits high release rates at lower temperature due to the dissociation of temperature-sensitive intermolecular interaction in the polymer complex. This gave hydrocortisone release control in an on-off manner without considerable lag time and it was possible to switch hydrocortisone on-off with one degree temperature fluctuation.

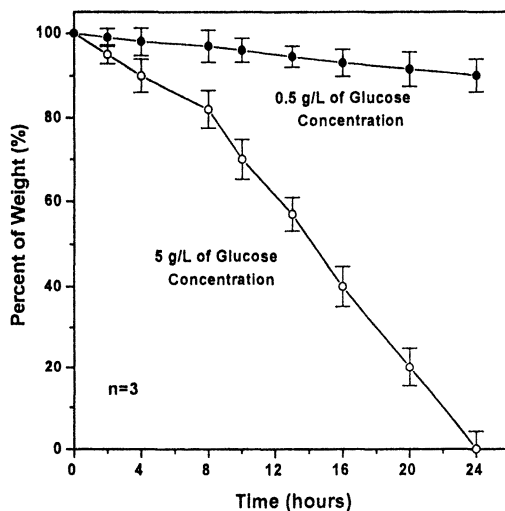


Figure 4. Disintegration of the polymer matrix in phosphate buffer solution at two glucose concentrations.

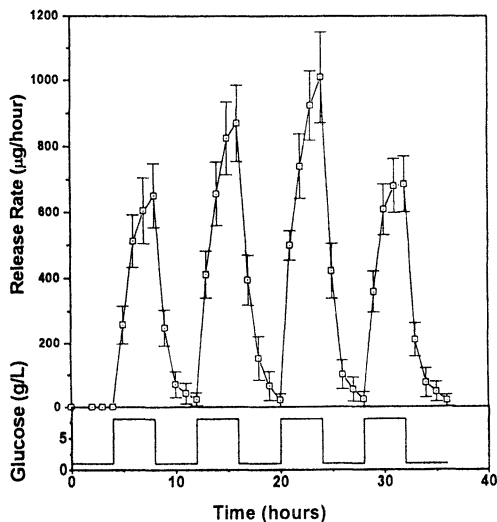


Figure 5. Insulin release from the insulin-loaded matrix in response to alternating change of glucose concentration.

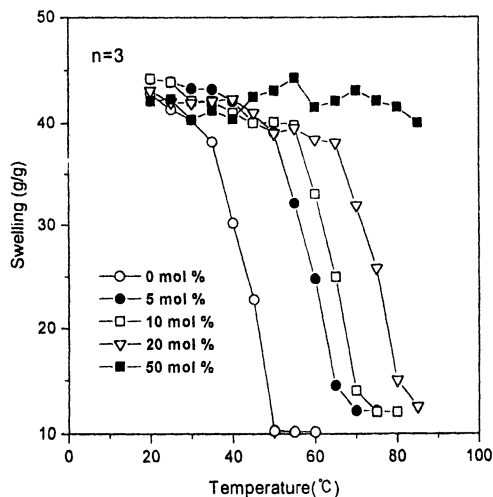


Figure 6. Equilibrium swelling change of poly(DMAEMA-co-EAAm) gel in response to temperature change.

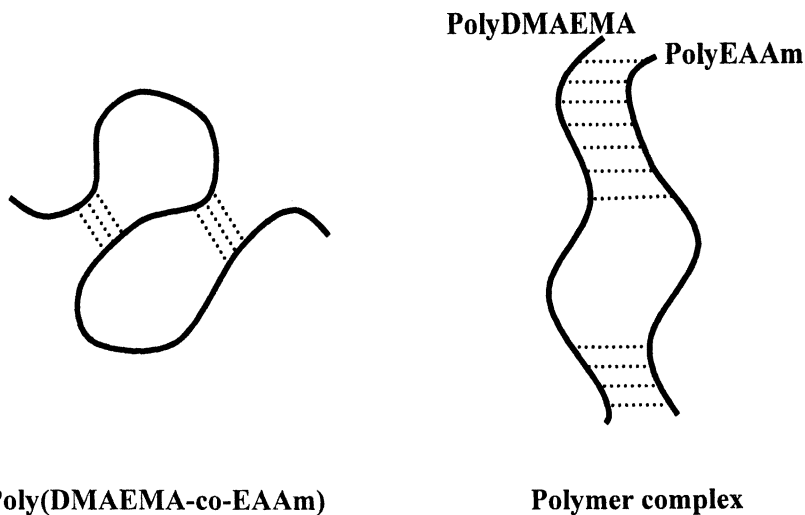


Figure 7. Schematic description of intra/intermolecular interaction in copolymer and polymer mixture.

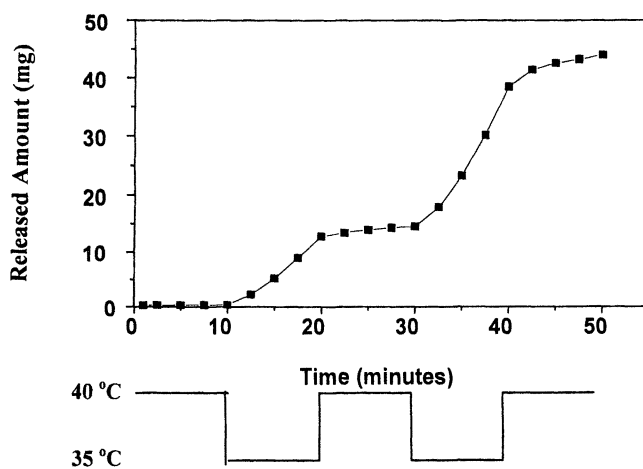


Figure 8. Release of hydrocortisone from the microparticle in response to pulsatile temperature change.

Conclusions

pH/temperature-sensitive polymer systems with functions resulting from both polymer-water and polymer-polymer interactions was demonstrated and a transition mechanism was proposed. The formation of hydrogen bond in the polymer system played an important role in determining the pH/temperature-induced phase transition. Using these polymer systems, the delivery systems for glucose-controlled insulin release and temperature-controlled release of hydrocortisone were designed and characterized. These polymer systems have a variety of potential applications in the area of drug delivery.

References

1. Siegel, R. A.; Firestone, B. A. *Macromolecules*, **1988**, 21, 3254.
2. Yuk, S. H.; Cho, S. H.; Lee, H. B. *J. Controlled Release*, **1995**, 37, 69.
3. Ricka, J.; Tanaka, T. *Macromolecules*, **1984**, 17, 2916.
4. Tanaka, T.; Nishio, I.; Sun, S. T.; Nishio, S. *Science*, **1982**, 218, 467.
5. Kwon, I. C.; Bae, Y. H.; Kim, S. W. *Nature*, **1991**, 354, 291.
6. Choi, O. S.; Yuk, S. H.; Jhon, M. S. *J. Appl. Polym. Sci.*, **1994**, 51, 375.
7. Heskins, M.; Guillet, J. E. *J. Macromol. Sci.-Chem.*, **1986**, A2(8), 1441.
8. Hoffman, A. S.; Afrassibi, A.; Dong, L. C. *J. Controlled Release*, **1986**, 4, 213.
9. Bae, Y. H.; Okano, T.; Kim, S. W. *Makromol. Chem., Rapid Commun.*, **1987**, 8, 481.
10. Bae, Y. H.; Okano, T.; Kim, S. W. *Makromol. Chem., Rapid Commun.*, **1988**, 9, 185.
11. Stayton, P. S.; Shimoboji, T.; Long, C.; Chilkoti, A.; Chen, G. H.; Harris, J. M.; Hoffman, A. S. *Nature*, **1995**, 378, 472.
12. Ilman, F.; Tanaka, T.; Kokufuta, E. *Nature*, **1991**, 349, 400.
13. Kim, S. W.; Bae, Y. H. Smart drug delivery system, in: Sam, A. P.; Fokkens, J. G. (Eds), *Innovation in drug delivery. Impact on Pharmacotherapy*, The Anselmus Foundation, Houten, The Netherland, 1995, ppl 12.
14. Aoki, T.; Kawashima, M.; Katono, H.; Sanui, K.; Ogata, N.; Okano, T.; Sakurai, Y. *Macromolecules*, **1994**, 27, 947.
15. Chen, G. H.; Hoffman, A. S. *Nature*, **1995**, 373, 49.
16. Feil, H.; Bae, Y. H.; Feijen, J.; Kim S. W. *Macromolecules*, **1993**, 26, 1259.
17. McCormick, C. L.; Nonaka, T.; Johnson, C. B. *Polymer* **1988**, 29, 371.
18. Cho, S. H.; Jhon, M. S.; Yuk, S. H.; Lee, H. B. *J. Polym. Sci. B: Polym. Phys.* **1997**, 35, 595.
19. Yuk, S. H.; Cho, S. H.; Lee, S. H., *Macromolecules*, **1997**, 30, 6856.
20. Russell, G. A.; Hiltner, P. A.; Gregonis, D. E.; deVisser, A. C.; Andrade, J. D., *Polym. Sci., Polym. Phys Ed.*, **1980**, 18, 1271.
21. Cho, S. H.; Jhon, M. S.; Yuk, S. H. *Eur. Polym J.* in press.

Chapter 24

Characterization of Poly(2-ethylacrylic acid) for Use in Drug Delivery

Jeffrey G. Linhardt¹ and David A. Tirrell²

¹Polymer Science and Engineering Department,
University of Massachusetts, Amherst, MA 01003

²Division of Chemistry and Chemical Engineering,
California Institute of Technology, Pasadena, CA 91125

The pH-dependent conformational transition of poly(2-ethylacrylic acid) [PEAA] and the interaction of PEAA with phosphatidylcholine bilayer membranes were investigated. The location and breadth of the conformational transition were shown to be dependent on the molecular weight and polydispersity of the sample. The pH-dependent destabilization and fusion of extruded large unilamellar vesicles (LUVs) by PEAA were characterized and reduction of either the chain length or the polymer concentration caused the fusion and contents release events to shift to lower pH values. Release of entrapped calcein was observed at pH values ca. 1 unit higher than those found to cause membrane fusion. Decreased levels of fusion were observed when the concentration of PEAA was lower than that of the lipid; however, quantitative release of encapsulated calcein could be effected at very low polymer concentrations (~3% w/w PEAA/lipid).

Thirty years of research on liposomal drug delivery systems is now beginning to pay off in the clinic. Several liposomal delivery systems, including antifungal and anticancer formulations, are currently being used to treat patients (1,2). The future promises development of more advanced drug carriers with researchers now focusing on liposomes that bear site-specific targeting information and that will effectively deliver different types of drug candidates such as recombinant proteins (3), antisense oligonucleotides (4), and cloned genes (5).

To date, liposomes have been successful in changing the biodistribution of drugs in the body by causing accumulation of the drug at the disease site. This has led to enhanced therapeutic activity and reduced toxicity when compared with that of the free drug. A significant advance was made by prolonging the circulation lifetime of liposomes through the use of the glycolipid monosialoganglioside (GM₁) (6) or the use

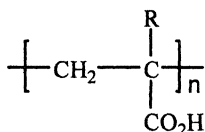
of a derivative of phosphatidylethanolamine bearing polyethylene glycol (PEG-PE) (7). These liposomes escape the leaky vasculature present at certain disease sites because of their ability to evade uptake by the mononuclear phagocytic system (MPS).

When designing liposomes capable of intracellular delivery of therapeutic agents, it is essential that liposomal fusion with the target cell occurs, and that the contents be delivered to the cytoplasm before undergoing lysosomal degradation. This is where responsive liposomes can be used to release the drug from the endosome before fusion with the lysosome occurs.

Strategies for the design of responsive liposome systems can utilize the lipid constituents of the membrane or other molecules (most commonly macromolecules) that disrupt the membrane in response to various stimuli. The use of phospholipids that form nonlamellar phases under certain conditions can be used for membrane destabilization (8,9). Diacyl lipids that are prone to cleavage of one of the acyl chains can also act as permeabilizing agents (10,11). Furthermore, inclusion of defect forming molecules in the membrane can effect membrane permeabilization (12).

Macromolecular approaches toward responsive liposome systems include using model peptides that mimic the actions of fusogenic proteins and synthetic polymers that act on membranes. Peptides derived from the fusion domains of the fusion protein of the influenza virus (13), and the sperm surface proteins fertilin (14) and PH-30 (15) have been used in destabilization and fusion of PC vesicles. Furthermore, membrane properties including fusogenicity, permeability, and the gel to liquid-crystalline phase transition temperature (T_m), have been altered by the use of synthetic polyelectrolytes (16-18). These polyelectrolytes include poly(acrylic acid) [PAA, **1a**] and poly(methacrylic acid) [PMA, **1b**] whose interactions with membranes are pH sensitive (18,19).

In this laboratory, we have studied the effect of poly(2-ethylacrylic acid) [PEAA, **1c**], a hydrophobic polyelectrolyte, on membranes. This polymer undergoes a conformational collapse when the pH of an aqueous solution is depressed and causes



1 a: R=H **b:** R=CH₃ **c:** R=CH₂CH₃

membrane leakage at low concentrations (<3% w/w PEAA/lipid). When present at higher concentrations (50% w/w PEAA/lipid), a structural reorganization from membrane vesicles at high pH to small polymer-lipid micelles at low pH occurs (20).

These properties have stimulated interest in the use of PEAA in the design of drug carriers for pharmaceutical applications. Thus far, PEAA has been used to create liposomes that respond to pH (21), temperature (21), light intensity (22,23), and concentration of a solute such as glucose (24). In this chapter, the pH-dependent solution properties of PEAA are examined, along with the pH-dependent interaction of PEAA with PC vesicles.

Molecular Weight Control

Our initial goal in the studies described herein was to prepare PEAA of well defined molecular architecture. We were especially interested in PEAA of low molecular weight (<8000) with narrow molecular weight distribution. PEAA was obtained from a bulk free-radical polymerization of 2-ethylacrylic acid (25). The polydispersity of the product was consistent with that expected for a free radical synthesis in which termination occurs primarily through disproportionation ($PDI \sim 2$ / PDI is the polydispersity index given by M_w/M_n). Solvent fractionation was used to reduce the polydispersity of PEAA as obtained from radical polymerization. The product was fractionated as follows: PEAA was dissolved in methanol and precipitated by the slow dropwise addition of ether. The precipitate was filtered and more ether was added to the filtrate to precipitate the next fraction. The fractions obtained are listed in Table I with their molecular weights as determined by gel permeation chromatography (GPC). The molecular weight of the samples decreases as the amount of ether in the solvent mixture increases. Weight-average molecular weights range from 4,800 to 32,000.

Table I. Molecular Weights^a of PEAA Samples Obtained from Solvent Fractionation

<i>Sample^b</i>	<i>M_w</i>	<i>M_n</i>	<i>PDI</i>
Unfractionated	32,000	14,000	2.2
1:1	23,000	16,000	1.4
2:1	11,800	8,400	1.4
6:1	8,000	6,200	1.3
10:1	5,000	4,400	1.2
Soluble	4,800	4,100	1.2

^aDetermined by GPC with PEO calibration

^bRatios in the sample column refer to the ether:methanol ratio used to precipitate each fraction. [Appears in Ref. 33]

Solution Conformation Properties of PEAA

Fluorescence studies with pyrene can be used to determine the polarity of the microenvironment of the fluorophore. The steady-state fluorescence intensity of pyrene increases upon transfer from a polar environment such as water, to a non-polar environment such as hexane. Thus pyrene has been useful in studying the conformational transition of polyelectrolytes in solution, by observing an increase in its peak 1 (373 nm) and peak 3 (384 nm) fluorescence intensities when the polymer chain goes from an extended hydrophilic coil to a more compact hydrophobic polymer coil (26). Figures 1A and 1B show the conformational transition for four different fractions of PEAA and for the unfractionated sample. As the molecular weight of the sample is lowered, the conformational transition occurs at lower pH.

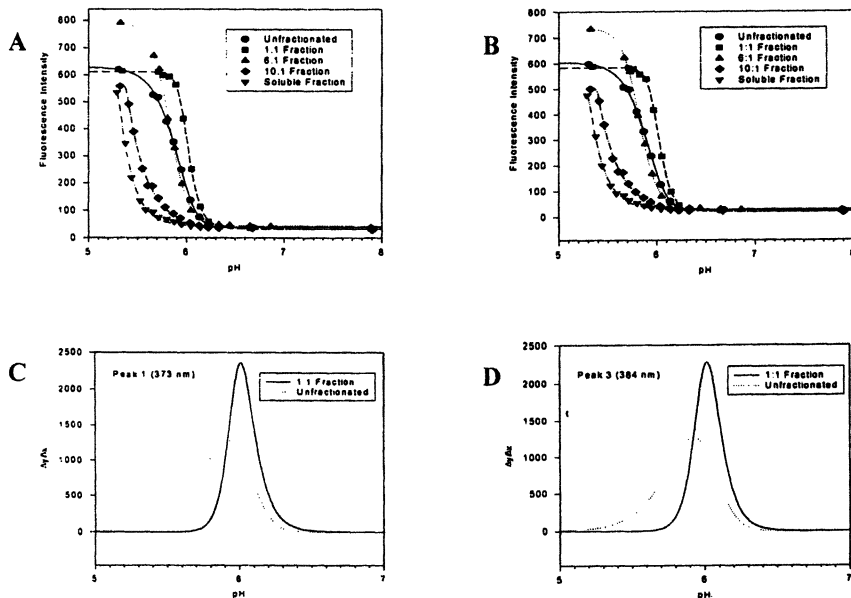


Figure 1. Fluorescence intensity at 373 nm (Peak 1,A) and 384 nm (Peak 3,B) for pyrene dissolved in phosphate-buffered solutions of PEEA of different molecular weights. First derivative plots for the 1:1 and the unfractionated samples demonstrate the effect of polydispersity on the transition width (Peak 1,C and Peak 2,D). [Appears in Ref. 33]

This result can be partially explained by comparison with titration data for PEEA in the same region. Unlike PAA, the ionization behavior of PMA (27) and PEEA (28) is strongly dependent on molecular weight in the transition region, where shorter chains are more highly charged at the same pH. Therefore, if one makes the assumption that the conformational collapse occurs at a given extent of chain ionization, shorter PEEA chains must be subjected to lower pH to induce collapse.

Since all of the fractions were of lower polydispersity than the unfractionated sample, we wanted to examine the effect of polydispersity on the breadth of the conformational transition. This was done by plotting the first derivative of the transition curves shown in Figures 1A and 1B (29). The derivative results in a peak whose maximum value was designated the transition midpoint, and whose full width at half maximum (FWHM) defined the transition width. Figures 1C and 1D show the first derivative plots for the 1:1 fraction and unfractionated samples, for which the number-average molecular weights are similar. Note that the width of the peak for the 1:1 fraction is narrower than that of the unfractionated sample, which we ascribe to the decrease in polydispersity (PDI of 1.4 vs. 2.2). Table II shows the transition widths and midpoints for each of the fractions.

Table II: Transition Midpoints and Widths Obtained from Fluorescence Measurements

Sample	Peak 1 (373 nm)		Peak 3 (384 nm)	
	FWHM	Transition pH	FWHM	Transition pH
Unfractionated	0.33	5.93	0.41	5.93
1:1	0.22	6.01	0.21	6.02
6:1	0.34	5.83	0.33	5.82
10:1	0.28 ^a	5.42	0.29 ^a	5.42
Soluble Fraction	0.22 ^a	5.34	0.23 ^a	5.34

^aFWHM value was obtained by doubling the pH difference between the midpoint (peak value) and the higher pH half maximum value of the first derivative plot.

pH is controlled by mixing appropriate ratios of monobasic and dibasic phosphate buffers (100 mM) [Appears in Ref. 33]

Characterization of PEEA Interactions with Bilayer Membranes

Optical Density Measurements and Transmission Electron Microscopy. Figure 2 compares the turbidity data obtained on mixtures of egg yolk phosphatidylcholine (EYPC) vesicles and PEEA, when the vesicles are prepared either by vortex hydration of a dried lipid film (MLVs; 100 nm to 10 μ m in diameter) or extrusion through a polycarbonate membrane (LUVs; 100 nm in diameter) (30). For MLVs, a smooth transition is observed as PEEA induces a structural reorganization from a turbid mixture of membrane vesicles to an optically clear solution of disc-like micelles, which is consistent with earlier experiments (20). However, when extruded LUVs were used for turbidity measurements, there was a large increase in the optical density

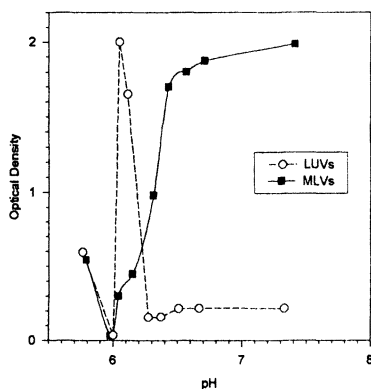


Figure 2. Turbidity measurements on mixtures of EYPC vesicles and PEEA, both at concentrations of 1 mg/mL. As the pH is reduced, MLVs undergo a smooth turbidity transition, while LUVs show a large increase in optical density prior to clarification. [Appears in Ref. 34]

of the suspension just prior to clarification (Figure 2). The interpretation of this large peak was that vesicle aggregation or fusion was occurring.

The answer to this question was sought using transmission electron microscopy (TEM). We wanted to determine the structures that were present in the PEAA/EYPC mixtures used in the turbidity studies, particularly those present where the abrupt increase in optical density occurred. Figure 3 shows a series of TEM micrographs that includes a control sample of extruded EYPC vesicles in PEAA solution at pH 8.3 (Figure 3A) and vesicles present in PEAA solutions at pH 6.1 at various times after mixing (Figures 3B-F). The vesicles in the control are ca. 100 nm in diameter, consistent with the size of the pores used for extrusion. When vesicles are added to a PEAA solution at pH 6.1, the size increases with time to a final average diameter five times larger (500 nm), indicating that vesicle fusion is occurring.

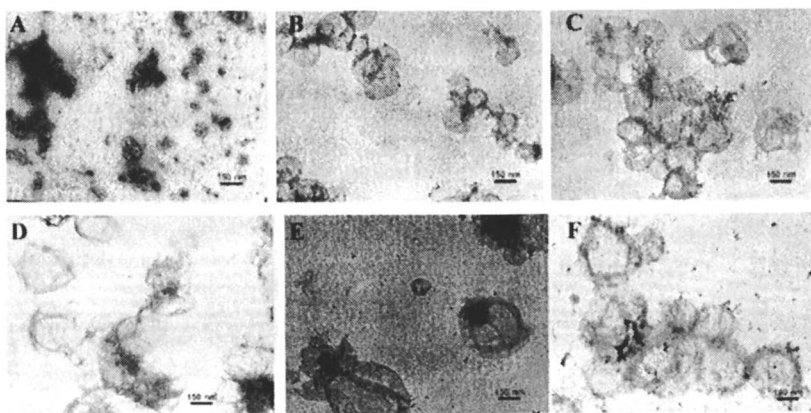


Figure 3. TEM micrographs of PEAA/EYPC vesicle mixtures stained with uranyl acetate at: B) 20 min, C) 50 min, D) 90 min, E) 180 min, and F) 1440 min after mixing at pH 6.1 where a maximum increase in optical density occurs; A) control sample prepared at pH 8.5, where the polymer-lipid interactions are weak or absent. [Appears in Ref. 34]

Fusion Assay and Contents Release. A lipid mixing fusion assay was performed to support data obtained from electron microscopy. This assay relies upon fluorescence resonance energy transfer (RET) which occurs when two chromophores are in close proximity and the fluorescence emission of one of the chromophores overlaps the fluorescence excitation of a second probe (13). For our experiment, we prepared labelled EYPC vesicles containing 1 mol% each of NBD-PE and Rh-PE, and mixed them with unlabelled EYPC vesicles at a ratio of 1:3. The fluorescence emission spectra obtained during a typical lipid mixing fusion assay are shown in Figure 4 (excitation wavelength for NBD-PE is 468 nm). At high pH, when the chromophores

are in close proximity, the fluorescence emission for NBD-PE is quenched, but that of Rh-PE is high. When membrane fusion is induced by lowering the pH of the solution, more bilayer area becomes available for dilution of the chromophores. As shown in Figure 4, this leads to an increase in the NBD-PE emission (525 nm) and a corresponding decrease in Rh-PE fluorescence emission at 585 nm.

The lipid mixing fusion results and electron microscopy data demonstrate the ability of PEAA to induce membrane fusion. This distinguishes PEAA from PAA and PMA, as the latter polymers cause vesicle aggregation (but no fusion) at lower pH (16,18).

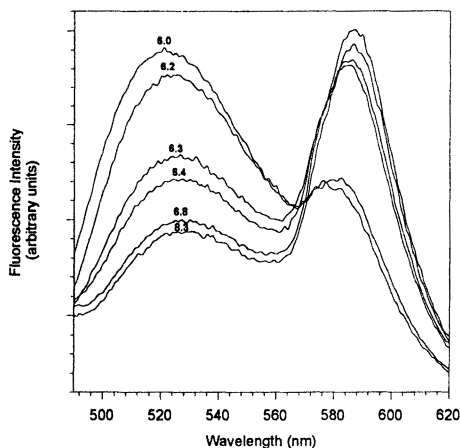


Figure 4. Fluorescence emission spectra of mixtures of PEAA and EYPC vesicles [containing 1 mol% of each NBD-PE (donor) and Rh-PE (acceptor)] at 6 pH values. At high pH, the fluorescence of NBD-PE at 525 nm is quenched by resonance energy transfer to Rh-PE. As the pH is lowered, the fluorescent probes diffuse apart and an increase in NBD-PE fluorescence is observed, along with a decrease in the Rh-PE emission at 585 nm. [Appears in Ref. 34]

In the body, there are many instances of membrane fusion events where material is neither lost from the cell nor from the fusing compartment (e.g. viral infection, fertilization, and endocytosis). There are relatively few demonstrations of such so called “leakless” fusion events in model membrane systems. In order to test for leakless fusion, we performed a contents release assay by observing the fluorescence increase associated with release of calcein from the interior of PC vesicles (26). Calcein was excited at 495 nm and the fluorescence emission at 525 nm was monitored. The results of this study showed that the membrane becomes permeable to encapsulated material 0.4–1.0 pH units higher than where fusion occurs, and that there is 100% release of the marker dye before fusion is induced (Figure 5).

A detailed study of the effects of molecular weight (MW) and concentration of PEAA on fusion and contents release was performed and the results are presented in Figures 5 and 6. Figure 5 shows that the transition midpoints (50% fusion or 50%

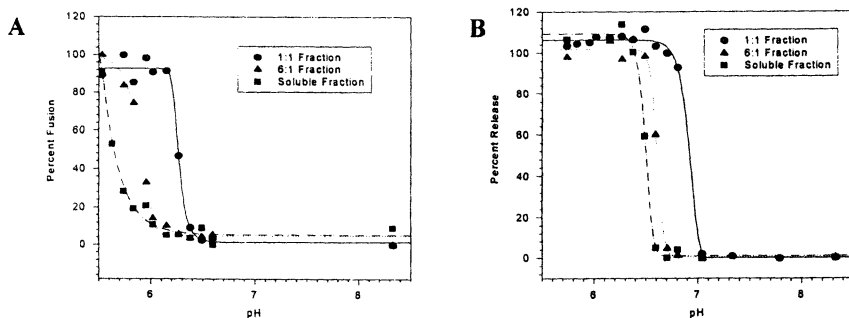


Figure 5. Effects of PEAA molecular weight on A) fusion and B) contents release. Samples were prepared as 3.3/1 w/w mixtures of PEAA to lipid. Release of encapsulated material occurs at pH values 0.43-0.96 pH units higher than those required for fusion.

Percent fusion was calculated for each point along the pH axis from the following equation: $\%Fusion = [(F_{meas} - F_o) / (F_{max} - F_o)] \times 100$ or $(\Delta F / \Delta F_{max}) \times 100$; where F_{meas} is the fluorescence intensity of NBD-PE at 530 nm, F_o is the fluorescence intensity in the quenched state, and F_{max} is the fluorescence intensity achieved by infinite probe dilution, determined by the addition of 40 μ L of 100 mM Triton X-100. Percent Release was also calculated by $(\Delta F / \Delta F_{max}) \times 100$ [Appears in Ref. 34]

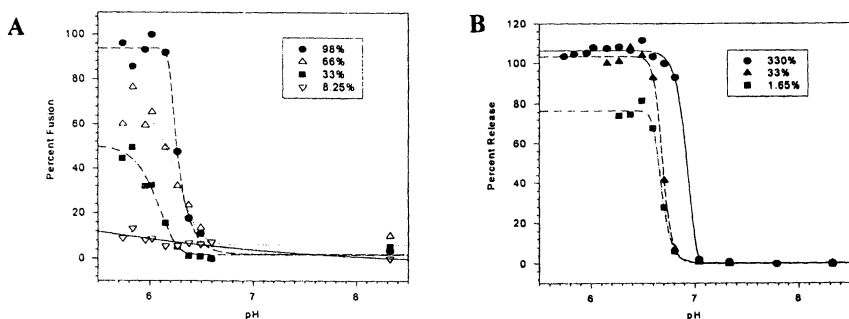


Figure 6. Effects of PEAA concentration on A) fusion and B) contents release. Percentages shown represent the weight of PEAA compared to lipid. The extent of membrane fusion is reduced as the concentration of PEAA is lowered below 100% and is not detected below concentrations of 16.5%. Release of encapsulated calcein is efficient down to low concentrations of PEAA; 80% release is observed at concentrations as low as 1.65%. [Appears in Ref. 34]

release) for both fusion and release are dependent upon MW, and that the transition occurs at lower pH for lower MW fractions. Figure 6 shows the effect of PEAA concentration on fusion and contents release. As the concentration of PEAA becomes lower than that of the lipid, percent fusion decreases until fusion can no longer be detected ($\leq 16.5\%$ w/w PEAA/lipid) [Figure 6A]. In contrast, very low polymer concentrations can effect efficient release of encapsulated calcein (80% release at 1.65% w/w PEAA/Lipid) [Figure 6B].

The results of the concentration study shown in Figure 6 are summarized in Table III. Calculations were performed that show that efficient delivery vehicles can be made with as few as 50-100 PEAA chains ligated to the exterior of the vesicle.

Table III. Concentration Dependence^a of Transition Midpoints for Fusion and Contents Release

Concentration wt % PEAA/EYPC	Transition pH		PEAA Molecule ^b Lipid Molecule	PEAA Strands ^c per Vesicle
	Fusion	Calcein Release		
330	6.27	6.94	1:8	10,600
98	6.25	---	1:27	3100
66	6.23	6.70	1:40	2100
33	6.10	6.68	1:80	1100
16.50	no fusion	6.67	1:160	530
8.25	no fusion	---	1:320	270
3.30	---	6.66	1:800	110
1.65	---	6.66	1:1600	55

^a1:1 fraction was used for the concentration study

^bRatios based on molar masses of 760 g/mol and 20,000 g/mol for lipid and PEAA, respectively.

^cNumber based on assumption of above molar masses, vesicles of 100 nm in diameter, and area per lipid in a bilayer = 70 Å² [Appears in Ref. 34]

Conclusions

The pH-dependent conformational collapse of PEAA was shown to depend upon molecular weight and polydispersity of the sample by affecting the location and breadth of the conformational transition, respectively. PEAA induces fusion of phosphatidylcholine LUVs upon acidification in aqueous solution. Transmission electron microscopy shows a large increase in the size of the vesicles when the pH of a PEAA/EYPC mixture is lowered to pH 6.1, which coincides with the abrupt increase in optical density. Fusion and contents release were observed to depend upon MW and concentration of PEAA; both events shifted to lower pH values with a reduction in MW or concentration. Release of contents occurred at pH values 0.4 to 1.0 pH units higher than those required for vesicle fusion. Future work will focus on PEAA-conjugated liposomes that have been developed in this laboratory (31,32) and will examine their efficacy as intracellular delivery vehicles.

Literature Cited

1. Allen, T. M. *Curr. Opin. Coll. Inter. Sci.* **1996**, *1*, 645-651.
2. Chonn, A.; Cullis, P. R. *Curr. Opin. Biotech.* **1995**, *6*, 698-708.
3. Weiner, A. *Immunomethods* **1994**, *4*, 201-209.
4. Dean, N.; McKay, R. *Proc. Natl. Acad. Sci. USA* **1994**, *91*, 11762-11766.
5. Miller, A. D. *Angew. Chem. Int. Ed.* **1998**, *37*, 1769-1785.
6. Gabizon, A.; Papahadjopoulos, D. *Proc. Natl. Acad. Sci. U.S.A.* **1988**, *85*, 6949.
7. Blume, G.; Cevc, G. *Biochim. Biophys. Acta* **1990**, *1029*, 91-97.
8. Allen, T.; Hong, K.; Papahadjopoulos, D. *Biochemistry* **1990**, *29*, 2976-2985.
9. Lai, M.-Z.; Duzgunes, N.; Szoka, F. *Biochemistry* **1985**, *24*, 1654-1661.
10. Ringsdorf, H.; Schlarb, B.; Venzmer, J. *J. Angew. Chem., Int. Ed. Engl.* **1988**, *27*, 113-158.
11. Haubs, M.; Ringsdorf, H. *Nouv. J. Chim.* **1987**, *11*, 151-156.
12. Anderson, V. C.; Thompson, D. H. *In Polymers at Interfaces: Macromolecular Assemblies*, in press.
13. Bailey, A. L.; Monck, M. A.; Cullis, P. R. *Biochim. Biophys. Acta* **1997**, *1324*, 232-244.
14. Martin, I.; Ruyschaert, J. M. *FEBS Letters* **1997**, *405*, 351-355.
15. Muga, A.; Neugebauer, W.; Hiramata, T.; Surewicz, W. K. *Biochemistry* **1994**, *33*, 4444-4448.
16. Fujiwara, M.; Grubbs, R. H.; Baldeschwieler, J. D. *J. Coll. Inter. Sci.* **1997**, *185*, 210-216.
17. Seki, K.; Tirrell, D. A. *Macromolecules* **1984**, *17*, 1692-1698.
18. Fujiwara, M.; Grubbs, R. H.; Baldeschwieler, J. D. *Polym. Prepr.* **1991**, *31*, 275.
19. Thomas, J. L.; You, H.; Tirrell, D. A. *J. Am. Chem. Soc.* **1995**, *117*, 2949-2950.
20. Thomas, J. L.; Tirrell, D. A. *Acc. Chem. Res.* **1992**, *25*, 336-342.
21. Tirrell, D. A.; Takigawa, D. Y.; Seki, K. *Ann. N.Y. Acad. Sci.* **1985**, *446*, 237-248.
22. You, H.; Tirrell, D. A. *J. Am. Chem. Soc.* **1991**, *113*, 4022-4023.
23. Ferritto, M. S.; Tirrell, D. A. *J. Am. Chem. Soc.* **1988**, *21*, 3117-3119.
24. Devlin, B. P.; Tirrell, D. A. *Macromolecules* **1986**, *19*, 2465-2466.
25. Ferritto, M. S.; Tirrell, D. A. *Macromol. Synth.* **1992**, *11*, 59-62.
26. Chen, T. S.; Thomas, J. K. *J. Polym. Sci.: Polym. Chem.* **1979**, *17*, 1103-1116.
27. Kawaguchi, S.; Takahashi, T.; Tajima, H.; Hirose, Y.; Ito, K. *Polym. J.* **1996**, *28*, 735-741.
28. Schroeder, U.K.O.; Langley, K.A.; Tirrell, D.A., unpublished results.
29. *Sigma Plot: Curve Fitting and Transform Manual*; Jandel Scientific, **1995**.
30. Hope, M. J.; Bally, M. B.; Webb, G.; Cullis, P. R. *Biochem. Biophys. Acta* **1985**, *858*, 161-168.
31. Maeda, M.; Kumano, A.; Tirrell, D. A. *J. Am. Chem. Soc.* **1988**, *110*, 7455-7459.
32. Kim, J.; Tirrell, D. A. *Macromolecules* **1999**, submitted for publication.
33. Linhardt, J. G.; Thomas, J. L.; Tirrell, D. A. *Macromolecules* **1999**, *32*, 4457-4459.
34. Linhardt, J. G.; Tirrell, D. A. *Langmuir* **2000**, in press.

Chapter 25

Synthesis and Characterization of Thermoreversible, Protein-Conjugating Polymers Based on *N*-Isopropylacrylamide

Hasan Uludag and Xiao-Dong Fan

Department of Biomedical Engineering, Faculty of Medicine and Dentistry,
University of Alberta, Edmonton, Alberta T6G 2G3, Canada

Thermoreversible, protein-conjugating polymers are being explored as drug carriers for controlled delivery of therapeutic proteins. Such polymers can be designed so that they (i) can conjugate to proteins without crosslinking agents, (ii) are soluble at a low temperature (so that chemical manipulations can be carried out in a solution state), and (iii) are insoluble at the physiological temperature to form a gelled state at a site of application. This study was intended to engineer thermoreversible *N*-isopropylacrylamide (NIPAM) polymers that contain protein-reactive *N*-acryloxysuccinimide (NASI) and hydrophobic methyl methacrylate (MMA) and ethyl methacrylate (EMA) units. NASI, MMA and EMA units were all shown to effectively reduce the lower critical solution temperature (LCST) of the polymers. NASI component was shown to undergo pH-dependent hydrolysis which can significantly influence the LCST. In experiments designed to assess the stability of polymer gels, gel stability was found to be inversely correlated with the LCST. In experiments designed to assess gel formation, NASI was found to have an unstabilizing effect on hydrogel formation, and MMA and EMA (<27% mole ratio) were not capable of facilitating gelation. We conclude that protein-reactive polymers can be engineered for LCST but this does not readily lend itself for polymer gelation.

Thermoreversible, protein-reactive polymers have attracted recent attention by the pharmaceutical industry due to their potential to act as novel carriers of therapeutic proteins. The thermoreversible (i.e., temperature-dependent solubility) character of the polymers allows one to carry out desired manipulations, such as mixing and injecting, in a solution state but eventually enables one to induce a phase separation simply by increasing the temperature above the solubility limit of the polymers.

The fact that such a phase separation is driven only by a temperature change is attractive since no other exogenous molecules need to be added to a pharmaceutical dosage form. The protein-reactivity of the polymers allows one to conjugate proteins to polymers without crosslinking agents, hence the possibility of altering the protein structure is reduced. In a protein-polymer conjugate, the polymer is expected to control the protein delivery kinetics and the exposure of biological tissues to the therapeutic protein. The physicochemical properties of the polymer then become critical and need to be engineered to control the protein delivery. In addition to controlled delivery formulations [1], the thermoreversible polymers have found applications for delivery of anti-thrombogenic agents on blood-contacting surface [2], and for cell transplantation [3].

Polymers of N-isopropylacrylamide (NiPAM) have been the most commonly studied thermoreversible polymer. A NiPAM homopolymer exhibits a lower critical solution temperature (LCST: temperature for soluble \leftrightarrow insoluble transition) of 30-32 °C in water [4]. LCST is believed to represent the temperature at which hydrophobic force (due to interaction of $-N-(CH_3)_2$ groups) causing insolubility in an aqueous environment is balanced by H-bonding between water and $-HN-$ groups that retains a polymer in solution. The hydrated polymer collapses to a globular state above LCST to form micellar structures. The LCST of NiPAM homopolymer can be effectively controlled by incorporating charged units, such as methacrylic acid, as well as hydrophobic units, such as butyl methacrylate [5-7]. Charged residues typically increase the LCST whereas hydrophobic residues lower the LCST. N-acryloxysuccinimide (NASI) was incorporated into NiPAM polymers to allow conjugation with amine groups [8,9], a side group common in proteins. The reaction of polymerized NASI with an amine is expected to proceed with a mechanism similar to reaction of succinimide esters of small molecules. The latter is well studied [10] and involves a nucleophilic attack at the carbonyl group adjacent to succinimide ring. The large size of (expected to cause steric resistance for conjugation), NiPAM/NASI copolymers did not hamper efficient protein conjugation [8]. The LCST of the polymer-protein conjugates was shown not to be different from the LCST of the polymer [8]. Despite some efforts to incorporate butyl methacrylates into NiPAM/NASI [3], no significant effort has been spent for engineering NiPAM/NASI polymers for controlled delivery applications.

The LCST of a polymer is particularly expected to play an important role for *in vivo* delivery of proteins. The LCST defines the upper limit to which conjugation reactions can be carried out in solution. The LCST is expected to influence the resiliency of a polymeric gel formed at the physiological temperature of 37 °C. In this paper, we have prepared polymers from NiPAM, NASI and alkyl methacrylates (AMAs), methyl methacrylate (MMA) and ethyl methacrylate (EMA). Our first aim was to study the dependence of LCST on the polymer composition. Our second aim was to investigate the hydrogel formation by the prepared polymers. Since the polymers are expected to be insoluble and possibly gel *in vivo*, the feasibility of hydrogel formation and the stability of the formed hydrogels have direct influence the drug delivery characteristics.

Experimental

Materials

NiPAM, MMA, EMA, acryloyl chloride, N-hydroxysuccinimide (NHS), benzoyl peroxide (BPO), 1,4-dioxane, diethyl ether and tetrahydrofuran (THF) were purchased

from Aldrich (Milwaukee, WI). Hexanes (85% n-hexane) was from Fisher (Fair Lawn, NJ). NASI was prepared in this lab by reacting acryloyl chloride with NHS, as described in [9]. The inhibitors in MMA and EMA were removed by distillation under a high vacuum before polymerization.

Polymer Synthesis

The preparation of NiPAM, NiPAM/NASI, NiPAM/NASI/MMA, and NiPAM/NASI/EMA polymers was adopted from a reported procedure [5]. All glassware used in polymerization were thoroughly washed and baked at 95 °C before assembly. As an example, 95/5 NiPAM/NASI polymer was prepared by dissolving 5.0g of NiPAM and 0.459g of NASI in 25 mL of dioxane, followed by the addition of 0.023g of BPO. The solution was purged with nitrogen for 30 minutes while stirring with a magnetic stirrer. After incubating at 70 °C for 22 hours, the polymer was precipitated by hexane and purified by dissolving the precipitate in THF and precipitating the solution by diethyl ether. The polymers were dried at 50 °C under the vacuum for one week.

Polymer Compositions

The composition of the synthesized polymers was routinely determined by the proton Nuclear Magnetic Resonance (NMR) spectroscopy. The chemical shifts for NiPAM, MMA and NASI were at 3.9 ppm, 3.6 ppm and 2.8 ppm, respectively. The peak areas were normalized for the number of hydrogens present in each peak. Due to the overlap of chemical shifts for NiPAM and EMA, elemental analysis for nitrogen was used to determine the composition of NiPAM/NASI/EMA polymers (i.e., nitrogen content can be used to calculate NiPAM mole ratio once NASI mole ratio is determined). A spectroscopic method was additionally used to determine the NASI content of the polymers [11]. Briefly, a polymer sample was reacted with excess 0.1 M NH_4OH to release all NHS from the NASI units. The change in absorbance at 260 nm was determined (Cary 50; Varian Inc.) and used as a measure of NASI concentration. A calibration curve was based on the aminolysis of NASI monomer.

Determination of NASI Hydrolysis Rate

The pH-dependent hydrolysis rate, k_{hyd} , of NASI in polymers was obtained by spectroscopy. The pH of the hydrolysis medium was controlled by using 0.1 M concentration of phosphate buffer (pH = 7.4 and 8.3), carbonate buffer (pH = 9.1 and 10.1) and citric acid buffer (pH = 3.2, 4.6 and 6.4). To calculate k_{hyd} , the kinetics of absorbance change at 260 nm was monitored and the data was analyzed by a pseudo-first order equation. In experiments where the extent of hydrolysis was measured in phosphate buffer, a 10 mg/mL polymer solution in dioxane was diluted 10-fold with either 0.1 M phosphate buffer (pH = 7.4) or 0.1 M NH_4OH . The relative absorbance at 260 nm (i.e., Abs. in phosphate buffer divided by Abs. in NH_4OH) was as a measure of hydrolysis.

Differential Scanning Calorimetry (DSC) and Spectroscopy for LCST

Differential Scanning Calorimetry. The Seiko model DSC 210/SSC5000 instrument was used for the DSC. The heating rate was 1 °C/minute, and polymer concentration was 3% w/v in 0.1 M phosphate buffer (pH = 7.4). 50 µL of polymer solution was sealed in DSC pans and heated from 0 to 50 °C. The thermograms were exported into SIGMAPLOT for analysis.

Spectroscopy. The polymers were dissolved at 10 mg/mL in 0.1 M phosphate buffer (pH = 7.4). 1 mL of polymer solution was added into a cuvette which was placed in a spectrophotometer (Ultraspect 2000; Pharmacia) equipped with a water-circulation cell. The water temperature was adjusted between 10 and 30 °C (in 0.5 °C increments every 10 minute) using a refrigerated/heated water circulator and the optical density (O.D.) was determined at 420 nm. Actual temperature of the samples was routinely measured using a digital thermometer. The data was fitted to a sigmoidal curve and the LCST was taken as the midpoint of the inflection point.

Water Uptake Ratio and Direct Observation of Hydrogel Formation

To determine the water uptake of polymeric gels, polymer films were cast from THF solution in PTFE dishes and dried under vacuum at 50 °C for 1 week. The films were carefully weighed and immersed into 0.1 M phosphate buffer (pH = 7.4). The samples in buffer were put into a temperature-controlled environment and the temperature was decreased from 35 °C by 1 °C every 24 hour. The experiment was terminated when polymer films were dissolved or disintegrated. To measure water uptake, the surface of polymer gels was carefully wiped with a soft paper towel to remove the free water and the weight of the gels was determined. The water uptake was calculated by: (wet weight/dry weight) x 100%. The observation of hydrogel formation was conducted under similar conditions except the temperature was increased from 10 to 37 °C (1 °C increase every 24 hour). The polymer solutions were prepared as 10 mg/mL in 0.1 M phosphate buffer (pH = 7.4). The solutions were photographed using an OLYMPUS D-600L Digital Camera every 24 hour.

Results and Discussion

NiPAM-based polymers have been prepared for protein conjugation in controlled drug delivery applications. Having an LCST lower than the physiological temperature of 37 °C, such polymers are expected to be insoluble and/or gel at an application site and localize the conjugated proteins. It is feasible to envision either an 'injectable' or 'implantable' mode of delivery for the prepared polymers. To design polymers with desired, predictable properties, we synthesized a variety of copolymers and terpolymers with different compositions. As expected, the composition of the prepared polymers was dependent on the monomer feed ratios during polymerization (**Figure 1**). With NiPAM/NASI polymers, the polymer NASI content was generally lower than the feed ratio. This observation was independent of the NASI assessment method (by NMR or aminolysis assay). The aminolysis assay

further confirmed the amine-reactivity of the prepared polymers. With NiPAM/NASI/AMA polymers, the polymer MMA content was similar to the feed ratio but the polymer EMA content was significantly higher than the feed ratio. The NASI content of NiPAM/NASI/AMA polymers was lower than the feed ratio (typical feed ratios of 2% gave a polymer NASI content of 0.9 - 1.5%). A detailed analysis of monomer reactivity ratios was not attempted because of relatively small sample size (see Ref. [6] for information on reactivity ratios).

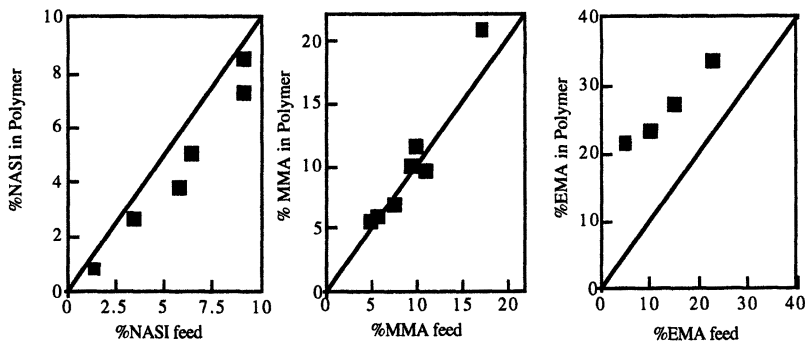


Figure 1. Composition of the synthesized NiPAM/NASI (left), NiPAM/NASI/MMA (center) and NiPAM/NASI/EMA (right) polymers. The straight line in each graph represents 1:1 ratio of monomer feed and final polymer composition. Note that the NASI feed ratio for the NiPAM/NASI/AMA polymers was maintained at ~2%.

Polymer Hydrolysis

The succinimide ester in NASI can undergo aminolysis with primary amines as well as hydrolysis in an aqueous environment. The aminolysis rate is dependent on the nature of the amine (pK_{as} , presence of steric groups, etc.) but is typically higher than the hydrolysis rate at a particular pH. Hydrolysis yields -COOH groups that can significantly influence the polymer properties due to electrostatic repulsion of ionized polymer. Because the NiPAM/NASI polymers will be utilized in an aqueous environment, the hydrolysis rate of the polymers was characterized (Figure 2). The fastest hydrolysis was seen at the highest pH of 10.1 for all samples and k_{hyd} decreased with a decrease in pH. This observation is comparable to the observations with succinimide esters of small molecules (e.g., biotin-N-hydroxysuccinimide [12]) and is indicative of the increased nucleophilicity of water at higher pHs [10]. As compared to NASI monomer, the hydrolysis of NASI in polymers was >100-fold slower (not shown). The k_{hyd} also appeared to be inversely related to NASI content of the polymer at pH=10.1. This is indicative of inter- and intra-molecular interactions among the NASI units in polymers and is consistent with relatively hydrophobic nature of this monomer (see below). The hydrolysis rate at pH = 7.4 (the pH where the remaining studies were carried out) was slow, and accounted for <5% hydrolysis of the total NASI groups after 4 hours (not shown).

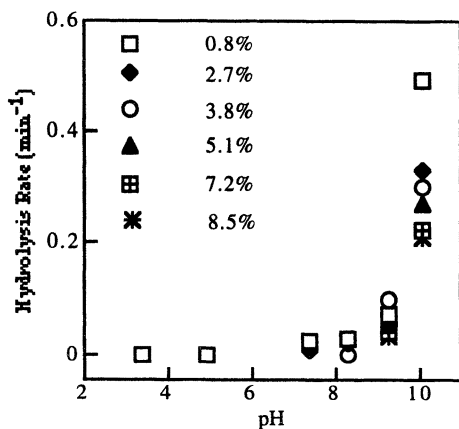


Figure 2. Hydrolysis of NiPAM/NASI polymers as a function of solution pH. The percentages correspond to the NASI mole ratio in polymers. Note that the hydrolysis rate for $\text{pH} < 7.4$ was relatively small, after which an exponential increase was noted. At the highest pH tested, %NASI content of the polymers was inversely related to the hydrolysis rate.

LCST of NiPAM/NASI Copolymers

Based on spectroscopy, an LCST of 26.7 °C was obtained for the NiPAM homopolymer (Figure 3). A small (1-2 °C) decrease in LCST was noted for the polymers with NASI content up to 3.8%, after which a significant decrease in LCST was observed. At higher NASI ratios, the transition from the soluble to insoluble state became more gradual (Figure 3). This is likely to reflect a heterogeneity in NASI composition of the polymers. There was a difference in the final O.D. obtained for the polymer samples; whereas NiPAM homopolymer had the highest O.D. above LCST (~3), the NASI-containing polymers had a lower O.D. (~2). This might be due to a gradual precipitation of NASI-containing polymers. When NiPAM/NASI copolymers were incubated in the phosphate buffer for a prolonged time (12 days), a significant increase in LCST was seen (Figure 3, insert). The change in LCST was dependent on the NASI content; whereas 7.2% NASI gave a ~14 °C increase in LCST, 3.8% NASI gave ~2 °C change. Figure 4 shows the DSC thermograms of the NiPAM/NASI polymers. A single endothermic peak indicative of a homogenous phase separation was obtained for the NiPAM homopolymer, unlike multi-step changes observed with crosslinked NiPAM networks [14]. With increasing NASI, the onset and the endothermic peak temperature showed a slowly decreasing trend. The maximum peak area appeared to get gradually broad and smaller, again indicating a more gradual phase transformation. Based on the comparison of O.D. and DSC measurements, the onset temperature of the endothermic peak, and not the peak temperature, appeared to correctly represent the LCST of the copolymers. This observation was unlike the previous observation [4,5] where the peak point of the endotherm was taken as the LCST. The transition enthalpy, ΔH , in DSC measurements also decreased at higher NASI content (not shown). Taken together, these results indicated that NASI primarily exerts a hydrophobic effect on the LCST of NiPAM polymer, but this effect was reversed by prolonged incubation and possible hydrolysis of the polymer in an aqueous environment.

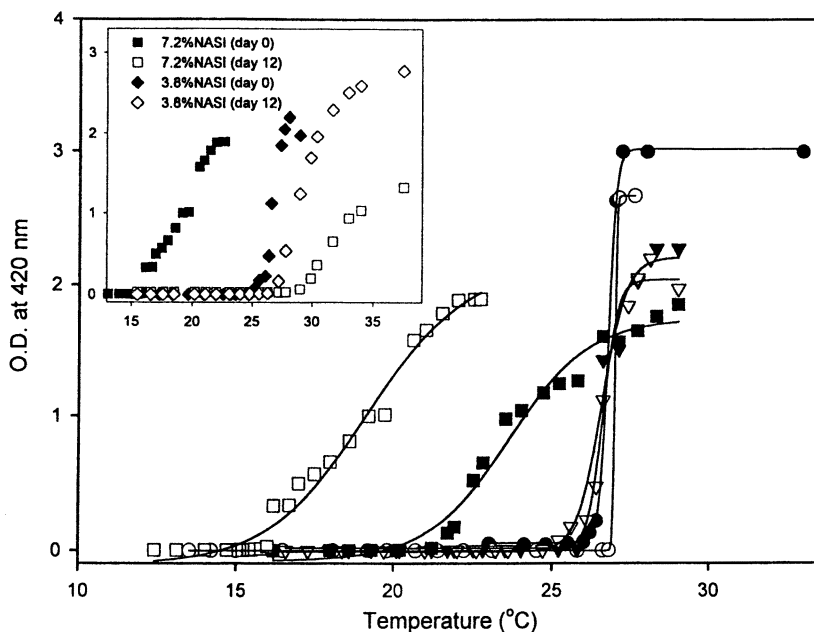


Figure 3. LCST of NiPAM/NASI copolymers. Open squares: 7.2% NASI, closed squares: 5.1% NASI, open triangles: 3.8% NASI, closed triangles: 2.7% NASI, open circles: 0.8% NASI, closed circles 0% NASI. The insert shows the changes in LCST after the chosen polymers were incubated for 12 days at 4 °C.

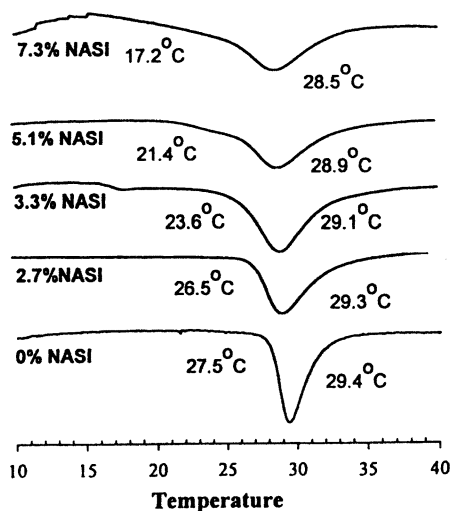


Figure 4. DSC thermograms for NiPAM/NASI polymers. The peak temperature and the onset temperature for the endothermic peak are indicated. Note that onset temperature is a more sensitive indicator of phase transition.

LCST of AMA-Containing Copolymers

Table 1 provides a summary of the LCST measurements for NiPAM/NASI/AMA polymers. The NASI content was kept constant at 1.0-1.3% so that the polymer LCST was not significantly affected (with or without hydrolysis). Incorporating MMA and EMA into the NiPAM/NASI copolymer reduced the LCST irrespective of the assessment method. The higher LCST temperature determined by the O.D. measurements was due to broad transition of the polymers with higher AMA content (similar to high NASI polymers in shown **Figure 3**). This result further confirms the feasibility of decreasing the LCST of NiPAM/NASI polymers in a controlled manner by incorporating hydrophobic monomer units into the polymer. As before, the onset temperature for endothermic peak was more sensitive to the AMA content of the polymers. Interestingly, the potency of hydrophobic EMA and MMA groups to lower LCST appeared to be similar. We anticipated EMA to be more effective in reducing the LCST because of an additional methylene in the alkyl chain. More studies are needed to determine whether a critical alkyl chain length exists after which the LCST becomes unproportionally lower.

Table 1. LCST of NiPAM/NASI/AMA terpolymers

%MMA	LCST by		LCST by DSC		%EMA	LCST by		LCST by DSC	
	Spectroscopy	Peak T.	Onset T.	Peak T.		Spectroscopy	Peak T.	Onset T.	Peak T.
5.6	24.8	28.8	24.5	21.5	24.6	27.7	22.0		
7.0	24.7	28.7	24.8	23.3	23.2	26.4	17.5		
9.7	23.4	28.0	24.2	27.2	21.5	24.3	15.4		
11.6	22.7	27.9	20.8						
20.9	19.9	27.2	17.2						

Hydrogels of NiPAM/NASI/AMA Polymers

It is clear that all of the polymers synthesized for this study was capable of displaying an LCST below the physiological temperature. This is a critical, but not the only requirement for the polymers to form a gel *in vivo*. It is also essential that the induced polymeric micelles exhibit sufficient self-association for gelation. Two approaches were taken to study hydrogel properties of the synthesized polymers. In the first approach (hydrogel dissolution study), a dry polymer film was prepared and the water uptake was determined as the temperature is lowered beyond the LCST. This approach aimed at determining the stability of gels as the driving force for dissolution becomes increasingly larger. In the second approach (hydrogel formation study), a polymer solution was prepared at a low temperature and the temperature was gradually increased above the LCST. This approach aimed at determining the polymer propensity to form a cohesive gel as the polymer loses water-solubility. It is important to note that time scale for these studies was significantly longer than LCST measurements (days vs. minutes).

The polymer films made up of NiPAM homopolymer exhibited a relatively small water uptake as the temperature was lowered to 30 °C, below which gels became highly swollen and dissolved within a 3 °C range (**Figure 5**). The dissolution temperature agreed with the LCST. The NiPAM/NASI films, on the other hand, dissolved immediately after being immersed in the buffer (solutions remaining cloudy)

and did not form gels irrespective of the NASI content (**not shown**). Presumably, small degree of NASI hydrolysis exerted sufficient repulsive forces for the dissolution of the film. Incorporating MMA to the NiPAM/NASI polymers (NASI mole ratio of 1.1-1.3%) enabled formation of stable gels under the experimental conditions (**Figure 5**). The higher the MMA content of the polymers, the lower the dissolution temperature was (i.e., more stable). It is interesting to note that MMA up to 11.6% was not able to offset the unstabilizing effect of NASI. By comparison, a NiPAM/MMA copolymer with 9.7% MMA but without NASI had a dissolution temperature 3-4 °C lower than a corresponding polymer (11.6% MMA) with 1% NASI. Only at a MMA mole ratio of 20.9% the polymer had a higher resiliency than the NiPAM homopolymer. The EMA also lowered the dissolution temperature and increased the maximum water uptake in a dose-dependent manner (**Figure 5**). The potency of EMA appeared to be the same as the MMA in stabilizing the hydrogel (compare polymers with MMA ratio of 20.9% and EMA ratio of 21.5%).

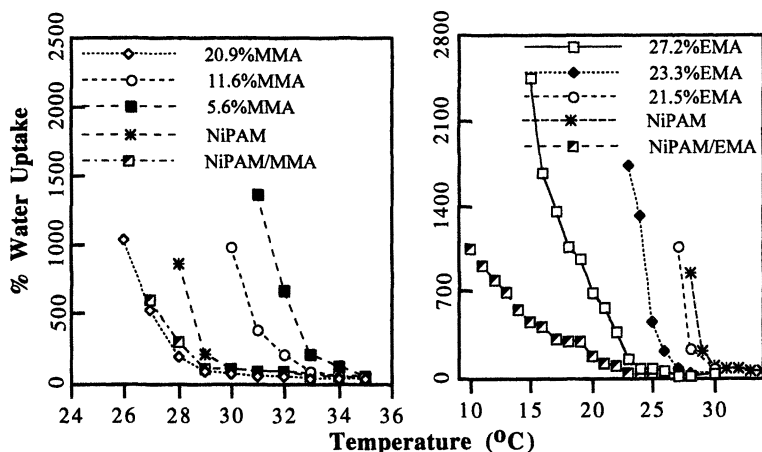


Figure 5. Water uptake by NiPAM/NASI/MMA (left) and NiPAM/NASI/EMA (right) polymer films as a function of temperature. The NiPAM/MMA and NiPAM/EMA had an AMA content of 9.7% and 26.3%, respectively.

We have additionally investigated the gelation of NiPAM/NASI/AMA polymers. The NiPAM homopolymer was observed to develop turbidity at 28 °C and to gel at 30 °C, but the gel readily separated from the solution phase and was typically a small fraction (<10%) of the solution volume. The NiPAM/NASI polymers (%NASI \leq 7.2) exhibited turbidity at the same temperature range, irrespective of NASI content, but did not gel at all. With NiPAM/NASI/AMA, turbidity was observed at 28-29 °C and 26-27 °C for MMA and EMA containing polymers, respectively. A small (<10% of volume) gel also formed within 2-3 °C of turbidity formation but no difference was observed among the polymers (irrespective of AMA unit or AMA mole ratio). The only notable difference was the NiPAM/EMA polymer that exhibited turbidity as early as 15 °C and gelled at 26 °C. The initial gel volume encompassed the total volume of the solution, but it gradually decreased as the temperature was increased to 37 °C. Taken together, the gelation experiments indicated that NASI-containing

polymers did not form a stable gel and that incorporation of chosen hydrophobic monomers did not facilitate gel formation.

Conclusions and Implications for Controlled Drug Delivery

The results presented here indicated that protein-conjugating polymers with tailored LCST can be synthesized using NiPAM, NASI and AMAs. Two common techniques, DSC and O.D. measurements, provided a similar measure of transition temperature, as long as the onset temperature of the endothermic peak, rather than the peak temperature, was employed in DSC. NASI, despite acting as a hydrophobic unit, was found to have an unstabilizing effect on gelation in an aqueous environment. As little as 1% NASI was sufficient for such an effect which was presumably due to the formation of -COOH groups. As much as 20% AMA was needed to offset the undesirable effect of NASI. The NASI in polymers is expected to be conjugated to therapeutic proteins and this might not change the LCST of the conjugates [8]. However, it is unlikely that all of the NASI will be consumed during conjugation. Strategies will need to be developed to control the fate of unconsumed NASI to control the conjugate LCST, as well as to eliminate adverse effects on conjugate gelation *in vivo*. As expected, hydrogel gel stability was positively correlated with the AMA content of the polymer but we found a significant difference in the hydrogel properties whether the gels were subjected to a temperature decrease or temperature increase (stability of already formed gels vs. propensity for gelation). One needs to study the NiPAM/NASI/AMA polymers with a clear understanding of the application at hand. The choice of the experimental system should depend whether the polymers will be subjected to gelation before application (i.e., implantable delivery) or are expected to gel after delivery (i.e., injectable delivery).

References

1. Bromberg L.E.; Ron E.S. *Advanced Drug Delivery Reviews* **1998**, 31, 197.
2. Gutowska, A.; Bae Y.H.; Jacobs, H.; Mohammed, F.; Mix, D.; Feijen, J.; Kim, S.W. *Journal of Biomedical Materials Research* **1995**, 29, 811.
3. S. Shimizu; M. Yamazaki; S. Kubota; T. Ozasa; H. Moriya, K. Kobayashi; M. Mikami; Y. Mori; S Yamaguchi. *Artificial Organs* **1996**, 20, 1232.
4. H. G. Schild, in *Water-Soluble Polymers*, ACS Press **1991**, 16, 249.
5. Feil, H.; Bae, Y.H.; Feijen, J.; Kim, S.W. *Macromolecules* **1993**, 26, 2496.
6. Brazel, C.S.; Peppas, N.A. *Macromolecules* **1995**, 28, 8016.
7. Chung, J.E.; Yokoyama, M.; Aoyagi, T.; Sakurai, Y.; Okano, T. *Journal of Controlled Release* **1998**, 53, 119.
8. Chen, J.P.; Hoffman, A.S. *Biomaterials* **1990**, 11, 631.
9. Pollack, A.; Blumenfeld, H.; Wax, M.; Gaughn, R.L.; Whitesides, G.M. *Journal of American Chemical Society* **1980**, 102, 6342.
10. Cline, G.W.; Hanna, S.G. *Journal of Organic Chemistry* **1988**, 53, 3583.
11. Miron, T.; Wilchek, M. *Analytical Biochemistry* **1982**, 126, 13544.
12. Grumbach, I.M.; Veh, R.W. *Journal of Immunological Methods* **1991**, 140, 205.
13. Kim, J.-C.; Bae, S.K.; Kim, J.D. *Journal of Biochemistry* **1997**, 121, 15.

Chapter 26

A Novel Composite Membrane for Temperature- and pH-Responsive Permeation

F. Yam¹, X. Y. Wu¹, and Q. Zhang²

¹Faculty of Pharmacy, University of Toronto, Toronto M5S 2S2, Canada
²Institute of Biomedical Engineering, Chinese Academy of Medical Sciences and Peking Union Medical College, Tianjin, China

A stimuli-sensitive composite membrane was prepared from nanoparticles of poly(N-isopropylacrylamide-co-methacrylic acid) and a hydrophobic polymer. The effects of temperature, solute size, and pH on the solute permeation through the membrane were studied. The permeation rate increased with increasing temperature or decreasing pH. A greater increase was found for larger molecules like vitamin B₁₂ than smaller ones. Both membrane hydration and solute partition, decreasing with increasing temperature, could not explain the increased permeability. Thus a gel-pore mechanism of permeation was proposed that the solutes could diffuse through the membrane *via* two pathways, namely the gel phase of the nanoparticles and the water-filled pores, depending upon the molecular size. The nanoparticles acted as nanovalves controlling the pore size of the membrane by their volume change. The SEM photographs evidenced the porous structure of the membrane when the nanoparticles collapsed.

The application of "intelligent" polymers to stimuli-responsive drug delivery has gained increasing interest (1), which partly stems from the observation that several disease states manifest themselves by a change in the physiological parameters of the body (2-5). For instance, inflammation and infections result in an elevated temperature at the local site (2,3), and the intracellular pH is lower than the extracellular pH in tumors (4). In the case of diabetes mellitus, the dose of insulin required varies with the time of the day and the glucose level (5). In addition, external stimuli may be introduced in a clinical setting. For example, hyperthermia (6) is applied to the tumor site to sensitize the cancer cells, resulting in a higher killing rate. In the meantime, the heat can stimulate the release of therapeutic agents from a thermosensitive delivery system. Therefore, it is desirable to design drug delivery

systems that can release drugs in response to the disease state or environmental stimuli.

Polymers of N-isopropylacrylamide (NIPAm) have found applications in stimuli-responsive drug delivery (7-10) and biotechnology (11-14), mainly because of their sharp thermal response. The linear polymer of NIPAm displays a lower critical solution temperature (LCST) (15) and the cross-linked polymers experience a drastic change in swelling at the volume phase transition temperature (T_{tr}) (16-19). Copolymers of NIPAm may exhibit response to other stimuli as well, such as pH and ionic strength (16,17,20-23). However, the use of NIPAm-based polymers for practical drug delivery has been hindered by two barriers, namely negative thermosensitivity and weak mechanical strength. The former is represented by a decreased release rate at a higher temperature due to shrinking of the polymers, and the latter is a common drawback of hydrogels that can readily absorb water up to several times their own weight.

To attain positive thermosensitivity, i.e., an increased release rate at a higher temperature, and higher mechanical strength, membrane systems have been developed (24-28). These systems are mainly prepared by chemical reactions such as grafting or in situ free radical polymerization, where the reaction conditions are unfavorable to the stability of therapeutic agents, especially biological products like proteins and polypeptides. Besides, purification is required to remove unreacted chemicals and initiator residues. There is a membrane system that is devoid of chemical reaction (29). However, it gives a transition temperature outside the physiological range. In this study, a novel composite membrane system was developed to overcome the above mentioned problems based on thermo- and pH-responsive nanoparticles and a hydrophobic polymer.

Materials and Methods

Materials

N-isopropylacrylamide (NIPAm, Eastman Kodak) was purified by recrystallization from hexane and toluene. Methacrylic acid (MAA, Aldrich) was made inhibitor free by distillation. N,N'-methylenebisacrylamide (BIS, Aldrich), sodium dodecyl sulfate (SDS, Mallinckrodt) and potassium persulfate (KPS, Aldrich) were used as received. Theophylline, acetaminophen, vitamin B₁₂, and chymotrypsin were purchased from Sigma and used as model drugs.

Synthesis and Characterization of Poly(NIPAm/MAA) Nanoparticles

Poly(NIPAm/MAA) nanoparticles were prepared by an aqueous dispersion polymerization process (16,17,30). NIPAm, MAA, and BIS were mixed in a mole ratio 1:0.1:0.068 to a total concentration of 135 mM. SDS was added to a concentration of 0.4 mM. After the mixture was heated to 70°C and purged with

nitrogen gas, the polymerization was initiated by the addition of a KPS solution to a concentration of 2.1 mM. The reaction was carried out at 70°C under a nitrogen blanket for 4 hours with constant stirring at 200 rpm.

The nanoparticles were purified by membrane dialysis against DDI water using Spectra/Por® dialysis tubing (Fisher Scientific) with a molecular weight cutoff of 12,000 to 14,000. The hydrodynamic size of the particles in various aqueous media was determined with a dynamic light scattering particle sizer (NICOMP Model 370) at temperatures from 15 to 60 °C.

Preparation and Characterization of Membranes

The membranes were prepared from a polymer solution or suspension. In a typical preparation, 0.31 g of dried nanoparticles were mixed with 24 g of absolute alcohol containing 0.69 g of ethylcellulose (viscosity 100, Dow Chemical Company). The mixture was stirred for 2-3 days and then poured into a glass ring to form a composite membrane. Control membranes were fabricated using the same method in the absence of the nanoparticles.

The contact angle of water on the membranes was measured using a goniometer (Model 100-00 Rame-Hart Inc.). The temperature in the sample chamber was controlled with a water bath (Haake D8). Small membrane samples were mounted in the chamber and equilibrated at a temperature of interest for 5 minutes prior to the measurements.

To determine the hydration degree of the membranes, the samples were equilibrated in dilute salt or buffer solutions for over 2 days at different temperatures. The samples were weighed after having been patted briefly with a tissue. The measurements were repeated ten times using different samples and the swelling ratio of the membrane was calculated as the weight ratio of the swollen membrane to the dry membrane. The thickness of the membranes was measured with a micrometer.

The swollen membrane samples were then freeze-dried, fractured, and mounted vertically on sample holders with a double-sided tape. The cross-sectional morphology of the samples was examined using a scanning electron microscope (Hitachi S-520).

Partition and Permeation Studies

The membrane samples were immersed in drug solutions of different concentrations for over 2 days. The drug concentration before and after immersion was measured by a diode array UV-Vis spectrophotometer (HP 8452A). The partition coefficient, i.e., the ratio of drug concentration within the membrane to that in the external medium, was computed from mass balance.

The amount of solute permeated through the membrane was measured using side-by-side diffusion cells with a jacket connected with a water bath (Haake D8). The initial drug concentration in the donor compartment was at least 100-fold greater than that in the receptor compartment. The solution was transported by a peristaltic pump to a flow cell and assayed by UV-Vis spectrophotometry. The permeability, defined

here as the product of diffusion (D) and partition coefficients (K) divided by the thickness of the membrane (h), was calculated according to Fick's first law of diffusion (31).

Results and Discussion

Volume Phase Transition of Poly(NIPAm/MAA) Nanoparticles

Figure 1 depicts that the diameter of the nanoparticles decreases with increasing temperature with a phase transition at $\sim 37^\circ\text{C}$ in distilled deionized (DDI) water and at $\sim 24^\circ\text{C}$ in pH 4 buffer. The reduction in diameter is up to 2.4-fold, corresponding to about 14-fold reduction in the volume. Such dramatic change in volume results from the hydrophobic interaction among the isopropyl groups in the NIPAm units, which is favored as the hydrogen bonding of structured water molecules is weakened at $T > T_{tr}$ (16-19). The downward shift in T_{tr} at a lower pH is due to a lower degree of ionization of the carboxyl groups in the MAA units, which increases the hydrophobicity of the polymer chains (16,17).

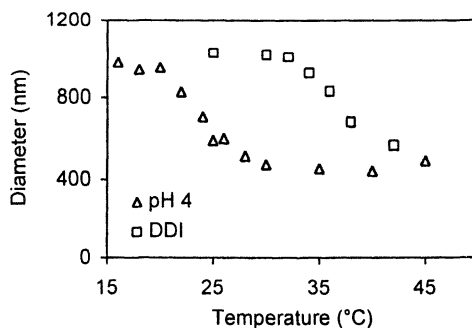


Figure 1. Diameters of the nanoparticles vs. temperature in DDI water and 0.05 M pH 4 buffer.

Properties of the Membrane

The contact angle of water on the surface of both composite and control (i.e., without the nanoparticles) membranes was in the range of $60\text{--}70^\circ$, implying a good biocompatibility of the membranes. Figure 2 shows that the increase in the relative contact angle, $CA_T/CA_{20^\circ\text{C}}$, is more profound for the composite membrane than the control one. This observation may be ascribed to the exposure of the nanoparticles to the surface. The particles become more hydrophobic at a higher temperature, leading to a greater increase in the surface hydrophobicity of the membrane. Although the

exposure of the nanoparticles is reflected by the surface property, no leakage of the nanoparticles was detected from the membranes used in this study. This is perhaps because the exterior surface of the membrane has denser structure than the interior, which is normally observed in polymeric membranes.

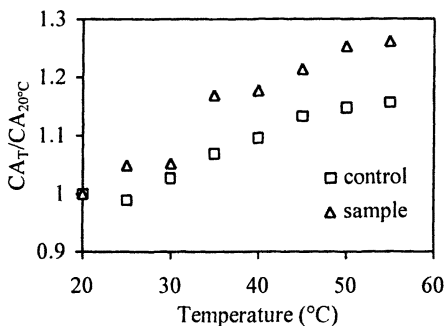


Figure 2. Relative contact angle of water vs. temperature for the membranes.

As illustrated by Figure 3, the swelling ratio of the composite membrane decreases with increasing temperature continuously with a transition at around 35°C, close to the T_r of the nanoparticles. The change in the swelling ratio at the transition is less than 10 wt%, while the variation in the membrane thickness is negligible. Compared with the particles that can swell up to 8-14 times their volume at $T < T_r$, this change is very small. Such insignificant change in swelling ratio can be attributed to small portion (~31 wt%) and entrapment of the particles, as well as the retention of the water in the membrane at $T > T_r$.

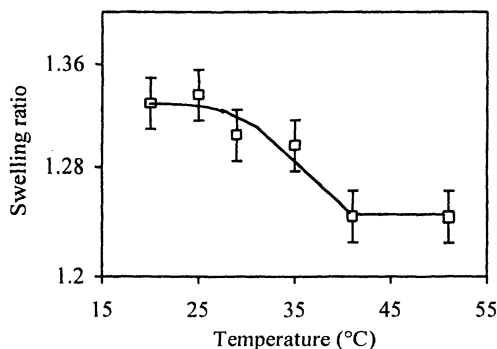


Figure 3. Swelling ratio of the composite membrane in 0.1 mM KCl vs. temperature. The variation in the membrane thickness with temperature is negligible.

The cross-sectional morphology of the composite and control membrane was revealed by the SEM photographs. Figures 4 reveals a porous structure in the

composite membrane (left) and a much denser structure in the control membrane (right). This may explain why the control membrane is even impermeable to small molecules such as acetaminophen and theophylline. In the composite membrane, the nanoparticles are either distributed within the pores or wrapped by the polymer matrix. Given that the nanoparticles swell at $T < T_{tr}$, the pores depicted in Figure 4 are likely occupied originally by the particles at the swollen state. In fact, visible traces of spheres at the edge of the pores suggest the initial position of the particles.

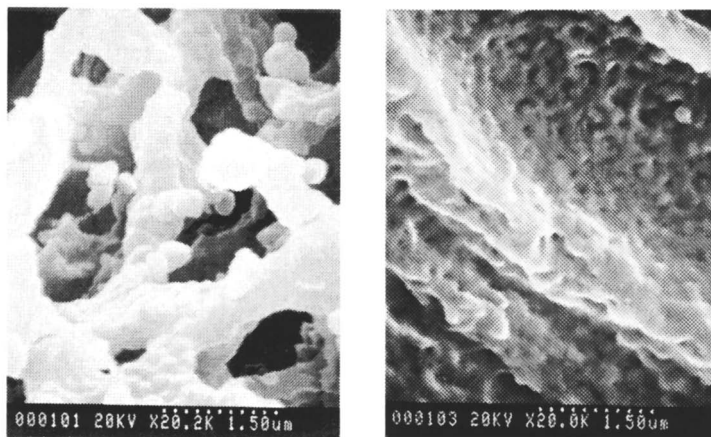


Figure 4. SEM photographs showing the cross-sectional morphology of the composite (left) and the control (right) membranes.

Permeation of Solutes

Effect of Temperature and Solute Size

Figure 5 shows that in 0.1 mM KCl solution, the permeability of acetaminophen through the composite membrane increases continuously with increasing temperature, with a transition at a temperature between 30 °C and 35 °C. A similar trend was also observed for acetaminophen and theophylline in DDI water. The transition coincides closely with the T_{tr} of the nanoparticles in DDI water. However, the permeability change with temperature is in the opposite direction to the change in the particle size and the membrane hydration.

Compared to acetaminophen and theophylline, the temperature dependence of permeability of vitamin B₁₂ (VB₁₂) is more significant. It was undetectable for two days in DDI water at room temperature, while increased to 1.6×10^{-6} cm/s at 45 °C. In a CaCl₂ (Figure 6) or KCl solution (Table I), the permeability of VB₁₂ was as follows: in 0.1 mM KCl, $2.94 \pm 0.03 \times 10^{-7}$ cm/s at 20 °C and $3.24 \pm 0.04 \times 10^{-6}$ cm/s at 45 °C; and in 0.1 mM CaCl₂, $3.63 \pm 0.01 \times 10^{-7}$ cm/s at 20 °C and $4.11 \pm 0.04 \times 10^{-6}$ cm/s at 45 °C. This result suggests that the effect of temperature on the permeability depends on the size of the solute.

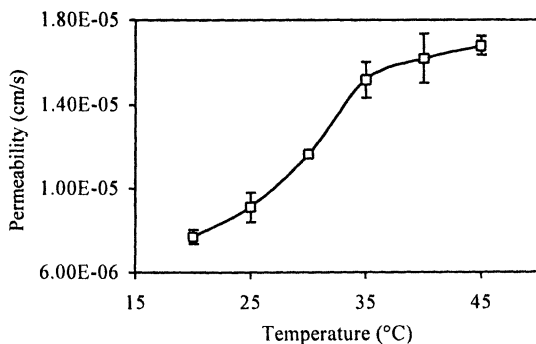


Figure 5. The permeability of acetaminophen vs. temperature in 0.1 mM KCl.

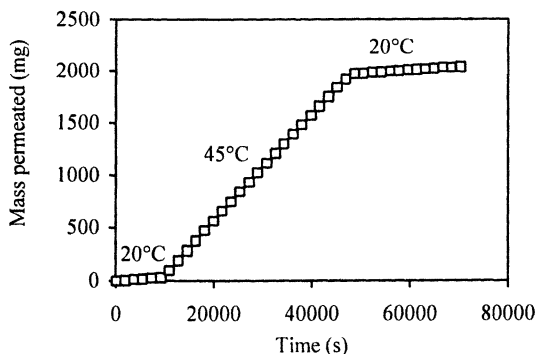


Figure 6. Permeation profile of vitamin B₁₂ across the composite membrane in a CaCl₂ solution ($\mu = 0.1$ mM) at 20°C and 45°C.

Table I. Permeability in 0.1 mM KCl and Molecular Size of the Solutes

Solutes	Molecular weight	R_h (Å)	Permeability at 45°C (cm/s)	$P_{45^\circ\text{C}}/P_{20^\circ\text{C}}$
Acetaminophen	151.16	2.4	1.68×10^{-5}	2.20
Theophylline	180.17	3.0	8.25×10^{-6}	2.88
Vitamin B ₁₂	1355.42	8.5	3.24×10^{-6}	11.0
Chymotrypsin	~20,000	~18	Undetectable	N/A

As shown in Table I, the permeability decreases with increasing molecular weight or decreasing hydrodynamic radius (R_h) of the molecules. As the molecular weight increases from 151 for acetaminophen to ~20,000 for chymotrypsin, the permeability

at 45 °C decreases from 1.68×10^{-5} to an undetectable level. The enhanced permeation of solutes of low molecular weights at 45 °C is relatively small, e.g., $P_{45^\circ\text{C}}/P_{20^\circ\text{C}} = 2.2$ for acetaminophen and 2.9 for theophylline. However, it becomes much greater as the molecular weight of the solute increases, e.g., $P_{45^\circ\text{C}}/P_{20^\circ\text{C}} = 11$ for VB₁₂. This result may be explained by the gel-pore mechanism presented later, which takes into account size exclusion and heterogeneity of the membrane.

Effect of pH

The permeability of theophylline in 0.05 M phosphate buffer solutions at 20°C and 45°C increased slightly in the range of pH 5 to pH 6, and then dropped at pH 7.4. The permeability ratio at two temperatures, $P_{45^\circ\text{C}}/P_{20^\circ\text{C}}$, increased with decreasing pH, suggesting that a reduction in pH enhances the thermoresponsive permeation. The effect of pH on the permeability of VB₁₂ is more remarkable and in a different pattern. As shown in Figure 7, the permeability of VB₁₂ at 45°C increases monotonously from pH 7.4 to pH 4. Such pH-dependent permeability may be attributed to the pH-dependent swelling of the nanoparticles, and the balance of solute permeation *via* two different pathways, namely gel phase of the nanoparticles and water-filled pores, as described in the next section.

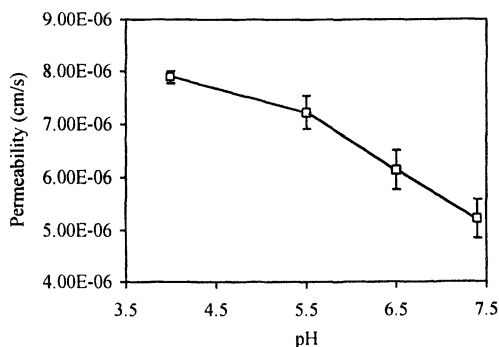


Figure 7. Permeability of vitamin B₁₂ vs. pH of the solution at 45°C. The pH of the solution was adjusted by titrating 0.1 M NaCl with 0.1 N NaOH and 0.1 N HCl.

Proposed Model of Permeation

As above presented, the solute permeation through the composite membrane increases with increasing temperature or decreasing pH, while the swelling of the membrane decreases with temperature. This observation violates the prediction by Yasuda's free volume theory (32), i.e., a smaller diffusion coefficient in a hydrogel with a lower swelling ratio. Unless the partition coefficient increases, offsetting the reduction in the diffusion coefficient, the permeability should decrease as the temperature is increased. However, like the swelling ratio, the partition coefficient

was also smaller at 45 °C (data not shown). Therefore, we have proposed the following gel-pore permeation mechanism for the composite membrane system.

The nanoparticles act as nanovalves that control the pore size by their volume change. At $T < T_{tr}$, or a higher pH, the swollen particles occupy the space and the pore size is minimal. Hence, the solutes mainly diffuse through the gel phase of the swollen nanoparticles. As the particles collapse at $T > T_{tr}$, or at a lower pH, the pores are opened up for solute to pass through, whereas the gel phase becomes more compact and thus less permeable to solutes (33). When the gain in the permeation rate in the pores exceeds the loss in the gel phase, the overall permeability exhibits a positive response. The extent of net increase in the permeability depends upon the solute size that determines its predominant pathway. For small solutes like acetaminophen and theophylline which can pass through both the pores and the gel phase, the increase in the pore volume compensates the reduced diffusion coefficient in the gel phase only with a small surplus, e.g. 2-3 fold. For large solutes like VB₁₂ which can only pass through the water-filled pores, generation of such pores exerts a great impact on the permeability. Macromolecules like chymotrypsin can neither pass through the gel phase nor the pores of the membrane because of size exclusion.

Conclusion

A novel composite membrane system was developed with temperature- and pH-responsive nanoparticles embedded in a polymeric matrix. The permeability of solutes through the membrane increased with increasing temperature with a transition similar to the T_{tr} of the nanoparticles, which was enhanced by a decrease in pH. The magnitude of stimuli-responsive permeation was affected by the solute size that determined the pathway of permeation. A gel-pore permeation mechanism was proposed involving pore formation by the volume change of the nanoparticles. The scanning electron micrographs provided structural evidence for the possibility of this mechanism.

Acknowledgement

The authors sincerely thank the financial support from the NSERC, Faculty of Pharmacy, University of Toronto; Fellowship to F. Yam from Parke-Davis and Merck Frosst; and the Visiting Scientist Award to Q. Zhang from the MRC (Canada)-NNSFC (China) Exchange Program.

References

1. Hoffman, A.S. In *Controlled Drug Delivery Challenges and Strategies*; Park, K., Ed.; American Chemical Society: Washington, DC, 1997; pp 485-498.
2. *Robbins Pathologic Basis of Disease*, 5th ed.; Robbins, S.L.; Kumar, V.; Cotran, R.S., Eds.; W.B. Saunders Company: Philadelphia, PA, 1994; pp 51-92.

3. Sherwood, L.; *Human Physiology From Cells to Systems*, 3rd ed.; Wadsworth Publishing Company: Belmont, CA, 1997; pp 121, 165.
4. Martin, G.R.; Jain, R.K. *Cancer Res.* **1994**, *54*, 5670-74.
5. Carlisle, B.A.; Koda-Kimble, M.A. In *Applied Therapeutics: the Clinical Use of Drugs*, 6th ed.; Young, L.Y.; Koda-Kimble M.A., Eds.; Applied Therapeutic Inc.: Vancouver, WA, 1995; Ch. 48.
6. Field, S.B.; Hand J.W. In: *An Introduction to the Practical Aspects of Clinical Hyperthermia*; Field, S.B.; Hand, J.W., Eds.; Taylor and Francis: London, 1990; pp 1-9.
7. Okano, T.; Bae, Y.H.; Kim, S.W. In *Pulsed and Self-Regulated Drug Delivery*; Kost, J., Ed.; CRC Press: Boca Raton, FL, 1990; pp 17-46.
8. Bae, Y.H.; Okano, T.; Kim, S.W. *J. Contr. Rel.* **1989**, *9*, 271-279.
9. Okano, T.; Bae, Y.H.; Jacobs, H., et al. *J. Contr. Rel.* **1990**, *11*, 255-65.
10. Dong, L.C.; Hoffman, A.S. *J. Contr. Rel.* **1990**, *13*, 21-31.
11. Stayton, P.S.; Shimoboji, T.; Long, C., et al. *Nature (London)* **1995**, *378*, 472-474.
12. Chilkoti, A.; Chen, G.; Stayton, P.S., et al. *Bioconjugate Chem.* **1994**, *5*, 504-507.
13. Okano, T.; Yamada, N.; Sakai, H., et al. *J. Biomed. Mater. Res.* **1993**, *27*, 1243-51.
14. Dong, L.C.; Hoffman, A.S. *J. Contr. Rel.* **1986**, *4*, 223-227.
15. Heskins, M.; Guillet, J.E. *J. Macromol. Sci. Chem.* **1968**, *2*, 1441-1455.
16. Wu, X.Y.; Lee, P.I. *Pharm. Res.* **1993**, *10*, 1544-47.
17. Huang, J.; Wu, X.Y. *J. Polym. Sci. Part A Polym. Chem.* **1999**, in press.
18. Tanaka, T. *Sci. Am.* **1981**, *244*, 124-138.
19. Dusek, K. Ed., *Responsive Gels: Volume Transition I & II*, Springer-Verlag, NY, 1993.
20. Chen, G.; Hoffman, A.S. *Nature (London)* **1995**, *373*, 49-52.
21. Velada, J.L.; Liu, Y.; Huglin, M.B. *Macromol. Chem. Phys.* **1998**, *199*, 1127-34.
22. Serres, A; Baudys, M; Kim, S.W. *Pharm. Res.* **1996**, *13*, 196-201.
23. Gutowska, A; Bark, J.S.; Kwon, I.C. et al. *J. Contr. Rel.* **1997**, *48*, 141-48.
24. Iwata, H.; Oodate, M.; Uyama, Y., et al. *J. Membr. Sci.* **1991**, *55*, 119-130.
25. Lee, Y.M.; Shim, J.K. *Polymer* **1997**, *38*, 1227-32
26. Spohr, R.; Reber, N.; Wolf, A., et al.. *J. Contr. Rel.* **1998**, *50*, 1-11.
27. Chun, S.W.; Kim, J.D. *J. Contr. Rel.* **1996**, *38*, 39-47.
28. Park, Y.S.; Ito, Y.; Imanishi, Y. *Langmuir* **1998**, *14*, 910-914.
29. Lin, Y.Y.; Chen, K.S.; Lin, S.Y. *J. Contr. Rel.* **1996**, *41*, 163-170
30. Wu, X.Y.; Pelton, R.H.; Hamielec, A.E., et al. *Colloid. Polym. Sci.* **1994**, *272*, 467-477.
31. Crank, J.; Park, G.S. In *Diffusion In Polymers*; Crank, J.; Park, G.S., Eds.; London Academic Press: London, 1968; pp 1-39.
32. Yasuda, H.; Lamaze, C.E.; Ikenberry, L.D. *Macromol. Chem.* **1968**, *118*, 19-35.
33. Palasis, M.; Gehrke, S.H. *J. Contr. Rel.* **1992**, *18*, 1-12.

Chapter 27

Glucose Monitoring via Reverse Iontophoresis

Neil Ackerman, Bret Berner, Jim Biegajski, Qiang Chen, Hilary Chen,
Tom Conn, Hardip Dehal, Tim Dunn, Al Ewing, Steve Fermi,
Russell Ford, Priya Jagasia, Yalia Jayalakshmi, Priti Joshi,
Brian Kersten, Ronald Kurnik, Tim Lake, Matt Lesho, Jan-Ping Lin,
David Liu, Margarita Lopatin, Lexa Mack, Heather Messenger,
Sam Morley, Michelle Oliva, Norman Parris, Russell Potts¹, Jeff Pudlo,
Michael Reidy, Pravin Soni, Janet Tamada, Michael Tierney,
Christopher Uhegbu, Prema Vijayakumar, Charles Wei,
Steve Williams, Don Wilson, and Christine Wu

Cygnus, Inc., 400 Penobscot Drive, Redwood City, CA 94063

Background

Frequent glucose monitoring is essential for people with diabetes to manage their blood glucose levels effectively. Present procedures for obtaining such information, however, are invasive and painful. Development of a painless approach would represent a significant improvement in the quality of life for people with diabetes. In addition, results from the DCCT^[1], UKPDS^[2] and Kumamoto Trials^[3] showed that a tight-control regimen, which uses aggressive therapy with frequent glucose measurements to guide the administration of insulin and oral agents, leads to a substantial decrease in the long-term effects of diabetes. Nevertheless, even as many as seven measurements per day were not sufficient to prevent an increase in hypoglycemic events in those patients who followed this aggressive therapy^[1]. The GlucoWatch[®] biographer provides a means to obtain painless and non-invasive measurements for up to 12 hours using a single blood measurement for calibration. A monitoring system that provides automatic and frequent measurement of glucose could provide a warning of impending hypoglycemia, potentially making aggressive diabetes management safer.

Each of the current techniques for measuring blood glucose concentrations has drawbacks. The most generally accepted method relies on extraction of small

¹Corresponding author.

aliquots of blood, obtained via a fingerstick. It is painful and invasive however, often resulting in poor patient compliance to a glucose-monitoring program. The measurement frequency of a typical user is not sufficient to achieve tight control. Implantation of biosensors or microdialysis tubing to sample from the subcutaneous tissue or peritoneal cavity is capable of providing frequent measurements ^[4,5]. However, poor biocompatibility, due to protein deposition, for example, limits the life of these devices, and the invasiveness of the method prevents wide acceptance. Near infrared spectroscopy, a non-invasive technique for blood glucose measurement ^[6,y], is not commercially established and requires large, expensive equipment. As such, there is no commercial device that allows non-invasive, frequent measurement of blood glucose.

Iontophoretic Glucose Extraction

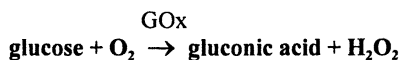
The non-invasive method described here extracts glucose through the skin using an applied potential (a process known as reverse iontophoresis), and measures the extracted sample using an electrochemical/enzymatic sensor. Iontophoresis is a technique whereby a constant, low-level electrical current ($0.3\text{mA}/\text{cm}^2$ in these studies) is conducted through the skin between an anode and cathode. Due to the applied potential, sodium and chloride ions (from beneath the skin) migrate towards the cathode and anode, respectively ^[8,9]. Uncharged molecules (e.g., glucose) are also carried along with the ions by convective (electroosmotic) transport. It is this convective flow that causes interstitial glucose to be transported across the skin ^[10]. The skin has a negative charge at neutral pH, and hence, there is greater net transport to the cathode. As a consequence, glucose is preferentially extracted at the cathode. Over the typical range of iontophoretic current densities ($0\text{--}0.5\text{ mA}/\text{cm}^2$), glucose extraction is linear with current density and duration of iontophoretic current ^[8,9].

The feasibility of iontophoretic glucose extraction has been demonstrated both *in vitro* ^[10] and in human subjects ^[11]. In the studies with human subjects, glucose extraction was measured by HPLC analysis. Changes in blood glucose levels correlated with glucose extracted into a buffer receiver solution over a 15 minute period of iontophoretic current application (current density of $0.3\text{ mA}/\text{cm}^2$). Calibration of the system was performed to account for possible biological variability in skin permeability. A single point calibration was found to compensate for this variability. The calibration was performed by taking a reading using a traditional blood glucose measurement method, and using this reading to calibrate all subsequent extraction readings. It was found that glucose transport correlates well with blood glucose in a linear fashion, however the sensitivity (i.e. the amount of glucose extracted compared to the blood glucose) varied among individuals and skin sites. The results of this feasibility study showed a mean correlation coefficient of 0.92, and a mean absolute relative error of 13% for the comparison of extracted to blood glucose values. The extraction process, however, yields a glucose concentration which is about 0.1% of that found in blood. Therefore, in contrast to the sensitivity

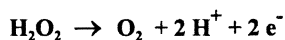
for glucose detection required for conventional fingerstick measurements, increased sensitivity is required to measure iontophoretically-extracted glucose.

Glucose Detection of the Iontophoretic Extraction

In the GlucoWatch® biographer the concentration of extracted glucose is measured by a biosensor. An amperometric, electrochemical-sensing chemistry was chosen as the most suitable for this application. The biological selectivity element in this biosensor is the enzyme glucose oxidase (GOx), which catalyzes the oxidation of glucose to gluconic acid. This enzyme is extremely selective towards glucose. To obtain a signal from this enzyme reaction, it must be coupled to the sensing electrodes. This is achieved by the direct detection of glucose oxidase-generated, hydrogen peroxide (H₂O₂).



The H₂O₂ is detected via an electrocatalytic oxidation reaction at a Pt-containing working electrode in the sensor, producing an electric current, and regenerating O₂.



Thus, for every glucose molecule extracted, two electrons are transferred to the measurement circuit. The magnitude of the resulting electric current is correlated to the amount of glucose collected through the skin.

The main challenge in developing the biosensor for measuring iontophoretically-extracted glucose is the small amount of glucose transported through the skin, and the resulting low concentration that must be accurately quantified. For example, at blood glucose level of 50 mg/dL, approximately 50 picomoles of glucose are extracted through the skin during three minutes of iontophoresis, resulting in a concentration at the biosensor of about 4 μM. This concentration is almost three orders of magnitude lower than the blood glucose concentration measured by typical fingerstick blood glucose monitors. The biosensor that has been developed for the GlucoWatch biographer has high sensitivity and low noise, resulting in an extremely low limit of detection for glucose. The operating principles of the electrochemical/enzymatic sensor are described in detail elsewhere^[12].

Operation of the GlucoWatch Biographer

A miniaturized device for the combined extraction and detection of glucose (the GlucoWatch biographer) is shown schematically in Figure 1. The extraction and detection is achieved using two hydrogel pads placed against the skin. The side of each pad away from the skin is in contact with separate iontophoretic and sensing electrodes. Two such electrode assemblies are required to complete the iontophoretic

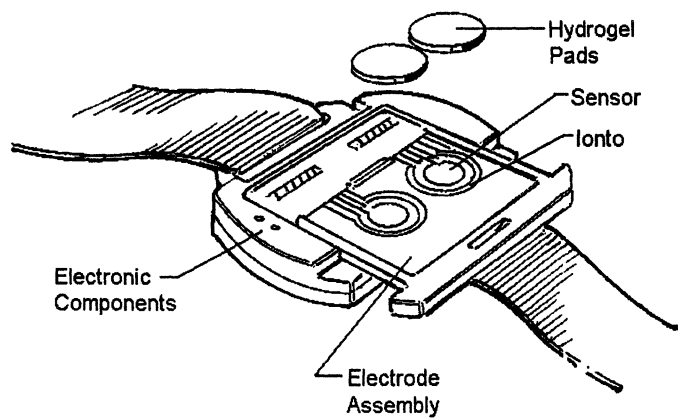


Figure 1. A schematic diagram of the GlucoWatch® biographer.

circuit. During operation, one iontophoretic electrode is cathodic (negatively charged) and the other anodic (positively charged), enabling the passage of current through the skin. As a consequence, glucose is collected in the hydrogel during the iontophoretic extraction period. The iontophoretic time interval is adjusted to minimize skin irritation and power requirements, yet extract sufficient glucose for subsequent detection. It has been found that an optimal time for extraction of glucose is about three minutes, under the conditions described here.

The hydrogel is composed of an aqueous salt solution in a crosslinked polymer containing the enzyme, glucose oxidase. As described above, this enzyme catalyzes the conversion of the glucose (in the presence of oxygen) to hydrogen peroxide and gluconic acid. The peroxide is subsequently detected at an electrochemical sensor.

Glucose exists in two forms: α -glucose and β -glucose, which differ only in the position of the hydroxyl group at the C-1 position in the six membered ring^[13,14]. These two forms (called anomers) are in a proportion of 37% and 63% for α and β forms at equilibrium, respectively. The same proportion of α - and β -glucose is also found in blood and interstitial fluid. As glucose enters the hydrogel, it diffuses throughout, but only the β -form of glucose reacts with the GOx enzyme. As the β -form is depleted, the α -form then converts (mutarotates) to the β -form to re-establish the equilibrium. The products of the GOx reaction (H_2O_2 and gluconic acid) also diffuse throughout the hydrogel.

On the side of the hydrogel away from the skin, and adjacent to the annular iontophoretic electrode, is the sensing electrode (see Figure 1). A sensing electrode is found at both the iontophoretic anode and cathode. Thus, there are two sensing electrodes, noted as sensor A and B. These circular sensing electrodes are composed of a platinum composite, and are activated by applying a potential of 0.3-0.8 V (relative to a Ag/AgCl reference electrode). At these applied potentials, a current is then generated from the reaction of H_2O_2 (generated from extracted glucose) which has diffused to the platinum sensor electrode. The measured current is proportional to the amount of H_2O_2 , and hence, extracted glucose.

The current (mA) utilized in iontophoresis potentially interferes with detection of the low current (nA) generated at each electrochemical sensor. Consequently, the iontophoretic and sensing electrodes are not activated at the same time. Instead, a typical situation is to have the iontophoresis proceed for about three minutes to collect an adequate amount of glucose. During this period about 10ng of glucose is typically extracted at the cathode. Iontophoresis is then stopped and the sensing electrodes are activated for typically seven minutes. This period of seven minutes is chosen so that all of the glucose (both α and β) has been converted to H_2O_2 , and that all of the hydrogen peroxide has diffused to the platinum electrode, and subsequently oxidized, to generate a current. Thus, all extracted glucose and H_2O_2 are consumed during this cycle. The integrated current (or charge) over this seven minute interval is then proportional to the total amount of glucose that entered the hydrogel during the iontophoresis interval. The iontophoresis polarity is reversed and cycle is then repeated^[15]. Thus, if sensor A is at the cathode during the first cycle, sensor B is the cathode during the second cycle. The combined cycle requires 20 minutes, and the

combined cathode sensor charge ($A + B$) is a measure of the glucose extracted. This 20-minute cycle is repeated throughout operation of the Glucowatch biographer.

An example of the sensor current vs. elapsed time during operation is shown in Figure 2. These results show that during iontophoresis the sensor current is zero. When the sensor circuits are then activated, H_2O_2 (converted from glucose) reacts with the platinum electrode to produce a current, which monotonically declines over the seven-minute detection cycle. During the initial period of sensor operation ($t < 90$ seconds), the current declines as $t^{-1/2}$, as predicted for diffusion to a planar electrode from a semi-infinite reservoir^[12]. Note that current is generated at both electrodes, even though glucose is primarily collected at the cathode. The anode signal is due to ascorbic and uric acids, which migrate solely to the anode. Ascorbate and urate are known to react directly with a platinum electrode and produce a signal that interferes with conventional blood glucose monitoring devices. During iontophoresis these anions collect only at the anode, while glucose is found primarily at the cathode. Hence, the unique ion selective nature of the GlucoWatch biographer prevents the interference of the electroactive species in the measurement of iontophoretically-extracted glucose.

Clinical Results

Biographers were applied to the lower forearm of human subjects with diabetes requiring insulin injection. Subjects included Type 1 and 2 diabetics using insulin. All subjects were 18 years of age, or older, and consisted of both males and females from a broad ethnic cross-section. As many as three GlucoWatch biographer measurements were obtained per hour. In addition, subjects obtained two capillary blood samples per hour, and the glucose concentration was determined using a Hemocue® Blood Analyzer (HemoCue Inc., Mission Viejo, CA). The blood glucose measurement obtained at three hours was used as a single point calibration. This calibration value was used to calculate the extracted blood glucose for all subsequent GlucoWatch biographer measurements. Measurements were continued for 12 hours, yielding a maximum of 23 paired measurements (not including the calibration point) comparing the GlucoWatch biographer and blood glucose values.

Results obtained with one subject are shown in Figure 3. These results show close tracking of GlucoWatch biographer and blood glucose values throughout the study. An analysis of the results for 46 watches, with 897 paired data point is shown in the Table. These results show that the GlucoWatch biographer yields a mean absolute error (MAE = absolute value of [Biographer glucose – Blood glucose]/Blood glucose) of 15.6%. In addition, the paired data yielded a correlation coefficient of 0.89. Finally, 96% of the data lie in the therapeutically relevant A+B region of the error grid analysis^[16]. The values obtained in this study are similar to those obtained for conventional blood glucose measuring devices^[17].

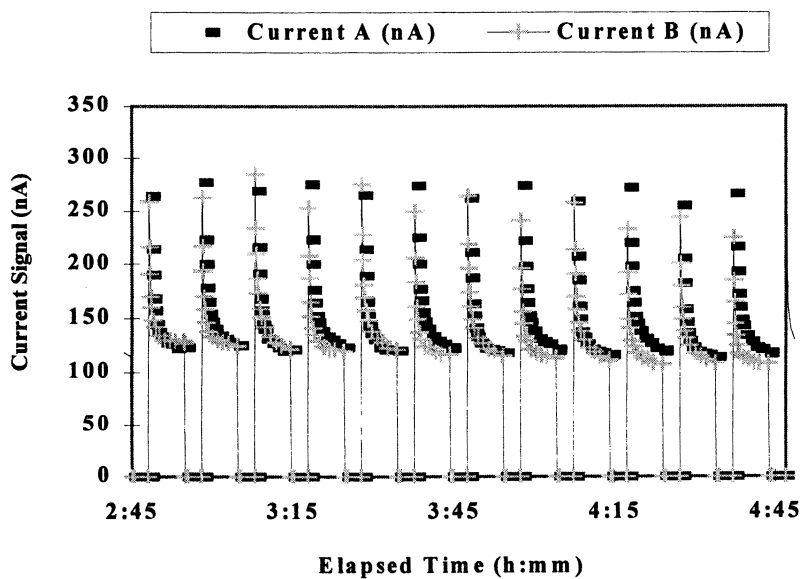


Figure 2. The current from both sensors (alternative cathode and anode) during two hours of operation on a human subject.

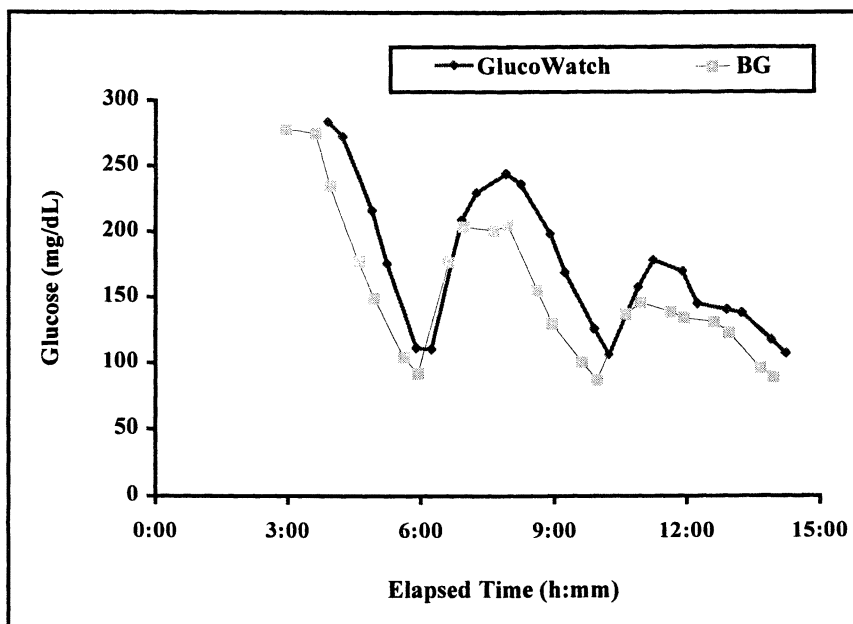


Figure 3. Glucose concentration vs. elapsed time for one subject as measured by the GlucoWatch biographer and the reference blood (BG) method.

Conclusion

In this study, the GlucoWatch biographer yields continuous measurements of glucose (3/hr) over a 12-hour period with accuracy and precision similar to existing, single-point blood measuring device. This non-invasive device holds promise to provide frequent glucose measurements to better guide insulin administration in diabetic subjects, and improved disease management.

Table. The Statistical Summary for GlucoWatch Biographer Results from 46 Subjects.

MAE (%)	Correlation Coefficient	Error Grid Analysis A + B region (%)
15.6	0.89	96

References

1. The Diabetes Control and Complication Trial Research Group *New England J. Medicine* **1993**, *329*, 977.
2. UK Prospective Diabetes Study (UKPDS) Group *Lancet* **1998**, *352*, 837-853.
3. Ohkubo, Y.; Kishikawa, H.; Araki, E.; Miyata, T.; Isami, S.; Motoyoshi, S.; Kojima, Y.; Furuyoshi, N.; Shichiri, M. *Diabetes Research & Clinical Practice* **1995**, *28*, 103-17.
4. Meyerhoff, C.; Bischof, F.; Sternberg, F.; Zier, E.; Pfeiffer, F. *Diabetologia* **1992**, *35*, 1087-1092.
5. Moatti-Sirat, D.; et al. *Diabetologia* **1992**, *35*, 224-230.
6. Arnold, M.A. *Current Opinions in Biotechnology* **1996**, *7*, 46-49.
7. Jagemann, K.; Fischbacher, C.; Danzer, K.; Muller, U. A.; Mertes, B. *Zietschrift fur Physicalische Chemie* **1995**, *191*, 179-190.
8. Pikal, M.J. *Adv. Drug Del. Rev.* **1992**, *9*, 201.
9. Dinh, S. M.; Luo, C.-W.; Berner, B. *AIChE Journal* **1993**, *39*, 2011.
10. Glikfeld, P.; Hinz, R. S.; Guy, R. H. *Pharm. Res.* **1989**, *6*, 988-990.

11. Tamada, J. A.; Bohannon, N. J. V.; Potts, R. O. *Nature Medicine* **1995**, *1*, 1198.
12. Kurnik, R.T.; Berner, B.; Tamada, J.A.; Potts, R.O. *J. Electrochem. Soc* **1998**, *145*, 4119.
13. Fessenden, R. J.; Fessenden, J. S. *Organic Chemistry*; Willard Grant Press: Boston, MA, 1979.
14. Morrison, R. T.; Boyd, R. N. *Organic Chemistry*; Allyn and Bacon, Boston, MA, 1973.
15. Kurnik, R. T.; Potts, R. O.; Tamada, J. A.; Tierney, M. J. *PCT WO97/24059*, Cygnus Inc., Redwood City, CA; *July 10, 1997*.
16. Clarke, W. L.; Cox, D. C.; Conder-Frederick, L. A.; Carter, W.; Pohl, S. L., *Diabetes Care* **1987**, *10*, 622.

Chapter 28

Self-Emulsifying Drug Delivery Formulations in the 21st Century: Challenges and Opportunities

Panayiotis P. Constantinides

SONUS Pharmaceuticals, 22026 20th Avenue SE, Bothell, WA 98021

In this chapter opportunities and challenges on the use of self-emulsifying drug delivery formulations for oral drug delivery and intestinal absorption enhancement are discussed. In the context of self-emulsifying formulations, the discussion includes both self-emulsifying drug delivery systems (SEDDS) and water-in-oil (W/O) microemulsions and case studies are presented where these systems have successfully been used to improve drug dissolution and oral absorption by overcoming solubility and membrane transport barriers. Drug development challenges such as excipient and vehicle selection, gelatin compatibility, physical and chemical stability, drug release, toxicity and safety, range of applicability and overall commercial viability are addressed. Future perspectives are discussed to further expand the application of these lipid drug carriers in oral drug delivery.

Lipid-based self-emulsifying formulations (Fig.1) have attracted much interest in recent years as novel oral dosage forms for improving drug solubilization and dissolution and/or intestinal absorption enhancement (1). Within the context of self-emulsifying formulations are self-emulsifying drug delivery systems (SEDDES) for lipophilic molecules and w/o microemulsions for water-soluble molecules. The latter systems contain mixtures of surfactants and oils with the aqueous phase being maintained to below 20% (w/w) in most practical applications (1). Use of oil-in-water (o/w) microemulsions is limited for oral administration since these systems, due to the presence of a large continuous aqueous phase, are not compatible with gelatin capsules. Thus, for convenience and better compliance, SEDDES which are isotropic mixtures of oils and surfactants with or without cosolvents (2-4) have largely replaced o/w emulsions for oral administration of water-insoluble drugs. In fact, administered in gelatin capsules these oily formulations will disperse in the GI tract to form a fine emulsion upon dilution with gastrointestinal fluids (3,4). The property of self-emulsification permits such formulations to be administered as “preconcentrates” and represent an efficient vehicle for the *in vivo* administration of emulsions. Under similar conditions, w/o microemulsions will invert to o/w emulsions/microemulsions (5). Unlike emulsions which are sensitive and metastable dispersed systems, SEDDES are physically stable solutions and fairly easy to manufacture.

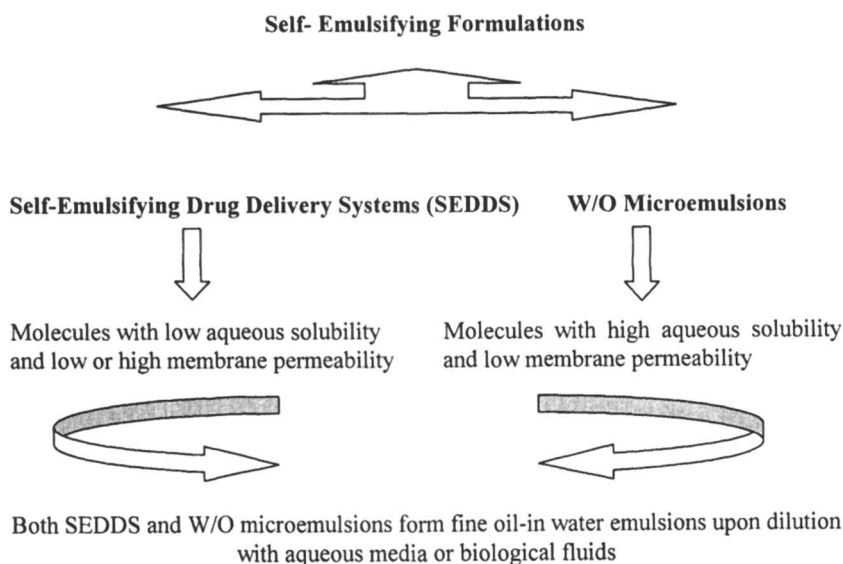


Figure 1. Self-Emulsifying formulations for oral drug delivery and absorption enhancement.

The design of effective self-emulsifying formulations of drugs, however, using well-defined and pharmaceutically acceptable excipients is still in its infancy with only few drug products on the market (6). Thus, the full drug delivery potential of self-emulsifying formulations has yet to be realized, particularly with water-soluble drugs/peptides. The purpose of this review article is to : a) present opportunities and case studies where self-emulsifying formulations can successfully be used to improve drug/solubilization and/or intestinal absorption of poorly absorbed drugs/peptides, and b) identify key drug development challenges and highlight of future research efforts to address these issues and rationally use this information to design orally active dosage forms.

Excipient and Vehicle Selection Considerations

Common excipients used to formulate self-emulsifying formulations are listed in Table I and include, glycerol and propylene glycol fatty acid esters, particularly C₈/C₁₀ mono-, di- and tri-esters, polyglycolized glycerides which are mixtures of glycerol and polyethylene glycol esters, polyoxyethylene fatty acid esters and castor oil derivatives, as well as phospholipids such as lecithin. Co-solvents such as ethanol, propylene glycol, and polyethylene glycol can also be used to aid drug solubilization (1). Criteria for their selection include, regulatory status, availability and cost, physical/chemical stability and compatibility with soft or hard gelatin capsules. Ternary phase diagrams of systems containing oil-surfactant(s)-water are used to identify SEDDS, o/w and w/o microemulsions (1,7). Physicochemical characterization include particle size, physical and chemical stability as well as *in vitro* drug release/dissolution studies (7). Vehicle selection for oral drug delivery is also based on drug solubility, membrane permeability and gelatin compatibility studies which are part of the preformulation work.

In reference to the gelatin compatibility studies, self-emulsifying formulation filled capsules are monitored for phase separation, precipitation, and whether the capsules become soft or brittle when stored under certain temperature and moisture conditions (8). The water moisture content and migration to/from the gelatin shell can be monitored by Karl-Fischer titration. Acid and peroxide value determination can be used to monitor hydrolytic and oxidative breakdown of the lipid components. Disintegration rates can be monitored using the USP physical test <701> for capsule disintegration (8). In one particular study (9) soft gelatin capsules when filled with microemulsion formulations with a hydrophilic phase range (w/w) of 10 to 40% and a lipophilic phase range of 90 to 60%, respectively, remained physically and chemically stable over temperatures between 2-8°C and 30°C/45%RH. At 40°C/75% RH, however, the capsules softened and acid and peroxide values increased (9). A glass transition of gelatin between 30°C and 40°C make extrapolations to shelf-life at room temperature difficult (8).

One can utilize the biopharmaceutics drug classification scheme based on drug solubility and membrane permeability (10) to properly select a suitable microemulsion system for drug solubilization and delivery. Thus, w/o microemulsions can be used with molecules having high aqueous solubility and low

Table I. Representative Excipients Commonly Used in Self-Emulsifying Drug Delivery Formulations

<i>Trade Name</i>	<i>Chemical Definition</i>	<i>HLB</i>
Arlacel 80	sorbitan oleate	4.4
Arlacel 186	monoolein: propylene glycol (90:10)	2.8
Capmul MCM	C ₈ /C ₁₀ mono-/diglycerides from coconut oil	5.5-6.0
Captex 200	C ₈ /C ₁₀ diesters of propylene glycol from coconut oil	oil
Centrophase 31	Liquid Lecithin	4.0
Cremophor EL	polyoxyethylene glycerol triricinoleate 35 DAC	13.5
Labrafil M 1944 CSD	primarily oleic acid (C _{18:1}) polyglycolysed glycerides from apricot kernel oil	3-4
Labrasol	C ₈ /C ₁₀ polyglycolyzed glycerides from coconut oil	14
Miglyol 812	C ₈ /C ₁₀ triglycerides from coconut oil	oil
Myvacet	distilled acetylated monoglycerides	oil
Poloxamer 407	polyoxyethylene-polyoxypropylene block copolymer (MW = 12,600)	18-23
Myverol 18-92	distilled sunflower oil monoglyceride (90% glyceryl linoleate)	3.7
Soybean Oil	primarily oleic (25%) and linoleic (54%) triglycerides	oil
Tagat TO	polyoxyethylene (25) glycerol trioleate	11.3
TPGS	d- α -tocopheryl-polyethylene glycol 1000-succinate	16-18
Tween 80	polyoxyethylene (20) sorbitan oleate	15

SOURCE: Adapted from Reference 6. Copyright 1995 Kluwer Academic/Plenum.

membrane permeability (Fig.1). Anticipated drug delivery benefits include, increased stabilization and protection against enzymatic hydrolysis as well as enhanced intestinal absorption (1).

Molecules with low aqueous solubility and low or high membrane permeability, can be formulated in SEDDS (Fig.1) to improve drug solubilization and dissolution with concomitant improvement in oral bioavailability (3,4). It has been shown that lipophilic drugs with high triglyceride solubility (≥ 100 mg/ml) and a high octanol:water partition coefficient ($\log P \geq 5$) are primarily absorbed through the lymphatic system (11,12) and are good candidates for formulation in SEDDS. Water-soluble molecules with high aqueous solubility (≥ 10 mg/ml) or a low octanol:buffer partition coefficient ($\log P < 1.0$) are suitable for formulation in w/o microemulsions (13). If necessary, the pH and/or the ionic strength of the aqueous phase can be properly adjusted to achieve the desired aqueous phase solubility. In reference to membrane permeability across intestinal tissues, molecules with low permeability can be defined as those having an ileal permeability value < 0.010 cm/h (13). Table II lists the preformulation studies that are necessary in order to properly select a suitable self-emulsifying vehicle for oral delivery. It should be emphasized, however, that in order to design efficient microemulsion systems to address specific drug delivery needs, computational modelling along with physicochemical studies are necessary to better understand and correlate drug structure with microemulsion composition and drug permeability.

Table II. Excipient and Vehicle Selection for Oral Drug Delivery based on Preformulation Data

<i>Physicochemical</i>	<i>Biopharmaceutical</i>
Drug solubility and stability (pH and temperature effects)	Membrane permeability across intestinal tissues
Octanol : water and oil:aqueous phase drug partitioning (pH and temperature effects)	Intestinal absorption from a solution
Gelatin compatibility (Excipients/Vehicle)	Enzymatic hydrolysis in the presence of intestinal enzymes
Plasma assay	Hepatic clearance and metabolism

General Formulation Development Challenges with Lipid-Based Vehicles

In regard to the lipid-based excipients which are natural polymers of varying degree of purity, it is necessary to set meaningful controls and specifications such as, batch-to-batch variability, purity, polymorphism, phase transitions and molecular

weight distribution. Typical specifications include: physical characteristics, such as appearance, odor and color, as well as chemical characteristics that include, viscosity, mass, density, refractive index, saponification, hydroxyl, iodine and acid values, water content and heavy metals.

Development and validation of suitable analytical and physicochemical methods to monitor drug stability, potency and release from self-emulsifying formulations, as well as, in process controls and finished product specifications need to be properly addressed. Analysis of lipid-drug formulations is not straightforward and the following methodology strategies can be considered (14) : i) direct analysis of intact lipid-drug particles, ii) dissolution of the particles followed by direct analysis which may involve temperature changes, addition of solvents, detergents, reducing or oxidising agents, or mechanical disruption, iii) dissolution of particles, separation of components, followed by individual analysis, and iv) use of lipid solvent extraction to separate components.

Development of dissolution methods for poorly soluble drugs in lipid-based vehicles that are presented as lipid-filled capsules is very challenging (15) since such matrices are not soluble in commonly used aqueous dissolution media. Although surfactants (16) or hydro-alcoholic media (17) have been used in some dissolution studies, it has been suggested that exposure of the gelatin shell to such media may induce physical and/or chemical changes resulting either from complex formation or crosslinking reactions. These interactions along with separation of poorly soluble drugs as metastable liquid crystals and dosage form and lipid floatation in the dissolution vessel will influence the solubility and disintegration time of the gelatin shell and/or true release kinetics of the drug. Due to the difficulties associated with the dissolution of lipid-based formulations, no official dissolution method has yet been established. Recently, however, a modified two-phase dissolution media system has been developed by considering the inherent immiscibility of aqueous phosphate buffer and 1-octanol and properly modulating dissolution hydrodynamics and the positioning of the formulation in the aqueous phase within the dissolution vessel (15). Using nifedipine as a model drug consistent and reproducible dissolution data was obtained with this modified two-phase dissolution media system (15). As new and reproducible dissolution methods for lipid-filled capsules emerge, it is likely that an official USP monograph will soon be established.

Additional points to consider when using lipid absorption enhancers in self-emulsifying formulations, particularly from a toxicological perspective, are (1,18): a) potential tissue irritation and/or damage, b) selectivity and reversibility of the action of the enhancer, c) effects of repeated administration, d) acute versus chronic toxicity, e) structural changes in the intestinal mucosa induced by the enhancer or its metabolite, and f) the overall safety of the enhancer. These effects may have serious toxicological implications which must be carefully evaluated with the necessary histological examination and the use of biochemical markers (1,18). A therapeutic window between the absorption enhancing and toxic dose need to be identified. A versatile absorption enhancer is perhaps the one combining a synthetic and a naturally occurring biopolymer that exhibits the ideal toxicological and bioavailability profile.

Oral Drug Delivery Opportunities with SEDDS

Data to date suggests that SEDDS when given orally can offer improvements in both the rate and extent of absorption of the encapsulated drug as well as consistency of the resulting plasma concentration profiles (3,4,6,19). It is believed that improvement in oral bioavailability is the result of eliminating poor dissolution as a barrier to drug absorption, and/or enhancing intestinal lymphatic drug transport (3,4,12). In addition, enhancement of drug absorption from SEDDS may be due to effects on membrane permeability, transit time or the metabolism of the drug (10,12). After oral administration and spontaneous self-emulsification in the GI tract, the components of the SEDDS will follow lipid metabolism pathways (1,12,20). Thus, enzymatic hydrolysis of the glycerides will generate fatty acids and monoglycerides. These lipids will then associate with bile salts to form mixed micelles incorporating the solubilized drug (20). Depending on the fatty acid composition of the excipient, the solubilized drug is ultimately systemically absorbed either via the portal vein or the lymphatic system (12).

The emphasis for oral drug delivery has centered around lipophilic peptide delivery, particularly of cyclosporine and protease inhibitors. A new cyclosporine formulation (Sandimmune Neoral®) has recently been developed and marketed by Novartis as an oral solution or a soft gelatin capsule. This new formulation is a microemulsion concentrate (SEDDS) and it contains Cyclosporin A, ethanol, corn oil mono-/di-/triglycerides, polyoxy (40) hydrogenated castor oil and propylene glycol. Upon dilution with aqueous media or biological fluids, Neoral® forms an o/w microemulsion (6,19, 21-23). In clinical studies, Neoral® has shown to produce reduced inter- and intra-subject variability in cyclosporine pharmacokinetics when compared to the original Sandimmune formulation (Table III, 6, 22).

Table III. Mean (CV%) Pharmacokinetic Parameters Following Twice-Daily Dosing with Sandimmune (SIM) or Sandimmune Neoral (SIMN) by Eleven Stable Renal Transplant Patients

<i>Parameter</i>	<i>SIM</i>	<i>SIM</i>	<i>SIMN</i>	<i>SIMN</i>
	<i>Fasting</i>	<i>Non-Fasting</i>	<i>Fasting</i>	<i>Non-fasting</i>
T_{max} (h)	2.1 (33.3)	2.6 (76.9)	1.5 (33.3)	1.2 (33.3)
C_{max} ($\mu\text{g/L}$)	663 (34.5)	528 (40.5)	997 (20.0)	892 (35.8)
C_{min} ($\mu\text{g/L}$)	78 (30.8)	92 (29.3)	94 (22.3)	100 (23.0)
AUC ($\mu\text{g}\cdot\text{h/L}$)	2645 (25.7)	2432 (24.3)	3454 (17.6)	3028 (19.7)
PTF %	261 (23.4)	212 (36.8)	317 (18.0)	309 (31.1)

All concentrations measured in whole blood at steady state; AUC was measured over a dosing interval; PTF = peak-trough fluctuation. SOURCE: Reproduced from Reference 6. Copyright 1995 Kluwer Academic/Plenum.

As can be seen from the data in Table III, Neoral® compared to the earlier formulation exhibits reduced t_{max} , increased C_{max} and AUC and thus improved oral

bioavailability with less variability with respect to consistency and extent of absorption. It is very likely, that the differences between these two formulations of cyclosporine and the improved pharmacokinetics of Neoral® are due to its ability to form a microemulsion in the GI tract (6, 21-23).

Drug Development Challenges with SEDDS

For SEDDS it has been shown that the oil/water partition coefficient of the drug and droplet size can modulate drug release (2,4). The higher the concentration of the emulsifier, the smaller the droplet size of the resulting emulsion and the faster the drug release (2,4). The absence of an aqueous phase in SEDDS as compared to o/w or w/o microemulsions can contribute to improved physical and chemical stability. Selecting, however, the most suitable system for a particular drug is challenging and requires a better understanding of their drug release and absorption characteristics.

Other product development issues with SEDDS in soft or hard gelatin capsules include: a) selection of vehicle where drug has maximum solubility, and b) hygroscopicity of the contents inducing dehydration of the gelatin shell or solute migration into the shell. Thus, there is a need to investigate solubility characteristics of the drug to be encapsulated particularly in relation to temperature and moisture effects in order to design fill liquid formulations which give optimum conditions for drug solubility, physical stability and enhanced bioavailability.

Oral Drug Delivery Opportunities with W/O Microemulsions

Water-in-oil microemulsions have been developed to overcome metabolic and physical barriers to water-soluble drug molecules, particularly peptides and proteins (1, 24-28). As illustrated in Table IV, several structurally unrelated water-soluble molecules showed enhanced absorption from w/o microemulsions incorporating medium-chain glycerol and/or propylene glycol fatty acid esters (Table I, 26).

At physiological pH, both calcein (6-carboxyfluorescein) and fluorescein isothiocyanate (FITC)-dextran are negatively charged whereas, the RGD peptide SK&F106760 and vancomycin are zwitterionic and positively charged, respectively. Calcein and the RGD peptide have very similar molecular weights of about 600, while vancomycin and FITC-dextran are larger molecules with molecular weights of about 1,500 and 4,500, respectively (Table IV). As can be seen from the data in Table IV significant intestinal absorption enhancement was observed with all investigated water-soluble molecules regardless of the size and/or charge of the molecule. Thus, w/o microemulsions enhance the duodenal absorption of polar molecules, up to about 5,000 molecular weight, in the dog (26).

In reference to the RGD peptide SK&F106760, enhanced bioavailability was also observed in the rat as shown in Fig. 2. Preformulation data with this peptide, both physicochemical and biopharmaceutical are listed in Table V (27).

Table IV. Molecules with Enhanced Intestinal Absorption from W/O Microemulsions Upon Intraduodenal Administration in Dogs

<i>Molecule</i>	<i>MW</i> (<i>charge, physiol. pH</i>)	<i>% Bioavailability</i> (<i>mean ± sem</i>)
Calcein	650 (negative)	6.3 ± 1.5 (solution) 29.3 ± 4.0 (ME)
RGD peptide	634 (zwitterion)	6.1 ± 1.1 (solution) 58.6 ± 13.6 (ME)
Vancomycin	1,450 (positive)	1.0 ± 0.5 (solution) 13.5 ± 2.9 (ME)
FITC-Dextran	4,400 (negative)	0.29 ± 0.04 (solution) 33.4 ± 4.0 (ME)

SOURCE : Reproduced from Reference 26 with permission from author.

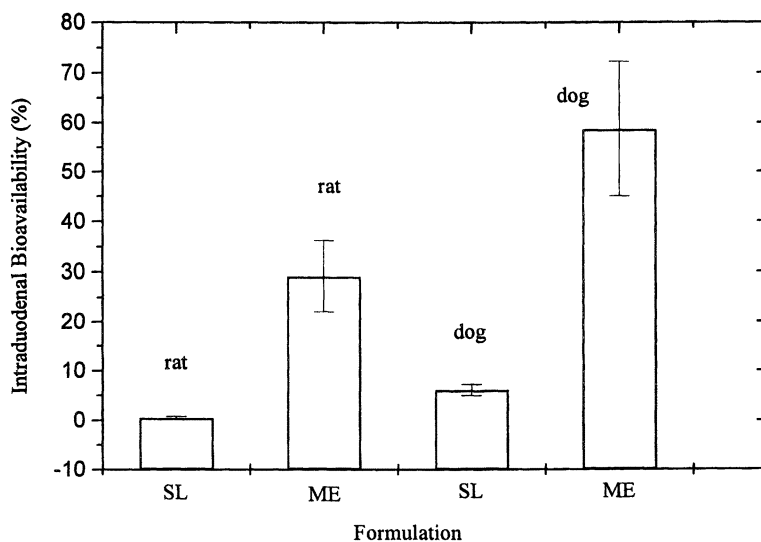


Figure 2. Intraduodenal bioavailabilities of the RGD Peptide SK&F 106760 in the rat and dog from a saline solution (SL) and w/o microemulsion (ME) formulations. The peptide dose (mg/kg) in the rat and dog were 10.0 (SL), 8.4 (ME) and 5.0 (SL), 3.0 (ME), respectively. The administered microemulsion volume was 3.3 and 0.250 ml/kg in the rat and dog, respectively. Bioavailability values represent mean ± sem (n=3, rat ; n=4, dog).

This peptide meets all criteria for encapsulation into a w/o microemulsion. Thus, as Table V indicates, SK&F106760 has high aqueous solubility, it partitions primarily into the aqueous phase, it has low membrane permeability and it is stable in intestinal fluids (27). Due to its poor membrane permeability the observed intraduodenal bioavailability from a saline solution is very low (Fig. 2 and Table V). Approximately a 60- and 10- fold bioavailability enhancement was observed in the rat and dog, respectively, from a w/o microemulsion incorporating medium-chain glycerides. The differences in the extent of absorption appear to be species specific, however, the relative levels of the excipients between the two w/o microemulsions were different. In addition, the observed differences may be due to the differences in the administered microemulsion volume which was 3.3 and 0.25 ml/kg, in the rat and dog, respectively.

Most of the work with w/o microemulsions has primarily been focused on preclinical research and although clinical development is being pursued at least with one peptide, 1-(3-mercaptopropionic acid)-8-D-arginine-vasopressin (dDAVP), MW = 1085, no clinical data has been published. Absorption studies of dDAVP in dogs (28) comparing enterically coated microemulsion capsules, non-coated microemulsion capsules and Minirin® dDAVP tablets (100 µg/capsule or tablet or ≈ 8.3 µg/kg), produced a pharmacologically significant Factor VIII response from the enterically coated capsules which was associated with increased plasma levels of dDAVP based on an immunoassay (28).

Drug Development Challenges with W/O Microemulsions

In addition to the general formulation development challenges with lipid-based vehicles discussed earlier, there are several development challenges that are specific to w/o microemulsions (1). These include, commercial viability, range of applicability, mechanism(s) of absorption enhancement, and toxicity/safety. For a commercially viable soft gelatin capsule formulation, the dose volume is restricted to about 0.5 ml/capsule or 0.010 ml/kg (for a 70 kg human). Most of the preclinical studies with w/o microemulsions, however, reported improved bioavailability at administered volumes that are at least an order of magnitude above the clinical dose thus making any comparisons with human dose difficult. It is not surprising that not all water-soluble drugs can be formulated in w/o microemulsions with a concomitant improvement of their intestinal absorption. For water-soluble drugs, in general, the higher the aqueous solubility or the water/oil partitioning, the higher the bioavailability (1). Therefore, water/oil partitioning studies using the corresponding microemulsion phases need to be conducted along with *in vitro* permeability studies and correlated to the observed oral bioavailability (1). The mechanisms by which w/o microemulsions enhance the oral bioavailability of water-soluble molecules are not well understood. The nature of the *in vivo* particle and site of drug release are largely unknown. Implication of lipid absorption pathways is not supported by known facts of lipid uptake into the intestinal mucosa. One of the proposed mechanisms is based on the lipid enhancer, such as medium-chain glycerides, inducing structural and

physical changes in the mucosal membrane thus resulting in significant permeability changes. This mechanism is supported by several *in vitro* studies showing that the permeability of paracellular markers is markedly affected by medium-chain glycerides. In regard to the development issues with absorption enhancers, these are discussed earlier along with other general formulation development challenges with lipid-based vehicles.

Table V. SK&F 106760 : Physicochemical and Biopharmaceutical Data

<i>Physicochemical</i>	<i>Biopharmaceutical</i>
Chemical Structure [cyclo(s,s)-(2-mercapto)benzoyl-N α -methyl-Arg-Gly-Asp-(2-mercapto)-phenylamide]	Membrane permeability : 0.002 cm/h in rabbit ileum (cutoff : 0.010 cm/h)
MW: 634 (acetate salt)	i.d bioavailability from saline solution : <1% (rat), \approx 6% (dog)
Charge: zwitterion (physiological pH)	enzymatic stability: stable in the presence of intestinal enzymes
Solubility (25 °C): 54 mg/ml in 0.010 M Tris pH 7.4 ; > 100 mg/ml in saline pH 6.0	plasma clearance in the rat (i.v. at 3.0 mg/kg) : 5.6 ± 1.7 ml/min/kg (hepatic blood flow in the rat: 69 ml/min x kg)
Oil/buffer partitioning (37 °C) : 13/87 (Capmul MCM: Ringer's buffer, 1:1)	Pharmacologic activity : Platelet aggregation inhibition
Plasma assay : HPLC fluorescence post-column derivatization	

Conclusions and Future Perspectives

Specific pharmacokinetic needs have been met with marketed drugs, such as cyclosporine Neoral® using SEDDS. These systems are likely to have increasing applications in the future as oral dosage forms of lipophilic drugs/peptides. Most of the work with w/o microemulsions has been focused on very productive preclinical research and early clinical development and their marketing potential has yet to be

proven. Development and validation of suitable analytical and physicochemical methods to monitor drug stability, potency and release from microemulsion formulations, as well as, in-process controls and finished product specifications need to be properly addressed. Further research and development is needed to establish a database on possible correlations between drug structure, microemulsion composition and intestinal permeability/absorption and to rationally use this information to design orally active dosage forms.

It is evident from the work reported to date that self-emulsifying formulations offer an attractive alternative for the oral administration of both lipid-soluble and water-soluble molecules. The aforementioned drug development challenges are more than compensated by the effectiveness of these lipid-based formulations in drug solubilization, improved physical and chemical stability and enhanced oral bioavailability. An opportunity area of increasing interest and future growth is the delivery and targeting of specific lipid excipients and/or other reported inhibitors of the intestinal P-glycoprotein using SEDDS in an effort to inhibit drug efflux and thus improve oral absorption (29). Many lipophilic drugs/peptides can benefit from this approach, including cancer chemotherapeutic agents (30), since P-glycoprotein is responsible for membrane transport and the development of multidrug resistance (MDR).

The growing interest in the commercial use of self-emulsifying formulations for the delivery of challenging molecules such as peptides/proteins and genes, is likely to stimulate further advancements in biomaterials and the development of synthetic or semi-synthetic and safer excipients and emulsifying agents. This will provide pharmaceutical formulators with a wider selection of excipients for oral dosage form development by overcoming current limitations of existing excipients in reference to drug solubility, physical/chemical stability and biocompatibility. A versatile emulsifying agent that exhibits the ideal toxicological and bioavailability profile will be a dream come through for pharmaceutical development.

References

1. Constantinides, P.P. *Pharm. Res.* **1995**, *12*, 1561.
2. Pouton, C.W. *Int. J. Pharm.* **1985**, *27*, 335.
3. Charman, S.A., Charman, W.N., Rogge, M.C., Wilson, T.D., Dutko, F.J., and Pouton, C.W. *Pharm. Res.* **1992**, *9*, 87.
4. Shah, N.H., Carvajal, M.T., Patel, C.I., Infeld, M.H. and Malick, A.W. *Int. J. Pharm.* **1994**, *106*, 15.
5. Constantinides, P.P. and Yiv, S.H. *Int. J. Pharm.* **1995**, *115*, 225.
6. Holt, D.W., Mueller, E.A., Kovarik, J.M., Van Bree, J.B. and Kutz, K. *Transplant. Proc.* **1994**, *26*, 2935.
7. Constantinides, P.P. and Scalart, J.P. *Int. J. Pharm.* **1997**, *158*, 57.
8. AAPS Symposium on *Hard and Soft Gelatin Capsules : Issues, Research and Outcome* 1997, Boston.

9. Sedlak, D., Szymkowiak, J., Saar, A., Owen, A.J., Brzezczko, A. and Bottom. C. A. *Proc. Int. Symp. Control. Rel. Bioactive Mater.* **1997**, 24, 271.
10. Amidon, G.L., Lennernas, H., Shah, V.P. and Crison, J.R. *Pharm. Res.* **1995**, 12, 413.
11. Charman, W.N., and Stella, V.J. *Int. J. Pharm.* **1986**, 34, 175.
12. Hauss, D. J., Fogal, S.E., Ficorilli, J.V., Price, C.A, Roy. T., Jayaraj, A.A. and Keirns, J.J. *J. Pharm. Sci.* **1998**, 87, 164.
13. Constantinides, P.P., Scalart, J.P., Lancaster, C.M., Marcello, J., Marks, G., Ellens, H. and Smith, P.L. *Pharm. Res.* **1994**, 11, 1385.
14. Weiner, A.L. *Encyclopedia of Pharmaceutical Technology*, **1991**, 8, 417.
15. Pillay, V. and Fassihi, R. *Pharm. Res.* **1999**, 16, 333.
16. Shen, P-C., Kim, S-I., Petillo, J.J. and Serajuddin, A.T.M. *J. Pharm. Sci.* **1991**, 80, 712.
17. Serajuddin, A.T.M., Sheen, P-C, Mufson, D., Bernstein, D.F. and Augustine, M.A. *J. Pharm. Sci.* **1988**, 77, 414.
18. Swenson, E.C. and Curatolo, W.J. *Adv. Drug Del. Rev.* **1992**, 8, 39.
19. Klyaschitsky, B.A. and Owen, A.J. *J. Drug Targeting* **1998**, 5, 443.
20. Smith, P.L., Wall, D.A and Wilson, G. In *Pharmaceutical Particulate Carriers: Therapeutic Applications*; Rolland, A., Ed. Marcel Dekker, New York, **1993**, pp. 109-166.
21. Mueller, E.A., Kovarik, J.M., van Bree, J.B., Terzloff, W., Grevel, J., and Kutz, K. *Pharm. Res.* **1994**, 11, 301.
22. Noble, S. and Markham, A. *Drugs* **1995**, 50, 924.
23. Neumayer, H.H., Budde, K., Faerber, L., Haller, P., Kohnen, R., Maibuecher, A., Schuster, A., Vollmar, J., Waiser, J., and Cuff, F.C. *Clin. Nephrol.* **1996**, 45, 326.
24. Lee, V.H.L., Yamamoto, A., and Kompella, U.B. *Crit. Rev. Ther. Drug Carrier Syst.* **1991**, 8, 91.
25. Sarciaux, J.M., Acar, L., and Sado, P.A. *Int. J. Pharm.* **1995**, 120, 127.
26. Owen, A., Nielsen, S., Matalonis, S., Sedlak, D. and Yiv, S. *AAPS Eastern Regional Meeting*, **1996**.
27. Constantinides, P.P., Lancaster, C.M., Marcello, J., Chiossone, D., Orner, D., Hidalgo, I., Smith, P.L., Sarkahian, A.B., Yiv, S.H. and Owen, A.J. *J. Control. Rel.* **1995**, 34, 109.
28. Nielsen, S., Yiv, S., Sturgis S., Unger, A., Tustian, A. and Owen, A. *Proc. Int. Symp. Control. Rel. Bioactive Mater.* **1994**, 21,
29. Wachter, V.J., Salphati, L., and Benet, L.Z. *Adv. Drug Deliv. Rev.* **1996**, 20, 99.
30. DeMario, M.D. and Ratain, M.J. *J. Clin. Oncol.* **1998**, 16, 2557.

Chapter 29

Polymeric Micelles for the Delivery of Poorly Soluble Drugs

Vladimir P. Torchilin and Volkmar Weissig

Department of Pharmaceutical Sciences, School of Pharmacy,
Bouve College of Health Sciences, Northeastern University, Boston, MA 02115

To improve the stability of pharmaceutical micelles and make them long-circulating, we have prepared new polymeric micelles from diacyllipid (phosphatidyl ethanol, PE) derivatives of polyethylene glycol (PEG-PE). PEG-PE micelles are extremely stable (very low CMC value) and can easily incorporate poorly soluble pharmaceuticals including both low-molecular-weight compounds and proteins, as well as diagnostic agents. Comparative studies on micellar and liposomal carriers demonstrated that, under certain circumstances, micelles proved to be superior carriers. Thus, the lipophilic cationic drug dequalinium cannot be loaded into liposomes, while it can be easily solubilized by PEG-PE micelles forming stable mixed micelles. The small size of micelles permits their easier penetration into tumors with small cutoff size. Protein-loaded micelles accumulate in subcutaneous Lewis lung carcinoma in mice better than larger protein-loaded liposomes.

The solubilization of drugs using micelle-forming surfactants may be advantageous for drug delivery purposes because of increased water solubility of sparingly soluble drug, enhanced permeability across the physiological barrier or substantial changes in drug biodistribution. Depending on the specific chemical design of the surfactant molecule and the administration route, the combination of the above factors may result in increased drug bioavailability and/or substantial reduction in toxicity and other adverse effects. The use of special amphiphilic molecules as surfactants can introduce the property of extended blood half-life of micelles upon intravenous administration. In addition, micelles may be made targeted by chemical attachment of a targeting moiety to their surface.

Low-molecular weight oligoethyleneglycol-based surfactants are widely used in pharmaceutical technology as solubilizers for poorly water-soluble or water-insoluble

drugs for parenteral and oral routes of drug delivery, for example, Polysorbate 80 (1,2). The main advantage of these surfactants for pharmacological applications is their reported low toxicity (3,4).

Micelles composed of low molecular weight surfactants are thermodynamically unstable in aqueous media and are subject to dissociation upon dilution. *In vivo*, this results in micelle collapse with subsequent precipitation of incorporated drug. The critical micelle concentrations of these surfactants are usually in the millimolar range. Hence, in terms of drug delivery carrier development, there is a need to find a new class of surfactant molecules able to form more stable micelles with lower CMC values. One of the possible candidates for this role, a class of amphiphilic polymers known to form polymeric micelles in aqueous solutions, have been proposed as drug carriers (5). The authors have suggested an approach in which a relatively hydrophobic drug is covalently attached to the polyaspartic acid polymeric block (polyAsp) of the PEG-(polyAsp) copolymer, thus resulting in an amphiphilic AB-type copolymer. This copolymer is able to form polymeric micelles with the hydrophobic block making up particle's core, while the PEG block forms a surrounding water-soluble shell. AB-type amphiphilic block-copolymers of PEG (molecular weight of 12 kDa) and poly(aspartyl adriamycin) with 20 aspartyl adriamycin units demonstrated blood half-life in mice > 5 hours, thus indicating a substantial increase in micelle stability (6). The hydrophilic PEG block of the micelle-forming copolymer may contribute to the preparation's decreased toxicity in a similar manner as for conventional Polysorbate surfactants. In addition, the presence of this polymer on the particle surface can contribute to its steric protection from interaction with some unwanted blood components and substantially prolong its circulation time.

An important advantage of polymeric micelles as drug carriers over other microparticulate carriers is their smaller size compared to liposomes and polymeric microspheres. This circumstance is important for selected drug administration routes (for example, percutaneous lymphatic delivery and extravasation into solid tumors). On the other hand, their surface properties still provide them with a prolonged half-life in the circulation and allow coupling of targeting moieties with the micelle surface.

Diacyllipid-PEG Conjugates as Micelle-Forming Polymeric Carriers for Therapeutic and Diagnostic Agents

The stability of micelles, in major part, depends on the strength of Van der Waals interactions between hydrophobic blocks forming the core of the particle and the molecular size of the hydrophilic block counterbalancing the non-water-soluble part of the macromolecule. Use of lipid moieties as hydrophobic blocks capping PEO chains can provide additional advantages for particle stability when compared with conventional amphiphilic polymer micelles since the existence of two fatty acid acyls might contribute considerably to the increase of the hydrophobic interactions between the polymeric chains in the micelle's core.

Diacyllipid-PEG conjugates have been introduced into the controlled drug delivery area as polymeric surface modifiers for steric protection of liposomes (7).

Interestingly, the diacyllipid-PEG molecule itself represents a characteristic amphiphilic polymer with a bulky hydrophilic (PEG) portion and a very short, but extremely hydrophobic, diacyllipid part. Typically for other PEG-containing amphiphilic block-copolymers, diacyllipid-PEG conjugates were found to form micelles in an aqueous environment (8). Proper size, surface coating and the ability to be loaded with sufficient quantities of drug or diagnostic agent makes PEG-lipid micelles a perfect choice for drug delivery. The supramolecular structure of PEG-diacyllipid micelles is similar to that of PEG-lipid-containing liposomes: both particulates possess a lipidic core surrounded by a hydrophilic PEG shell. As a consequence, one may expect similar *in vivo* properties, including half-life in the blood. Macrophage-evading properties might be an important issue not only for intravenous drug carriers, but also for other administration routes.

A series of PEG-phosphatidylethanolamine (PEG-PE) conjugates were synthesized using egg PE (transphosphatidylated) and N-hydroxysuccinimide esters of methoxy-PEG succinates (molecular weight of 2 kDa, 5 kDa and 12 kDa) (9). HPLC-based gel permeation chromatography showed these polymers forming micelles of different size in an aqueous environment (Figure 1A). The stability of the polymeric micelles was confirmed using the same method: no dissociation into individual polymeric chains was found upon the chromatography of serially diluted samples of PEG(5 kDa)-PE up to a polymer concentration of ca. 1 $\mu\text{l/ml}$, which corresponds to a nanomolar/micromolar CMC value (Figure 1B). PEG-PE micelles can efficiently incorporate some sparingly soluble and amphiphilic substances. For example, a spectral analysis of the micellar HPLC peak shows that polymeric micelles can incorporate the topoisomerase II inhibitor ellipticine, a substance with water solubility 1.5 $\mu\text{g/ml}$, at the drug:PEG-PE molar ratio = 1:25 (9). The most successful examples of hydrophobic substance incorporation into PEO-lipid micelles were different amphiphilic lipid derivatives. Thus, the fluorescent lipid probe rhodamine-PE incorporates into micelles up to a 2:1 drug:PEG-PE molar ratio (9). One can suggest that the most successful therapeutical applications of PEG-lipid polymeric micelles as drug carriers would require the use of the appropriate hydrophobized prodrugs.

During biodistribution experiments *in vivo*, ^{111}In -labeled PEG-PE micelles demonstrated half-life times up to 2.5 h in mice (9). This value is long enough comparing with the majority of non-surface-modified particulates, but somewhat shorter than for PEG-containing liposomes. Several circumstances might explain this difference: first, particles might extravasate from the vasculature due to their considerably smaller size compared with liposomes (see the last Section). Another possibility is an exchange of the amphiphilic label with the plasma proteins possessing affinity to lipidic moieties (such as albumin).

In experiments on lymphatic imaging (10), we have incorporated amphiphilic chelating probes $\text{Gd}^{(111)\text{In}}$ -DTPA-PE and ^{111}In -DTPA-SA into PEG(5 kDa)-PE micelles (20 nm in diameter) and successfully used these particulate agents in experimental percutaneous lymphography, using γ -scintigraphy and MR imaging in rabbits. The popliteal lymph node can be visualized within seconds after injection.

It may be possible to improve the efficacy of micelles as contrast medium by increasing the quantity of carrier-associated reporter metal (such as Gd or ^{111}In), and thus enhancing the signal intensity. We have tried to solve this task by using so called

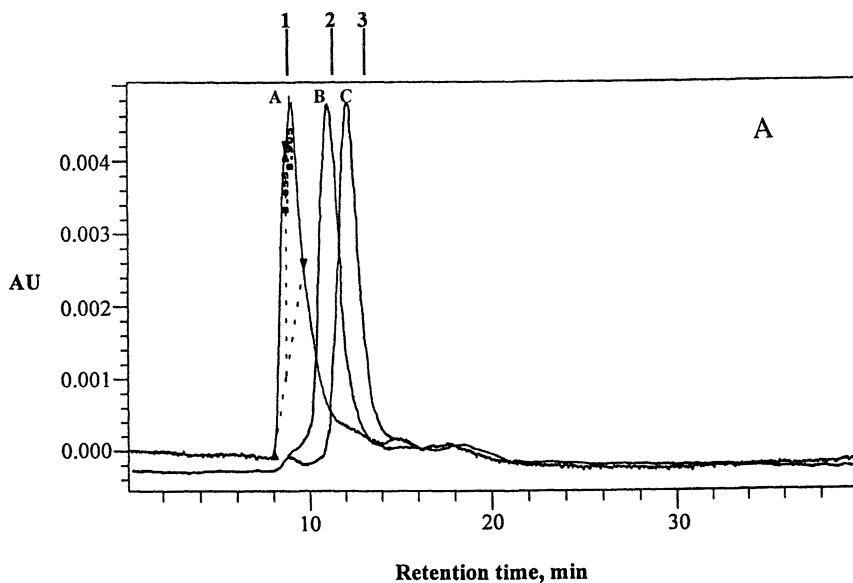
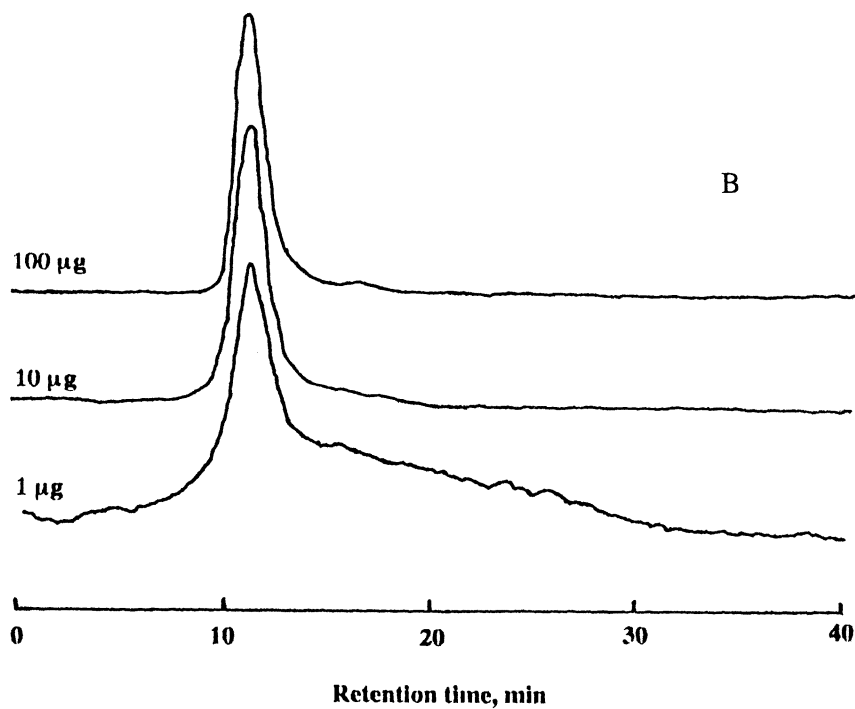


Figure 1. A - HPLC-based gel permeation chromatography of micellar forms of PEG-PE conjugates with different molecular weights of PEG blocks. A - 12 kDa; B - 5 kDa; C - 2 kDa. Retention times of molecular weight standards: 1 - Blue Dextran (2,000 kDa); 2 - thyroglobulin (669 kDa); 3 - amylase (200 kDa). Column: Shodex Protein KW-804; solvent PBS, pH 8.0; detection - 215 nm. B - HPLC-based gel permeation chromatography of serial dilutions of PEG(5 kDa)-PE micelles. Total amount of the polymer injected is indicated. Sample volume - 100 μ l; other conditions - as in B. (Reproduced from reference 9.)

Figure 1. *Continued.*

amphiphilic chelating polymers (11). To increase the loading of micelles and liposomes with reporter metals, we have suggested and experimentally designed a new family of soluble single-terminus modified polymers containing multiple chelating groups and suitable for incorporation into liposomes and micelles. The approach is based on the use of CBZ-protected polylysine (PL) with free terminal amino-group, which is derivatized into a reactive form with subsequent deprotection and incorporation of DTPA residues, and was initially suggested by us for heavy metal load on proteins and antibodies (12). Using the polylysine N-terminus modification chemistry, we developed a pathway for the synthesis of amphiphilic polychelator N, α -(DTPA-polylysyl)glutaryl phosphatidyl ethanolamine (DTPA-PL-NGPE). This polychelator easily incorporates into the micelle core (Figure 2) in the process of carrier preparation, and sharply increases the number of chelated Gd or other heavy metal atoms attached to a single lipid anchor.

Diagnostic Iodine-Containing Micelles for Computed Tomography

Computed tomography (CT) represents an imaging modality with high spatial and temporal resolution. The diagnostic value of CT might be significantly increased when contrast agents are used to attenuate tissues and organs of interest. Since providing diagnostically acceptable imaging requires the iodine concentration on the order of millimoles per ml of tissue (13), large doses of low-molecular-weight CT contrast agent, such as iodine-containing organic molecules, are normally administered to patients. The selective enhancement of blood upon such administration is brief due to rapid extravasation and clearance. A material whose distribution is limited to the blood pool should possess a size larger than fenestrated capillaries (> 10 nanometers), resistance to phagocytosis, and the radiopaque moiety structurally incorporated within the particulate.

Recently, we have described some preliminary results on the synthesis and *in vivo* properties of a block-copolymer of methoxy-poly(ethylene glycol) (MPEG) and iodine-substituted poly-L-lysine (14,15). This copolymer easily micellizes in solution forming stable and heavily iodine-loaded particles (up to 35% of iodine by weight) with a size below 100 nm. First, MPEG-PA NHS ester was prepared from MPEG-PA, NHS and dicyclohexylcarbodiimide, and then converted into MPEG-PA-poly(CBZ)lysine diblock copolymer by reaction with poly(CBZ)lysine. The product of this reaction was "deprotected" by removing CBZ-groups with HBr in acetic acid. Then, 2,3,5-triiodobenzoic acid NHS ester was prepared by reacting of 2,3,5-triiodobenzoic acid, dicyclohexylcarbodiimide and NHS. To prepare MPEG-PA-poly[ϵ ,N-(2,3,5-triiodobenzoyl)]-L-lysine, both synthesized components were conjugated in the presence of triethylamine to yield a MPEG-propionic acid(PA)-poly[ϵ ,N-(2,3,5-triiodobenzoyl)]-L-lysine (MPEG-iodolysine)block-copolymer. The formation of iodo-micelle formation from MPEG-iodolysine is shown on Figure 3.

The final micellar agent was injected intravenously into rats and rabbits, and the X-ray signal was monitored from several organs using a CT scanner. A significant enhancement of 3 to 4-fold in the blood pool (aorta and heart) was observed in rats for at least a period of 2 hours following the injection. Another important feature of the

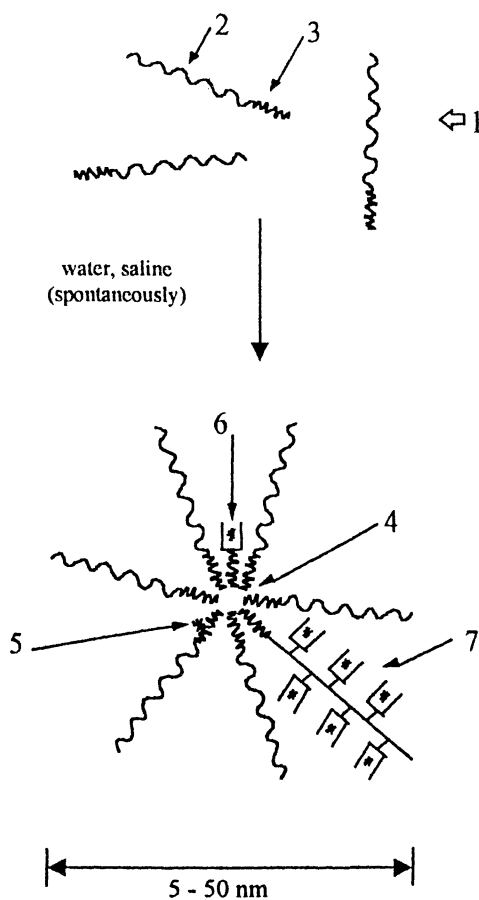


Figure 2. Schematic structures of micelle formation and loading with a contrast agent. Micelle is formed spontaneously in aqueous media from amphiphilic compound (1) the molecule of which consists of distinct hydrophilic (2) and hydrophobic (3) moieties. Hydrophobic moieties form the micelle core (4). Contrast agent (asterisk; gamma- or MR-active metal-loaded chelating group, or heavy element, such as iodine or bromine) can be directly coupled to the hydrophobic moiety within the micelle core (5), or incorporated into the micelle as an individual monomeric (6) or polymeric (7) amphiphilic unit.

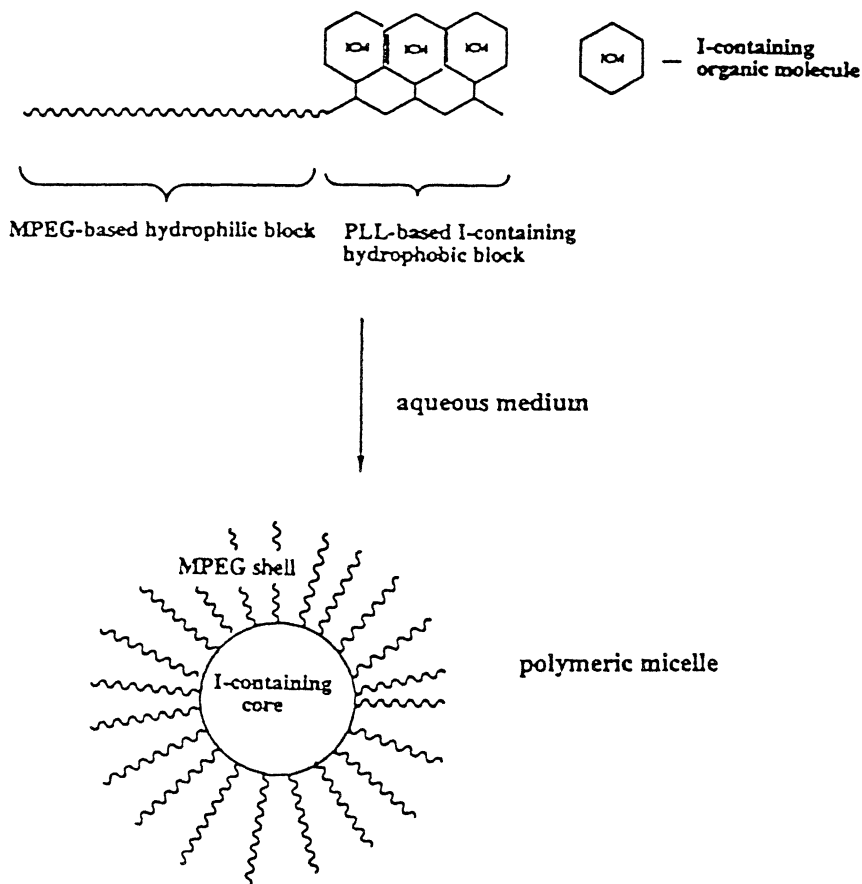


Figure 3. Schematic formation of iodine-containing polymeric micelles (ICPM) for blood pool CT imaging. (Reproduced from reference 14.)

iodo-micelles is their proven ability to slowly dissociate into unimers and gradually be cleared from the body via the kidneys. Micelles with such properties might find a certain clinical utility for the diagnostic CT imaging of the blood pool.

Micellar Form of Dequalinium

In certain cases, micelles may better serve as a delivery system for some hydrophobic and/or amphiphilic drugs than liposomes, which are traditionally used for this purpose. One of the known examples of this kind is connected with a solubilization system for a "bola"-like lipophilic cation dequalinium (16). Dequalinium (DQA), a topical antimicrobial agent, also drew considerable interest as a potential anticarcinoma drug. It was shown to be very effective in prolonging the survival of mice with intraperitoneally implanted carcinoma MB49 (17). Delocalized lipophilic cations were also shown to increase the sensitivity of carcinoma cells to radiation and photodynamic therapy (18,19). Unfortunately, a severe drawback of these agents is their limited solubility (20).

DQA stock solutions are commonly prepared in NaCl-free buffer solutions or distilled water at a concentration between 10 and 100 mM using a bath-type sonicator. However, even at very low salt concentrations around 20 mM NaCl, the formation of large aggregates was observed. At 150 mM NaCl more than 95% of the initially solubilized DQA could be removed from the solution as precipitate by simple centrifugation. To overcome solubility problems of DQA, we attempted the incorporation of DQA into liposomes and micelles made of PEG(5000)-DSPE.

To prepare DQA-liposomes, equal quantities of dequalinium chloride and PC were solubilized in chloroform:methanol (1:1, v/v) and dried using a rotary evaporator. After addition of NaCl-free buffer (5 mM HEPES) or distilled water, the sample was probe sonicated until a clear opaque solution was obtained. Alternatively, DQA-liposomes can be prepared by the addition of NaCl-free buffer, containing octylglycoside(OG), to the dry lipid/DQA mixture obtained as described with subsequent extensive dialysis against NaCl-free buffer. To prepare micelles, equal quantities of PEG(5000)-DSPE and dequalinium chloride were solubilized in methanol and dried with a rotary evaporator, followed by addition of OG-containing HBS (5 mM HEPES, 0.14 M NaCl, pH 7.4). Then, the dialysis was carried out and a minor precipitate of a non-incorporated DQA was removed by centrifugation and filtration. Vesicle size was determined by photon correlation spectroscopy with the Coulter™ Model N4 + Submicron Particle Analyzer.

In the absence NaCl, up to 50 mol % DQA could be incorporated into small 50 nm phosphatidylcholine (PC) liposomes made by probe sonication. Prepared under identical conditions, DQA alone, without phospholipid, forms significantly larger vesicles. These so-called DQAsomes (21) have a diameter between 100 and 600 nm. Therefore, the formation of liposomes with narrow size distribution from DQA/PE strongly suggests the association of DQA with the PC bilayer. However, all attempts to prepare DQA/PC mixed vesicles by the detergent dialysis method failed, since DQA is quantitatively removed from the original phospholipid/DQA mixture during dialysis. This indicates that the association of DQA with the bilayer membranes is not

stable. All attempts to incorporate DQA into various liposomes either by dialysis or sonication in the presence of salt also failed.

However, in striking contrast to liposomes, micelles made from PEG(5000)-PE effectively incorporate DQA in physiological NaCl solution. We prepared PEG-PE micelles in 5 mM HEPES, 0.15 mM NaCl, pH 7.4, by OG dialysis at an initial equimolar ratio of PEG(5000)-DSPE and DQA. After removing non-incorporated DQA by centrifugation and filtration, the PEG-DSPE micelles contained ca 30 mol % DQA. PEG-DSPE micelles with and without DQA had similar size (around 10 nm) and size distribution pattern. The total concentration of micellar solubilized DQA in the sample was 2 mM. At this concentration, DQA immediately forms aggregates larger than 5 μm when diluted with saline from a 10 mM aqueous stock solution. No such aggregates of DQA were detectable even after storage of the micelle preparation for over one week at 4°C. Even dialysis over more than one week did not reduce the DQA content in these micelle preparations.

Figure 4 represents a hypothetical structure of PEG-PE micelles with incorporated DQA. DQA is a dicationic compound resembling bola-form electrolytes, that is, it has a symmetrical molecule with two charge centers separated at a relatively large distance. These bola-like molecule might be able to bend in the middle and incorporate into the micelle's core. So, in certain situations micelles and not liposomes may appear to be carriers of choice for some poorly soluble compounds. This might be possible due to more favorable orientation of a drug molecule within the carrier particle.

Accumulation of Protein-Loaded Micelles in Tumor

In other cases, however, it is the small size of micelles which makes them superior compared to liposomes. Thus, we recently reported the use of PEG-PE micelles for the effective delivery of an artificially hydrophobized protein to a solid tumor, Lewis lung carcinoma, in mice (22).

The transport efficacy and accumulation of microparticulates, such as liposomes and/or micelles, in the tumor interstitium is determined to a great extent by their ability to penetrate the leaky tumor vascular endothelium (23,24). Diffusion and accumulation parameters were recently shown to be strongly dependent on the cutoff size of tumor blood vessel wall, and the cutoff size varies for different tumors (25).

In a general case, the biodistribution of a microparticulate carrier-associated anticancer drug depends on its circulation time in blood (summarized in (26) using liposomes as an example). Thus, it was repeatedly confirmed that long-circulating PEG-grafted liposomes demonstrate an increased accumulation in implanted tumors (27). Later, however, it was found that in some cases even the use of long-circulating liposomes could not provide their sufficient accumulation in certain tumors. A recent report (28) showed that coating 100 nm liposomes with PEG did not result in an increased accumulation of liposome-encapsulated drug in a subcutaneously established murine Lewis lung carcinoma. This phenomenon may be explained by the low vascular permeability (small cutoff size) of some tumors. In those cases, drug carriers smaller in size than liposomes may provide more efficient drug delivery into tumors. Here, we demonstrate that micelle-incorporated protein accumulates to a

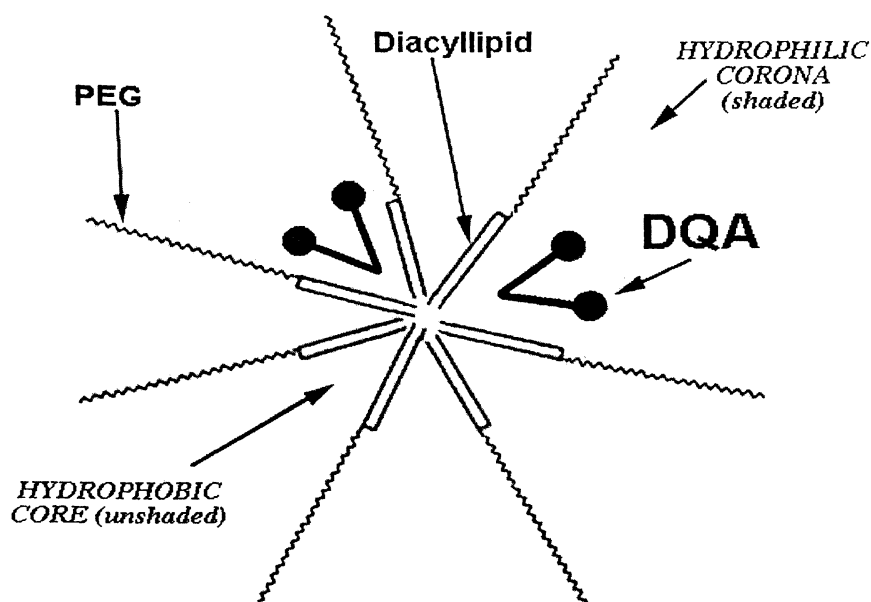


Figure 4. Hypothetical structure of DQA incorporated into PEG-based micelles. (Reproduced from reference 16.)

higher extent in subcutaneously established murine Lewis lung carcinoma than the same protein in larger liposomes.

We used soybean trypsin inhibitor (STI, MW 21,500 kDa) in our experiments. To achieve STI incorporation into liposomes and micelles, the protein was artificially hydrophobized via the interaction with N-glutaryl-PE (NGPE) as in (29). To follow protein biodistribution and clearance, we pre-modified STI with residues of diethylene triamine pentaacetic acid (DTPA), and DTPA-modified protein was loaded with ^{111}In after its incorporation into liposomes or micelles.

For micelle preparation, PEG(5000)-DSPE was solubilized in chloroform. After chloroform removal on a rotary evaporator, a required quantity of NGPE-DTPA-STI in OG solution was added to dried micelle-forming components. Sonication for five minutes using a bath sonicator yielded a clear solution. The detergent was removed by dialysis for 3 days against HBS. Sterically protected long-circulating liposomes (egg phosphatidylcholine: cholesterol : PEG-DSPE = 8 : 2 : 1, molar ratio) were prepared by drying a lipid solution in chloroform with a rotary evaporator, followed by addition of a required quantity of NGPE-DTPA-STI in OG solution. Final lipid concentration was 16 mg/ml. Liposomes obtained by overnight dialysis against HBS were sized by multiple passing through polycarbonate filters until 95% of the liposome population had an average diameter between 95 and 110 nm. Size and size distribution of liposome and micelle samples were determined by photon correlation spectroscopy with the CoulterTM Model N4+ MD sub-micron particle analyzer.

Mice were inoculated s.c. into rear flank with Lewis lung carcinoma cells and, after tumors reached ca. 5 mm in size (usually after 18-25 days), mice were injected i.v. into the tail vein with 0.1 ml of liposome or micelle sample (2 mg of lipid/polymer and ca. 20 μCi of ^{111}In per mouse). Mice were sacrificed in groups of 5 after 1, 4 and 23 hours, organs were harvested and the radioactivity was determined in a gamma-counter.

The incorporation of lipid-modified protein into liposomes and micelles is schematically shown in Figure 5. An important property of micelles as drug carriers is their size, which normally varies between 5 and 50 nm, thus filling the gap between individual molecules (size around and below 1 nm) as drug carriers and nanoparticles, such as liposomes, with a size around 100 nm and above. As follows from our data, we could easily incorporate hydrophobized STI into both 100 nm PEG-liposomes and 15 nm PEG5000-DSPE micelles at levels where the protein does not influence the size of either carrier.

While liposome stability in diluted aqueous solutions does not differ from that in more concentrated solutions (30), micelles are known to dissociate upon dilution, the extent of dissociation being dependent on the critical micellation concentration (CMC). However, PEG-lipid-based micelles are remarkably stable upon dilution (9). Figure 6 presents an HPLC-based gel permeation chromatography of serial dilutions of PEG-5000-DSPE micelles with incorporated STI. It can be seen that micelles are still present at a concentration of 140 nM, indicating an extremely low, nanomolar, CMC value, which is for many other low-molecular-weight surfactants in the millimolar range. This led us to expect that STI-loaded PEG-lipid micelles will remain intact even being diluted with a large volume of blood.

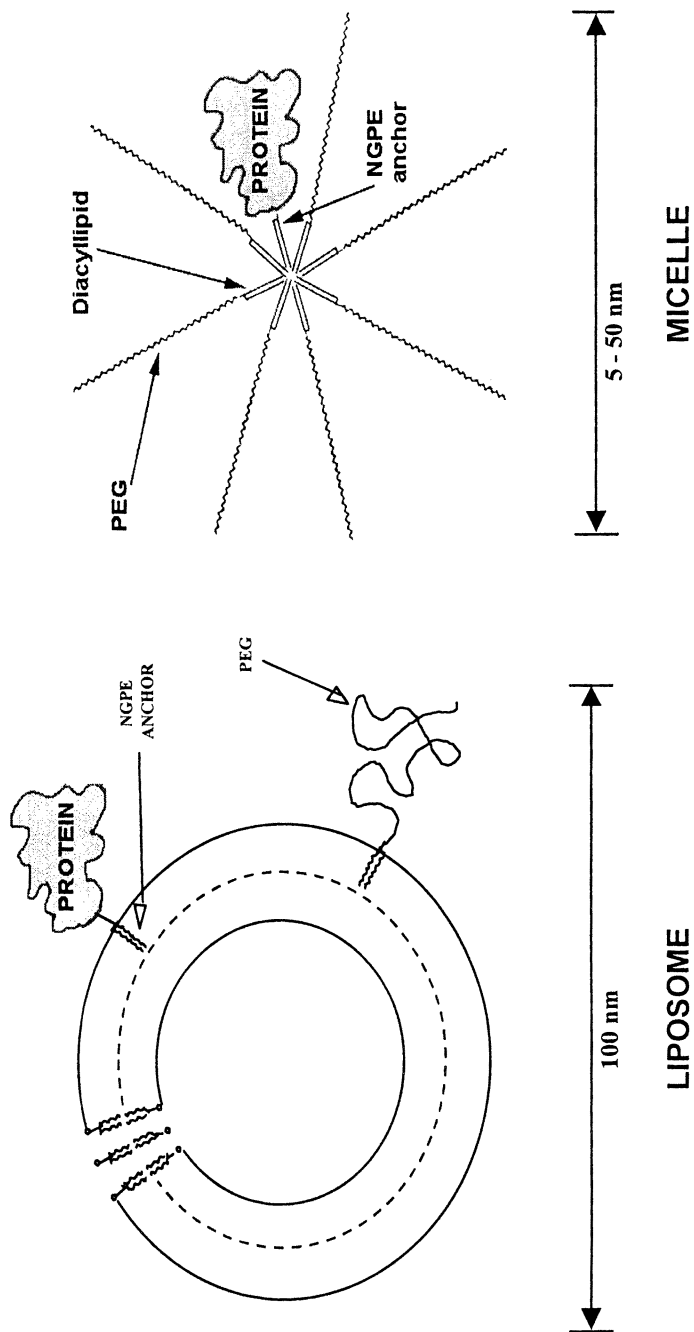


Figure 5. Principal structure of a long-circulating liposome and a polyethyleneglycol-diacetyl lipid micelle with incorporated hydrophobized protein. (Reproduced from reference 22.)

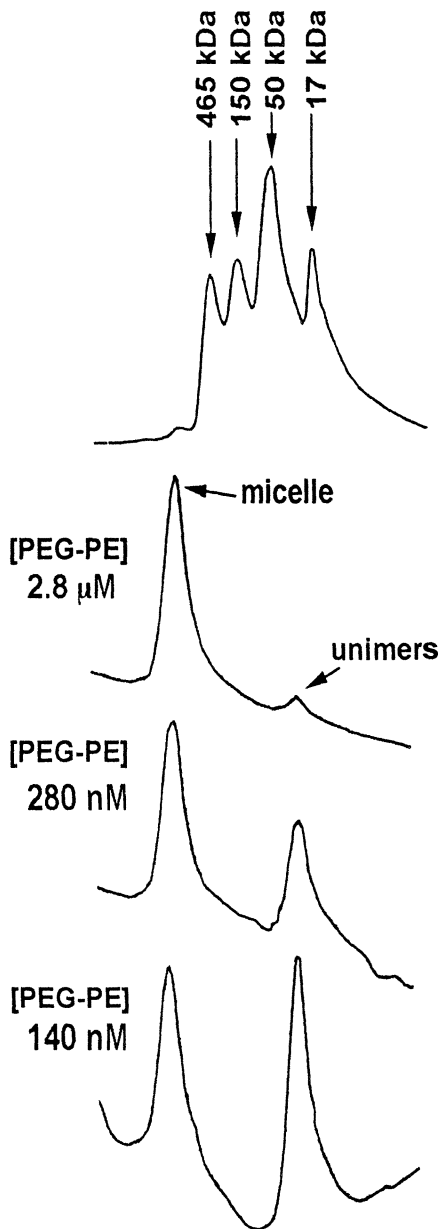


Figure 6. HPLC-based gel permeation chromatography of serial dilutions of PEG5000-DSPE micelles with incorporated STI. Sample volume 20 μ l. Column: Shodex Protein KW-804. Solvent HBS, pH 7.4. Detection at 215 nm. (Reproduced from reference 22.)

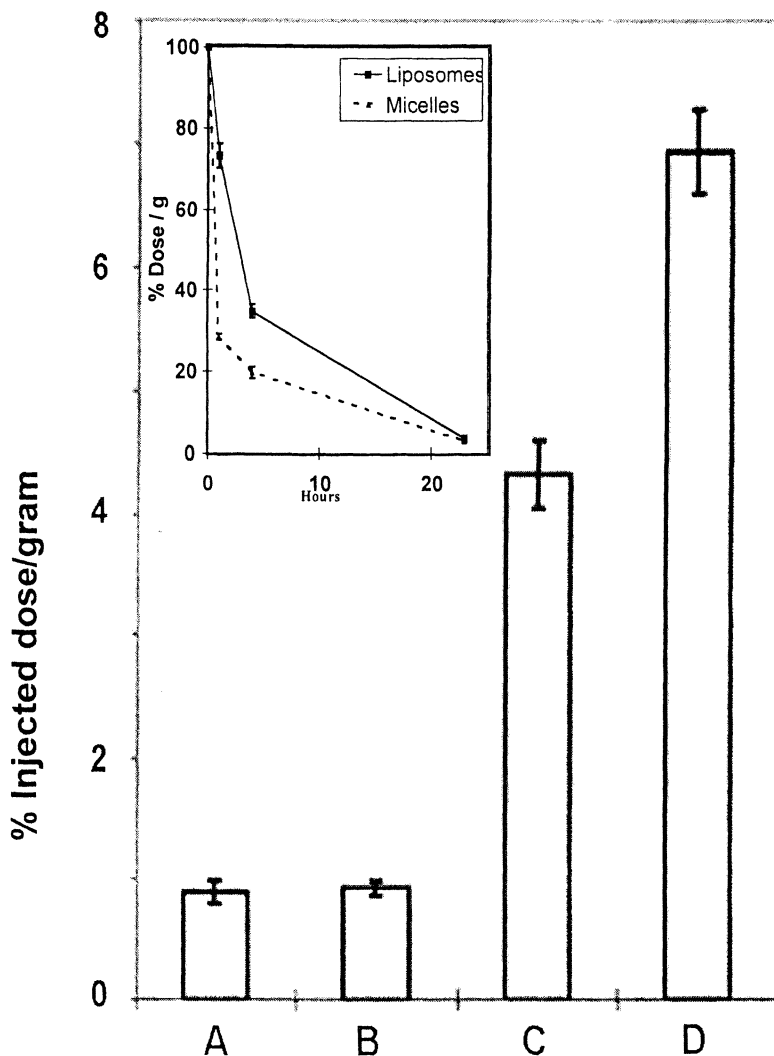


Figure 7. Tumor accumulation 23 hours after i.v. injection of native STI (A), NGPE-DTPA-STI (B), NGPE-DTPA-STI anchored in 100 nm long-circulating liposomes (C) and micellar-bound NGPE-DTPA-STI (D). Insert: Blood clearance of NGPE-DTPA-STI anchored in long circulating liposomes and PEG5000-DSPE micelles. (Reproduced from reference 22.)

Animal experiments revealed different biodistribution patterns of all tested preparations - free STI, STI-liposomes and STI-micelles. The native protein demonstrates the expected fastest disappearance from the blood and the maximum accumulation in the liver and spleen. Both micelles and liposomes demonstrate clear longevity in the blood, however, liposomes seem to stay in the circulation longer than micelles. Thus, after 1 hour, blood concentration of liposomes is still ca. 75 % dose/g, but only ca. 30% dose/g for micelles. Micelles also accumulate somewhat faster in the spleen, while the liver accumulation pattern looks very similar for both carriers.

The longevity of PEG-micelles and PEG-liposomes, together with their slow clearance via liver and spleen, naturally result in their improved accumulation in the tumor compared with the native STI. Even more important is the fact that despite faster blood clearance, micelles accumulate in the tumor significantly better than liposomes, delivering more STI (Figure 7).

This result confirms that the efficacy of passive delivery to solid tumors is not only controlled by the exposure level outside of extravasation but also by the more complex relationship between the tumor's microvascular permeability and the size of a drug carrier. Our results suggest that in certain tumors (such as subcutaneously established murine Lewis lung carcinoma) small-size micelles provide better delivery of a drug (protein) than larger long-circulating liposomes.

References

1. Tengamnuay, P.; Mitra, A.K. *Pharm. Res.* **1990**, *7*, 127-133.
2. Martinez-Coscolla, A.; Miralles-Loyola, E.; Garrigues, T.M.; Sirvent, M.D.; Salinas, E.; Casabo, V.G. *Drug Res.* **1993**, *43*, 699-705.
3. Magnusson, G.; Olsson, T.; Nyberg, J.-A. *Toxicol. Lett.* **1986**, *30*, 203-207.
4. Port, C.D; Garvin, P.J.; Ganote, C.E. *Toxicol. Appl. Pharmacol.* **1978**, *44*, 401-411.
5. Yokoyama, M.; Inoue, S.; Kataoka, K.; Yui, N.; Sakurai, Y. *Makromol. Chem., Rapid Commun.* **1987**, *8*, 431-435.
6. Kwon, G.S.; Yokoyama, M.; Okano, T.; Sakurai, Y.; Kataoka, K. *Pharm. Res.* **1993**, *10*, 970-974.
7. Klibanov, A.L.; Maruyama, K.; Torchilin, V.P.; Huang, L. *FEBS Lett.* **1990**, *268*, 235-238.
8. Lasic, D.D.; Woodle, M.C.; Martin, F.J.; Valentincic, T. *Period. Biol.* **1991**, *93*, 287-290.
9. Trubetskoy, V.S.; Torchilin, V.P. *Adv. Drug Delivery Rev.* **1995**, *16*, 311-320.
10. Trubetskoy, V.S.; Frank-Kamenetsky, M.D.; Whiteman, K.R.; Wolf, G.L.; Torchilin, V.P. *Acad. Radiol.* **1996**, *3*, 232-238.
11. Trubetskoy, V.S.; Torchilin, V.P. *J. Liposome Res.* **1994**, *4*, 961-980.
12. Slinkin, M.A.; Klibanov, A.L.; Torchilin, V.P. *Bioconj. Chem.* **1991**, *2*, 342-348.
13. Wolf, G.L. In *Handbook of Targeted Delivery of Imaging Agents*; Torchilin, V.P., Ed.; CRC Press: Boca Raton, FL, 1995, 3-22.
14. Trubetskoy, V.S.; Gazelle, G.S.; Wolf, G.L.; Torchilin, V.P. *J. Drug Targeting* **1997**, *4*, 381-388.

15. Torchilin, V.P.; Frank-Kamenetsky, M.D.; Wolf, G.L. *Acad. Radiol.* **1999**, *6*, 61-65.
16. Weissig, V.; Lizano, C.; Torchilin, V.P. *J. Liposome Res.* **1998**, *8*, 391-400.
17. Weiss, M.J.; Wong, J.R.; Ha, C.S.; Bleday, R.; Salem, R.R.; Steele, Jr., G.D.; Chen, L.B. *Proc. Natl. Acad. Sci. USA* **1987**, *84*, 5444-5448.
18. Teicher, B.A.; Holden, S.A.; Jacobs, J.L.; Abrams, M.J.; Jones, A.G. *J. Biol. Chem.* **1986**, *35*, 3365-3369.
19. Oseroff, A.R.; Ohuoha, D.; Ara, G.; McAuliffe, D.; Foley, J.; Cincotta, L. *Proc. Natl. Acad. Sci. USA* **1986**, *83*, 7929-7933.
20. Sun, X.S.; Wong, J.R.; Song, K.; Hu, J.; Garlid, K.D.; Chen, L.B. *Cancer Res.* **1994**, *54*, 1465-1471.
21. Weissig, V.; Lasch, J.; Erdos, G.; Meyer, H.; Rowe, T.C.; Hughes, J. *Pharm. Res.* **1998**, *15*, 334-337.
22. Weissig, V.; Whiteman, K.R.; Torchilin, V.P. *Pharm. Res.* **1998**, *15*, 1552-1556.
23. Yuan, F.; Leunig, M.; Huang, S.K.; Berk, D.A.; Papahadjopoulos, D.; Jain, R.K. *Cancer Res.* **1994**, *54*, 3352-3356.
24. Yuan, F.; Dellian, M.; Fukumura, M.; Leunig, M.; Berk, D.A.; Torchilin, V.P.; Jain, R.K. *Cancer Res.* **1995**, *55*, 3752-3756.
25. Hobbs, S.K.; Monsky, W.L.; Yuan, F.; Roberts, W.G.; Griffith, L.; Torchilin, V.P.; Jain, R.K. *Proc. Natl. Acad. Sci. USA* **1998**, *95*, 4607-4612.
26. Gabizon, A.A. *Adv. Drug Delivery Rev.* **1995**, *16*, 285-294.
27. Papahadjopoulos, D.; Allen, T.M.; Gabizon, A.; Mayhew, E.; Matthay, K.; Huang, S.K.; Lee, K.-D.; Woodle, M.C.; Lasic, D.D.; Redemann, C.; Martin, F.J. *Proc. Natl. Acad. Sci. USA* **1991**, *88*, 11460-11464.
28. Parr, M.J.; Masin, D.; Cullis, P.R.; Bally, M.B. *J. Pharmacol. Exp. Ther.* **1997**, *280*, 1319-1327.
29. Weissig, V.; Lasch, J.; Klibanov, A.L.; Torchilin V.P. *FEBS Lett.* **1986**, *202*, 86-90.
30. Lasic, D.D. *Liposomes from Physics to Applications*; Elsevier: Amsterdam, The Netherlands, 1993, p 54.

Chapter 30

The Role of Plasma Lipoproteins as Carriers of Water-Insoluble Compounds: Biological and Physiological Consequences

Kishor M. Wasan, Manisha Ramaswamy, Allison L. Kennedy,
Kathy Peteherych, and Wesley Wong

Faculty of Pharmaceutical Sciences, The University of British Columbia,
2146 East Mall Avenue, Vancouver, British Columbia V6T 1Z3, Canada

Abstract

The plasma lipoprotein distribution of potential drug candidates to date has not commonly been investigated. For some hydrophobic drug candidates, attainment of similar plasma free drug levels has not been associated with uniform production of pharmacological activity in different animal species. It is well-known that plasma lipoprotein lipid profiles vary considerably between different animal species. In addition, human disease states can significantly influence plasma lipoprotein profiles, resulting in altered therapeutic outcomes. Current research has shown that lipoprotein association of drug compounds can significantly influence their pharmacological and pharmacokinetic properties. The focus of this paper will be to review the factors that influence the interaction of one model hydrophobic compound, cyclosporine (CsA), and compounds incorporated into lipid-based vesicles with lipoproteins and the implications of altered plasma lipoprotein concentrations on the pharmacological behavior of these compounds.

Introduction

Lipoproteins are a heterogeneous population of macromolecular aggregates of lipids and proteins that are responsible for the transport of lipids through the

vascular and extravascular fluids from their site of synthesis or absorption to peripheral tissues.^{1,2} These lipids, which include triacylglycerols (TG), cholesteryl esters (CE) and phospholipids (PL) are delivered from the liver and intestine to other tissues in the body for storage or catabolism in the production of energy. Lipoproteins are also known to be involved in a number of other biological processes including coagulation, tissue repair, and as carriers of a number of hydrophobic compounds within the systemic circulation.³⁻⁵

It has been well documented that disease states significantly influence circulating lipoprotein content and composition. Therefore, it appears possible that changes in the lipoprotein profile would affect not only the ability of a compound to associate with lipoproteins but also affect the distribution of the compound within the lipoprotein subclasses. The result of such an effect could lead to alterations in the pharmacokinetics and pharmacological action of the drug.

The focus of this paper will be to review the factors that influence the interaction of one model hydrophobic compound, cyclosporine (CsA), and compounds incorporated into lipid-based vesicles with lipoproteins and the implications of altered plasma lipoprotein concentrations on the pharmacological behavior of these compounds.

Lipoprotein Structure and Function

Lipoproteins are spherical particles consisting of a nonpolar lipid core (TG and CE) surrounded by a surface monolayer of amphipathic lipids (PL and unesterified cholesterol) and specific proteins called apolipoproteins. A number of different phospholipids are incorporated into the coat of the lipoprotein. The most abundant of these phospholipids is phosphatidylcholine, which is also utilized as a substrate in the esterification of cholesterol to cholesterol ester by the enzyme lecithin cholesterol acyltransferase. Since lipids, in general, have lower buoyant densities than proteins, lipoproteins with a larger amount of lipid relative to protein will have a lower density than lipoproteins with a smaller lipid-to-protein ratio.

Plasma lipoproteins are classified and separated according to their density and are divided into five main categories: triglyceride-rich lipoproteins which includes chylomicrons and very low-density lipoproteins (VLDL), intermediate density lipoproteins (IDL), low-density lipoproteins (LDL) and high-density lipoproteins (HDL).

Chylomicrons are the largest of the lipoproteins (diameter of approximately 100-1000 nm) and are found in greatest abundance after a meal. They are synthesized by the intestine and are core-rich in TG derived from dietary fat. VLDL are the next largest lipoproteins (diameter of approximately 30-80 nm) and are also rich in TG. They are synthesized mainly by the liver but may also be synthesized to a lesser degree by the intestine. IDL, whose lipid core is comprised mainly of CE with some TG, are the resultant product of VLDL metabolism. However, LDL, are the product of IDL metabolism in which almost all of the remaining TG have been hydrolyzed to produce a lipoprotein with a core comprised almost entirely of CE. LDL are the second smallest lipoproteins (diameter of approximately 18-25 nm) and

are the major carrier of cholesterol (mostly in the form of CE). HDL is the smallest of the lipoproteins with a diameter of approximately 7 to 12 nm.

Lipoproteins as Novel Carriers of Cyclosporine (CsA)

CsA is a cyclic polypeptide of fungal origin discovered in the early 1970s and approved for use in 1983.⁶ It interacts with the intracellular protein cyclophilin, which inhibits the calcium dependent translocation of nuclear transcription factors, which are necessary for interleukin-2 gene transcription. Since interleukin-2 is required for the proliferation of T-lymphocytes cyclosporine is capable of diminishing the immune response.^{6,7} However, despite its effectiveness as an immunosuppressant, the use of CsA is limited by renal toxicity, which is characterized by a rise in serum creatinine and a decrease in the glomerular filtration rate.⁸

A number of laboratories, including ours, have shown CsA to associate with lipoproteins upon incubation in human plasma,⁹⁻¹¹ resulting in a modification of its pharmacological activity. De Kippel *et al.*¹² and Nemunaitis *et al.*¹³ have reported decreases in CsA activity in patients that have elevated plasma triglyceride levels, while de Groen and coworkers have observed increases in cyclosporine toxicity in those with hyperlipidemia.¹⁴ Lemaire and coworkers have observed enhanced antiproliferative effects of CsA when the drug was associated with low-density lipoproteins that were not evident when the drug was associated to either very low-density (VLDL) or high-density lipoproteins (HDL).¹⁵ Gardier and coworkers observed that heart transplant patients with high total plasma cholesterol levels demonstrated increased CsA association with plasma low-density lipoproteins (LDL) and an increased CsA-induced renal toxicity compared to normolipidemic controls.¹⁶ In addition, Arnadottir and coworkers observed elevations in CsA-induced renal toxicity in kidney transplant patients who exhibited increases in plasma cholesterol concentration.¹⁷ Taken together, these studies provide substantial evidence suggesting that plasma lipoprotein lipid levels have a major impact on influencing the efficacy and toxicity of CsA.

Factors that Influence CSA Interactions with Plasma Lipoproteins

The association of CsA with plasma lipoproteins appears to have a major impact on the drug's efficacy and safety, particularly since it is often administered to patients with abnormal lipid metabolism (i.e. hypo/hypercholesterolemia and/or hypertriglyceridemia). Our laboratory has investigated two different characteristics of dyslipidemic plasma, which may influence the association of CsA with plasma lipoproteins and thus modify its pharmacokinetics and pharmacodynamics. These two characteristics are (1) changes in the rate of transfer of esterified cholesterol and triglycerides between different lipoprotein classes and (2) changes in plasma lipoprotein lipid and protein content.

(1) Influence of Cholesteryl Ester Transfer Protein (CETP)

A change in protein-mediated transfer of esterified cholesterol and triglycerides between different lipoprotein classes is an important feature of dyslipidemic plasma. Zilversmit and Morton demonstrated that this transfer was facilitated by lipid transfer protein, often referred to as cholesteryl ester transfer protein (CETP).¹⁸ Our laboratory has hypothesized that since the human body may recognize hydrophobic compounds as lipid-like particles, then an increase in CETP concentration and activity may facilitate the movement of compounds, such as CsA, among different lipoprotein classes.¹⁹ When CsA was incubated in human plasma with or without additional supplementation of CETP for 60 minutes at 37^o C, increases in CETP concentration resulted in an increased percentage of CsA recovered in the HDL/lipoprotein deficient plasma (LPDP) fraction (Table 1).¹⁹

Table 1. Effect of CETP on the Distribution of CsA into Plasma lipoproteins.

Amount of CETP ^a (ug protein)	HDL/LPDP (%) ^b	LDL/VLDL (%) ^b
0	51 +/- 1	49 +/- 5
0.5	57 +/- 4*	43 +/- 4
1.0	59 +/- 3*	40 +/- 1*
2.0	61 +/- 1*	38 +/- 1*

Data were expressed as mean +/- standard deviation (n=6). *p<0.05 vs. HDL/LPDP or LDL/VLDL fraction at CETP = 0. CsA, cyclosporine; CETP, cholesteryl ester transfer protein; HDL, high density lipoproteins; LPDP, lipoprotein deficient plasma; LDL, low density lipoproteins; VLDL, very low density lipoproteins. ^aamount of exogenous CETP added to 1 ml of human plasma. Endogenous CETP concentration was 1 µg protein / ml of human plasma for all test samples. All incubations were carried out for 60 minutes in pooled human plasma. ^bpercent of initial cyclosporine incubated in human plasma. Total recovery > 98%. Adopted from reference 19.

Additional experiments that were designed to directly measure the potential role of CETP to facilitate CsA transfer demonstrated that CETP-mediated percent transfer of CE among HDL and LDL particles in human plasma was significantly different from that of CsA (Table 2).¹⁹ The differences in the percent transfer of CE versus CsA may be attributed to an ability of CETP to transfer lipid and drug separately. Furthermore, differences could be attributed to the ability of HDL and LDL particles to accumulate a higher amount of CE than CsA.

Furthermore, when CETP-mediated transfer of CE between HDL and LDL was inhibited by TP2 (a monoclonal antibody directed against CETP), only the transfer of CsA from LDL to HDL was significantly decreased (Table 2).¹⁹ These results suggest that the transfer of CsA from LDL to HDL is partially facilitated by CETP while the transfer of CsA from HDL to LDL is not facilitated by CETP but by

other plasma factors and/or spontaneous transfer. This notion is supported by the work of Hughes and co-workers, who hypothesize that the plasma distribution of CsA is determined by factors other than simple diffusion between lipoprotein particles.²⁰

These findings suggest that the distribution/redistribution of CsA among plasma lipoproteins facilitated by CETP may serve as a possible mechanism for determining the ultimate fate of these compounds.

Table 2. Percent transfer of CE and CsA between lipoproteins, in the presence or absence of a monoclonal antibody (TP2) directed against CETP in human plasma.

Treatment	HDL to LDL % kt ^a		LDL to HDL % kt ^a	
	CE	CsA	CE	CsA
Without TP2	18 +/- 3.5	8.6 +/- 1.4	12.5 +/- 1.8	19.8 +/- 6.1
With TP2	2.2 +/- 0.9*	10.3 +/- 2.2	2.9 +/- 1.4*	7.5 +/- 2.6*

Data were expressed as mean +/- standard deviation (n=6). *p<0.05 vs. without TP2. CE, cholesteryl ester; CsA, cyclosporine; CETP, cholesteryl ester transfer protein; HDL, high-density lipoproteins; LDL, low density lipoproteins. ^apercent fraction of labeled CE and CsA transferred per unit time. Adopted from reference 19.

(2) Influence of Lipoprotein Concentration and Composition

A second feature of dyslipidemic plasma is the increase and/or decrease in plasma lipoprotein cholesterol and triglyceride concentrations. Since CsA associates with plasma lipoproteins following their administration, our laboratory has hypothesized that changes in lipoprotein concentration and composition would alter the lipoprotein distribution of CsA.

Our laboratory reported that broad plasma dyslipidemias (Table 3) and specific increases in LDL and VLDL lipid levels (Table 4) resulted in an increasing amount of CsA recovered in these fractions and a significant decrease in the amount of CsA recovered in the HDL fraction (Tables 3 and 4).⁹ Furthermore, the amount of drug recovered in the nonlipoprotein fraction remained unchanged. These findings suggest that CsA lipoprotein distribution may be partially regulated by plasma lipoprotein cholesterol and to a lesser extent triglyceride concentrations. It further suggests that the redistribution of drug from one lipoprotein class (HDL) to another (LDL or VLDL) could be influenced by different disease states and adjunct therapies such as Intralipid infusion, where lipoprotein plasma concentrations and composition are altered.²¹

Table 3. Distribution of CsA at 1000 ng/ml within normolipidemic and dyslipidemic plasma from different human subjects following incubation for 60 minutes at 37°C.

Plasma Type	Lipoprotein fraction, % ^a		
	VLDL/LDL	HDL	LPDP
Normolipidemic	31.9 +/- 3.6	44.4 +/- 4.2	19.7 +/- 3.1
Hypercholesterolemic	46.3 +/- 7.7 ^b	20.9 +/- 7.7 ^d	20.9 +/- 2.6
Hypertriglyceridemic	54.3 +/- 13.1 ^c	20.0 +/- 4.6 ^d	18.9 +/- 7.3
Hypercholesterolemic + Hypertriglyceridemic	55.3 +/- 9.2 ^c	20.1 +/- 3.7 ^d	12.9 +/- 5.0 ^b

Data expressed as mean +/- standard deviation (n=6 patients in each group). ^bp<0.05, ^cp<0.01, ^dp<0.001 vs. normolipidemic plasma type. CsA, cyclosporine; VLDL, very low-density lipoproteins; LDL, low-density lipoproteins; HDL, high-density lipoproteins; LPDP, lipoprotein deficient plasma. ^apercent of initial CsA concentration incubated. Plasma types: normolipidemic (total cholesterol = 100-200 mg/dL and total triglyceride = 100-200 mg/dL), hypercholesterolemic (total cholesterol = 250-300 mg/dL), hypertriglyceridemic (total triglyceride = 350-500 mg/dL), hypercholesterolemic + hypertriglyceridemic (total cholesterol = 250-300 mg/dL and total triglyceride = 350-500 mg/dL). Total CsA recovery was greater than 88%. Adopted from reference 9.

In addition, we observed that increasing the TG: total cholesterol (TC) ratio within VLDL and HDL resulted in more CsA recovered in the VLDL fraction but less CsA recovered in the HDL fraction.⁹ However, increases in the HDL TG: TC ratio increased the amount of drug recovered in the HDL fraction.⁹ These findings suggest that not only lipid mass (TC and TG) and lipoprotein composition but also the type of lipoprotein in which these changes occur is another possible factor in determining to which lipoprotein CsA associates. Since transplantation patients exhibit lipid disturbances, including decreased cholesterol levels and/or elevated triglyceride levels, these results may provide an explanation for the unpredictable and inconsistent pharmacokinetics and pharmacodynamics of CsA following administration.

Compounds Incorporated into Lipid-Based Vesicles

A number of studies have investigated the interaction of liposomes and lipid-complexes with plasma lipoproteins. Surewicz *et al.* have reported the formation of thermally stable complexes when anionic phospholipids (such as dimyristoylphosphatidylglycerol [DMPG]) are co-incubated with apolipoprotein AI.²² Scherphof demonstrated the transfer of phosphatidylcholine from small

Table 4. Distribution of CsA at 1000 ng/ml within plasma from three different patients following incubation for 60 minutes at 37°C.

Patient Profile	Lipoprotein fraction, % ^a				TC mg/dl	TG mg/dl
	VLDL	LDL	HDL	LPDP		
Patient I	13+/-6	27+/-0.4	47+/-5	8+/-1	113	79
Patient II	17+/-6	34+/-5	41+/-8	5+/-1	179	167
Patient III	19+/-7	41+/-3 ^b	28+/-2 ^{b,c}	7+/-1	235	394

Data expressed as mean +/- standard deviation (n=6 replicates). ^bp<0.05 vs. patient I; ^cp<0.05 vs. patient II. CsA, cyclosporine; VLDL, very low-density lipoproteins; LDL, low-density lipoproteins; HDL, high-density lipoproteins; LPDP, lipoprotein deficient plasma; TC, total cholesterol; TG, total triglyceride. ^apercent of initial CsA concentration incubated. Adopted from reference 9.

unilamellar vesicles to HDL.²³ Our laboratory has recently investigated the interaction of three different compounds incorporated into lipid-based vesicles with plasma lipoproteins.

(1) Amphotericin B Lipid Complex (ABLC)

Preliminary studies were conducted in which ABLC (composed of dimyristoylphosphatidylcholine [DMPC] and DMPG) was incubated in human serum for 60 minutes at 37°C. Following incubation the serum was separated into its lipoprotein and lipoprotein-deficient fractions by density gradient ultracentrifugation and percent of AmpB and DMPG recovered in each fraction was determined by high-pressure liquid chromatography (HPLC). Greater than 90% of the original concentration of AmpB and 80% of DMPG from the original formulation incubated in serum were recovered in the HDL fraction.⁵

Recent studies have shown that when ABLC was incubated in human plasmas of varying lipid concentration and lipoprotein composition, the majority of AmpB was recovered in the HDL fraction.²⁴ We further showed that differences in lipid coat content (free cholesterol and PL) carried by HDL influenced the distribution of ABLC within plasma of different human subjects.²⁴

(2) Liposomal Annamycin

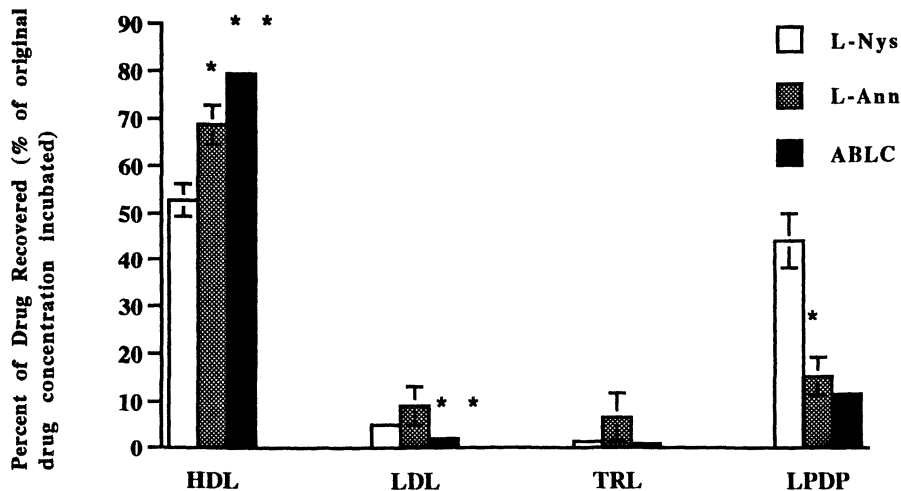
When liposomal annamycin (composed of DMPC and DMPG) at different concentrations (5-20 µg annamycin per ml) was incubated in human plasma for 60 minutes at 37°C greater than 67% of the initial annamycin concentration incubated was recovered in the HDL fraction.²⁵ We further observed that elevation of plasma LDL-cholesterol or VLDL-triglyceride concentrations increased the percent recovery of annamycin in these lipoprotein fractions.²⁵

(3) Liposomal Nystatin

When liposomal nystatin (composed of DMPC and DMPG) at 20 μg nystatin per ml was incubated in human plasmas of varying lipid and lipoprotein concentrations for 5 minutes at 37^o C 24 to 53% of the original nystatin concentration incubated was recovered in the HDL fraction. Furthermore, it was observed that as the amount of HDL protein decreased the percent of nystatin recovered within this fraction decreased following the incubation of liposomal nystatin.²⁶ These findings suggest that the preferential distribution of nystatin into plasma HDL may be a function of the HDL protein concentration.

Taken together these findings along with our observations using ABLC and liposomal annamycin suggest that lipid-based vesicles containing DMPG may have the ability to target compounds specifically to HDL due to the ability of DMPG to complex with apolipoprotein AI (Figure 1). Therefore, any DMPG-drug complex introduced into human plasma, initially either as an intact liposome or as a lipid-drug complex would likely increase the level of distribution of that drug into HDL. However, additional factors such as HDL particle size, charge and total surface area may also influence the distribution of the drug into HDL.

Figure 1. Distribution of Liposomal Nystatin, Liposomal Annamycin and Amphotericin B lipid complex (20 μg of drug/ml) within human plasma following incubation for 60 minutes at 37^o C.



Abbreviations: L-Nys, liposomal nystatin; L-Ann, liposomal annamycin; ABLC, amphotericin B lipid complex; HDL, high-density lipoproteins; LDL, low-density lipoproteins; TRL, triglyceride-rich lipoproteins; LPDP, lipoprotein deficient fraction. Data presented as mean \pm standard deviation (n=3 for L-Nys & ABLC, n=5 for L-Ann), *p<0.05 vs. L-Nys, **p<0.05 vs. L-Ann.

Implications of Altered Lipid and Lipoprotein Metabolism

Disturbances in lipid metabolism (e.g. hypertriglyceridemia and hypocholesterolemia) commonly occur during infection or when the immune system has been depressed. Studies have indicated several mechanisms by which infection causes the increase of TG: (1) increased hepatic de novo synthesis of fatty acids leading to increased secretion of VLDL, (2) increased adipose tissue lipolysis with the mobilized fatty acid being reesterified into TG in the liver and then resecreted as VLDL rather than being oxidized, and (3) decreased levels of lipoprotein lipase (an enzyme responsible for the hydrolysis of TG into free fatty acids and glycerol) leading to decreased clearance of TG-rich VLDL. Furthermore, cancer cells appear to require additional cholesterol for the formation of new membrane material and metabolism requirements, as evidenced by the development of hypocholesterolemia and a decrease in plasma LDL cholesterol concentrations in leukemia patients.

Since a number of hydrophobic compounds, not just CsA, predominantly associate with plasma lipoproteins upon incubation in plasma, changes in plasma TG and cholesterol concentrations could affect not only the plasma distribution of these compounds, but may also have a bearing on their pharmacokinetics and pharmacodynamics. Understanding how variations in plasma lipid concentrations affect hydrophobic drug interactions with lipoproteins could help explain the changes in the pharmacokinetics and pharmacodynamics of these compounds when administered to patients that exhibit modifications in their lipid and lipoprotein metabolism.

Conclusions

Lipoproteins serving as drug carriers within the systemic circulation should be considered as a possible mechanism of delivery for hydrophobic drugs to specific tissue sites. Furthermore, the ability to target compounds specifically to one lipoprotein subclass over another potentially modifies the pharmacokinetics and pharmacological action of these compounds.

Acknowledgements

The authors of this paper would like to thank the Medical Research Council of Canada and Tilak Technologies for providing funding for this research.

Literature Cited

- (1) Davis, R.A.; Vance, J.E. In: *Biochemistry of lipids, lipoproteins and membranes*. 1996, 473.
- (2) Harmony, J.A.K.; Aleson, A.L.; McCarthy, B.M. In: *Biochemistry and biology of plasma lipoproteins*. 1986, 403.
- (3) Mbewu, A.; Durrington, P.N. *Atherosclerosis* 1990, 85, 1.
- (4) Durrington, P.N. In: *Lipoproteins and Lipids*. 1989, 255.

- (5) Wasan, K.M.; Cassidy, S.M. *J. Pharm. Sci.* **1998**, *87*, 411.
- (6) Borel, J.F.; Kis, Z.L. *Transplant. Proc.* **1991**, *23*, 1867.
- (7) Wiederrecht, G.; Lam, E.; Hung, S.; Martin, M.; Sigal, W. *Ann. N.Y. Acad. Sci.* **1993**, *696*, 9.
- (8) Bennett, W.M. *J. Am. Acad. Dermatol.* **1990**, *23*, 1280.
- (9) Wasan, K.M.; Pritchard, P.H.; Ramaswamy, M.; Wong, W.; Donnachie, E.M.; Brunner, L.J. *Pharm. Res.* **1997**, *14*, 1613.
- (10) Awani, W.N.; Kasiske, B.L.; Heim-Duthoy, K.; Vennkateswara, R.K. *Clin. Pharmacol. Ther.* **1989**, *45*, 41.
- (11) Awani, W.N.; Sawchuk, R.J. *Drug Metab. Disp.* **1985**, *13*, 133.
- (12) De Kippel, N.; Sennesael, J.; Lamote, J.; Ebinger, G.; De Keyser, J. *Lancet* **1992**, *339*, 1114.
- (13) Nemunaitis, J.; Deeg, H.J.; Yee, G.C. *Lancet* **1986**, *i*, 744.
- (14) de Groen, P.C.; Akasmit, A.J.; Rakela, J.; Forbes, G.S.; From, R.A.F. *N. Engl. J. Med.* **1987**, *317*, 861.
- (15) Lemaire, M.; Tillement, J.P. *J. Pharm. Pharmacol.* **1982**, *34*, 715.
- (16) Gardier, A.M.; Mathe, D.; Guedeny, X.; et al. *Ther. Drug Monitoring* **1993**, *15*, 274.
- (17) Arnadottir, M.; Thysell, H.; Nilsson-Ehle, P. *Am. J. Kidney Dis.* **1991**, *17*, 700.
- (18) Morton, R.E.; Zilversmit, D.B. *J. Lipid Res.* **1982**, *23*, 1058.
- (19) Wasan, K.M.; Ramaswamy, M.; Wong, W.; Pritchard, P.H. *J. Pharmacol. Exp. Ther.* **1998**, *284*, 599.
- (20) Hughes, T.A.; Gaber, A.O.; Montgomery, C.E. *Ther. Drug Monitoring* **1991**, *13*, 289.
- (21) Wasan, K.M.; Grossie, V.B., Jr.; Lopez-Berestein, G. *Antimicrob. Agents Chemother.* **1994**, *38*, 2224.
- (22) Surewicz, W.K.; Epand, R.M.; Pownall, H.J.; Hui, S.W. *J. Biol. Chem.* **1986**, *261*, 16191.
- (23) Scherphof, G.; Van Leeuwen, B.; Wilschut, J.; Damen, J. *Biochim. Biophys. Acta* **1983**, *732*, 595.
- (24) Kennedy, A.L.; Wasan, K.M. *Pharm. Res.* **1999**, submitted.
- (25) Wasan, K.M.; Morton, R.E. *Pharm. Res.* **1996**, *13*, 462.
- (26) Cassidy, S.M.; Strobel, F.W.; Wasan, K.M. *Antimicrob. Agents Chemother.* **1998**, *42*, 1878.

Chapter 31

Polymeric Lipid Nanosphere Composed of Hemocompatible Phospholipid Polymers as Drug Carrier

Kazuhiko Ishihara

Department of Materials Science, Graduate School of Engineering,
The University of Tokyo, Hongo, Bunkyo-ku, Tokyo 113-8656, Japan

The amphiphilic water-soluble polymers having phosphorylcholine group in the side chain were prepared by the polymerization of 2-methacryloyloxyethyl phosphorylcholine (MPC) with *n*-butyl methacrylate(BMA). The poly(MPC-co-BMA)s could form aggregate in water, which was confirmed from surface tension measurement of the aqueous solution. The hydrophobic compounds were solubilized in the poly(MPC-co-BMA) aqueous solution and remained stable even when the solution was stored at room temperature for more than 12 months. It is suggested that the hydrophobic parts of the MPC polymer became attracted to each other and formed an aggregate structure. According to the fluorescent spectroscopic results, the MPC polymer had a hydrophobic domain in water. The structure of the aggregate seems to be a polymeric lipid nanosphere. The physical structure of the polymer aggregate was stable even in the presence of a plasma protein. Moreover, the polymer aggregate could not activate platelets. These results indicate that the MPC polymer aggregate did not have any adverse effect on the blood components and could be used as a novel drug carrier in the bloodstream.

Molecular assemblies consisting of phospholipids, such as liposomes and lipid microspheres have the potential to carry bioactive molecules in the living organisms because of their excellent blood compatibility(1-3). Although many studies have been carried out to understand their effectiveness on the drug delivery systems, most of the efforts failed because of the lack of mechanical and chemical stability. The bioactive molecules entrapped in the inner phase easily leach out shortly after injection. Thus, the stability of these phospholipid assemblies must be improved. Polymerization of these phospholipids seems to be one of the most effective methods for this improvement(4,5). As another stabilization method of the molecular assemblies, the combination of polymers with these phospholipid assemblies has been reported(6,7).

The 2-methacryloyloxyethyl phosphorylcholine (MPC) which possesses both phosphorylcholine group and methacrylate unit can copolymerize with a hydrophobic monomer and the water-insoluble copolymers are obtained(8,9). It has already been reported that protein adsorption and platelet adhesion were suppressed even when blood contacted the surface of the MPC copolymer, that is, the MPC copolymer showed excellent blood compatibility(10-13). The blood compatibility is one of the important properties for drug carriers which are directly injected into blood stream. From these points of view, we tried to improve the solubility in water of the MPC copolymer and use it as a drug carrier for hydrophobic drugs like the lipid nanosphere.

In this report, the preparation of the water-soluble MPC copolymer with a hydrophobic moiety and evaluation of its basic properties as a hydrophobic drug carrier are reported.

Materials and Method

Materials

MPC was synthesized by the previously reported method and recrystallized from acetonitrile(8). Poly[MPC-co-n-butyl methacrylate(BMA)](PMB)s were prepared by conventional radical polymerization (8). The chemical structure of the obtained PMB, was confirmed by ¹H-NMR and FTIR spectroscopies. The composition of MPC unit in the polymer was determined by phosphorus analysis. The molecular weight was determined by size-exclusion chromatography using the Tosoh. The number-averaged molecular weight (M_n) was calculated by comparison of the elution times of the sample with the poly(ethylene oxide) (PEO) standard. The chemical structure and synthetic results of PMB are indicated in Figure 1 and Table 1, respectively. Fluorescence probes such as perylene (Pe), pyrene (Py), anilinoanthracene (AN), 1,6-diphenyl-1,3,5-hexatriene (DPH), and 1-(2-(5'-carboxyxazol-2'-yl)-6-aminobenzofuran-5-oxy)-2-(2'-amino-5'-methylphenoxy)ethane-N,N,N',N'-tetraacetic acid penta-acetoxymethyl ester (Fura 2-AM) were commercially available reagents and used without further purification. Bovine serum albumin (BSA) was obtained from Sigma Co., Ltd.

General Measurements

The surface tension of the aqueous solution of PMB with various concentrations was measured by the Wilhelmy method with DCA-100 from Orientech, Tokyo, Japan. The temperature was controlled at 22 ° C. An ¹H-NMR spectrum was obtained with a JEOL α -500 high-resonance spectrometer. The fluorescence spectrum was recorded with a FP-750 spectroscopy, JASCO, Tokyo, Japan. The circular dichroism spectrum was recorded using a J-720W, JASCO, Tokyo, Japan.

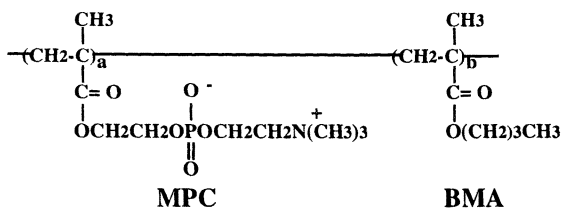


Figure 1. Structure of PMB.

Table 1. Synthetic result of PMBs

Code	Mole fraction of MPC in feed	Mole fraction of MPC in polymer ^{a)}	Yield (%)	$M_n \times 10^{-5}$ ^{b)}	Solubility in water ^{c)}
Poly(MPC)	1.0	1.0	89.2	0.80	++
PMB80	0.80	0.71	69.0	1.2	++
PMB60	0.60	0.52	61.0	1.5	++
PMB30	0.30	0.27	79.0	3.8	-
PMB30W	0.30	0.30	75.0	0.54	++

a) Unit mole fraction of MPC was determined by phosphorus analysis.

b) Estimated by size exclusion chromatography with PEO standard.

c) One milligram polymer was soluble(++) or (insoluble) in 1 mL water at 25 °C.

Solubilization of Hydrophobic Fluorescence Probe

The PMB30W was dissolved in pure water to make a 0.1 g/dL solution. An excess amount of fluorescence probe was suspended into the solution and the suspension was shaken 5 min at room temperature (about 21 ° C). The supernatant was then carefully filtered off using the Millipore filter with 0.45 μm pore diameter and the fluorescence intensity of the filtrate was measured at room temperature. The same procedure was carried out using pure water and poly(MPC) aqueous solution instead of the PMB30W solution. The fluorescence intensities of these solutions were compared to determine the solubilization ability of the PMB30W.

Measurement of Cytoplasmic Calcium Ion Concentration of Platelet

A human platelet suspension was prepared. A fluorescent probe for Ca²⁺ concentration measurement, Fura 2-AM was loaded into the platelets by incubating the platelet suspension with 5 μM Fura 2-AM in HBSS at 37 ° C for 45 min. The platelets were then washed with HBSS and resuspended in HBSS at a final concentration of 2 x 10⁸ cells/mL. The platelet suspension was recalcified, so that the external calcium concentration was adjusted to 1 mM with CaCl₂/HBSS just 5 min before the following experiment. One min after measurement, HBSS containing poly(MPC) , PMB30W, PEO, or poly(N-vinyl pyrrolidone)(PVPy) (21 g/dL, 11 μL) was added to 400 μL of the platelet suspension. The platelet suspension was excited at both 340 and 380 nm, and emission was measured at 500 nm. The change in the [Ca²⁺]_i in platelets (Δ[Ca²⁺]_i) was measured for 1 min after addition of various polymers. The bar graph show the mean value with a standard deviation, and the comparative analysis was performed using the Student's *t*-test.

Results and Discussion

Structure of PMB30W in Water

Water-solubility of the PMBs was strongly dependent both MPC unit composition and the molecular weight. Since the MPC unit was extremely hydrophilic, a polymer having about 0.7 unit mole fraction of hydrophobic BMA unit could be dissolved in water by lowering the molecular weight. The solubility of the MPC unit is quite unique compared with other non-ionic hydrophilic vinyl monomer units such as acryl amide, N-vinyl pyrrolidone.

Figure 2 demonstrates the concentration dependence of the surface tension of an aqueous solution containing poly(MPC) and PMBs. The surface tension did not change in the case of the poly(MPC) in the concentration range from 10^{-5} to 10^{-1} g/dL, that is, the same as that of pure water. On the other hand, the surface tension of the PMB aqueous solution strongly depended on the polymer concentration. Particularly, in the case of PMB30W case, it decreased from the 10^3 g/dL level and became constant over 10^{-2} g/dL. This result indicated that PMB30W in water could aggregate and form a micelle-like structure when the concentration was above 10^{-2} g/dL. The diameter of the PMB30W aggregate was 23 ± 5 nm, which was determined by a dynamic light scattering measurement at 0.01 g/dL. The PMB30W aggregates may solubilize hydrophobic compounds.

In Table 2, the ratio of the solubility of the hydrophobic fluorescent probe in water and aqueous solutions of PMB30W or poly(MPC) is summarized at the polymer concentration of 0.1 g/dL. Though every fluorescent probe tested could not dissolve in water, the solubility was increased more than 500 times in the presence of PMB30W.

To determine the interaction between the polymer chains of PMB30W in water, the $^1\text{H-NMR}$ spectra were measured at various temperatures. In Figure 3, the representative spectra of PMB30W in D_2O at 0.01 g/dL are shown. The characteristic peaks of PMB30W, that is, choline methyl in the side chain and α -methyl in the backbone were observed at 3.0-3.5 ppm and 0.5-1.5 ppm, respectively. The temperature dependence of the NMR intensity attributed to the α -methyl of the backbone versus that attributed to choline methyl in the MPC unit is shown in Figure 4. The value was almost constant in the temperature range between 20 to 60 °C, however, it significantly increased at 75 °C. The intensity of the $^1\text{H-NMR}$ signal corresponded to a functional group strongly dependent on the environment surrounding the functional group(14). If the specific functional group located on the surface of the polymeric aggregate faces the solvent, the intensity of $^1\text{H-NMR}$ signals of the functional group should be constant. On the other hand, if the functional group is located on the inside of the polymeric aggregate, the intensity of the NMR signals is weak compared with that located on the surface. Therefore, the ratio of the intensity of the NMR signals relates the functional groups located at the surface versus those located on the inside of the aggregate and represents the structure of the polymeric aggregate in the water. As shown in Figure 4, the ratio of NMR signals attributed to the choline methyl versus the α -methyl dramatically increased between 60 °C and 75 °C. This corresponded to the structure change of the PMB30W aggregates in this temperature range. The hydrophobic interaction became weak above 60 °C(15). It is considered that the structure change of the PMB30W aggregates corresponded to the decrease in the hydrophobic interactions. In other words, the dominant force for aggregation of the PMB30W molecules is the hydrophobic interactions. This is, the hydrophobic compounds can then be encapsulated and stabilized in the PMB30W aggregates.

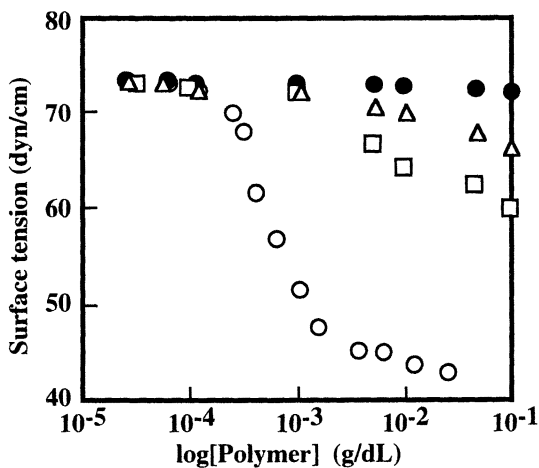


Figure 2. Surface tension of aqueous solution containing water-soluble MPC polymer. (●) poly(MPC), (△) PMB80, (□) PMB60, and (○) PMB30W.

Table 2. Solubilization of hydrophobic compounds in the PMB30W aqueous solution

Compound	Ratio of fluorescence intensity	
	PMB30W/water	PMB30W/Poly(MPC)
Py	530	80
Pe	5400	2700
AN	5800	1100
DPH	490	600

[Polymer] = 0.1 g/dL in water at room temperature.

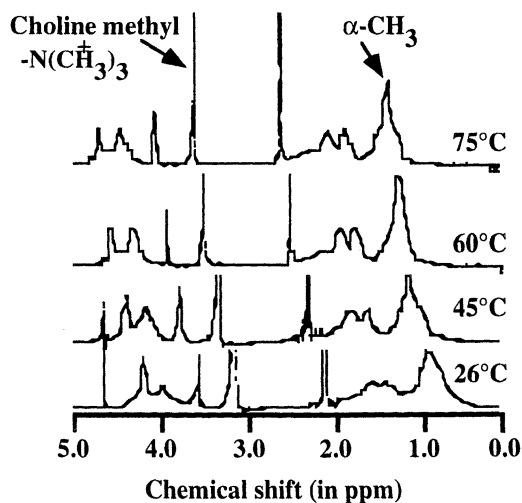


Figure 3. $^1\text{H-NMR}$ spectra of D_2O solution containing 0.01g/dL PMB30W at various temperatures.

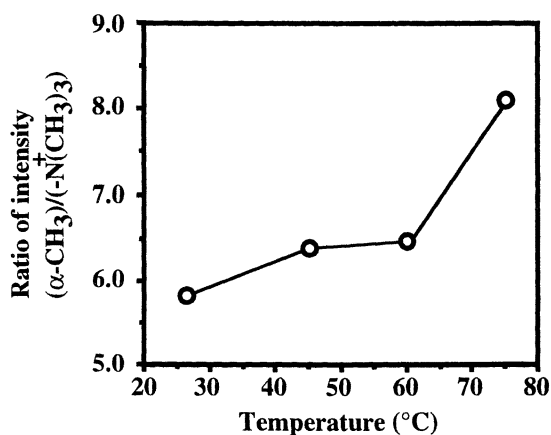


Figure 4. Ratio of $^1\text{H-NMR}$ intensity attributed to α -methyl vs choline methyl in PMB30W at various temperatures.

Solubilization of Hydrophobic Compounds with PMB30W Aggregate

The hydrophobic fluorescent probe could be solubilized in the PMB30W aggregate by stirring. Table 2 summarizes the ratio of the fluorescence intensity of the fluorescent probe in an aqueous solution of PMB30W versus that in pure water as every fluorescent probe tested here hardly dissolved in water and the fluorescence intensity was quite low. On the other hand, a strong fluorescence intensity was observed in the presence of PMB30W. That is, the amount of the fluorescent probe dissolved in water increased with the addition of PMB30W and the fluorescent probes could locate on the inside of the PMB30W aggregate. The chemical structure of the fluorescent probe did not affect the solubilization ability of the PMB30W aggregate. This result was important because the PMB30W aggregate could contain various drugs on the inside of the aggregate.

The stability of the molecular assemblies under biological conditions is important when they apply to a drug carrier.

Figure 5 shows the ratio of the fluorescence intensity of Pe solubilized in PMB30W aggregates in the presence of BSA. The fluorescence intensity did not change in the BSA range from 0 to 6 mg/mL. This BSA concentration was the 10% level of plasma because when the concentration of BSA was much higher, the fluorescence due to BSA became dominant and that of Pe could not be recognized. The physical structure of the PMB30W aggregate was maintained even in the BSA solution. As a comparison with them, the PMB30W aggregate, the polymeric lipid nanosphere, could be used as a drug carrier.

Interaction between PMB30W Aggregate and Blood Components

Hemocompatibility is one of the most important factors required for drug carriers used in the bloodstream. We have already reported that when the PMB30, which is insoluble in water, coated the polymer substrate, the surface showed protein adsorption resistive properties(11,12,16). Moreover, another water-soluble MPC polymer, poly(MPC-co-styrene) with a 0.5 MPC unit mole fraction, could stabilize the enzyme. The activity of horse-radish peroxidase (HRP) in the MPC polymer solution was maintained at the initial level even when it was stored at room temperature for 20 days(17). Under the same conditions, the activity of HRP in PBS immediately disappeared within 3 days. The reason for such stabilization is not understood at the present time. However, we considered one possibility, that is, the water structure in the MPC polymer solution is quite unique compared with other aqueous solutions containing conventional water-soluble polymers such as PVPy and PEO(18). In the case of the MPC polymer, bound water on the polymer chains was less than that on the other polymer chains. This means that the MPC polymer can mildly interact with water molecules in direct contact with phosphorylcholine groups in the MPC units. Therefore, when the MPC polymer came in contact with proteins, it could not induce denaturation of the proteins. However, many more investigations are needed to clarify this point.

Figure 6 indicates the cytoplasmic free calcium ion concentration of platelets in the presence of various water-soluble polymers including PMB30W. The

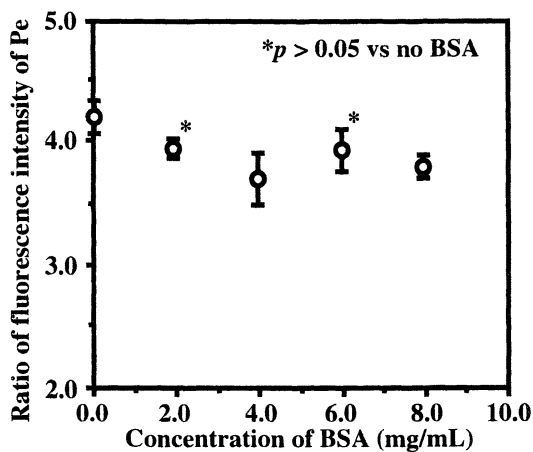


Figure 5. Relationship between concentration of BSA and fluorescence intensity of perylene solubilized in PMB30W aggregate. [PMB30W] = 0.1 wt%.

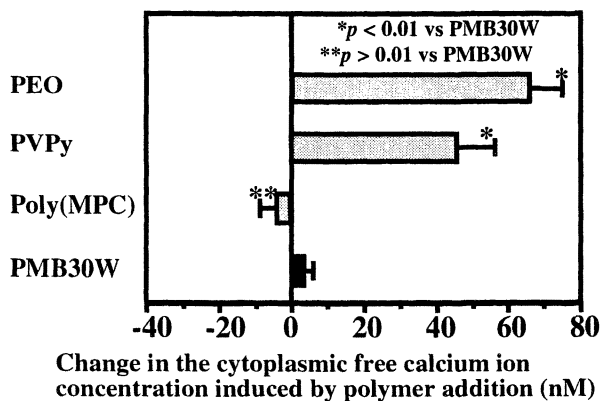


Figure 6. Change in cytoplasmic-free calcium ion concentration of platelets by addition of various water-soluble polymers.

cytoplasmic-free calcium ion concentration reflects to the degree of platelet activation(19). When the free calcium ion concentration is low, platelet activation hardly occurs. The PMB30W aggregates induced less activation of platelets compared with PVPy and PEO. We also noted that the cytoplasmic-free calcium ion concentration increased above 1000 nM by the addition of a strong activator such as thrombin(13). Every water-soluble polymer induced a small change in this value, however, it should be prevented when the polymer is used as a drug carrier in the bloodstream. Therefore, the PMB30W is a more suitable polymer for this purpose than PVPy and PEO.

Juliano et al. reported the interaction between the polymeric phospholipid liposome and platelets(20,21). The coagulation ability of the platelets did not change after the polymeric liposome composed of the phosphatidylcholine derivative was added. This means that the phosphorylcholine group has no adverse effects on the platelet functions. As shown in the NMR spectra of the PMB30W aggregate in D₂O, the surface was covered with phosphorylcholine groups. Therefore, the PMB30W aggregate cannot significantly interact with platelets.

Conclusions

A novel amphiphilic polymer composed of MPC with a phosphorylcholine group and hydrophobic BMA was prepared. The polymer, PMB30W, could be water-soluble when the molecular weight of the polymer was below 0.54×10^5 , but is still a stable aggregate even in the presence of proteins. The aggregate solubilized hydrophobic compounds and stably maintained them. Blood compatibility of the PMB30W aggregates was excellent compared with the other water-soluble polymers. These results lead us to the conclusion that the PMB30W is a promising biomaterial as a drug carrier which can be injected into the bloodstream.

Acknowledgement

This study was partially supported by the Shiseido Science and Technology Research Foundation.

References

1. Patel, H.M. *Biochem. Soc. Trans.* **1985**, 13, 513.
2. Gregoriadis, G. *Trend Biotech.* **1985**, 3, 235.
3. Mizushima, Y. *Drug Exp. Clin. Res.* **1985**, 11, 595.
4. Regen, S.L.; Aingh, S.; Oehme, G.; Singh, M. *J. Am. Chem. Soc.* **1982**, 104, 791.
5. Hub, H.H.; Hupfer, B.; Koch, H.; Ringsdorf, H. *Angew. Chem. Int. Ed. Engl.* **1982**, 19, 938.

6. Sunamoto, J.; Sato, T.; Hirota, M.; Fukushima, K.; Hiratani, K.; Hara, K. *Biochim. Biophys. Acta* **1987**, *898*, 323.
7. Ishihara, K.; Nakabayashi, N. *J. Polym. Sci., Part A: Polym. Chem.* **1991**, *29*, 831.
8. Ishihara, K.; Ueda, T.; Nakabayashi, N. *Polym. J.* **1990**, *22*, 355.
9. Ueda, T.; Oshida, H.; Kurita, K.; Ishihara, K.; Nakabayashi, N. *Polym. J.* **1992**, *24*, 1259.
10. Ishihara, K.; Aragaki, R.; Ueda, T.; Watanabe, A.; Nakabayashi, N. *J. Biomed. Mater. Res.* **1990**, *24*, 1069.
11. Ishihara, K.; Ziats, N.P.; Tierney, B.P.; Nakabayashi, N.; Anderson, J.M. *J. Biomed. Mater. Res.* **1991**, *25*, 1397.
12. Ishihara, K.; Oshida, H.; Ueda, T.; Endo, Y.; Watanabe, A. Nakabayashi, N. *J. Biomed. Mater. Res.* **1992**, *26*, 1543.
13. Iwasaki, Y.; Mikami, A.; Kurita, K.; Yui, N.; Ishihara, K.; Nakabayashi, N. *J. Biomed. Mater. Res.* **1997**, *36*, 508.
14. Ohno, H.; Seki, N.; Tsuchida, E. *Makromol. Chem.* **1984**, *185*, 329.
15. Tnaford, C.; *Hydrophobic Effect*; Wiley-Interscience: New York, 1980.
16. Ishihara, K.; Nomura, H.; Mihara, T.; Kurita, K.; Iwasaki, Y.; Nakabayashi, N. *J. Biomed. Mater. Res.* **1998**, *39*, 323.
17. Sakaki, S.; Ishihara, K.; Nakabayashi, N.; In *Advances in Polymeric Biomaterials Science*; Akaike, T.; Okano, T.; Akashi, A.; Terano, M.; Yui N., Eds.; CMC: Tokyo, 1997; p167.
18. Fukumoto, K.; Iwasaki, Y, Nakabayashi, N.; Shindo, Y, Ishihara, K. *Polym. Preprint, Jpn* **1998**, *47*, 3048.
19. Feinstein, M.B.; Egan, J.J.; Shaafi, R.I.; White, J. *Biochem. Biophys. Res. Commun.* **1983**, *113*, 598.
20. Juliano, R.L.; Hsu, M.J.; Peterson, D.; Regen, S.L.; Singh, A. *Exp. Cell. Res.* **1983**, *146*, 422.
21. Bonte, F.; Hsu, M.J.; Papp, A.; Wu, K.; Regen, S.L.; Juliano, R.L. *Biochim. Biophys. Acta* **1987**, *900*, 1.

Chapter 32

Solubility Considerations and Design of Controlled Release Dosage Forms

Gopi M. Venkatesh¹

SB Pharmaceuticals, 1250 S. Collegeville Road, Collegeville, PA 19426

The presentation describes four different approaches taken at SB for developing controlled release dosage forms. 1. A buffer-based, membrane-coated dosage form was developed for a potent anti-hypertensive agent, which has a poor solubility above pH=4 and undergoing extensive first pass metabolism on oral administration. 2. Buffer crystals were polymer coated, drug layered by a slurry process and then over-coated with a more permeable polymer blend. These capsule formulations provide *in vitro* release rates of 30-50 mg/hr for 6-8 hrs. 3. Marumerized matrix beads containing a thrombolytic agent were coated with semi-permeable and enteric polymers. Mixtures of uncoated and differently coated beads were filled into capsules, thus providing distinctly different pulsatile release profiles. 3. A novel easy-to-scale up and cost effective CR technology (capsule and bilayer tablets) based on dry granulation and Thermal Infusion Process was developed for drug substances with an aqueous solubility varying from 1 mg/ml to 1-2 g/ml. 4. Multi-tablet dosage forms based on wet granulation and membrane coating, exhibiting pulsatile release profiles are also described.

Controlled release (CR) dosage forms offer a significant potential for enhancing patient compliance and clinical efficacy, and for decreasing adverse side effects and treatment costs relative to immediate release dosage forms. Additionally, the development of novel CR technologies may extend patent protection for a product and thus provide economic value to the company. Hence, extensive research efforts have been directed toward the development of oral controlled release solid dosage

¹Current address: Eurand, 845 Center Drive, Vandalia, OH 45377.
E-mail: gvenkatesh@eurand.com.

forms for marketing of new as well as existing products. As a consequence, the know-how now exists to develop systems that can deliver most therapeutic agents, at desired rates for extended periods ranging from a few hours to a few days (1-4). These systems encompass simple matrix or film coated beads and tablets and sophisticated delivery systems such as osmotic delivery or multi-layer tablets and site-specific polymeric devices. However, the usefulness of such systems is somewhat limited by short GI transit times, permeability- and/or solubility-limited drug absorption, especially in the colon etc. Still, it appears possible to maximize therapeutic efficacy of most drugs while using simple controlled release dosage forms provided efforts are made to understand the characteristics of the drug substance (permeability, pH-dependent solubility) and dosage forms (release rate, effect of transit times), and how these impact the absorption rate, elimination rate, and plasma concentration, thereby establishing an *in vitro/in vivo* correlation. This presentation describes four novel and distinctively different approaches taken to formulate and release drugs that possess different pH dependent solubilities and moisture sensitivities. Three of the four approaches emphasize the use of multi-unit solid dosage forms, recognizing the advantages that a multi-particulate dosage form offers over a monolithic tablet formulation in terms of more consistent GI transit time, less dose dumping potential, and flexibility of blending unit dosage forms with distinctly different release profiles.

I. CR Buffer Bead Dosage Forms

A buffer-based, membrane-coated controlled release delivery system was developed for fenoldopam mesylate (5), a highly potent intravenous anti-hypertensive agent with a rapid onset of action and a short elimination half-life. Following oral administration, fenoldopam undergoes an extensive first pass metabolism, resulting in about 5% bioavailability with a marked inter-subject variability possibly due to its pH dependent solubility profile and poor absorption in the colon. The drug's solubility varies from about 10 mg/ml in simulated gastric fluid (SGF) to about 0.03 mg/ml in simulated intestinal fluid (SIF). The estimated release rate required from the CR device was 25-35 mg of fenoldopam per hour over an 8 hr period to maintain an effective blood level of 5-10 ng/ml. The *in vitro* and *in vivo* data, generated during preliminary screening experiments, on membrane-coated matrix tablets and marumerized beads, containing acidifying buffers to provide an acidic environment, suggested the need to membrane coat buffer crystals prior to drug layering in order to provide a constant acidic environment within drug loaded beads.

Membrane Coating and Drug Layering

In order to provide a constant acidic environment within the slurry coated beads, buffer crystals were membrane coated (sub-coat) with a polymer system which is less permeable under acidic conditions. A slurry coating process was developed

using an aqueous slurry of fenoldopam mesylate/PVP/buffer (solid content up to 60%) to load drug onto the membrane coated buffer crystals, and these slurry coated beads were further coated (over-coat) with a polymer system which is more permeable than the sub-coat membrane. These coating experiments were carried out using a Glatt GPCG 5/9 fluid bed granulator equipped with an expansion chamber and a 7" Wurster insert (5). The Eudragit polymers L100, S100, RLPM and RSPM were dissolved in an aqueous alcoholic solution with triethyl citrate as the plasticizer. When a coating solution containing a mixture of Eudragit RSPM and L100 or S100 was needed, the two polymers had to be separately dissolved and then blended. Tartaric acid crystals (#16 mesh) were coated with a polymer blend, Eudragit RS/S, which would severely restrict water ingress at acidic pHs, and the polymer blend, Eudragit RL/L or RS/L, which was more permeable than the sub-coat membrane system, was used for the over-coat. Initial experiments optimizing the inlet and product temperatures, flow rate, atomization pressure, fluidization level, binder level, as well as the solid content of the aqueous slurry, were carried out in order to obtain multiples-free slurry coated beads. The processed beads were filled into hard gelatin capsules.

Mechanism of Action

Water penetrates through the permeable over-coat, dissolves buffer crystals in the fenoldopam slurry coat, and then penetrates the less permeable sub-coat membrane, thus establishing micro-channels. The dissolved buffer slowly diffuses out through the sub-coat and slurry-coated fenoldopam layers. In doing so, more drug is dissolved. To provide for the decreased solubility of fenoldopam in SIF, both sub-coat and over-coat membranes were partly composed of an enteric polymer (e.g. a blend of Eudragit RL or RS with L or S polymer).

Release Profiles from Slurry-coated Beads and Conclusions

Prototype controlled release formulations were screened for dissolution profiles of fenoldopam as well as the buffer. The release of fenoldopam was monitored using validated HPLC methods and SGF as the mobile phase for the SGF samples and SIF as the mobile phase for the SIF samples (detection at @ 210 nm). The dissolution method was a two-stage procedure wherein the dosage form was released in SGF for 2 hours and then in SIF for an additional 6 hours (the media was changed every hour to minimize degradation of fenoldopam in alkaline media). The in-vitro release profiles from two prototype formulations in hard gelatin capsules, having a sub-coat of 70/30 RSPM/S100, are presented in Figure 1. These capsule formulations provide *in vitro* release rates of 30-50 mg/hr for 6 to 8 hr. The 70/30 Eudragit RSPM/L100 over-coat seems to provide more desirable release profiles for both fenoldopam and the buffer, while the 70/30 RLPM/L100 over-coat seems to provide an overall increased release of fenoldopam. In either case, the buffer release is much faster than that of fenoldopam, and the release of fenoldopam is not complete within 8 hours. There are alternate ways to achieve a faster as well as complete release of fenoldopam, which include increasing the buffer to drug ratio and using less water soluble fumaric or succinic acid crystals as the buffer. However, the technology

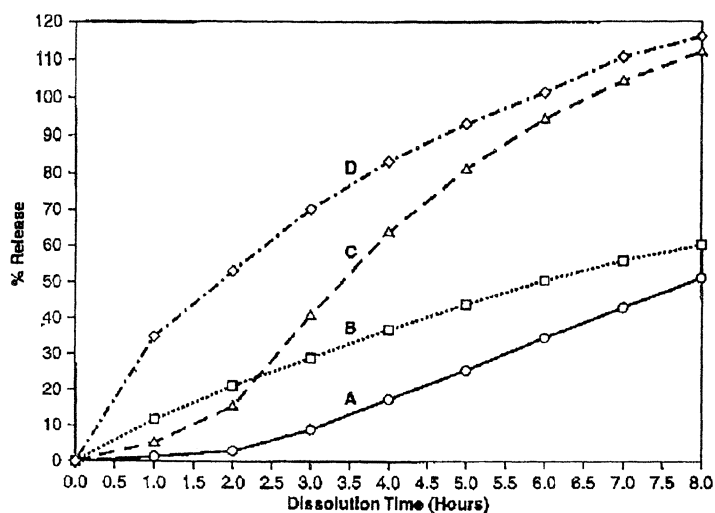


Figure 1. Release profiles from slurry-coated tartaric acid crystals: beads with 70/30 Eudragit RS/S sub-coat, buffered slurry and 70/30 RS/L over-coat [fenoldopam (A) and tartaric acid (C)], and beads with 70/30 RS/S sub-coat, non-buffered slurry and 70/30 RL/L over-coat [fenoldopam (B) and tartaric acid (D)] (Venkatesh, G.M., *Pharm. Develop. Techn.* **1998**, 3, 477 (With permission from Marcel Dekker, Inc.)).

described here using tartaric acid as the buffer will be highly useful for applying it to weakly basic drug substances with less stringent pH-dependent solubility profiles.

II. CR Marumerized Bead Dosage Forms

Membrane coated marumerized bead CR technology was applied to a potent thrombolytic antagonist (compound A), for the management of cardiovascular and renal diseases. 80-85% of the orally administered drug was absorbed, though over 90% of it was excreted unchanged with an elimination half-life of about an hour. Consequently, frequent repeated dosing of 400 mg tablets was required. Gastric and intestinal infusion studies with aqueous solutions indicated that the drug was well absorbed throughout the GI tract. A steady plasma concentration of 1 ug/ml for 12 hrs was estimated to be required for maximum therapeutic efficacy. Furthermore, the drug's aqueous solubility increases with increasing pH (0.25, 2.28 and 7.9 mg/ml at pHs of 1.2, 4.5 and 7.5, respectively).

Extrusion-Speronization and Dissolution Testing

High drug content immediate and sustained release matrix beads were manufactured using a Luwa extruder and marumerizer system. A wet granulated mass suitable for extrusion-speronization was prepared by blending, in a Hobart mixer, 80 parts of the drug, 10 parts of Avicel PH101 and 10 parts of PVP (K-30) added as a 10% solution. The wet mass was extruded using a 1.0 mm screen with constant feeder (80 rpm) and extruder (33 rpm) speeds. The extrudate was immediately processed in a spheronizer at 985 rpm for 15 min with a dusting of Avicel PH102, and beads were dried in a hot air oven at 50°C for 17 hr. #16-20 mesh beads were collected. Sustained release beads were manufactured by coating marumerized beads with Eudragit RL and L polymers or their blends using a Granu-Glatt. Beads with inherent sustained release characteristics, without a subsequent membrane coating, were prepared by replacing Avicel with a 85/15 blend of Methocel E4M/E15. Dissolution testing of bead formulations, both uncoated and coated, was performed in media of different pHs using USP Apparatus 1 (Baskets@ 100 rpm and UV detection at @272 nm).

Results and Conclusions

The uncoated and differently coated marumerized bead formulations exhibited varying pH-dependent dissolution profiles (i.e., pulsatile release profiles over a period of 3-4 hours) when tested in media with different pH values (Figure 2). In order to meet the projected b.i.d. regimen, blends of IR and differently coated beads were filled into hard gelatin capsules. Optimization of the blend compositions was intended to be done following establishment of an *in-vitro/in-vivo* correlation.

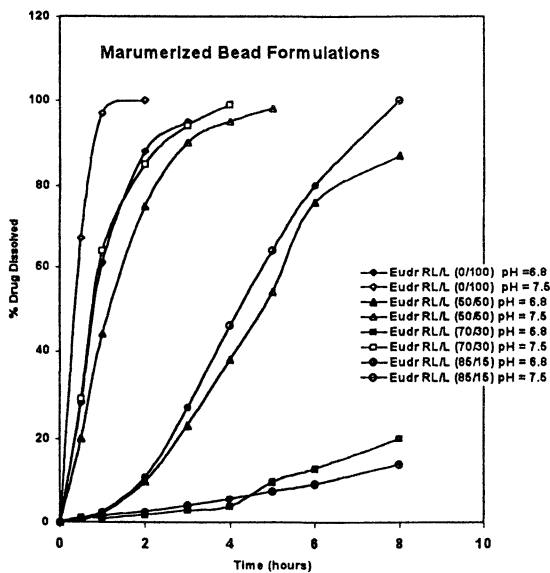


Figure 2. *In vitro* release profiles for CR marumerized bead formulations

III. CR Dosage Forms Based on Thermal Infusion Process

A novel, easy-to-scale up, and cost-effective controlled release technology (6,7) based on dry granulation and an optional thermal infusion process was developed. This technology was applied to a variety of drug substances differing widely in their aqueous solubility characteristics (e.g. aqueous solubility varying from <1 mg/ml to > 1 g/ml). A roller compaction process was found to be particularly useful for moisture- and heat-sensitive drug substances.

Roller Compaction and Thermal Infusion Process

The dry granulation process involves blending the drug substance with suitable excipients (including dissolution rate controlling matrices), roller compacting, milling the compacts thus obtained and sieving to obtain granules with desired particle size distributions. These granules are optionally subjected to thermal infusion (a mild heat treatment at 5-15°C below the melting temperature of the dissolution rate controlling matrix. The granules containing glyceryl behenate, Compritol™, a hydrophobic waxy material used as a dissolution rate controlling excipient, become more uniformly coated upon thermal infusion. In the dosage forms containing a highly water soluble polymer, such as poly(ethylene oxide), (Polyox™ WSR), the drug particles are embedded in the Polyox matrix. On contact with the dissolution medium, Polyox rapidly gels and controls the release of the active. The granules with or without the thermal treatment are filled into hard gelatin capsules or blended with additional excipients and compressed into tablets. Illustrations to follow will include bilayer and conventional tablet formulations of a combination product and capsule formulations of a freely water soluble (1-2 g/mL) compound D. The two layers of the bilayer tablet formulation was individually engineered to contain either a fairly water soluble compound B or a highly soluble compound C. The *in vitro* release from these delivery systems (tablets and capsules) is largely diffusion controlled.

In vitro/in vivo Data from Combination Products

The dissolution testing of bilayer and conventional tablet formulations (refer to Table I for formulation details) was performed in USP Apparatus 1 (baskets@ 100 rpm) in deaerated water and amounts of compounds B and C dissolved were monitored by HPLC and inductively coupled plasma (ICP) emission spectroscopy, respectively.

The release profiles for Formulas A to C are presented in Figure 3. The release of moderately water soluble compound B is slower than that of freely water soluble compound C from the bilayer and conventional tablet formulations. For example, less than 40% of compound B from Formula A was released in 8 hr while about 90% of the compound C was released by design in 6 hr. The pilot scale clinical data comparing plasma concentrations of the two compounds from three different formulations in human volunteers are presented in Figure 4.

Table I: Formulations of Compounds B and C

<i>Formula A</i>	<i>Formula B</i>	<i>Formula C</i>
Layer 1: 710mg of compound A1 mix Layer 2: 290mg of comp. B Mix	Layer 1:573mg of A3 Mix + 155mg of A granules Layer 2:290mg of B3 Mix	510mg of A3 Mix + 206.7mg of A granules + 290mg B Mix
A: Roller compacted granules of 95.67 parts of compound B, 3.33 parts of Compritol and 1.00 part of colloidal silica (Immediate Release)	B: Compression Mix consisting of TIPped blend of 148.8 parts of compound C + 141.2 parts of Compritol	
A1: Compression Mix consisting of 620 parts of A granules TIPped + 90 parts of Avicel PH102	B1: Roller compacted granules of 148.8 parts of compound C, 63.9 parts of Compritol and 2.1 part of colloidal silica	
A2: 600 parts of A granules + 20 parts of Compritol TIPped	B2: 214.8 parts of B1 granules + 53 parts of Compritol TIPped	
A3: Compression Mix consisting of 620 parts of A2 (TIPped) granules + 90 parts of Avicel PH102	B3: Compression Mix consisting of 267.8 parts of B2 (TIPped) granules + 20 parts of Avicel PH102 and 2.2 parts of magnesium stearate	

Accelerated Stability and Dissolution Data for CR. Capsule Formulations

Roller compacted granule formulations of compound D with distinctly different release profiles (about 80% in 4 hr. or 80% in 8 hr.) were developed by incorporating compound D and different ratios of HPMC E4M and Polyox WSR. The dissolution testing of these capsule formulations was performed in USP Apparatus 1 (baskets@ 100 rpm) in 900 ml of 0.1N HCl and monitored by HPLC. The marginal effect of the thermal treatment on the release profiles of the capsule formulation containing a high molecular weight (~5 M) thermoplastic polymer is evident from Table II. Polyox is known to depolymerize at accelerated temperature and humidity conditions resulting in faster dissolution rates, which can be stabilized by incorporating butylated hydroxytoluene (BHT).

IV. CR Multi-tablet Dosage Forms

Multi-tablet dosage forms are also described for orally active compound E, based on wet granulation and membrane coating, exhibiting pulsatile release profiles. The active being a mesylate salt of a dicarboxylic acid, exhibits low solubility in SGF, solubility approaching zero with increasing pH and solubility rapidly increasing with further increase in pH above pH=6.8.

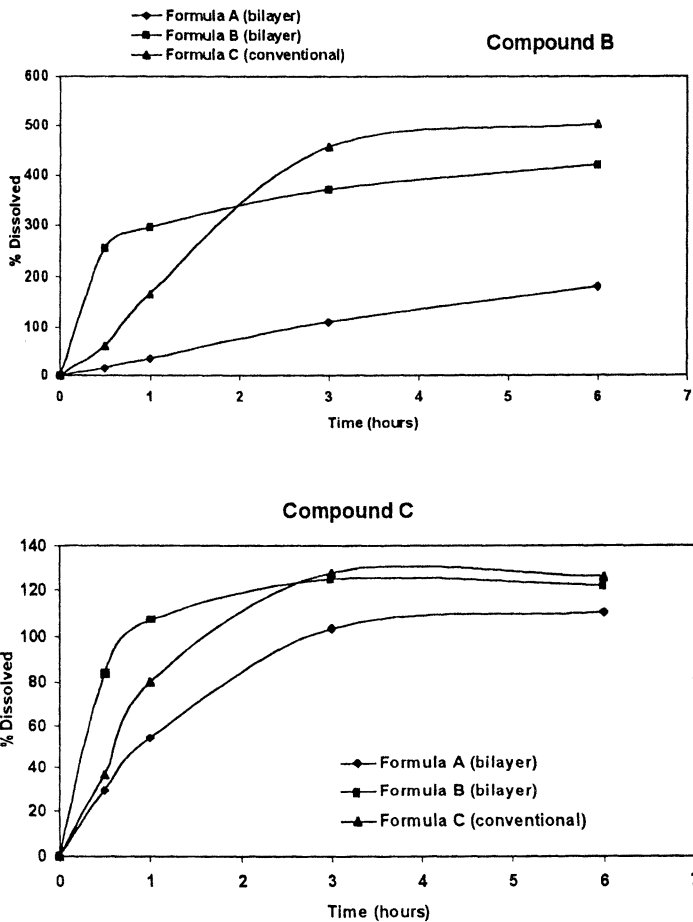


Figure 3. *In vitro* release profiles for CR bilayer and conventional tablet formulations (combination product).

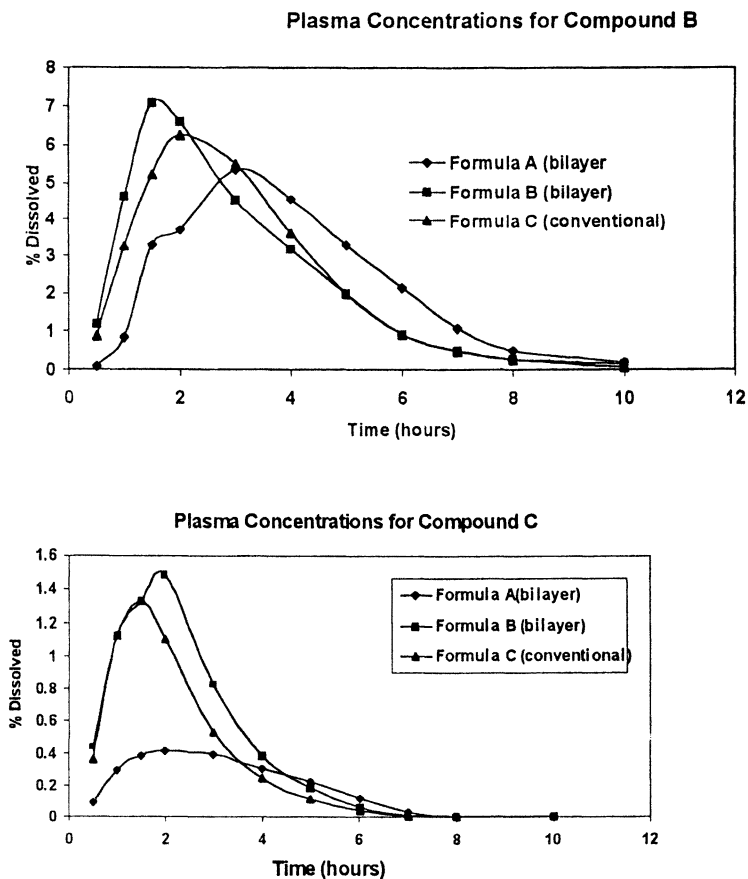


Figure 4. Plasma concentrations for CR bilayer and conventional tablet formulations (combination product).

Table II : Dissolution Profiles of Compound D

<i>Stability Condition</i>	<i>% Dissolved</i>			
	<i>1 hr</i>	<i>2 hr</i>	<i>4 hr</i>	<i>8 hr</i>
Formula A (40% Polyox/10% HPMC) UnTIPed				
Initial	29	43	59	77
30°C/60%RH, 4 mo	29	40	58	80
30°C/60%RH, 10 mo	28	42	62	88
40°C/75%RH, 4 mo	28	42	61	87
Formula B (40% Polyox/10% HPMC) TIPed				
Initial	23	35	51	73
30°C/60%RH, 4 mo	25	34	50	79
30°C/60%RH, 10 mo	29	42	60	83
40°C/75%RH, 4 mo	27	39	57	82

Manufacture of Tablet Cores and Coating

Tablet formulations based on a hydrophilic matrix system [ratio of drug to gelling polymer (85/15 Methocel E4M/Methocel E15 blend) varied from 3:2 to 3:5 and lactose and Avicel PH102 used as the soluble and wicking excipients, respectively] was developed to produce 25 and 50 mg strength tablet cores (refer to Table III for typical formulations). The drug, polymers and Avicel PH101/impalpable lactose (if present) were granulated in a high shear granulator using a 10% PVP (Povidone K-30) solution and dried in a fluid bed drier. The dry milled granules were blended with magnesium stearate and compressed into tablets

Table III : CR Tablet Formulations of Compound E

<i>Ingredient, mg</i>	<i>Formul A</i>	<i>Formul B</i>	<i>Formul C</i>	<i>Formul D</i>	<i>Formul E</i>
Intragranular					
Drug	30.60	30.60	30.60	30.60	30.60
Methocel E4M	42.68	34.53	26.01	26.01	26.01
Hydro. Lactose		4.42	19.62	5.12	
Avicel PH102					9.70
PVP (K 30)	3.50	3.50	3.50	3.50	3.50
Extragranular					
Avicel PH102				4.50	
Mag stearate	0.68	0.68	0.68	0.68	0.68

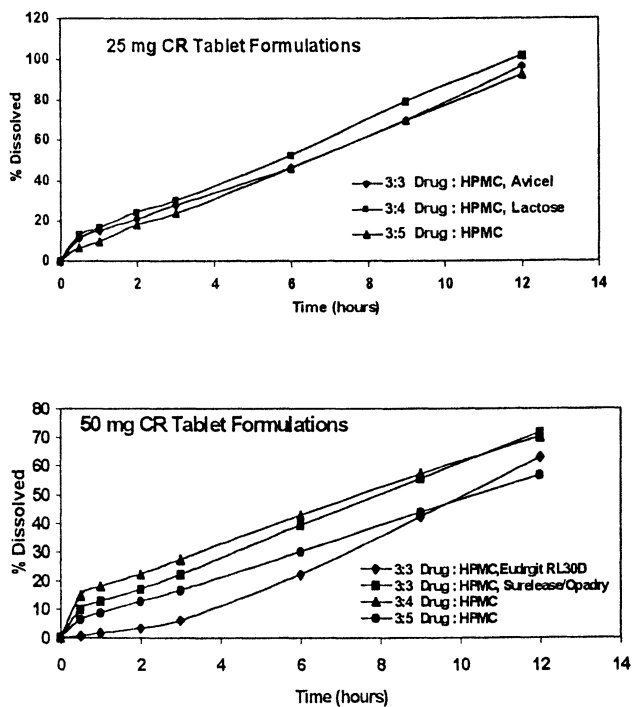


Figure 5. *In vitro* release profiles for CR matrix tablet formulations in SIF.

on a rotary tablet press. These tablets were coated with a semi-permeable EudragitRL30D or L30D or a 80/20 Surelease/Opadry White using a coating pan

Dissolution Profiles of Matrix Tablet Formulations

Dissolution testing in SGF, SIF or in SGF for 2 hr followed by testing in SIF. was performed using USP Apparatus 1 (baskets@ 100 rpm). 25 mg tablet cores of Formulas C and D were found to exhibit pulsatile release profiles. In contrast, the release profiles for 25 mg matrix tablet cores of Formulas A, B and E, presented in Figure 5 (top), indicate formulations with alternate drug to polymer ratios providing similar, almost zero-order release profiles. Figure 5 also illustrates distinctly different release profiles in SIF from 50 mg tablets, uncoated and differently coated. Opadry White in the Surelease/Opadry coating rapidly dissolved on contact with the dissolution medium producing micro-pores for the passage of the dissolved drug. The enteric polymer on the Eudragit L30D coated tablet dissolved in the medium at a pH > 6 resulting in a pulsatile release profile. Based on these and other observations, we can conclude that the multi-tablet approach would permit appropriate modulations of *in vitro* release profiles for targeting to different regions of the gastrointestinal tract to maximize therapeutic efficacy.

Conclusions

Four different approaches were presented for developing controlled release dosage forms for therapeutic agents of varying pH-solubility profiles and hydrolytic stability. The dosage forms comprise of membrane coated drug layered buffer crystals, marumerized beads, thermally treated dry granulation tablets or capsules and multi-tablets.

Acknowledgments

The author wishes to record his appreciation and gratitude to Robin Roman and Nagesh Palepu for technical discussion and for their encouragement and to several colleagues notably C. Lentine, G. Olson, R. Leposki, I. Gonzalez, J. Jushchysyn, M. McLoughlin, S. Craig who willingly provided technical support.

References

1. Banaker, U.V. *Manufacturing Chemist* **1994**, January, 14.
2. Hwang, S.J.; Park, H.; Park, K., *Critical Reviews in Therapeutic Drug Carrier Systems* **1998**, 15, p 243.
3. Ahuja, A.; Khar, R.K.; Ali, J., *Drug Develop. Ind.Pharm.* **1997**, 23, p 489.
4. Watts, P.J.; Illum, L., *Drug Deveop. Ind. Pharm.* **1997**, 23, p 893.
5. Venkatesh, G.M., *Pharm. Develop. Techn.* **1998**, 3, 477.
6. Venkatesh, G.M.; Palepu, N.R., *PharmSci Supple.* **1998**, 1, p S-207 (2557).
7. Venkatesh, G.M.; Palepu, N.R. USP 5,690,959, November 25, 1997.

Chapter 33

Polymer Therapeutics into the 21st Century

Ruth Duncan

Centre for Polymer Therapeutics, The School of Pharmacy,
University of London, 29–39 Brunswick Square,
London WC1N 1AX, United Kingdom

Polymeric drugs, polymer-drug conjugates, polymer-protein conjugates and polymeric micelles covalently entrapping drugs have been termed “polymer therapeutics”. Respectively they display inherent pharmacological activity, act as polymeric prodrugs and provide the opportunity to design targetable drug-carriers. During the last two decades polymer therapeutics have already begun to find clinical use as new anticancer therapies, as a treatment for multiple sclerosis, and they are under clinical development as an anti-AIDS therapy. Increasing awareness of the practicalities of industrial development of polymer therapeutics has led to exponential growth in this field and this will undoubtedly continue into the next century. More novel polymeric architectures (e.g. dendrimers, block copolymers and stars) will make the transition into clinical development as anticancer and antiviral polymeric drugs, and drug carriers. Completion of the ‘Human Genome Project’ in 2002, and the increased understanding of the molecular basis of disease that this will bring, will accelerate the need for safe, bioresponsive polymer constructs that can effectively facilitate intracytoplasmic delivery of the medicines of the future - peptide/poynamide drugs, antisense oligonucleotides and gene therapeutics. Moreover, it is likely that only synthetic, multicomponent polymeric systems can help turn these approaches into much needed convenient-to-use, and practical to develop medicines for routine use.

Background

The first pioneering attempts to develop pharmacologically active polymers and polymeric drug-carriers were made 20 - 30 years ago (1,2). Two factors limited successful progress at that time. First, failure to anticipate the fact that polymer heterogeneity in form, particularly dispersity of molecular weight in a given preparation, would impact the biological and toxicological activity of a polymer. And second, the fact that design of multicomponent polymer systems was almost uniquely within the domain of the polymer chemist. In the 1970s there was

relatively little input from the biological disciplines - now acknowledged to be essential for preparation of effective polymer therapeutics. In addition, the development of polymer-drug conjugates throughout the 1980s was extremely slow due to the perception that these conjugates were simply an extension of the drug delivery portfolio encompassing liposomes, immunoconjugates and microparticles. Liposomes and microparticles were the height of fashion and were seen as uncomplicated formulations that could be quickly 'reduced to practice' for both controlled drug release and targeting. This dogma undoubtedly impeded the progress of the polymer-drug conjugate into the clinic, the latter being merely viewed as the "overly complex sibling" not worthy of investment of time and money. "Nice science but too complicated to be developed"

Early enthusiasm in the fields of polymer-drug conjugates and polymeric micelles, particularly that spawned by the work of Ringsdorf and colleagues (3,4), gave birth to a number of important research programmes world-wide that have now progressed into pre-clinical development and clinical trial (5-7). Parallel studies in the 1980's investigating polymer-protein conjugates also made steady progress, and both styrene-maleic anhydride-neocarzinostatin (SMANCS) (reviewed in 8) and polyethylene glycol (PEG) - L-asparaginase (reviewed in 9,10) were approved by Regulatory Authorities in Japan and the USA respectively for routine clinical use as antitumour agents during the last decade.

This truly interdisciplinary science is now benefiting enormously from the collaborative efforts of chemistry, biology, medicine and all aspects of the pharmaceutical sciences.

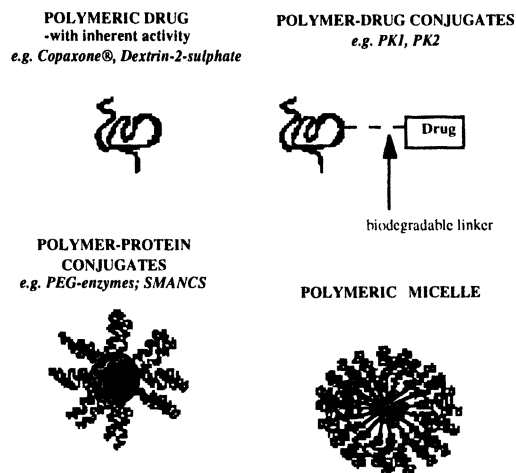


Figure 1. Schematic describing polymer therapeutics

The field encompassing polymeric drugs, polymer-drug conjugates, and polymeric micelles entrapping drugs by covalent linkage has been termed "polymer therapeutics" (Figure 1). The phrase was coined as these compounds are often considered as "new chemical entities" by Regulatory Authorities rather than a multipurpose drug delivery formulation. Today there is increased understanding that polymer therapeutics are rationally designed macromolecular drugs, prodrugs

and delivery systems, more usefully viewed as “simpler” synthetic analogues of biomolecules like immunoconjugates and fusion proteins. They are also emerging as a synthetic alternative to viral vectors. This awareness, the transfer of polymer-protein conjugates to market, and the difficulties encountered whilst developing liposomal and antibody-drug conjugates as anticancer agents (this field did not unfold as rapidly as first anticipated) has given rise to widespread confidence that significant opportunities exist for the commercialisation of polymer therapeutics, and this is predicted to grow further into the 21st Century.

Current Status

Polymeric drugs

Several polymeric drugs have already progressed through various stages of clinical development. Copaxone[®] (glatiramer acetate for injection) is a random copolymer of four amino acids now marketed in several countries as a new treatment for multiple sclerosis (11). The sulphated polysaccharide, dextrin-2-sulphate has been shown to block infection of T-cell lines by laboratory-adapted strains of HIV-1 (12) and recently dextrin-2-sulphate has shown potential in early clinical trials as an anti-AIDS treatment (13).

Polymer-drug conjugates

The polymer-drug conjugates so far most extensively studied are anticancer conjugates based on copolymers of N-(2-hydroxypropyl)methacrylamide (HPMA) (reviewed in 14,15). Four conjugates have now progressed into early clinical testing and the Phase I results obtained with HPMA copolymer-Gly-Phe-Leu-Gly-doxorubicin (PK1, FCE 28068) have recently been reported (16). We have shown that when given once every three weeks PK1 displays greatly reduced toxicity compared to free doxorubicin, and shows evidence of activity in chemotherapy refractory patients. Its maximum tolerated dose (MTD) was found to be 320 mg/m² (doxorubicin equivalent) and this is 4-5 times higher than the usual clinical dose of free doxorubicin (60-80 mg/m²). In the Phase I trial there was no evidence of the PK1-related cardiotoxicity (despite individual cumulative doses of up to 1680 mg/m² doxorubicin-equivalent), and the dose limiting toxicity was bone marrow suppression (16). PK1 is currently undergoing Phase II evaluation for treatment of breast, colon and non small cell lung cancer.

HPMA copolymer-doxorubicin containing additionally galactosamine (to mediate liver targeting) (PK2, FCE 28069) and HPMA copolymer-paclitaxel (PNU 166945) are currently undergoing Phase I/II testing (17,18) and preliminary reports suggest both have antitumour activity in man. A fourth compound has recently started Phase I evaluation, and this is an HPMA copolymer conjugate containing a camptothecin analogue (19).

The encouraging early clinical observations involving HPMA copolymers have verified capability to:-

- (i) transfer a novel polymeric carrier into man without evidence of polymer-related toxicity or immunogenicity

(ii) obtain a good correlation between the pharmacokinetics, pharmacology and toxicity of the polymer conjugates in animals and man (this in itself validates the pre-clinical biological development approach)

(iii) to design novel polymer-drug conjugates with reduced non-specific toxicity and the capacity to display antitumour activity in chemotherapy refractory patients

To help determine the clinical pharmacokinetics of PK1 and PK2 HPMA copolymer analogues were prepared that are suitable for radioiodination using [123 I] iodide or [131 I]iodide and thus can be used as probes for gamma camera imaging (20-22). These imaging analogues were the first polymeric gamma camera probes to progress to the clinic.

Polymeric micelles

Block copolymers prepared from a hydrophilic and hydrophobic block spontaneously form polymeric micelles in aqueous solution. Although the opportunities for drug delivery have long been known (23) it has taken some years to develop systems that have real clinical potential. Kataoka and colleagues (7, 24-26) have described poly(ethylene glycol-aspartate) block copolymer-doxorubicin conjugates that form micelles of 20-60 nm in diameter containing covalently attached doxorubicin and also free doxorubicin in the core. These micellar aggregates display prolonged circulation times, tumour targeting by the enhanced permeability and retention (EPR) effect and impressive antitumour activity in solid tumour models and they are currently in pre-clinical development in Japan.

Polymer therapeutics: the pharmacokinetic consequences

There are many polymer-drug and polymer-protein conjugates currently under study as potential treatments for a variety of disease indications. However, it has become clear that the *polymer component* is frequently the most important factor governing biodistribution, elimination, and metabolism of the conjugate. The only exceptions being instances where a conjugated ligand has been chosen specifically to introduce a targeting aspect to the conjugate, or when the protein drug is able to over-ride the influence of the polymer component (reviewed in 10).

Polymer conjugation to proteins (particularly PEGylation) modifies both the clinical pharmacokinetics (usually prolonging plasma circulation times), and pharmacodynamics, reduce the immunogenicity and has resulted in new forms of protein drug (of equivalent potency) that can be administered using more convenient dosing regimens. Polymer-protein drugs have the added advantage that they can be safely administered to patients exhibiting hypersensitivity reactions towards the original protein.

At the cellular level, conjugation of a low molecular weight drugs to a polymer has been successfully used to limit drug uptake to endocytic internalisation. This restricts cellular entry of drug to the lysosomotropic route (27) (Figure 2).

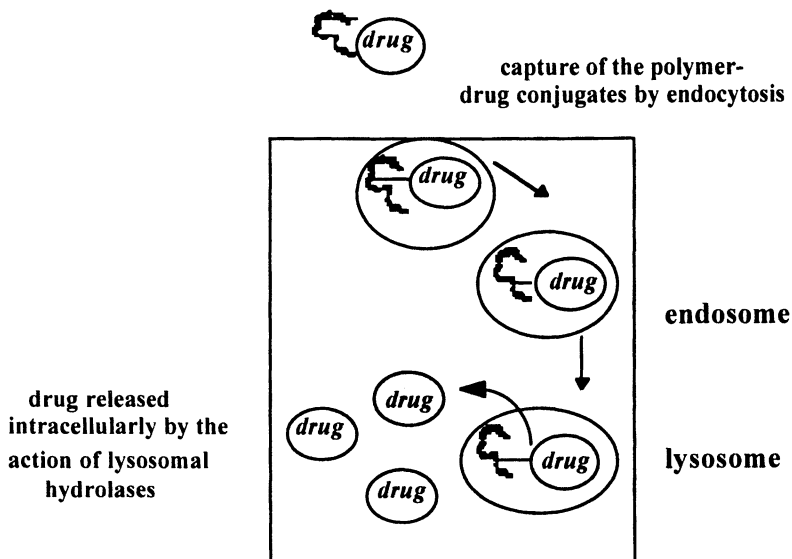


Figure 2 Schematic representation of lysosomotropic delivery

The advantages that lysosomotropic delivery bring include:-

- (i) restriction of drug uptake to endocytosis thus preventing the ubiquitous body distribution that often causes non-specific toxicity
- (ii) controlled rate of liberation of the bioactive species intracellularly by the design of an appropriate covalent polymer-drug linkage maximising pharmacological activity
- (iii) long circulation allowing either passive targeting by the EPR effect or receptor-mediated targeting after conjugate modification to include additionally a cell-specific localising ligand
- (iv) the opportunity to circumvent resistance mechanisms (like multiple drug resistance in cancer chemotherapy) by delivery of drugs via an intracellular compartment rather than by transmembrane passage (reviewed in 5)

To the Future

Challenges

As we move into the 21st Century, it is clear that polymer therapeutics are becoming an established addition to the armoury of pharmaceuticals that can be used to treat life-threatening disease. This is however just the beginning. Considerable scope remains for improved molecular engineering, and much more advanced polymer therapeutics will be needed in the future.

Many clinical challenges remain. In the UK last year cancer (in its many forms) overtook cardiovascular disease as the most common cause of mortality and it is predicted to do so in the USA within the next 3 years. Cancer, cardiovascular disease and CNS-related diseases, particularly in the ageing population, all demand effective therapy and appropriate polymer therapeutics could provide the answer. Completion of the Human Genome Project in 2002 will give further clues to the precise molecular basis of many diseases and with this information design of specific 'gene-targeted' therapeutics (including antisense and gene therapy) can only increase. Both these concepts, however, rely heavily on the existence of adequate delivery systems if they are to be successful. Another clinical area of extreme importance is the observed emergence of resistance to current therapy for common infective diseases such as tuberculosis. Targetable polymeric anti-infective agents may have a role to play here too.

In my opinion, three particularly important areas relating to polymer therapeutics will be highlighted for intensive exploration in the next few years:-

(i) second generation anticancer therapies

(ii) polymers as components of intracytoplasmic delivery systems (the totally synthetic viral vector that can be used clinically is achievable, but we are still far from an effective system that can be useful *in vivo*)

(iii) novel polymeric architectures for:- controlled drug delivery; cell-specific targeting; as vectors that can cross biological barriers as viruses so often do, and as multicompartiment microcontainers for combination chemotherapy

Tumour targeting using the EPR effect - second generation anticancer polymer therapeutics

Over the last two decades, one of the most significant advances in our understanding of tumour targeting has been the realisation that circulating macromolecular drugs, polymeric micelles and PEGylated liposomes passively localise in solid tumour tissue by the mechanism Maeda and colleagues called the EPR effect (8). Contrary to the dogma that "macromolecules and particulates cannot penetrate tumours", unambiguous evidence from many laboratories has confirmed that the hyperpermeability of angiogenic vasculature of solid tumours, combined with the decreased lymphatic drainage of tumour tissue compared to normal tissue results in significant drug targeting to tumours when using macromolecular and liposomal carriers that have a relatively long plasma residence time (comment in 28). For example, tumour : blood ratios of up to 2500 were measured in a rabbit tumour model for the polymer-protein conjugate SMANCS (29,30), and HPMA copolymer-doxorubicin conjugates display tumour accumulation ranging from 2-20% dose/g in various tumour models (31,32). The B16F10 tumour area under the curve (AUC) of HPMA copolymer-doxorubicin was 17-fold higher than seen following administration of an equi-dose of free doxorubicin (31) and due to the increased MTD of doxorubicin conjugate, higher doses could be administered resulting in increased AUC values displaying targeting of > 70-fold.

The nature and extent of EPR-mediated targeting in clinical setting will ultimately govern whether or not any polymer therapeutic will be successful in the

treatment of micrometastases, established solid tumours and of course tumours of diverse cellular origin. Clinical imaging by gamma camera or positron emission tomography (PET) is probably the only way to understand the EPR effect in patients and studies are ongoing to this end. Quantitative experiments in animal tumour models designed to calibrate the magnitude of the EPR effect in tumours at different stages of development, of different type (origin, primary, metastases) and at different locations (normal tissue environment has a part to play) are only just beginning. As are the investigations to compare the effect of polymer architecture - linear versus branched - on tumour uptake and retention to that seen for globular proteins.

Certainly, the magnitude and heterogeneity of vascular permeability in solid tumour tissue is a complex issue. It is already clearly shown using certain animal models that some tumour domains have little or no blood circulation for long periods of time and visualisation with fluorescent labelled polymers indicates polymer percolation out of vessels to be regio-dependent. In addition, larger macromolecules and larger liposomes extravasate poorly in some established tumours models (33). However, this does not detract from the many observations that show a substantial improvement in tumour drug localisation (much more than can be achieved with the parent compound) using vectors able to localise selectively by EPR targeting. Moreover, this improved targeting also correlates well with significantly improved pharmacological activity in many models.

Observation that larger (0.5 -1.0 g), longer established mouse tumours and also human xenograft tumours frequently display lower extents of EPR targeting (in the range 1-5 % dose/g) than smaller tumours (< 0.5 g) of the same type (typically 8 - 20 % dose/g) (32) suggests considerable opportunity for the use of polymer therapeutics to treat micrometastatic disease that is so often is impossible to handle with surgery, radiotherapy or conventional chemotherapy. The observed tumour-size dependency of EPR targeting also counsels caution when proposing general rules for the EPR effect using data obtained from tumours of one size and one origin.

Interestingly, in the B16F10 and sarcoma 180 tumour models it has been demonstrated that EPR-mediated targeting of HPMA copolymers is governed solely by the plasma concentration of circulating polymer across a wide molecular weight range (15,000 - 800,000 Da) (34,35). The smaller (less than ~ 40,000 Da) polymers that are excreted rapidly accumulate less well than higher Mw polymers (> 40,000 Da) which showed progressive tumour uptake that was not molecular weight dependent across a wide range. Therefore, it must be concluded that all the HPMA copolymer anticancer conjugates (Mw ~ 30,000 Da) currently undergoing clinical trial which display a plasma $t_{1/2\alpha}$ of 1-2 h in animals and man are by no means optimised in terms of their potential for tumour targeting. Although non-biodegradable PEG and HPMA copolymers cannot be safely used at higher molecular weights for fear of potential systemic accumulation leading to storage-disease syndrome toxicity, the search is already on to identify 'safe' biodegradable polymeric carriers providing greater versatility for use across a much wider molecular weight range (36). These carriers would give an opportunity to promote EPR-mediated targeting, and additionally they might provide new platforms for the delivery of drugs that require repeated (even daily) administration such as cardiovascular agents or anti-inflammatory drugs.

In the near future, polymer-anticancer systems currently in pre-clinical development are expected to enter Phase I clinical trial. These include HPMA copolymer-platinates (37), poly glutamic acid-paclitaxel (38) and a pluronic block copolymer formulation entrapping doxorubicin (39). All have potential to target tumours by the EPR effect.

Acknowledging that most cancer chemotherapy is today given as a drug combination, it is highly likely that the next decade will bring a new generation of polymeric antitumour approaches involving combinations of polymer drug conjugates (maybe some of the polymer drug conjugates already in the clinic today will simply be combined), polymer conjugates bearing two drugs on a single polymeric chain or indeed combinations of polymer-drug and polymer-enzyme. The latter concept is called polymer directed enzyme prodrug therapy (PDEPT) and administration of the polymer-enzyme 5 h after a polymer-drug conjugate has already shown ability to cleave rapidly the drug from polymer outside tumour cells providing very high localised concentrations within the tumour interstitium (40).

Bioresponsive polymers for intracytoplasmic delivery

Rational design of the first polymer therapeutics for cancer therapy has only been possible with an understanding of polymer biocompatibility, macromolecular pharmacokinetics at the whole organism level and with an understanding of endocytosis and the lysosomotropic route for drug delivery. For successful transfer of macromolecular drugs (including antisense, antigene, ribozyme, gene and peptide and protein drugs) to the cytoplasmic compartment of the cell additional biological barriers must be considered, in particular the cell membrane and the membranes surrounding endosomal and lysosomal vesicles (Figure 3). Synthetic constructs designed for intracytoplasmic delivery will, by necessity, incorporate membrane penetration features seen in natural macromolecules (toxins and transport proteins) and of courses viruses. Over the last decade many attempts have been made to identify, and lately custom synthesise, polymers that can promote cytoplasmic transfer of macromolecules, particularly DNA. Cationic polymers such as poly-L-lysine were initially chosen to promote transfection due to their ability to complex and condense anionic plasmid DNA (41,42). However, many key challenges still remain and these are the focus for intensive investigation in many groups. It is unlikely that an effective synthetic intracytoplasmic vector suitable for *in vivo* or indeed routine clinical use will emerge quickly. An optimum vector will not be identified by random screening and many excellent studies are currently investigating the structure activity relationships of polymeric materials in terms of their ability to contribute one particular function to the design of a successful "synthetic viral mimetic". It is doubtful whether a single polymer will be able to provide all the necessary attributes and more probably a multicomponent terpolymer system or supramolecular system will be needed.

Many of the essential polymer features required for a viral mimetic are common to those needed for a lysosomotropic system, but several are unique. The following checklist may provide a useful guide:-

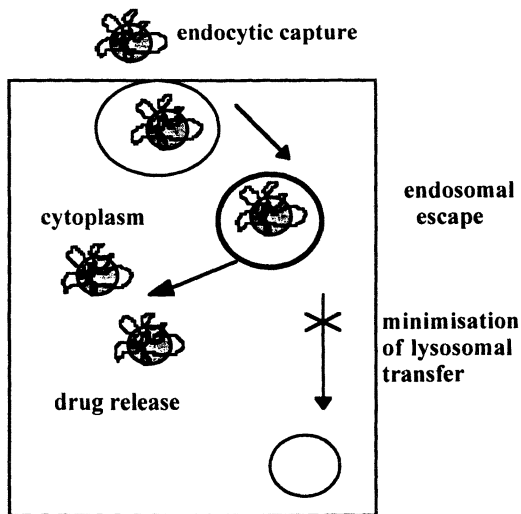


Figure 3 Schematic of synthetic intracytoplasmic delivery system

- biocompatible polymer (preferably biodegradable)
- able to carry the “drug” payload in transit
- able to protect the payload against inactivation during transport
- avoid liver and lung uptake (unless this is the target)
- target appropriate cell type
- enter the cell by endocytosis (unless trans- cell membrane passage is possible)
- ***able to exit the endosome***
- deliver (at the optimum rate) the “drug” intracellularly

And not least, as often forgotten in the academic sector, the vector must be:-

- suitable for scale-up manufacture (reproducibly)
- characterisable by validated methods

- amenable to preparation as a convenient to use formulation

One of the most interesting challenges is identification of totally synthetic polymers that can, quantitatively and rapidly elicit endosomal escape. Thus they could function a synthetic fusogenic peptide in the viral mimetic. Behr and colleagues have shown that polyethyleneimine (PEI) can breach the endosomal membrane. PEI seems to act as a 'proton sponge', and once internalised into the endosome it swells in the acidic environment inducing osmotic rupture of the vesicle (43). Together with Ferruti and colleagues, we have shown that polyamidoamines (PAAs) can be designed to cause pH-dependent membrane rupture *in vitro* (44) and *in vivo* (45). PAAs will have an interesting role to play in intracytoplasmic delivery as these biocompatible, biodegradable polymers (46) have been designed such that they are not hepatotropic after i.v. injection, and they also accumulate in solid tumours by the EPR effect (45).

It is unlikely that the viral mimetic of the future (Figure 4) will be a single polymer chain. Probably at least 3 separate components will be required and still further tailoring may be needed depending on the exact nature of the drug carried and its intended intracellular pharmacological target. Additional targeting elements might include nuclear localising sequences to assist delivery of nucleus-targeted drugs to their site of action.

Novel polymeric architectures

Synthetic chemistry provides vast scope for preparation of new materials and supramolecular systems. Comprehensive review is beyond the scope of this article, but a glance at the literature appearing monthly confirms this fact. Increased marriage of synthetic chemistry with a desire to achieve biomimicry, and to create novel biomedical materials is already beginning to accelerate the appearance of many interesting new systems. Early consideration of polymer biocompatibility and an early reflection as to the likely costs and feasibility of scale-up manufacture will ensure that

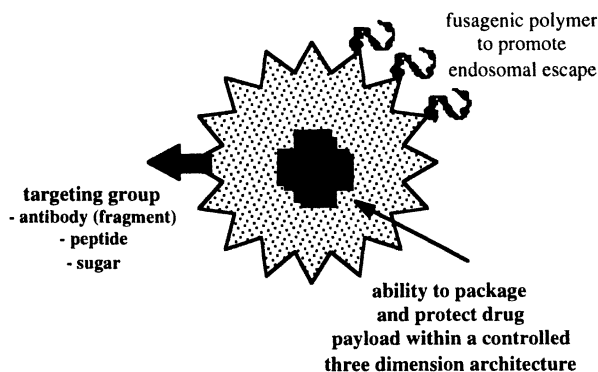


Figure 4 Schematic of a multicomponent synthetic viral vector

energy is first directed towards those systems with a realistic potential for commercialisation. All novel polymers that are water soluble, biodegradable and

that can be well tolerated in the biological environment are potential candidates for development as a drug delivery platform.

The plethora of hyperbranched polymers and dendrimers (reviewed in 47) that have appeared over the last decade afford potential advantages as polymeric drugs and drug carriers compared with the linear polymers used today. Dendrimers display narrow polydispersity, the possibility to tailor-make their surface chemistry, and the reduced structural density in the intramolecular core is amenable to host-molecule entrapment with opportunities for subsequent controlled release (48). Comparison of the cytotoxicity of several families of dendrimer *in vitro* (49) has confirmed that like other polycations cationic dendrimers are toxic and probably not suitable for i.v. administration *in vivo*. However, anionic surfaces were generally biocompatible and we selected the anionic polyamidoamine (PAMAM) sodium carboxylate dendrimer generation 3.5 (described by Tomalia and colleagues and reviewed in (50)) as a carrier for cisplatin. The resultant dendrimer platinate had a platinum loading in the range 20-25 wt%, was highly water soluble and displayed the ability to target B16F10 tumours *in vivo* by the EPR effect. This led to significant antitumour activity in this tumour model which does not respond to cisplatin at its MTD (51,52).

PAMAM dendrimers have also shown potential as gene delivery agents (53), and recently experiments conducted to examine the ability of radioiodinated PAMAM dendrimers (of different generation and surface functionality) to cross the adult rat intestine *in vitro* (54) showed that anionic PAMAM dendrimers pass to the serosal side of this tissue much faster than neutral linear polymers such as HPMA copolymers, anionic linear polymers, and indeed considerably faster than tomato lectin which adheres strongly to the mucosal surface and has often been used as an oral bioadhesive. Understanding of the potential uses of dendrimers and highly branched polymers as drug carriers for oral and systemic administration is still evolving and will undoubtedly emerge as an important area in the future.

Concluding remarks

Polymer therapeutics have come a long way. Those compounds that have successfully progressed into clinical testing, and moreover to market, have given credibility to this new field. Industry now has confidence that polymeric drugs and conjugates can be manufactured reproducibly, and is evolving sophisticated new analytical methods to characterise these complex (often supramolecular) systems.

Rational design rather than screening is the key to success. Systematic evaluation of each component is required to optimise and assemble an effective system. Much information on the structure-activity relationships of polymers in terms of their biological activity and pharmacokinetics is already available in the literature, but it should be remembered that combination of components will often change the behaviour of the system as a whole. Thus demanding ongoing refinement at each step. Reflection backwards will help design of effective new systems in the future. A new era for polymeric therapeutics is dawning!

References

1. Ringsdorf, H. *J. Polym. Sci. Polym. Symp.* **1975**, 51, 135.
2. Regelson, W. In *Water soluble polymers II*; Bikales, N., Ed.; Plenum Press: New York, **1973**; pp 161-177.

3. Gros, L.; Ringsdorf, H.; Schupp, H. *Angew.Chemie Int. Ed. Eng.* **1981**, *20*, 301.
4. Ahlers, M.; Muller, W.; Reichert, A.; Ringsdorf, H.; Venzmer, J. *Angew.Chemie Int. Ed. Eng.* **1990**, *29*, 1269.
5. Duncan, R. *Anti-Cancer Drugs* **1992**, *3*, 175-210.
6. Putnam, D.; Kopecek, J. *Adv.Polym.Sci.* **1995**, *122*, 55.
7. Kwon, G.; Kataoka, K. *Adv. Drug.Del.Rev.* **1995**, *16*, 295.
8. Maeda, H. In *Polymer Site-Specific Pharmacotherapy*; Domb, A.J., Ed.; John Wiley & Sons Ltd: New York, **1994**; pp 95-116.
9. Nucci, M. L.; Shorr, D.; Abuchowski, A. *Adv. Drug Delivery Rev.* **1991**, *6*, 133.
10. Duncan, R.; Spreafico, F. *Clinical Pharmacokinetics* **1994**, *27*, 290.
11. Lobel, R.; Riven- Kreitman, R.; Ameselent, A.; Piunchasi, J. *Drugs of the Future* **1996**; *2*, 131.
12. Shaunak, S.; Gooderham, N.I.; Edwards, R.I.; Payvandi, N.; Javon, C.M.; Baggett, N.; MacDermot, J.; Weber, J.N.; Davies, D.S. *Br. J. Pharmacol.* **1994**, *113*, 151.
13. Shaunak, S.; Thornton, M.; John, S.; Toe, I.; Peers, E.; Mason, P.; Krausz, T.; Davies, D. S. *AIDS* **1998**, *12*, 299.
14. Duncan, R.; Dimitrijevic, S.; Evagorou, E.G. *S.T.P. Pharma Sci* **1996**, *6*, 237.
15. Brocchini, S.; Duncan, R. In *Encyclopedia of Controlled Drug Delivery*; Mathiowitz, E., Ed.; Wiley: New York, **1999**, in press.
16. Vasey, P. A.; Kaye, S. B.; Morrison, R.; Twelves, C.; Wilson, P.; Duncan, R.; Thomson, A.H.; Murray, L.S.; Hilditch, T.E.; Murray, T.; Burtles, S.; Fraier, D.; Figerio, E.; Cassidy, J. *Clin Cancer Res.* **1999** *5*, 83.
17. Kerr, D.; Seymour, L.; Boivin, C.; Julyan, P.; Doran, J.; David, M.; Anderson, D.; Christodoulou, C.; Daryani, S.; Young, A.; Hesslewood, S.; Ferry, D. *Proceed. 3rd Int'l. Symp. on Polymer Therapeutics*, London, **1998**; p23.
18. Huniunk, W. B.; Terwogt, J. M.; Dubbelman, R.; Valkenet, L.; Zurlo, M.; Schellens, J.; Beijnen, J. *Proceed. 3rd Int'l. Symp. on Polymer Therapeutics* London, **1998**.
19. Caiolfa, V.R.; Zamal, M.; Fiorini, A.; Frigerio, E.; D'Argy, R.; Ghiglieri, A.; Farao, M.; Angelucci, F.; Suarato, A. *Proceed. of the Intl. Symp. on Recent Advances in drug Del. Systems*, Salt Lake City **1999**; p46.
20. Pimm, M.V.; Perkins, A.C.; Duncan, R; Ulbrich K. *J. Drug Targeting* **1993**; *1*, 152.
21. Pimm, M.; Perkins, A.; Duncan, R.; Ulbrich, K.; Strohal, J. *J. Drug Targeting* **1996**; *3*, 375.
22. Pimm, M.; Perkins, A.; Duncan, R.; Ulbrich, K.; Strohal, J. *J. Drug Targeting* **1996**; *3*, 385.
23. Horpel, G.; Klesse, W.; Ringsdorf, H.; Schmidt, B. *IUPAC Proceed. Int. Symp. on Macromolecules* Amherst Massachusetts **1982**; p346.
24. Kataoka, K.; Kwon, G.; Yokoyama, M.; Okano, T.; Sakurai, Y. *J. Cont.Rel.* **1993**; *24*, 119.
25. Kwon, G.; Yokoyama, M.; Okano, T.; Sakurai, Y. Kataoka K. *Pharm. Res.* **1993**; *10*, 970.

26. Yokoyama, M.; Fukushima, S.; Uehara, R.; Okamoto, K.; Kataoka, K.; Sakurai, Y.; Okano, T. *J. Cont. Rel.* **1998**; *50*, 79.
27. DeDuve, C.; De Barsy, T.; Poole, B.; Trouet, A.; Tulkens, P.; Van-Hoof, F. *Biochem. Pharmacol.* **1974**; *23*, 2495.
28. Muggia, F. M. *Clin. Cancer. Res.* **1999**; *5*, 7.
29. Iwai, K.; Maeda, H.; Konno, T. *Cancer Res.* **1984**; *44*, 2114.
30. Maeda, H.; Ueda, M.; Morinaga, T.; Matsumoto, T. *J. Med. Chem.* **1985**; *28*, 455.
31. Seymour, L.; Ulbrich, K.; Styger, P.; Brereton, M.; Subr, V.; Strohalm, J.; Duncan, R. *Br. J. Cancer* **1994**; *70*, 636.
32. Duncan, R.; Sat, Y. *Ann. Oncol.* **1998**; *9* (S2), 149.
33. Yuan, F.; Dellian, M.; Fukumura, D.; Leunig, M.; Berk, D.; Torchilin, V.; Jain, R. *Cancer Res.* **1995**; *55*, 3752.
34. Seymour, L.W.; Miyamoto, Y.; Brereton, M.; Styger, P.S.; Maeda, H.; Ulbrich, K.; Duncan, R. *Eur. J.Cancer* **1995**; *5*, 766.
35. Noguchi, Y.; Wu, J.; Duncan, R.; Strohalm, J.; Ulbrich, K.; Akaike, T.; Maeda, H. *Jap. J. Cancer Res.* **1998**; *89*, 307.
36. German, L.; Hirst, D.; Duncan, R. *Proceed. of the Intl. Symp. on Recent Advances in Drug Delivery Systems, Salt Lake City, USA 1999*; p212.
37. Gianasi, E.; Wasil, M.; Evagorou, E.G.; Keddle, A.; Wilson, G.; Duncan, R. *Eur. J. Cancer* **1999**; in press.
38. Li, C.; Yu, D.; Inoue, T.; Yang, D.; Milas, L.; Hunter, N.; Kim, E.; Wallace, S. *Anticancer Drugs* **1996**; *7*, 642.
39. Batrakova, E.; Dorodnych, T.; Klinskii, E.; Kliushnenkova, E.; Shemchukova, O.; Goncharova, O.; Ajakov, S.; Alakhov, V.; Kabanov, A. *Br. J. Cancer* **1996**; *74*(10), 1545.
40. Satchi, R.; Connors, T.A.; Duncan, R. **1999**; *Proceed. Intl. Soc. for Control. Rel. Bioactive Mater.* Boston **1999**; in press.
41. Wu, G.; Wu, C. *J. Biol.Chem.* **1987**; *262*, 4429.
42. Zauner, W.; Ogris, M.; Wagner, E. *Adv. Drug Del. Rev.* **1998**; *30*, 97.
43. Boussif, O.; Lezoualch, F.; Zanta, M.A.; Mergny, M.D.; Scherman, D.; Demeneix, B.; Behr, J.P. *Proc. Nat. Acad. Sci. USA.* **1995**; *92*, 7297.
44. Richardson, S. C. W.; Ferruti, P.; Duncan, R. *J. Drug Targeting*, **1999** in press
45. Richardson, S. C. W.; Mann, S.; Ferruti, P.; Duncan, R. *Proceed. Intl. Soc. for Control. Rel. Bioactive Mater.* **1999**; in press.
46. Ferruti, P.; Duncan, R.; Richardson, S., 1998. Tailor-made soluble polymer carriers. In Gregoriadis, G., McCormack, B. (eds.) *Targeting of Drugs: Stealth Therapeutic Systems* (New York: Plenum Press) pp 207-224.
47. G.R. Newkome, C.N. Moorefield and F. Vögtle, *Dendritic molecules*, VCH Publishers Inc. New York, 1996. pp 1-261.
48. Jansen, J. F. G. A.; de Brabander-van den Berg, E.M.M.; Meijer, E. W. *Science* **1994**; *266*, 1226.
49. Malik, N.; Wiwattanapatapee, R., Klopsch, R.; Lorenz, K.; Frey, H.; Weener, J.W.; Meijer, E. W.; Paulus, W.; Duncan, R. *J. Controlled Rel.* **1999**; in press.

50. Tomalia, D.A.; Esfand, R. *Chem & Ind.*, **1997**, 11, 416.
51. Malik, N.; Evagorou, E.G.; Duncan, R. *Anticancer Drugs* 1999; submitted
52. Malik, N.; Evagorou, E.G.; Duncan R. *Proceed Int'l. Symp. Control. Rel. Bioact. Mater.* **1997**, 24, 107.
53. Kukowska-Latallo, J. F.; Bielinska, A. U.; Johnson, J.; Spindler R.; Tomalia, D. A.; Baker, R, Jr. *Proc.Natl.Acad.Sci.USA*, **1996**; 93, 4897.
54. Wiwattanapatapee, R.; Carreno-Gomez, B.; Malik, N.; Duncan, R. **1998**; *J. Pharm. Pharmacol.* 50, 99.

Chapter 34

Controlled Release from Ordered Microstructures Formed by Poloxamer Block Copolymers

Lin Yang and Paschalis Alexandridis

Department of Chemical Engineering,
State University of New York at Buffalo, Buffalo, NY 14260–4200

The *in vitro* release kinetics of a low molecular weight hydrophilic drug from hydrogels consisting of Poloxamer poly(ethylene oxide)-poly(propylene oxide) block copolymer spherical micelles, and from tablets formulated from bulk (water-free) Poloxamer are reported. Sustained drug release has been achieved. Our experiments showed the drug release kinetics to depend on two contributions: (i) diffusion of the drug molecules through the water channels present in the gel microstructure ($\sim\sqrt{t}$), and (ii) release concurrent with the erosion/dissolution of the Poloxamer gel matrix ($\sim t$). The drug release profiles determined experimentally for Poloxamer hydrogels were fitted to an equation which included both a diffusion and an erosion term. The two contributions were quantified and were correlated to the apparent diffusion coefficient of the drug in the gel matrix and to the erosion rate of the gel matrix. The matrix erosion rate was measured independently, and the drug released due to the erosion effect was thus estimated. The release of hydrophilic drug from Poloxamer tablets followed closely the erosion mechanism (zero order release kinetics), however, the diffusion mechanism was still active due to the formation of a thin hydrogel layer at the tablet surface. The interplay between the self-assembled microstructures present in Poloxamer block copolymer hydrogels and the drug molecules can be utilized in controlled delivery applications.

Poloxamers (also known as Pluronic®) are triblock copolymers consisting of poly(ethylene oxide) (PEO) and poly(propylene oxide) (PPO) blocks. PEO is water-soluble (hydrophilic) while PPO is sparsely soluble in water (hydrophobic). Poloxamers are thus amphiphilic and, when present in aqueous solutions above a certain concentration (CMC: critical micellization concentration) and/or temperature (CMT: critical micellization concentration), they tend to self-assemble into spherical micelles having a hydrophobic PPO core which is “protected” by a hydrophilic PEO

corona (1). At high (e.g., >20%) concentrations, and/or above a certain temperature, Poloxamers can form hydrogels. It is now known that these "gels" are lyotropic liquid crystals and have different microstructures (based on, e.g., spherical, cylindrical or planar micelles), depending on the Poloxamer molecular weight, PEO/PPO block ratio, and Poloxamer concentration, the temperature, and the presence of additives (2).

The ability to form micelles and hydrogels renders Poloxamers useful in a variety of applications (3). A number of Poloxamers have been approved for pharmaceutical use. Poloxamer micelles can be used, e.g., as drug delivery vehicles, with the drug molecules solubilized in the hydrophobic PPO core. Encouraging results have been reported where the entrapment of peptide and protein drugs into Poloxamer micellar microcontainers reduces toxicity, prolongs their residence time, and protects them against degradation (4,5). Poloxamer hydrogels have also been used as an artificial barrier in transdermal drug delivery, taking advantage of their reverse thermal gelation property (i.e., a gel forms from a liquid solution upon increasing the temperature) and the improved diffusivity of the drug in the Poloxamer gel due to the presence in the gel microstructure of continuous water channels (6,7). Sustained release and improved bioavailability have been reported in Poloxamer-based ocular or intranasal delivery systems, resulting from their strong bioadhesiveness and prolonged clearance time (8).

The kinetics of drug release from the Poloxamer matrix is a central issue in all applications of Poloxamers in drug delivery systems. In vitro zero-order (i.e., linear function of time) release of both small-molecule (9) and protein (4) drugs from Poloxamer hydrogels into aqueous surroundings has been reported. At the same time, drug release which is linear to the square root of time (10) has been observed in many studies which utilized isopropylmyristate (IPM), a solvent used to emulate the properties of skin, as the receptor phase. It has been recognized that the drug release kinetics can be affected by the physicochemical properties (such as pKa) of the drug, as well as by the properties of the Poloxamer gel (such as the Poloxamer concentration and the presence of additives (11)). However, very few investigations have addressed the mechanism of drug release from Poloxamer gels, taking into account the fact that these gels are well organized lyotropic liquid crystals, and recognizing that this microstructure can affect the drug release.

We have carried out extensive studies characterizing the formation of Poloxamer micelles (12), the solubilization in such micelles (13), and the microstructure of Poloxamer gels under equilibrium conditions (14), and have recently examined the kinetics of Poloxamer gel formation and dissolution (15). In this context, we have observed that, following the penetration of water in bulk Poloxamer, the block copolymer molecules self-assemble into different lyotropic liquid crystalline structures according to the water concentration gradient; these hydrogels swell with water linearly to the square root of time (15). Water-soluble drug molecules present in Poloxamer hydrogels (or in bulk Poloxamer tablets) can be released in the aqueous solution via diffusion through the free water channels present in the gel, or via the erosion (dissolution) of the Poloxamer gel matrix (16). While physico-chemical properties of the drug, such as solubility, partition coefficient, and size, always play an important role on the apparent release kinetics, we expect the gelation and dissolution properties of the Poloxamer to contribute to, and even control the release kinetics.

In the present study we report the *in vitro* release kinetics of a low molecular weight hydrophilic model drug, caffeine, from Poloxamer hydrogels and from tablets formulated from bulk (initially water-free) Poloxamer. The contributions to the release kinetics of the diffusion of the drug molecules out of the gel and of the erosion (dissolution) of the Poloxamer matrix have been quantified. The release characteristics of the gels are contrasted to those of the tablets.

Materials and Methods

Materials

The Pluronic F127 (Poloxamer 407) poly(ethylene oxide)-poly(propylene oxide)-poly(ethylene oxide) block copolymer was a gift from BASF Corp. Pluronic F127 has a nominal molecular weight of 12600 and 70% PEO content. The polymer is available as flakes (part of the PEO is in crystalline form at room temperature). Ethyl acetate, acetone, and cobalt nitrate 6-hydrate were purchased from J. T. Baker, and Ammonium thiocyanate from Fisher Scientific. Caffeine (of purity more than 99.9%) was purchased from Sigma. Water of Milli-Q quality was used in all experiments.

Preparation of Poloxamer Hydrogels

An appropriate amount of caffeine was dissolved in water at room temperature. Bulk Pluronic F127 was then mixed with the aqueous caffeine solution to obtain the desired Poloxamer weight percentage. The mixture was left in a refrigerator (4 °C) for two days (with occasional stirring) until a clear homogeneous liquid solution was obtained. The caffeine-loaded aqueous Poloxamer solution was then poured into a cylindrical mold with a 0.68 cm height and a 1.17 cm radius. A strong gel formed in less than 5 minutes when the Poloxamer water solution was placed into a chamber thermostated at 37 °C. The microstructure of this hydrogel consists of spherical block copolymer micelles (of radius of about 10 nm) packed in a cubic lattice (17).

Preparation of Poloxamer Tablets

A homogeneous mixture of caffeine and Pluronic F127, with 20 wt% dispersed caffeine loading and a total Poloxamer + caffeine weight of about 1 g, was placed into a tablet mold with a 1.3 cm radius, and was compressed using a manual press under 2500 pounds of pressure for 2 minutes. The height of the resulting tablet was about 0.75 cm. The density of the tablet was approximately 0.97 g/mL (for comparison, the density of the bulk block copolymer is 1.04 g/mL).

Release Experiments

In vitro release studies of caffeine from Poloxamer hydrogels or tablets were conducted in beakers containing 300 mL water for the gels (and 500 mL water for the tablets) at 37 °C. The stirring rate was 20 rpm, controlled by a Barnant series 20 mixer located 2 cm above the gel (or tablet) surface. The Poloxamer gels/tablets were fixed at the bottom of the dissolution cell with only one side exposed to the aqueous medium. 10 mL samples of the solution were removed at certain time intervals (to

determine the caffeine concentration), and equal amounts of water were added (to keep the total solution volume constant). The amount of caffeine present in the aqueous solution was detected at 272.5 nm using a Beckman DU-70 spectrophotometer.

Assay of Poloxamer Concentration (18)

A series of Pluronic F127 aqueous solutions were prepared, with Poloxamer concentrations ranging from 0.01 to 0.08 wt%. A cobalt thiocyanate reagent (dye solution) was prepared by dissolving 4.6 g of cobalt nitrate 6-hydrate and 20 g of ammonium thiocyanate in 100 mL water. 0.5 mL of a Pluronic F127 solution, 0.5 mL cobalt thiocyanate dye solution, and 1.5 mL ethyl acetate were mixed well in a 14 mL centrifuge tube, and were then centrifuged for 10 min at 12000 rpm, using a Sorvall RC-5B Refrigerated Superspeed Centrifuge, DuPont Instruments. After the centrifugation, the upper two layers were aspirated by a pipette, without disturbing the pellet that was formed by the Pluronic and dye complex. The pellet and the centrifuge tube were washed with about 5 mL ethyl acetate and were then centrifuged for 4 min at 10500 rpm. This washing-centrifugation process was repeated five times, until the aspirated ethyl acetate became colorless. The pellet was then dissolved in 1.5 mL acetone and the absorbance was measured at 333 nm using a Beckman DU-70 spectrophotometer. A calibration curve of absorbance vs Pluronic F127 concentration was thus obtained. The Pluronic F127 concentrations of the samples withdrawn during the release experiments were measured following the above procedure.

Measurement of Caffeine Partition Coefficient in Poloxamer Micelles (19)

The partition coefficient of caffeine between the F127 micellar (S_m) and aqueous phases (S_w) was determined from the ratio of the caffeine solubility in a micellar solution to that in an aqueous solution. In this study, excess amount of caffeine was added to pure water and to a series of aqueous Pluronic F127 solutions with F127 concentrations ranging from 0.01 to 15 wt% at 23 °C. Following an equilibration period of about one month, the undissolved caffeine was separated from the saturated solution by filtering twice with paper filter. The solubility of caffeine in the saturated solutions was measured by UV at 272.5 nm.

Results and Discussion

Partition Coefficient of Caffeine in Pluronic F127

Caffeine is a non-charged low-molecular weight (194.19) molecule with relatively good water solubility, 1 g in 46 mL water at room temperature (20). The release of drug from the hydrogel can be a result of diffusion of the drug molecules through the aqueous domains present in the hydrogel structure, or a consequence of the erosion (dissolution) of the gel matrix. Therefore, the location of the caffeine molecules in the Poloxamer hydrogel will affect the drug release mechanism. If the majority of the caffeine molecules were to partition into the hydrophobic core of the Poloxamer micelles, then the diffusion mechanism would be insignificant due to the very small

amount of caffeine dissolved in the water channels occurring between adjacent micelles in the Poloxamer hydrogel. In this case, the caffeine would be released in the solution primarily due to the erosion of the Poloxamer gel matrix. On the other hand, if most caffeine molecules were present (dissolved) in the water channels of the Poloxamer gel and the partition of caffeine in the micelles was negligible, then the release mechanism of caffeine would be controlled both by the diffusion of caffeine molecules through the water channels, and by the release of caffeine concurrent with the erosion of Poloxamer gel matrix (see Figure 1).

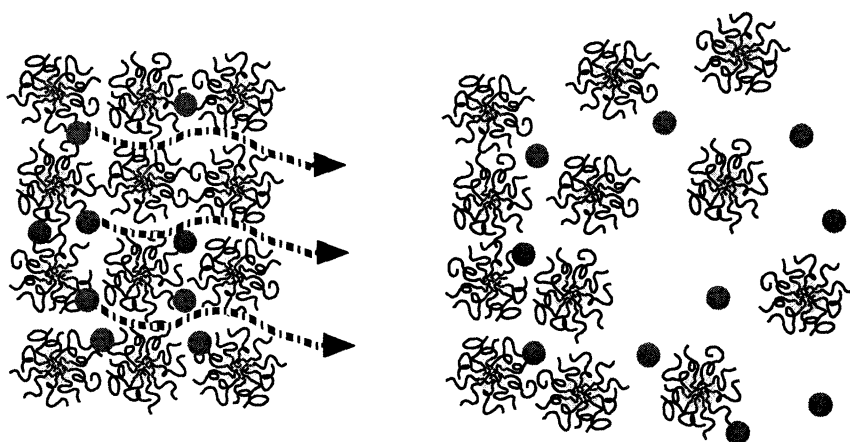


Figure 1. Schematic of diffusion (left) and erosion (right) release mechanisms of a hydrophilic drug from Poloxamer hydrogels.

In order to elucidate the above, we measured the solubility of caffeine in aqueous Pluronic F127 solutions and compared it to the caffeine solubility in plain water. From Figure 2, where the caffeine solubility is plotted vs the F127 concentration, we can see that the caffeine solubility remained almost independent of the F127 concentration, up to about 12 wt% F127. When the F127 concentration was increased further to 15%, the caffeine solubility decreased to some extent. This is most likely a result of the decrease in the amount of water available for solvation of the drug. As shown in Figure 1 (filled circles), when the caffeine solubility is expressed in terms of only the water present in the solution, then the solubility values at high F127 content approach those observed at low F127 contents. From the fact that the caffeine solubility in the Pluronic F127 solution remained independent of the F127 concentration, we can conclude that the partition of caffeine into the hydrophobic micellar core is negligible. Therefore, both diffusion and erosion mechanisms need to be considered in the release of caffeine from the Poloxamer hydrogels.

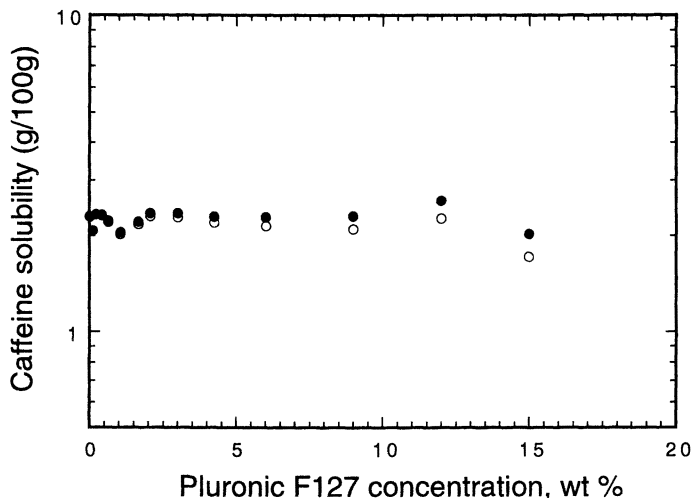


Figure 2. Caffeine solubility vs Pluronic F127 concentration: (o) caffeine solubility in aqueous F127 solution expressed in terms of the overall (caffeine + water) solution content; (•) caffeine solubility expressed in terms of only the water amount.

Diffusion and Erosion Mechanisms of Controlled Release

In order to describe the release of caffeine from the Pluronic gel, and to ascribe our observations to the diffusion and erosion mechanisms, we utilized the following expression (16):

$$A = M_1 + M_2 t^{1/2} + M_3 t \quad (1)$$

Here, A is the amount of caffeine (per unit area) released from the gel matrix, and M_1 , M_2 and M_3 are constants. In this model, the first term accounts for the retardation of the drug release due to the induction time needed for the polymer disentanglement. The second term describes the Fickian-type (first order) diffusion of drug from the Pluronic hydrogel. The third term results from the (zero order) release of the drug upon the erosion/dissolution of the gel matrix.

According to a model proposed by Higuchi (23), the constant of the diffusion term, M_2 , can be expressed as:

$$M_2 = 2 C_0 (D_{app} / \pi)^{1/2} \quad (2)$$

where C_0 is the initial caffeine concentration in the gel matrix, and D_{app} is the apparent diffusion coefficient of caffeine in the gel matrix.

The erosion/dissolution term of Equation 1, M_3 , can be related to the dissolution rate of gel matrix, and can be expressed as:

$$M_3 = C_0 k / C_{p0} \quad (3)$$

where C_0 is the initial caffeine concentration in the gel matrix, C_{p0} is the Poloxamer concentration in the gel matrix, and k is the dissolution rate constant of the gel matrix. k can be obtained independently from the caffeine release, by measuring the change of Poloxamer concentration in the dissolution medium.

Controlled Release of Caffeine from Poloxamer Hydrogel

Representative data for the release of caffeine from Poloxamer hydrogels are shown in Figure 3, where the amount of released caffeine per unit area is plotted vs time for a 20 wt% Pluronic F127 gel with 2.2% caffeine dissolved. The drug release achieved was almost immediate ($M_1 \approx 0$). In the Poloxamer hydrogel, the block copolymer molecules are already solvated and arranged in spherical micelles that actually repel each other. So, given the opportunity (i.e., the driving force originating from the concentration gradient), these micelles are immediately released in the solution, together with the accompanying drug.

The caffeine release profile in the experiment shown in Figure 3 obviously deviates from the zero-order kinetics. The microstructure of the Poloxamer hydrogels which we studied is based on block copolymer micelles arranged in a liquid crystalline lattice which allows domains of free water to be present between adjacent micelles (2). This lyotropic liquid crystalline structure makes it possible for small drug molecules with relatively high water solubility, such as caffeine, to diffuse out from the gel matrix. As a result, diffusion is an important mechanism and manifests itself in the release profile of Figure 3. Meanwhile, the solvated block copolymer micelles which make up the hydrogel can dissolve into the aqueous solution. Caffeine present in the gel matrix will then be released concurrently with the disintegration of gel matrix. Consequently, in the release of low molecular weight hydrophilic drugs from Poloxamer hydrogels we expect to have both diffusion and erosion. The caffeine release profile obtained from the experiment of Figure 3 can be fitted nicely ($R = 0.9999$) to Equation 1 which considers both diffusion and erosion effects.

The dissolution rate constant (k) of 20 wt% F127 gel containing 2.2% dissolved caffeine was obtained by determining the concentration of Pluronic F127 in the dissolution medium over the course of the dissolution experiment. The amount of caffeine released due to the dissolution of F127 matrix was estimated from Equation 3, under the assumption that the caffeine amount in the gel matrix remained constant during the dissolution process. The caffeine release profile which can be attributed to the erosion of the gel matrix is also plotted in Figure 3. The amount of caffeine released due to the F127 gel matrix erosion is up to 40% smaller than the measured

overall caffeine release. This result indicates that during the release process of caffeine from a Pluronic hydrogel, the diffusion of caffeine from the gel matrix through the water channels is an active mechanism and makes significant contributions. Moreover, with the diffusion of caffeine from the gel matrix, the caffeine concentration remaining in gel matrix will decrease with time. Thereby, the assumption of constant caffeine concentration would lead to an over-estimation of the erosion contribution, especially at the later stages of the gel matrix dissolution process (where from the two curves shown in Figure 3 it appears that the erosion becomes more dominant).

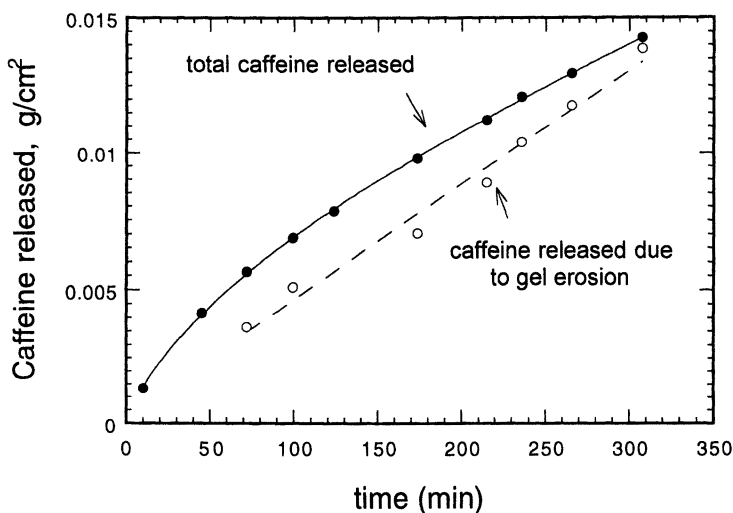


Figure 3. Caffeine release profile from 20 wt% Pluronic F127 hydrogel with 2 wt% dissolved caffeine. Fitting of the caffeine release data to Equation 1 results in the expression: $A = -0.0008 + 0.000655 t^{1/2} + 0.0000117 t$.

The apparent diffusion coefficient of caffeine in the 20 wt% F127 hydrogel matrix was obtained from the fitting of the caffeine release profile to Equation 1, and then from relating the constant M_2 to the apparent diffusion coefficient, based on Equation 2. The caffeine diffusion coefficient is thus estimated to $1.15 \cdot 10^{-5} \text{ cm}^2/\text{s}$. This result is much higher than the $8.2 \cdot 10^{-10} \text{ cm}^2/\text{s}$ caffeine diffusion coefficient reported for ethyl cellulose dry film with 20% plasticizer (24). The high caffeine diffusion coefficient observed in the Pluronic hydrogel matrix can be attributed to the high (80%) water content and to the well defined liquid crystalline structure which allows the free dissolved caffeine to diffuse out more easily. The $1.15 \cdot 10^{-5} \text{ cm}^2/\text{s}$ diffusion coefficient measured in this study for caffeine is comparable to the $0.755 \cdot 10^{-5} \text{ cm}^2/\text{s}$ diffusion coefficient reported for diclofenac sodium in a 20 wt% F127 hydrogel (6).

It is notable that, under our experimental conditions, it took more than 5 hours to totally release all of the caffeine loaded in 1 gram of 20 wt% F127 hydrogel. This shows the potential of Poloxamer hydrogels as a sustained drug delivery system.

Controlled Release of Caffeine from Poloxamer Tablet

An alternative formulation of caffeine involves its compounding with water-free flake-like Poloxamer. A representative release profile of caffeine from such a tablet formed by bulk Pluronic F127 is shown in Figure 4. The overall release profile follows closely zero order kinetics, indicating the dominance of the erosion mechanism in the drug release process. However, Equation 1, which includes a diffusion term, still provides the best fit to the experimental data.

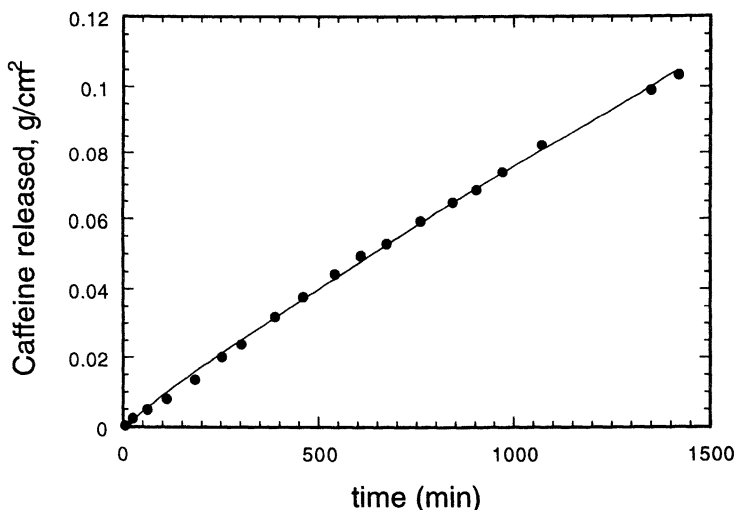


Figure 4. Caffeine release profile from Pluronic F127 tablet loaded with 20 wt% dispersed caffeine. Fitting of the caffeine release data to Equation 1 results in the expression: $A = -0.0024 + 0.00051 t^{1/2} + 0.000062 t$.

When a Poloxamer water-free tablet is placed into an aqueous solvent, water penetrates into the bulk block copolymer, the PEO and PPO blocks of the block copolymer segregate (one being water-soluble and the other not), and the block copolymers self-organize into regions of different lyotropic liquid crystal microstructure which is a function of the local water concentration (14,15). A Poloxamer hydrogel layer is thus formed *in situ*, and simultaneously dissolves into water. From our previous static dissolution studies (15), we found that the gel layers

became more extensive with the progress of dissolution time, and their widths were proportional to the square root of time. The development of these gel layers is controlled by two competing factors: (i) the dissolution (erosion) of the gel matrix adjacent to the solution, which consumes the gel layer, and (ii) the transfer of Poloxamer from the bulk water-free state into the hydrogel, which causes the hydrogel layer to grow to the expense of the bulk polymer.

Under conditions of stirring, the dissolution of the gel matrix is accelerated, thereby the thickness of the gel layer in the current tablet experiments is smaller than what we had observed in the static dissolution experiments (15). The near-zero order release from the Poloxamer tablet shown in Figure 4 results from the dominant erosion effect of the Poloxamer gel matrix in the presence of the solvent. The diffusion mechanism is still present, but becomes less important due to the thinner gel layer; thereby smaller amounts of caffeine are available for the diffusion process.

Conclusions

Sustained drug release can be achieved from formulations based on Poloxamer poly(ethylene oxide)-poly(propylene oxide)-poly(ethylene oxide) block copolymers which can form hydrogels consisting of close-packed spherical, cylindrical or planar micelles.

The release of a hydrophilic low-molecular weight drug from Poloxamer lyotropic liquid crystalline hydrogels or from bulk (initially water-free) Poloxamer tablets is based on the combination of two contributions: (i) diffusion of the drug molecules through the water channels present in the hydrogel structure, which is a linear function of \sqrt{t} , and (ii) release of the drug concurrent to the erosion/dissolution of the Poloxamer gel matrix, which is a linear function of t . The release profile of such drugs fits very well to the model proposed in Equation 1 which includes both a diffusion term and an erosion term.

By comparing the caffeine released due to matrix erosion to the overall amount of caffeine released, we provide evidence that the diffusion of caffeine from the Poloxamer hydrogels has an important contribution to the overall release process. In the Poloxamer tablet formulation, the diffusion contribution becomes less important due to the much thinner gel layer formed during the tablet dissolution process. The release kinetics of caffeine from Poloxamer tablets are almost zero-order (erosion controlled).

This study aims in understand the drug release from block copolymer lyotropic liquid crystal structures in the context of the diffusion and erosion mechanisms. Hydrophilic or hydrophobic drugs, small or big molecules, and colloidal particles such as proteins and peptides, are expected to have different release profiles due to the different contributions of these two mechanisms. The dissolution conditions, such as temperature, solvent and stirring/shear rate, also have important effects on the release of drug from Poloxamer formulations. These subjects are currently under investigation in our laboratory. The aim is to utilize the interplay between the drug molecules and the self-assembled microstructures into controlled delivery applications.

Literature Cited

1. Alexandridis, P.; Hatton, T. A. *Colloids Surf.* **1995**, *96*, 1-46.
2. Alexandridis, P. *Curr. Opin. Colloid Interface Sci.* **1997**, *2*, 478-489.
3. Alexandridis, P. *Curr. Opin. Colloid Interface Sci.* **1996**, *1*, 490-501.
4. Wang, P. L.; Johnston, T. P. *Int. J. Pharm.* **1995**, *113*, 73-81.
5. Katakam, M.; Ravis, W. R.; Banga, A. K. *J. Controlled Release* **1997**, *49*, 21-26.
6. Mohamed, F. A. *Pharma Sciences* **1995**, *5*, 456-460.
7. Lu, G.; Jun, H. W. *Int. J. Pharm.* **1998**, *160*, 1-9.
8. Zhou, M.; Donovan, M. D. *Int. J. Pharm.* **1996**, *135*, 115-125.
9. Desai, S. D.; Blanchard, J. *J. Pharm. Sci.* **1998**, *87*, 226-230.
10. Chi, S. C.; Jun, H. M. *J. Pharm. Sci.* **1991**, *80*, 280-283.
11. Paavola, A.; Yliruusi, J.; Rosenberg, P. *J. Controlled Release* **1998**, *52*, 169-178.
12. Alexandridis, P.; Holzwarth, J. F.; Hatton, T. A. *Macromolecules* **1994**, *27*, 2414-2425.
13. Hurter, P. N.; Alexandridis, P.; Hatton, T. A. *Surfactant Sci. Ser.* **1995**, *55*, 191-235.
14. Alexandridis, P.; Olsson, U.; Lindman, B. *Langmuir* **1998**, *14*, 2627-2638.
15. Yang, L.; Alexandridis, P. *Polym. Prepr.* **1999**, *40*, 349-350.
16. Harland, R. S.; Gazzaniga, A.; Sangalli, M. E.; Colombo, P.; Peppas, N. A. *Pharm. Res.* **1988**, *5*, 488-494.
17. Holmqvist, P.; Alexandridis, P.; Lindman B. *J. Phys. Chem. B* **1998**, *102*, 1149-1158.
18. Ghebeh, H.; Handa-Corrigan, A.; Butler, M. *Anal. Biochem.* **1998**, *262*, 39-44.
19. *Merck Index*, Merck Research Laboratories, Merck & Co., Inc., NJ, **1996**.
20. Suh, H.; Jun, H.W. *Int. J. Pharm.* **1996**, *129*, 13-20.
21. Robinson, J. R. *Sustained and Controlled Release: Drug Delivery Systems*, Marcel Dekker, New York, **1975**.
22. Park, K. *Controlled Drug Delivery: Challenges and Strategies*, American Chemical Society, Washington DC, **1997**.
23. Higuchi, W. I. *J. Pharm. Sci.* **1962**, *51*, 802-804.
24. Siepmann, J.; Ainaoui, A.; Vergnaud, J. M.; Bodmeier, R. *J. Pharm. Sci.* **1998**, *87*, 827-832.

Chapter 35

Supramolecular-Structured Polymers for Drug Delivery

Tooru Ooya and Nobuhiko Yui¹

School of Materials Science, Japan Advanced Institute of Science
and Technology, 1-1 Asahidai, Tatsunokuchi, Ishikawa 923-1292, Japan

Polyrotaxanes as a supramolecular-structured polymer were characterized aiming at a drug carrier, a drug permeation enhancer, an implantable material, and a stimuli-responsive material. Biodegradable polyrotaxanes exhibit their supramolecular architectures: many α -cyclodextrins (α -CDs) are threaded onto a single poly(ethylene glycol) (PEG) chain capped with biodegradable bulky end-groups. Further, a stimuli-responsive polyrotaxane, in which many β -CDs are threaded onto a triblock-copolymer of PEG and poly(propylene glycol) (PPG) capped with fluorescein-4-isothiocyanate, was designed as a novel smart material.

Supramolecular sciences have been getting fascinating field whereby nanostructures in nature are constructed by self-assemblies of small molecules (1). A family of polyrotaxanes has been recognized as a molecular assembly in which many cyclic compounds are threaded onto a linear polymeric chain capped with bulky end-groups (1). The name of rotaxane was given from the Latin words for wheel and axle, and thus it refers to a molecular assembly of cyclic and linear molecules. Inclusion complexation of α -cyclodextrins (α -CDs) threaded onto poly(ethylene glycol) (PEG) has been well studied as a polypseudorotaxane by Harada *et al.* since 1990 (2). Our recent studies have focused on the design of biodegradable polyrotaxanes aiming at biomedical and/or pharmaceutical applications. This paper deals with the structural characteristics of our designed polyrotaxanes as a supramolecular-structured polymer and their feasibility for biomedical and/or pharmaceutical applications.

Biodegradable Polyrotaxanes for Drug Delivery

During last two decades, water-soluble and/or biodegradable polymers have been widely demonstrated as polymeric carriers for biologically active agents (3).

¹Corresponding author.

Chemical immobilization of any drug onto a water-soluble polymeric backbone via biodegradable spacer has been a general strategy to design polymeric drug carriers since Rigsdorf proposed his idea on a polymeric drug carrier in 1975. We have proposed the design of biodegradable polyrotaxanes as novel candidates for drug carriers. The most attractive character of such a polyrotaxane will involve the control of drug release utilizing the dissociation of the supramolecular structure (Figure 1). Generally, drugs in polymeric prodrugs were covalently bound to the polymeric mainchain via biodegradable moieties. Those macromolecular prodrugs are to provide prolonged release action of the drugs by the hydrolysis or biological scission of the covalent bonds (4). In our approach, drugs can be introduced to α -CDs via another biodegradable spacers in the polyrotaxane. Thus, regulating the degradability of the terminal degradable moiety and the spacers, it may be likely that the terminal moieties of the polyrotaxanes are firstly degraded by hydrolytic enzymes to release the drug-immobilized α -CDs. The covalent bonds between the drug and the α -CDs are then subjected to hydrolysis to release the active drugs.

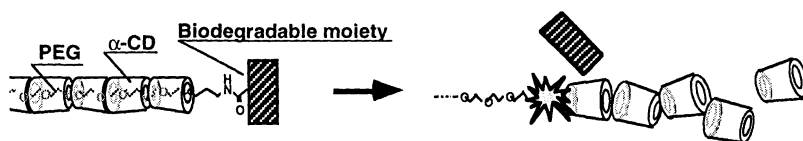


Figure 1. α -CD release via terminal hydrolysis of the polyrotaxane.

Synthesis of Biodegradable Polyrotaxanes and Drug-Polyrotaxane Conjugates

We have synthesized a series of biodegradable polyrotaxanes in which many α -CDs are threaded onto a PEG chain capped with an L-phenylalanine (L-Phe) moiety via a peptide linkage (5-8). The synthesis was carried out by i) preparing a polypseudorotaxane consisting of α -CD and amino-terminated PEG as previously reported by Harada *et al.* (9,10), and ii) capping both terminals of amino-groups in the polypseudorotaxane with benzyloxycarbonyl (Z-) L-Phe-succinimide in dry DMSO. The obtained polyrotaxanes were hydroxypropylated using propylene oxide in a 1N NaOH solution, and Z-groups were deprotected with palladium-carbon. The hydroxypropylation of the α -CDs improved the solubility of the polyrotaxanes in a phosphate-buffered saline. The purity of the polyrotaxanes was evaluated by $^1\text{H-NMR}$ and GPC (7). The threading of α -CDs onto a PEG chain has been confirmed by detecting the hydrophobic cavity of α -CDs when the terminal peptide linkages were cleaved by papain (5, 6).

The conjugation of the polyrotaxane with a model drug (theophylline) was carried out (11). Hydroxyl groups of the hydroxypropylated (HP)- α -CDs in the polyrotaxane (ca. 20-22 α -CDs were threaded onto PEG, $M_n=4000$, with the degree of HP substitution being 8-9/ α -CD) were activated by 4-nitrophenyl chloroformate in DMSO/pyridine at 0°C . The coupling of *N*-aminoethyl-theophylline-7-acetoamide with the activated polyrotaxane was carried out using DMSO/pyridine (1:1) as a

solvent. Z-groups were deprotected to obtain a drug-polyrotaxane conjugate (Figure 2). The synthesis was confirmed by $^1\text{H-NMR}$ and GPC. The number of HP- α -CDs in the drug-polyrotaxane conjugate was determined to be ca. 13-14 by $^1\text{H-NMR}$ spectrum. From the GPC peaks, one theophylline molecule was found to be introduced into every two α -CD molecules in the drug-polyrotaxane conjugate.

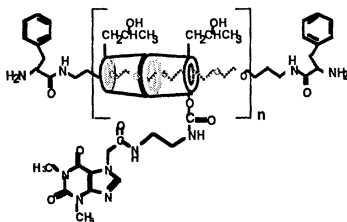


Figure 2. Schematic representation of the drug (theophylline) polyrotaxane conjugate.

Drug Release from Biodegradable Polyrotaxanes via Supramolecular Dissociation and its Relation to Solution Properties

Table 1. Solution Parameters Determined by Light Scattering Measurements

Sample	The Number of HP- α -CDs	Association Number	$A_2 \cdot 10^4$ ($\text{ml} \cdot \text{mol}^{-2} \cdot \text{g}^{-2}$)
Drug-polyrotaxane conjugate	13 - 14	6	-8.03
Polyrotaxane	20 - 30	2	3.40
L-Phe-terminated PEG	0	46	0.25

NOTE: \bar{M}_n of the used PEG is 4000 for all samples. The number of HP- α -CDs was determined by $^1\text{H-NMR}$.

Solution parameters of the polyrotaxane and the drug-polyrotaxane conjugate, which were determined by static light scattering measurements, were summarized in Table. 1. Association number of the polyrotaxane and the drug-polyrotaxane conjugate was found to be much smaller than that of L-Phe-terminated PEG. This result indicates that hydroxyl groups in HP- α -CDs participate in preventing the association of such a supramolecular-structured polymer. The second virial coefficient (A_2) value is a measure of the extent of polymer-polymer or polymer-solvent

interaction. Polymers are avoiding one another as a result of their van der Waals "excluded volume" when the A_2 value is large, and they are attaching one another in preference to the solvent when it is small or negative. Taking the characteristics of the A_2 value into account, it is suggested that the polyrotaxanes are considered to exhibit a loosely packed association, presumably due to their supramolecular structure. On the other hand, L-Phe-terminated PEG seems to exhibit a tightly packed association, because the terminal hydrophobic moieties can associate easily due to the flexibility of the PEG chains (12). In addition, the drug-polyrotaxane shows less association state with strong molecular interaction of theophylline (11). Furthermore, the ratio of hydrodynamic radius and radius of gyration (R_H/R_g) of the polyrotaxane revealed an anisotropic shape, indicating its rod-like structure (data not shown) (12). The rod-like structure of the polyrotaxane is likely to affect the reduced association state.

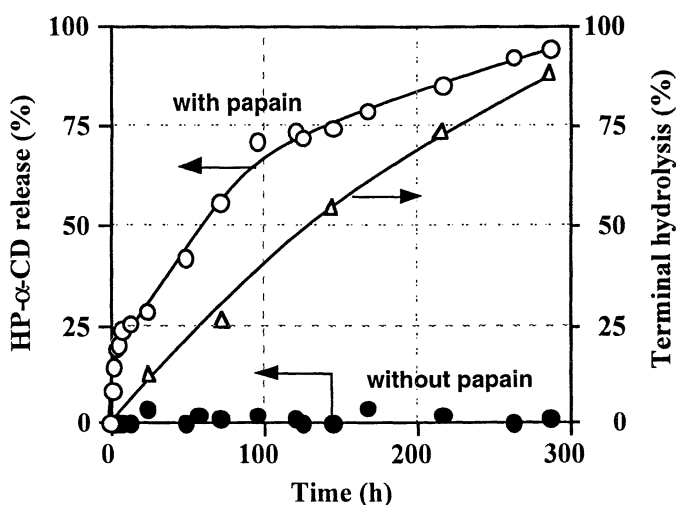


Figure 3. HP- α -CD release via terminal hydrolysis of the polyrotaxane in the presence of papain as a model enzyme

As for the polyrotaxane, HP- α -CD was found to be released by the terminal hydrolysis in the presence of papain as a model enzyme (Figure 3). The terminal hydrolysis in the polyrotaxanes proceeded to over 85 %, in contrast to the limited hydrolysis in L-Phe-terminated PEG (~50%) (12). Taking the A_2 values of the polyrotaxane into account (Table. 1), the complete dissociation of the polyrotaxanes by hydrolysis may be due to the less association state related to the rod-like structure. On the other hand, the high association state of L-Phe-terminated PEG with strong molecular interaction is considered to decrease the accessibility of papain to the terminals. *In vitro* degradation of the drug-polyrotaxane conjugate by papain was examined in order to clarify the terminal hydrolysis of the drug-polyrotaxane

conjugate and drug-immobilized HP- α -CDs (drug-HP- α -CDs) release. As shown in Figure 4, the release of drug-HP- α -CD from the drug-polyrotaxane conjugate was found to be completed around 200 h. HP- α -CD release from the polyrotaxane proceeded to reach 100% at 320 h under a similar experimental condition. Considering the solution properties of the drug-polyrotaxane conjugate as mentioned above, these results indicate that the association of the conjugate does not induce the steric hindrance but rather enhances the accessibility of enzymes to the terminal peptide linkages. Presumably, the terminal peptide linkages in the drug-polyrotaxane conjugate are likely to be exposed to the aqueous environment as a result of the specific association nature.

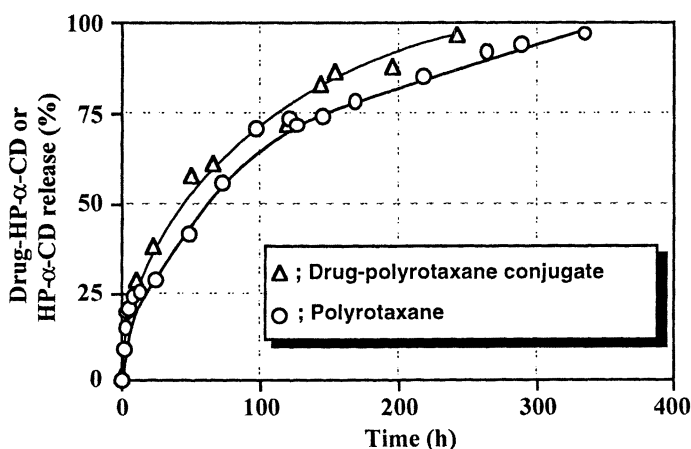


Figure 4. Drug-HP- α -CD release from the drug-polyrotaxane conjugate in comparison with HP- α -CD release from the polyrotaxane.

Potential of the Polyrotaxanes as a Drug Penetration Enhancer

Cellular response to synthetic polymers is of fundamental importance to their possible therapeutic application as pharmacologically active polymers and polymeric carriers for biologically active molecules (13). Our recent studies revealed that our designed polyrotaxanes have the ability of enhancing the fluidity of red blood cell ghosts, although the mixture of the constituent molecules (HP- α -CD + L-Phe-terminated PEG) shows less effect (8, 14). Here, the potential of the polyrotaxanes as a drug penetration enhancer is described in relation to the effects of the polyrotaxane structure on cellular interaction.

Effect of the Polyrotaxanes on Drug Permeation through Hairless Rat Skin

Our previous studies revealed that the treatment of skin stratum corneum with the polyrotaxanes induces the preferential extraction of polar lipid components but maintains ordered lipid bilayers in the stratum corneum (15). This finding indicates that the structure of the polyrotaxane is important for the effective interaction with the skin stratum corneum as well as red blood cell ghosts (8, 14). Indomethacin (IND) permeation through hairless rat skin treated with the polyrotaxanes was evaluated using a two-chamber cell at 37°C for 18 h. The enhanced permeation of IND through the full-thickness skin was observed when the skin surface was pre-treated with the polyrotaxane solution in PBS at 37°C for 18 h (16). Increased permeability coefficient (P, cm/sec) values were obtained, corresponding to a decrease in the bound water content. Therefore, the interaction of the polyrotaxanes with the stratum corneum may induce an enhanced IND permeation. Similar effects were observed when the dermis side of the skin was pre-treated with the polyrotaxane solution under the same condition (16). This suggests the possibility of the polyrotaxane penetration into not only the stratum corneum but also subcutaneous tissue. We have not determined yet how the polyrotaxanes can increase the permeability coefficient: whether it is a partition- or diffusion-controlled mechanism. Because the polyrotaxanes were degraded into their constituent molecules by a protease (data not shown), the selection of biodegradable moieties seems to enable the appropriate metabolism of polyrotaxanes after they have penetrated into subcutaneous tissues.

Biodegradable Polyrotaxanes for Tissue Engineering

Biodegradable polymers have been studied as implantable materials for cell growth and tissue regeneration (17). Aliphatic polyesters such as poly(L-lactic acid) (PLA) is a representative of implantable materials for tissue engineering. However, high crystallinity of PLA reduces water intrusion into the crystalline regions resulting in incomplete hydrolysis; crystalline oligomers remain in the tissue for a long time. Such a complex situation causes chronic inflammatory reactions at the implanted sites (18). Our next concern of biodegradable polyrotaxanes is in the design of implantable materials for tissue engineering. A novel design for biodegradable polymers has been proposed by constructing a supramolecular structure of a polyrotaxane; α -CDs threaded onto a PEG chain are capped with benzyloxycarbonyl (Z-) L-Phe via ester linkages (19). The most favorable characteristics of the polyrotaxanes as implantable materials will involve their excellent biocompatibility, mechanical properties and instantaneous dissociation properties. The polyrotaxane may have high crystallinity which is due to intermolecular hydrogen bonds between the hydroxyl groups of the α -CDs. This high crystallinity is postulated to be disappeared due to terminal hydrolysis, although the crystallinity of aliphatic polyesters usually increases as a result of their hydrolysis. The hydrolysis of the ester linkage in a certain PEG terminal will trigger rapid dissociation of the supramolecular structure into α -CDs, PEG and Z-L-Phe, thus, this may not induce any inflammatory reactions.

Supramolecular Dissociation of Biodegradable Polyrotaxanes with Ester Linkages

The biodegradable polyrotaxane with ester linkages as a terminal stopper has been synthesized and characterized (19). *In vitro* hydrolysis of the polyrotaxane was performed, and the α -CD release via terminal hydrolysis was evaluated by HPLC using a reverse phase column. As for the supramolecular dissociation of the polypseudorotaxane (without the Z-L-Phe moiety), it was found that α -CD release was completed within 10 min in the buffer at any pH (Figure 5a). On the other hand, as for the polyrotaxane, the completion of the α -CD release required several days (Figure 5b). These results indicate that the supramolecular dissociation of the polyrotaxane was prolonged in comparison with the polypseudorotaxane. Further, the α -CD release rate at pH 8.0 was found to be faster than those at pH 7.4 and 5.7 (Figure 5b). The terminal hydrolysis at each pH was well correlated with the α -CD release behavior (data not shown). Taking these results into account, it is suggested that the terminal hydrolysis of the polyrotaxane is a dominant process in the supramolecular dissociation. Recently, it was found that the induction period observed before the onset of hydrolysis in the polyrotaxanes was prolonged by chemical modifications of α -CDs such as acetylation. This finding enables us to design implantable materials which are to be disappeared in a predicted period.

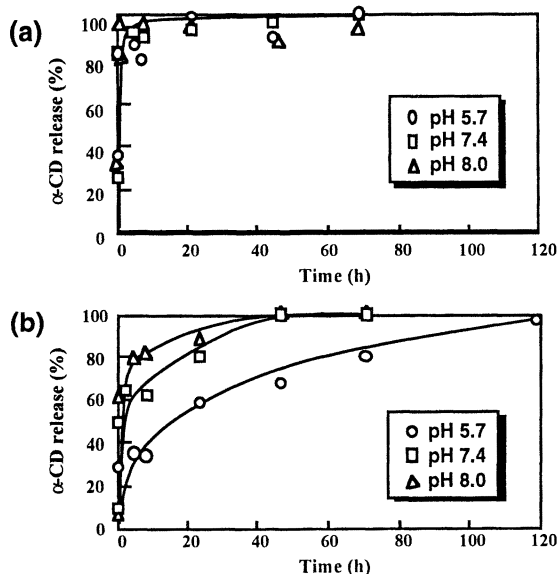


Figure 5. Cumulative α -CD release (%) from the polypseudorotaxane (a) and the polyrotaxane (b).

Feasibility of Polyrotaxanes for Stimuli-Responsive Materials

New synthetic methods have been investigated over the past two decades in order to design "intelligent" or "smart" materials which exhibit large property changes in response to small physical or chemical stimuli. Our alternative concern regarding polyrotaxanes is how such a molecular assembly can be utilized as a material with molecular dynamic functions: threading of many CDs onto a polyrotaxane might change the location along a linear polymeric chain in response to external stimuli which would be perceived as the action of mechanical pistons (20). Because the driving force for such inclusion complexation of CDs with a polymeric chain is due to intermolecular hydrogen bonding between neighboring CDs as well as steric fittings and hydrophobic interaction between host and guest molecules, several stimuli such as temperature and dielectric change may be used to control the assembled state of the CDs onto a polyrotaxane (Figure 6).

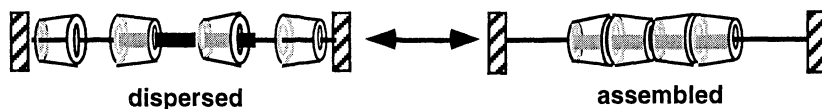
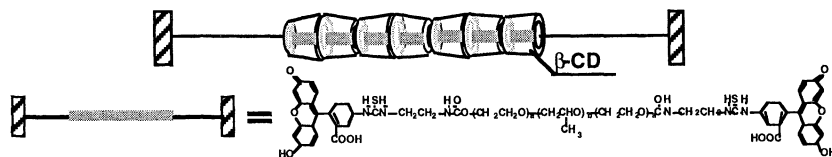


Figure 6. Stimuli-responsive change in CD location in a polyrotaxane.

Synthesis and Characterization of a Polyrotaxane Consisting of β -Cyclodextrins and a Poly(ethylene glycol)-Poly(propylene glycol) Triblock-Copolymer



Scheme 1. A polyrotaxane in which many β -CDs are threaded onto the triblock-copolymer capped with fluorescein-4-isothiocyanate (FITC)

A polyrotaxane, in which many β -CDs are threaded onto PEG-*block*-PPG-*block*-PEG triblock-copolymer ($\bar{M}_n = 4200$, PPG segment $\bar{M}_n = 2250$, PEG segment $\bar{M}_n = 975 \times 2$) named Pluronic[®] P-84 capped with fluorescein-4-isothiocyanate (FITC), was synthesized as a model of stimuli-responsive molecular assemblies (21). Terminal hydroxyl groups of the triblock-copolymer were modified to obtain amino-terminated triblock-copolymer. The polypseudorotaxane between the amino-terminated triblock-

copolymer and β -CDs was prepared in 0.1 M phosphate buffered saline at 40 °C. The terminal amino-groups in the polypseudorotaxane were allowed to react with FITC in DMF at 5 °C to obtain the polyrotaxane (Scheme 1). In this condition, a side reaction of β -CDs and FITC was prevented (21, 22). The threading of β -CDs in the polyrotaxane was confirmed by GPC, $^1\text{H-NMR}$ and 2D NOESY NMR spectroscopies using a 750 MHz FT-NMR spectrometer (21). The number of β -CDs in the polyrotaxane was determined to be ca. 7 from the $^1\text{H-NMR}$ spectrum.

Change in the Location of β -CDs in Response to Temperature

The interaction of β -CDs with terminal FITC moiety was analyzed by means of induced circular dichroism (ICD) measurement in 0.01 N NaOH at 25°C (21). A positive ellipticity $[\theta]$ of the polyrotaxane around 490 nm decreased when the temperature increased from 20 to 40 °C. This result indicates that the interaction between β -CD and the terminal FITC moiety is considered to decrease with increasing temperature. The interaction of β -CD hydrophobic cavity with the PPG segment of the triblock-copolymer was analyzed by means of 750MHz $^1\text{H-NMR}$ spectroscopy. With increasing temperature, the peak of the methyl protons in the PPG segment shifted to the lower field and slightly broadened for the polyrotaxane (21). The methyl proton peak shifted to the lower field is considered to be due to the interaction between the methyl protons of propylene glycol (PG) units and the cavity of the β -CDs. Assuming that the shifted methyl proton peak is the included methyl protons with β -CDs, the number of β -CDs located on the PG units can be estimated (21). As a result, it is considered that ca. 5.2 β -CD molecules were localized on the PPG segment at 50 °C, although ca. 1.3 β -CD molecules existed on the PPG segment at 10 °C. It was found that the association number of the polyrotaxane was decreased although that of the model triblock-copolymer was slightly increased from 35 °C to 50 °C (23). These results indicate that the dissociation behavior of the polyrotaxane may be related to the localization of β -CDs along the triblock-copolymer. Thus, stimuli-responsive polyrotaxanes can be one of candidates to create novel smart materials acting in a similar manner to natural chemomechanical proteins of myofibrils where myosin headpeices slide along actin filaments to initiate the contraction process.

Conclusions

It is concluded that our designed biodegradable polyrotaxanes were demonstrated to be promising as a drug carrier as well as a drug permeation enhancer, and an implantable materials for tissue engineering (24, 25). Stimuli-responsive polyrotaxanes will provide new fields of smart materials which are constructed by mimicking natural supramolecular assemblies. Supramolecular dissociation of the polyrotaxanes by their terminal hydrolysis will be the most unique characteristic when considering biomedical and pharmaceutical applications. Further, effective interaction of the polyrotaxanes with cellular systems is considered to be related to the supramolecular structure. These polyrotaxanes are designed as to be degraded after meanwhile or by completing their medical functions in living body, and thus, to be excreted as soluble compounds. In near future, biodegradable and/or stimuli-

responsive polyrotaxanes will enable us to achieve novel biomedical and pharmaceutical properties.

Acknowledgement

The authors are grateful to Mr. Fujita, H., Mr. Kamimura, W., Mr. Watanabe, J. and Mr. Kumeno, T. (JAIST) for their help in the experiments on biodegradable polyrotaxanes. A part of this study was financially supported by a Grant-in-Aid for Scientific Research (B) (No.851/09480253) and a Grant-in-Aid for Scientific Research on Priority Areas "New Polymers and Their Nano-Organized System" (No. 277/09232225), from The Ministry of Education, Science, Sports and Culture, Japan.

References

- Gibson, H. W.; Marand, H. *Adv. Mater.* **1993**, *5*, 11.
- Harada, A. *Adv. Polym. Sci.* **1997**, *133*, 141.
- Advances in Polymeric Systems for Drug Delivery*; Okano, T.; Yui, N.; Yokoyama, M.; Yoshida, R., Eds.; Gordon & Breach Sci. Pub.: Yverdon, 1994.
- Ulbrich, K.; Konak, C.; Tuzar, Z.; Kopecek, J. *Makromol. Chem.* **1987**, *188*, 1261.
- Ooya, T.; Mori, H.; Terano, M.; Yui, N. *Macromol. Rapid Commun.* **1995**, *16*, 259.
- Yui, N.; Ooya, T. In *Advances Biomaterials in Biomedical Engineering and Drug Deliver*; Ogata, N.; Kim, S. W.; Okano, T., Eds., Springer, Tokyo, 1996; pp 333-334.
- Ooya, T.; Yui, N. *J. Biomater. Sci. Polym. Edn.* **1997**, *8*, 437.
- Yui, N.; Ooya, T.; Kumeno, T. *Bioconjugate Chem.* **1998**, *9*, 118.
- Harada, A.; Kamachi, M. *Macromolecules* **1990**, *23*, 2821.
- Harada, A.; Li, J.; Kamachi, M. *Nature* **1992**, *356*, 325.
- Ooya, T.; Yui, N.; *J. Controlled Release*, **1999**, *58*, 251.
- Ooya, T.; Yui, N. *Macromol. Chem. Phys.* **1998**, *199*, 2311.
- Rihová, B. *Adv. Drug Deliv. Rev.* **1996**, *2*, 176.
- Ooya, T.; Yui, N. *J. Biomater. Sci. Polym. Edn.* **1998**, *9*, 313.
- Kamimura, W.; Ooya, T.; Yui, N. *J. Controlled Release* **1997**, *44*, 295.
- Ooya, T.; Sugawara, H.; Yui, N. *Jpn. J. Drug Deliv. Syst.* **1997**, *12*, 89.
- Langer, R.; Vacanti, J. P. *Science*, **1993**, *260*, 920.
- Biomedical Applications of Polymeric Materials*; Tsuruta, T., Ed.; CRC Press, New York 1993.
- Watanabe, J.; Ooya, T.; Yui, N. *Chem. Lett.*, **1998**, 1031.
- Fujita, H.; Ooya, T.; Kurisawa, M.; Mori, H.; Terano, M.; Yui, N. *Macromol. Rapid Commun.* **1996**, *171*, 509.
- Fujita, H.; Ooya, T.; Yui, N. *Macromolecules* **1999**, *32*, 2534.
- Fujita, H.; Ooya, T.; Yui, N. *Macromol. Chem. Phys.* **1999**, *200*, 706.
- Fujita, H.; Ooya, T.; Yui, N. *Polym. J.* **1999**, in press.
- Ooya, T.; Yui, N. *Crit. Rev. Ther. Drug Carrier Syst.*, **1999**, *16*, 289.
- Ooya, T.; Yui, N. *S. T. P. Pharma. Sci.* **1999**, *9*, 129.

Chapter 36

Fentanyl-Loaded Poly(L-lactide-co-glycolide) Microspheres for Local Anesthesia

Hai Bang Lee¹, Gilson Khang², Jin Cheol Cho²,
John M. Rhee², and Jung Sik Lee³

¹Biomaterials Laboratory, Korea Research Institute of Chemical Technology,
P.O. Box 107, Yusung, Taejeon, 305-606 Korea

²Department of Polymer Science and Technology, Chonbuk National University,
Dukjin-ku, Chonju, 560-756 Korea

³Research Center, Samchundang Pharmaceuticals Company, Ltd., P.O. Box 289,
Youngdeungpo, Seoul, 150-037, Korea

Fentanyl-loaded biodegradable poly(L-lactide-co-glycolide) (PLGA) microspheres (MSs) were prepared to study the possibility for long-acting local anesthesia. We developed the fentanyl citrate (FC, highly water-soluble), and fentanyl base (FB, slightly water-soluble)-loaded PLGA (75:25 by mole ratio of lactide to glycolide) MSs by means of novel W'/O/O and conventional O/W methods, respectively. The influence of several preparation parameters, such as emulsifier types and concentrations, molecular weights and concentrations of PLGA, initial drug loading, etc., has been observed in the release pattern of fentanyl. The release of FC and FB in *in vitro* was more prolonged over 15 and 30 days, respectively, with close to zero-order pattern by controlling the preparation parameters. Mechanisms of the release pattern of fentanyl-loaded PLGA MSs were discussed.

The development of long-acting local anesthetics is needed for post-operative analgesia and control of chronic pain of cancer patients. Several attempts have been made to prolong the action of local anesthetic. A typical example is a transdermal therapeutic system of fentanyl, Durogesic[®] (Alza Co. USA).¹⁻⁴ The treatment of acute pain requires strong opioids, whereas it is not indicated for the treatment of acute pain as postoperative pain, since it is not possible to individualize and titrate the dose to an effective and safe level in painful conditions requiring short-term treatment. That is to say, it is difficult to precisely control the fentanyl release rate through skin. Therefore, the localized delivery of fentanyl to the pain site may be introduced to overcome the difficulties associated with transdermal therapy. It would deliver the drug at a continuous rate and reduce the administration difficulties.

Recently, one of the most significant candidates for the study of a biodegradable polymeric controlled release system is poly(L-lactide-co-glycolide) (PLGA) due to its

controllable biodegradability and relatively good biocompatibility.⁵ However, it is not easy to design a suitable formulation for the controlled release of drug for the desired period of time because the drug release is affected by many factors, such as polymer molecular weight, monomer composition, drug particle, size and distribution of microspheres (MSs), preparation method, and etc.⁶ These parameters determined the properties of the resulting biodegradable product which govern the release patterns of the drug.

In this study, we demonstrated the possibility of the fentanyl citrate (FC, highly water soluble) and fentanyl base (FB, slightly water soluble) loaded MSs for local anesthesia with the precise and effective control of fentanyl administration over 15 days. FC and FB loaded PLGA MSs were prepared by means of the novel W'/O/O and conventional O/W solvent evaporation method, respectively. Also, the effects of the preparation condition on morphology and size of MSs were investigated, and the *in vitro* release patterns of fentanyl were observed by high performance liquid chromatography (HPLC) and scanning electron microscope (SEM), respectively.

Experimental

Polymerization of PLGA Copolymer

PLGA (75:25) was synthesized by direct condensation from 75 mole percent of L-lactide (Boehringer Ingelheim, Germany) and 25 mole percent of glycolide (Boehringer Ingelheim) under low pressure nitrogen atmosphere with 150 ppm of catalyst as stannous octoate (Wako Chem. Co. Japan) in toluene at 165 °C. The average molecular weight (MW) obtained was 27, 55, and 87 kg/mole, with controlling reaction times of 1.5, 2.5 and 3.5 hrs, respectively. Molecular weight distribution was 1.5 ~ 1.98 by the measurement of gel permeation chromatography (GPC, Waters Co., USA) using standard polystyrenes.

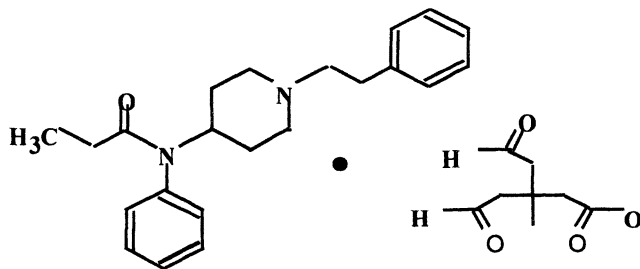


Figure 1. Chemical structure of FC.

Preparation of FC-loaded MSs by Novel W'/O/O Method

FC (Smith MacFarlan Pharm Co., UK, Figure 1) was dissolved in acetic acid glacial (W'). PLGA was dissolved in acetonitrile (MeCN) containing aluminum stearate as an emulsifier (O). After the adding of W' to O, they were thoroughly mixed with a sonicator at 4W for 30 sec (W'/O). The W'/O emulsion was poured into mineral oil (O) with Span 80 (W'/O/O) at 350 rpm. After solvent evaporation for 24 hours at 35 °C, MSs were filtered and washed three times with n-hexane, and then freeze-dried.

Morphology and size of FC/PLGA were observed by SEM. Cross-sectional morphology of MSs was obtained by imbedding the MSs in an aqueous 30 % gelatin gel containing 5 % glycerin. After 1 day drying in vacuum, a sharp surgical blade was used to cut the hardened gel. Figure 2 shows a schematic diagram of this experiment. The conditions of preparation and the characteristics of FC/PLGA MSs are listed in Table 1.

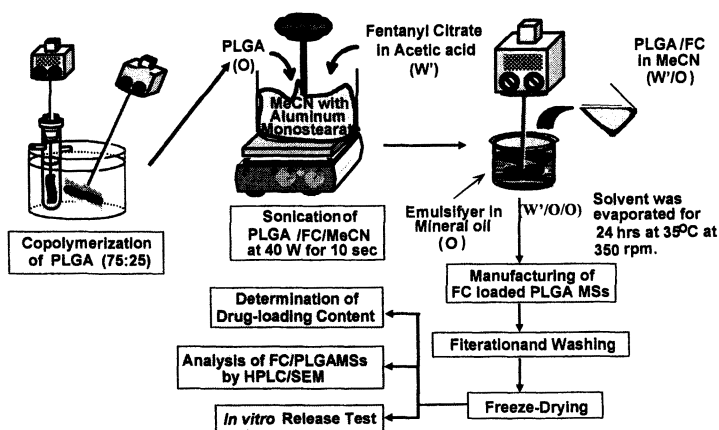


Figure 2. Schematic diagram of FC/PLGA MSs fabrication and analyzing method.

Table 1. The Conditions of Preparation and Characteristics of FC/PLGA MSs.

Batch No	PLGA Conc. (w/v %)	Span 80 Conc. (w/v %)	AlSt ^a Conc. (w/v %)	Theor. Load'g (%)	Load'g Eff. (%)	MSs Size (μm)
FC-1	1	1	0.1	20	37.4	40 ~ 400
FC-2	1	1	0.2	20	49.4	52 ~ 350
FC-3	1	1	0.4	20	50.9	58 ~ 300
FC-4	1	1	0.4	5	34.9	49 ~ 183
FC-5	1	1	0.4	10	30.2	38 ~ 115
FC-6	2.5	1	0.4	20	65.9	59 ~ 380
FC-7	0.66	1	0.4	20	54.8	33 ~ 334
FC-8	1	0.66	0.4	20	62.3	48 ~ 369
FC-9	1	0.2	0.4	20	73.1	60 ~ 413

a: aluminum stearate

Measurement of FC Content and In Vitro Release of FC/PLGA MSs

In order to measure FC content in MSs, 5 mg of FC/PLGA MSs was dissolved with 1 mL of dichloromethane and then added to 10 mL of phosphate buffered saline (PBS, pH 7.4). The supernatant in the mixture was analyzed by HPLC. For the *in vitro* test, an appropriated amount of PLGA/FC MSs was placed in 5 mL of PBS solution in a

constant temperature bath at 37 °C. Samples were withdrawn at a scheduled time and analyzed by HPLC^{7, 8} (wave length: 230 nm; the composition of mobile phase: 24 % of MeCN, 31 % of MeOH, and 45 % of H₂O by volume).

Preparation of FB-loaded MSs by Conventional O/W Method

FB (Smith MacFarlan Pharm Co.) and PLGA were dissolved in methylene chloride (O, oil phase) with appropriate concentration. The oil phase was poured into 1 wt % gelatin (polyvinylalcohol (PVA), or Tween 40) as an emulsifier in aqueous solution (W, water phase). After solvent evaporation for 24 hrs, MSs were washed three times with 0.2 wt % gelatin solution, and then freeze-dried. Morphology and size of FB/PLGA MSs were observed by SEM. The conditions of preparation and the characteristics of FB/PLGA MSs are listed in Table 2.

Table 2. The Conditions of Preparation and Characteristics of FB/PLGA MSs.

<i>Batch No</i>	<i>PLGA MW (kg/mole)</i>	<i>Initial Drug Loading (%)</i>	<i>Polymer Conc. (w/v %)</i>	<i>Emulsifier Types</i>	<i>Load'g Eff. (%)</i>	<i>MSs Size (μm)</i>
FB-1	27	20	5.7	Gelatin	60.3	12 ~ 93
FB-2	27	20	5.7	PVA	29.3	10 ~ 85
FB-3	27	20	5.7	Tween 40	19.6	9 ~ 107
FB-4	27	10	5.7	Gelatin	40.2	28 ~ 101
FB-5	55	10	5.7	Gelatin	17.9	24 ~ 118
FB-6	87	10	5.7	Gelatin	16.1	29 ~ 135
FB-7	27	10	10	Gelatin	54.8	22 ~ 123
FB-8	27	5	5.7	Gelatin	39.2	17 ~ 85
FB-9	27	10	5.7	PVA	5.5	12 ~ 89
FB-10	27	10	10	PVA	11.6	15 ~ 112
FB-11	55	10	10	PVA	12.8	13 ~ 110
FB-12	87	10	10	PVA	18.9	18 ~ 127

In Vitro Release of FB/PLGA MSs

For the *in vitro* test, an appropriated amount of FB/PLGA MSs was placed in 5 mL of phosphate buffered saline (PBS, pH 7.4) in a constant temperature bath at 37 °C. Samples were withdrawn at a scheduled time and analyzed by HPLC⁹ (wave length: 205 nm; the composition of mobile phase: 50 % of MeCN, and 50 % of 0.05 M phosphate buffer).

Results and Discussions

The Effect of Preparation Parameters on FC Release of FC/PLGA MSs

In order to increase FC release and loading efficiency compared with conventional O/O and W/O/W methods, the novel W'/O/O method has been developed. In the case of the O/O method, FC crystals can be seen on the MSs surfaces, resulting in initial

burst effects, but no FC crystals on the FC/PLGA MSs surface could be observed using the W'/O/O method (Figure 3).

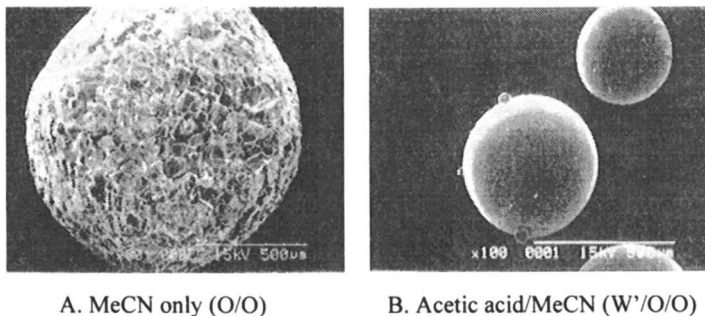


Figure 3. Effect of manufacturing methods as O/O and W'/O/O on surface morphology of FC/PLGA MSs (Original magnification: $\times 80$, bar: 500 μm).

It appears that the hydrophobic nature of PLGA forced out hydrophilic FC. Consequently, low loading of FC (below 10 %; results were not shown) was observed in the O/O method, whereas higher FC loading (above 50 %) could be reached in the W'/O/O method (see Table 1).¹⁰ The size of FC/PLGA MSs obtained was in the range of 50 ~ 350 μm . The FC was released near zero-order rate for 15 days from the three batches (Batch Nos. FC-3, 4, and 5).

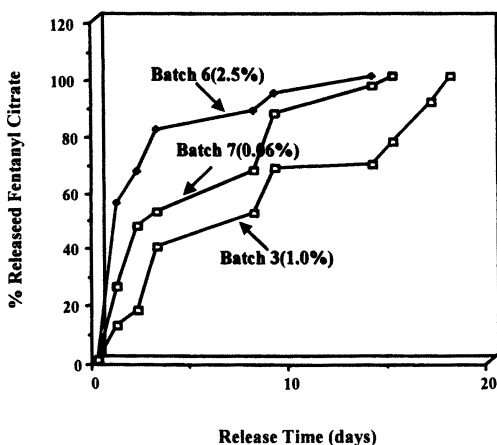


Figure 4. Effect of the concentration of PLGA release with 20 % of FC initial loading content (FB-6: 2.5 %, FB-7: 0.66 %, and FB-3: 1.0 %).

Figure 4 shows the effect of PLGA concentration on FC release. The slowest release rate of FC was observed in 1.0 w/v % of PLGA concentration. Figure 5 shows the changes of the cross-sectional view of MSs with the variation in PLGA concentration. It can be observed that the increasing of PLGA concentration results in high solution viscosity and decreases porosity. This is expected since the optimum FC release is dependent on the PLGA concentrations.

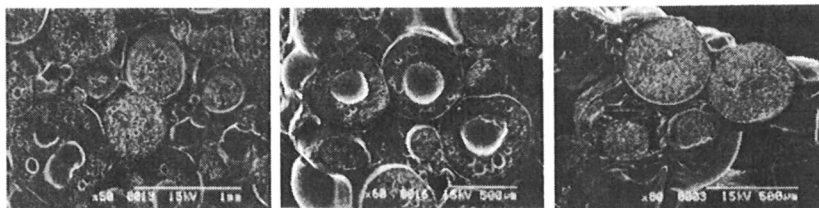


Figure 5. Effect of the concentration of PLGA on porosity in FC/PLGA MSs (Left to right - FC-7: 0.66 %, FC-3: 1.0 %, and FC-6: 2.5 %).

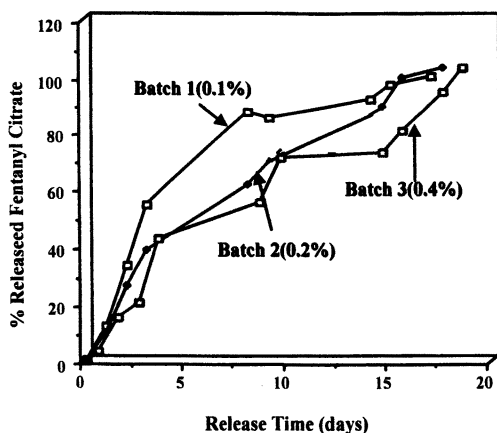


Figure 6. Effect of the different concentrations of aluminum stearate with 1.0 w/v % of PLGA concentration on FC release (FC-1: 0.1 wt %, FC-2: 0.2 wt %, and FC-3: 0.4 wt % of aluminum stearate).

Figure 6 shows the effect of aluminum stearate as an emulsifier in MeCN. The released amount of FC was slower with increasing aluminum stearate concentration.

¹¹ To investigate the effect of the concentration of Span 80 as an emulsifier in mineral oil phase, FC-3, 8, and 9 were prepared with the different concentrations (Figure 7). The higher concentration of Span 80, the slower of a controlled release rate was observed. It might be suggested that the increased concentration of emulsifiers, such

as aluminum stearate and Span 80 can be stabilized to form FC-loaded PLGA MSs, resulting in a more stable release pattern.

The Effects of Preparation Parameters on FB Release of FB/PLGA MSs

The conventional O/W method was applied to fabricate FB-loaded PLGA MSs since FB is a slightly water-soluble drug. Figure 8 shows the effect of emulsifier types on FB release. Morphologies and cross-sectional views of FB/PLGA MSs with

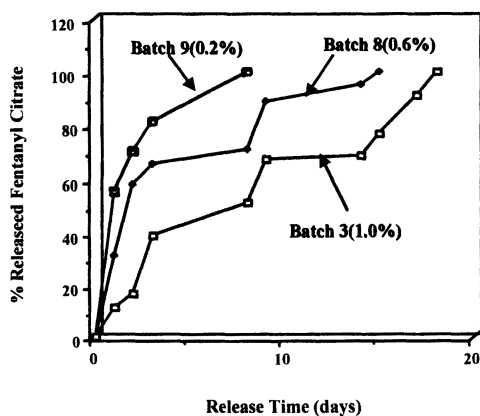


Figure 7. Effect of the different concentrations of Span 80 with 16.5 w/v % of PLGA concentration on FC release (FC-9: 0.2 wt %, FC-8: 0.6 wt %, and FC-3: 1.0 wt % of Span 80).

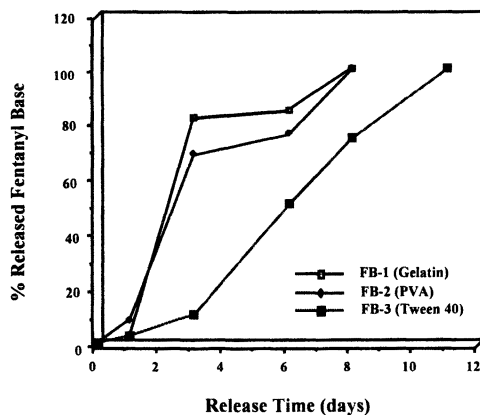


Figure 8. The effect of emulsifier types on FB release.

different emulsifiers were observed, as shown in Figure 9. The size of FB/PLGA MSs was in the range of 10 ~ 150 μm . The lowest porosity and nonporous surface morphology of MSs was obtained by using gelatin emulsifier.¹² Drug loading efficiency ranked in order of gelatin > PVA > Tween 40 (Table 2). From these results, it might be suggested that gelatin is a stable emulsifier in a FB/PLGA system. Figure 10 shows the effect of initial FB loading on FB release. In the case of 20 % FB loading, an initial burst effect was observed, whereas FB was released for 40 days from 5 % FB loading.

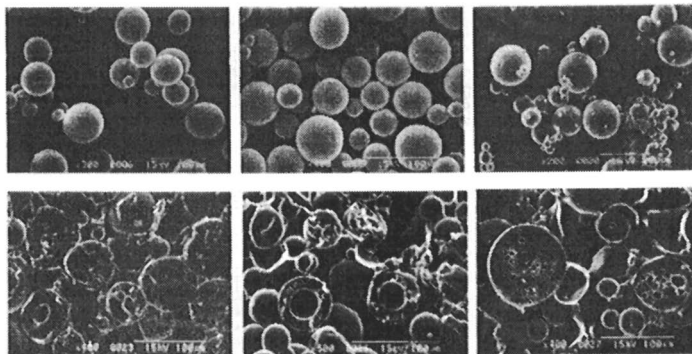


Figure 9. The surface morphology and cross-sectional views of FB/PLGA MSs with different emulsifiers (Left to right - FB-1: Gelatin, FB-2: PVA, and FB-3: Tween 40).

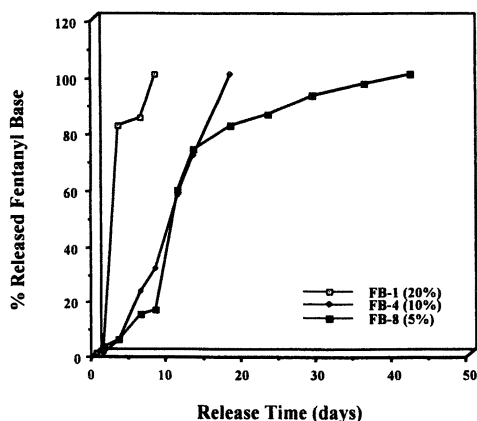


Figure 10. The effect of initial FB loading on FB release.

Figure 11 shows the effect of PLGA concentrations using 1.0 wt % of PVA as an emulsifier. It can be observed that the released amount of FB was slower with higher PLGA concentration. Increasing the concentration of PLGA results in an increase in MSs size due to increased viscosity of the organic phase. In order to investigate the effect of molecular weights of PLGA, the amounts of 27, 55, and 87 kg/mole were used on FB release in 1 wt % of PVA. The FB release rate reduced by the higher molecular weight of PLGA resulted in higher viscosity (results were not shown).

Conclusions

The release of FC in *in vitro* was successfully performed over 15 days with close to zero-order release pattern under experimental conditions (FC-3) of 20 % of initial FC content, 0.4 wt % of aluminum stearate, 1 wt % of Span 80, 0.7mL of acetic acid, and 1 wt % of PLGA concentration. The surface morphology and cross-sectional view of FC/PLGA MSs prepared with the W/O/O method were a nonporous surface and a hollow and porous structure, respectively. This novel W/O/O preparation method might be applicable to highly water-soluble, small drugs for designed controlled release.

To obtain the sustained FB delivery with effective and precise control, FB-loaded PLGA MSs were fabricated using the simple O/W method. The size of FB/PLGA MSs was in the range of 10 ~ 150 μm , and the morphology and cross-sectional views of MSs were the nonporous surface and porous structure, respectively. The release of FB in the *in vitro* was more prolonged over 40 days by controlling the fabrication parameters with close to zero-order pattern.

Studies on the *in vivo* animal experiment for FC and FB/PLGA MSs are in progress.

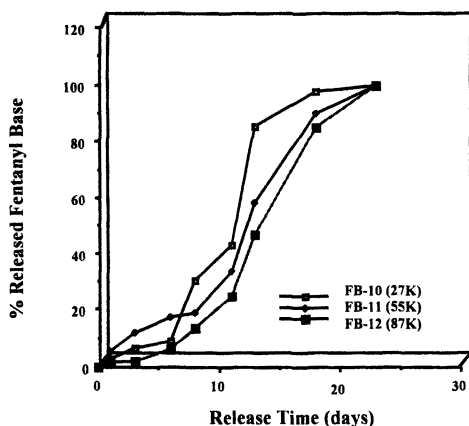


Figure 11. The effect of PLGA concentrations using 1.0 wt % of PVA as an emulsifier on FB release.

Acknowledgment This work was supported by the Korea Ministry of Health and Welfare (Grant No.: HMP-95-G-2-33).

References

1. Poklis, A. *Clinical Toxicology* **1995**, 33(5), 439.
2. Southan, M.A. *Anti-Cancer Drugs* **1995**, 6(Suppl. 3), 29.
3. Miguel, R.; Kreitzer, J.M.; Reinhart, D.; Sebel, P.S.; Bowie, J.; Freedman, G.; Eisenkraft, J.B. *Anesthesiology* **1995**, 83(3), 470.
4. Dewell, W.M.; Khandaghabadi, M.; D'Souza, M.J.; Solomon, H.M. *Am. J. Hosp. Pharm.*, **1994**, 12, 243.
5. Cho, J. C.; Khang, G.; Rhee, J. M.; Kim, Y. S.; Lee, J. S.; Lee, H. B. *Polymer (Korea)*, to appear **1999**
6. Khang, G.; Cho, J. C.; Lee, J. W.; Rhee, J. M.; Lee, H. B. *Bio-Med. Mater. Engineering*, to appear **1999**
7. Gupta, S.K.; Southam, M.; Gale, R.; Hwang, S.S. *J. Pain Symp. Management* **1992**, 7(Suppl), S17.
8. Seilinger, K.; Lanzo, C.; Sekut, A. *J. Pharm. Biomed. Anal* **1994**, 12, 243.
9. Bansal, R.; Aranda, J. V. *J. Liq. Chrom. & Rel. Technol.* **1996**, 19(3), 353
10. Splenlehauer, G.; Veillard, M.; Benoit, J.P. *J. Pharm. Sci.* **1986**, 75(8), 750.
11. Sandrap, P.; Moes, A. *J. Int. J. Pharm.* **1993**, 98, 157.
12. Jeffery, H.; Davis, S. S.; O'Hagan, D. T. *Int. J. Pharm.* **1991**, 77, 169
13. Ogawa, Y.; Yamamoto, M.; Okada, H.; Yashiki, T.; Yamamoto, T. *Chem. Pharm. Bull.* **1984**, 36, 1294.

Chapter 37

Ionic Cross-Linked Polyphosphazene Microspheres

Alexander K. Andrianov, Jianping Chen, Sameer S. Sule,
and Bryan E. Roberts

Avant Immunotherapeutics, Inc., 119 Fourth Avenue, Needham, MA 02494

Ionic cross-linked polyphosphazene microspheres were prepared under mild conditions by a simple aqueous coacervation process utilizing aluminum and calcium salts as cross-linking reagents. Hydrolytic degradability of the obtained hydrogel microspheres was shown to be sensitive to the type of the ionic cross-linker. It was demonstrated that microsphere size distribution can be controlled by the conditions of the coacervation step and is only slightly affected by the concentration of the ionic cross-linker under the conditions studied. The method potentially allows the use of designed polyphosphazene polyelectrolytes to prepare microspheres with desired physico-chemical and biological properties.

Polymeric hydrogel microspheres have been used extensively in the development of advanced drug delivery systems and controlled release technologies [1]. In particular, polyphosphazene hydrogel microspheres are of interest as carriers for a variety of prophylactic and therapeutic agents because of potential biocompatibility and the fact that phosphazene polymers can be designed to generate any combination of properties needed for specific biomedical applications [2]. Microspheres based on some phosphazene polyelectrolytes, such as poly[di(carboxylatophenoxy)phosphazene] (PCPP) also display powerful immunostimulatory properties, that makes them an ideal candidate as a vaccine delivery vehicle [3].

Recently we described a simple aqueous based method of preparing polyphosphazene hydrogel microspheres with controlled microsphere size distribution [4]. In this process aqueous polyphosphazene solutions are coacervated using solution of sodium chloride followed by cross-linking of the coacervated microdroplets with calcium ions to produce ionic cross-linked microspheres.

The advantages of this method are in its simplicity, reproducibility and that it avoids the use of organic solvents, heat, and also allows the microsphere size to be varied by a simple manipulation of the experimental conditions.

This paper reviews the potential of the coacervation method in the preparation of polyphosphazene hydrogel microspheres with specific characteristics, such as desired biological activity of the carrier polymer and controlled degradability. Particularly, we expand the scope of the microencapsulation method to include preparation, characterization and study of the hydrolytic stability of aluminum cross-linked polyphosphazene microspheres and discuss properties of some of the potential matrix forming polyphosphazenes.

Experimental

Materials.

PCPP-sodium salt was prepared using the synthetic method described elsewhere [5, 6]. Poly(dichlorophosphazene) was reacted with sodium salt of propyl p-hydroxybenzoate and the obtained product was subjected to the alkaline hydrolysis. The weight-average molecular weight (M_w) of the polymer was determined as described previously [7] and was equal to 860,000 g/mol. Fluorescein isothiocyanate labeled bovine albumin, FITC-BSA (Sigma Chemical Co., St. Louis, MO) contained 11.2 moles of FITC per 1 mole of BSA and was used as received. Dulbecco's phosphate buffered saline, PBS (pH 7.4) was purchased from Sigma Chemical Co., St. Louis, MO. All other chemicals were reagentgrade.

Analytical Methods.

The molecular weight of the polymer was determined by gel permeation chromatography (510 HPLC pump, Waters, Milford, MA) in an aqueous phase using Dawn DSP-F multi-angle laser light scattering detector, MALLS (Wyatt Technology, Santa Barbara, CA), Waters 410 refractive index detector (Waters, Milford, MA) and Ultrahydrogel Linear column (Waters, Milford, MA) as described previously [7]. Phosphate buffered saline PBS (pH 7.4) was employed as a mobile phase.

The particle size distribution of the microspheres was analysed by a Malvern Mastersizer S Particle Sizer (Malvern Instruments, Southborough, MA) using a 300RF lens and a small volume dispersion unit. The coacervate microdroplets and the microspheres were studied using Olympus CK-2 inverted microscope (Olympus, Japan). Microspheres loaded with FITC-BSA were also investigated using an Olympus BH-2 fluorescent microscope (Olympus, Japan). Efficiency of microencapsulation was determined using a F-2000 Hitachi fluorescence spectrometer (Hitachi, Japan).

Microsphere Preparation.

Aqueous PCPP-salt solutions were prepared by dissolving the polymer in water and diluting with deionized water and PBS (pH 7.4) to a final concentration of 0.2% (w/v). Aluminum lactate (Aldrich Chemical Company, Milwaukee, WI) solution was prepared in deionized water, 8% (w/v) and adjusting the pH of the solution to 6.7 using NaOH. The coacervate of PCPP was prepared in sodium chloride solution as described elsewhere [4]. The droplets were cross-linked by the addition of the coacervate dispersion to 8% aluminum lactate or 8.8% calcium chloride solution. The suspension was stirred for one hour, and the microspheres were collected and washed with water on a 0.45 μm Nalgene filter (Nalge Company, Rochester, NY).

Encapsulation of FITC-BSA.

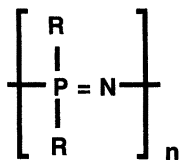
FITC-BSA was encapsulated in the aluminum cross-linked PCPP microspheres. 4 ml of 0.2% (w/v) PCPP-sodium salt solution was mixed with 0.3 ml of 0.5% (w/v) aqueous solution of FITC-BSA. To this solution, 7.4 ml of 6.22% (w/v) aqueous solution of sodium chloride was added and the mixture was shaken. After 8 minutes of incubation when a significant amount of microspheres was observed, the coacervate was poured slowly into a 500 ml of 8% (w/v) aluminum lactate solution and stirred for 30 minutes. The obtained microspheres were collected and washed with water on a 0.45 μm filter.

The efficiency of encapsulation of FITC-BSA in the microspheres was then determined. The microspheres were filtered through a 0.45 μm Millipore Millex-HV hydrophilic PVDF filter (Millipore Corporation, Bedford, MA). The filtrate was then analyzed using a F-2000 Hitachi fluorescence spectrometer (λ_{ex} 492nm, λ_{em} 514nm) to determine the concentration of FITC-BSA in solution.

Results and Discussion

Polyphosphazenes as Drug Delivery Vehicles.

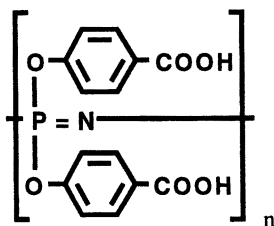
Polyphosphazenes present a rare opportunity as polymers for biomedical and specialty applications due to the versatile molecular design, ease of structural manipulations for these macromolecules, and a sophisticated spectrum of physical, chemical, and biological properties. The term polyphosphazenes covers a large family of organometallic polymers containing a backbone consisting of alternating phosphorus and nitrogen atoms with two organic side groups attached to each phosphorus atom:



Fundamental developments in polyphosphazene synthesis yielded synthetic pathways allowing a choice of a tremendous variety of substituents to be introduced in the polymer to create macromolecular structures with versatility that cannot be achieved using traditional polymerization or polycondensation techniques [2]. Since physico-chemical and biological properties of polyphosphazenes are determined to a great extent by the structure of polymer side groups and their combinations, polyphosphazenes can be designed to display customized and potentially unique sets of characteristics. Furthermore the peculiarity of this class of polymers is not only in the tremendous number of structures that can be synthesized, but also in the phosphorus-nitrogen backbone, which has a remarkable skeletal flexibility manifested in specific polymers having some of the lowest glass transition temperatures known in polymer chemistry. Due to its hydrophilicity, the phosphazene backbone can also serve as an ideal starting point for designing water-soluble and hydrophilic polymers, or can be rendered hydrolytically degradable when combined with appropriate side groups. This structural versatility combined with the unique character of the phosphorus-nitrogen backbone make polyphosphazenes especially attractive for targeting specific applications, especially biological. Polyphosphazenes, for example, were investigated and showed potential as materials for matrices for microcapsules and microspheres, protein and drug delivery vehicles, immunostimulants, bioinert medical devices and implants [2].

Phosphazene polyelectrolytes (polyphosphazenes containing ionic or ionizable groups) are a new rapidly developing class of phosphazene polymers which display some remarkable biological and physico-chemical properties that differentiate these synthetic polymers from conventional polyelectrolytes. In particular, some phosphazene polyelectrolytes demonstrate the ability to form inter- and intramolecular hydrogen bonds under physiological conditions and exhibit unusual ionic selectivity. Polyelectrolytes have been designed and synthesized to have high charge density, high hydrophobicity, biodegradability and high pKa values.

One of the most important functional properties of phosphazene polyelectrolytes uncovered to date is the ability of some of these polymers to form aqueous based coacervation systems and some peculiar gel forming characteristics mimicking those



PCCP

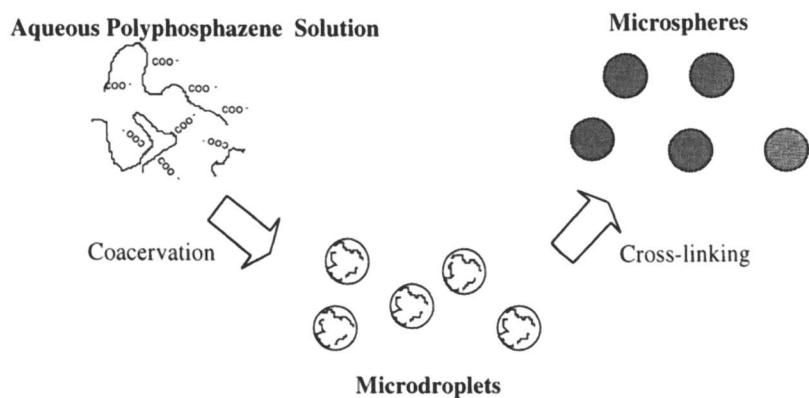
of natural products, such as alginate [4, 8]. These properties prompted the use of phosphazene polyelectrolytes, such as PCPP, in a number of patented aqueous microencapsulation techniques demonstrating the potential of these polymers as carriers for the delivery of vaccines, proteins, other biologics and drugs. The advantages of these methods are in the simplicity of preparation, mild conditions of encapsulation, and the ability to control microsphere size distribution.

Preparation of Polyphosphazene Microspheres by Aqueous Coacervation.

It was reported previously that aqueous solutions of PCPP can form a coacervate phase when treated with solutions of sodium chloride at room temperature [4]. A phase diagram established for a PCPP - NaCl - water shows that the separation of a macromolecular solution into two immiscible liquid phases - a concentrated polyphosphazene coacervate phase and a polymer deficient phase, can take place in a relatively wide range of polymer and salt concentrations and results in the formation of polymer coacervate microdroplets of spherical shape in the broad size range [4]. Though such systems are in dynamic equilibrium and relatively unstable, the advantage of PCPP as a coacervate forming material is in the ability of this polyphosphazene polyelectrolyte to form stable ionotropic gels almost instantaneously when exposed to calcium ions in aqueous solutions (Scheme 1). Addition of multivalent ionic cross-linker usually does not change the coacervate microdroplet size and shape despite changes in the ionic composition of the solution. At the same time, presence of significant quantities of sodium ions does not affect ionic gelation of PCPP and does not have an adverse effect on already formed microspheres despite the possibility of gel destabilizing ion-exchange reactions. The microspheres have spherical shape, typically, with a narrow size distribution (Figure 1). Microspheres of different sizes can be prepared by varying the conditions of coacervation, such as polymer and salt concentration and time of incubation in sodium chloride solutions (Figure 2).

Preparation of Microspheres with Variable Hydrolytic Stability.

Hydrogel microspheres with degradable matrices present a significant interest in the delivery of high molecular weight peptide and protein drugs [1]. The release of the encapsulated agent in such systems can be controlled not only by the permeability of the matrix, but also by the rate of matrix erosion determined by the stability of the polymer backbone and cross-linker. Polyphosphazenes, including polyphosphazene polyelectrolytes, can be synthetically designed to degrade with a predetermined rate [9]. However, ionic cross-linking of polyelectrolyte chains with multivalent ions presents another simple and attractive technique for the development of bioerodible hydrogels [10], since different degrees of stability of the ionic bridges can be achieved using different multivalent cations [11]. Polyphosphazene ionotropic hydrogel microspheres is an example of a protein delivery system where the choice of a multivalent cross-linker can have a potentially dramatic impact on the release and erosion properties of the matrix. Originally, coacervation based microencapsulation process was developed for PCPP utilizing calcium chloride as a cross-linking reagent. The resulting calcium cross-linked



Scheme 1. PREPARATION OF POLYPHOSPHAZENE MICROSPHERES

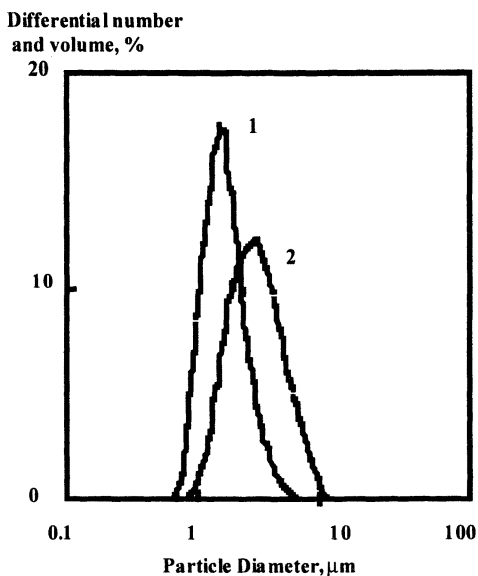


Figure 1. Particle size distribution of PCPP hydrogel microspheres by number (1) and by volume (2).

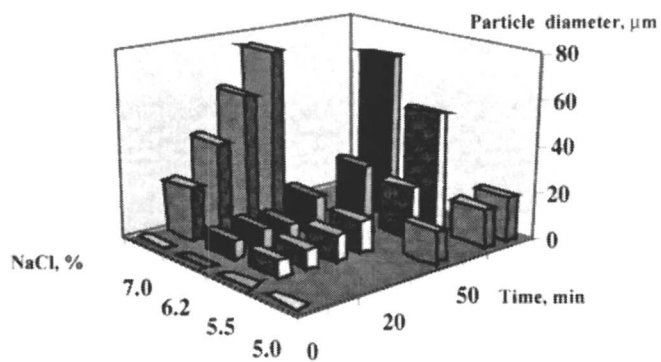


Figure 2. Effect of the coacervation conditions on the microspheres mean diameters (Data are from reference [4]).

microspheres are usually characterized by high sensitivity to the ionic environment and can readily erode and dissolve in the solutions with high concentrations of salts of monovalent ions. In order to develop microspheres with superior stability in the solutions with higher ionic strength a number of aluminum salts were investigated as cross-linking agents for the PCPP microspheres. As a result of this study aluminum lactate was shown to be an effective cross-linker producing microspheres with a narrow size distribution, both by volume and by number with a little effect of aluminum lactate concentration on the size distribution. The analysis of microspheres obtained under the same conditions and cross-linked with aluminum lactate solutions of different concentrations (1%, 4% and 6% (w/v)) demonstrated that the increase in the concentration of the cross-linker resulted in a somewhat more narrow particle size distribution of microspheres and complete prevention of the formation of aggregates (Figure 3).

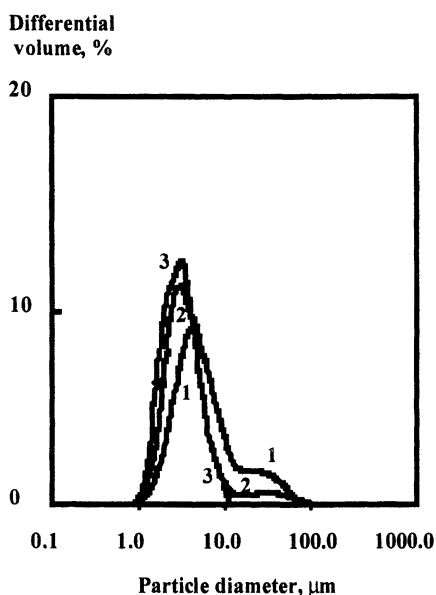


Figure 3. Particle size distribution of PCPP hydrogel microspheres cross-linked with different concentrations of aluminum lactate (1) 1% (2) 4% (3) 6%

Stability of the aluminum cross-linked PCPP microspheres in PBS was studied by incubating the microspheres in PBS (pH 7.4). Contrary to calcium cross-linked PCPP microspheres, the aluminum based PCPP microspheres were found to be stable for at least 1 month. Figure 4 shows the particle size distribution of the microspheres before and after incubation in PBS for 24 hours. As seen from the figure the microsphere size distribution profiles are practically identical. These

results demonstrate the potential of this system to prepare ionic hydrogel microspheres stable in aqueous solutions at neutral pH. Studies are now ongoing to prepare microspheres with a combination of cross-linkers.

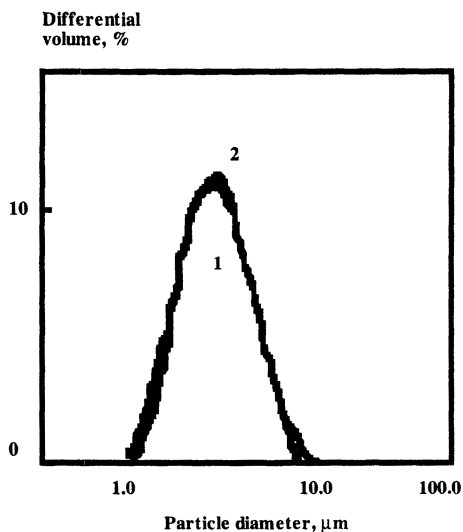
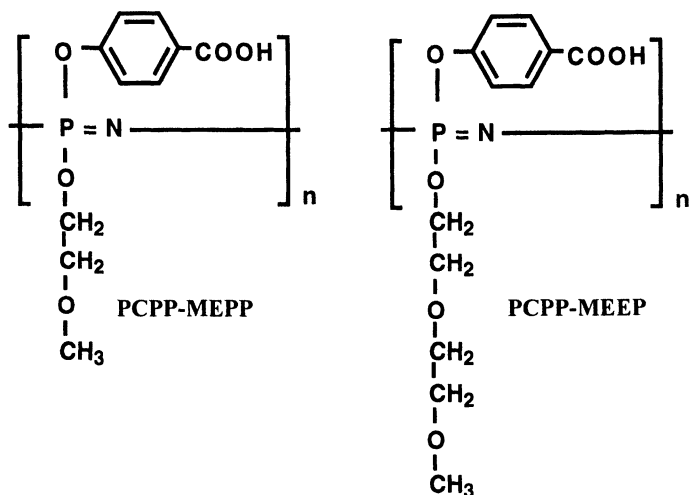


Figure 4. Particle size distribution of PCPP hydrogel microspheres before (1) and after (2) incubation in PBS (pH 7.4) for 24 hrs.

Microsphere Matrix Properties.

The versatility of the matrix properties can be achieved via utilization of designed phosphazene polyelectrolytes. The realization of this potential can be especially dramatic in case of some phosphazene polyelectrolytes which were shown to be effective in modulating biological responses related to host defense mechanisms against a variety of disease causing agents. PCPP, for instance, was demonstrated to be a potent immunostimulant inducing high level of protective antibodies against a number of vaccine antigens [3, 12]. It was shown, however, that the immunostimulating activity of PCPP (Figure 5) can be significantly improved through the manipulation of the macromolecular structure and the synthesis of new polyphosphazene derivatives [13]. There is an indication that the utilization of such chemical modification approaches can lead not only to greatly enhanced antibody levels, but also to the stimulation of cell mediated responses. This expands the potential applications of the designed polyphosphazenes, and



ELISA TITER, 10^{-4}

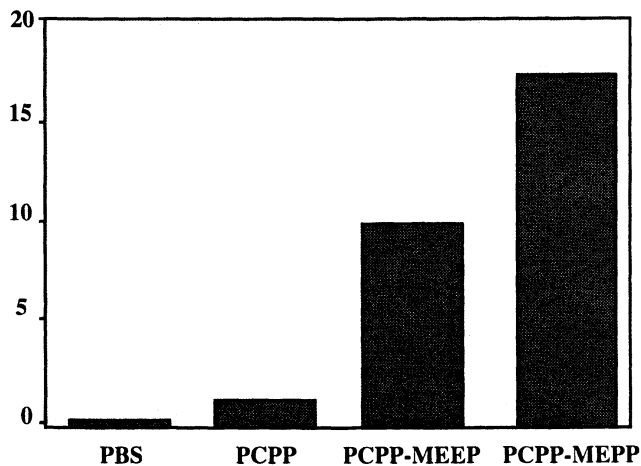


Figure 5. Serum IgG titers after subcutaneous immunization of Balb/C mice with 5 μg of Split X-31 influenza adjuvanted with various polyphosphazene polyelectrolytes (week 3 data).

polyphosphazene based microspheres, beyond vaccines to immunotherapeutic treatment of cancer and persistent infections.

Conclusions

The elucidation of novel polymeric derivatives with superior biological activity, bioinert carrier properties, and advanced functional characteristics can be potentially achieved by the extension of conventional combinatorial chemistry approaches to the design of phosphazene polymers. Although polyphosphazene synthesis is somewhat more involved than that of common petro-chemical polymers, it offers a unique synthetic flexibility not available for other classes of polymers. Polyphosphazenes of almost unlimited structural varieties can be synthesized including mixed substituent copolymers in which several differentside groups can be introduced in a polymer structure by simultaneous or sequential substitution. Significant advances were also made in the development of the synthetic methods with a focus on a precise control of macromolecular structure and molecular weight distribution, as well as monitoring of the molecular parameters during the polymer transformation [6]. The synthesized libraries of polyphosphazenes can be evaluated for functional and biological properties and further refined utilizing computational chemical modeling to rationalize the design of phosphazene polymers for specific applications.

References

1. Park, K.; Shalaby, W. S. W.; Park, H. *Biodegradable Hydrogels for Drug Delivery*; Technomic Publishing Co., Inc.: Lancaster-Basel, 1993.
2. Allcock, H. R. In *Biodegradable Polymers as Drug Delivery Systems*; Chasin, M., Langer, R., Eds.; Marcel Dekker, Inc.: New York, 1990, pp 163-193.
3. Payne, L. G.; Jenkins, S. A.; Andrianov, A. K.; Roberts, B. E. In *Vaccine Design*; Powell, M. F., Newman, M. J., Eds.; Plenum Press: New York, 1995, pp 473-493.
4. Andrianov, A. K.; Chen, J.; Payne, L. G. *Biomaterials* **1998**, *19*, 109-115.
5. Allcock, H. R.; Kwon, S. *Macromolecules* **1989**, *22*, 75-79.
6. Andrianov, A. K.; Le Golvan, M. P.; Svirkin, Y. Y.; Sule, S. S. *Polymer Preprints* **1998**, *39*, 220-221.
7. Andrianov, A. K.; LeGolvan, M. P. *J. of Appl. Polym. Sci.* **1996**, *60*, 2289-2295.
8. Cohen, S.; Baño, M. C.; Visscher, K. B.; Chow, M.; Allcock, H. R.; Langer, R. *J. Am. Chem. Soc.* **1990**, *112*, 7832-7833.

9. Andrianov, A. K.; Payne, L. G.; Visscher, K. B.; Allcock, H. R.; Langer, R. *J. of Appl. Polym. Sci.* **1994**, *53*, 1573-1578.
10. Prasad, M. P.; Kalyanasundaram, M. *J. Appl. Polym. Sci.* **1993**, *49*, 2075-2079.
11. Axelos, M. A. V.; Mestdagh, M. M.; Francois, J. *Macromolecules* **1994**, *27*, 6594-6602.
12. Payne, L. G.; Jenkins, S. A.; Woods, A. L.; Grund, E. M.; Geribo, W. E.; Loebelenz, J. R.; Andrianov, A. K.; Roberts, B. E. *Vaccine* **1998**, *16*, 92 - 98.
13. Andrianov, A. K.; Sargent, J. R.; Sule, S. S.; Le Golvan, M. P.; Woods, A. L.; Jenkins, S. A.; Payne, L. G. *Journal of Bioactive and Compatible Polymers* **1998**, *13*, 243-256.

Chapter 38

Polysaccharide as a Drug-Coating Polymer

Ki-Young Lee, Kun Na, and Yu-Eun Kim

Department of Biochemical Engineering, Chonnam National University,
300 Yongbongdong Puk-gu, Kwangju City, 500-757 Korea

Many polysaccharides were examined as a potential drug containing material. Microspheres were prepared using lactan acetate. Lactan acetate microspheres(LAM) were used as a pH-sensitive drug carrier. The swelling capacity of LAM at pH 7.4 was much greater than that at pH 1.2. The in vitro release rate of indomethacin at pH 7.4 was approximately 10 times faster than that at pH 1.2. Nanoparticles were prepared using guar acetate by a dialysis method. The particle sizes of guar acetate nanoparticle I (GAN I) and II (GAN II) were 250.78 ± 185.13 nm and 718 ± 145.90 nm, respectively. The size of GAN depended on the polymer concentration. GAN I released the drug (indomethacin) more rapidly compared to GAN II. Alginate beads coated with dextran acetate released the drug considerably more under presence of dextranase. Alginate beads coated with dextran acetate can be used as a colon targeting system.

Introduction

There has been significant interest in using biopolymers, such as polysaccharides and proteins, as biodegradable hydrogels for drug delivery¹. The use of hydrophilic polysaccharides as matrices for controlled release has received considerable attention, since their ingestion produced almost no adverse dietary, physiological or toxic effect in animals and humans. Albin et al. reported slow release indomethacin (IND) formulations based on polysaccharides². Santucci et al. reported that gellan was suitable for formulation of sustained-release beads³. A large number of polysaccharides are able to form physical gels after simple modification⁴. Lactan, guar gum and dextran were acetylated. Lactan acetate was known to have pH-sensitivity and dextran was known to be degradable by dextranase in colon^{5,6}. As a basic model drug, we chose IND. It is one of most potent nonsteroidal anti-inflammatory drugs (NSAIDs) for the treatment of rheumatoid arthritis, osteoarthritis, and acute gouty arthritis. The focus of this paper is preparation of various polysaccharides in

microspheres, nanoparticles and beads and use them as a coating material for controlled drug delivery.

Experiment

Materials

IND, dextran, dextranase, guar gum, alginate and dichloromethane (DCM) were purchased from Sigma Chemical Co. (USA). Formamide, glutaraldehyde, coconut oil and pyridine were purchased from Junsei (Japan). Acetic anhydride was purchased from Lancaster Synthetic Co.(England). Lactan gum was obtained from fermentation of *Rahnella aquatilis* in our laboratory.

Preparation of polysaccharide acetate

Polysaccharide acetate was prepared as follows. Two grams of polysaccharide was suspended in 20 ml of formamide and dissolved by vigorous stirring at 50 °C. Pyridine (60 ml) and acetic anhydride (150 ml) were added and the mixture was stirred at 54 °C for 48hr. Polysaccharide acetate was obtained after reprecipitation from water (200 ml)⁷.

Preparation of lactan acetate microspheres (LAM)

To prepare LAM, 40 mg of lactan acetate was dissolved in 5 ml of DCM. Then, the solution was stirred at room temperature for 1 hr. To form microspheres, the solution was dropped slowly into 50 ml of double-distilled water and vigorously stirred to evaporate the solvent for 2 hr at room temperature. And the residual solvent was removed by evaporation for 30 min. LAM were harvested by centrifugation at 3000 g for 10 min and then freeze-dried to obtain microspheres. Microspheres containing IND were also prepared, and their morphology was examined using a scanning electron microscope (SEM, JEOL, JSM 5400, Japan).

Preparation of IND-loaded guar acetate nanoparticle (GAN)

IND (40 mg) was dissolved in 5 ml of DMSO (dimethylsulfoxide) and GAN I (40 mg) or GAN II (80 mg) were added. The solution was dialyzed in distilled water using a dialyze membrane (M.W. cut-off of 12,000). The water was replaced five times during 5 hr of dialysis, followed by two more changes in the next 4 hr. The resulting solution was freeze-dried.

Photon Correlation Spectroscopy (PCS) Measurements

For particle size measurement, Zetasizer 3000 (Malvern Instruments, U.K.) with a He-Ne laser beam was used at the wavelength of 633 nm and at 25°C (scattering angle of 90°).

Powder X-ray Diffractometry (XRD) study

Samples were exposed to CuK α radiation (40 kV x 30 mA) in a wide angle

X-ray diffractometer (D/MAX-1200, Rigaku, Japan). The instrument was operated in the step scan mode in increments of 0.02° (2θ).

Preparation of alginate beads including IND

The mixture of 4 ml of coconut oil and 20 mg of IND was subjected to ultrasonic treatment to obtain a drug-dispersed oil phase. The drug-dispersed oil phase was ground into colloidal fineness. Alginate aqueous solution (2 w/v %) was added to the colloidal emulsion. The O/W emulsion bead was transferred dropwise using a syringe (26 gauge) to 1 % (w/v) of calcium chloride aqueous solution. Alginate beads were obtained within 5 min (Fig. 1).

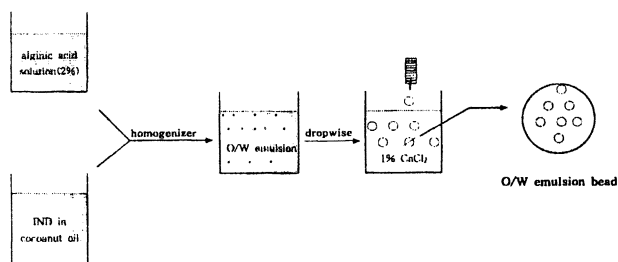


Fig.1 Schematic diagram for the preparation of alginate beads.

Coating of alginate beads with dextran acetate and crosslinked dextran

Alginate beads were coated with dextran acetate solubilized in dichloromethane by a typical solvent evaporation method as shown in Fig. 2(a). Resulting beads were air-dried. Dextran was crosslinked with glutaraldehyde, and alginate beads were added to the crosslinked dextran solution. This solution was stirred and the resulting beads were air-dried (Fig.2(b)).

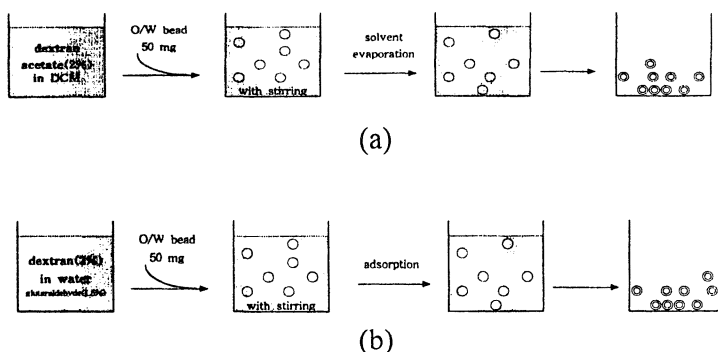


Fig. 2 Preparation of alginate beads coated with (a) dextran acetate or (b) cross-linked dextran.

Results and Discussion

Preparation of polysaccharide acetate

Hydrophobic polysaccharide acetate was synthesized by replacing hydrogen atoms with acetyl groups. The FT-IR spectra of lactan acetate showed the presence of acetate groups, indicated by C=O stretching (wave number 1753 cm^{-1}), CH_3 deformation (1381 cm^{-1}) and O=C=O bonds (599 cm^{-1}) and reduction of hydrophilic OH groups (3500 cm^{-1})⁵.

IND release from LAM

The major factor in controlling the drug release pattern was the pH-dependent swelling behavior of the microspheres. The pH-sensitive swelling behavior of lactan acetate pellets was measured (Fig. 3(a)). The swelling of lactan acetate pellets at pH 7.4 was much greater than that at pH 1.2. Yuk et al.⁸ reported that pH sensitive drug release pattern was due to diffusion of the drug from the capsule network and the escape of drug from the surface, which disintegrated after swelling depending on the chemical composition of the capsule network and pH of the release media. Under acidic conditions (e.g., pH 1.2), carboxylic groups were protonated and lactan acetate microspheres were shrunken. Under neutral conditions (e.g., pH 7.4), however, the concentration of negatively charged carboxylic group in lactan acetate microspheres increased, leading to a drastic increase in swelling. IND release experiments were performed at two pH conditions for 12 hr. Fig. 3(b) shows the release pattern from microspheres with the drug loading of 41 %. The drug is not released from the microspheres. However, at pH 7.4 the overall release rate increased as a result of the ionization of carboxylic groups at neutral pH. After drug release, microspheres at pH 1.2 maintained a spherical shape, but the microspheres at pH 7.4 disintegrated completely (Fig. 4).

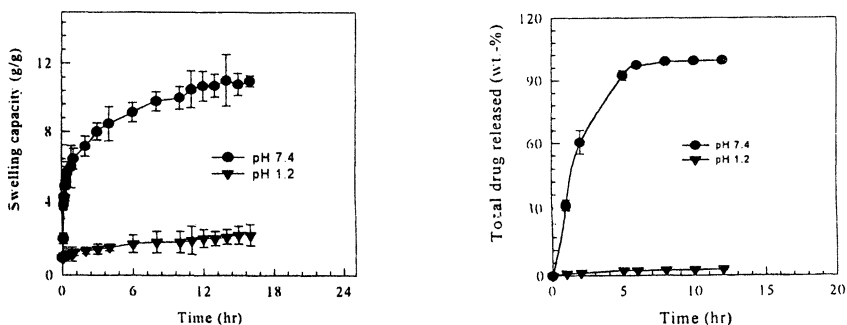
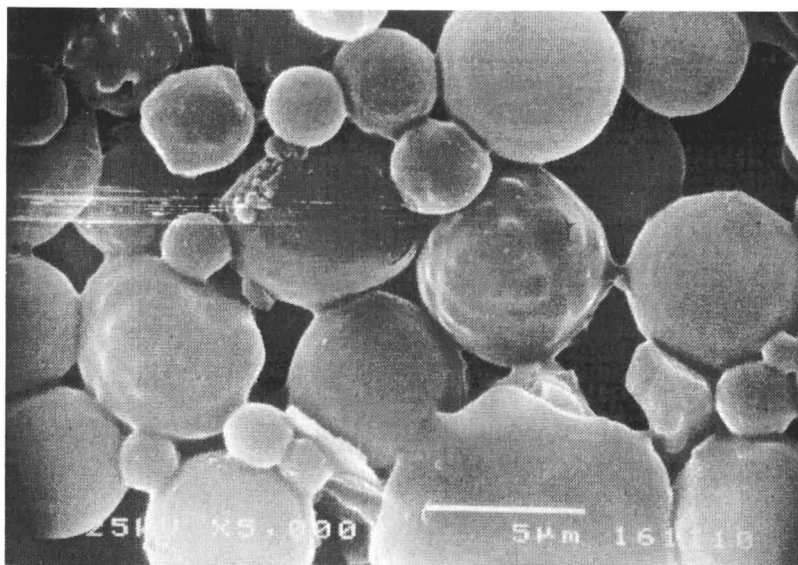
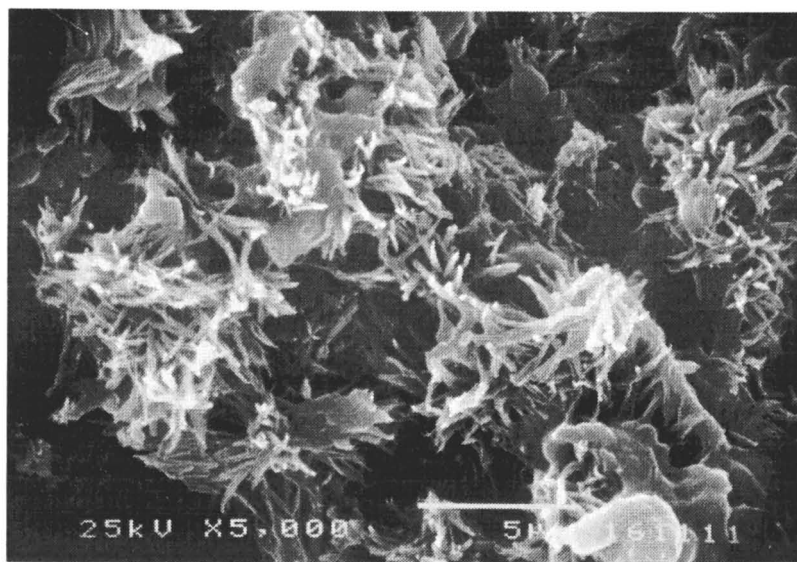


Fig. 3 The swelling (a) and drug release (b) kinetics of lactan acetate at pH 1.2 and 7.4. (Reproduced with permission from reference 5).



(a)



(b)

Fig. 4 SEM pictures of lactan acetate microspheres after drug release at pH 1.2 (a) and at pH 7.4 (b) for 24 hr (Reproduced with permission from reference 5).

Physical state of the drug in GAN

Figure 5 shows particle size distributions of GAN I and II. The sizes of GAN I and II in distilled water were 250.78 ± 185.13 nm and 718 ± 145.9 nm respectively, as measured by photon correlation spectroscopy. When the polymer concentration was decreased, the particles became smaller. The physical state of the drug in nanoparticles was examined by powder X-ray diffraction studies. Powder X-ray diffraction patterns of GA (a), IND (b), a physical mixture of the drug (15 %) and GA nanoparticles (c), GAN I (d) and GAN II (e) are shown in Fig. 6. GA exhibited an amorphous aspect, while IND was shown to have a crystalline structure. For the physical mixture of the drug (15%) and GA, crystalline structure of IND was observed. However, in GAN I, polymorphic change occurred with a decrease in the degree of crystalline state in the formulation developed, suggesting that IND is dispersed in an amorphous form in the polymer network. Similar findings were reported previously for other hydrophobic drugs such as hydrocortisone⁹.

IND Release from GAN

The release profiles from different formulations were compared with that of IND powders (Fig. 7). When IND powders and formulated IND were tested for release in vitro, 90% of nonformulated IND was released within 3 hr. For GAN I and GAN II, 54 % and 21 % of IND were released within 3 h, while 87 % and 83 % were released after an additional 24 h, respectively. Consequently GAN I (small nanoparticles) displayed more rapid initial drug release, compared to the larger particles probably due to their greater surface area per unit mass.

Enzyme-sensitive drug release

Figure 8 shows drug release patterns at pH 1.2 or 7.2 in the absence of dextranase. At pH 1.2 all formulations showed negligible drug release. At pH 7.2, IND release were 50 %, 35 %, and 25 % from alginate beads, alginate beads coated with crosslinked dextran (CD), and beads coated with dextran acetate (DA), respectively. Figure 9 shows drug release pattern at pH 7.2 in the presence of 1.61 U/mg or 4.84 U/mg of dextranase. At 4.84 U/mg of dextranase, 80 % of IND was released from DA coated leads after 12 hr. Figure 10 shows drug release patterns in the absence and presence of dextranase. Drug release from alginate beads coated with dextran acetate reached 95 % in 7 hr. Since dextranase is known to be present in colon, alginate beads with dextran acetate have a potential as a colon targeting material.

Conclusions

In this work, various polysaccharides were examined as a coating polymer for microbeads. Lactan gum showed pH-sensitive property, which may be used for enteric coating. Drug release from alginate bead coated with dextran acetate was dependent on the presence of enzyme. This property can be used to develop colon-targeted drug delivery systems.

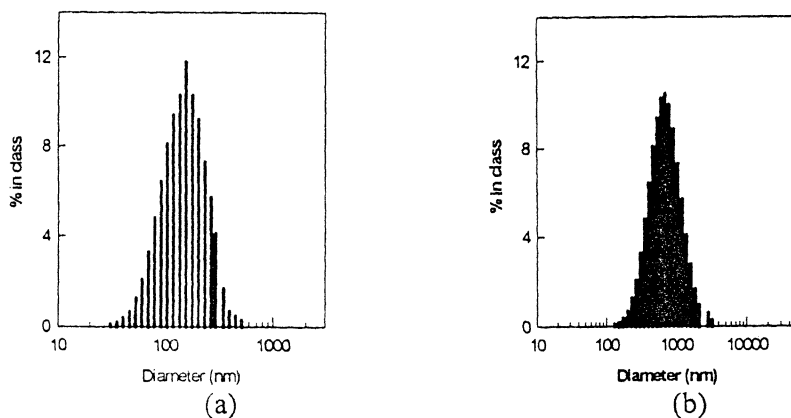


Fig. 5 Particle size distribution of GAN I (a) and II (b).

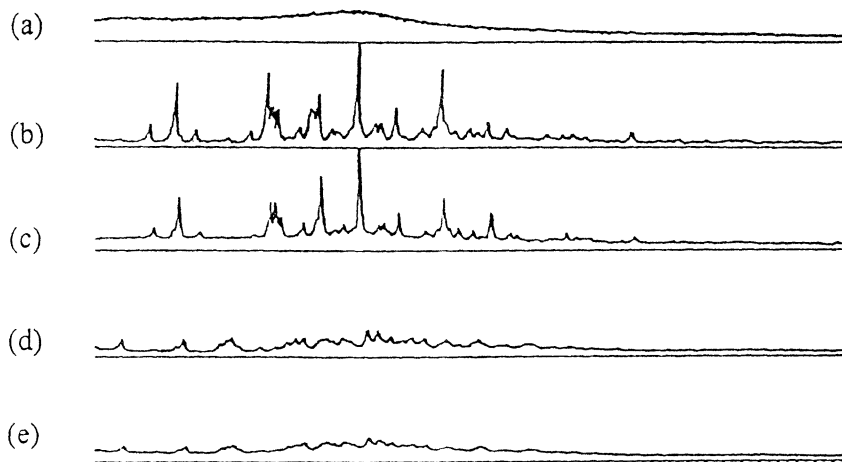


Fig. 6 Powder X-Ray diffraction patterns of GA(a), IND(b), physical mixture of GAN and IND (c), GAN I(d) and GAN II (e).

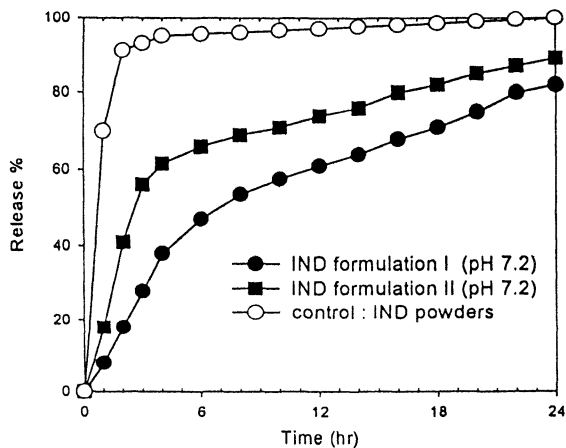


Fig. 7 Release of IND in the GAN I and GAN II at pH 7.2.

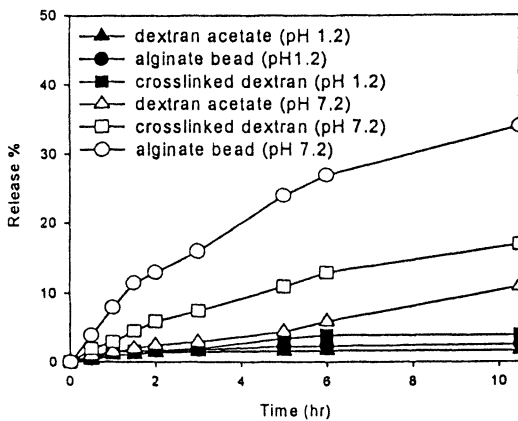


Fig. 8 Release of IND from alginate beads, beads coated with dextran acetate or cross-linked dextran.

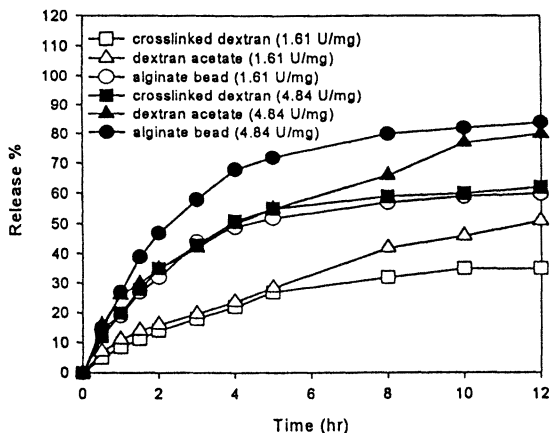


Fig. 9 Release of IND from alginate bead, bead coated with dextran acetate or cross-linked dextran. (Number within bracket indicate dextranase concentration)

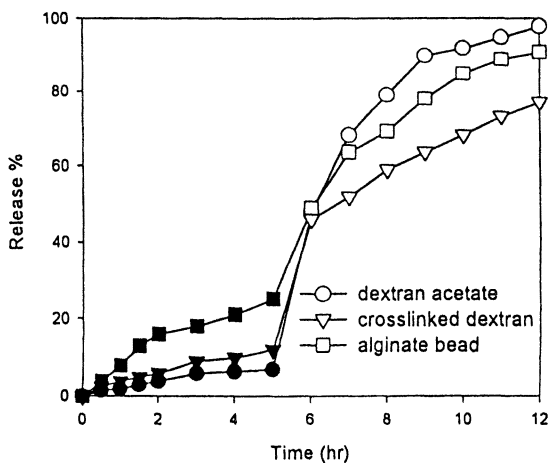


Fig. 10 Release of IND from alginate beads, beads coated with dextran acetate and beads coated with crosslinked dextran. At 5 hr, 3.225 U/mg of dextranase was added.

References

- (1) Park, K.; Shalaby, W. S; Park H. In: *Biodegradable hydrogels for drug delivery*; Technomic Publishing Inc. , 1993.
- (2) Albin P.; Markus A.; Pelah Z.; Ben-Zvi Z. *J. Controlled Release* **1995**, 36, 109
- (3) Santucci E.; Alhaique F.; Carafa M. ; Coviello T., *J. Controlled Release* **1996**, 42, 157
- (4) Linton, J.D.;Ash S. G.; Huybrechts, In: *Microbial Polysaccharides* ; Stockton Press **1991** .
- (5) Na, K.; Lee K.Y., *Drug Development and Industrial Pharmacy*, **1998**, 24(6) 563
- (6) Hirsh, S., Schehlmann, V., Kolter, K., and Bauer, K. H., *Marcomol. Symp.* **1995**, 99, 209
- (7) Motozato Y.; Ihara H.; Tomoda T.; Hirayama, *J. Chromatogr.*, **1986**, 355, 434
- (8) Yuk, S. H., C. H. Cho, B. C. Shin, and H. B. Lee, . *Eur. Polym. J.* 1996, 32: 101-104.
- (9) Chavalier, M., J. P. Benoit, and Thies, *J. Pharm. Pharmacol.*, 1986, 38; 249-253.

Chapter 39

Preparation of Blood-Compatible Nanoparticles Bearing Phosphorylcholine Group

Kazuhiko Ishihara¹, Tomohiro Konno², Kimio Kurita²,
Yasuhiko Iwasaki³, and Nobuo Nakabayashi³

¹Department of Materials Science, Graduate School of Engineering,
The University of Tokyo, Hongo, Bunkyo-ku, Tokyo 113-8656, Japan

²College of Science and Technology, Nihon University,
Chiyoda-ku, Tokyo 101-8356, Japan

³Institute of Biomaterials and Bioengineering,
Tokyo Medical and Dental University, Chiyoda-ku, Tokyo 101-0062, Japan

The biodegradable poly (L-lactic acid) (PLA) nanoparticles covered with 2-methacryloyloxyethyl phosphorylcholine (MPC) polymer were prepared by the solvent evaporation technique with the amphiphilic water-soluble MPC polymer as the emulsifier. The diameter of the nanoparticles was approximately 200 nm, which was determined by atomic force microscopy and dynamic light scattering. X-ray photoelectron spectroscopy analysis indicated that the surface of the nanoparticles was fully covered with the MPC polymer. The amount of plasma protein bovine serum albumin adsorbed on the nanoparticles coated with the MPC polymer was significantly smaller compared with that on the polystyrene nanoparticles. The PLA nanoparticles coated with the MPC polymer is suggested to be a safer drug carrier in the bloodstream. One of the anticancer drugs, adriamycin (ADR), could be adsorbed on the nanoparticles through a hydrophobic interaction. Even when the nanoparticles were stored in PBS for 5 days, 40 % of the ADR still remained on the surface. We concluded that the nanoparticles coated with the MPC polymer are useful as a novel adsorption-type drug carrier, which could be applied through the bloodstream.

A drug delivery system should achieve the maximum physiological effects during pharmaceutical treatment using the minimum amount of a drug. For this purpose, safer drug carriers such as polymer aggregates, liposomes, and nanoparticles are needed (1-6). Nanoparticles are especially effective carriers of drugs since they are quite stable in living organisms (1, 2, 7). In general, biodegradable polymers have

been used as the material of choice for preparing the nanoparticles (2-5, 7). Therefore, we used the biodegradable poly (L-lactic acid) (PLA) as the core of the nanoparticles.

There are two loading methods for a drug in a nanoparticle system (8). One is the encapsulation of the drug in the nanoparticles, and the other is the adsorption of the drug on the surface of the nanoparticles (Figure 1). The adsorption method is very convenient and simple because many drugs have a hydrophobic component part in their molecule or structure. Moreover, the drugs can be easily loaded onto the nanoparticles by mixing after the preparation of the nanoparticles. Therefore, we chose the rational adsorption of a drug as the loading method.

When normal nanoparticles are injected into the bloodstream, they are immediately phagocytized by the cells of the mononuclear phagocytic systems because their biocompatibility and blood compatibility is quite poor (9). Therefore, the surface modification of the nanoparticles with blood compatible material is important in order to prolong the circulation period in the bloodstream.

We have synthesized 2-methacryloyloxyethyl phosphorylcholine (MPC) polymers with attention to the structure of a biomembrane and reported that the MPC polymers showed excellent blood compatibility (10), i.e., suppression of protein adsorption and platelet adhesion. The MPC polymers have been studied as modifier materials to improve the blood compatibility of medical devices (11).

In this communication, the biodegradable PLA nanoparticles coated with the MPC polymer were prepared and the effectiveness of the MPC polymer/PLA nanoparticles as a drug carrier were then evaluated.

Materials and Methods

Materials

MPC was synthesized by a previously reported method (11). Water-soluble poly (MPC-co-BMA) with a 0.30 MPC unit mole fraction (PMB30W) was prepared by a conventional radical polymerization technique using *t*-butyl peroxy neodecanoate as the initiator. The number-averaged molecular weight (M_n) of the PMB30W was 5.0×10^4 which was determined by light scattering. PLA ($M_n = 2 \times 10^4$) was purchased from Wako Pure Chemicals, Ltd., Osaka, Japan, and used without further purification. Polystyrene nanoparticles were purchased from Polysciences, Inc., Warrington, PA, USA (average diameter = 202 nm). Bovine serum albumin (BSA) and adriamycin-hydrochloride (ADR) were purchased from Sigma Chemicals, St. Louis, MO, USA, and used without further purification.

Preparation of Nanoparticles

In a sample tube, 50 mL of an aqueous solution containing a given amount of PMB30W was placed stirred at 400 rpm with cooling in an ice bath. PLA (25 mg) was dissolved in 2.5 mL methylene dichloride and the solution was dropped into the

PMB30W aqueous solution. The mixture was sonicated using a probe-type generator for 30 min and kept under reduced pressure for 2 h to evaporate the methylene dichloride. The formed nanoparticles were fractionated by centrifugation at 10,300 g at 4 °C for 30 min. The nanoparticles as a precipitate were resuspended with distilled water and centrifuged again under the same conditions. This procedure was repeated three times to completely remove any free PMB30W. The nanoparticles were finally freeze-dried.

Characterization of the PMB30W/PLA Nanoparticles

One drop of the PMB30W/PLA nanoparticle suspension prepared with 1.0 mg/mL of PMB30W was spread on a glass plate. It was dried in air at room temperature, and then dried in vacuo. The morphology of PMB30W/PLA nanoparticles was observed using atomic force microscopy (AFM, SPI-3800, Seiko, Chiba, Japan). The surface of the nanoparticles was analyzed using an X-ray photoelectron spectroscope (XPS, ESCA-200, Scienta, Uppsala, Sweden). The size distribution and the ζ -potential of the PMB30W/PLA nanoparticles were determined using an electrophoretic light scattering (ELS, ELS-700, Otsuka Electronics, Ltd., Tokyo, Japan) with a 90° scattering angle in phosphate-buffered saline (PBS, pH7.4; ionic strength, 0.10 M).

Determination of Amount of BSA Adsorbed on the PMB30W/PLA Nanoparticles

BSA was dissolved in PBS at a concentration of 20 mg/mL. The polystyrene nanoparticles or the PMB30W/PLA nanoparticles was dropped into the BSA solution and the concentration of the particle suspension was 0.18 mg/mL. After the solutions were incubated for 30, 60, and 180 min at 37 °C, the mixed suspensions were fractionated by centrifugation. The amount of BSA adsorbed on the PMB30W/PLA nanoparticles or polystyrene nanoparticles was determined using a microBCA protein assay reagent kit, Pierce, Rockford, IL, USA by comparison of the concentration of BSA in the supernatant with that of the original BSA solution.

Adsorption of Adriamycin onto the Nanoparticles

ADR was dissolved in a small amount of ethanol and then diluted with distilled water. The ADR solution was mixed with the PMB30W/PLA nanoparticle suspension prepared with 1.0 mg/mL of PMB30W. The final concentration of ADR was adjusted to 6×10^{-4} g/dL. After incubation for 2 days at room temperature, the suspension was centrifuged to precipitate the nanoparticles for removing the free ADR. The precipitated nanoparticles were sufficiently rinsed with distilled water until free ADR in the supernatant was not detected by fluorescence spectroscopy. After the nanoparticles (ADR/PMB30W/PLA nanoparticles) was freeze-dried to determine the amount of adsorbed ADR using the following procedure. The nanoparticles were dissolved in methylene dichloride, and the concentration of ADR adsorbed on the obtained nanoparticles was calculated from the fluorescence intensity

of the methylene dichloride solution. The excited wavelength (λ_{ex}) and emission wavelength (λ_{em}) of the ADR were 470 nm and 585 nm, respectively.

***In vitro* ADR Release from Nanoparticles.**

One mL of PBS (ionic strength 1.0 M) was added to 9 mL of an ADR/PMB30W/PLA nanoparticles suspension (1.0 mg/mL) in a centrifugation tube. The suspension was immediately centrifuged at 10,300 g and 37 °C for 30 min. The fluorescence intensity of the ADR in the supernatant was measured. The nanoparticles were resuspended with the supernatant and incubated at 37 °C. The suspension was repeatedly centrifuged for a given period and the fluorescence intensity then measured.

Cell Assay of Activity of ADR/PMB30W/PLA Nanoparticles.

Human premyelocytic leukaemia cell lines (HL-60) cells were cultured in growth medium consisting of RPMI 1640 (GIBCO BRL, Rockville, MD USA) with 10 % heat-inactivated fetal bovine serum supplemented with 10 mg/mL penicillin, 25 mg/mL streptomycin, and amphotericin B in 0.85 % saline, at 37 °C in a humidified atmosphere of 5 % CO₂ and 95 % air. In the cell culture dish with HL-60 cells at an initial density of 1×10^6 cells/well, ADR solution (final concentration: 4.0×10^{-7} mol/L), ADR/PMB30W/PLA nanoparticles (3.8×10^{-4} g/mL, the same ADR concentration), or PMB30W/PLA nanoparticles (3.8×10^{-4} g/mL) was added at 37 °C. After given period, number of vital cell was determined by the trypan blue dye exclusion test and monitored with phase-contrast microscope.

Results

The PMB30W/PLA nanoparticles could be prepared by the solvent evaporation technique using the PMB30W bearing the phospholipid polar group, which served as both an emulsifier and a surface modifier. Figure 2 is a schematic representation of the PMB30W/PLA nanoparticle. The PMB30W was stably immobilized on the surface of the PLA nanoparticle. That is, an interlocking network was formed between the hydrophobic segments and the PLA chains.

An AFM view of the PMB30W/PLA nanoparticles prepared in 1.0 mg/mL of PMB30W aqueous solution is shown in Figure 3. It was observed by AFM that the nanoparticle had a spherical shape with a 100-300 nm diameter. The size and distribution of the nanoparticles were also measured with ELS. The ELS measurement results are summarized in Table 1. A weight average diameter of nanoparticles prepared in 1.0 mg/mL of PMB30W solution was 215 ± 35 nm. The results of ELS corresponded to those of the AFM observations. The ζ -potential of the nanoparticles is also summarized in Table 1. The nanoparticles prepared in 0.01 mg/mL PMB30W aqueous solution had a highly negative ζ -potential in PBS. On the

Encapsulation type drug carrier



Adsorption type drug carrier

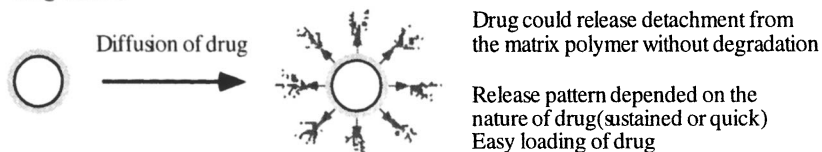


Figure 1. Loading of drug in/on the polymeric drug carrier.

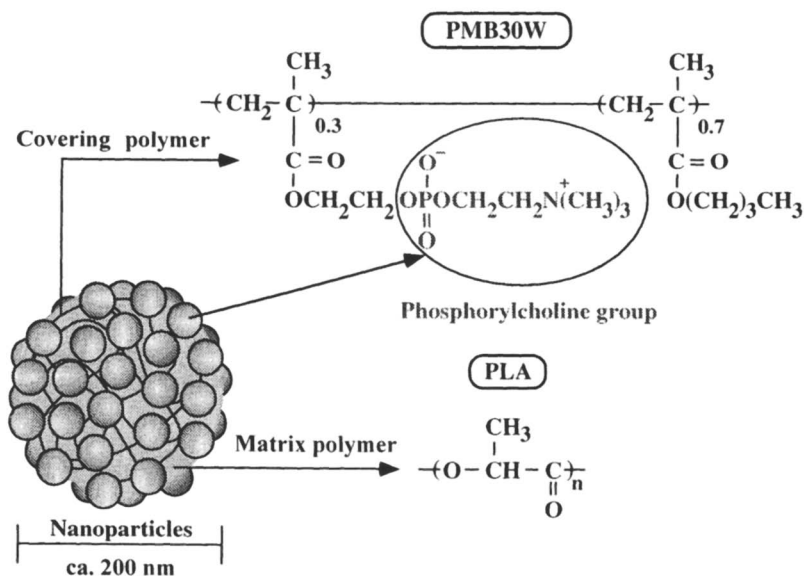


Figure 2. Schematic representation of the PLA nanoparticle covered with the MPC polymer.

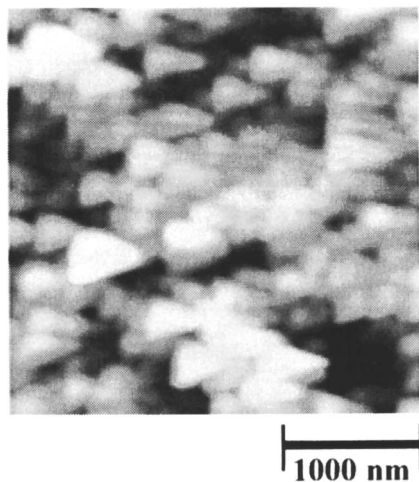


Figure 3. AFM view of the PMB30W/PLA nanoparticles.

Table 1. Characterization of nanoparticles covered with the PMB30W

<i>Concentration of PMB30W (mg/mL)</i>	<i>ζ-potential (mV)</i>	<i>Diameter (weight average) (nm)</i>	<i>Diameter (Number average) (nm)</i>
0.01	- 41	207 \pm 49	183 \pm 35
0.10	- 10	199 \pm 57	168 \pm 36
1.00	- 8.2	215 \pm 35	201 \pm 29

other hand, the ζ -potential of the nanoparticles increased in an increase of PMB30W concentration.

The XPS spectra of C_{1s} and P_{2p} on the surface of the nanoparticles are shown in Figure 4. In the case of the PLA nanoparticles prepared with 0.01 mg/mL of PMB30W, there was no phosphorous peak, and the strong peak attributed to the carbonyl carbon at 288 eV was observed. On the other hand, those prepared with 1.0 mg/mL of PMB30W had a phosphorous peak due to the MPC unit. Therefore, in the following study, the PMB30W/PLA nanoparticles prepared with 1.0 mg/mL of PMB30W were used.

Figure 5 shows the amount of BSA adsorbed on the polystyrene nanoparticles and PMB30W/PLA nanoparticles. The amount of BSA adsorbed on the polystyrene nanoparticles was higher than that on the PMB30W/PLA nanoparticles and increased with an increase in the incubation time. The α -helix content of native BSA which was determined with a Circular Dichroism spectroscopy was 50 %, and that which contacted the PMB30W/PLA nanoparticles was very similar to the level as that of the native BSA (Data not shown).

The ADR could be adsorbed onto the PMB30W/PLA nanoparticles. After the unadsorbed ADR was repeatedly removed by centrifugation, the amount of ADR that remained on the surface was 0.3 g/g-nanoparticles. Figure 6 indicates the release profile of adsorbed ADR from the nanoparticles in PBS with pH 7.4. The release of ADR continued for about 30 h. Within the first 12 h, 50 % of adsorbed ADR was released in the medium, and after 30 h, more than 60 % of initial amount of ADR was released.

Figure 7 indicates the relationship between the survival ratio of HL-60 cells and incubation time. In the case of ADR addition, the percentage of survival cells versus control (no addition) decreased gradually. On the other hand, the addition of the ADR/PMB30W/PLA nanoparticles showed a delay of cell response slightly compared with that of ADR solution. The PMB30W/PLA nanoparticles did not affect on the cells. These results indicated that the pharmaceutical effects of ADR/PMB30W/PLA nanoparticles were dependent on the diffusion of ADR from the nanoparticles. Moreover, the PMB30W/PLA nanoparticles did not affect to the proliferation and metabolism of HL-60 cells.

Discussion

The PLA nanoparticles prepared using PMB30W by the solvent evaporation technique were stably dispersed in an aqueous media. This indicates that the hydrophilic MPC units are located on the surface of the nanoparticles as shown in Figure 2. The PMB30W functioned as an emulsifier for the methylene dichloride solution containing PLA. The results from the XPS analysis indicated that the phosphorylcholine groups were located on the surface of the PMB30W/PLA nanoparticles. Moreover, a decrease in the intensity of the carbonyl carbon peaks and an increase in that of the methylene carbon peaks (285 eV) indicated that the PMB30W (polymethacrylate) was concentrated at the surface of the nanoparticles.

The biocomponents including the plasma protein have a slightly negative charge. Therefore, the positive charged nanoparticles are not suited for general administration. Also, the nanoparticle with a large negative ζ -potential is easily taken up by the

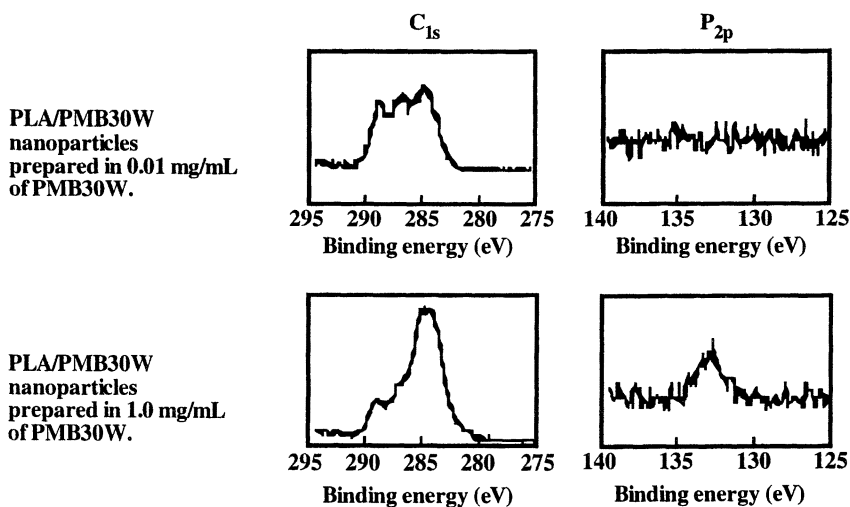


Figure 4. XPS spectra of PMB30W/PLA nanoparticles prepared in 0.01 mg/mL or 1.0 mg/mL PMB30W aqueous solution.

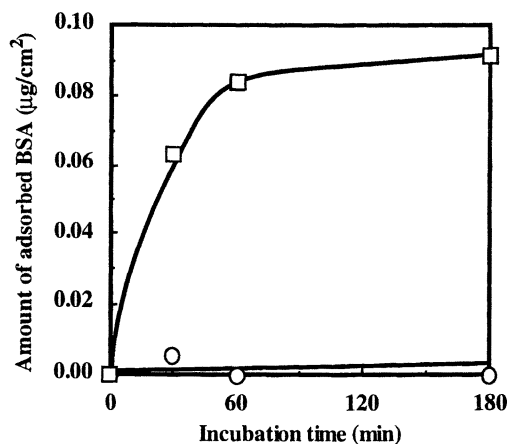


Figure 5. Amount of adsorbed BSA on (□) polystyrene nanosphere and (○) PMB30W/PLA nanoparticles in PBS (pH7.4) at 37 °C. BSA concentration was 20 μg/mL, polystyrene nanosphere (diameter; 200 nm) and PMB30W/PLA nanoparticles (diameter; 200 nm which was determined with dynamic light scattering and atomic force microscope) concentration was 1.0×10^5 μg/mL, respectively.

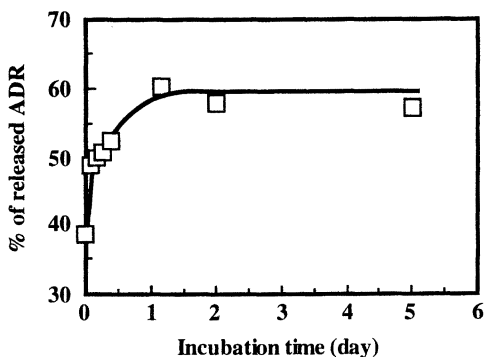


Figure 6. Release of ADR from ADR/PMB30W/PLA nanoparticles in PBS (pH 7.4; ion strength, 0.1 M) at 37 °C.

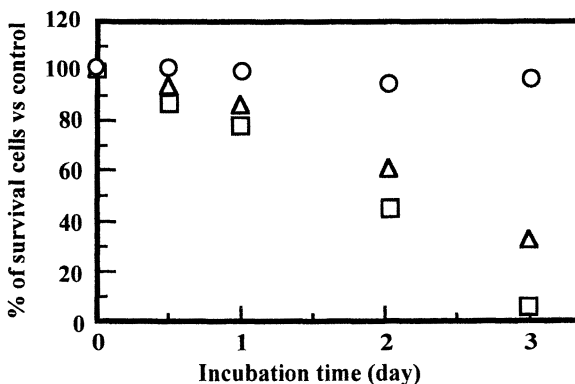


Figure 7. The percent of survival cells as against control that was determined by trypan blue dye exclusion test. Addition of (○) PMB30W/PLA nanoparticles, (△) ADR/PMB30W/PLA nanoparticles, and (□) ADR solution. Concentrations of ADR and each nanoparticle were 4.0×10^7 M and 3.8×10^{-4} g/mL, respectively.

reticuloendothelial systems (RES) after intravenous injection (7). That is, the PMB30W/PLA nanoparticles, which have a lightly anionic ζ -potential surface, satisfied one of the requirements for blood compatibility.

It has been reported that the water-insoluble poly (MPC-co-BMA) membrane has a 0.5 mV ζ -potential and a weak interaction with plasma proteins (12, 13). Protein adsorption is one of the most important phenomena for determining the blood compatibility of the drug carriers. As shown in Figure 5, the BSA was immediately adsorbed on the polystyrene nanoparticles. On the other hand, the adsorption of BSA hardly occurred on the PMB30W/PLA nanoparticles. From the CD spectra of BSA in the presence of the PMB30W/PLA nanoparticles, the α -helix content of BSA contacted with the nanoparticles was almost at the same level as that of the native BSA (approximately 50 %) (Data not shown). These results indicated that the PMB30W/PLA nanoparticles did not induce any conformational change in the BSA even when the BSA contacted the nanoparticles. It is very important to inhibit the thrombus formation when they are introduced into the bloodstream.

Sugiyama et al. prepared microspheres composed of MPC and methyl methacrylate and found an effective suppression of the adsorption of both BSA and human serum γ -globulin. They presumed that the surface layer of the microspheres adsorbed much water, and the surface of the microsphere formed a partial hydrogel structure (14, 15). We have already reported that the MPC polymer surface effectively reduces protein adsorption (10, 13) and considered the reason of these phenomena. Since the water state on the MPC polymer surface is maintained as natural, proteins in contact with the surface can immediately detach. That is, the surface, which has a higher content of free water, mildly interacts with the blood components (12, 16). Therefore, the PMB30W/PLA nanoparticles were expected to have weak interactions with the blood components, and not cause the opsonization which ultimately leads to phagocytosis.

The ADR could be adsorbed onto the surface of the nanoparticles through the hydrophobic interaction in aqueous medium. Fifty % of the adsorbed ADR was rapidly released by dilution with PBS. That is, the ADR solubility is considered to increase by dilution with PBS. This is because the phosphorylcholine head group of the MPC unit is electrically neutral and stable to ions, due to forming an inner ion complex as zwitter ions. The ADR could be retained by a simple adsorption method on the nanoparticles. An *in vitro* activity test using the HL-60 cells clearly indicated that the ADR/PMB30W/PLA nanoparticles could inhibit the cell proliferation whereas the PMB30W/PLA nanoparticles were inert to the cells.

It is concluded that the PMB30W/PLA nanoparticles effectively suppressed the unfavorable interactions with biocomponents. The PMB30W can potentially improve the blood compatibility of the PLA nanoparticles, and the PMB30W/PLA nanoparticles have the strong possibility of a long circulatory half-life which could result in be a safer adsorption-type drug carrier in living organisms.

Acknowledgements

This study was partially supported by the Shiseido Science and Technology Research Foundation and Grants-in-Aid for Scientific Research from the Ministry of Education, Japan (09480250).

References

1. Maruyama, A.; Ishihara, T.; Adachi, N.; Akaike, T. *Biomaterials* **1994**, *15*, 1035.
2. Ogawa, Y. *J. Biomater. Sci. Polymer Edn.* **1997**, *8*, 391.
3. Boury, F.; Marchais, H.; Benoit, J.P.; Proust, J.E. *Biomaterials* **1997**, *18*, 125
4. Coombes, A.G.A.; Tasker, S.; Lindblad, M. Holmgren, J.; Hoste, K.; Toncheva, V.; Schacht, E.; Davies, M.C.; Illum, L. *Biomaterials* **1997**, *18*, 1153.
5. Peracchia, M.T.; Gref, R.; Minamitake, Y.; Domb, A.; Lotan, N.; Langer, R. *J. Controlled Release* **1997**, *46*, 223.
6. Yokoyama, M.; Fukushima, S.; Uehara, R.; Okamoto, K.; Kataoka, K.; Sakurai, Y.; Okano, T. *J. Controlled Release* **1998**, *50*, 79.
7. Vittaz, M.; Bazile, D.; Spenlehauer, G.; Verrecchia, T.; Veillard, M.; Puisieux, F.; Labarre, D. *Biomaterials* **1996**, *17*, 1575.
8. Maruyama, A.; Ishihara, T.; Kim, J.S.; Kim, S.W.; Akaike, T. *Bioconjugate Chem.* **1997**, *8*, 735.
9. Voronov, I.; Santerre, J.P.; Hinek, A.; Callahan, J.W.; Sandhu, J.; Boynton, E.L. *J. Biomed. Mater. Res.* **1998**, *39*, 40.
10. Ishihara, K.; Oshida, H.; Endo, Y.; Ueda, T.; Watanabe, A.; Nakabayashi, N. *J. Biomed. Mater. Res.* **1992**, *26*, 1543.
11. Ishihara, K.; Ueda, T.; Nakabayashi, N. *Polym. J.* **1990**, *22*, 355.
12. Ishihara, K.; Nomura, H.; Mihara, T.; Kurita, K.; Iwasaki, Y.; Nakabayashi, N. *J. Biomed. Mater. Res.* **1998**, *39*, 323.
13. Ueda, T.; Ishihara, K.; Nakabayashi, N. *J. Biomed. Mater. Res.* **1995**, *29*, 381.
14. Sugiyama, K.; Aoki, H. *Polym. J.* **1994**, *26*, 561.
15. Sugiyama, K.; Mitsuno, S.; Shiraishi, K. *J. Polym.Sci. A: Polym. Chem.* **1997**, *35*, 3349
- Lu, D.R.; Lee, S.J.; Park, K. *J. Biomater. Sci. Polymer Edn.* **1991**, *3*, 147.

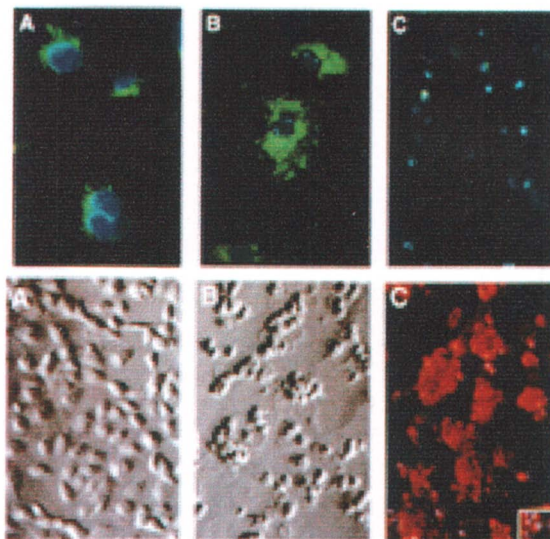


Figure 7. Cell-apoptosis induced by SGP. a) Fluorescence microscopy of normal dermal microvessel endothelial cells A). Same cells treated with 1 mM SGP, for 30 min (B) and for 2 hours (C). The nuclei are stained blue, and the mitochondria are stained green. b) Normal human Kaposi's sarcoma cells using Hoffman modulated phase contrast microscopy as same conditions described above. These show the condensed nuclei and cell membrane blebbing characteristic of apoptosis.

Author Index

- Ackerman, Neil, 273
Agarwal, Rajesh, 54
Ainaoui, A., 90
Alexandridis, Paschalis, 364
Allen, Theresa M., 100
Amidon, Gordon L., 46
Andrianov, Alexander K., 395
Bass, Paul, 78
Baughman, Robert A., 54
Berner, Bret, 273
Biegajski, Jim, 273
Blau, Sigal, 78
Borchardt, Ronald T., 36
Chen, Hilary, 273
Chen, Jianping, 395
Chen, Qiang, 273
Cho, Jin Cheol, 385
Cho, Sun Hang, 232
Conn, Tom, 273
Constantinides, Panayiotis P., 284
Dehal, Hardip, 273
Dokka, S., 193
Duan, M. X., 65
Duncan, Ruth, 350
Dunn, Tim, 273
Ellerby, H. Michael, 139
Ewing, Al, 273
Fan, Xiao-Dong, 253
Faroonsargn, D., 193
Fermi, Steve, 273
Fix, Joseph A., 14
Ford, Russell, 273
Gombotz, Wayne R., 110
Gonze, Mark, 54
Guo, J. H., 65
Guo, Wenjin, 212
Han, Hyo-kyung, 46
Hashida, Mitsuru, 201
Ishihara, Kazuhiko, 324, 417
Iwasaki, Yasuhiko, 417
Jagasia, Priya, 273
Jayalakshmi, Yalia, 273
Joshi, Priti, 273
Junginger, H. E., 25
Keller, Gilbert-André, 168
Kennedy, Allison L., 314
Kersten, Brian, 273
Khang, Gilson, 385
Kim, Yu-Eun, 407
Kiyota, Taira, 139
Kohen, Ron, 78
Kong, Qingzhong, 220
Konno, Tomohiro, 417
Kotze, A. F., 25
Kurita, Kimio, 417
Kurnik, Ronald, 273
Lake, Tim, 273
Larson, Gretchen M., 184
Lee, Hai Bang, 385
Lee, Jin Ho, 232
Lee, Jung Sik, 385
Lee, Ki-Young, 407
Lee, Kyung-Dall, 184
Lee, Robert J., 212
Lee, Sannamu, 139
Lencer, W. I., 149
Leone-Bay, Andrea, 54
Lesho, Matt, 273
Li, Wenlu, 168
Lillehei, Kevin, 220
Lin, Jan-Ping, 273
Linhardt, Jeffrey G., 243
Liu, David, 273
Liu, Yang, 220
Lopatin, Margarita, 273
Lu, Lichun, 124
Lueßen, H. L., 25
Luo, Q., 193
Ma, H., 65
Mack, Lexa, 273
Madara, J. L., 149
Merlin, D., 149
Messenger, Heather, 273
Mikos, Antonios G., 124
Money, Sam, 54
Mooney, David J., 157
Morley, Sam, 273
Mrsny, Randall J., 1, 168
Na, Kun, 407
Nakabayashi, Nobuo, 417

- Ng, Ka-yun, 220
Nishikawa, Makiya, 201
Oliva, Michelle, 273
Ooya, Tooru, 375
Ouellette, A. J., 149
Ouriemchi, E. M., 90
Park, Kinam, 1
Parris, Norman, 273
Peteherych, Kathy, 314
Peter, Susan J., 124
Peters, Martin C., 157
Pettit, Dean K., 110
Potts, Russell, 273
Pudlo, Jeff, 273
Ramaswamy, Manisha, 314
Reidy, Michael, 273
Rhee, John M., 385
Rivera-Schaub, Theresa, 54
Roberts, Bryan E, 395
Rojanasakul, Yon, 193
Rosado-Gray, Connie, 54
Rubinstein, Abraham, 78
Sako, Kazuhiro, 14
Sawada, Toyohiro, 14
Selsted, M. E., 149
Seo, Jung Ki, 232
Shi, X., 193
Soni, Pravin, 273
Stamatas, Georgios N., 124
Sugihara, Gohsuke, 139
Sule, Sameer S., 395
Takakura, Yoshinobu, 201
Tamada, Janet, 273
Thanou, M., 25
Thrombe, Avinash G., 69
Tierney, Michael, 273
Tirrell, David A., 243
Torchilin, Vladimir P., 297
Uhegbu, Christopher, 273
Uludag, Hasan, 253
Venkatesh, Gopi M., 335
Vergnaud, J. M., 90
Verhoef, J. C., 25
Vijayakumar, Prema, 273
Wang, Binghe, 36
Wasan, Kishor M., 314
Wei, Charles, 273
Weissig, Volkmar, 297
Williams, Steve, 273
Wilson, Don, 273
Wong, Wesley, 314
Wu, Christine, 273
Wu, X. Y., 263
Yam, F., 263
Yamashita, Fumiyoshi, 201
Yang, Lin, 364
Ye, J., 193
Yui, Nobuhiko, 375
Yuk, Soon Hong, 232
Zhang, Q., 263
Zheng, C. X., 65
Zuo, Y., 65

Subject Index

- A**
- Absorption barriers, gastrointestinal application, 25–26
 - Absorption enhancers, systemic toxic effects, 32
 - Absorption enhancing effect
 - carbomer, 27
 - chitosans, 30
 - Acetaminophen
 - in vitro release mechanism from drug:PEG:polymer matrix tablets, 20*t*
 - in vitro release profile from PEO and HPMC matrix tablets, 20*f*
 - permeability and molecular size of solutes, 269*t*
 - permeability through composite membrane, 268
 - permeability vs. temperature, 269*f*
 - release from HPMC matrix sustained-release tablets, 17*f*
 - Acid-labile liposomes, behave like viruses, 187
 - N*-Acryloxysuccinimide (NASI)
 - determination of hydrolysis rate, 255
 - reduce LCST, 253
 - unstabilizing effect on gelation, 262
 - Active specific immunotherapy, brain tumors, 220–229
 - Acyclovir, amino acid ester prodrugs, 49–51
 - Acyloxyalkoxy cyclic prodrugs, apparent permeation values, 41
 - Adhesive antioxidant enzymes, experimental colitis in the rat, 78–89
 - Administration route, controlled release dosage form, 3
 - Adriamycin (ADR)
 - adsorbed onto PMB30W/PLA nanoparticles, 423
 - anticancer drug, 417
 - release from ADR/PMB30W/PLA nanoparticles in PBS, 425*f*
 - Aggregate structure, MPC polymer, 324
 - Aggregation modes in buffer, SGP and its analogs, 147
 - Alginate, increase growth factor loading, 163
 - Alginate beads
 - coated with dextran acetate, 407
 - coating with dextran acetate and crosslinked dextran, 409–410
 - diagram for preparation, 409*f*
 - encapsulation system for growth factors, 161
 - Alkaline phosphatase activity
 - marrow stromal cells cultured on PPF substrates, 136*f*
 - osteoblastic phenotype markers, 135
 - Aluminum crosslinked PCPP microspheres, stability, 402
 - Aluminum lactate, crosslinker producing microspheres with narrow size distribution, 402
 - Aluminum stearate, emulsifier in MeCN, 390*f*
 - Amine reactivity, NiPAM/NASI/AMA polymers, 257
 - Amino acid ester, peptide carrier mediated membrane transport, 50
 - Amino acid ester prodrugs, acyclovir and zidovudine, 49–51
 - Amino acid sequences
 - capable of directing proteins to distinct organelles, 171*t*
 - mutation, 170
 - trafficking signals, 170
 - 4-Aminophenylacetic acid (4-APAA), luminal acidification, 51
 - Amphiphathic polymer, migration, 176
 - Amphiphilic water-soluble polymers, poly(MPC-*co*-BMA)s, 324–334
 - Amphotericin B lipid complex
 - distribution within human plasma following incubation, 321*t*
 - incubated in human plasmas, 320
 - Amphotericin, reduction in dose-limiting kidney toxicities, 105

- Anesthesia, fentanyl-loaded PLGA microspheres, 385–394
- Angiogenesis
development and wound healing, 159
peptide growth factors, 160
potential growth factors, 159
protein growth factors, 157
transplanted cell engraftment, 157–166
- Anion-conductive channels within liposomes, neutrophil α -defensins, 150
- Anion-selective channels, eukaryotic cell membranes in vitro, 155
- Antennapedia protein, transit across cellular membranes and into cytoplasm, 177
- Anthracyclines, liposomal drugs and vascular permeabilities, 105
- Antibody-targeted liposomes, classical and stealth, 106
- Anticancer conjugates, HPMA copolymer, 356
- Anticancer drugs
ADR, 417
DQA, 305–306
rate of drug release, 107
second generation, 355–357
targeted liposomes, 106
- Anticoagulation, plasma heparin levels, 54
- Anti-Factor Xa, oral heparin delivery in humans, 62
- Antigenicity, potential delivery vectors, 179
- Antihypertensive agent, buffer-based, membrane-coated dosage form, 335
- Antimicrobial activity, α -defensins, 150
- Antimicrobial peptides, cryptidins 2 and 3, 149–156
- Antioxidant activity, rat small intestine and colon, 78
- Antioxidant enzyme
local attachment to colonic mucosa, 83
ulcerated tissues, 87
- Antisense oligonucleotides, gene therapy, 105
- Antitumor activity, dendrimer platinate, 360
- Antitumor immune response
development, 228
presence of established intracranial tumor, 221
subcutaneous administration of irradiated tumor cells and cytokines, 228
vaccinating with a mixture of i9L and IFN- γ , 223–224
- Antiviral prodrugs, carrier-mediated transport, 46
- Apical membranes of epithelial cells, solute transport, 155
- Apoptosis, induction, 147
- Apparent permeation values, cyclic prodrugs of opioid peptides, 41
- Aqueous pores, peptide and peptide mimetic permeation, 37
- Arphamenine A, potent inhibitor for peptide transporters in renal brush border membrane vesicles, 51
- Arthritis treatment, NSAID, 407
- Artificial organs, tissue engineering, 6
- Asialoglycoprotein receptors
branched galactose oligomers, 202
hepatocytes, 201
- Aspirin, plasma drug level obtained with various dosage forms, 96*f*
- Autocrine factor, peptide and protein therapeutics, 7
- B**
- Bacterial escape from endosomes, macromolecular and gene delivery, 188
- Betamethasone
local treatments, 80, 83
MPO activity levels and TNF α concentrations, 87
- BFE, *see* Bulk-fluid endocytosis (BFE)
- bFGF, active in normal and pathological processes, 159

- Bilayer and conventional tablet formulations in vitro release profiles, 343*f*
 plasma concentrations, 344*f*
- Bilayer membrane holding SGP, electric current profiles, 144*f*, 146*f*
- Bile salts, effect on once-a-day dosage forms, 16
- Binding properties, polycarboxophil and carbomer, 27
- Binding site barrier, ligand-targeted liposomes, 106
- Bioactivity conservation, PEGylated etanercept, 117
- Bioadhesion, dosage forms on GI wall, 90, 91
- Bioadhesion systems, GI wall, 97
- Bioavailability
 carbomer and buserelin, 28
 water-soluble drugs in w/o microemulsions, 293–294
- Biochemical markers, inflammation severity, 87
- Biocompatibility
 controlled release dosage form, 3
 monolithic dosage forms, 91
 silicone implants, 6
- Biodegradable hydrogels, drug delivery, 407
- Biodegradable polymer substrates, TGF- β 1, 129–132
- Biodegradable polyrotaxanes
 drug delivery, 375–379
 drug release via supramolecular dissociation, 377–379
 supramolecular architectures, 375
 synthesis, 376–377
 tissue engineering, 380–381
 with ester linkages, supramolecular dissociation, 381
- Biodegradable sutures, PGLA, 158
- Biodistribution
 animal experiments, 312
 carriers after intravenous injection, 202
 glycosylated carriers, 202–205
¹¹¹In-labeled PEG–PE micelles, 299
 liposomal association of drugs, 100
 liposomal formulation of PGE₁, 206
- Bioerodible polymers, drug release, 91
- Biological activity, protein or peptide therapeutics, 10
- Biomembranes, interaction with proteins, 146
- Biopharmaceutical feasibility, controlled release formulation, 72–74
- Biosensors, glucose-monitoring program, 274
- Biotin–streptavidin bridge, enhanced levels of gene expression, 190
- Bladders, engineered, 158
- Blister fluid, drug profile, 95
- Block copolymer lyotropic liquid crystal structures, diffusion and erosion mechanisms, 373
- Block copolymer micelles, disintegration of gel matrix, 370
- Blood compatibility
 MPC, 418
 MPC copolymer, 325
 phosphorylcholine group, 417–427
 PMB30W aggregates, 333
- Blood components, interaction with PMB30W, 331–333
- Bloodstream, MPC polymer as safe drug carrier, 417
- Bone growth factors, polymeric delivery vehicles, 124–138
- Bone regeneration cascade, controlled release of TGF- β 1 to a bone defect, 125
- Bone tissue engineering, TGF- β 1, 125
- Bone-regenerating properties, chitosan, 29
- Brain tumors
 immunotherapy, 220–229
 inhibitory influence on development of antitumor immune response, 225–226
 repressive effect on immune system, 229
- Breast cancer cells
 targeted cytotoxin delivery, 181
 transport of fluorescent heregulin to nuclei, 172*f*
- Bronchial secretion, drug profile, 95

- BSA, adsorbed on polystyrene
nanosphere and PMB30W/PLA
nanoparticles in PBS, 424*f*
- Buffer, GI activity of insulin in IIOP, 66
- Buffer bead dosage forms, controlled
release delivery system, 336–339
- Buffer crystals, polymer coated, drug
layered, 335
- Bulk-fluid endocytosis (BFE),
membrane-
associated uptake pathway, 169
- Burst effect, TGF- β 1, 124
- Buserelin
absorption enhancing effect, 27–28
intraduodenal administration in rats,
29*t*
mean serum concentrations after
intraduodenal application, 28*f*, 31*f*
potency of chitosan HCl to increase
absorption, 30
- n*-Butyl methacrylate (BMA),
polymerization, 324
- C
- Caco-2 cell
intestinal epithelium model, carbomer
activity, 27
overexpression of hPEPT1
transporters, 51
- Caco-2/hPEPT1 cells, nonpeptide amino
acid–nucleoside esters, 50
- Caco-2 intestinal epithelium model,
permeability of paracellular markers,
30
- Caco-2 permeability, feasibility of
controlled release for drug candidate,
69
- Caffeine
controlled release from Poloxamer
hydrogel, 370–372
controlled release from Poloxamer
tablet, 372
in vitro release kinetics from
Poloxamer, 366–373
partition coefficient in Pluronic F127,
367–368
solubility vs. Pluronic F127
concentration, 369*f*
- Cancer drugs, targeting, 4, 6
- Cancer vaccines, treatment of brain
tumors, 221
- Capsule formulations, accelerated
stability and dissolution data, 342
- Carbomer
co-application of buserelin, 28
inhibition activity, 27
mucoadhesive properties, 26–27, 34
proteolytic enzyme inhibiting and
paracellular permeation enhancing
properties, 34
- Carbopol, mucosal penetration enhancer,
25
- Carbopol 934P, *see* Carbomer
- Cargo molecule, versatility, 182
- Carrier backbones, poly(amino acids),
203
- Carrier-mediated transport, antiviral
prodrugs, 46
- Carrier proteins, molecular nature, 47
- Catalase
activity in the mucosa/submucosa of
the small intestine, 78
cationization, 80
- Cationic peptides, α -defensins, 150
- Cationization of proteins, residence time
in target organs, 87
- Cationized antioxidant enzymes
colonic mucosa, 78
local treatment of colitis, 87
- Cationized catalase and SOD
cationization quantification, 81
local treatments, 80, 83
treatment of experimental colitis, 79
- Cationized proteins
activity and net charge, 82*t*
attachment to rat intestinal mucosa, 80
- Cell apoptosis, induced by SGP, 148(a)*f*
- Cell biology, controlled release drug
delivery systems, 2
- Cell death, necrosis (passive) or apoptosis
(active), 147
- Cell-mediated immunity, polypeptide
delivery of antigenic proteins, 190
- Cell permeation, cyclic prodrugs, 40

- Cell populations, transplantation on biodegradable polymer matrices, 158
- Cell-specific targeting, drugs and genes with glycosylated liposomes, 201–211
- Cell-surface receptors, modified cellular pathways, 10
- Cell survival, vascularization, 158–159
- Cell transfection, living viruses, 3
- Cell transplantation
 cells on macroporous matrices, 158
 engineering organs, 157–158
 polymer matrices, 164
- Cellular membrane permeability, passive membrane transport, 46
- Cellular targeting
 gene therapy, 3
 therapeutic macromolecules, 177
- Cellular uptake pathways, proteins, 169
- Cellular uptake time courses, [³²P]DNA complexed with liposomes, 209
- CETP, *see* Cholesteryl ester transfer protein (CETP)
- α -CH₃, chemical shift, 237*t*
- Channel formation
 cryptdin-based, 155
 SGP-related proteins, 145–146
- Chemical conjugation, drugs, 205
- Chemical linkers
 cyclic prodrugs of peptides and peptide mimetics, 43
 preparation of cyclic prodrugs, 38–39
 susceptible to esterase metabolism, 36
- Chemotherapeutic drugs, liposomal carriers, 100
- Chimera, targeted delivery, 179
- Chimera delivery vehicle, targeting sequence, 176
- Chinese hamster ovary (CHO) cells, hPEPT1 transporter, 50
- Chitosan
 absorption enhancing effects, 34
 carrier of plasmids in gene delivery, 29
 chemical representation, 29*f*
 mucoadhesion, 29
 paracellular permeability, 30
 source and properties, 28–30
- Chitosan derivatives
 novel permeation enhancers, 30–33*f*
 transmucosal absorption of hydrophilic macromolecules, 25–35
- Chitosan HCl, permeability of ¹⁴C-mannitol in Caco-2 intestinal epithelia, 32
- Cholesteryl ester transfer protein (CETP), plasma distribution of CsA, 317–318
- Chronic pain, genes encoding pain-killing proteins, 8
- Chronobiology, oral delivery systems, 15
- Chymotrypsin, permeability and molecular size of solutes, 269*t*
- Circulation time in blood, biodistribution of anticancer drug, 306
- Cl⁻ channels, down electrochemical gradient into crypt lumen, 150–151
- Clinical applications, potential, 179–182
- Clinical imaging, EPR effect in patients, 356
- Clinical pharmacokinetics, polymer conjugation to proteins, 353
- Coacervation method, preparation of polyphosphazene microspheres, 399–401
- Colicin, nonpolar membrane environment, 139
- Colon
 absorption of once-a-day dosage forms, 23, 70
 drug absorption, 14
 fluid content and drug release profiles, 17
- Colon inflammation
 cationized and native catalase, SOD, BSA, and commercial drugs, 86*t*
 quantification, 81
- Colon targeting system, alginate beads coated with dextran acetate, 407
- Colonic mucosa
 attachment of antioxidant enzymes, 79
 attachment of cationized catalase and SOD, 83
- Composite membrane, temperature and pH responsive permeation, 263–272
- Computed tomography (CT), diagnostic value, 302

- Conformational studies, phenylpropionic acid-based cyclic prodrugs, 40–41
- Constant release rate, validity for physiological conditions, 232
- Controlled release
- challenges in technologies, 6–8
 - current technology, 3–6
 - diffusion and erosion mechanisms, 369–370
 - important factors, 4–6
 - interdependent factors in system design, 5*f*
 - oral dosage, 90–97
 - pH/temperature-sensitive polymers, 232–242
 - present and future, 2–12
 - solubility considerations and design, 335–347
- Controlled release feasibility assessment, early drug candidate, 71–75
- Controlled release prototypes, rapid development, 75–76
- Coumarinic acid-based prodrugs
- ability of RGD analogs to permeate membranes, 42–43
 - solution structures and passive diffusion, 40
- Critical micelle concentration (CMC), surfactants, 298
- Crosslinked network, temperature-induced phase transition, 238
- Crosslinked poly(acrylic acid) derivatives
- absorption enhancers, 26–28
 - structure, 27*f*
- Crosslinking, binding interactions with mucosal tissues, 26
- Cross-sectional morphology, composite membrane, 267–268
- Cryogenic nonaqueous process, PLGA microsphere processing technology, 160
- Cryptdin
- neutrophil products with antimicrobial properties, 149
 - Paneth cells, 149–156
 - reversible Cl⁻ secretory response, 151–153
- Cryptdin 1–6, amino acid sequences, 154*f*
- Cryptdin 2 and 3, secretory response, 155
- Cryptdin 3
- channels in T84 cell membranes, 153*f*
 - dose dependency of Cl⁻ secretion, 152*f*
 - ion conductances and Cl⁻ secretion, 154
- Cryptdin peptides, structure–function relationships, 154–155
- Crystallinity, intermolecular hydrogen bonds, 380
- CsA, *see* Cyclosporine (CsA)
- CT, *see* Computed tomography (CT)
- CTL, *see* Cytotoxic lymphocytes (CTL)
- Cyclic prodrugs
- chemical linkers used in preparation, 38–39
 - permeation of biological barriers, 36
- Cyclization of linear peptides, metabolic stability and barrier permeability, 43
- Cyclization strategies, permeation of biological barriers, 36
- α -Cyclodextrins (α -CD), threaded onto PEG, 375
- β -Cyclodextrins (β -CD), change in location in response to temperature, 383
- Cyclosporine (CsA)
- distribution into plasma lipoproteins, 317*t*
 - distribution within normolipidemic and dyslipidemic plasma, 319*t*
 - distribution within plasma following incubation, 320*t*
 - interaction with compounds in lipid-based vesicles with lipoproteins, 314–323
 - interactions with plasma lipoproteins, 316–319
 - lipoprotein concentration and composition, 318–319
 - lipoproteins as novel carriers, 316
- Cystolic delivery, endosomolytic activity of LLO into pH-sensitive liposomes, 189
- Cytochrome P450, metabolism of peptides and peptide mimetics, 37

- Cytoplasmic free calcium ion concentration, 331–333
- Cytosolic delivery
 macromolecules with modified liposome formulations, 184–192
 membrane-impermeant macromolecules, 185–186
 strategies, 187–188
- Cytotoxic activity, infiltrating mononuclear cells, 228
- Cytotoxic agent, delivery to sensitive location, 181
- Cytotoxic lymphocytes (CTL), i9L plus IFN- γ , 220
- Cytotoxicity
 analysis of spleen cells from primed and unprimed rats, 227*f*
 dendrimers, 360
- D
- Defective genes, therapeutic approaches, 7–8
- α -Defensins
 cryptidins, 149–156
 soluble inducers of channel-like activity, 151
 structure and function, 150
- β -Defensins, epithelial cells of the intestine and respiratory tract, 150
- Degradative enzymes, effect on once-a-day dosage forms, 16
- Delicate macromolecules, polymers as safe absorption enhancers, 26–33
- Dendrimers, advantages as polymeric drugs, 360
- Dequalinium (DQA)
 incorporated into PEG-based micelles, 307*f*
 micellar form, 305–306
- Development strategy, drug candidate, 70–71
- Diabetes, glucose monitoring, 273
- Diacyllipid-PEG conjugates
 micelle-forming polymeric carriers, 298–302
 steric protection of liposomes, 298
- Diffusion coefficient, caffeine in F127 hydrogel matrix, 371
- Diffusion dominated drug release, HPC, HEC, and HPMC tablets, 20
- Diffusion mechanism, release of caffeine from Poloxamer gel, 369–370
- Diffusional transport, nutrients and waste products, 158
- N,N'*-Dimethylaminoethyl methacrylate (DMAEMA), glucose-controlled insulin delivery system, 232–242
- Dipeptides, basolateral and apical membrane transport, 52
- Dissolution media system, modified two-phase, 289
- Dissolution methods, poorly soluble drugs in lipid-based vehicles, 289
- Dissolution profiles, compound D, 345*t*
- Dissolution testing, CR marumerized bead dosage forms, 339
- DNA complexes, transfection activity of folate-PEI and folate-PEG-PEI, 216
- DNA delivery, glycosylated carriers, 206–210
- DNA/liposome complexes, inhibitory effect of galactose on transfection activity, 208*f*
- Docking proteins, transport of proteins with targeting sequences, 176
- Dosage
 delayed release and controlled release, 2
 development of controlled release forms, 3
- Dosage form
 effect of shape, 94–95
 in vitro performance, 72–74
- Dose strengths, development of early drug candidates, 70
- Doxorubicin
 decrease in cardiac toxicities, 105
 drug release rate, 103
 liposome carrier, 102
 stealth liposomes, 103
- DQA, *see* Dequalinium (DQA)
- Drug candidate, considerations in early development, 70–71

- Drug coating polymer, polysaccharide, 407–416
- Drug delivery, PEEA, 243–252
- Drug delivery problems, liposomal carriers, 100–109
- Drug layering, slurry coated beads, 336–337
- Drug modalities
drug delivery approaches, 9
next millennium, 9
- Drug penetration enhancer, potential of polyrotaxanes, 379–380
- Drug permeation through skin, polyrotaxanes, 380
- Drug pharmacokinetics, liposome encapsulation, 102–103
- Drug–polyrotaxane conjugates
drug–HP- α -CD release, 379*f*
synthesis, 376–377
- Drug properties, controlled release dosage form, 3
- Drug release
kinetics, 91, 92, 94, 95*f*
pH-dependent swelling of microspheres, 410
- Drug screening, small molecule drugs, 9
- Drugs, maximum tolerated dose, 104
- Drugs and genes with glycosylated liposomes, cell-specific targeting, 201–211
- Drugs of intermediate solubility, association with liposomes, 101
- Dry granulation, controlled release technology, 341
- DVT prevention model, oral SNAC/heparin, 59
- Dyslipidemic plasma, plasma lipoprotein cholesterol and triglyceride concentrations, 318–319
- E
- Efflux transporters, multidrug resistance protein, 37
- Egg yolk phosphatidylcholine (EYPC) vesicles
fusion assay and contents release, 248–251
turbidity data, 247–248
- EMA, *see* Ethyl methacrylate (EMA)
- Encapsulation methods, release growth factors while maintaining biological activity, 160
- Endocrine factors, peptide and protein therapeutics, 7
- Endocytic compartments
macromolecular degradation by hydrolases, 186
mechanism to overcome the membrane barrier, 187
- Endogenous antioxidant capacity, rat colonic mucosa/submucosa, 83
- Endoplasmic reticulum (ER) targeting signals
lipid biosynthesis, protein production and N-linked glycosylation, 174
proteins, 174–175
- Endosomal escape, synthetic polymers, 359
- Endosomes, interruption of the intracellular signal, 169
- Endothelial cell specificity, VEGF, 159
- Engineering organs, cell transplantation, 157–158
- Entrapped calcein, release, 243
- Enzymatic barrier
peptide and protein absorption, 26
peptide transport, 37
- Enzyme, modified cellular pathways, 10
- Enzyme-sensitive drug release, dextran acetate or crosslinked dextran, 412
- Epithelial cells, antimicrobial peptides, 150
- ER, *see* Endoplasmic reticulum (ER)
targeting signals
- Erosion dominated drug release, tablets made from PEO, 20
- Erosion mechanism, release of caffeine from Poloxamer gel, 369–370
- Esterase metabolism, chemical linkers, 38
- Esterase-sensitive cyclic prodrugs, RGD analogs, 43*f*
- Etanercept, control and PEGylated, tryptic peptide maps, 118*f*

- Ethyl acrylamide (EAAm), glucose-controlled insulin delivery system, 232–242
- Ethyl methacrylate (EMA), reduce LCST, 253
- Excipients
 oral drug delivery, 288*t*
 self-emulsifying formulations, 286–288
- Experimental colitis
 induction, 80
 rat, adhesive antioxidant enzymes, 78–89
- Extrusion spherization, CR
 marumerized bead dosage forms, 339
- EYPC, *see* Egg yolk phosphatidylcholine (EYPC) vesicles
- F
- Fabricated PLGA/PEG blend
 microparticles, SEM and fluorescence micrograph, 127*f*
- FB, *see* Fentanyl base (FB)
- FC, *see* Fentanyl citrate (FC)
- Feasibility assessment
 appropriate drug candidates for novel drug-delivery approaches, 69
 controlled release of a particular drug candidate, 75
- Fenoldopam, release profiles, 337–339
- Fenoldopam mesylate, controlled release delivery system, 336–339
- Fentanyl base (FB), local anesthesia, 386
- Fentanyl base (FB)/PLGA microspheres
 preparation and characteristics, 388*t*
 surface morphology and cross-sectional views, 392*f*
- Fentanyl base (FB) release
 emulsifier types, 391*f*
 initial FB loading, 392*f*
- Fentanyl citrate (FC)
 chemical structure, 386*f*
 local anesthesia, 386
 release and loading efficiency, 388–391
- Fentanyl citrate (FC)/PLGA microspheres
 effect of manufacturing methods on surface morphology, 389*f*
 fabrication and analyzing method, 387*f*
 preparation and characteristics, 387*t*
- Fibroblasts, growth factors, 160
- First-in-class, molecules with new pharmacology, 70
- First-pass metabolism, sustained release dosage form, 70
- FITC–BSA, *see* Fluorescein isothiocyanate-labeled bovine serum albumin (FITC–BSA)
- Fluidity of red blood cell ghosts, polyrotaxanes, 379
- Fluorescein isothiocyanate-labeled bovine serum albumin (FITC–BSA), co-encapsulated porogen, 124–138
- Flux measurements, Caco-2 monolayers, 73
- Folate conjugated poly-L-lysine, receptor-specific transfection in cultured tumor cells, 213
- Folate conjugation
 receptor-mediated endocytosis, 213*f*
 tumor-specific targeted drug delivery, 212
- Folate receptor, targeted gene delivery, 212–219
- Folate–PEI and Folate–PEG–PEI
 characterization, 216
 synthesis, 214*f*
 transfection activities of DNA complexes, 216
- Food effects
 OCAS absorption, 21
 therapeutic efficacy, 14
- Freeze dried modification, carbomer, 34
- Full drug release, dimension of dosage form, 94
- Functional polymers, controlled release drug delivery systems, 2
- Functional vasculature, transplanted matrix, 157
- Fusion protein, ability to coalesce two tightly apposed membranes, 187

Fusogenic peptides, gene expression, 209–210

G

Galactosylated cationic liposomes, DNA complexes, 206–209

Galactosylated cationic poly(amino acid), biodistribution of DNA/liposome complexes, 209–210

Gal-C4-Chol, chemical structure, 204*f*

GAN, *see* Guar acetate nanoparticle (GAN)

Gastrointestinal tract

altered drug release profiles, 17
influence on drug release, 15
kinetics of drug release, 91
performance of once-a-day dosage forms, 16*f*, 21
peroral route of peptide or protein administration, 25–26
site specific delivery, 15

Gastrointestinal transit time, oral controlled drug delivery, 4

Gel-forming matrix tablets
pseudo zero-order drug release, 19
sustained-release formulation, 18

Gel matrix
diffusion and erosion, 368
dissolution, 373

Gel network, degree of freedom of polymer chain, 238

Gel nicardipine hydrochloride tablets, pharmacokinetic parameters, 23*t*

Gel-pore permeation mechanism
composite membrane system, 271
solute diffusion through membrane, 263

Gel tablets

in vitro and *in vivo* release
performance, 21, 22*f*
pharmacokinetic parameters, 22*t*

Gelatin capsules
in vitro release profiles, 337
SEDDS, 285, 291

Gelatin compatibility studies, self-emulsifying formulation filled capsules, 286

Gelatin shell, solubility and disintegration time, 289

Gelation

induced polymeric micelles, 260
NiPAM/NASI/AMA polymers, 261

Gelation index, PEO matrix tablets with filler, 19

Gene delivery

approaches, 2, 7–8
glycosylated carriers, 206–210
ideal system, 3
nonviral liposomal vectors, 107
role of targeting, 218

Gene expression

cellular control, 193
inhibitory effect of peptides, 198

Gene products, delivery approaches, 2

Gene regulation, nuclear transcription factors, 193

Gene therapy

antisense oligonucleotides, 105
liposomal carriers, 100
parenteral injection and syringable microparticulate delivery systems, 3

Gene transfer vector system, targeting to the folate receptor, 212–219

Generally regarded as safe (GRAS) materials, polymers, 4

Generic controlled release technology, applicable to variety of potential drugs, 76

Genetic manipulation studies, growth and development of organs and tissues, 6

Genetic material, protective mechanism, 8

Glioma cells, immunotherapy, 221

Glucose detection, iontophoretic extraction, 275

Glucose monitoring, reverse iontophoresis, 273–282

Glucose-sensitive insulin release, insulin-loaded matrix, 236–238

GlucoWatch biographer

clinical results, 278
current from both sensors, 279*f*

- glucose concentration vs. elapsed time, 280*f*
 operation, 275–278
 painless and noninvasive measurement, 273
 schematic diagram, 276*f*
 statistical summary of results, 281*f*
- Glycolipid monosialoganglioside, circulation lifetime of liposomes, 243
- Glycosylated carriers, drug delivery, 205–206
- Glycosylated liposomes
 biodistribution, 203–204
 comparison with glycosylated poly(amino acids), 201–211
- Glycosylated poly(amino acids) comparison with glycosylated liposomes, 201–211
 in liver PC and NPC cells, 204*f*
 LMW drug carriers, 202–203
- Golgi apparatus targeting signals, processing and sorting proteins, 175
- GRAS, *see* Generally regarded as safe (GRAS) materials
- Growth factor
 binding to cognate receptors at surface of target cell, 169
 delivery from tissue engineering matrices, 157–166
 encapsulated within alginate beads, 161
- functional vasculature, 159–160
 NLS motifs, 170
 potential unwanted introduction, 177
- Growth factor encapsulation, double emulsion technique, 160
- Growth factor release, ¹²⁵I-labeled, 164*f*
- Guar acetate nanoparticle (GAN)
 drug release rate, 407
 particle size distribution, 413*f*
 physical state of the drug, 412
 powder X-ray diffraction patterns, 413*f*
- H
- Half-life
 appropriate for drug delivery approaches, 69
 circulating serum concentrations of IL-15 and PEG-IL-15, 119
 drugs in liposome aqueous interior, 104
 superoxide radical and hydrogen peroxide, 87
 systemic administration of antioxidant enzymes, 79
- Hemocompatible phospholipid polymers, drug carriers, 324–334
- Hemolysins, thiol-activated, pore-forming, 189
- Heparin
 APTT response in rats following a single colonic dose, 57*f*
 description, 54
 GI absorption in rats and monkeys, 56–62
 microsphere-encapsulated, 55
 oral delivery, 54–63
- Heregulin, translocation through plasma membrane, 177
- High throughput screening, drug discovery process, 69
- HIV protease inhibitors, cytochrome P450, 37
- HIV-1 TAT protein, transit across cellular membranes and into cytoplasm, 177
- Host defense against microbes, α -defensins, 150
- hPEPT1 transporter, prodrug delivery, 46–53
- Human Genome Project
 small molecular drugs, 9
 therapeutic application and disease-causing defective genes, 7–8
- Human plasma, CsA incubation with or without supplementation of CETP, 317
- Human trabecular bone, replacement by porous composite material, 125
- Human tumors, folate receptor, 212
- Hydrocortisone
 release from microsphere, 241*f*
 temperature-controlled release, 238

Hydrogel

- low water environments, 17
- microstructures, 365
- NiPAM/NASI/AMA polymers, 260–262
- Ploxamer, 364–374
- Hydrogel gel stability, AMA content, 262
- Hydrogel microspheres
 - degradable matrices, 399
 - hydrolytic degradability, 395
- Hydrogen bonds, hydrophobic
 - contribution to LCST, 234, 238
- Hydrolysis, NiPAM/NASI polymers, 257, 258*f*
- Hydrophilic compounds, paracellular permeation, 32
- Hydrophilic drugs
 - aqueous interior of liposomes, 101
 - rate of drug release, 104
- Hydrophilic macromolecules, peroral delivery, 25–26
- Hydrophilic peptides, paracellular pathway, 37
- Hydrophobic blocks, capping PEO chains, 298
- Hydrophobic compounds
 - changes in plasma TG and cholesterol concentrations, 322
 - solubilization in PMB30W aqueous solution, 329*t*
 - solubilization with PMB30W aggregate, 331
- Hydrophobic drugs
 - hydrophobic acyl chain region of phospholipid bilayer, 101
 - solubilized in liposomal membranes, 104
- Hydrophobic fluorescence probe, solubilization, 327
- Hydrophobic helical hairpin, colicin A folding structure, 139
- Hydrophobic peptides, passive diffusion via transcellular pathway, 37
- Hyperbranched polymers, advantages as polymeric drugs, 360
- Hypoglycemic effect, IOP by oral administration, 65–68

I

- IC, *see* Intracranial (IC) tumor
- IFN- γ , *see* Interferon- γ (IFN- γ)
- IOP, *see* Insulin in oil preparation (IOP)
- Immunomodulatory effect
 - antitumor immune response, 226–227
 - tumor, 220–221
- Immunostimulant, PCPP, 403–405
- Immunotherapy, treatment of brain tumors, 220–229
- Implantable materials, cell growth and tissue regeneration, 380
- Import peptide (IP), cellular delivery of NLS peptides, 196
- In vitro–in vivo correlation, feasibility, 74
- Inclusion complexation, α -CDs threaded onto PEG, 375
- Incubation time, survival ratio of HL-60 cells, 423
- Indomethacin (IND)
 - enhanced permeation, 380
 - NSAID, 407
 - release from alginate beads, 414*f*
 - release from alginate beads coated with dextran acetate or crosslinked dextran, 415*f*
 - release from GAN, 412, 414*f*
 - release from LAM, 410
- Inflammation in experimental colitis, systemic treatment with SOD, 79
- Inflammatory processes, antioxidant profiles of organ tissues, 78
- Inflammatory reactions, rapid dissociation of supramolecular structure, 380
- Inhibitory peptides
 - design, 196
 - effect on NF- κ B-dependent luciferase gene expression, 199*f*
 - nuclear translocation of NF- κ B, 198
 - suppression of LPS-induced TNF α production, 199*f*
- Injectable lipid-based systems, side effects, 2
- Insertion mechanism, pore-forming colicins, 139–140

- Insulin**
 chitosan and colonic absorption, 30
 glucose monitoring, 273
 hypoglycemic effect of IIOP, 65–68
 plasma concentrations after nasal administration, 34*f*
 pulmonary and gastrointestinal routes, 4
- Insulin delivery system, glucose-controlled**, 236–238
- Insulin in oil preparation (IIOP)**
 effects of buffer of different pH on stability, 66*t*
 hypoglycemic effect of oral administration, 65–68
 serum glucose of diabetic rats, 67*f*
 serum glucose of normal mice, 68*f*
 serum insulin of diabetic rats, 67*f*
- Insulin-loaded matrix, preparation**, 236
- Insulin release**
 alternating glucose concentration, 239*f*
 alternating rate, 238
 glucose-controlled, 237*f*
- Intelligent polymers, stimuli-responsive drug delivery**, 263
- Interferon, systemic side effect issues**, 7
- Interferon- γ (IFN- γ), vaccination**, 220
- Interleukin, systemic side effect issues**, 7
- Intestinal absorption, w/o microemulsions upon intraduodenal administration**, 292*t*
- Intestinal absorption enhancement, self-emulsifying drug delivery formulations**, 284
- Intestinal absorption mechanism, amino acid ester prodrugs**, 49–51
- Intestinal crypt, anatomy**, 150–151
- Intestinal epithelia**
 crypts of lieberkuhn, 149
 permeability, 31–32
 regulated Cl⁻ secretion, 151
- Intestinal mucosa, permeation of peptides and peptide mimetics**, 36–38
- Intestinal peptide transporters, stereoselectivity**, 47
- Intestinal tissues**
 engineered, 158
 membrane permeability, 288
- Intra/intermolecular interaction, copolymer and polymer mixture**, 240*f*
- Intracellular bacteria, new cystolic delivery strategy**, 188–190
- Intracellular delivery**
 growth factors and polypeptide hormones and toxins, 10–11
 therapeutic agents, design of responsive liposome systems, 244
- Intracellular organelles**
 targeted delivery, 179
 targeting macromolecular therapeutics, 168–183
- Intracellular protein trafficking, fate of conjugated or chimeric therapeutic molecules**, 168
- Intracellular signal, down-regulation mechanism**, 169
- Intracellular targeting vectors, design**, 177–182
- Intracellular trafficking signals, nucleus and other organelles**, 170–176
- Intracranial (IC) tumor cell implantation before vaccination**, 225
 immunotherapy, 220
- Intracytoplasmic delivery**
 bioresponsive polymers, 357–359
 synthetic system, 358*f*
- Iodine-containing micelles**
 blood pool CT imaging, 304*f*
 CT, 302–305
- Iodine-substituted poly-L-lysine, synthesis and in vivo properties**, 302
- Ion channels**
 modified cellular pathways, 10
 peptides, 145–146
- Ion conductive pores, rabbit defensin NP-1**, 150
- Ionically crosslinked polyphosphazene microspheres**, 395–406
- Iontophoretic glucose extraction, noninvasive measurement of blood glucose**, 274–275
- Irradiated 9L-glioma cells (i9L), vaccination**, 220
- N-Isopropylacrylamide (NIPAM) characterization of polymers**, 254

synthesis and characterization of thermoreversible protein-conjugating polymers, 253–262
 thermal response of polymers, 264

K

Kaposi's sarcoma

ER delivery for selective cell apoptosis, 181
 widespread apoptosis, 147

Kidney cells, fluorescent markers targeted to nuclei, 172*f*

L

Lactan acetate, swelling and drug release kinetics, 410*f*

Lactan acetate microspheres (LAM) after drug release, 411*f*
 pH-sensitive drug carrier, 407

Lactan acetate pellets, pH-sensitive swelling behavior, 410

LAM, *see* Lactan acetate microspheres (LAM)

Large unilamellar vesicles (LUV) fusion of phosphatidylcholine, 251
 optical density, 247–248
 pH-dependent destabilization and fusion, 243

LCST, *see* Lower critical solution temperature (LCST)

Leakless fusion, contents release assay, 249

Lewis lung carcinoma, PEG–PE micelles for delivery of hydrophobized protein, 306–312

Lipid absorption enhancers, self-emulsifying formulations, 289

Lipid-based self-emulsifying formulations, oral dosage forms, 285

Lipid-based vehicles, general formulation development challenges, 288–289

Lipid-based vesicles, compounds incorporated, 319–321

Lipid bilayers

cyclic prodrugs, 43–44

SGP that forms a pore, 139–148

Lipid-degrading enzymes, targeted delivery, 181

Lipid–drug formulations, analysis, 289

Lipid metabolism, implications of disturbances, 322

Lipophilic cationic drug dequalinium, PEG–PE micelles, 297

Lipophilic drugs, lymphatic system, 288

Lipophilic peptide delivery, oral drug delivery, 290

Lipoprotein

involvement in biological processes, 315

percent transfer of CE and CsA, 318*t*

structure and function, 315–316

Lipoprotein association of drug compounds, pharmacological and pharmacokinetic properties, 314

Lipoprotein metabolism, implications of disturbances, 322

Lipoprotein profile, alterations in drug pharmacokinetics and pharmacological action, 315

Liposomal anamycin distribution within human plasma following incubation, 321*t*
 incubated in human plasma, 320

Liposomal carriers, solving drug delivery problems, 100–109

Liposomal drug(s), potential uses, 104–106

Liposomal drug delivery systems choice of drugs, 101
 clinical development, 100–101
 clinical use, 243
 problems, 186

Liposomal nystatin distribution within human plasma following incubation, 321*t*
 incubated in human plasmas, 321

Liposome(s)

accumulation of drug at disease site, 243

improving on the current generation, 106–107

interaction with cells, 185–186

- interactions of drugs, 102*f*
 - poor pharmacokinetic properties and rapid uptake by phagocytic cells, 189
 - solubilize drugs and protect them from degradation, 100
 - Liposome-based products, clinical development, 101
 - Liposome formulations
 - bacterial mechanisms, 188–189
 - drug clearance rate, 103
 - modified, 184–192
 - Liposome stability, diluted aqueous solutions, 308
 - Listeriolysin O (LLO)
 - pH-dependent hemolytic activity, 189
 - protein secreted by intracellular parasite to escape from endocytic compartment, 188–189
 - Listeriosomes*
 - deliver molecules of molecular mass up to 50 kD, 189
 - nonviral, nonbacterial liposome, 189–190
 - Live vectors, neutralizing immunological responses, 3
 - LLO, *see* Listeriolysin O (LLO)
 - LMWA, *see* Low molecular weight antioxidant (SMWA) compounds
 - Loading methods, drug in nanoparticle system, 418
 - Local anesthesia
 - chronic pain of cancer patients, 385
 - fentanyl-loaded PLGA microspheres, 385–394
 - Localization of drugs, passive targeting, 103
 - Long-circulating liposomes
 - increased plasma concentration vs. time, 103
 - structure, 309*f*
 - Low molecular weight antioxidant (LMWA) compounds, defense mechanisms, 78
 - Lower critical solution temperature (LCST)
 - AMA-containing copolymers, 260
 - NiPAM/NASI copolymers, 258, 259*f*
 - NiPAM/NASI/AMA terpolymers, 260*t*
 - thermoreversible polymers, 253
 - LPS-induced TNF α gene expression, inhibition, 198
 - Luminal enzymes, degradation of perorally administered peptides, 26
 - Lung tissue, drug profile, 95
 - LUV, *see* Large unilamellar vesicles (LUV)
 - Lymphatic imaging, percutaneous lymphography, 299
 - Lyotropic liquid crystalline structure diffusion, 370
 - Ploxamer, 365
 - Lysosomal compartment, macromolecular degradation by hydrolases, 186
 - Lysosomal hydrolases, ligand to mannose-6-phosphate receptors in *trans*-Golgi apparatus, 175
 - Lysosome targeting signals, proteins, 175–176
 - Lysosomotropic delivery
 - advantages, 354
 - schematic representation, 354*f*
- ## M
- Macromolecular cargo, delivery to cytoplasm of specific cells, 177
 - Macromolecular drugs
 - parenteral dosing, 54
 - pulmonary and gastrointestinal routes, 4
 - target sites for therapeutic effectiveness, 184
 - transfer to cytoplasmic compartment of the cell, 357
 - Macromolecular prodrugs
 - characterization, 205
 - prolonged release action of drugs, 376
 - Macromolecular therapeutics, targeting, 168–183
 - Macromolecules
 - access to cytoplasm, 182
 - cytosolic delivery, 184–192

- Macropores, ingrowth of granulation tissue from the host, 158
- Magic bullets, therapeutic treatment at specific cells or tissues, 168
- Mammalian cells, SGP-induced apoptosis, 147
- Mannose receptors, macrophages, 201
- Marker, targeted drug delivery to tumors, 212
- Marrow stromal cells
 - cultured on PPF substrates with TGF- β 1-loaded PLGA/PEG microparticles, 134*f*
 - cultured on PPF/ β -TCP substrates in vitro, 125
 - proliferation and osteoblastic differentiation, 124
 - response to released TGF- β 1, 132–135
- Marrow stromal osteoblast culture, TGF- β 1 released from biodegradable polymer microparticles, 129–135
- Marumerized bead(s)
 - acidifying buffers, 336
 - CR technology, 339
- Marumerized bead formulations, in vitro release profiles, 340*f*
- Mass transport limitation, size regulation, 159
- Mathematical model, calculation of drug absorption, 74
- Matrix properties, phosphazene polyelectrolytes, 403
- Matrix tablet(s), low water environments, 17
- Matrix tablet formulations
 - dissolution profiles, 347
 - in vitro release profiles, 346*f*
- Mechanical stress, OCAS formulations, 20–21
- Membrane(s)
 - liposome barrier, 185–186
 - temperature and pH responsive permeation, 263–272
- Membrane-bound organelles, mammalian cells, 170
- Membrane coating, constant acidic environment, 336–337
- Membrane fusion events, contents release assay, 249
- Membrane partition characteristics, cyclic prodrugs, 41–42
- Membrane permeability, amino acid ester prodrugs, 50, 51
- Membrane permeation, cyclization strategies, 38
- Membrane perturbation, SGP-related proteins, 146
- Membrane properties, altered by synthetic polyelectrolytes, 244
- Membrane transport, L-configuration of amino acid, 51
- Membrane voltage, defensin-associated pores, 150
- Metabolic barrier, luminal and membrane-bound enzymes, 25–26
- Metabolic lability, hydrolytic pathways, 36
- Metabolism, influence on bioavailability, 73
- 2-Methacryloyloxyethyl phosphorylcholine (MPC)
 - blood compatibility, 418
 - polymer covering PLA, 417
 - polymerization, 324
 - protein adsorption on polymer surface, 426
 - surface tension of aqueous solution, 329*f*
- Methoxy-poly(ethylene glycol) (MPEG), synthesis and in vivo properties, 302
- Methyl methacrylate (MMA), reduce LCST, 253
- Mice, serum glucose with IOP, 67
- Micelle(s)
 - accumulation in tumor, 312
 - delivery of poorly soluble drugs, 297–313
- Micelle collapse, precipitation of incorporated drugs, 298
- Micelle formation and loading with contrast agent, schematic structures, 303*f*
- Micelle-forming surfactants, solubilization of drugs, 297

- Microemulsion system, drug solubilization and delivery, 286
- Microencapsulation, hydrolytic stability of aluminum crosslinked polyphosphazene microspheres, 396
- Micrometastatic disease, polymer therapeutics, 356
- Microparticles
 biodegradable polymers, 125, 126
 in vitro degradation, 129
 transport efficacy and accumulation in tumor interstitium, 306
- Microspheres
 effect of coacervation conditions on mean diameters, 401*f*
 formation, 238
 ionically crosslinked, 395–406
 matrix properties, 403–405
 nonuniform drug distribution, 161
 preparation method, 235*f*
 variable hydrolytic stability, 399–403
- Microvasculature, generating, 159
- Mimetic drugs, development, 8–9
- Mitochondrial proteins, encoded by nuclear genes, 173
- Mitochondrial targeting signals, proteins, 173–174
- MMA, *see* Methyl methacrylate (MMA)
- Model peptides, mimic fusogenic proteins and synthetic polymers that act on membranes, 244
- Molecular assembly
 polyrotaxanes, 375
 stability under biological conditions, 331
- Molecular targeting, nuclear transcriptional regulators, 193–200
- Molecular weight, PEEA samples obtained from solvent fractionation, 245*t*
- Molecular weight control, PEEA, 245
- Monkeys, GI absorption of SNAC/heparin, 56–62
- Monolithic dosage forms, biocompatible polymer, 91
- Mononuclear cell, cytotoxic and proliferative activity, 226–227
- Mononuclear cell infiltration
 antitumor response and vaccination, 228
 determination at site of tumor cell challenge, 225–226
 induced tumor, vaccination, 220
 tumor, 226*t*
- Mononuclear phagocytic systems, nanoparticles injected into bloodstream, 418
- MPC, *see* 2-Methacryloyloxyethyl phosphorylcholine (MPC)
- Mucoadhesive properties, polymers, 26
- Mucosa/submucosa layer of intestine
 antioxidant enzyme activities, 82*t*
 small intestine, antioxidant enzymes, 78
- Mucosal epithelial cells, hPEPT1 peptide transporter, 46
- Mucosal penetration enhancers, safe, 25–35
- Mucosal transport barrier, hydrophilic macromolecules, 25–26
- Mucus layer, diffusion of peptides, 26
- Multi-tablet dosage forms, orally active compound, 342–347
- N
- N-terminal PEGylation,
 PEG–muGM–CSF, 113–114, 115
- Nanoparticle(s)
 composite membrane system, 271
 covered with PMB30W,
 characterization, 422*t*
 drug carriers, 417
 pore size of membrane, 263
- Nanoparticle diameter vs. temperature, 266*f*
- Nasal administration, absorption efficiency of TMCs, 33–34*f*
- NASI, *see* *N*-Acryloxysuccinimide (NASI)
- Negatively-charged membranes,
 adherence of cationized proteins, 87

- Neutrophils, oxygen-independent killing of bacteria, 150
- NF- κ B
 EMSA studies, 197*f*
 inhibition of nuclear translocation, 196–198
 transcription factor involved in immune and inflammatory disorders, 194
- NF- κ B-dependent reporter gene expression, inhibition, 198
- NiPAM/NASI polymers, DSC thermograms, 259*f*
- NLS, *see* Nuclear localization amino acid sequences (NLS)
- Nonparenteral macromolecular drug delivery, clinical challenge, 54
- Nonprotein mimetic drugs, development, 8–9
- Nonsteroidal anti-inflammatory drugs (NSAID), arthritis treatment, 407
- Noveon AAI, *see* Polycarbophil
- NSAID, *see* Nonsteroidal anti-inflammatory drugs (NSAID)
- Nuclear localization amino acid sequences (NLS)
 deletion or mutation, 179
 nuclear targeting of macromolecules, 169
- Nuclear localization signals, clusters of basic amino acids lysine and arginine, 170
- Nuclear targeting, cellular conditions, 173
- Nuclear targeting capacity, classes of human proteins, 180*t*
- Nuclear targeting signals, proteins, 170–173
- Nuclear translocation, NF- κ B, 194
- Nucleolus, gene transcription, rRNA processing and nascent ribosomal subunit assembly, 170
- Numerical models, kinetics of drug release, 91
- O
- OCAS, *see* Oral controlled absorption system (OCAS)
- Oil/water partition coefficient, drug release, 291
- Oil-in-water (o/w) microemulsions, not compatible with gelatin capsules, 285
- Oligonucleotide drugs
 delivery, 7–8
 nonparenteral delivery, 3
- Once-a day oral delivery systems
 future challenges and opportunities, 24*t*
 representative, 16*t*
 requirements, 14
- Opioid peptides
 cyclic prodrug strategies, 36, 39–42
 paracellular pathway, 37
- Optimal release profiles, development of early drug candidates, 70
- Oral absorption, peptides and peptide mimetics, 36–45
- Oral administration
 drug delivery route, 4
 fenoldopam, 336
- Oral bioavailability
 formulated in SEDDS, 288
 intestinal drug absorption and first-pass drug metabolism, 46
- Oral controlled absorption system (OCAS)
 future challenges and opportunities, 23, 24*t*
 hydration and drug release in small intestine and colon, 18*f*
 in vitro and in vivo release performance, 21, 22*f*
 minimal food effects, 14
 once-a-day dosing, 18–24
 pharmacokinetic parameters, 22*t*, 23*t*
- Oral controlled release prototypes, feasibility assessment and rapid development, 69–77
- Oral delivery systems
 controlled release, 14–24
 heparin, 54–63
 insulin, 65–68
 representative plasma profiles, 15*f*
- Oral dosage
 consistency throughout gastrointestinal tract, 17
 constant plasma drug level, 90–97

- Oral drug delivery, self-emulsifying drug delivery formulations, 284
- Oral heparin
absorption from GI tract, 55
chemical structures of delivery agents, 57*f*
efficacy studies, 59–62
formulation development, 55
- Oral SNAC/heparin
DVT clot formation and treatment, 60*f*, 61*f*
GI absorption, 56–62
human clinical studies, 62
mean dose-dependent prolongation of anti-Factor Xa activity, 62*f*
- Ordered microstructures, controlled release, 364–374
- Organelles, targeting macromolecular therapeutics, 168–183
- Osmotically driven delivery systems, limited water availability, 17
- Osteoblastic phenotype markers, alkaline phosphatase activity and osteocalcin production, 135
- Osteocalcin production
marrow stromal cells cultured on PPF substrates, 137*f*
osteoblastic phenotype markers, 135
- Ovarian carcinomas, folate receptor, 212
- Oxidative damage, ROS, 79
- P
- P-Glycoprotein, substrate activity, 42
- Paneth cell α -defensins, intestinal Cl⁻-secreting crypt epithelial cells, 151–154
- Paneth cell cryptdins, natural pore-forming proteins, 149–156
- Paracellular pathway, hydrophilic peptides and peptide mimetics, 37
- Paracellular transport of hydrophilic compounds, protonated chitosan, 30
- Paracrine factor, peptide and protein therapeutics, 7
- Parenteral dosing, macromolecular drugs, 54
- Partition coefficient, feasibility of controlled release for drug candidate, 69
- Passive targeting
large solid tumors, 106
reduced clearance rate of liposomal drugs, 103
- Patent issues, early drug candidates, 70, 74
- PCPP, *see*
Poly[di(carboxylatophenoxy)phosphazene] (PCPP)
- PEAA, *see* Poly(2-ethylacrylic acid) (PEAA)
- PEAA/EYPC vesicle mixtures
fluorescence emission spectra, 249*f*
stained with uranyl acetate, 248*f*
- Peak-associated side effects, therapeutic efficacy, 14
- PEG, *see* Poly(ethylene glycol) (PEG)
- PEG5000–DSPE micelles, serial dilutions, 310*f*
- PEG–IL–15
MALDI–TOF mass spectroscopy results, 121*f*
proliferation of T-cells, 119
size exclusion HPLC, 120*f*
- PEG–IL–15 antagonist
activity, 119–121*f*
characterization, 114–115
- PEG–micelles and PEG–liposomes, longevity, 312
- PEG–PE, *see* PEG-phosphatidylethanolamine (PEG–PE)
- PEG–phosphatidylethanolamine (PEG–PE) conjugates
gel permeation chromatography of micellar forms, 300*f*, 301*f*
polymeric micelles, 299
- PEGylated etanercept, characterization of solution and affinity, 117*t*
- PEGylated proteins
characterization, 112–113
clinical use, 113
purification, 112
- PEGylation
approaches to minimize activity loss, 111*t*

- PEG backbones and conjugation chemistries available, 111*t*
 protein products, 120
 rationale, 110–111
 tool to enhance protein delivery, 110–123
- PEI, *see* Polyethylenimine (PEI)
- Penetratins, translocation of macromolecules across plasma membrane, 177
- Penetration enhancers, mucosal, 25–35
- Peptide
 cryptidins, 149–156
 entrapment efficiency of liposomes, 105
 oral absorption, 36–45
 stable solution structures, 10
 translocation into membrane, 142–143
- Peptide drugs
 delivery approaches, 2
 nonparenteral delivery, 3, 6–7
 selectivity, 9
 understanding structures, 10
- Peptide growth factors, angiogenesis, 160
- Peptide mimetic(s), oral absorption, 36–46
- Peptide mimetic transport, pathways across intestinal mucosa, 37*f*
- Peptide transporter
 nonpeptidyl substrates, 49–52
 peptidyl substrates, 47–49
 structural modification of drugs, 47
 structure–transport relationship, 52
 structures of nonpeptidyl substrates, 49*f*
 structures of peptidyl substrates, 48*f*
- Peptide transporter-mediated intestinal absorption, amino acid ester prodrugs, 51
- Permeabilizing agents, diacyl lipids, 244
- Permeation
 proposed model, 270–271
 through membrane, 263–272
- Peroral delivery, hydrophilic macromolecules, 25–26
- Peroxisome targeting signals, proteins, 174
- PGLA, *see* Poly(lactic-*co*-glycolic) acid (PGLA)
- pH-mediated degradation, protection within liposomes, 104
- pH-sensitive liposomes, behave like viruses, 187
- pH-sensitive polymers, self-regulated drug delivery systems, 3–4
- pH/temperature-induced phase transition, poly(DMAEMA-*co*-EAAm), 234–236
- pH/temperature-responsive polymer system
 controlled drug release device, 232–242
 polymer–water and polymer–polymer interactions, 233
- Pharmacodynamics, polymer conjugation to proteins, 353
- Pharmacological feasibility, controlled release
 formulation, 74
- Phase separation, driven only by temperature change, 254
- Phase transition, pH/temperature-induced, 242
- Phenylpropionic acid-based cyclic prodrugs
 cell permeation, 40
 lipophilic character, 40
- Phosphatidylcholine bilayer membranes, interaction with PEAA, 243–252
- Phosphazene polyelectrolytes
 biological and physico-chemical properties, 398–399
 immunostimulatory properties, 395
- Phosphazene synthesis, synthetic flexibility, 405
- Phospholipid assemblies, stability, 324
- Phosphorus–nitrogen backbone, polyphosphazenes, 398
- Phosphorylcholine group
 blood-compatible nanoparticles, 417–427
 PMB30W/PLA nanoparticles, 423
- Physical entrapment, drugs, 206

- Physicochemical and biopharmaceutical data, RGD peptide SK&F106760, 294*t*
- Physicochemical feasibility, controlled release formulation, 72
- Physiologic influences, once-a-day controlled release dosage forms, 16–18
- PLA, *see* Poly(L-lactic acid) (PLA)
- Plasma drug level
dosage forms, 95–97
erodable dosage form, 93–94
oral dosage forms with controlled drug release, 90–97
rate of drug release, 92
simple and multidose, 94–95
therapeutic efficacy, 14
- Plasma lipoproteins
categories, 315
lipid profiles, 314
role as carriers of water-insoluble compounds, 314–323
- Plasma membrane, growth factor and polypeptide hormone translocation, 176
- Plasma membrane translocations, cellular conditions, 173
- Plasma nicardipine, oral dosing of controlled-release nicardipine hydrochloride, 17*f*
- Plasma protein, water-insoluble poly(MPC-*co*-BMA) membrane, 426
- Plasma protein bovine serum albumin, adsorbed on MPC polymer, 417
- Plasmid DNA, nonviral delivery vehicles, 105
- Platelets
cytoplasmic-free calcium ion concentration with water-soluble polymers, 332*f*
interaction with polymeric phospholipid liposome, 333
measurement of cytoplasmic calcium ion concentration, 327
- PLGA, *see* Poly(lactide-*co*-glycolide) (PLGA); Poly(L-lactic-*co*-glycolic acid) (PLGA)
- Pluronic F127, Poloxamer 407 block copolymer, 366
- Pluronic F127 hydrogel, caffeine release profile, 371*f*
- Pluronic F127 tablet, caffeine release profile, 372*f*
- PMB
structure, 326*f*
synthetic result, 326*t*
- PMB30W
aggregate, interaction with blood components, 331–333
¹H-NMR spectra of D₂O solution, 330*f*
interaction between polymer chains in water, 328
ratio of ¹H-NMR intensity attributed to α -methyl vs. choline methyl, 330*f*
relationship between concentration of BSA and fluorescence intensity of perylene, 332*f*
structure in water, 327–328
- PMB30W/PLA nanoparticles
AFM view, 422*f*
XPS spectra, 424*f*
- Polar drugs, intestinal absorption, 46
- Poloxamer
applications, 365
block copolymers, ordered microstructures, 364–374
triblock copolymers, 364
- Poloxamer hydrogels
block copolymer micelles arranged in liquid crystalline lattice, 370
controlled release of caffeine, 370–372
diffusion and erosion release mechanisms of hydrophilic drug, 368*f*
layer formation in situ, 372–373
- Poloxamer matrix, kinetics of drug release, 365
- Polyacrylate, transmucosal absorption of hydrophilic macromolecules, 25–35
- Polyamidoamines (PAA), pH-dependent membrane rupture, 359
- Polycarophil
inhibition activity, 27
mucoadhesive properties, 26–27

- Poly[di(carboxylatophenoxy)phosphazene] (PCCP) hydrogel microspheres
 crosslinked with aluminum lactate, 402*f*
 immunostimulatory properties, 395
 particle size distribution, 400*f*, 403*f*
 structure, 398*f*
- Polydispersity, effect on conformational transition, 246
- PolyDMAEMA, stereochemical configuration, 236
- PolyDMAEMA and polyEAAm, insulin delivery system, 232–242
- Poly(DMAEMA-*co*-EAAm)
 citric-phosphate buffer solution, 235*f*
 equilibrium swelling change, 240*f*
- Poly(2-ethylacrylic acid) (PEAA)
 characterization for use in drug delivery, 243–252
 concentration dependence of transition midpoints, 251*t*
 concentration effect on fusion and contents release, 250*f*
 design of drug carriers, 244
 interactions with bilayer membranes, 247–251
 molecular weight effect on fusion and contents release, 250*f*
 pH-dependent conformational collapse, 251
 solution conformation properties, 245–246
- Poly(ethylene glycol) (PEG)
 biomedical field, 110–111
 chemistry and solubility, 110
 coating delivery systems, 6
 conjugation of proteins, 110–123
 OCAS system, 18
 PLGA blend to form microparticle carriers, 125
 TGF- β 1, 124–138
- Poly(ethylene glycol) (PEG) conjugation, reduction or alteration in biological activity, 111
- Poly(ethylene glycol)–diacyllipid micelle, structure, 309*f*
- Polyethyleneimine (PEI)
 compact charge complexes with plasmid DNA, 213
 endosomal membrane, 359
- Poly(ethylene oxide) (PEO), OCAS system, 18
- Poly(ethylene oxide) (PEO)–filler matrix tablets, gelation index, 19*t*
- Poly(ethylene oxide)–poly(propylene oxide)–poly(ethylene oxide), Poloxamer block copolymers, 364–374
- Poly(L-lactic acid) (PLA)
 biodegradable nanoparticles, 417
 implantable materials for tissue engineering, 380
 nanoparticle covered with MPC polymer, 421*f*
- Poly(lactic-*co*-glycolic) acid (PLGA)
 degradation following tissue development, 158
 tissue engineering materials, 157
- Poly(lactic-*co*-glycolic) acid (PLGA) matrices
 biological activity of VEGF, 163*f*
 fabrication process with incorporated growth factor, 162*f*
 formed by gas-foaming/particulate leaching process, 162*f*
 growth factor delivery, 161–164*f*
- Poly(lactic-*co*-glycolic) acid (PLGA) microspheres, protein encapsulation, 160–161
- Poly(DL-lactic-*co*-glycolic acid) (PLGA) copolymers
 cumulative release kinetics of TGF- β 1, 133*f*
 decrease of WAMW in PLGA/PEG microparticles, 130*f*
 distribution of FITC-BSA, 131*f*
 microparticle carriers for bioactive molecules, 125
 TGF- β 1, 124–138
- Poly(L-lactide-*co*-glycolide) (PLGA), fentanyl-loaded biodegradable microspheres, 385
- Poly(L-lactide-*co*-glycolide) (PLGA) concentration

- change in FC/PLGA microspheres, 390*f*
- effect on FB release, 393*f*
- effect on FC release, 389*f*
- Polymer(s)
 - safe drug carriers, 26–33
 - self-regulated drug delivery systems, 3–4
- Polymer–anticancer systems, preclinical development, 357
- Polymer directed enzyme prodrug therapy, polymer drug conjugates, 357
- Polymer–drug conjugates, current status, 352–353
- Polymer LCST, in vivo delivery of proteins, 254
- Polymer matrix in phosphate buffer solution, disintegration, 239*f*
- Polymer–polymer interactions, zipper-like effect, 238
- Polymer system, pH/temperature-responsive, 232–242
- Polymer therapeutics
 - challenges, 354–355
 - clinical use, 350
 - history, 350–351
 - into the 21st century, 350–363
 - pharmacokinetic consequences, 353–354
 - schematic, 351*f*
- Polymeric architectures, novel, 359–360
- Polymeric delivery vehicles, bone growth factors, 124–138
- Polymeric drug(s), current status, 352
- Polymeric drug carrier, loading of drug, 421*f*
- Polymeric gels, water uptake, 256
- Polymeric lipid nanosphere, hemocompatible phospholipid polymers, 324–334
- Polymeric micelles
 - current status, 353
 - delivery of poorly soluble drugs, 297–313
- Poly(NIPAm/MAA) membrane
 - cross-sectional morphology, 268*f*
 - properties, 266–268
 - relative contact angle of water vs. temperature, 267*f*
 - swelling ratio vs. temperature, 267*f*
- Poly(NIPAm/MAA) nanoparticles, volume phase transition, 266
- Polypeptide hormones
 - binding to cognate receptors at surface of target cell, 169
 - NLS motifs, 170
 - potential unwanted introduction, 177
- Polypeptide translocation, mechanism, 177
- Polyphosphazene
 - drug delivery vehicles, 397–399
 - synthetic pathways, 398
- Polyphosphazene microspheres
 - ionically crosslinked, 395–406
 - preparation by aqueous coacervation, 399–401
 - protein delivery system, 399–402
- Polyphosphazene polyelectrolytes, subcutaneous immunization with influenza, 404*f*
- Poly(propylene fumarate) (PPF)
 - injectable material for filling skeletal defects, 125
 - marrow stromal cells, 124
- Polypseudorotaxane, cumulative α -CD release, 381*f*
- Polyrotaxane
 - cumulative α -CD release, 381*f*
 - feasibility as stimuli-responsive materials, 382–383
 - HP- α -CD release, 379*f*
 - implantable materials, 380
 - in presence of papain, HP- α -CD release via terminal hydrolysis, 378*f*
 - interaction with cellular systems, 383
 - stimuli-responsive change in CD location, 382*f*
 - supramolecular-structured polymer, 375–384
- α -Polyrotaxane, CD release via terminal hydrolysis, 376*f*
- β -Polyrotaxane
 - CD and a triblock copolymer, synthesis and characterization, 382–383

- CD threaded onto triblock copolymer, 382*f*
- Polysaccharide, drug coating polymer, 407–416
- Poorly soluble drugs, polymeric micelles, 297–313
- Pore-forming domains, form ion channels into planner lipid, 147
- Pore-forming proteins, Paneth cell cryptdins, 149–156
- PPF, *see* Poly(propylene fumarate) (PPF)
- Predictive methods, consideration of drug delivery or sustained release option, 70
- Prodrug strategies
 cyclic, 38*f*
 hPEPT1 transporter, 46–53
 oral absorption of peptides and peptide mimetics, 36–45
 peptides and peptide mimetics, 38
 structure–transport relationship of peptide transporters, 52
- Proliferation analysis, spleen cells from primed and unprimed rats, 227*f*
- Prostaglandin E₁ (PGE₁), effective administration, 205
- Protease inhibitors, peptide drug absorption, 27
- Protein
 cellular uptake pathways, 169
 entrapment efficiency of liposomes, 105
 translocation into membrane, 145
- Protein adsorption, blood compatibility of drug carriers, 426
- Protein chemistry, controlled release drug delivery systems, 2
- Protein conjugation
 NiPAM-based polymers, 256
 thermoreversible, 253–262
- Protein delivery, PEGylation, 110–123
- Protein design, sequence selection, 144
- Protein drugs
 delivery approaches, 2
 nonparenteral delivery, 3, 6–7
 selectivity, 9
 understanding structures, 10
- Protein folding, protein and peptide therapeutics, 10
- Protein-loaded micelles, accumulation in tumor, 306–312
- Protein reactivity, conjugate proteins to polymers without crosslinking agents, 254
- Protein release rates, polymer blends, 124
- Protein translocation
 across membranes, 176–177
 intramitochondrial, 173
- Proton sponge, osmotic rupture of the vesicle, 359
- Prototype(s), rapid development, 69–77
- Prototype formulations, clinical studies, 75–76
- Pyrene, fluorescence intensity in phosphate-buffered solutions of PEAA, 246*f*
- R
- Rat
 experimental colitis, 78–89
 GI absorption of SNAC/heparin, 56–62
- Rat colon, FITC-labeled cationized BSA (F-BSA), 84*f*
- Rat colonic mucosa, cationized and noncationized catalase and SOD, 85*f*
- Rat intestinal mucosa, attachment properties of cationized proteins, 83
- Rat intestine
 evaluation of total antioxidant capacity, 79–80
 relative reducing power, 81
- Reactive oxygen species (ROS), GI tissues, 78
- Receptor-mediated endocytosis (RME)
 interruption of intracellular signal, 169
 uptake pathway for growth factors and polypeptide hormones, 169
- Recombinant biotechnology, small molecular drug candidates, 9
- Recombinant human transforming growth factor- β 1 (TGF- β 1)

- biodegradable polymer blends,
 124–138
 controlled release from PLGA/PEG
 blend, 124
 Red blood cell ghosts, fluidity, 379
 Regional absorption
 drugs in human GI tract, 73*f*
 sustained release formulations, 70
 Regional permeability of drugs,
 physicochemical properties, 72–73
 Release kinetics, TGF- β 1 from
 PLGA/PEG microparticles, 126–129
 Renal peptide transporters,
 stereoselectivity, 47
 Replacement tissues and organs, tissue
 engineering, 157
 Reporter metals, micelles and liposomes,
 302
 Retention time, plasma drug level, 90
 Retrieval motifs, ER, 174
 Reverse iontophoresis, glucose
 monitoring, 273–282
 RGD peptide mimetics
 coumarinic acid-based cyclic prodrug
 strategy, 42–43
 cyclic prodrug strategies, 36
 orally bioavailable derivative with *in vivo*
 efficacy, 43
 paracellular pathway, 37
 RME, *see* Receptor-mediated endocytosis
 (RME)
 Roller compaction, dry granulation
 process, 341
 ROS, *see* Reactive oxygen species (ROS)
- S**
- Salbutamol sulphate
 kinetics of drug release and plasma
 drug level, 93–94
 plasma drug level with Ventolin and
 erosion-controlled release dosage
 form, 93*f*
 Sandimmune Neoral (SIMN),
 pharmacokinetic parameters, 290*f*
 Secretory response, epithelial barrier, 151
 Self-emulsifying drug delivery
 formulations
 challenges and opportunities, 284–296
 oral administration of lipid-soluble
 and water-soluble molecules, 295
 oral drug delivery and absorption
 enhancement, 285*f*
 Self-emulsifying drug delivery systems
 (SEDDS)
 drug development challenges, 291
 lipophilic molecules, 285
 oral drug delivery opportunities,
 290–291
 Self-regulating drug delivery systems,
 validity for physiological conditions,
 232
 SGP, *see* Small globular protein (SGP)
 Side effects
 difficulty in prediction, 74
 injectable lipid-based systems, 2
 Signal peptides
 hydrophobicity over 20–30 amino
 acids, 174
 protein targeting to mitochondrial
 matrix, 173
 Silicone implants, biocompatibility, 6
 Site-specific PEGylation, etanercept, 114,
 115–119*f*
 SK&F106760
 encapsulation into w/o microemulsion,
 291–293
 intraduodenal bioavailabilities, 292*f*
 Skeletal defects, PPF combined with a
 vinyl monomer and an initiator, 125
 Skin stratum corneum, polyrotaxanes,
 380
 Slurry coated beads
 fenoldopam mesylate/PVP/buffer,
 336–337
 release profiles, 337–339
 Slurry-coated tartaric acid crystals,
 release profiles, 338*f*
 Small globular protein (SGP)
 amino acid sequence and helical wheel
 representation, 140*f*
 amino acid sequence of three mutants,
 145*f*

- circular dichroism and Trp-fluorescence
- behavior, 142*f*
- conformations, 141
- de novo* design and synthesis, 139–148
- expected folding state and open umbrella state, 140*f*
- α -helical contents and molecular weights, 141*t*
- related proteins, synthesis, 143–147
- stability, 141
- targeted form to treat cancer, 147
- Small molecular drug(s),
 - pharmacokinetic and pharmacodynamic profiles, 8
- Small molecule drug candidates, delivery systems, 15
- Smart polymers
 - limitations on practical application, 4
 - response to small physical or chemical stimuli, 382
 - self-regulated drug delivery systems, 3–4
 - supramolecular assemblies, 383
- SNAC/heparin
 - oral, 56–59
 - pharmacodynamic/kinetic profiles following oral administration in monkeys, 58*f*
- SOD, *see* Superoxide dismutase (SOD)
- Solubility
 - caffeine in aqueous Pluronic F127, 368
 - controlled release dosage forms, 335–347
 - feasibility of controlled release for drug candidate, 69
- Solutes
 - membrane permeation, 268–270
 - permeation of composite membrane, 270–271
- Solution parameters, determined by light scattering measurements, 377*t*
- Solvent evaporation, PMB30W/PLA nanoparticles, 420
- Soybean trypsin inhibitor, incorporation into liposomes and micelles, 308
- Span 80, effect of concentration on FC release rate, 391*f*
- Sperm nuclei, expression of introduced somatic genetic material, 8
- Spheres, dimensions and time for full release, 94*t*
- Spleen weight, mice treated with PEG– μ GM–CSF, μ GM–CSF or PBS, 116*f*
- Stealth liposomes
 - antibody-targeted, 106
 - doxorubicin, 105
 - increased plasma concentration vs. time, 103
- Stereoselectivity, intestinal and renal peptide transporters, 47
- Sterically stabilized liposomes, longer circulation times, 185
- Stimuli-responsive drug delivery, intelligent polymers, 263
- Stimuli-responsive polyrotaxane, novel smart material, 375
- Stimuli-sensitive composite membrane, temperature and pH responsive permeation, 263–272
- Storage defects, potential therapy for diseases, 181
- Storage stabilities, liposomes, 104
- Strategy, early drug candidate development, 70–71
- Structural rigidity, PEO gel, 21
- Structure information, peptides, and proteins, 10
- Subcutaneous vaccination, i9L + IFN- γ , 227–228
- Substrate activity, cyclic prodrugs, 41–42
- Substrate specificity, peptide transporters, 52
- Substrates of peptide transporters, therapeutic drugs, 47
- Sugar receptors, glycosylated delivery systems, 201
- Superoxide dismutase (SOD)
 - activity in the mucosa/submucosa of the small intestine, 78
 - cationization, 80

- Supramolecular dissociation,
 biodegradable polyrotaxanes with
 ester linkages, 381
- Supramolecular structure
 dissociation, 376
 drug delivery, 375–384
- Surface tension, PMB aqueous solution,
 328
- Surfactants, damage to GI membranes, 56
- Survival cells, trypan blue dye exclusion
 test, 425*f*
- Swelling, lactan acetate pellets, 410
- Swelling ratio, composite membrane, 267
- Syndiotactic triads, polyDMAEMA, 236
- Synthesized NiPAM polymers,
 composition, 257*f*
- Synthetic methods, polyphosphazenes,
 405
- Synthetic viral mimetic, designed for
 intracytoplasmic delivery, 357
- Systemic immunosuppressive effect,
 tumor cells, 228
- T**
- Tablet cores and coating, manufacture,
 345–347
- Tablet formulations
 bilayer and conventional, 341
 compound B and C, 342*t*
 compound E, 345*t*
- Target cells
 cytosolic space, 184
 introduction of macromolecules into
 cytoplasm, 169
- Targeted delivery
 chimeras, 179
 treatment of disease, 181
- Targeted gene delivery, via folate
 receptor, 212–219
- Targeted liposomal therapy,
 improvements, 106
- Targeted prodrug design, membrane
 transporters for polar nutrients, 46–47
- Targeted therapeutics, specific tissues,
 182
- Targeting
 controlled release dosage form, 3
 EPR-mediated, 355–357
 intracellular sites, 10–11
 nonliving vectors, 3
 specific tissues and cells, 4, 6
- Targeting factors, proteins, 176
- Targeting macromolecular therapeutics,
 specific cell organelles, 168–183
- Targeting vectors
 idealized, 178*f*
 intracellular, 177–182
- Technological feasibility, controlled
 release formulation, 74
- Temperature-sensitive polymer complex,
 preparation, 236
- TGF- β 1, see Recombinant human
 transforming growth factor- β 1 (TGF- β 1)
- Theophylline
 conjugation with polyrotaxane,
 376–377
 permeability and molecular size of
 solutes, 269*t*
 permeability through composite
 membrane, 268
 pH-dependent permeability, 270
- Therapeutic efficacy
 controlled release delivery system,
 336
 drug release rate, 104
 multi-tablet approach, 347
 once-a-day oral dosage, 14
- Thermal infusion process
 CR dosage forms, 341–342
 dry granulation process, 341
- Thermoreversible protein-conjugating
 polymers, synthesis and
 characterization, 253–262
- Thermosensitivity, membrane systems,
 264
- Thrombolytic agent, marumerized matrix
 beads, 335
- Thrombolytic antagonist, CR
 marumerized bead dosage forms, 339
- Tight junctions
 chitosan activity, 30–31
 threshold value at charge density of
 polymer, 32

- Tissue damage by hydroxyl radicals, cationization of catalase, 79
- Tissue engineering
 biodegradable polyrotaxanes, 380–381
 drug delivery vehicles, 6
 gas-foaming/particulate leaching method, 161
 matrices, growth factor delivery, 157–166
 use of alginate, 161
 use of microspheres, 160–161
- Toxicity
 absorption enhancer, 289
 cationic lipids, 105
 liposome encapsulation of drugs, 102
 novel polymers on Caco-2 cells, 32
 protease inhibitors, 27
 toxins and enzymes delivered as cargo, 179
- Trafficking signals, amino acid sequences, 170
- Transfection activity
 DNA complexes, free folate, 217*f*
 folate-PEG-PEI, 218
- Transfection efficiency, nonliving vectors, 3
- Transfection of KB cells, folate conjugates of PEI, 217*f*
- Transforming growth factor- β 1 (TGF- β 1)
 controlled release from biodegradable polymer microparticles, 126–129
 cumulative release kinetics, 128*f*
 marrow stromal osteoblast culture, 129–135
 release kinetics, 126–129, 132
- Translocation mechanisms, aqueous solution into lipid bilayers, 144
- Transplanted cell, reconstitution of functional tissue mass, 157–158
- Transplanted cell engraftment, angiogenesis, 157–166
- Transport structures, organelles, 176
- N*-Trimethyl chitosan (TMC)
 permeability of 14 C-mannitol in Caco-2 intestinal epithelia, 32
 synthesis, 31*f*
- Trimethyl chitosan (TMC) chloride
 concentration-dependent transport enhancement ratios, 33*f*
 enhancement of nasal insulin absorption in rats, 33–34*f*
- N*-Trimethyl chitosan (TMC) chloride, mucosal penetration enhancer, 25
- N,N,N*-Trimethyl chitosan (TMC) chloride, targeted peptide drug delivery, 31–32
- Tripeptide peroxisomal signal, extreme carboxyl terminus of peroxisomal proteins, 174
- Trp fluorescence, quenching by various *n*-doxylstearic acids in the presence of egg PC liposomes, 143*f*
- Trypsin cleavage, PEGylation of etanercept, 117
- Tumor, immunomodulatory effect, 225–226
- Tumor accumulation, injection of STI formulations, 311*f*
- Tumor cell specific delivery, folate conjugates, 213
- Tumor-induced immunosuppression, patients with malignant glioma and tumor-bearing animals, 228
- Tumor targeting, EPR effect, 355–357
- Tumor vaccine
 efficacy in preventing tumor development, 223–224
 efficacy in treating established tumor, 224–225
- Turbidity data, EYPC vesicles, 247–248
- U
- Ulcerated tissues, antioxidant enzyme therapy, 87
- Unfolding step, passage through pores/pathways, 176
- Unwanted cells, destruction by intracellular targeting technology, 181
- V
- Vaccination
 at or after tumor cell challenge, 228
 i9L + IFN- γ , 227–228

- time relative to tumor cell challenge, 224
 with i9L + IFN- γ , survival of animals with IC tumor cells, 224*f*
- Vaccines**
 liposomal carriers, 100
 liposomes as antigen carriers, 105–106
- Valacyclovir (L-Val-ACV)**
 initial uptake rate in untransfected Caco-2 cells and transfected Caco-2/hPEPTI cells, 51*t*
 peptide transporter-mediated absorption mechanism, 51
- Vascular endothelium, liposome drug delivery, 105**
- Vascular network, critical for large organs and tissues, 164**
- Vascular permeability**
 reduced clearance rate of liposomal drugs, 103
 solid tumor tissue, 356
- Vascularization**
 cell survival, 158–159
 engineered tissues, 159
 forming tissues, challenge in tissue engineering, 159
 growth factors from tissue engineering matrix, 157
- Vasculature permeability, liposomal drugs into diseased tissues, 103**
- Vectors**
 appropriate cargo components, 179
 intracellular targeting, 177–182
- VEGF**
 blood vessel formation, 159
 delivered from porous tissue engineering scaffolds, 164
- Vehicle selection, oral drug delivery, 286–288**
- Ventolin, immediate release dosage form, 93**
- Viral fusion protein, incorporation into liposomes, 187–188**
- Viral mimetic, essential polymer features, 357–359**
- Viral vectors**
 compared to liposomal vectors, 105
 genetic material delivery and uptake, 8
 multicomponent synthetic, 359*f*
- Viruses, paradigm for intracellular delivery, 187**
- Vitamin B₁₂**
 permeability and molecular size of solutes, 269*t*
 permeability through composite membrane, 268
 permeation profile, 269*f*
 pH-dependent permeability, 270*f*
- W**
- Wall permeability, amino acid ester prodrugs, 50*t***
- Warfarin, replacement for heparin, 55**
- Water uptake, NiPAM/NASI/MMA and NiPAM/NASI/EMA polymer films, 261*f***
- Water-in-oil (w/o) microemulsions**
 drug development challenges, 293–294
 oral drug delivery opportunities, 291–293
 water-soluble molecules, 285
- Water-insoluble compounds, carried in plasma lipoproteins, 314–323**
- Wound healing**
 cell targeting specificity, 181
 chitosan, 29
- Z**
- Zidovudine, amino acid ester prodrugs, 49–51**